ISOLATION, STRUCTURE DETERMINATION AND TOTAL SYNTHESIS OF

POTENTIAL CANCER CHEMOTHERAPEUTIC AGENTS FROM

NATURAL SOURCES

by

ROBERT A. BRITTON

B.Sc., University of Waterloo, 1996

A THESIS SUBMITTED IN PARTIAL FULFILMENT OF

THE REQUIREMENTS FOR THE DEGREE OF

DOCTOR OF PHILOSOPHY

in

THE FACULTY OF GRADUATE STUDIES

(Department of Chemistry)

We accept this thesis as conforming

to the required standard

THE UNIVERSITY OF BRITISH COLUMBIA

September, 2002

© Robert A. Britton, 2002

In presenting this thesis in partial fulfilment of the requirements for an advanced degree at the University of British Columbia, I agree that the Library shall make it freely available for reference and study. I further agree that permission for extensive copying of this thesis for scholarly purposes may be granted by the head of my department or by his or her representatives. It is understood that copying or publication of this thesis for financial gain shall not be allowed without my written permission.

Department of ___CHEMISTRY___

The University of British Columbia
Vancouver, Canada

Date ___Sept. 7/2002___

Abstract

The ultimate goal in the chemotherapeutic treatment of cancer is the development of drugs that are highly effective against tumor cells and have little or no effect on healthy cells. Key to this pursuit is the identification of differences that exist between the life cycle of normal and cancerous cells. Thus, the discovery of new small molecule inhibitors of enzymes that regulate cellular growth and division should provide a better understanding of these biological processes and perhaps lead to more selective cancer treatments.

Mitosis, or cell division, is disrupted by antimitotic agents, which correspondingly have become the most promising chemotherapeutics in cancer treatment. Recently, the Caribbean soft coral *Erythropodium caribaeorum* was shown to be a good source of eleutherobin, a potent antimitotic agent. Having procured eleutherobin from this source, synthetic manipulations of the natural material provided a series of eleuthoside congeners, which were assayed for antimitotic activity. A remarkable relationship between the $\Delta^{2',3'}$ olefin and eleuthoside biological activity was highlighted by these studies.

The G2 checkpoint is one of a series of checkpoints that temporarily halt cell cycle progression in order to allow for repair of damaged DNA. It has been demonstrated *in vitro* that the inhibition of this checkpoint, in combination with a DNA damaging agent, selectively potentiates the killing of cancer cells. Extracts of the Brazilian ascidian *Didemnum granulatum* demonstrated G2 checkpoint inhibition activity. Fractionation of these extracts resulted in the isolation of isogranulatimide. In order to unambiguously confirm the structural assignment of this substance, generate sufficient material for biological testing and investigate the effect of structure on its biological activity, an efficient synthesis of isogranulatimide and several congeners was developed.

Concurrently, two new analogues of okadaic acid, a potent protein phosphatase inhibitor, have been isolated from the sponge *Merriamum oxeato*, collected in Jervis Inlet, British Columbia. These substances displayed pronounced G2 checkpoint inhibition activity and represent the first examples of diarrhetic shellfish poisons (DSP) in the Northeastern Pacific Ocean.

A total synthesis of 13-methoxy-15-oxozoapatlin, a G2 checkpoint inhibitor *and* antimitotic agent, has also been completed. Employing a linear sequence of 22 synthetic transformations, a renewable source of this structurally complex pentacyclic diterpene has been realized. The completion of this synthesis relied on the development of new synthetic methods useful in the construction of bicyclo[3.2.1]octanes.
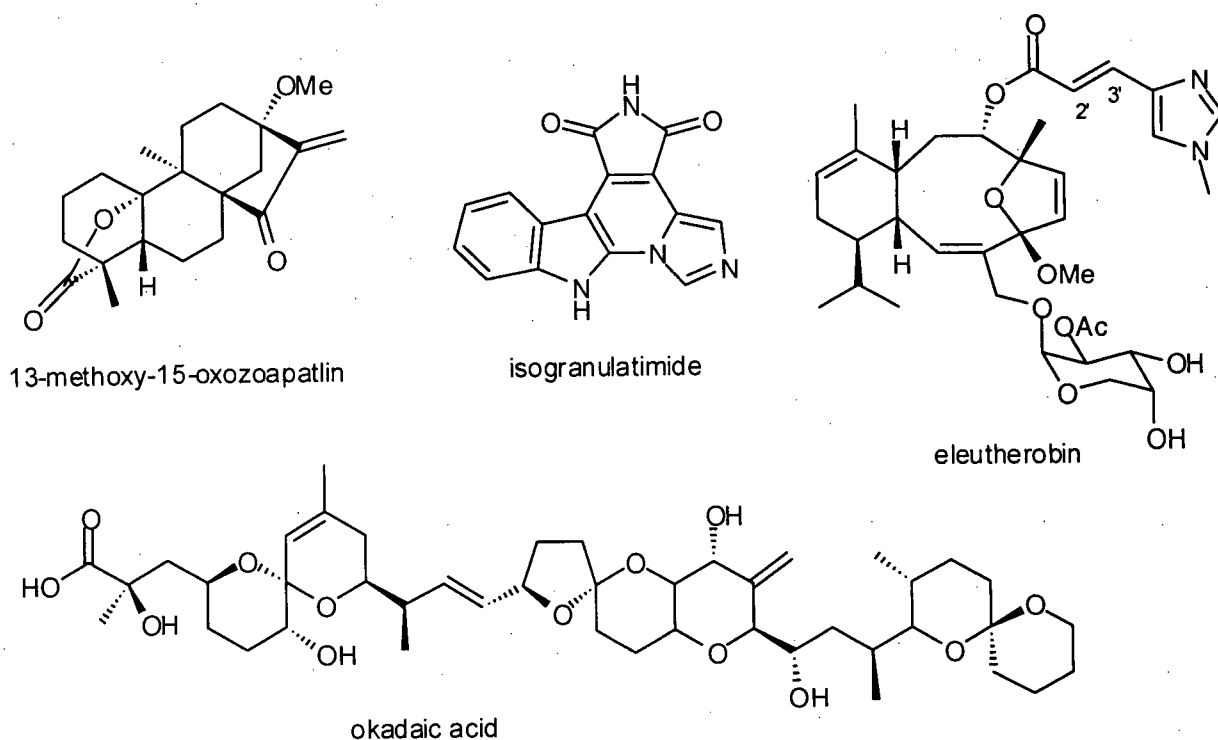
13-methoxy-15-oxozoapatlin

isogranulatimide

eleutherobin

okadaic acid

TABLE OF CONTENTS

LIST OF TABLES

LIST OF FIGURES

LIST OF ABBREVIATIONS

α	-	below the plane of the ring or 1,2 relative position
Ac	-	acetyl
AIBN	-	azobisisobutyronitrile
anal.	-	analysis
AMU	-	atomic mass units
APT	-	attached proton test
β	-	above the plane of a ring or 1,3-relative position
BOC	-	butoxycarbonyl
br	-	broad
Bu	-	butyl
calcd	-	calculated
COSY	-	(^{1}H-^{1}H)-homonulcear correlation spectroscopy
C–X	-	carbon number X
C	-	Celcius
δ	-	chemical shift in parts per million from tetramethylsilane or 1,5-relative position
Δ	-	denotes position of olefin
DCI	-	desorption chemical ionization
DDQ	-	2,3-dichloro-5,6-dicyano-1,4-benzoquinone
DCC	-	1,3-dicyclohexyldicarbodiimide
DIBAL	-	diisobutylaluminum hydride
DMA	-	N,N-dimethylacetamide
DME	-	dimethyl ether
DMAP	-	4-dimethylaminopyridine
DMF	-	N,N-dimethylformamide
DMPU	-	N,N-dimethylproptleneurea
DMS	-	dimethyl sulfide
DMSO	-	dimethyl sulfoxide
DNA	-	deoxyribonucleic acid
DSP	-	diarrhetic shellfish poisons
d	-	doublet or donor
dd	-	doublet of doublets
EA	-	elemental analysis
EI	-	electron impact
E	-	entgegen (configuration)
ed.	-	edition
ED., Eds.	-	editor, editiors
ELISA	-	enzyme linked immuno sorbant assay
ε	-	1,6-relative position
equiv.	-	equivalent(s)
EOM	-	ethoxymethyl
Et	-	ethyl
FAB	-	fast atom bombardment
γ	-	1,4-relative relationship
g	-	gram
GGPP	-	geranylgeranyl pyrophosphate
GLC	-	gas-liquid chromatography

h	-	hour(s)
HMBC	-	(^{1}H-^{13}C) heteronuclear multiple bond coherence
HMQC	-	(^{1}H-^{13}C) heteronuclear multiple quantum coherence
HOHAHA	-	homonuclear Hartmann Hahn
HPLC	-	high performance liquid chromatography
HRMS	-	high resolution mass spectroscopy
H–X	-	hydrogen number X
Hz	-	hertz
IC_{50}	-	inhibitory concentration (for 50% of a biological sample)
IR	-	infrared
J	-	coupling constant in hertz
KHMDS	-	potassium 1,1,1,3,3,3,-hexamethyldisilazide
L	-	liter
LDA	-	lithium diisopropylamide
LiHMDS	-	lithium 1,1,1,3,3,3-hexamethyldisilazide
LiTMP	-	lithium 2,2,6,6-tetramethylpiperidine
MS	-	mass spectroscopy
m	-	multiplet
mp	-	melting point
m	-	meta
MOM	-	methoxymethyl
MHz	-	megahertz
Me	-	methyl
μg	-	microgram(s)
μL	-	microliter(s)
μM	-	micromolar
mg	-	milligram(s)
mL	-	milliliter(s)
mm	-	millimeter(s)
mmol	-	millimole(s)
min	-	minute(s)
MTOC	-	mitotic organizational center
M	-	molar
mol.	-	molecular
mp53	-	lacking a functioning p53 tumor suppressor gene
nM	-	nanomolar
-ve	-	negative
N	-	normal
NIS	-	*N*-iodosuccinimide
NMR	-	nuclear magnetic resonance
NOE	-	nuclear Overhauser enhancement
NP	-	normal phase
1D NOESY	-	one dimensional nuclear Overhauser and exchange spectroscopy
p	-	para
pH	-	$-\log_{10}[\text{H}^+]$
Ph	-	phenyl
ppm	-	parts per million
PMP	-	1,2,2,6,6-pentamethylpiperidine
PhNTf$_2$	-	*N*-phenyltrifluoromethanesulfonimide

+ve	-	positive
PPTS	-	pyridinium *p*-toluenesulfonate
Pr	-	propyl
PKC	-	protein kinase C
pyr	-	pyridine
q	-	quartet
R	-	rectus (configuration)
R_F	-	retention factor
RP	-	reverse phase
SCUBA	-	self contained underwater breathing apparatus
s	-	singlet
S	-	sinister (configuration)
sec	-	secondary
t	-	triplet
t	-	tertiary
TBAF	-	tetrabutylammonium fluoride
TBS	-	*tert*-butlydimethylsilyl
tert	-	tertiary
Tf	-	trifluoromethanesulfonyl
TFA	-	trifluoroacetic acid
THF	-	tetrahydrofuran
TLC	-	thin layer chromatography
3D	-	three dimensional
TMS	-	trimethylsilyl
SEM	-	(2-trimethylsilylethoxy)methyl
$TMSCHN_2$	-	trimethylsilyldiazomethane
TESOTf	-	triethylsilyl trifluoromethanesulfonate
TMSOTf	-	trimethylsilyl trifluoromethanesulfonate
TOCSY	-	total correlation spectroscopy
Ts	-	toluenesulfonyl
uv	-	ultraviolet
UBC	-	University of British Columbia
US	-	United States (of America)
v/v	-	volume to volume ratio
λ	-	wavelength
w/v	-	weight to volume ratio
wtp53	-	with functioning p53 tumor suppressor gene
•	-	coordination or complex
±	-	racemic

ACKNOWLEDGEMENTS

1. Cancer and Chemotherapy

1.1 Introduction

Tragically, one in three Canadians and three out of four households in Canada will be affected by cancer.[1] In the year 2001 alone, the Canadian Cancer Society reported 134,100 new incidents of cancer and 65,300 deaths related to this disease.[1] Ominously, since cancer primarily affects the elderly, the aging of our population is projected to result in a 70% increase in the incidence of cancer by 2015.[1] Therefore, it is not surprising that the treatment of this dreaded disease is at the forefront of current scientific research.

Cancer is a general term that encompasses over 100 different diseases involving the uncontrolled growth of abnormal cells.[2] Thus, while normal cells propagate in an organized manner, regulated by the necessity to maintain healthy bodily function or repair damaged tissue, cancerous cells reproduce without provocation, creating a mass of cells known as a tumor. The movement or metastasis of cancer cells from a primary tumor to healthy tissues and organs throughout the body occurs readily through the blood stream or lymph system.[1] In this manner cancer spreads, leaving a trail of destruction in its wake. Currently, prostate cancer is the most frequently diagnosed primary tumor in men and breast cancer accounts for almost one third of cancerous tumors reported in women. In fact, one out of nine Canadian women will be diagnosed with breast cancer in their lifetime.[1]

Cancer remains the leading cause of premature death among Canadians.[1] However, owing largely to the development of more specific and efficacious treatments for this disease, the survival rate for cancer patients has risen from 20% in the early 20th century to a current level of approximately 50%.[1,3] This dramatic increase has coincided with improvements in surgical techniques, X-ray equipment, blood transfusions and antibiotics.[3] Moreover, while traditional

treatment of cancer by surgery or radiotherapy often eradicated the primary tumor but ultimately failed to treat metastatic cancer cells, a combination of these treatments and chemotherapy has emerged as a viable alternative. In this manner the former therapies focus on the removal of the primary tumor and are complimented by the chemotherapeutic treatment of metastatic cancer cells.

Since cancerous cells divide and multiply in an uncontrolled manner, these cells are typically more metabolically active than normal cells. Thus, while healthy cells spend a considerable amount of time resting, waiting for cellular cues to begin division, cancerous cells may grow without restraint. This disparity between cancer and healthy cells has formed the basis for most current cancer chemotherapeutic strategies, which target metabolically active cells. Unfortunately, an often treatment-limiting side effect of such therapies involves the unfortunate destruction of other rapidly dividing cells, including those of bone marrow and the gastrointestinal tract.[2] Moreover, once solid tumors (i.e. colon, rectum, lung and breast tumors) attain a certain size, their metabolic activity abates, resulting in a low proportion of dividing cells and a consequent indifference to chemotherapeutic treatment.[2]

The first documented treatment of cancer by chemical means was reported in 1865, when potassium arsenite was noted to elicit a positive response when administered to a patient with leukemia.[4] However, modern cancer chemotherapy owes its roots to pioneering work carried out during World War II at Yale University, where nitrogen mustards, derivatives of highly toxic mustard gas, displayed clinical effectiveness in treating a patient with terminal lymphosarcoma.[4] It is of some consternation, however, that after more than 50 years of drug development, the side effects of bone marrow toxicity and drug resistance reported for this first recipient of cancer chemotherapy are still observed in patients today.

The present trend in cancer chemotherapy, which involves the development of new drugs that exploit the subtle disparities between normal and cancerous cells, has relied on our evolving

recognition of differences between the life cycle for healthy and cancerous cells. The two primary events in cell proliferation are DNA replication and cell division. To ensure the fidelity of these events, the cell cycle is divided into four sequential phases and a quiescent state known as G0.[5] Owing to deprivation of certain growth factors, cells may exit their normal cycle of DNA replication and cell division and enter G0, in which fundamental cellular metabolism is depressed. Alternatively, the stimulation of these growth factors can signal a cell to re-enter this active cycle.
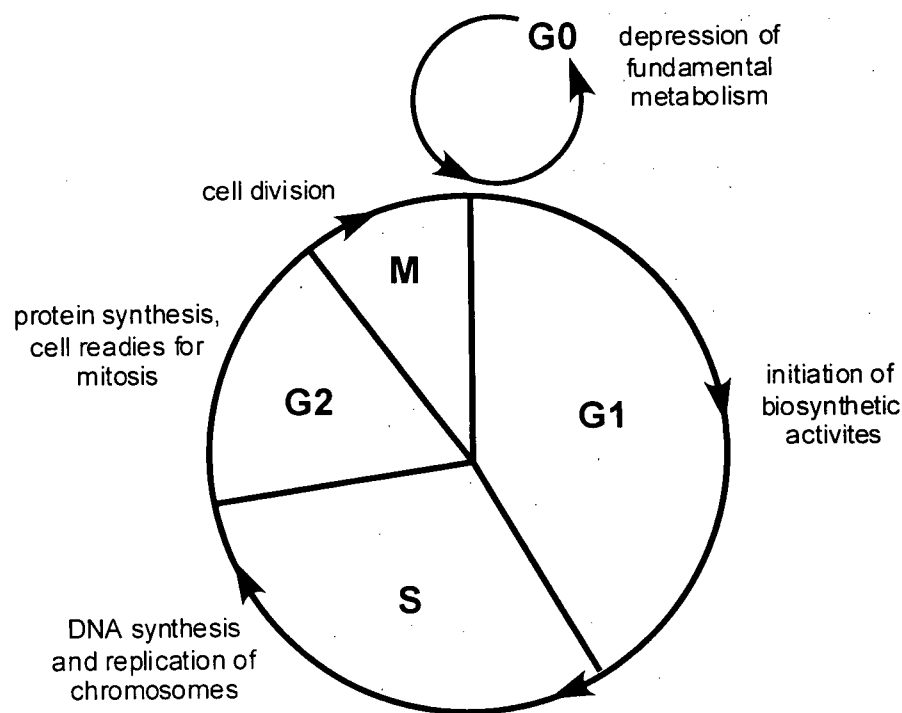
Figure 1.1. The cell cycle.

As outlined in Figure 1.1, the first phase of the cell cycle is the G1 phase. At this stage the cell must assess the viability of committing to another full round of division. Once G1 phase is initiated, genes for cell-cycle proteins are transcribed and translated in preparation for DNA synthesis. It is not surprising then that cancer cells have a number of mutated proteins typically involved in regulating the cellular progression through G1 phase.[5] Thus, the inability of these

proteins to inhibit the progress of cancerous cells facilitates the unabated growth of tumors. Entering S phase, cells begin the process of duplicating their entire genome, a task that must be completed before initiating a period of active protein synthesis, known as G2 phase. The final stage of the cell cycle, M phase or mitosis, involves breakdown of the nuclear envelope and separation of chromosomes into two identical units, which contain all the genetic information required for cell vitality. Subsequent migration of these daughter chromosomes to opposite ends of the cell is followed by their enclosure within new nuclear envelopes and, eventually, cell division.

Since cancerous cells propagate more rapidly than normal cells, and consequently spend more time in the cell cycle, drugs that interact with and ultimately kill dividing cells have demonstrated clinical effectiveness in the treatment of cancer.[3] In particular, antimitotic agents or compounds that disrupt cell division, have been effective in this regard.[6] Moreover, the recent discovery of new, more selective antimitotic agents and the elucidation of their unique modes of action has fueled interest in this method of chemotherapy.

1.2 Cancer chemotherapeutics and mitosis

Although a number of proteins are crucial to mitosis, a key to the potency of most antimitotic agents lies in their interaction with α and β tubulin, essential components of microtubules.[7] During mitosis, microtubules or spindle fibers emanate from microtubule -organizational centers (MTOC's) at the spindle poles of the cell. The growth of microtubules relies on the dynamic assembly and disassembly of α and β tubulin, monomeric proteins comprised of roughly 450 amino acid units (Figure 1.2).[7] It is noteworthy that the rate of depolymerization of tubulin is much greater than the rate polymerization. Thus, the growth and contraction of microtubules continues until the propagating end is stabilized or 'capped' by a

cellular component.[7] In particular, a complex of DNA and proteins known as a kinetochore, which functions to hold two sister chromatids together, stabilizes the growing microtubule. Once attached to the kinetochore, microtubules undergo contraction, during which the sister chromatids are pulled apart and delivered to the MTOC's at opposite ends of the cell. Thus, microtubules play a pivotal role in transporting the daughter chromosomes to the spindle poles, a necessary event in prelude to cell division. It is not surprising then, that the interaction of small molecules with the dynamic assembly and disassembly of microtubules results in abrogation of cell division and eventually cell death.[7] While certainly these antimitotic agents would also prove toxic to healthy dividing cells, the larger population of dividing cancer cells imparts selectivity to this mode of cancer treatment.
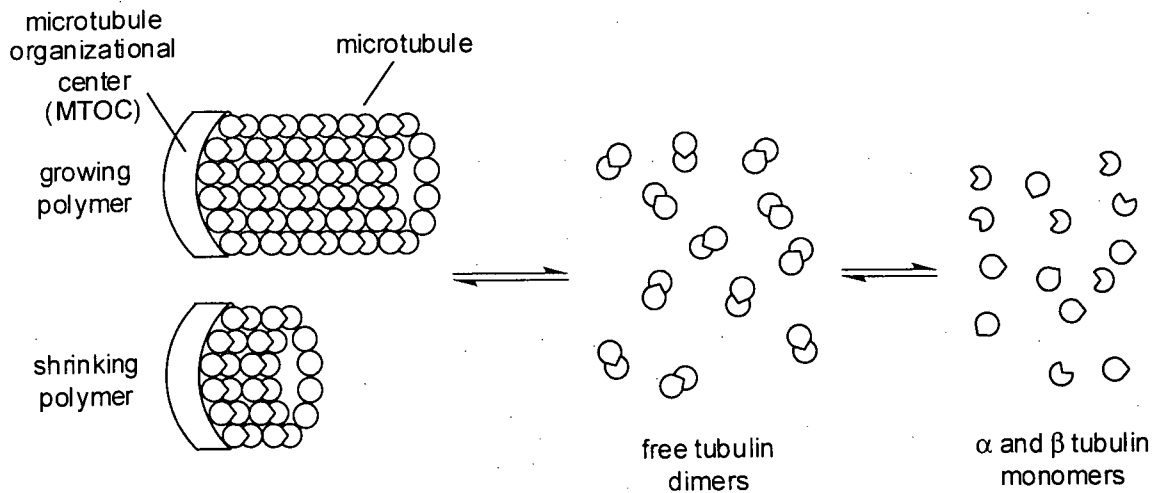
Figure 1.2. Dynamic assembly and disassembly of microtubules.
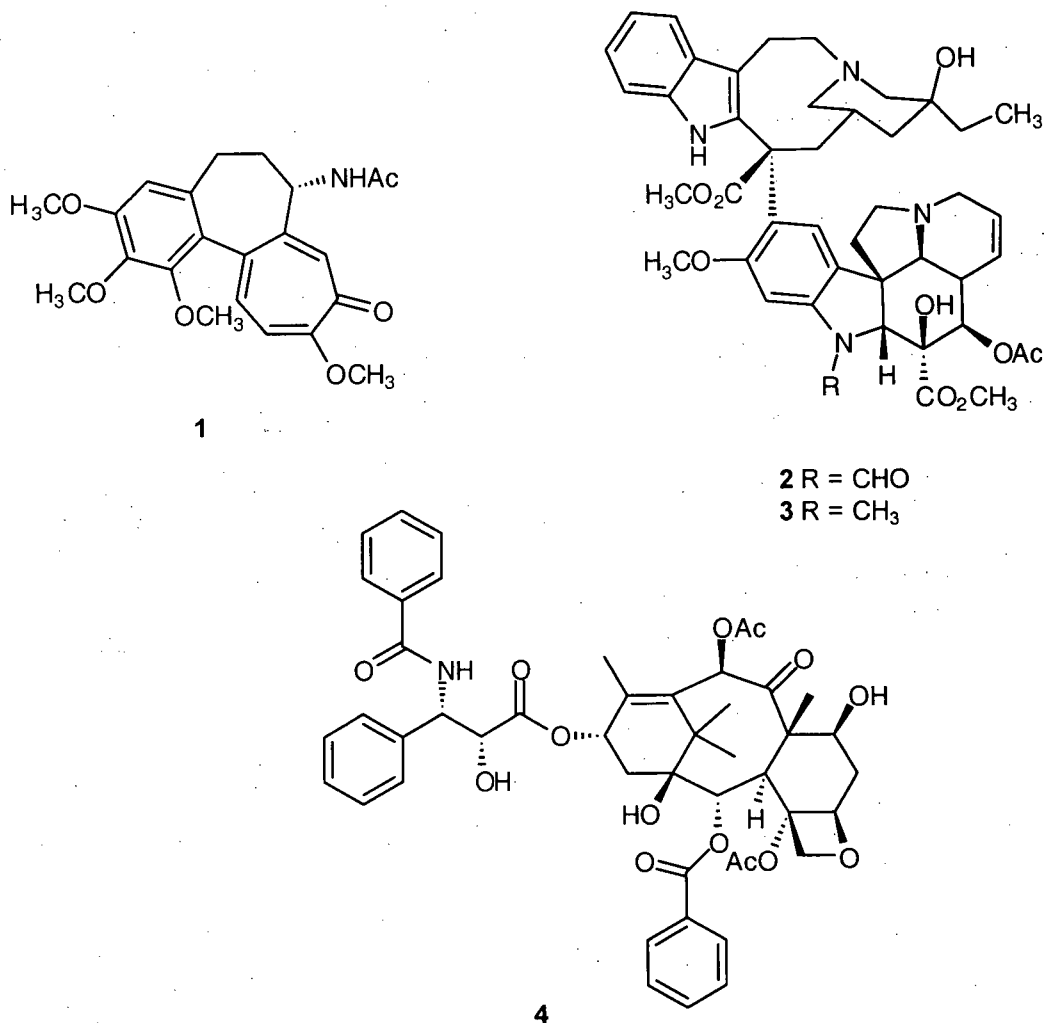
Figure 1.3. Antimitotic agents.

The first antimitotic agent to be characterized as such was colchicine (**1**) (Figure 1.3), which had traditionally found use in the treatment of inflammatory diseases.[8] It was demonstrated that colchicine (**1**) disrupts mitosis by binding tightly to tubulin and inhibiting the assembly of microtubules.[9] Thus, colchicine (**1**) is regarded as an inhibitor of microtubule assembly and as the progenitor of a family of compounds with similar biological activities that bind to tubulin at the "colchicine site". A second family of compounds that inhibit microtubule assembly through their interactions with tubulin are the vinca alkaloids. Through their reversible binding to the "vinca domain" on tubulin, compounds such as vincristine (**2**) and vinblastine (**3**)

inhibit the formation of microtubules and consequently compromise cell vitality.[9] Three decades of successful treatment of cancer patients with these antimitotic vinca alkaloids has validated this form of chemotherapy.[9]

More recently, a family of antimitotic agents that bind to tubulin and stabilize the formation of microtubules has been discovered. Taxol (**4**) (Figure 1.3), isolated from the Pacific yew tree *Taxus brevifolia*,[10] was the first microtubule stabilizing agent to be identified and has become an invaluable chemotherapeutic in the treatment of cancer. It is noteworthy that the interaction of antimitotic agents with the "taxol binding site" on tubulin results in dramatic polymerization of tubulin monomers and consequently the formation of spectacular arrays of microtubules, not necessarily originating at MTOC's.[9] While a number of drugs that inhibit mitosis by the same mechanism as taxol (**4**) have been reported, numerous side effects detract from the clinical utility of these potent cytotoxins.[11] Furthermore, a variety of cancers have demonstrated resistance to these drugs or become resistant through over-expression of P-glycoprotein, a cellular pump that mediates drug efflux.[11] Additionally, the development of taxol resistance through increased expression of tubulin isotypes and mutational modification of α and β tubulin structure has resulted in a decrease in the potency of these drugs after prolonged exposure.[11] Therefore, investigations geared towards the discovery of new antimitotic agents with improved biological activity towards taxol resistant cancers is well warranted and may indeed lead to improvements in cancer chemotherapy.

1.3 Cancer chemotherapeutics and the G2 checkpoint

The ultimate goal in the chemotherapeutic treatment of cancer is to develop drugs that are highly effective against tumor cells and have little or no effect on healthy cells. Recent discoveries of clear genetic differences between healthy and cancerous cells have presented a

number of unique opportunities to selectively target cancer cells by taking advantage of their genetic abnormalities. In the last decade, it has been discovered that roughly one half of human cancers involve a mutated or disrupted p53 tumor suppressor gene.[12] While not essential to the growth of normal cells, p53 is required for the detection of DNA damage and the initiation of cell cycle arrest to permit the repair of DNA. Thus, the development of chemotherapeutics that target cells lacking proper p53 function should provide selectivity in the treatment of cancer.[13]

Normal cells respond to DNA damage by activating checkpoints that temporarily halt growth and division to allow time for the repair of DNA.[14,15] The G1 checkpoint facilitates DNA repair before DNA replication in S phase and the G2 checkpoint permits DNA repair before the daughter chromosomes are segregated in mitosis. In this manner, the propagation of genetic abnormalities is prevented. Cells with mutated p53 tumor suppressor genes (mp53), approximately 50% of all solid tumor cancer cells, are unable to activate the G1 checkpoint in response to DNA damage.[16] However, their G2 checkpoint, although weaker than that in normal cells,[17] still provides an opportunity to repair damaged DNA and to successfully proceed into mitosis. Thus, inhibitors of the G2 checkpoint, when used alone, should have no effect on normal or cancerous cells. When used in combination with a DNA damaging agent, these inhibitors should have little effect on the ability of normal cells to survive, however, they should dramatically increase the killing of mp53 cancer cells. The expectation of this result derives from the fact that normal cells are still capable of activating their G1 checkpoint to repair damaged DNA and their G2 checkpoint is typically strong, and would therefore require a higher dose of G2-checkpoint-inhibitor-to-be-effectively-blocked. Alternatively, cancerous cells with a mutated p53 tumor suppressor gene (mp53), lack a G1 checkpoint and have a weak G2 checkpoint and should consequently be forced into a premature and lethal mitosis.

While very few G2 checkpoint inhibitors are known, two classes of compounds have serendipitously been discovered to elicit this effect, namely the purine analogues (e.g. caffeine

(5)[18,19] and pentoxyfylline (6)[20]) and the bis-indole maleimide alkaloids (e.g. staurosporine (7)[21] and UCN-01 (8)[22]) (Figure 1.4). In a variety of paired cell lines differing only in their p53 status, G2 checkpoint inhibitors induced greater sensitivity to DNA damage in cells with a mutated p53 tumor suppressor gene (mp53) than in those with a healthy tumor suppressor gene (wtp53).[23,24] For example, treatment of mp53 MCF-7 breast cancer cells with pentoxyfylline (6) in combination with the DNA damaging agent cisplatin resulted in a 30-fold increase in cell death when compared to treatment of these cells with cisplatin alone.[25] Unfortunately, the known G2 checkpoint inhibitors are of limited clinical use because they interact with a broad range of other cellular processes. Staurosporine (7) and UCN-01 (8) are nonselective kinase inhibitors and the purine alkaloids (e.g. 5 and 6) have multiple pharmacological activities. Consequently, none of the substances belonging to these families of compounds are sufficiently selective G2 checkpoint inhibitors to evaluate the principle of this combination therapy *in vivo*. However, the demonstration that even imperfect G2 checkpoint inhibitors can potentiate the cytotoxicity of DNA-damaging agents in a manner specific for mp53 cancer cells suggests that a rational search for novel G2 checkpoint inhibitors could yield agents with greater specificity and potency than those presently known.
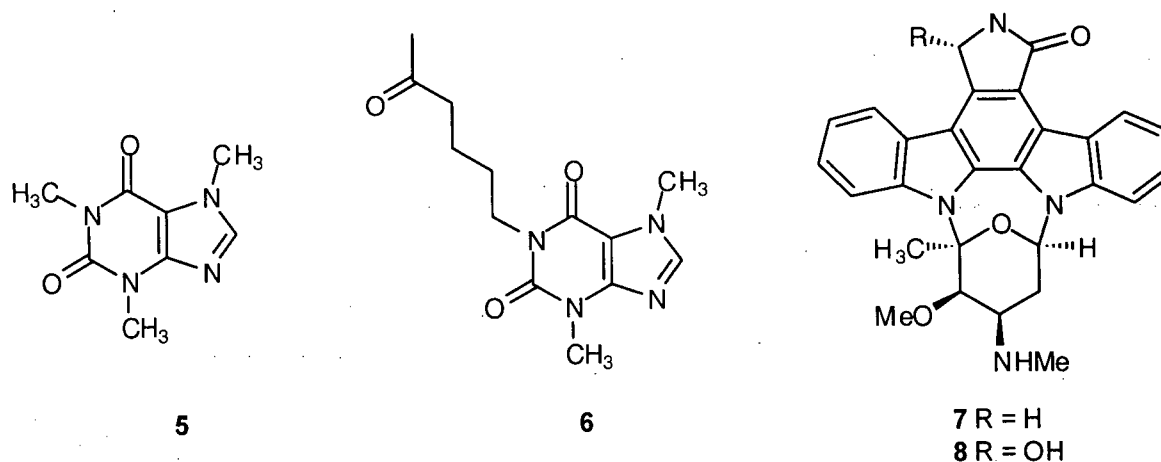
Figure 1.4. Inhibitors of the G2 checkpoint.

In this regard, the first high-throughput bioassay designed for rapid identification of G2 checkpoint inhibitors has recently been developed in the Department of Biochemistry and Molecular Biology at UBC.[26] Roberge and coworkers have reported that subjection of MCF-7 breast cancer cells lacking p53 function (mp53) to DNA-damaging γ-irradiation resulted in prolonged cellular arrest in G2, while DNA repair ensued. However, when treated with the G2 checkpoint inhibitors caffeine (**5**) or UCN-01 (**8**), approximately 60% of the G2 arrested cells progressed directly onto mitosis.[26] In this manner, the reversibility of DNA-damage induced G2 arrest was clearly demonstrated.

From these results, an assay for small molecule inhibitors of the G2 checkpoint has evolved.[26] As depicted in Figure 1.5, DNA damage is induced in a population of mp53 MCF-7 breast cancer cells through the action of γ-irradiation emitted by a ^{60}Co source. While individual cells certainly subsist in distinct phases of their life cycle when treated with γ-irradiation, after a sufficient amount of time has elapsed, synchronous arrest in G2 phase occurs. Thus, after a period of 16 hours, both the antimitotic agent nocodazole and a compound to be assayed for G2 checkpoint inhibition activity are added to the cells. If the added substance exhibits G2 checkpoint inhibition activity, the cells will be released from G2 and blocked in mitosis by the agency of nocodazole. Alternatively, if the added substance does not affect the G2 checkpoint, the cells will remain arrested in G2. To distinguish between cells arrested in G2 or mitosis, an enzyme-linked immuno sorbant assay (ELISA) was developed that recognizes a phosphorylated form of nucleolin present only during mitosis. In this manner, mitotic cells become significantly stained and can thus be visually differentiated from cells arrested in G2.

DNA damage

MCF-7 breast cancer cells with mutated p53 tumor supressor gene

16 hours

cells arrest in G2 phase

addition of a potential G2 checkpoint inhibitor and the antimitotic agent nocodazole

active G2 checkpoint inhibitor

cells arrest in mitosis and are detected by ELISA assay

inactive G2 checkpoint inhibitor

cells remain arrested in G2 phase (not detected in ELISA assay)

Figure 1.5. A novel, high-throughput assay for the detection of G2 checkpoint inhibitors.[26]

1.4 Current proposal

In the pursuit of new, more efficacious cancer chemotherapeutics, scientists have traditionally turned to nature for leads. Recently, however, owing to the ability of combinatorial chemistry and genomic-based technologies to rapidly construct new libraries of small molecules, there is an emerging perception that the significance of natural products in drug discovery is diminishing.[27,28] However, this notion remains to be substantiated, as there is currently no counterpart to the inherent structural diversity and biological activity of natural products in the available libraries of synthetic compounds.[29] In fact, of the 520 new drugs reported between 1983 and 1994, 40% of these were natural products or derivatives thereof.[28] Thus, while certainly new venues for drug discovery will aid the progression of disease control, the future role of natural products in drug discovery is secure.

The isolation of natural products has also contributed significantly to the burgeoning development of synthetic chemistry witnessed in the latter half of the 20th century. In this regard, natural products provide challenging target structures, the synthesis of which tests the rigor of synthetic methods and ingenuity in strategic planning. Moreover, the necessity to overcome obstacles accessory to such pursuits continues to fuel the development of new synthetic

methodologies. The synthesis of natural products also provides a venue for the construction of congeneric libraries of these substances, such that the role of structure in their biological activity may be accurately assessed.

The research described in this document details the isolation, structure determination, synthetic transformations and total syntheses of natural products that bear potential as novel cancer chemotherapeutics. In particular, studies directed towards the isolation and structure elucidation of natural product inhibitors of the G2 checkpoint and mitosis have been combined with the development of new synthetic methods for the construction of their carbocyclic and heterocyclic frameworks. The results gathered from this pursuit have identified potential leads for the chemotherapeutic treatment of cancer and generated renewable sources and structural congeners of these materials, facilitating their further exploitation in preclinical trials.

1.5 References

(1)   These statistics and facts about cancer were compiled by the Canadian Cancer Society in 2001 and detailed in a report published online at www.cancer.ca.

(2)   Pratt, W. B.; Ruddon, R. W.; Ensminger, W. D.; Maybaum, J. *The Anticancer Drugs, Second Edition*; Oxford University Press: New York, 1994.

(3)   Carter, S. K.; Bakowski, M. T.; Hellmann, K. *Chemotherapy of Cancer, Second Edition*; John Wiley & Sons: Toronto, 1981.

(4)   See reference 2, and references cited therein.

(5)   Hung, T. D.; Jamison, T. F.; Schreiber, S. L. *Chemistry and Biology* **1996**, *3*, 623.

(6)   Hamel, E. *Med. Res. Rev.* **1996**, *16*, 207.

(7)   Downing, K. H. *Annu. Rev. Cell Dev. Biol.* **2000**, *16*, 89.

(8)   Hastie, S. B. *Pharmac. Ther.* **1991**, *51*, 377.

(9)   See reference 6, and references cited therein.

(10) Wani, M. C.; Taylor, H. L.; Wall, M. E.; Coggon, P.; McPhail, A. T. *J. Am. Chem. Soc.* **1971**, *93*, 2325.

(11) Roberge, M.; Cinel, B.; Anderson, H. J.; Lim, L.; Jiang, X.; Xu, L.; Bigg, C. M.; Kelly, M. T.; Andersen, R. J. *Cancer Res.* **2000**, *60*, 5052.

(12) Stewart, Z. A.; Pietenpol, J. A. *Journal of Mammary Gland Biology and Neoplasia* **1999**, *4*, 389.

(13) For references regarding the potentiation of cell death by combination treatments involving DNA damaging agents and G2 specific cell cycle checkpoint inhibitors see: (a) Weinert, T.; Lydall, D. *Seminars Cancer Biol.* **1993**, *4*, 129. (b) Nurse, P. *Cell* **1997**, *91*, 865.

(14) Hartwell, L.; Weinert, T.; Kadyk, L.; Garvick, B. *Cold Spring Harbor Symp. Quant. Biol.* **1994**, *4*, 129.

(15) Kaufmann, W. K.; Paules, R. S. *FASEB J.* **1996**, *10*, 238.

(16) Kastan, M. B.; Onyekwere, O.; Sidransky, D.; Vogelstein, B.; Craig, R. W. *Cancer Res.* **1991**, *51*, 6304.

(17) Paules, R. S.; Levedakou, E. N.; Wilson, S. J.; Innes, C. L.; Rhodes, N.; Tlsty, T. D.; Galloway, D. A.; Donehower, L. A.; Tainsky, M. A.; Kaufmann, W. K. *Cancer Res.* **1995**, *55*, 1763.

(18) Busse, P. M.; Bose, S. K.; Jones, R. W.; Tolmach, L. J. *Radiat. Res.* **1978**, *76*, 292.

(19) Downes, C. S.; Musk, S. R. R.; Watson, J. V.; Johnson, R. T. *J. Cell Biol.* **1990**, *110*, 1855.

(20) Andreassen, P. R.; Margolis, R. L. *Proc. Natl. Acad. Sci. U. S. A.* **1992**, *89*, 2272.

(21) Tam, S. W.; Schlegel, R. *Cell Growth Differ.* **1992**, *3*, 811.

(22) Wang, Q.; Fan, S.; Eastman, A.; worland, P. J.; Sausville, E. A.; O'Conner, P. M. *J. Natl. Cancer Inst. (Bethesda)* **1996**, *88*, 956.

(23) Yao, S.-L.; Akhtar, A. J.; McKenna, K. A.; Bedi, G. C.; Sidransky, D.; Mabry, M.; Ravi, S. J.; Collector, M. I.; Jones, R. J.; Sharkis, S. J.; Fuchs, E. J.; Bedi, A. *Nat. Med.* **1996**, *2*, 1140.

(24) Bunch, R. T.; Eastman, A. *Clin. Cancer Res.* **1996**, *2*, 791.

(25) Fan, S.; Smith, M. L.; Rivet, D. J.; Duba, D.; Zhan, Q.; Kohn, K. W.; Fornace, J. A.; O'Conner, P. M. *Cancer Res.* **1995**, *55*, 1649.

(26) Roberge, M.; Berlinck, R. G. S.; Xu, L.; Anderson, H. J.; Lim, L.; Curman, D.; Stringer, C. M.; Friend, S. H.; Davies, P.; Vincent, I.; Haggarty, S. J.; Kelly, M. T.; Britton, R.; Piers, E.; Andersen, R. J. *Cancer Res.* **1998**, *58*, 5701.

(27) Harvey, A. L. *Trends Pharmacol. Sci.* **1999**, *20*, 196.

(28) Bindseil, K. U.; Jakupovic, J.; Wolf, D.; Lavayre, J.; Leboul, J.; van der Pyl, D. *Drug Discov. Today* **2001**, *6*, 840.

(29) Wessjohann, L. A. *Curr. Opin. Chem. Biol.* **2000**, *4*, 303.

2. Total Synthesis of the G2-Checkpoint Inhibitor and Antimitotic Diterpenoid (±)-13-Methoxy-15-oxozoapatlin

2.1 Terrestrial diterpenoids

Diterpenoids are perhaps the preeminent family of terrestrial natural products. Members of this family, whose biosynthesis involve the intermediacy of geranylgeranyl pyrophosphate (GGPP) (1), include some of the most important chemotherapeutics in use to date. Moreover, the complexity and diversity of diterpenoid structures is unparalleled within the realm of natural products.[1] Thus, the pharmaceutical potential attributed to these unique carbocycles has fueled a longstanding interest in their isolation and structure determination. Due, in large part, to the association between structural complexity and biological activity, the synthesis of terrestrial diterpenes has also attracted much attention and continues to provide a rigorous testing ground for synthetic planning and methodologies.

Although a number of pharmaceutically significant terrestrial diterpenes have been reported, none have received the attention afforded to taxol (2) (Figure 2.1). Originally isolated from the bark of the pacific yew tree *Taxus brevifolia* in 1971,[2] taxol (2) exhibited *in vitro* activity as an anti-tumor agent in studies carried out at the US National Cancer Institute. It was later shown that taxol (2) affects cell mitosis by microtubule polymerization, at the time, a unique mode of action for anti-tumor compounds.[3] This biological property, reported in 1979, attracted the interest of both natural product and synthetic chemists alike, and since this time over 100 structurally related analogues of taxol (2) have been reported from various species of *Taxus*.[4] Additionally, synthetic efforts towards this diterpene have culminated in 6 total syntheses.[5]

Diterpenes have also been implicated as the active ingredients in a number of traditional folk medicines. Extracts of the ornamental tree *Ginkgo biloba*, a member of the world's oldest species of tree, have been used since antiquity to delay the degeneration of faculties normally experienced in old age. The active constituents of these extracts have been characterized as a mixture of terpenoids and flavonoids. In particular, the ginkgolide diterpenes (e.g. ginkgolide A (**3**)),[6] have demonstrated significant antagonistic activity towards the platlet-activating factor (PAF), a key component of numerous physiological processes.[7] The combination of a ring cleavage and several structural rearrangements highlight the biosynthesis of these remarkable heterocycles from GGPP (**1**), providing a structural complexity that has proved an intimidating challenge for chemical synthesis.[8]
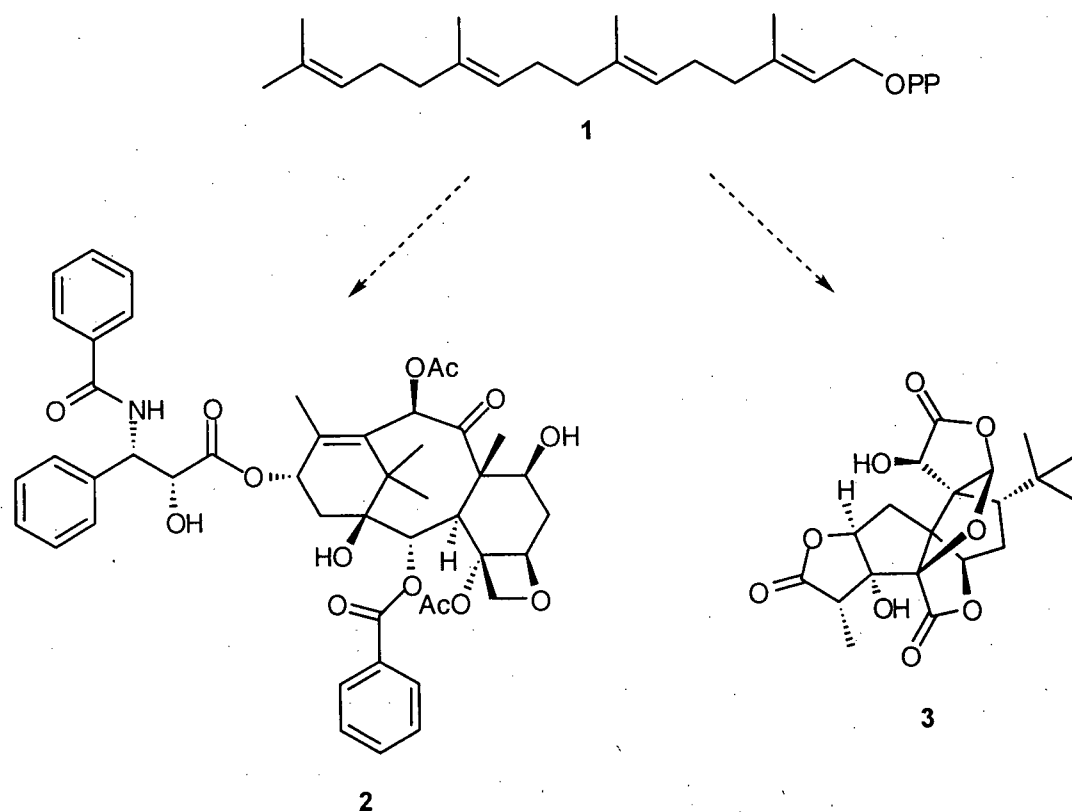
Figure 2.1. Biologically active terrestrial diterpenoids.

One of the most thoroughly studied families of terrestrial diterpenoids, however, has displayed little pharmaceutical potential. The tetracyclic diterpenes commonly referred to as the *ent*-kaurenoids and their biosynthetic progeny, the gibberellins, have received much attention due to their agronomical potential. The gibberellins (e.g. **4**, Scheme 2.3) were originally isolated from the fungus *Gibberella fujikuroi* and shown to be the causative agent of the "baka-nae" (literally: stupidly overgrown seedling) rice disease typified by excessive stem and leaf elongation.[9] They have since been found in plants, where not suprisingly, they act as growth hormones. The biosynthesis of gibberellins from *ent*-kaurene (**5**) has been the subject of numerous reports and will be discussed, along with that of other *ent*-kaurene derived diterpenes, in the following section.

4   **5**
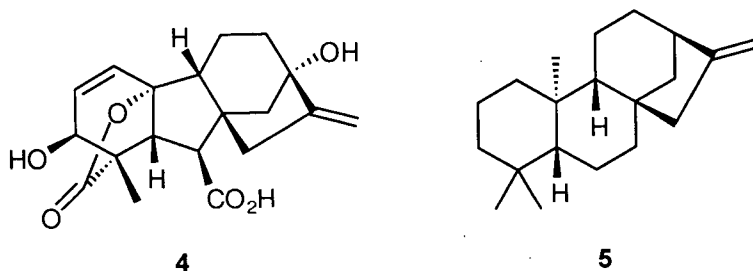
2.1.1 Biosynthetic pathway for *ent*-kaurenoids and related compounds

The biogenesis of *ent*-kaurene (**5**) and related compounds are outlined in Schemes 2.1 to 2.4. As detailed, the biosynthetic events that lead to **5** are initiated by the protonation of GGPP (**1**), which results in a transannular cyclization, producing either copalyl pyrophosphate (**6**) or labdadienyl pyrophoshate (**7**). As the most common stereochemistry observed among cyclic diterpenoids is that of **7**, the kaurenoids derived from **6** are considered enantiomeric. As such, the prefix *ent* is used to denote the absolute stereochemistry of this family of compounds.[4] In

proceeding from copalyl pyrophosphate (6) to ent-kaurene (5), a loss of diphosphate is followed by a second cyclization event, which generates the tricycle 8 (Scheme 2.2). Reaction between the terminal olefin function and the tertiary cation present in 8, produces the tetracycle 9, which possesses a bridging 5-membered ring with a stereochemical configuration opposite to that of ent-kaurene (5). A 1,2-alkyl shift, or Wagner-Meerwein rearrangement, then generates a tertiary cation and in so doing expands the 5-membered carbocyclic ring in 9 and, consequently, contracts the original 6-membered ring. This process effectively provides the ent-kaurenoid stereochemistry and is followed by the loss of a proton to afford ent-kaurene (5). Incredibly, the biosynthetic sequence of events that proceed from copalyl pyrophosphate (6) to 5 are catalyzed by a single enzyme.[4]
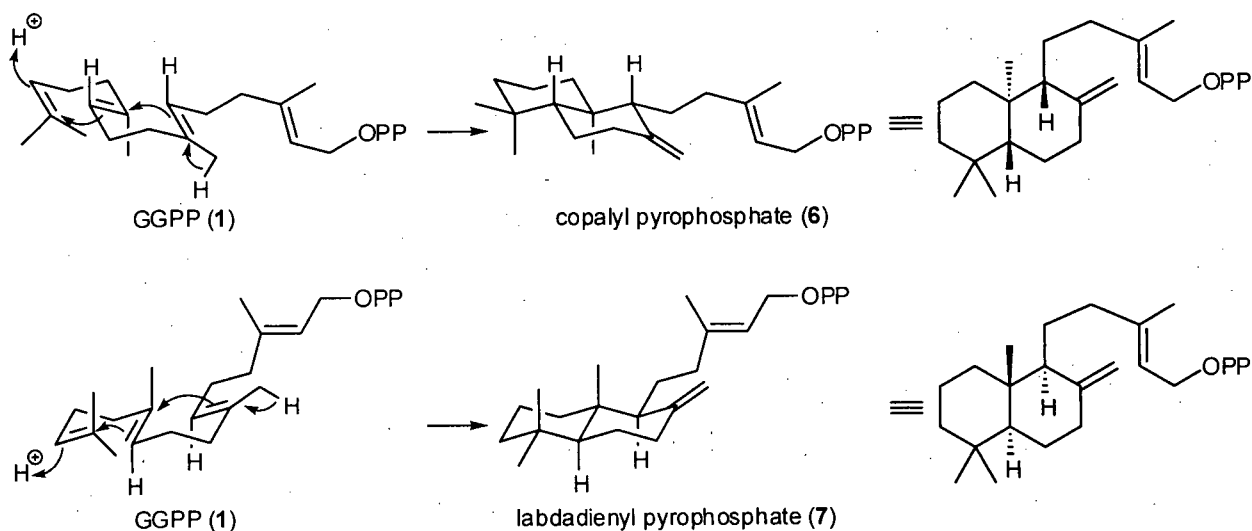
Scheme 2.1. Biosynthesis of copalyl pyrophosphate (6) and labdadienyl pyrophosphate (7) from GGPP (1).
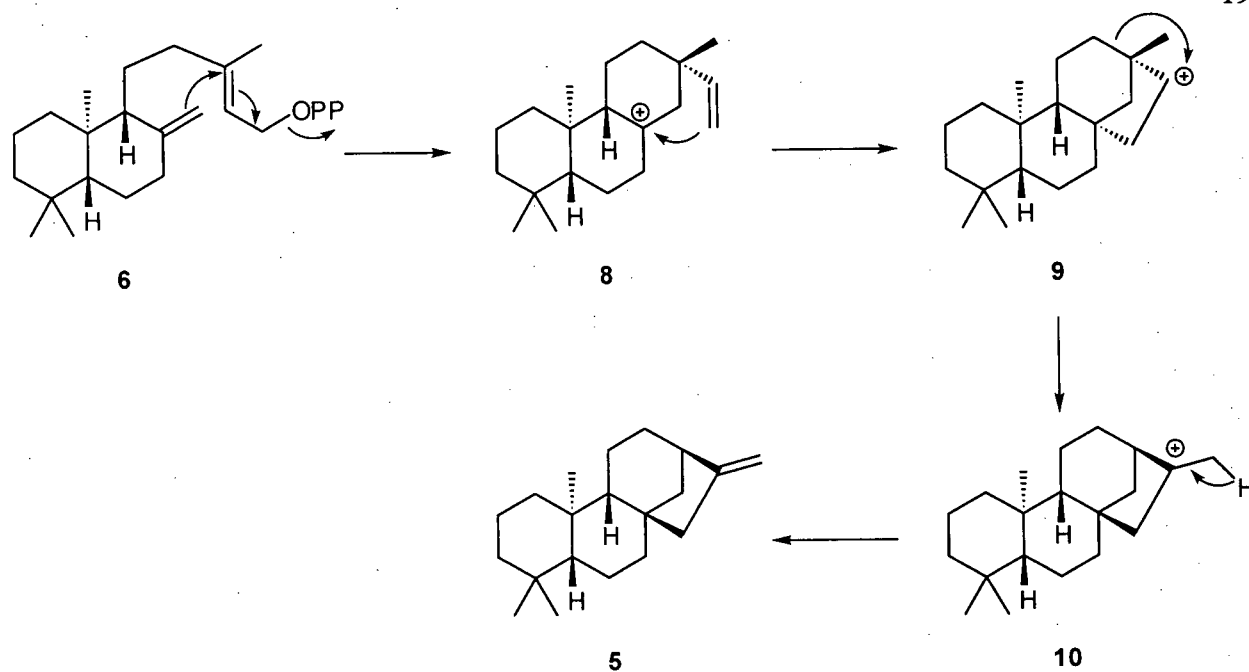
Scheme 2.2. Biogenesis of *ent*-kaurene (**5**) from copalyl pyrophosphate (**6**).

While *ent*-kaurene (**5**) serves as an intermediate in the production of many natural diterpenes, the aforementioned agronomical potential of the gibberellins (e.g. **4**) has motivated a thorough study of the biosynthesis of this important family of plant growth hormones.[10] Thus, oxidation at both C-7 and C-18 of *ent*-kaurene (**5**) provides *ent*-7-hydroxykaurenoic acid (**11**) (Scheme 2.3). Enzyme assisted generation of the secondary cation **12** is followed by a ring contraction, affording gibberellic acid-12 (**13**).[11] The tetracyclic acid **13** is one of the simplest members of the gibberellin family, all of which share a common tetracyclo[10.2.1.0^{4,12}.0^{5,10}]tetradecane, or gibbane, skeleton.[11,12] Further action of oxidative enzymes results in transformations that eventually provide the tetracyclic lactone gibberellic acid (**4**), the first gibberellin to be structurally characterized.[4,11]
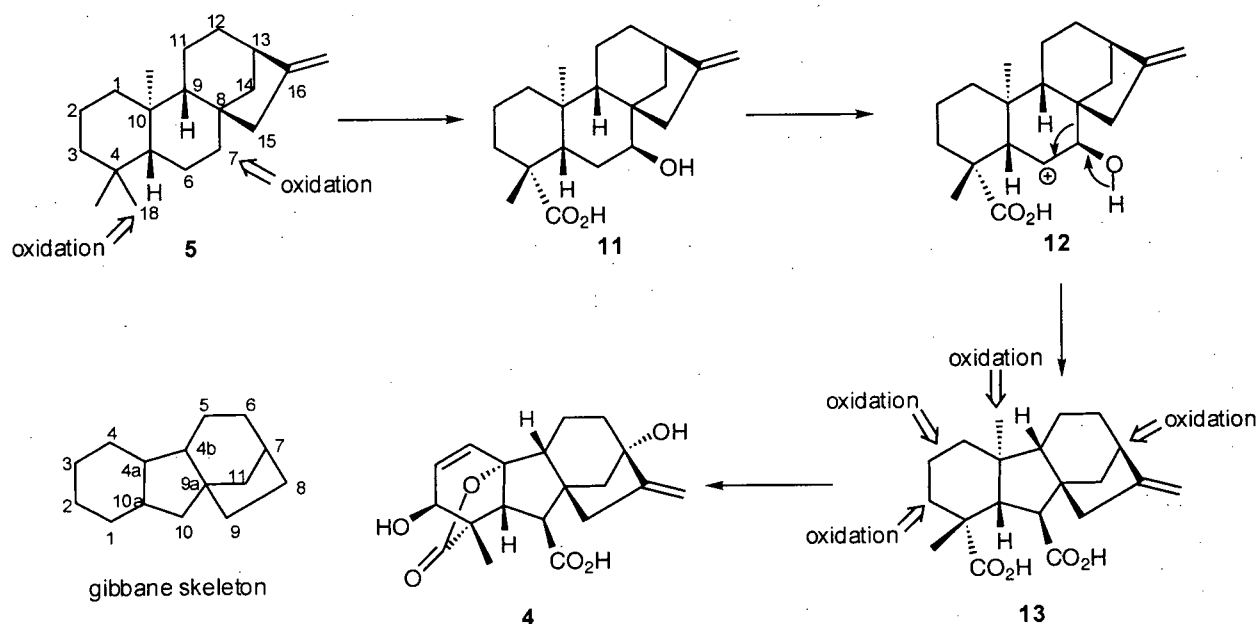
Scheme 2.3. Biosynthesis of gibberellic acid (**4**) from *ent*-kaurene (**5**).

The diterpenoid *ent*-kaurene (**5**) also plays a key role in the biogenesis of a series of tetracyclic lactones, similar in structure to the gibberellins, known as rearranged *ent*-kaurenes or zoapatlins. Although less is known about this process, the isolation and synthetic interconversions of members of this family have helped piece together the biosynthetic events detailed in Scheme 2.4. It is believed that an enzymatic oxidation at both C-9 and C-18 of *ent*-kaurene (**5**) affords stenlobin (**14**), which has been isolated from the stem and leaves of *Viguiera stenloba*.[13] Generation of the tertiary cation **15** is followed by a C-10 → C-9 methyl migration and concomitant lactonization, yielding the tetracyclic lactone zoapatlin (**17**). This proposed biogenesis has been supported by the biomimetic transformation of **14** into zoapatlin (**17**).[13] Delgado and co-workers have demonstrated that the treatment of **14** with two equivalents of $BF_3 \cdot OEt_2$, to promote the formation of the cationic intermediate **15**, results in a structural rearrangement and the subsequent production of zoapatlin (**17**) in moderate yield.[13]
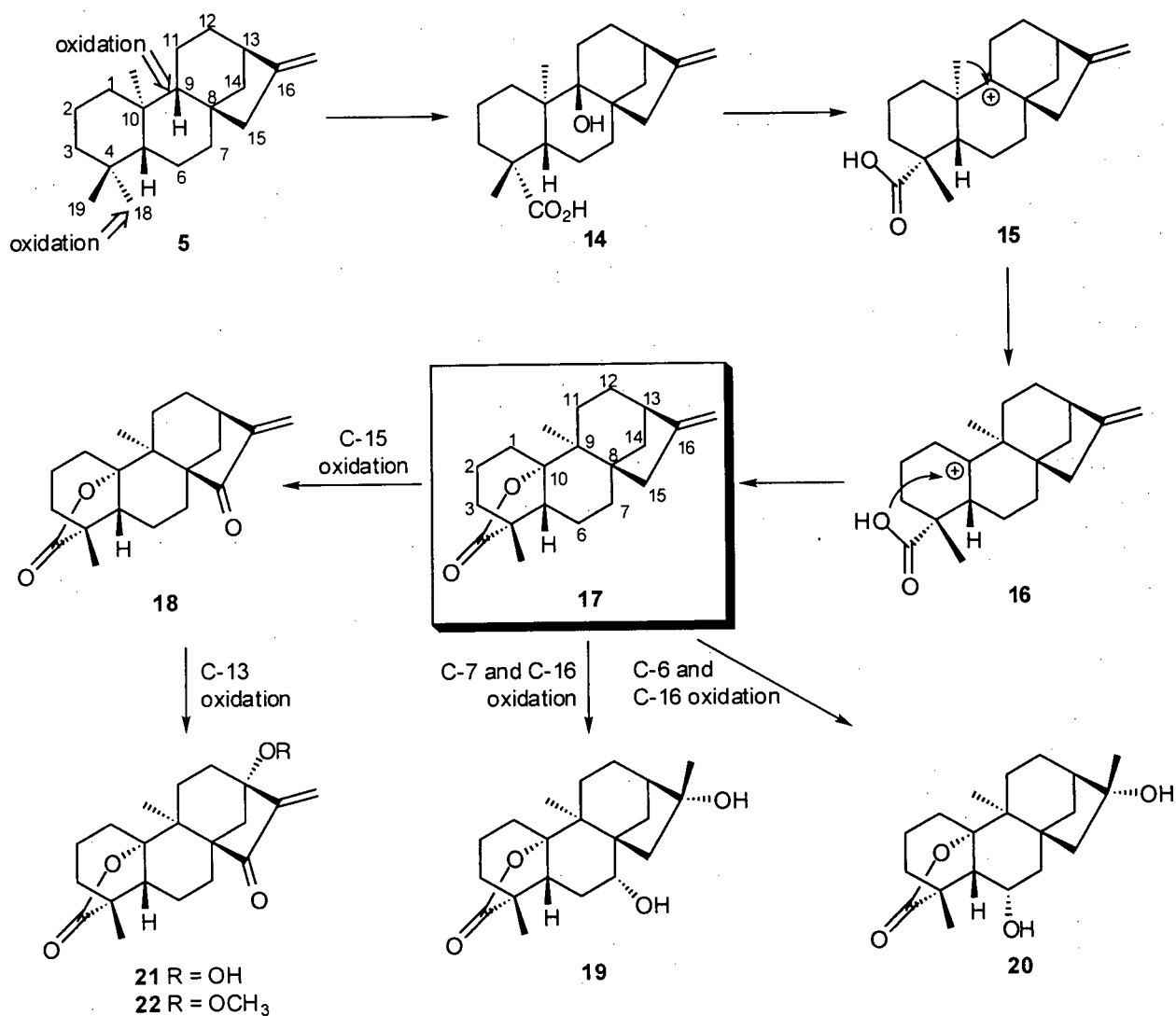
Scheme 2.4. Biosynthesis of zoapatlin (**17**) and related natural products from *ent*-kaurene (**5**).

Originally isolated in 1970 from the Mexican shrub *Montanoa tomentosa* by Caballero and co-workers,[14] the erroneous Chemical Abstracts reference to zoapatlin (**17**) as a *sesquiterpene* lactone, has led to confusion in the nomenclature of these compounds.[15] This original report was repeatedly overlooked and a compound identical in structure to zoapatlin (**17**) was later isolated from the stem and leaves of *Tetrachyron orizabaensis* and hence termed tetrachyrin.[16] Additionally, a report by Herz and co-workers regarding the isolation and structure determination of eupatalbin (**19**) and eupatoralbin (**20**), from *Eupatorium album*, incorrectly

stated these compounds were of a new skeletal type.[17] More recently, however, the term zoapatlin has been recognized for this class of compounds, which now includes 15-oxozoapatlin (**18**) isolated from *Viguiera maculata*.[18] The structural assignment of **18** and its biosynthetic relationship to zoapatlin (**17**) was confirmed through an allylic oxidation of the latter substance (SeO$_2$, then CrO$_3$-pyridine), which yielded a product with physical and spectroscopic properties identical to those of **18**. More recently, 13-hydroxy-15-oxozoapatlin (**21**) and 13-methoxy-15-oxozoapatlin (**22**), both isolated from the root bark of the South African tree *Parinari curatellifolia*, have been added to the family of zoapatlin diterpenes.[19,20] Owing to a unique biological activity profile expressed by the 15-oxozoapatlins (e.g. **18, 21** and **22**), their isolation and structure determination has spawned new interest in these diterpenes.

2.1.2 G2 checkpoint inhibition and antimitotic properties of 15-oxozoapatlins

Originally isolated in 1996, 13-methoxy-15-oxozoaptlin (**22**) demonstrated broad-spectrum activity against a panel of cultured human cancer cell lines.[20] The biological activity of **22** was reportedly related to its interference with the cell cycle transition from G2 phase to mitosis and mediated by a covalent reaction between a cellular component (such as a sulfhydryl-containing protein) and the α,β-unsaturated ketone moiety in **22**. More recently, Roberge and co-workers have demonstrated that 13-hydroxy-15-oxozoapatlin (**21**) is in fact both a G2 checkpoint inhibitor and an antimitotic agent.[21] At low micromolar concentrations (IC$_{50}$ = 10 μM), **21** causes breast cancer cells arrested at the G2 checkpoint by ionizing radiation to be released into mitosis. Additionally, it was discovered that those cells that were able to overcome the G2 checkpoint (approximately 22% of cells) became blocked in mitosis. The requirement of an α,β-unsaturated ketone functionality for G2 checkpoint inhibition activity was also investigated through the

synthesis and biological testing of the β-mercaptoethanol adduct (23) (eq. 1). It is noteworthy that when cells arrested at the G2 checkpoint were treated with 23, no increase in the number of mitotic cells was observed. However, this compound retained the cytotoxicity expressed by the parent diterpene 21. This data suggests that the regions of 21 responsible for checkpoint inhibition activity and cytotoxicity may indeed be separable. Taken together, through the synthesis of a series of compounds similar in structure to 21 and 22, a window of opportunity exists whereby the G2 checkpoint inhibition activity of the 15-oxo-zoapatlins may be enhanced, while their inherent cytotoxicity is reduced. As part of our studies directed at the isolation and synthesis of G2 checkpoint inhibitors and antimitotic agents, we chose to develop a synthesis of 13-methoxy-15-oxozoapatlin (22) that would be amenable to the construction of various analogues. The successful completion of this goal would set the stage for investigations into the effect of structure on the biological activity of these compounds.

(1)
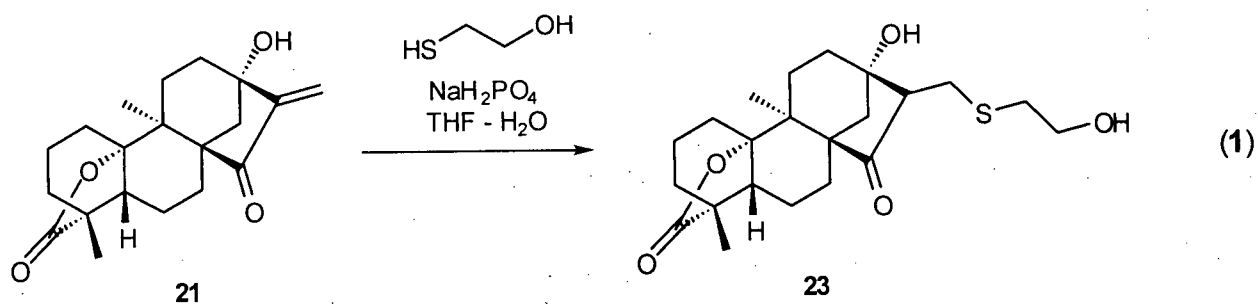
2.2 Proposal for the synthesis of (±)-13-methoxy-15-oxozoapatlin (22)

Although there is an abundance of literature reports regarding the syntheses of kaurene and related diterpenoids, the zoapatlins have been thus far neglected in this regard. This is, perhaps, due to a lack of biological activity demonstrated by the zoapatlins in the earlier disclosures on their isolation. However, as a result of the recent discovery that 13-hydroxy-15-oxozoapatlin (21) acts as both an *in vitro* G2 checkpoint inhibitor and antimitotic agent, a study directed towards the synthesis of these unique compounds is well warranted. Furthermore, while the zoapatlin skeleton is indeed similar to that of *ent*-kaurene (5), the structural differences between these frameworks (*vide infra*) are sufficient to justify targeting the zoapatlins as a testing ground for new synthetic methods and planning. Thus, through the successful synthesis of (±)-13-methoxy-15-oxozoapatlin (22), a greater scope of knowledge in diterpenoid synthesis and a renewable supply of these biologically significant compounds would be realized.

2.2.1 Construction of bicyclo[3.2.1]octane ring systems

A fundamental difference between the kaurenes (e.g. 5) and the zoapatlins (e.g. 22) is the *trans* B-C ring fusion present in the latter family of compounds (Figure 2.2). This stereochemical feature necessitates that the B ring (as described in Figure 2.2) adopt a chair conformation in the kaurenes and a boat conformation in the zoapatlins. Not suprisingly, analysis of molecular models of (±)-13-methoxy-15-oxozoapatlin (22) indicated that the ring strain resulting from this *trans* ring fusion would lead to considerable challenges in the assembly of the bicyclo[3.2.1]octane or C-D ring system of this molecule.
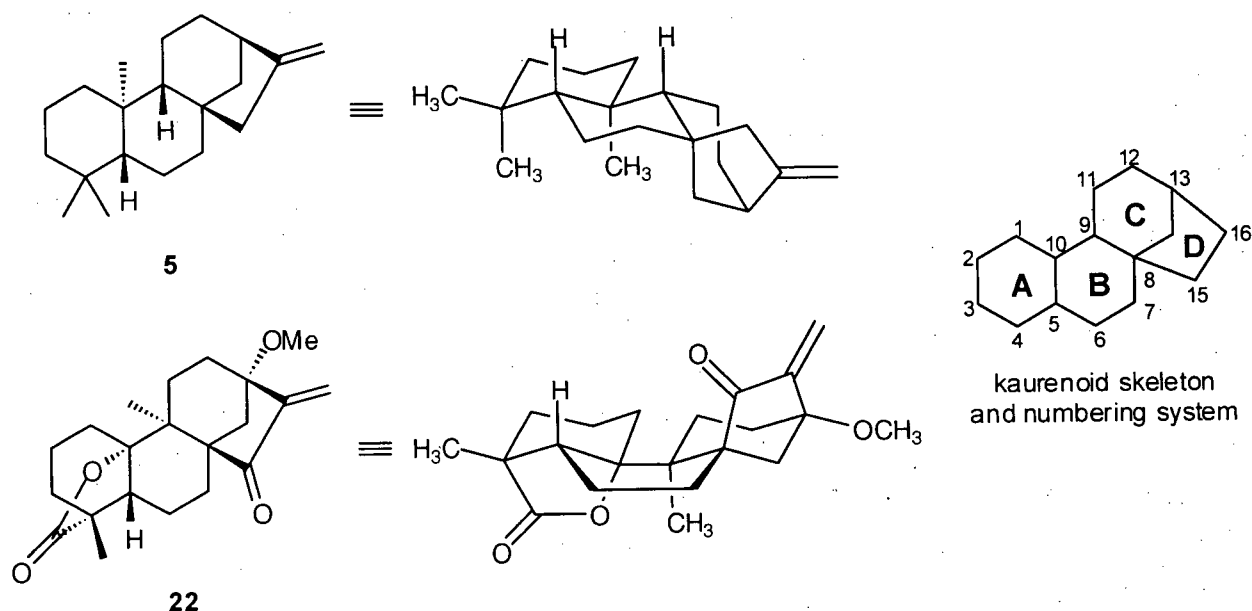
Figure 2.2. Representative 3D structures of *ent*-kaurene (**5**)
and 13-methoxy-15-oxozoapatlin (**22**).

From a number of reviews on the syntheses of *ent*-kaurene (**5**) and related natural products,[22,23] it was apparent that the key obstacle encountered in such an endeavor is in fact the construction of the bicyclo[3.2.1]octane, or C-D ring system. Therefore, a great amount of effort has focused on the development of synthetic methodology useful in this regard. Since the construction of bicyclo[3.2.1]octanes has recently been reviewed,[24] only a brief description of synthetic methods potentially applicable to the synthesis of (±)-13-methoxy-15-oxozoapatlin (**22**) will be presented here.

The first preparation of a bicyclo[3.2.1]octane skeleton dates back to 1903.[25] However, the development of practical methods for the construction of this carbon framework were delayed until the 1960s, when the isolation of numerous diterpenes bearing this structural motif attracted synthetic interest. In one of the original syntheses of kaurene (**24**), Ireland and co-workers employed an aldol reaction to effect the formation of the C-D rings (Scheme 2.5).[26] Thus, hydroboration and oxidation of the tricyclic olefin **25**, afforded the ketone **26**, along with

the regioisomer **27**. Deprotection of the latent aldehyde functionality in **26** under acidic

conditions, was accompanied by an aldol reaction, producing the desired tetracyclic kaurene

skeleton as a mixture of the diastereomeric alcohols **28**. Subsequent functional group

manipulations afforded the ketone **29**, which was subjected to Wittig olefination conditions to

provide kaurene (**24**). While useful in the synthesis of kaurene (**24**), this methodology suffers

somewhat in general practicality as it is both lengthy and uneconomical, providing **24** in only

11% yield over the sequence of reactions that initiated with the tricyclic olefin **25**.
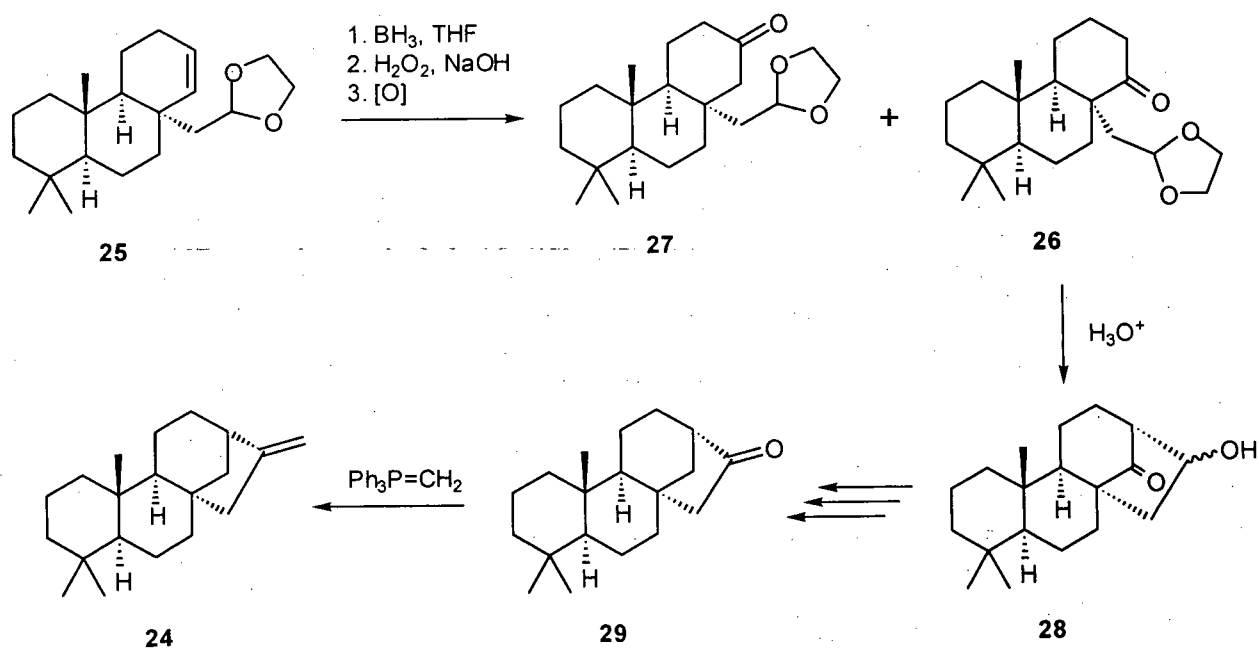
Scheme 2.5. Synthesis of the bicyclo[3.2.1]octane motif in kaurene (**24**).

In the synthesis of steviol (**30**), Mori and co-workers have reported an extension of the

above methodology that bears practical implications for a synthesis (±)-13-methoxy-15-

oxozoapatlin (**22**) (Scheme 2.6).[27] It was reported that treatment of the ketone **31** with acid

effected both removal of the acetal protecting group and a subsequent aldol reaction, affording a

mixture of diastereomeric alcohols that were directly oxidized to the diketone **32**. Subjection of

the diketone **32** to reductive ketone coupling conditions, or a pinacolic cyclization, provided the

isomeric α-hydroxy ketones **34** and **35**. Presumably, the production of **34** and **35** from the diketone **32** proceeds via alternative modes of fragmentation of the pinacol diol **33**. Wittig olefination of the α-hydroxy ketone **35**, followed by hydrolysis of the ester functionality provided steviol (**30**). Although numerous methods exist for the construction of bicyclo[3.2.1]octane fragments, this work represents one of the few examples whereby the final product includes an angular hydroxyl group at the C-D ring fusion, a prerequisite for the synthesis of the oxygenated zoapatlins **21** and **22**.
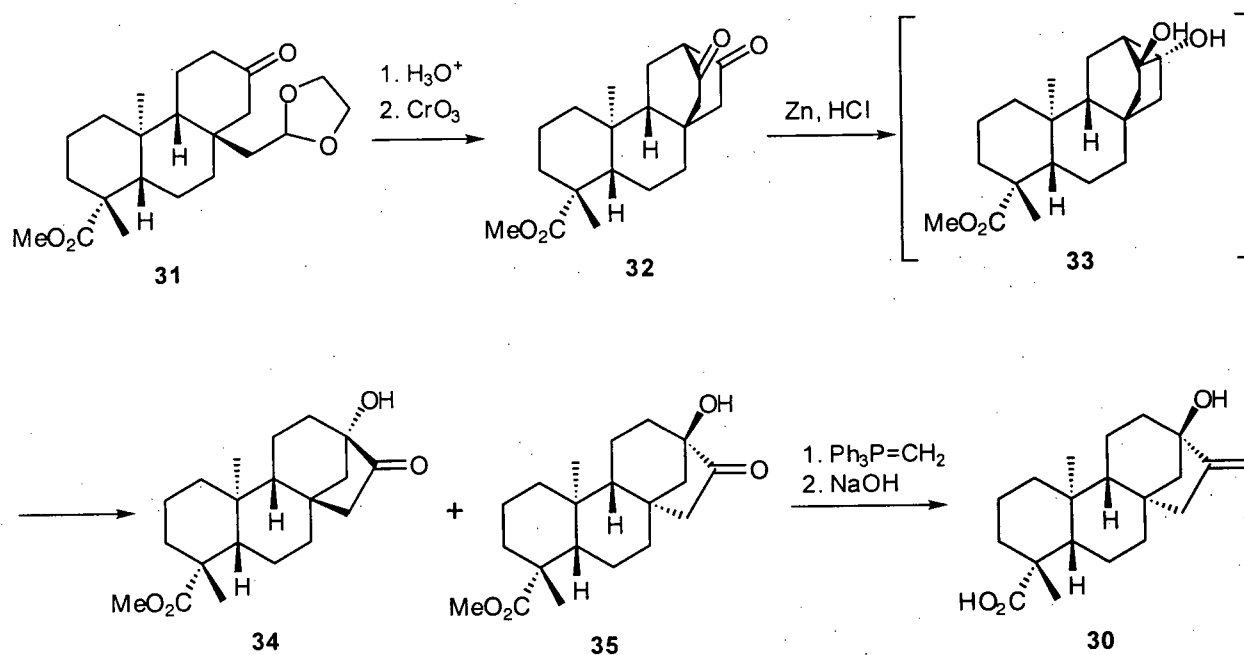
Scheme 2.6. Synthesis of steviol (**30**) by Mori and co-workers.

Corey and co-workers have also employed a pinacolic cyclization in the production of the bicyclo[3.2.1]octane fragment of **36**, analogously functionalized by a bridgehead hydroxyl moiety (Scheme 2.7).[28] Thus, it could be shown that gradual addition of the keto aldehyde **37** to a mixture of magnesium turnings and dimethyldichlorosilane in THF produced both the *cis-* and

trans-diols **38**. Oxidation of the mixture of diastereomeric alcohols provided the α-hydroxy

ketone **36** in excellent overall yield.
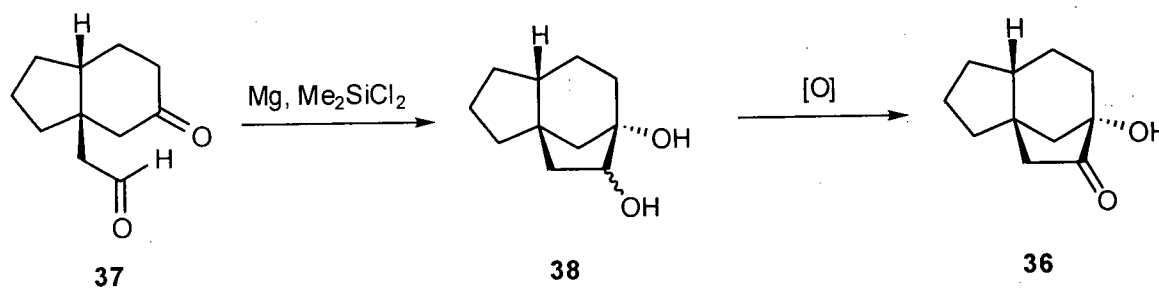
Scheme 2.7. Pinacolic cyclization of the keto-aldehyde **37**.

More recently, reductive free radical cyclization reactions have been employed to effect

the construction of the bicyclo[3.2.1]octane framework. In the context of this structural motif,

the intramolecular addition of a vinyl radical to an activated double bond was first applied

successfully in the synthesis of bicyclic ketone **39** (eq. 2).[29] Ramanathan and co-workers

demonstrated that upon generation of a vinyl radical from the vinyl iodide **40**, a regioselective

cyclization, involving the formed radical and the carbon at the β-position of the enone function,

produced **39** in excellent yield.

(2)
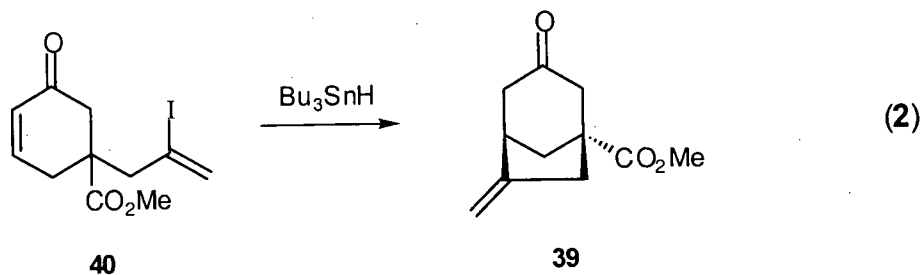
Photochemical 2 + 2 cycloadditions of allene and suitably functionalized enones have

found much use in the synthesis of the bicyclo[3.2.1]octane skeleton.[30] Corey and co-workers

recently demonstrated the potential of this reaction in the synthesis of the tricycle **41** (Scheme

2.8).[31] Thus, it was reported that irradiation of a solution of allene and the enone **42** provided the

tricyclic ketone **43** in excellent yield. The facial selectivity of the 2 + 2 cycloaddition is a key

feature of this reaction, as the *trans*-ring fusion of the decalin core of **43**, generated by this

process, relates well to the B-C ring system in the zoapatlins (see Figure 2.2). Manipulation of

the ketone function in **43** eventually yielded the secondary mesylate **44**, which, upon treatment

with Lewis acid underwent a skeletal rearrangement to provide the bicyclo[3.2.1]octane

containing carbocycle **45**. Reduction of the alkyl chloride function in **45** completed the sequence,

affording the tricyclic olefin **41** in an overall yield of 65% from the enone **42**. Although the

series of transformations that led to the successful construction of **41** proceeded in high yield, the

number of synthetic steps required by this sequence detracts from its potential application in the

final stages of a total synthesis of zoapatlin.
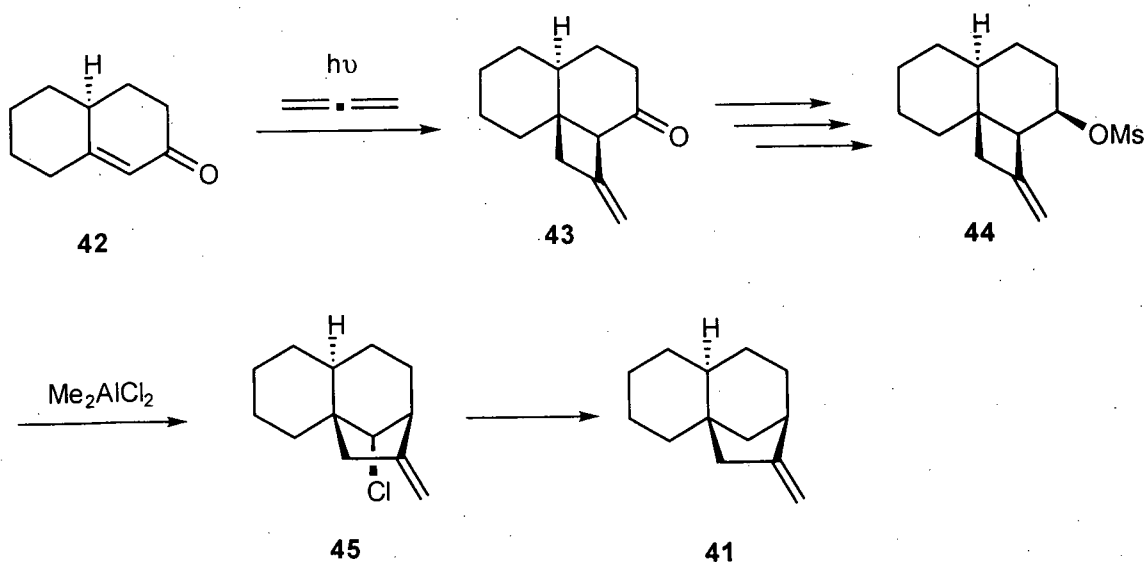
Scheme 2.8. Application of a photochemical 2 + 2
cycloaddition in the synthesis of bicyclo[3.2.1]octanes.

2.2.2 Retrosynthetic analysis: construction of the D ring of (±)-13-methoxy-15-oxozoapatlin (22)

The methodologies disclosed above, and other such methods developed for the synthesis of bicyclo[3.2.1]octanes, are generally suitable for a synthesis of (±)-13-methoxy-15-oxozoaptlin (22). However, the successful completion of our goals relied on a concise synthetic strategy that would be jeopardized by the number of synthetic transformations and/or low overall yields reported for these processes. Thus, the sequence of reactions that was required for the construction of the bicyclo[3.2.1]octane fragment of 22 would address both the *trans* B-C ring fusion *and* the inclusion of a bridgehead methoxyl moiety in a concise manner. It was our contention, that the enone 46 (eq. 4) would serve as an advanced intermediate in such an endeavor.

$$(4)$$

22   **46**
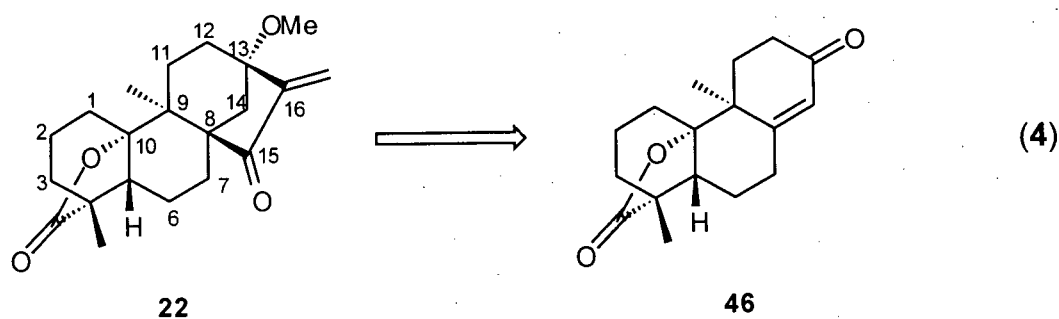
The choice of the enone 46 as a precursor to (±)-13-methoxy-15-oxozoapatlin (22) has a logical basis in that this substance includes the salient structural and stereochemical features required to access 22. Notably, through a successful sequence of synthetic transformations, the C-13 ketone should provide an avenue to the C-13-methoxyl function in 22. Additionally, the activated olefin should function as a handle for the construction of the bicyclo[3.2.1]octane and, necessarily, the *trans* B-C ring fusion. While deferment of the assembly of the

bicyclo[3.2.1]octane fragment of **22** to the later stages of the synthesis presents certain risk, this choice seemed reasonable as the structural features inherent in the tricyclic enone **46** would aid in addressing the stereochemical issues at hand (*vide infra*).

The conjugate addition of organometallic reagents, particularly organocuprates, to enones is a well-established reaction for the creation of carbon-carbon single bonds.[32] Unfortunately, studies have shown that the conjugate addition of organocuprates to $\Delta^{1,9}$-2-octalones (e.g. **50**), which closely resemble the B-C rings of the enone **46**, provide exclusively the *cis* fused octalones (e.g. **53**, eq. 5).[33] In fact, even the addition of bulky substituents (e.g. *t*-butyl in **51**) and cuprate coordinating alkoxy groups (e.g. -CH_2OCH_3 in **52**) has had little effect on the stereochemical outcome of this process.

$$1.\ Me_2CuLi$$
$$2.\ H_3O^+$$

(5)

50 R = H
51 R = *cis* *t*-Butyl
52 R = *trans* CH_2OCH_3

53 R = H (88%)
54 R = *cis* *t*-Butyl (62%)
55 R = *trans* CH_2OCH_3 (50%)
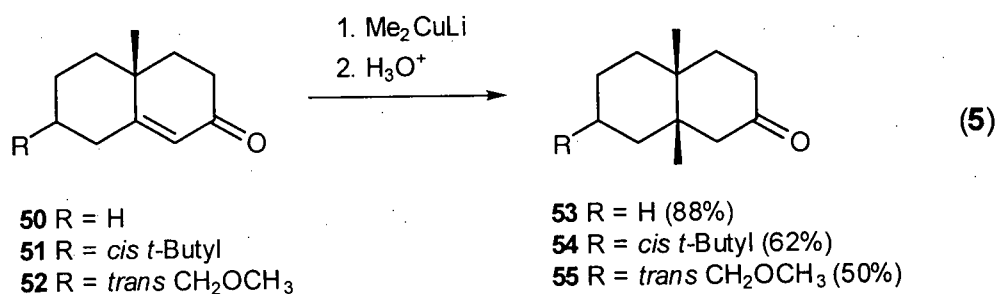
It was anticipated, however, that an oxy-Cope rearrangement would address our key concerns in the construction of bicyclo[3.2.1]octane fragment of **22**. This reaction involves the sigmatropic rearrangement of a 1,5-dien-3-ol (e.g. **56**) to provide a δ,ε-unsaturated ketone (e.g. **57**) and has been applied with tremendous success to the synthesis of a number of complex structural motifs (eq. 6).[34] The driving force for this rearrangement resides in the greater thermodynamic stability of the formed carbonyl C=O double bond relative to the C=C double bond in the starting material. In fact, these reactions are considered irreversible,[34] a feature that distinguishes them from classical [3,3] sigmatropic rearrangements.

$$\text{56} \xrightarrow{\text{heat}} \text{57} \rightleftharpoons \text{57} \qquad (6)$$
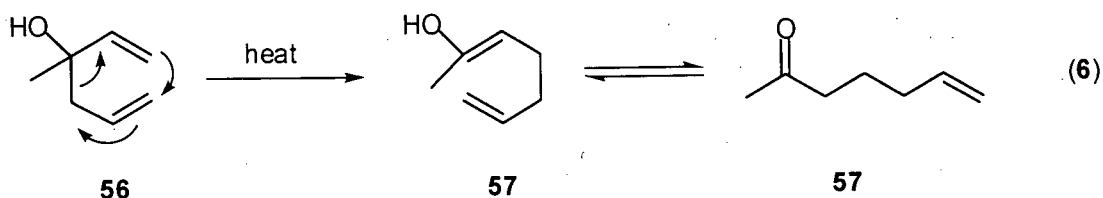
A more recent variant of this process, the anionic oxy-Cope, was discovered in 1975 when enormous rate accelerations for the oxy-Cope reaction were observed following the conversion of the tertiary allylic alcohol into the corresponding potassium alkoxide.[35] The weakening of the α-bonds in alkoxides has been brought forward as an explanation for the rate enhancement observed in the anionic oxy-Cope reaction.[36] More important from a practical perspective, is the fact that the increased rate of the anionic variant of the oxy-Cope allows these reactions to proceed at or below room temperature. This improvement has led to an overall increase in the versatility of the oxy-Cope reaction and, consequently, its application to complex natural product synthesis.[36]

Unless steric, electronic and/or structural features of the reactant dictate otherwise, the chair-like transition state conformations commonly adopted for this process result in a near quantitative transmission of asymmetry from the 1,5-dien-3-ol (e.g. **58**) to the ketone product (e.g. **61**, Scheme 2.9). Thus, while generation of the potassium alkoxide of **58** may lead to either transition state **59** or **60**, the product ratio of 96:4 for the anionic oxy-Cope adducts **61** and **62**, respectively, clearly indicates the overwhelming preference for a chair-like transition state in this reaction.[37]
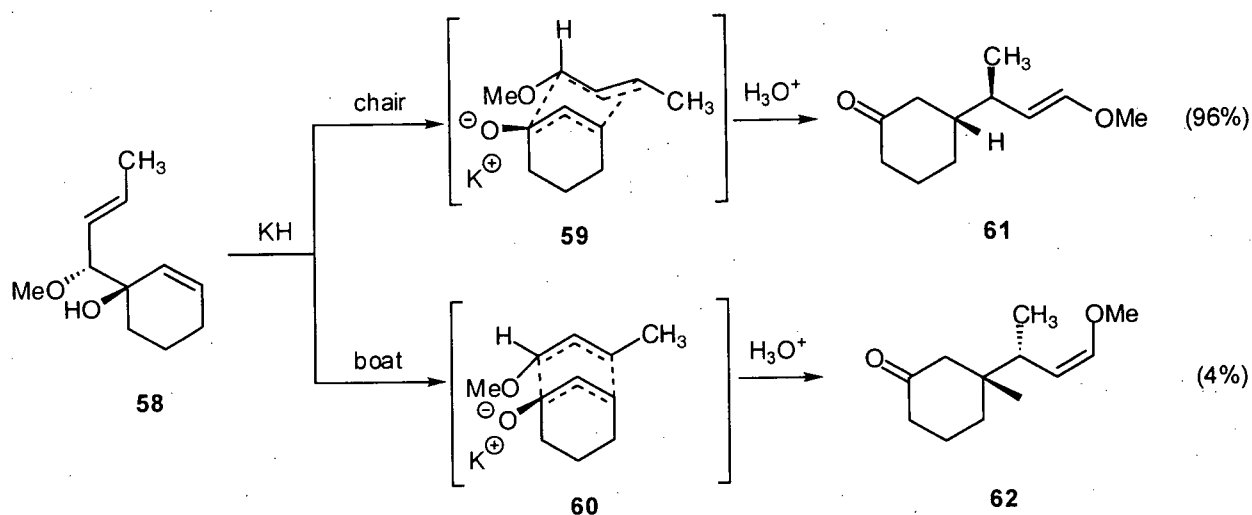
Scheme 2.9. Chair versus boat transition states in the anionic oxy-Cope reaction.

There are, however, examples in which boat-like transition states predominate due to unfavorable steric interactions present in the corresponding chair-like transition state. For example, White and co-workers have found that an anionic oxy-Cope rearrangement of the *trans*-divinylcyclohexanol **63** leads to a 1:1 mixture of the cyclodecenones **66** and **67**.[38] Presumably, the chair-like transition state **64**, which provides the Z isomer **66**, is sufficiently destabilized by the 1,3-diaxial interactions between the TMS substituent and the oxyanion so as to make the typically disfavored boat-like transition state **65** competitive.
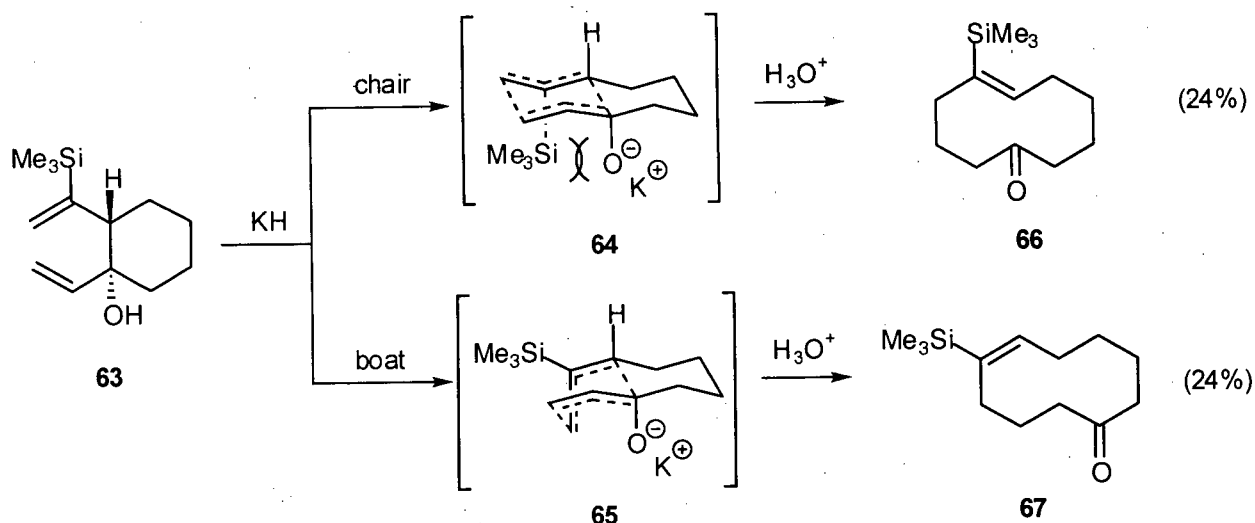
Scheme 2.10. Destabilization of a chair-like transition state in the anionic oxy-Cope reaction.

One of the most common methods for the construction of 1,5-dien-3-ols, the oxy-Cope precursor, involves the 1,2-addition of allylic organometallic agents to α,β-unsaturated carbonyl systems. In particular, the addition of allyl Grignard reagents to enones is well suited for this purpose.[36] It is noteworthy, however, that the facial selectivity expressed by the 1,2-addition of such reagents to cyclic enones is critical, as the stereochemical outcome of the corresponding oxy-Cope reaction will be dictated by the former event.

Analysis of molecular models of the enone **46** reveals that the two faces of the ketone function have decidedly distinct steric environments. It was anticipated that the addition of a suitably functionalized allyl anion to this substrate would occur with preference from the β-face of the molecule. As depicted in Scheme 2.11, the C-4a methyl substituent partially hinders the α-face of the ketone, thus favoring nucleophilic addition to the β-face of this function. The stereochemical outcome of this reaction is crucial, however, as only the 1,2-addition adduct **68** has the requisite stereochemistry to participate in an oxy-Cope reaction that would result in a *trans*-B-C ring fusion.
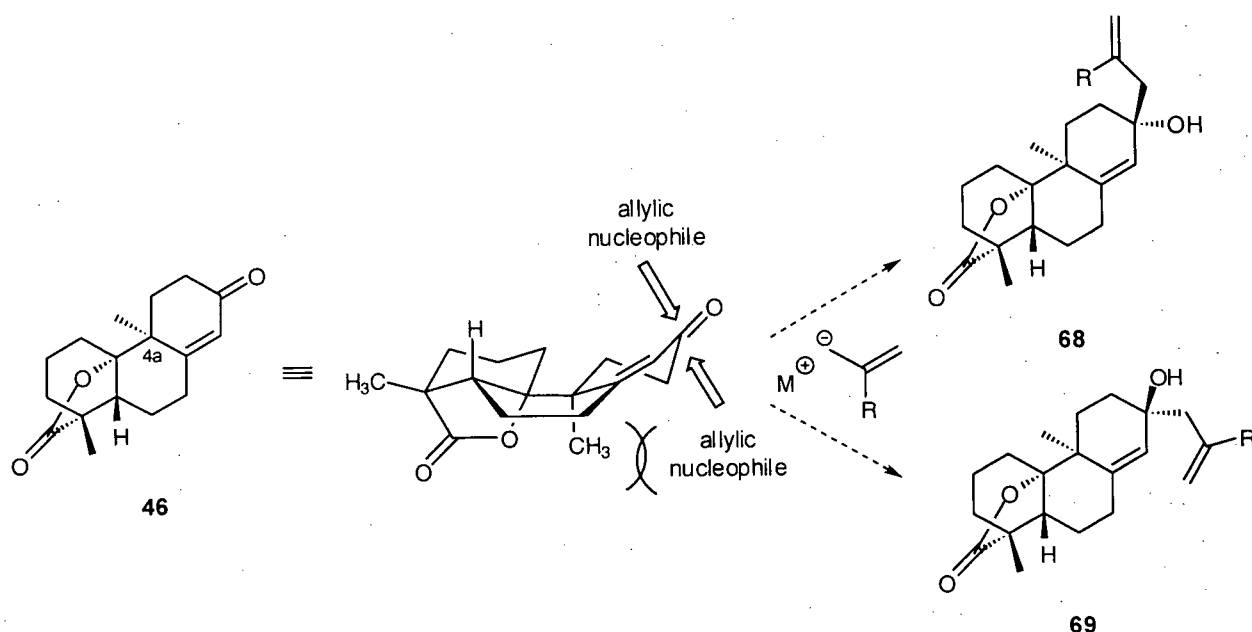
Scheme 2.11. Approach of allylic nucleophile to the enone **46**.

The anionic oxy-Cope event, as outlined in Scheme 2.12, should proceed via the boat-like transition state **70B** to afford, upon workup, the ketone **72** (Scheme 2.12). While the corresponding chair-like transition structure for this reaction suffers from severe non bonded interactions, there is ample evidence in the chemical literature to support a rearrangement by the former process. Furthermore, through judicious choice of the allyl anion employed in the 1,2-addition sequence, the terminal olefin function in the oxy-Cope adduct **72** could be transformed into a vinyl nucleophile. In this way, an intramolecular cyclization event between the olefinic and carbonyl functions present in **72** would complete the annulation sequence and provide the requisite zoapatlin skeleton **73**.
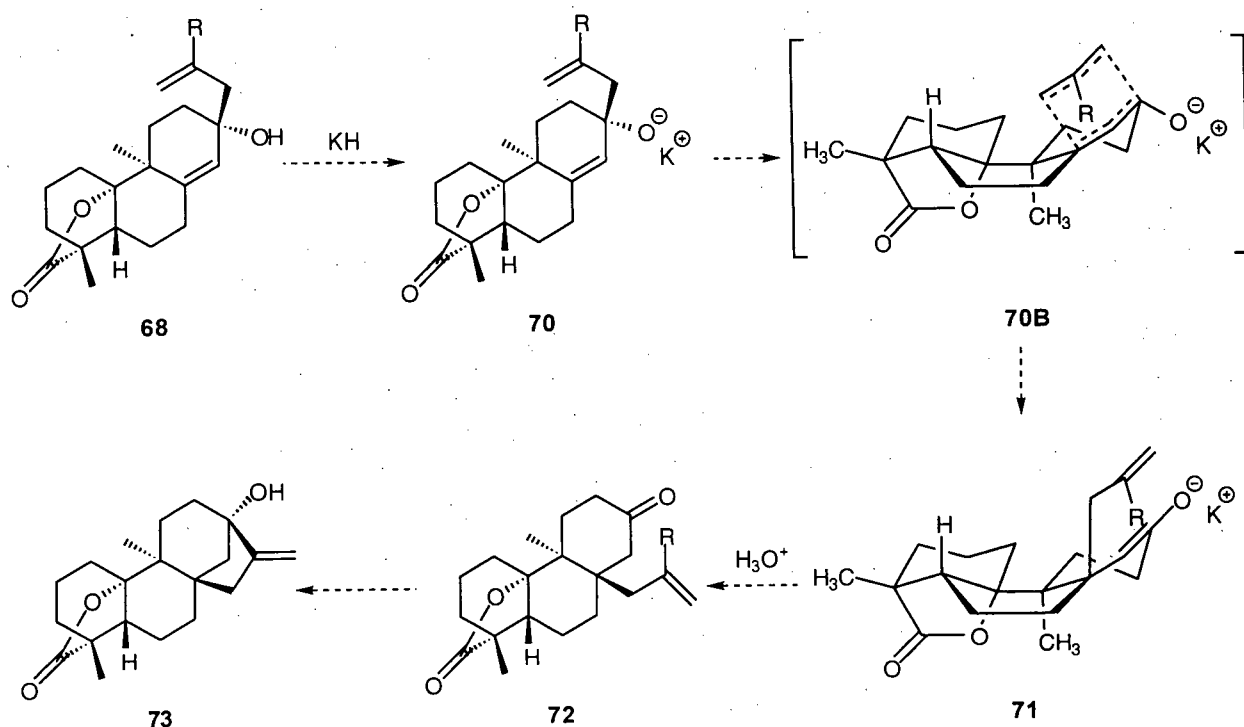
Scheme 2.12. Potential application of the anionic oxy-Cope reaction in the synthesis of **22**.

Recently, Piers and co-workers have disclosed both the preparation and synthetic uses of a number of bifunctional reagents.[39] In particular, the utility of 2,3-bis(trimethylstannyl)propene (**75**), a reagent that serves effectively as the synthetic equivalent of the d^2,d^3-prop-1-ene synthon **74**, has been highlighted (Scheme 2.13).[40] These researchers demonstrated that upon addition of a solution of MeLi to **75**, the allyllithium species **76** is generated in a quantitative manner. This highly reactive reagent may add directly to carbonyl compounds (e.g. **79**) or, upon generation of the corresponding the allylcopper(I) reagent **77**, engage in conjugate additions with α,β-unsaturated ketones (e.g. **78**). Therefore, through the choice of suitable reaction conditions, the allyllithium **76** or allylcopper(I) species **77** efficiently transfer the 2-(trimethylstannyl)allyl group in a 1,2- or 1,4-sense, respectively, to α,β-unsaturated carbonyl compounds.[41]

The 1,2- and 1,4-addition products **80** and **81**, that bear the 2-(trimethylstannyl)allyl group, further serve as useful intermediates for a variety of subsequent synthetic transformations.

Notably, through the conversion of the vinylstannane function in these molecules into a vinyl iodide, a facile process, the synthetic potential of these substances is increased dramatically. In particular, vinyl iodides such as **82** undergo $CrCl_2/NiCl_2$-mediated (Nozaki-Kishi)[42,43] coupling reactions with a variety of electrophiles. As expressed in Scheme 2.13, a $CrCl_2/NiCl_2$-mediated cyclization involving the vinyl iodide and ketone functions in **82** provides the bicycle **83**, as a mixture of diastereomers, in excellent yield.
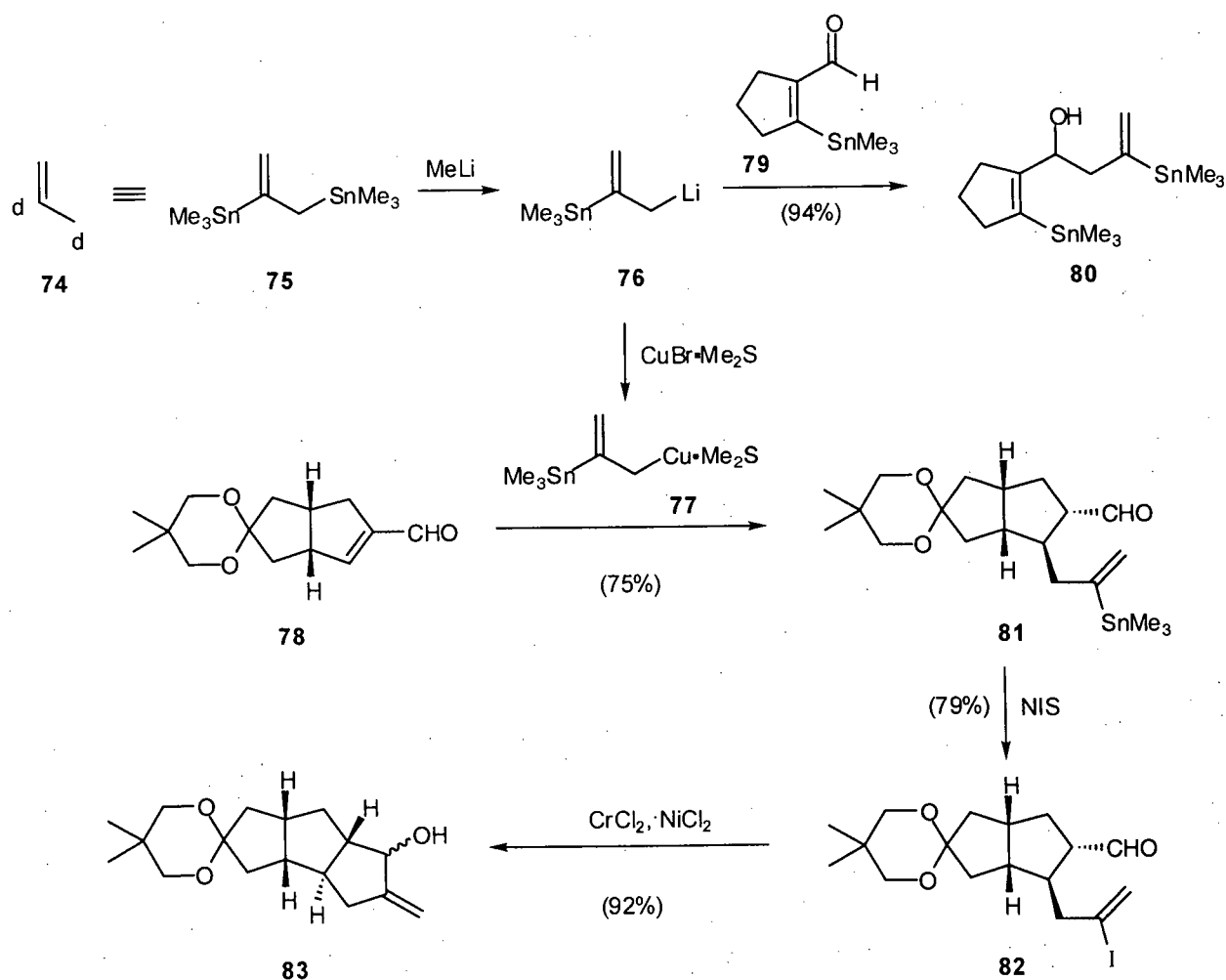
Scheme 2.13. Applications of the bifunctional reagent 2,3-bis(trimethylstannyl)propene (**75**).

In the context of a synthesis of (±)-13-methoxy-15-oxozoapatlin (**22**), it was anticipated that the allyllithium species **76** would react in a 1,2-fashion with the ketone function of the enone **46** (Scheme 2.14). Nonbonded interactions between the nucleophile **76** and the angular methyl group at C-9, were expected to impart selectivity in this reaction. In this regard, the 1,2-addition of the allyllithium reagent **76** should occur preferentially via addition to the β-face of the ketone function in **46**, yielding the α-tertiary alcohol **85**. Upon generation of the potassium alkoxide **86**, an anionic oxy-Cope rearrangement should proceed through a boat-like transition state (see Scheme 2.12) affording, upon workup, the vinylstannane **87**. Following conversion of the vinylstannane **87** into the vinyl iodide **88**, an intramolecular Nozaki-Kishi reaction should generate the tertiary alcohol **73**. Thus, through the proposed sequence of synthetic transformations, both key concerns in the synthesis of the bicyclo[3.2.1]fragment of **22** are addressed. Namely, the *trans*-B-C ring fusion would be controlled by a [3,3] sigmatropic rearrangement and the required bridgehead hydroxyl function will be generated by an intramolecular cyclization event. The completion of the synthesis, that is the conversion of the tertiary alcohol **73** into (±)-13-methoxy-15-oxozoapatlin (**22**), has precedent in the biomimetic synthesis of 15-oxozoapatlin (**18**) from zoapatlin (**17**) (*vide supra*).
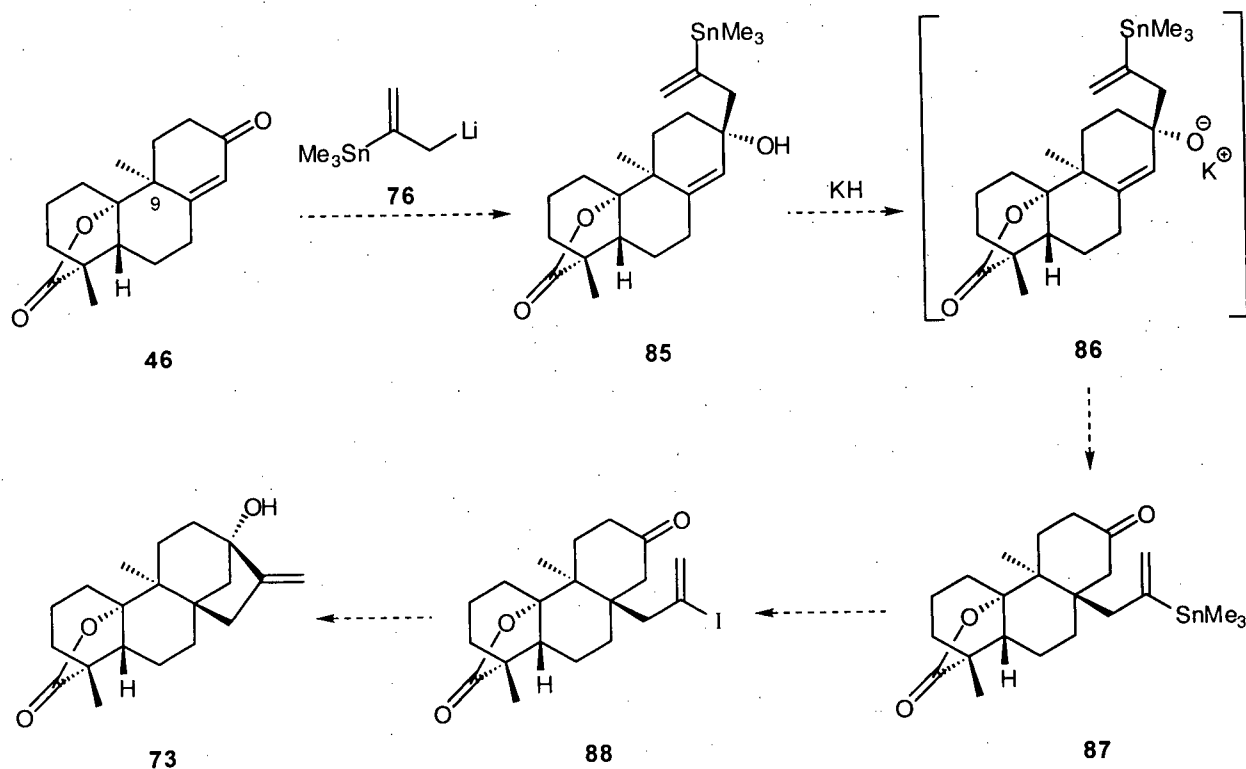
Scheme 2.14. Synthetic proposal for the bicyclo[3.2.1]octane
fragment of (±)-13-methoxy-15-oxozoapatlin (**22**)

2.2.3 Retrosynthetic analysis: construction of the C-ring and γ-lactone of (±)-13-methoxy-15-oxozoapatlin (22)

With the enone **46** established as a key intermediate in our proposed synthesis of (±)-13-methoxy-15-oxozoapatlin (**22**), it was essential to devise a straightforward synthetic plan for the construction of the former compound. In retrosynthetic terms, it seemed the bond disconnections that would most simplify this structure included the scission of the C-ring olefin and the elimination of the γ-lactone, thus providing the bicyclic diketone **90** as a suitable precursor (Scheme 2.15). In a forward sense, there exists precedent for an intramolecular aldol condensation[44] that would result in the formation of the C-ring and, consequently, the enone

functionality requisite for the proposed anionic oxy-Cope sequence. Additionally, the carboxylic acid moiety in the tricyclic enone **91** is ideally situated to engage in an electrophilic lactonization as a means of constructing the γ-lactone. While there exist two possible modes of electrophilic lactonization for this substrate, namely γ- or δ-lactonization, it was anticipated that under kinetically controlled conditions the formation of the γ-lactone should predominate.[45] Thus, the desired enone **46** would be accessed in only three synthetic transformations from the bicyclic diketone **90**. It is noteworthy that the sequential order of aldol condensation and iodolactonization reactions was chosen on the assumption that the basic conditions employed in the former reaction would result in destruction of the lactone function if the sequence of events were reversed.
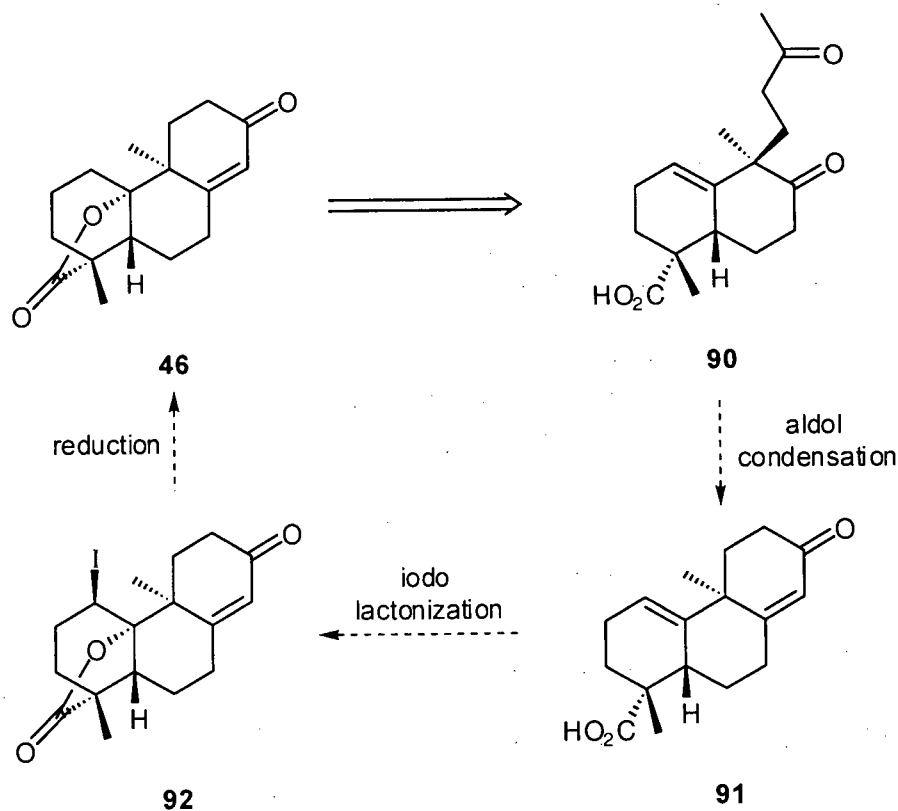
Scheme 2.15. Retrosynthesis and synthetic proposal for construction of the enone **46**.

2.2.4 Retrosynthetic analysis: construction of the A-B ring system of (±)-13-methoxy-15-oxozoapatlin (22)

As delineated in Scheme 2.15, the bicyclic diketone **90** represents the first key intermediate in the proposed synthesis of (±)-13-methoxy-15-oxozoapatlin (**22**). It was believed that a convergent assembly of the decalin core of the diketone **90** could be achieved by a Diels-Alder reaction between the diene **93** and methacrolein (**94**) (Scheme 2.16). Previous reports involving the cycloaddition of similar dienes in the construction of the decalin system of the natural product dysidiolide (**95**) lend credence to this proposal. In fact, a Diels-Alder process has been applied successfully to the construction of the decalin framework of this important protein phosphatase inhibitor in three separate syntheses (eq. 7).[46-48]

major Diels-Alder adduct   **95**   (7)
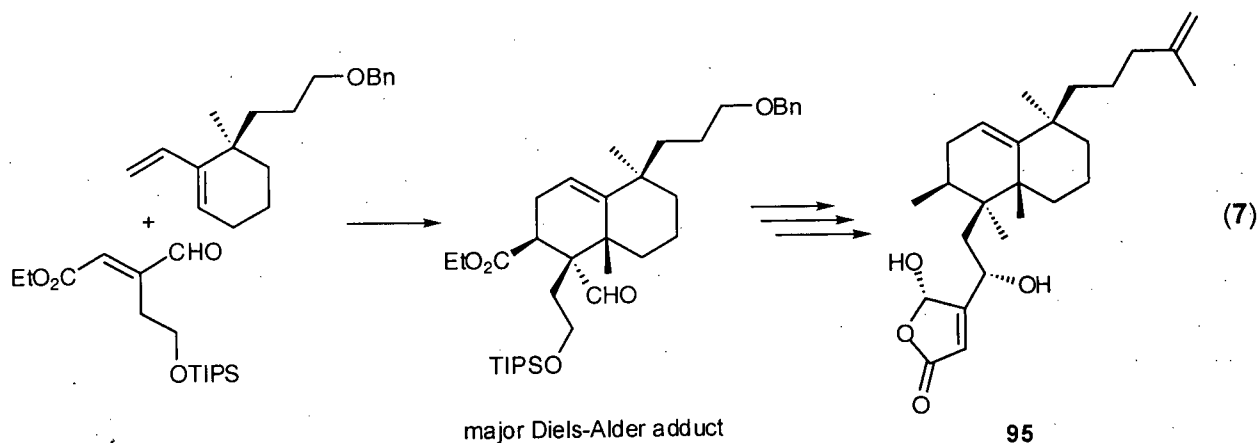
It was our contention that the single stereogenic center present in the diene **93** would govern the facial selectivity of the Diels-Alder reaction. Thus, based on the differing steric demands of the methyl and 3,3-(ethylenedioxy)butyl groups at C-2 in **93**, the cycloaddition of this substrate with methacrolein (**94**) should occur predominantly from the α-face (as shown). Based on precedent established in the syntheses of dysidiolide (**95**) and analogous cycloadditions between similarly substituted dienes and dienophiles,[49] the regioselectivity of the Diels-Alder

reaction was expected to be as shown. Finally, the stereoselectivity of the Diels-Alder reaction should be controlled by the preference for such processes to occur by an *endo*-transition state.[50] Thus, through the facial selectivity governed by the C-2 appendages in the diene **93** and the regio- and stereoselectivity typified by reactions of similar dienes and dienophiles, it was anticipated that of the possible eight diastereomeric products of this reaction, the desired bicycle **96** would predominate. Conversion of the bicycle **96** into the desired diketo acid **90** should be readily accomplished by hydrolysis of the ketal functions and oxidation of the aldehyde moiety. The results derived from application of the plan devised for the synthesis of (±)-13-methoxy-15-oxozoapatlin (**22**), as described here and above, are presented in the following sections.
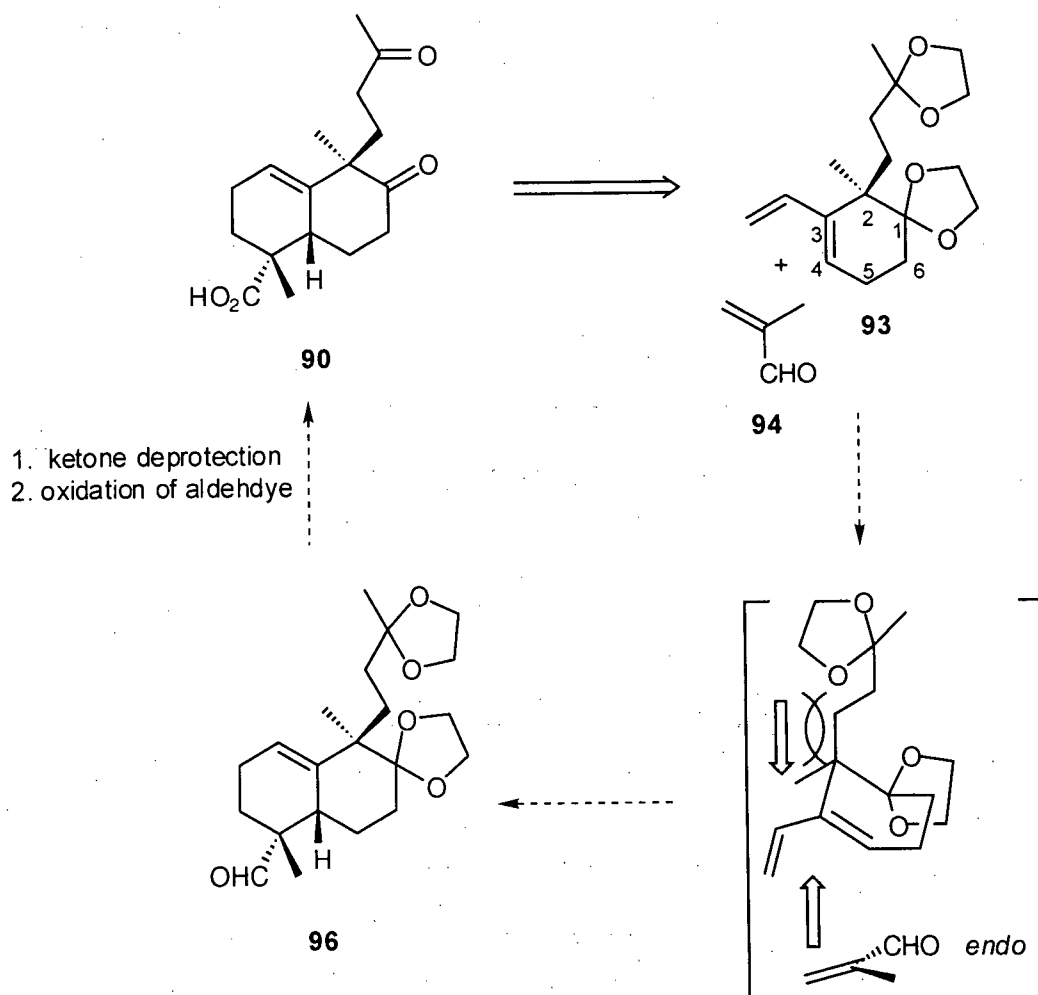
Scheme 2.16. Retrosynthesis and synthetic proposal for construction of the bicyclic ketone **90**.

2.3 Synthesis of (±)-15-methoxy-13-oxozoapatlin (22)

A summary of the key synthetic transformations proposed for the total synthesis of (±)-13-methoxy-15-oxozoaptlin (22) is outlined in Scheme 2.17. Thus, a Diels-Alder cycloaddition between the diene 93 and methacrolein (94) was expected to provide the bicyclic aldehyde 96. Unveiling of the latent ketone functions in 96, followed by an intramolecular condensation should afford the tricyclic enone 91. It was then expected that a sequence of reactions involving oxidation of the aldehyde function in 91 to the corresponding carboxylic acid and subsequent electrophilic lactonization would provide the tricyclic γ-lactone 46. A 1,2-addition of the allyllithium reagent 76 to the enone carbonyl in 46 should then furnish the tertiary alcohol 85, which is structurally predisposed to undergo an anionic oxy-Cope rearrangement that would afford the *trans-syn-trans*-fused tricycle 87. Conversion of the vinyl stannane moiety in 87 into a vinyl iodide and a subsequent intramolecular Nozaki-Kishi reaction involving the vinyl iodide and ketone functions in 88 should produce, in a straightforward manner, the tetracyclic lactone 73. Conversion of the tetracycle 73 into (±)-13-methoxy-15-oxozoapatlin (22), and hence completion of the synthesis, relies on the methylation of the bridgehead hydroxyl function in the former substance and an allylic oxidation of the exocyclic olefin.

If successful in implementation, the total synthesis of the G2 checkpoint inhibitor and antimitotic diterpene (±)-13-methoxy-15-oxozoapatlin (22) will represent the first total synthesis of any member of the zoapatlin family of natural products. Additionally, the methodology devised for the construction of the bicyclo[3.2.1]octane fragment of 22 would add significantly to the literature relating to the synthesis of this structural motif. More importantly, however, a renewable source of 22 and, consequently, a means to generate analogues of this potentially useful cancer chemotherapeutic will be realized.
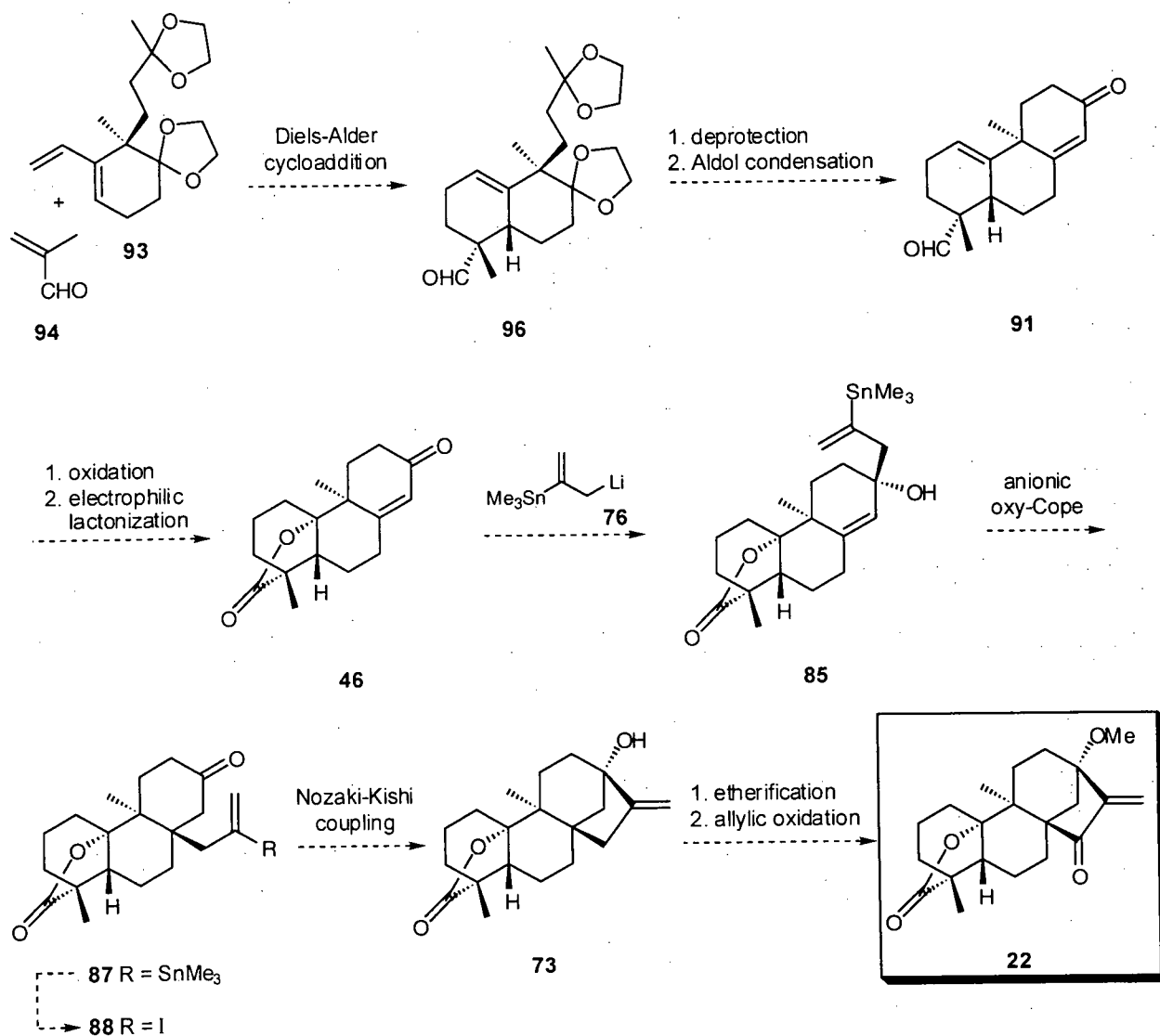
Scheme 2.17. Key transformations proposed for the
synthesis of (±)-13-methoxy-15-oxozoapatlin (**22**).

2.3.1 Synthesis of the diene 93

As delineated in a discussion of the retrosynthetic analysis of (±)-13-methoxy-15-
oxozoapatlin (**22**) (*vide supra*), the first key intermediate in the proposed synthesis of this
desirable substance is the diene **93**. It was anticipated that the diene function of **93** could be
introduced through the 1,2-addition of vinylmagnesium bromide to the ketone **94** and subsequent

dehydration of the resultant tertiary alcohol, a sequence of reactions that has proven successful in the construction of similar dienes (eq. 8).[47] The ketone **94** should, in turn, arise from a chemoselective protection of the known trione **95**. While precedent for this transformation exists, the protection of the trione **95** poses certain challenges. Under the acidic conditions typically required for ketal formation, this substrate is well known to participate in an intramolecular aldol condensation.[51]

95   94   93   (8)
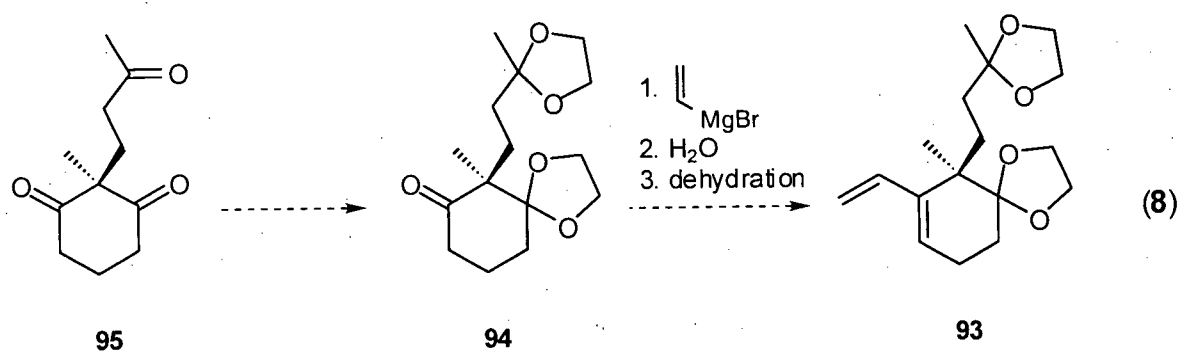
Recently, however, Ohshima and co-workers[52] disclosed that a selective protection of the trione **96** can be achieved efficiently using Noyori's method[53] (eq. 9). Thus, the Lewis acid catalyzed ketalization of **96** proceeds in excellent yield when 1,2-bis(trimethylsilyloxy)ethane (**97**) is employed for this transformation, avoiding destructive intramolecular aldol condensations. Although isomerizations (e.g. **98** → **99**) have been reported when these reactions are carried out on larger scale,[54] an investigation along this avenue of ketone protection was a logical starting point for the synthesis of the diene **93**.

96   98   99   (9)

(TMSOCH$_2$)$_2$ (97)
TMSOTf, CH$_2$Cl$_2$

(77%)
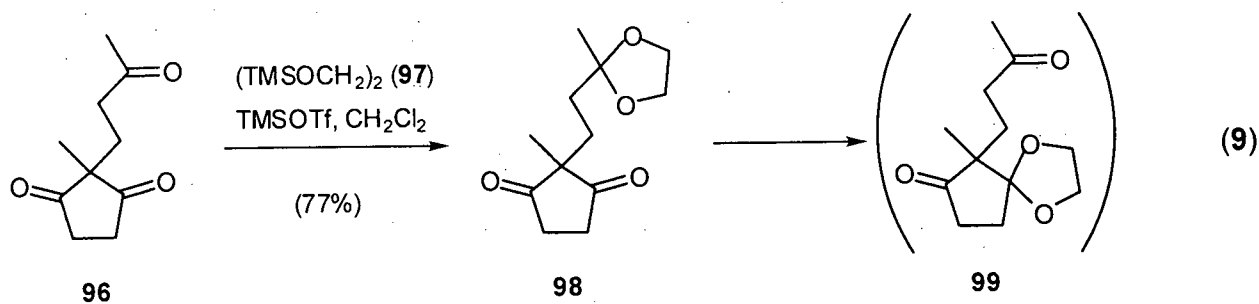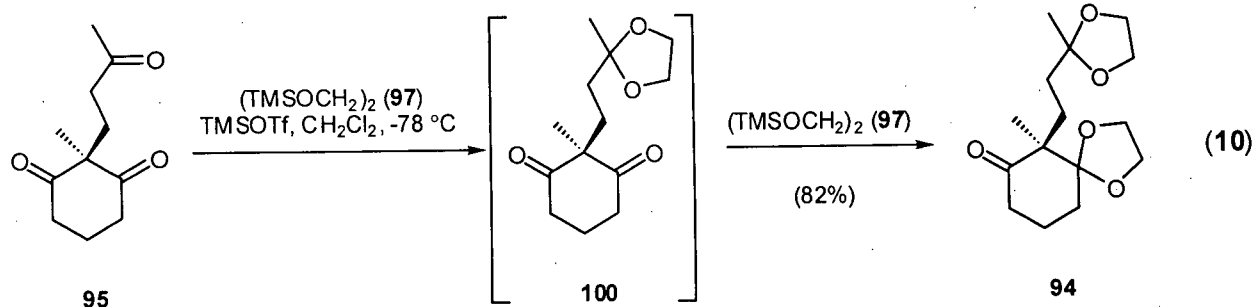
Thus, the total synthesis of (±)-13-methoxy-15-oxozoapatlin (**22**) commenced with treatment of a CH_2Cl_2 solution of the trione **95**[55] with *two* equivalents of 1,2-bis(trimethylsilyloxy)ethane (**97**) and a catalytic amount of TMSOTf. It was hoped that under these conditions, a chemoselective protection of both the side-chain carbonyl and one of the endocyclic carbonyl functions in **95** would be accomplished. Unfortunately, upon workup, a number of products, which included the monoketal **100**, the diketal **94**, and compounds isomeric in the position(s) of the ethylene ketal(s) were isolated (eq. 10). Variation in reaction time and the number of equivalents of TMSOTf had little effect on this unsatisfactory result. However, it could be shown that through the addition of *one* equivalent of 1,2-bis(trimethylsilyl)oxy)ethane (**97**) and a catalytic amount of TMSOTf to the trione **95**, the monoketal **100** was produced in good yield. From this result, a stepwise procedure reproducible in both yield and scale emerged. A catalytic amount of TMSOTf was added to a solution of the trione **95** and *one* equivalent of **97**. After the mixture had been stirred for one hour, an additional equivalent of **97** was added and, following a further three hours, workup of the reaction mixture provided the diketal **94** in excellent yield. Spectroscopic data collected on this substance fully supported the structural assignment. The IR spectrum of **94** exhibited a carbonyl stretching absorption (1713 cm^{-1}). Additionally, the ^{13}C NMR spectrum recorded for **94** included one carbonyl resonance at δ 210.1, two O-C-O carbon resonances (δ 114.0 and 109.8) and four oxymethylene carbon resonances (δ 65.2, 65.1, 64.7 and 64.6). Further evidence supporting the proposed structure was gathered from

the ^{1}H NMR spectrum recorded for **94**, which displayed an 8-proton multiplet from δ 3.98-3.85

that could be assigned to the protons on the two ethylene ketals in **94**. In addition, two 3-proton

singlets at δ 1.28 and 0.98 were attributed to the two methyl groups in the diketal **94**. That

neither of the methyl groups resonated above 2 ppm in the ^{1}H NMR spectrum, a diagnostic

resonance for methyl ketones, aids in assigning the structure of **94** as shown in eq. 10.

It had been anticipated that the addition of vinylmagnesium bromide to the ketone **94**

would result in the generation of the tertiary alcohol **101**, which, upon dehydration would

provide access to the diene **93** (eq. 11). Unfortunately, though a great deal of effort was

expended in this regard, it could be shown that vinylmagnesium, vinylcerium,[47] and vinyllithium

reagents would not effect the desired 1,2-addition. In fact, in all cases only starting material was

recovered from these reactions. This unpropitious result is most likely due to the steric

interference created by the methyl and 3,3-(ethylenedioxy)butyl groups adjacent to the ketone

function in **94**, impeding approach of the vinyl nucleophiles. Thus, it is likely that deprotonation

and consequently enolate formation, effected by the basic reagents precluded the desired 1,2-

addition.

$$\text{(11)}$$

It could be shown, however, that the ketone **94** undergoes facile deprotonation with

lithium diisopropylamine (LDA) to provide the enolate **102** (eq. 12). Treatment of this enolate

with N-phenyltrifluoromethanesulfonimide[56] (PhNTf$_2$) resulted in the formation of the enol

triflate **103** in excellent yield (eq. 12). It was our contention that the vinyl triflate moiety in **103** would provide a useful handle for further functionalization. For example, these groups are well known to participate in Pd(0) catalyzed coupling reactions with vinyl or aryl halides.[57] Additionally, McMurry and co-workers have demonstrated that enol triflates engage in regio- and stereospecific couplings with a wide variety of organocuprate reagents.[58]

$$\textbf{94} \xrightarrow{\text{LDA, THF, -78 °C}} \textbf{102} \xrightarrow[\text{(80%)}]{\text{PhNTf}_2} \textbf{103} \qquad (12)$$

The spectral data acquired on the enol triflate **103** was in full accord with the structural assignment of compound. The IR spectrum of **103** displayed no C=O stretching absorptions, indicating that the ketone function in **94** had indeed reacted. The ^{1}H NMR spectrum of **103** exhibited a 1-proton doublet of doublets at δ 5.67 that was assigned to the alkenyl proton. Additionally, the ^{13}C NMR spectrum included two resonances at δ 152.1 and 116.6, characteristic of the olefinic carbons in the enol triflate function in **103**. The successful incorporation of the trifluoromethanesulfonyl group was confirmed by the presence of a quartet $(J_{C\text{-}F} = 320 \text{ Hz})$ at δ 118.2, attributed to the CF$_3$ carbon, in the ^{13}C NMR spectrum of **103**.

Presumably as a result of steric encumberance, the enol triflate **103** was unreactive towards organocuprate reagents. However, the conversion of this material into the diene **93** could be effected cleanly and in near quantitative yield through a cuprous chloride (CuCl) accelerated, Pd(0) catalyzed Stille coupling reaction with tributylvinyltin (eq. 13).[59] The conditions employed for this transformation, developed by Liebeskind and co-workers,[59a,59b] have been applied successfully to a wide range of Stille coupling reactions and have been shown to be especially

useful for cases involving sterically congested substrates.[59c] That the diene **93** was indeed the

product of this reaction was confirmed by analysis of the spectral data obtained for this material.

The ^{1}H NMR spectrum of **93** displayed, for the diene function, four olefinic proton resonances at

δ 6.23, 5.78, 5.27 and 4.88. In particular, the two resonances at δ 5.27 and 4.88 were attributed to

the olefinic methylene protons and showed geminal coupling to one another ($J = 2$ Hz) as well as

coupling to the adjacent olefinic methine ($J = 17$ and 11 Hz, respectively). The latter two

couplings indicated the *trans* and *cis* nature of the methylene protons with respect to the adjacent

methine. Furthermore, a weak coupling ($J = 0.9$ Hz) between the endocyclic and exocyclic

olefinic methines confirmed connectivity of the two alkene units in this molecule. The ^{13}C NMR

spectrum of **93** included the expected four olefinic carbon resonances at δ 142.9, 136.7, 122.2

and 113.6, which, by analysis of a separate APT experiment and ^{13}C NMR peak heights, were

confirmed to be a quaternary carbon, two methines and one methylene, respectively.

(13)

103　　　　　**93**
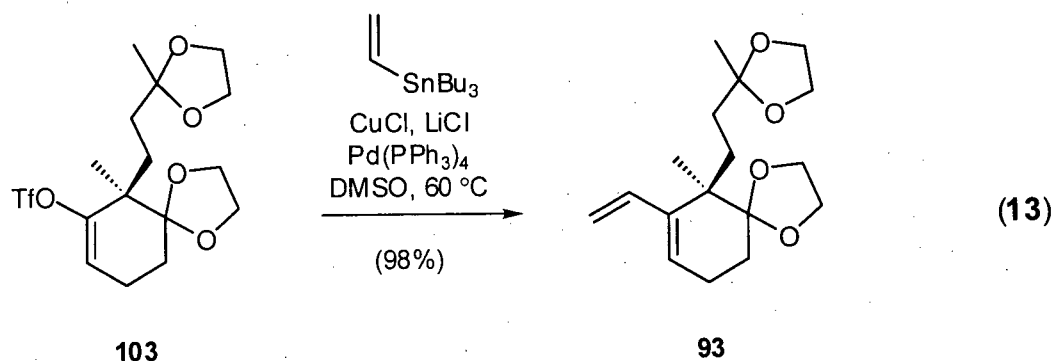
At this point, an essential intermediate in the proposed synthesis of ($\pm$)-13-methoxy-15-

oxozoapatlin (**22**), namely the diene **93**, had been obtained in a straightforward and high-yielding

manner. With an efficient synthesis of **93** established, an adequate quantity of this material

required to explore the proposed Diels-Alder reaction could be accessed. The results from these

studies are presented in the following section.

2.3.2 Synthesis of the bicyclic diketone 109

A summary of our investigations geared towards the production of the bicyclic aldehyde 96 via the Diels-Alder reaction of diene 93 with methacrolein (94), is presented in Table 2.1. While not included in this brief summary, the use of dienophiles other than methacrolein (94) was briefly explored. Unfortunately, both methacrylic acid (104) and ethyl methacrylate (105) were unsuitable for this transformation. Notably, the Lewis acid catalyzed or neat reactions of these dienophiles (i.e. 104 and 105) with the diene 93 provided complex mixtures of products with an overall poor mass balance. It could be shown, however, that simply stirring a solution of the diene 93 in methacrolein (94) overnight at room temperature provided a 3:2 mixture of the diastereomeric aldehydes 96 and 106 in quantitative yield (Table 2.1, entry 1). When a solution of 93 in 94 was heated to reflux, the diene 93 was consumed in less than one hour; however, the ratio of the diastereomeric aldehydes decreased to 1:1. As a higher degree of stereoselectivity had been anticipated for this process (vide supra), these results were quite disappointing. Fortunately, investigations focusing on the action of various Lewis acid mediators for this cycloaddition (Table 2.1, entries 3 to 7) revealed that EtAlCl$_2$, when employed stoichiometrically, provided more acceptable yields of the bicycle 96.[47] Moreover, the ratio of 96 to 106 could be further optimized by reducing the reaction temperature to -95 °C. In this manner, the desired bicyclic aldehyde 96 was produced in a yield of about 60%. It is noteworthy, that in the BF$_3$·OEt$_2$ mediated Diels-Alder reaction (entry 3) the sense of stereoselectivity for this process was reversed, providing the undesired bicyclic aldehyde 106 as the major product.
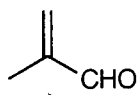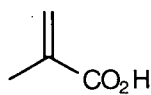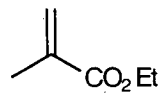
94   104   105

Table 2.1. Synthesis of the bicyclic aldehydes **96** and **106**.

$$(14)$$
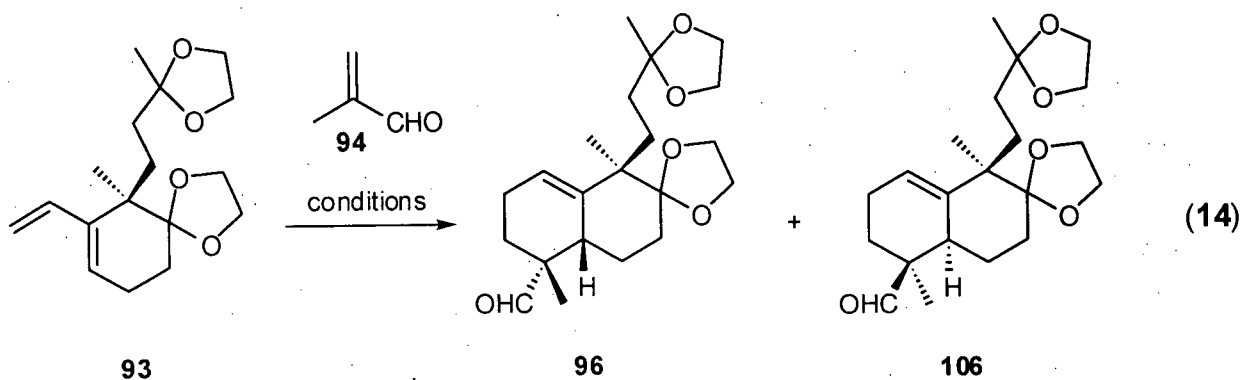
entry	Lewis acid (equiv.)	solvent	temp. (°C)	% yield[a]	product ratio (**96:106**:other diastereomers)[b,c]
1	none	methacrolein	20	100	3:2:0
2	none	methacrolein	67	100	1:1:0
3	BF$_3$·OEt$_2$ (1.0)	CH$_2$Cl$_2$	-78	90	2:4:1
4	TMSOTf (1.1)	CH$_2$Cl$_2$	-78	ND[d]	decomposition[e]
5	TiCl$_4$ (1.0)	CH$_2$Cl$_2$	-78	ND[d]	complex mixture[f]
6	AlCl$_3$ (1.05)	CH$_2$Cl$_2$	20	5[g]	1:1:0
7	EtAlCl$_2$ (1.1)	CH$_2$Cl$_2$	-78	96	8:5:0
8	EtAlCl$_2$ (1.1)	THF	-78	0	decomposition[e]
9	EtAlCl$_2$ (1.1)	hexane	-78	80	1:1:0
10	EtAlCl$_2$ (0.1)	CH$_2$Cl$_2$	-78	10[g]	8:5:0
11	EtAlCl$_2$ (5.0)	CH$_2$Cl$_2$	-78	0	decomposition
12	EtAlCl$_2$ (1.1)	CH$_2$Cl$_2$	-95	90	2:1:0

[a] Isolated yield of the mixture of diastereomers. [b] Determined by ^{1}H NMR analysis on the mixture of diastereomers. [c] Other diastereomers were not characterized. [d] ND : not determined. [e] ^{1}H NMR analysis indicated the ethylene ketals had been removed in the mixture of products. [f] The crude mixture of products included at least 6 compounds structurally different from **96**. [g] Approximately 90% of the starting material was recovered.

That the EtAlCl$_2$ mediated Diels-Alder reaction between the diene **93** and methacrolein (**94**) required greater than stoichiometric amounts of Lewis acid to run to completion (see entries 10 and 12) was not particularly surprising. A number of reports have indicated that during such transformations, the Lewis acid may complex preferentially to the starting material (e.g. methacrolein (**94**)) or the product.[60,61] In the former case, these reactions can be carried out with a catalytic amount of Lewis acid, as a molecule of starting material will dissociate the Lewis acid from the product and in so doing reintroduce the Lewis acid to the catalytic cycle. However, in the latter case, the preferential coordination of the Lewis acid to the product effectively removes

the Lewis acid from the catalytic cycle, and thus, in these situations, Lewis acids act as cycloaddition mediators only.

Unfortunately, the diastereomeric aldehydes **96** and **106** were inseparable by practical chromatographic procedures. Therefore, structural identification of these substances relied on the eventual purification and characterization of their chemical derivatives. Thus, when the crude mixture containing the aldehydes **96** and **106** was dissolved in ether and the resultant solution was treated with diisobutylaluminum hydride (DIBAL),[62] the alcohols **107** and **108** were produced. Fortuitously, these diastereomeric substances were separable by flash chromatography on silica gel. In this manner, the alcohols **107** and **108** were obtained in isolated yields of 53 and 27%, respectively, from the diene **93** (Scheme 2.18).

Analysis of the spectroscopic data collected for the alcohol **107**, the more polar of the two diastereomeric alcohols, yielded no conclusive evidence that its structure was as assigned. Nuclear Overhauser enhancement (NOE) difference experiments were also unable, in an unambiguous manner, to confirm the relative stereochemistry in the bicyclic core of this molecule. Furthermore, although both **107** and **108** exist as crystalline solids, recrystallization of these substances from a variety of solvents and mixed solvent systems did not generate crystals suitable for X-ray analysis. However, the stereochemical assignment of **107**, and hence the Diels-Alder adduct **96**, was confirmed through X-ray crystallographic analysis of a chemical derivative of **107** (*vide infra*). Nevertheless, while not configurationally conclusive, the spectral data collected for **107** was indeed consistent with the assigned structure. The IR spectrum displayed a stretching absorption at 3506 cm^{-1} (O-H). The ^{1}H NMR spectrum of **107** included an olefinic proton resonance (δ 5.42) and three 3-proton singlets (δ 1.28, 0.94 and 0.93), attributable to the olefinic methine and three methyl groups in the structure **107**, respectively. Additionally, the ^{13}C NMR spectrum of **107** exhibited only two olefinic carbon resonances (δ 141.3 and 120.5).

Moreover, the molecular formula of **107** was confirmed by a high-resolution mass spectrometric

measurement on the molecular ion.
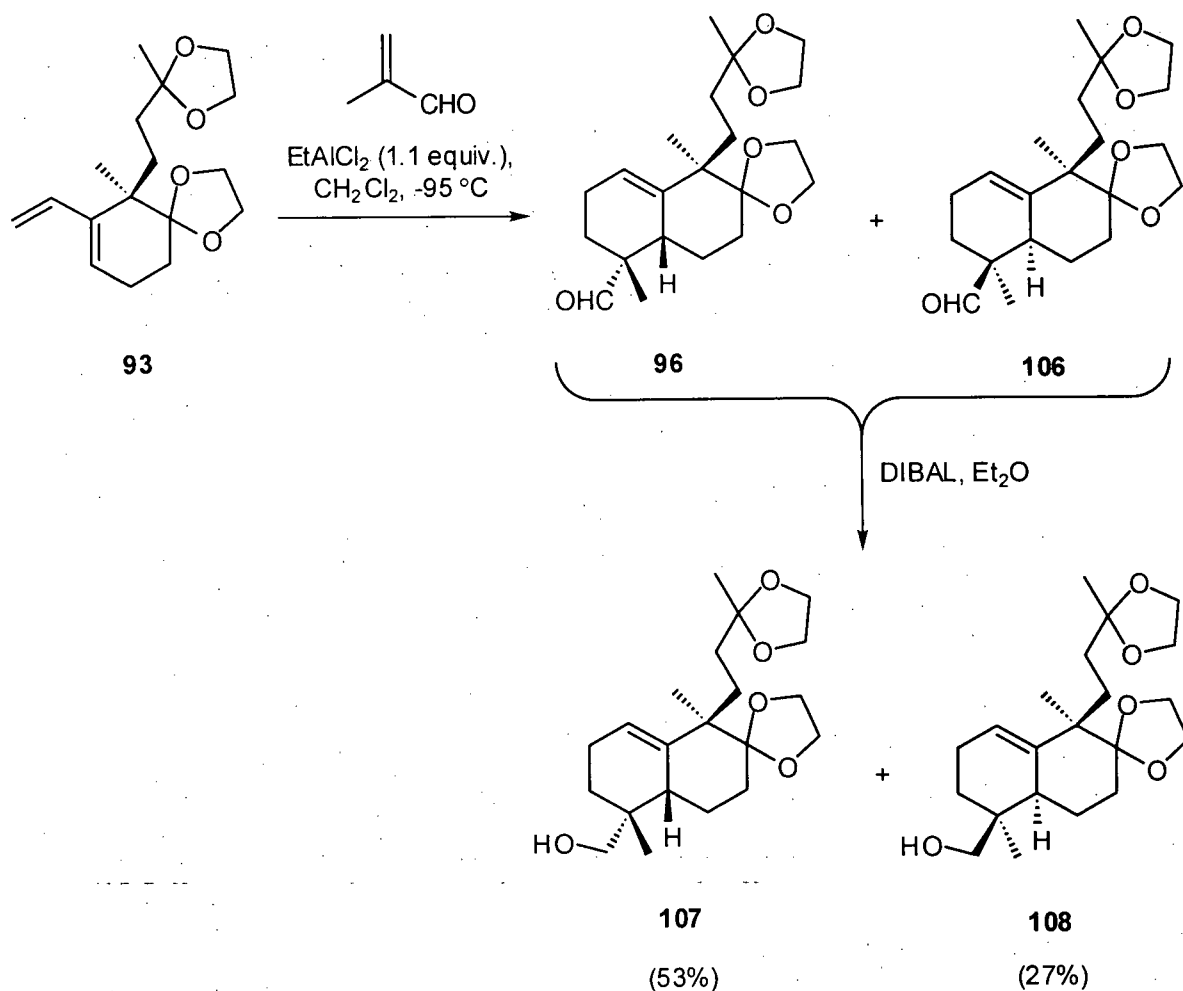
Scheme 2.18. Synthesis of the alcohols **107** and **108**.

Similarly, analysis of the spectral data collected on the alcohol **108** was inconclusive in

verifying the relative configuration of this compound. However, the IR spectrum included a

broad absorption at 3505 cm^{-1} (O-H) confirming the presence of the alcohol function in **108**. The

^{1}H NMR spectrum of **108** displayed a 1-proton multiplet in the olefinic region (δ 5.50) and three

3-proton singlets (δ 1.32, 1.07 and 0.90), which correspond to the olefinic methine and the three

methyl groups in this substance, respectively. The ^{13}C NMR spectrum contained the expected 21

signals. In particular, two olefinic carbon resonances (δ 141.1 and 118.3) confirmed the presence of a single olefin function in the alcohol **108**. While this data was not useful for the determination of the relative configuration of the stereogenic centers in compound **108**, literature precedent established for similar Diels-Alder reactions led to the reasonable conclusion that the minor product from this cycloaddition was substance **106**, and, consequently, that the minor product from the reduction of the mixture of diastereomeric aldehydes was **108**. While realizing that the structural assignment of these substances (i.e. **107** and **108**) was tentative, we decided to proceed, in the manner outlined (*vide supra*), with the major product from the Diels-Alder – reduction sequence, compound **107**.

Hydrolysis of the ethylene ketal functions in the bicyclic alcohol **107** was achieved smoothly by refluxing a solution of this material in acetone-H_2O with an equivalent of *p*-toluenesulfonic acid,[63] providing the dione **109** in quantitative yield (eq. 15). Fortunately, the dione **109** is a solid (mp 109 °C) which could be recrystallized from ether to provide crystals suitable for an X-ray crystallographic study.[64] As expected, a single crystal X-ray analysis of **109** (see Figure 2.3 and Appendix 2.1) showed conclusively that the relative configuration of this molecule was as assigned. Furthermore, the structures of the synthetic precursors to this molecule, namely the alcohol **107** and the Diels-Alder adduct **96**, were thus confirmed in an unambiguous manner.

107   **109**   (15)

55
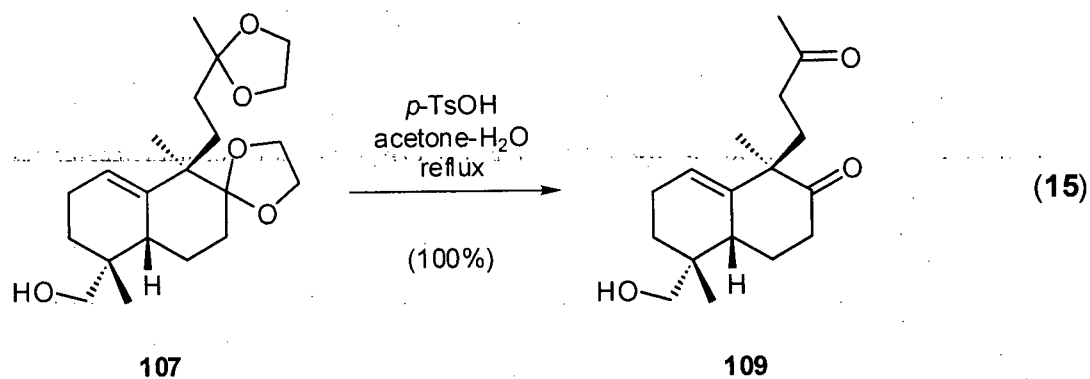
With the dione **109** in hand, a key intermediate in the proposed synthesis of (±)-13-methoxy-15-oxozoapatlin (**22**) had been accessed. It was originally anticipated that this dione would bear a formyl group, and not a hydroxymethyl function, at C-5 (see Figure 2.3 for numbering). Unfortunately, however, the sequence of reactions required to obtain the desired bicyclic diketone necessitated the reduction of the aldehyde function to facilitate product purification. In any event, the synthesis of diketone **109** was accomplished in a reasonable overall yield from the diene **93**. Furthermore, X-ray crystallographic analysis carried out on **109** proved essential in unambiguously confirming the structure of **109** and, consequently, the continuation of our studies towards the synthesis of **22**. The key synthetic events that would follow, as outlined in the retrosynthetic analysis of **22** (*vide supra*), included an intramolecular aldol condensation and an electrophile lactonization reaction. The results of this pursuit are summarized in the following section.
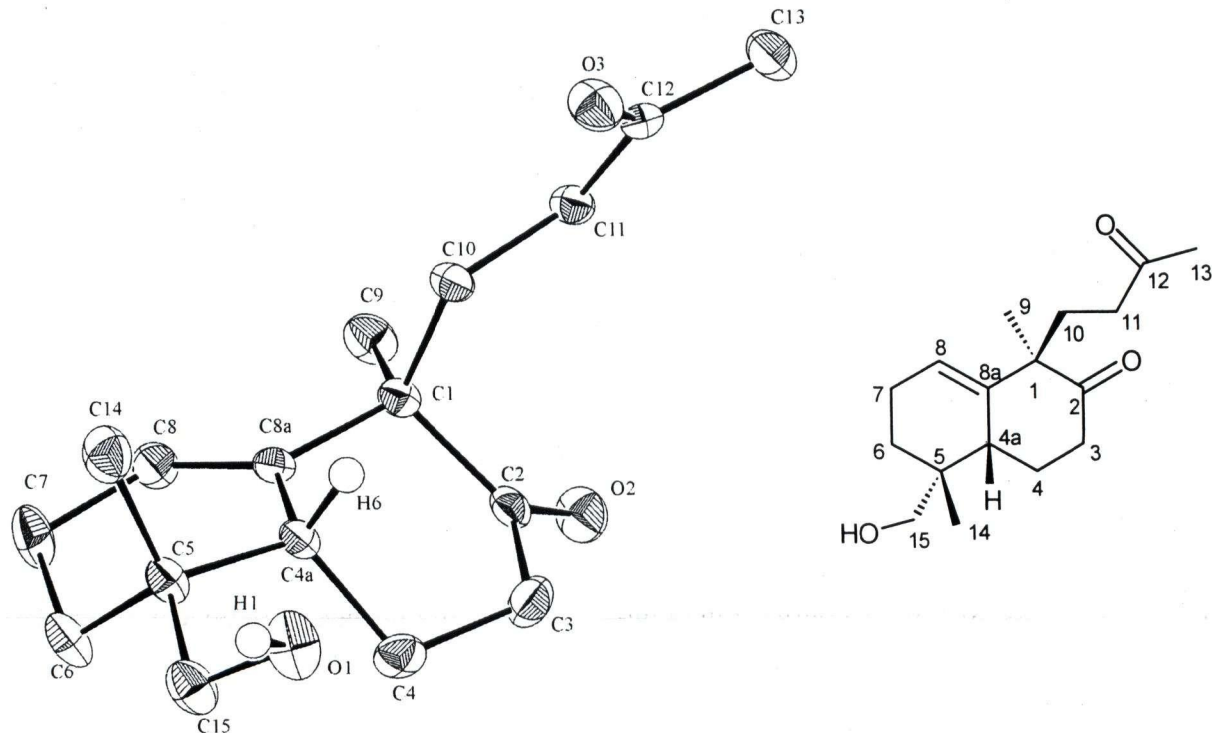
Figure 2.3. X-ray crystal structure of the dione **109**.

2.3.3 Synthesis of the tricyclic γ-lactone 46

46
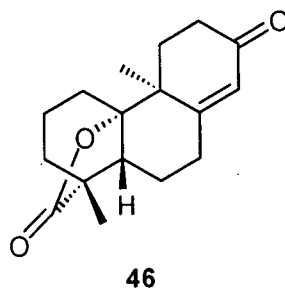
The synthesis of the tricyclic lactone **46** followed closely the proposed sequence of events outlined in the retrosynthetic analysis of this key intermediate (*vide supra*). Thus, after some experimentation, it was shown that an intramolecular aldol condensation of the dione **109** could be effected cleanly and efficiently through the treatment of a methanolic solution of this substance with excess NaOH (eq. 16). In this manner, the tricyclic alcohol **110** was accessed in excellent yield. Spectroscopic data collected on this material fully supported the formation of the enone **110**. The IR spectrum of **110** displayed a strong C=O stretching absorption at 1651 cm^{-1}, characteristic for a conjugated ketone, and a strong O-H stretching absorption at 3413 cm^{-1}. The ^{1}H NMR spectrum included two olefinic proton resonances (δ 5.78 and 5.58) and two 1-proton doublets that correspond to the hydroxymethyl function (δ 3.41 and 3.25). Further evidence for a successful condensation came from the disappearance of the 3-proton singlet (δ 2.10) assigned to the methyl ketone in the dione **109**. The ^{13}C NMR spectrum of **110** exhibited one enone carbonyl resonance (δ 199.1) and four olefinic carbon resonances at δ 174.3, 145.5, 125.1 and 119.0, which, by analysis of a separate APT experiment, were confirmed to be two trisubstituted olefinic carbons and two olefinic methine carbons, respectively. Additionally, the deshielded alkene carbon resonance at δ 174.3 is typical for the β-carbon of an α,β-unsaturated ketone function. From a more qualitative standpoint, it was noted, during TLC analysis of the enone **110**, that this substance absorbed UV light (λ = 254 nm) further supporting the presence of a conjugated enone function in the molecule.

(16)

NaOH, MeOH, rt

(90%)

109   110
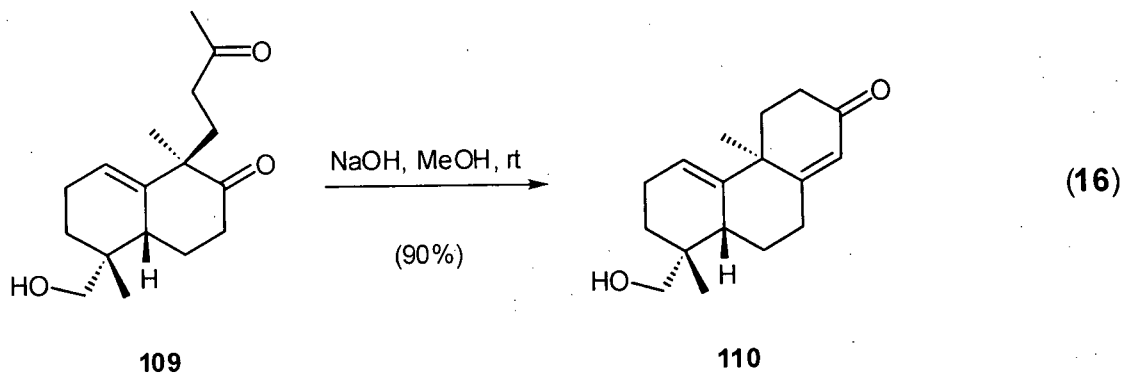
Conversion of the alcohol **110** into the aldehyde **91** was a straightforward process. Thus,

employing Ley's conditions,[65] the primary alcohol function in enone **110** was cleanly oxidized,

providing aldehyde **91** in excellent yield. Analysis of the IR spectrum of **91** supported the

structural assignment as the O-H stretching absorption observed in that of **110** was replaced by a

strong aldehyde C=O stretching absorption at 1718 cm^{-1}. Additionally, the ^{1}H NMR spectrum of

91 included a 1-proton singlet at δ 9.53 corresponding to the aldehyde proton. The ^{13}C NMR

spectrum displayed two carbonyl resonances (δ 205.7 and 198.6) as well as the other 15 carbon

signals anticipated for **91**. Moreover, an APT experiment revealed that the correct number of

methylene and quaternary carbons (11) and methyl and methine carbons (6) were present.

TPAP, NMO
CH$_2$Cl$_2$

(87%)

(17)

110   91
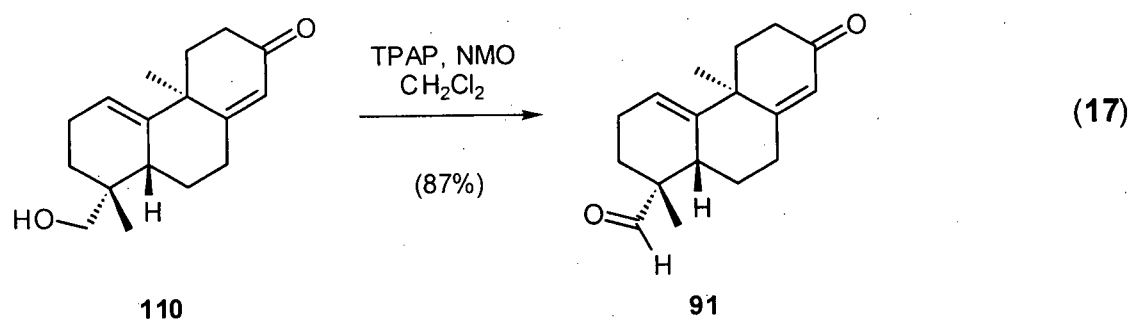
At this point, the stage was set to explore the oxidation - electrophilic lactonization

sequence. The results of our efforts in this regard are summarized in Scheme 2.19. To this end,

oxidation of the aldehyde function in **91** to the corresponding carboxylic acid proceeded

smoothly under standard conditions.[66] However, due to the large increase in polarity that

accompanied the formation of the carboxylic acid **111**, the chromatographic purification of this material was a tedious endeavor. Consequently, the crude carboxylic acid **111** was used in the next synthetic transformation without purification. Sequential treatment of an acetonitrile-H_2O solution of the acid **111** with $NaHCO_3$ and an excess of I_2[67] provided, after workup and subsequent column chromatography, the iodo lactone **92** in excellent overall yield from the aldehyde **91**. The conditions employed for this transformation reportedly provide kinetic control over the cyclization process, a necessary feature in our approach to ($\pm$)-13-methoxy-15-oxozoapatlin (**22**). In particular, the addition of base ($NaHCO_3$) significantly reduces the reversibility of this reaction, providing exclusively the iodo lactone that arises from a stereospecific *anti* addition of the carboxylate nucleophile to the iodine-double bond complex **112**.[45] More importantly, under kinetic (basic) conditions the acquisition of γ-lactones is preferred over δ-lactones, a prerequisite with regards to a synthesis of **22**.

Analysis of spectral data obtained for the iodo lactone **92** confirmed the stereo- and regioselective nature of the iodolactonization. The IR spectrum of **92** included two strong C=O stretching absorptions at 1771 and 1661 cm^{-1}, characteristic of a γ-lactone carbonyl and an α,β-unsaturated ketone, respectively. The ^{1}H NMR spectrum of **92** displayed only one olefinic proton resonance, a 1-proton singlet at δ 5.82, that could be assigned to the α-proton in the enone function. Additionally, a 1-proton doublet at δ 4.45 was attributed to the iodomethine proton at C-5. The ^{13}C NMR spectrum of **92** included two resonances at δ 196.5 and 178.7, which correspond to the enone and γ-lactone carbonyls, respectively. Also, a resonance at δ 85.8, typical of an acyloxy carbon, was established to be a quaternary carbon through an APT experiment, and thus assigned to the ring fusion carbon C-4b, confirming the presence of a γ-lactone.
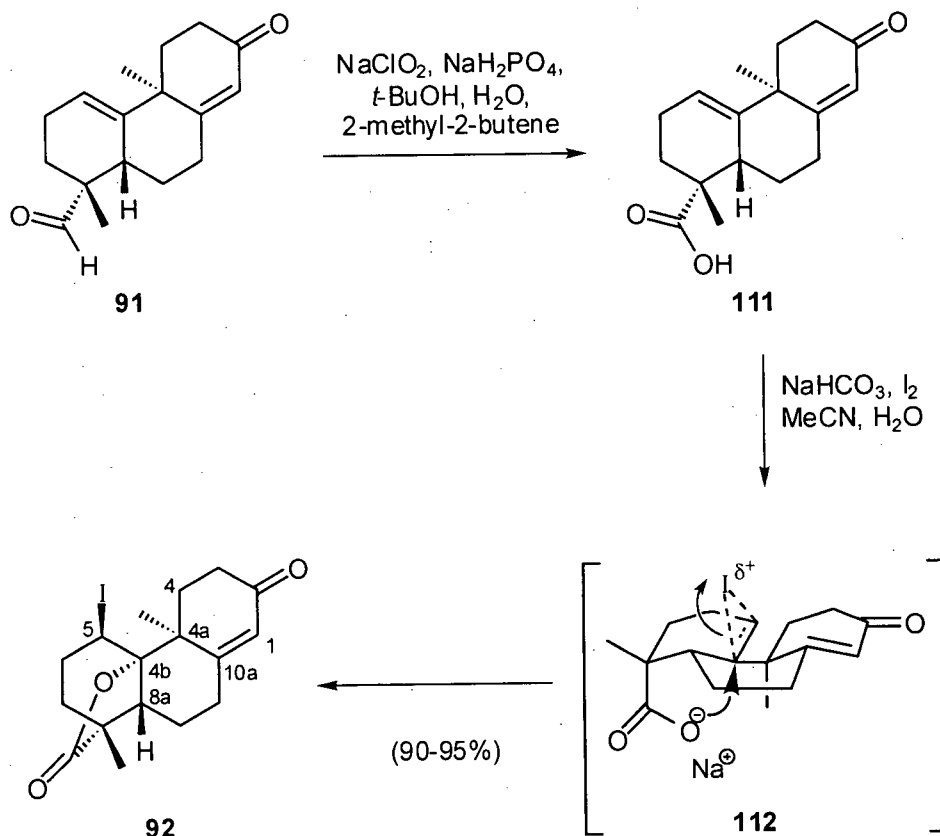
Scheme 2.19. Transformation of the aldehyde **91** into the iodo lactone **92**.

A fortuitous dispersion of resonances in the ^{1}H NMR spectrum of **92** provided ideal circumstances for an exhaustive spectroscopic investigation of this substance. A thorough analysis of data acquired from a series of APT, HMBC, HMQC and COSY experiments allowed for the complete assignment of the proton and carbon resonances in the ^{1}H and ^{13}C NMR spectra of **92** (see Experimental, Tables 2.3 and 2.4). Moreover, a series of 1D NOESY experiments also provided information regarding the relative configuration of each chirality center of the carbocyclic core of this substance. In particular, irradiation of a 3-proton singlet at δ 1.17, assigned to the methyl appendage at C-8, resulted in enhancements of a number signals, including the β-proton at C-7 (δ 1.84) and the angular proton H-8a (δ 3.03). Similarly, irradiation of the angular proton H-8a (δ 3.03) resulted in enhancements of signals corresponding to the

protons on the methyl group at C-8 and the β-proton at C-7. That the signal corresponding to the

iodomethine proton H-5 was not enhanced during these experiments suggested that the iodine at

C-5 was indeed axially oriented, as anticipated from a mechanistic analysis of the

iodolactonization reaction. Further evidence to support this assumption was derived from the

irradiation of the signal at δ 4.45 (H-5) which caused the enhancements of the α-protons at C-6

and C-4. Taken together, these results confirm the iodine at C-5 is indeed axially oriented and

that the structure of 92 is as shown.
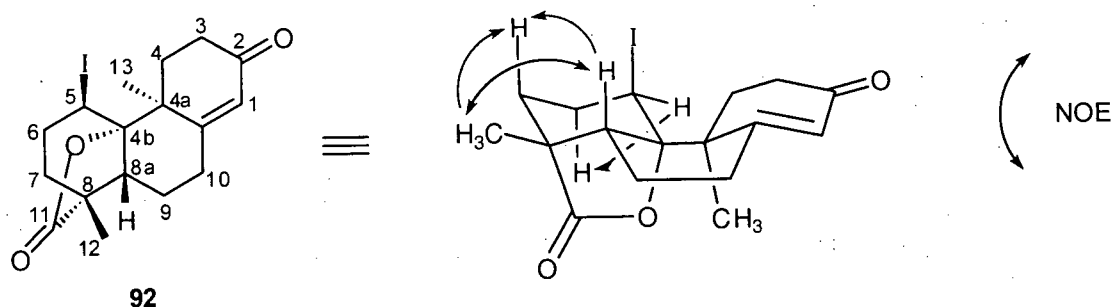
Figure 2.4. NOE correlations for the iodo lactone 92.

At this stage, all that remained to access the key tricyclic lactone intermediate 46 was

reduction of the iodomethine function in 92. It was anticipated that treatment of 92 with Bu₃SnH

and AIBN in refluxing benzene would smoothly furnish the desired γ-lactone 46.[67] However, in

the event, it was somewhat surprising to observe the formation of a second major product. Thus,

when the reaction was carried out at a concentration of 0.05 M with respect to the Bu₃SnH, the

desired γ-lactone 46 was isolated in only 61% yield (eq. 18). In addition to 46, a byproduct of

this reaction whose spectral data resembled that of the iodo lactone 92, was isolated in

approximately 30% yield. In order to optimize the production of the γ-lactone 46, it was

imperative to determine the structure of this byproduct and the mechanism by which it was

produced.

An array of spectroscopic experiments was employed to gather information about the structure of this unknown compound. From low resolution mass spectrometric analysis, the molecular ion for this substance was determined to be 274 AMU. As the γ-lactone **46** shares the same molecular weight and both compounds derive from the iodo lactone **92**, it could be concluded that the byproduct was a structural isomer of **46**. The ^{1}H NMR spectrum of the byproduct included an olefinic proton resonance at δ 5.77, corresponding to the enone methine, and 1-proton doublet at δ 4.75. The latter of these two signals was difficult to interpret, resembling both in coupling and chemical shift the iodomethine proton (H-5) in the iodo lactone **92** (δ 4.45, Figure 2.4). However, as mass spectrometric analysis had confirmed the isomeric nature of the byproduct and the γ-lactone **46**, it was clear that this resonance could not relate to an iodomethine function. Evidence eluding to the structure of the byproduct was gathered from both ^{13}C NMR and APT experiments on this substance. The ^{13}C NMR spectrum included two carbonyl resonances at δ 197.6 and 176.8 as well as resonances attributed to the enone olefinic carbons at δ 168.2 and 125.5. These signals confirmed the presence of both the lactone and the enone functions in the byproduct. Interestingly, the signal in the ^{13}C NMR spectrum of the iodo lactone **92** that had corresponded to the acyloxy carbon (C-4b) resonated at δ 85.8 and was replaced in that of the byproduct by a resonance at δ 75.0. Moreover, analysis of the APT experiment indicated that this signal corresponded to a methine carbon. Taken together, these data suggested that a structural rearrangement had occurred, whereby a scission of the acyl carbon - oxygen bond of the γ-lactone function in **46** was accompanied by bond formation between the adjacent carbon (e.g. C-5) and this oxygen, thus creating a δ-lactone. Further evidence in support of this hypothesis came from the IR spectrum of the byproduct, which displayed two strong C=O stretching absorptions at 1746 and 1666 cm^{-1}. These data are consistent with the typical stretching absorptions for a δ-lactone and enone carbonyl,

respectively. It was thus proposed that the structure of the byproduct is that depicted for the

tetracyclic δ-lactone **113** (eq. 18).
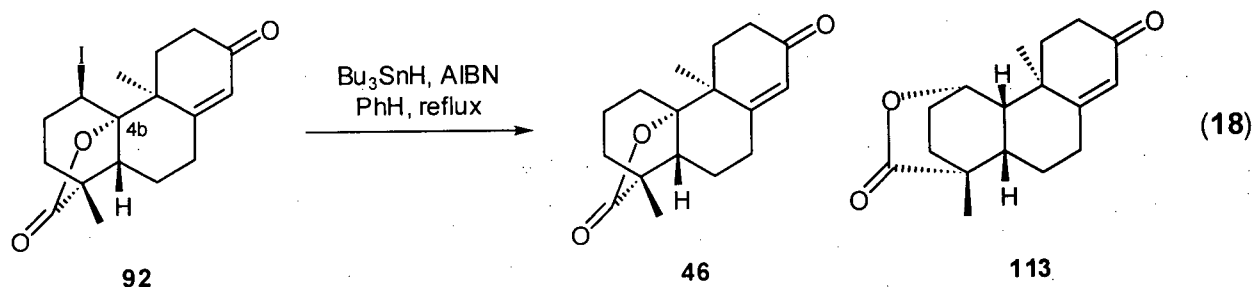
[Bu₃SnH] (M)	Yield (%) 46	Yield (%) 113
0.05	61	30
0.1	79	10
0.25	89	0

In order to unambiguously confirm the structure of the byproduct **113** a thorough

spectroscopic investigation of this material was carried out. Analysis of the results gathered from

HMBC, HMQC, COSY and APT experiments allowed for the complete assignment of all carbon

and proton resonances in the molecule (see Experimental, Tables 2.5 and 2.6). Additionally, a

series of 1D NOESY experiments were crucial in establishing the relative configuration of the C-

4b and C-8a centers (Figure 2.5). In particular, irradiation of the 3-proton singlet at δ 1.14 (H-

12), resulted in the enhancement of a multiplet at δ 1.98 that could be assigned to the angular

proton H-8a. Additionally, irradiation of a doublet at δ 4.75 (H-5) resulted in the enhancement of

a doublet at δ 1.89 (H-4b). Furthermore, irradiation of the doublet at 1.89 (H-4b) caused an

enhancement of the both the signals corresponding to H-5 (δ 4.75) and H-8a (δ 1.98). Thus, the

structure of the byproduct was confirmed to be that of the tricyclic δ-lactone depicted in Figure

2.5.
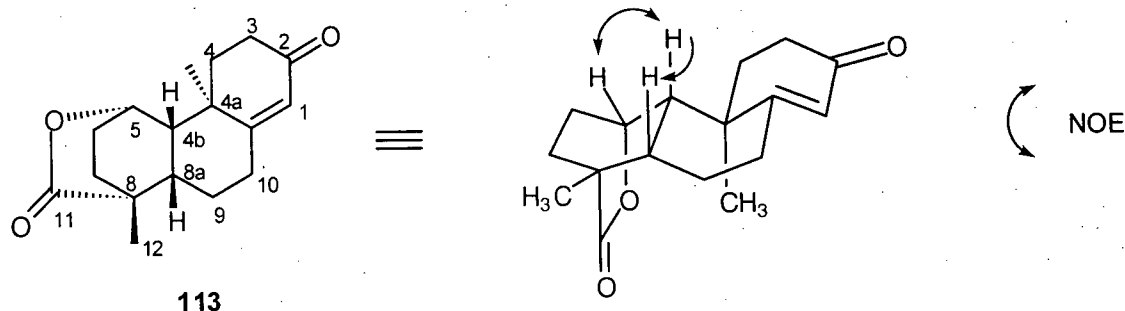
Figure 2.5. NOE correlations for the δ-lactone 113.

Recently in an analogous transformation of a gibberellin diterpenoid, Mander and co-workers reported a similar finding.[68] These researchers found that the radical mediated reduction of the alkyl iodide function in the tetracyclic lactone 114 resulted in a rearrangement, affording the δ-lactone 115. This report represented the first example of such a process in the literature (eq. 19).

$$\tag{19}$$
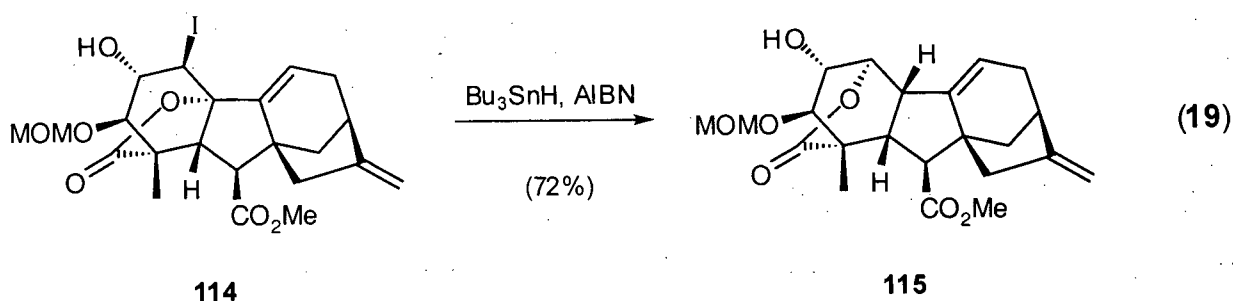
More recently, Crich and co-workers have exploited the radical mediated β-(acyloxy)alkyl rearrangement in the ring expansion and contraction of a variety of bromo and iodo lactones.[69] These researchers proposed that during the Bu_3SnH mediated reduction of halolactones (e.g. 116), the initially formed radical intermediate 117 might undergo a β-(acyloxy)alkyl migration. This rearrangement is expected to proceed via the mechanism depicted in Scheme 2.20, which involves the intermediacy of a three-center-three-electron transition structure (e.g. 118). However, that such rearrangements are not reported more frequently

suggests that the rate of radical migration is often low and in most cases cannot compete with the rate of reduction of the initially formed alkyl radical (e.g. **117**) by stannyl hydride. It is noteworthy that in the two known cases (e.g. **92** → **113** and **114** → **115**) in which this unanticipated rearrangement has occurred, the structure of the iodo lactone starting materials (e.g. **92** and **114**) are very similar. The relief of ring strain inherent in the γ-lactone moieties of both **92** and **114** is likely the driving force for the observed rearrangements. Fortunately, since the radical rearrangement is reportedly a slow process, an increase in the concentration of stannyl hydride should facilitate the formation of the desired γ-lactone by 'trapping' the initially formed alkyl radical prior to rearrangement. Thus, the production of the δ-lactone **113** should be avoided by an increase in concentration of Bu₃SnH.
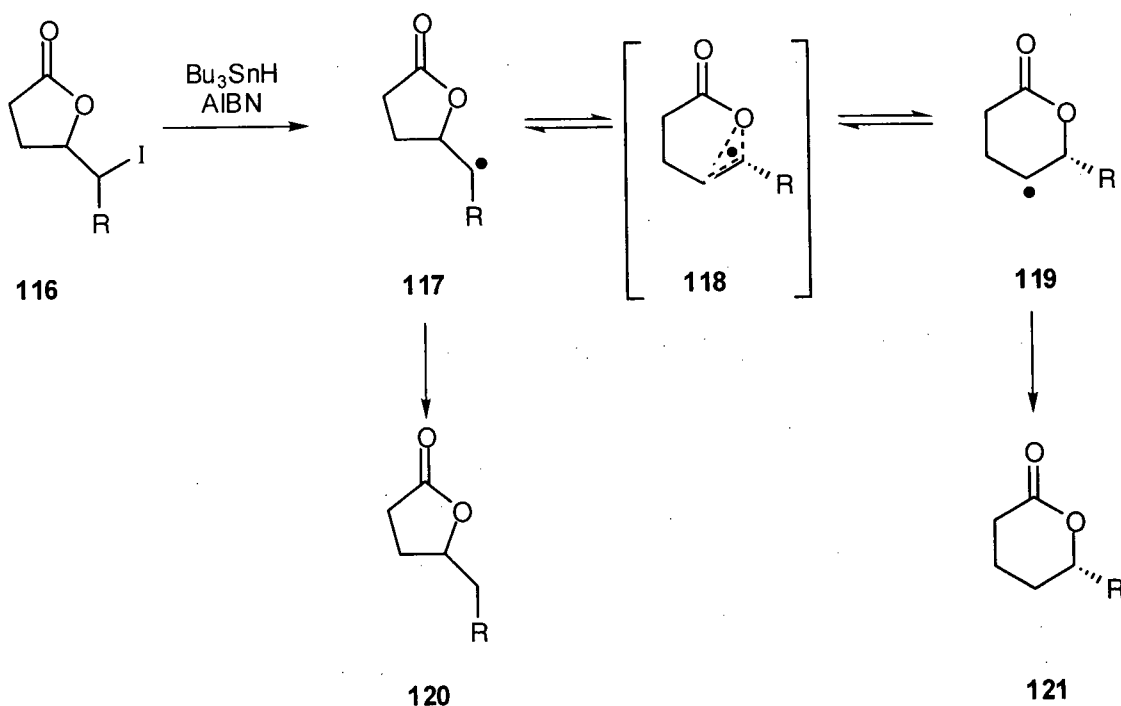
Scheme 2.20. Mechanism of the radical β-(acyloxy)alkyl migration.

Experimentally, it could be shown that increasing the concentration of Bu$_3$SnH to 0.1 M, in the reduction of the iodo lactone **92**, had a direct effect on the isolated yields of both the γ-lactone **46** and the byproduct **113**. Furthermore, when the reaction was carried out with a stannyl hydride concentration of 0.25 M, the desired γ-lactone **46** was formed exclusively (eq. 18). The spectral data obtained for **46** were in full accord with its structure. The IR spectrum of **46** showed strong C=O stretching absorptions at 1770 and 1667 cm^{-1} for the γ-lactone and enone carbonyls, respectively. The ^{1}H NMR spectrum of **46** included one olefinic proton resonance at δ 5.77. Additionally, the ^{13}C NMR spectrum displayed two carbonyl carbon resonances at δ 197.9 (enone) and 179.4 (γ-lactone) as well as two olefinic carbon resonances at δ 170.4 and 124.6. Further evidence for the presence of a γ-lactone moiety in **46** was garnered from analysis of an APT experiment carried out on this material. By this method, the acyloxy carbon resonance at δ 88.6 was confirmed to be a quaternary carbon.

46
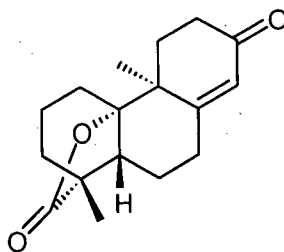
With an efficient synthesis of the γ-lactone **46** established, our next objective became the investigation of the proposed anionic oxy-Cope reaction (*vide supra*). The results of methodological studies and the unsuccessful attempt to apply these methods to the synthesis of (±)-13-methoxy-15-oxozoapatlin (**22**) are presented in the following section.

2.3.4 Investigations of the anionic oxy-Cope reaction involving alkenylstannanes
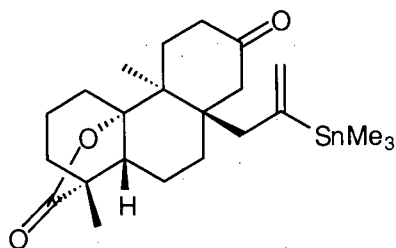
87

While it was anticipated that the anionic oxy-Cope reaction outlined in the retrosynthetic analysis of (±)-13-methoxy-15-oxozoapatlin (**22**) would yield access to the desired *trans-trans* fused tricycle **87**, it seemed prudent to first investigate this reaction on a model system. Due to the minimization of both steric interactions and conformational constraints in cyclohexenone (**122**), this simple carbocycle was selected as a suitable substrate to examine the efficacy of the proposed methodology. In this regard, addition of the known allyllithium species **76**[40] to cyclohexenone (**122**) resulted in the production of the tertiary alcohol **123** in excellent yield (eq. 20). A summary of experimental conditions employed to attempt the oxy-Cope reaction, or its anionic variant, is presented in Table 2.2. Unfortunately, treatment of the tertiary alcohol under standard anionic oxy-Cope conditions (see entries 1 and 2) resulted, upon workup, in the recovery of starting material. Additionally, attempts to effect a thermal oxy-Cope reaction were notably unsuccessful and led to the decomposition of this material (entries 3 to 5). However, a series of base-mediated reactions in hot xylene indicated that a narrow window of experimental temperatures exists, whereby the desired anionic oxy-Cope reaction (i.e. **123** → **124**) can be effected and decomposition of the starting material and/or the product is minimized. Thus, when the reaction mixture was maintained at 100 °C, the tertiary alcohol **123** was transformed into the known ketone **124**,[41] albeit in low yield (entry 7). It is noteworthy that while no reaction occurred at lower temperatures, an increase in temperature to 135 °C led exclusively to decomposition

materials that were not investigated further. While these results were somewhat discouraging, it

is noteworthy that the transformation of **123** into **124** represents, to the best of our knowledge,

the first example of an oxy-Cope rearrangement involving an alkenyl stannane.

Table 2.2. Summary of conditions employed to attempt the conversion of **123** into **124**.

(20)
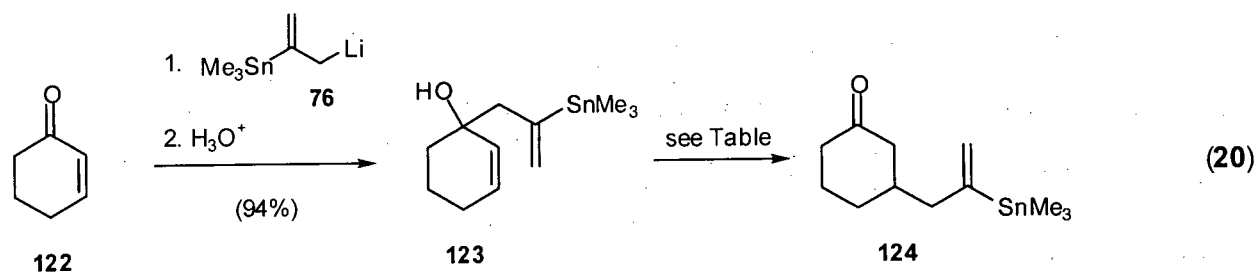
entry	solvent	additive	temp (°C)	reaction outcome
1	THF	KH	67	recovered **123**
2	THF	KH, 18-crown-6	67	recovered **123**
3	Diglyme	none	162	decomposition
4	NMP	none	200	decomposition
5	xylene	none	150	decomposition
6	xylene	KH, 18-crown-6	75	recovered **123**
7	xylene	KH, 18-crown-6	100	27% yield of **124**
8	xylene	KH, 18-crown-6	130	decomposition

In spite of the disappointing results outlined above, it was decided to attempt the

application of this sequence of transformations to the construction of the γ-lactone **87**. To this

end, treatment of the tetracyclic lactone **46** with the bifunctional allyllithium reagent **76** resulted

in the production of a 3:1 ratio of the two diastereomeric alcohols **85** and **126**, in a combined

yield of 67% (eq. 21). Unfortunately, unambiguous spectroscopic evidence that the 1,2-addition

of **76** to the ketone function of the γ-lactone **46** had occurred preferentially, as anticipated, from

the β-face of the molecule could not be obtained by a number of NOE experiments on the

diastereomeric alcohols **85** and **86**. Regardless, these substances could be separated by silica gel chromatography and subjected, individually, to conditions expected to effect an anionic oxy-Cope rearrangement. The results derived from these endeavors were quite disheartening. While a number of different experimental protocols, including those that had successfully converted **123** into **124**, were investigated, the oxy-Cope rearrangements of these substances led to decomposition or to the recovery of starting materials. At this point it was clear that our approach to the synthesis of (±)-13-methoxy-15-oxozoapatlin (**22**) would need to be re-evaluated.

(21)
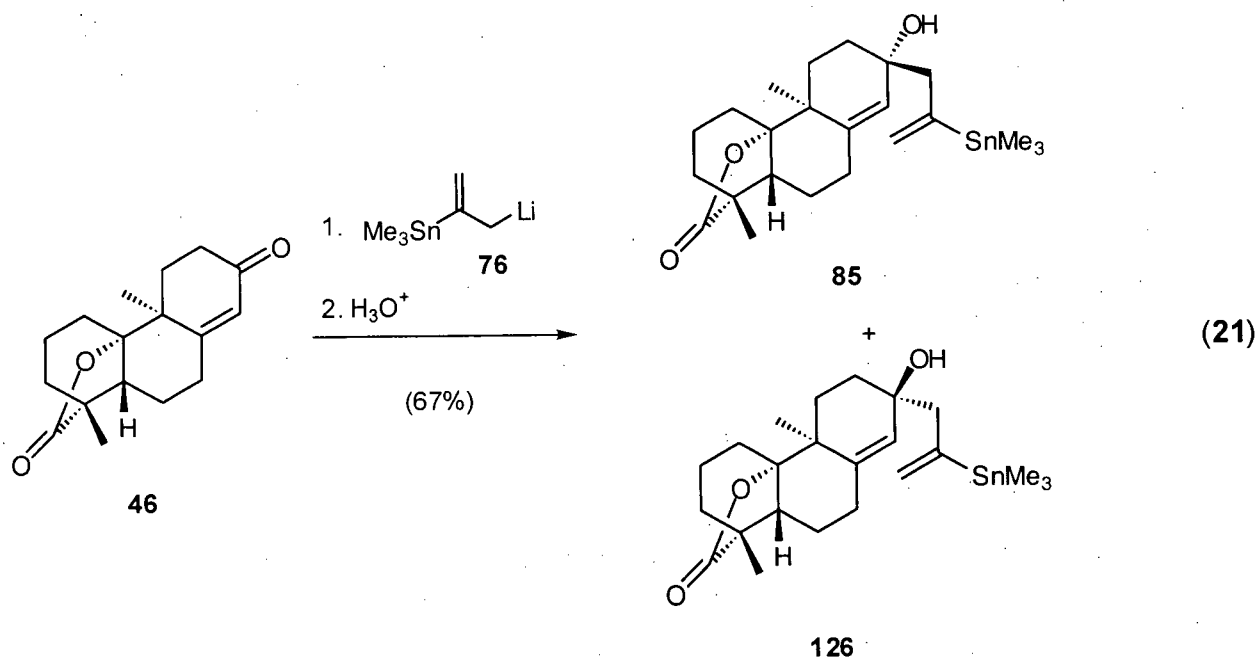
2.3.5 A modified retrosynthetic analysis for (±)-13-methoxy-15-oxozoapatlin (22)

Over the last 2 decades, applications of radical reactions in organic synthesis have increased dramatically.[70,71] In particular, the reaction of carbon-centered radicals with a variety of functional groups has proved advantageous over traditional carbon-carbon bond forming procedures. Namely, these radicals are extremely reactive yet the conditions by which they are

generated are relatively mild. Additionally, radical additions are generally irreversible and proceed via early, reactant like, transition states, making this process ideally suited for the formation of quaternary carbon centers.[72] Thus, it was anticipated that an intramolecular radical cyclization might represent a practical alternative to the oxy-Cope reaction, providing access to the bicyclo[3.2.1]octane fragment of (±)-13-methoxy-15-oxozoapatlin (**22**).

It was our contention that a synthesis of (±)-13-methoxy-15-oxozoapatlin (**22**) should necessarily take advantage of the efficient manner in which the enone **46** had been assembled. The construction of this tricyclic lactone, via which four of the requisite six carbon chirality centers present in **22** had been secured, required only 11 synthetic transformations and had proceeded in an overall yield of 25% from the known trione **95**. Furthermore, while cognizant of alternative synthetic methods to assemble the bicyclo[3.2.1]octane fragment of **22** from the enone **46** (*vide supra*), it remained our contention that the bifunctional reagent **76** could play a pivotal role in the development of a novel approach to such systems.

A modified synthetic plan for the construction of **22** from the γ-lactone **46** is presented in Scheme 2.21. The first synthetic event in the revised synthetic plan, namely the deconjugation of the enone function of **46**, was anticipated to be a facile process. As depicted, the γ-lactone function in the parent enone **46** acts as a conformational lock, such that the three carbocyclic rings (A,B,C) preferentially adopt chair, boat, and half chair conformations, respectively. On the other hand, in the β,γ-unsaturated ketone **127** the three rings assume chair, half chair, and chair conformations. Through computational modeling it could be shown that the difference in the relative energies of these substances was approximately 10 kcal/mol, with the β,γ-unsaturated ketone **127** being thermodynamically preferred.[73] From this, it was expected that the treatment of the enone **46** with base, under equilibrating conditions, should provide access to the β,γ-unsaturated ketone **127**.[33] Addition of the allyllithium species **76** (*vide supra*) to **127** would result in 1,2-addition of the allyl group to the ketone moiety in the latter substance. Through analyses

of relevant molecular models, it was anticipated that the C-4a methyl substituent would hinder the approach of the allyl lithium species **76** to the α-face of the ketone function in **127**, and thus impart some degree of facial selectivity to this process. At this point, the vinylstannane function could be transformed into a vinyl iodide,[41] a well-established process, providing **129**. The vinyl iodide and endocyclic olefin functions in **129** are thus ideally situated to engage in an intramolecular 5-*exo*-trig radical cyclization.
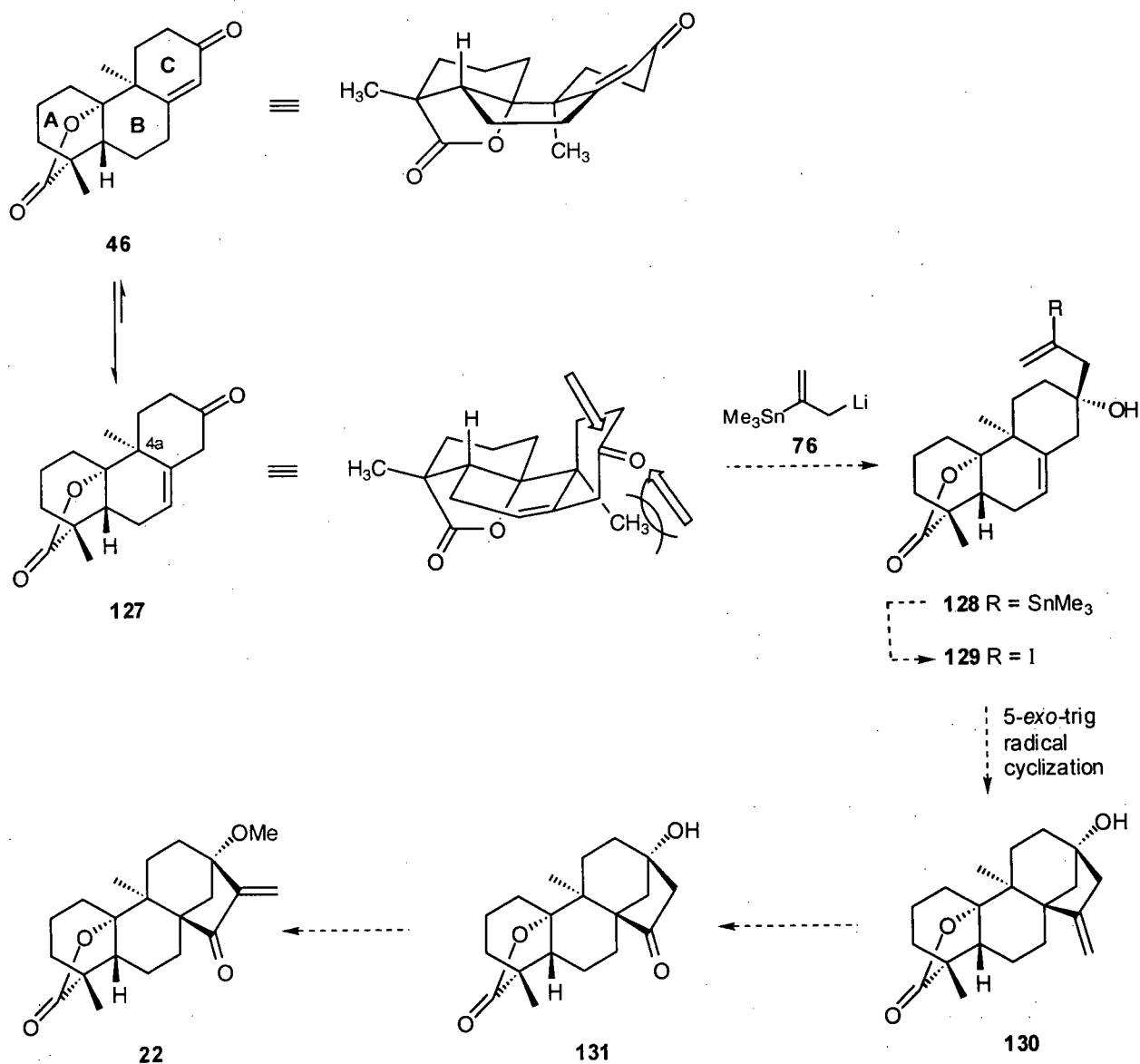
Scheme 2.21. Revised outline for the synthesis of (±)-13-methoxy-15-oxozoapatlin (**22**).

It is well documented that the regioselectivity for radical cyclizations is often very high.[70] This statement is supported by experimental details gathered from the cyclization of the 5-hexenyl radical, which produces the 5-*exo*-trig product at a rate 50 times faster than that of the 6-*endo*-trig product. Additionally, due to the early transition state for such processes and the extremely reactive nature of the vinyl radical, formation of the strained bicyclo[3.2.1]octane moiety of **130** should be possible by such methods. With **130** in hand, it was anticipated that cleavage of the exocyclic olefin would yield the ketone **131**, from which (±)-13-methoxy-15-oxozoapatlin (**22**) could be accessed.

2.3.6 Investigation of radical cyclization methods in the construction of the tetracyclic core of (±)-13-methoxy-15-oxozoapatlin (22)

As delineated in the revised retrosynthetic analysis of (±)-13-methoxy-15-oxozoapatlin (**22**) (Scheme 2.21), our immediate concern was the deconjugation of the α,β-unsaturated ketone function in the tricyclic lactone **46**. To this end, treatment of a solution of the lactone **46** in anhydrous *t*-BuOH with excess *t*-BuOK resulted in the rapid consumption of starting material and, upon acidic workup, the isolation of a compound that curiously absorbed UV light ($\lambda = 254$ nm). As the deconjugation of the enone function in **46** would be expected to result in the loss of UV absorbance, that this reaction had produced a single, UV absorbing product in excellent yield was somewhat unsettling. Additionally, analysis of the ^{1}H NMR spectrum of this material (initially) indicated that it possessed three olefinic protons. Clearly, this material was not the desired β,γ-unsaturated ketone **127**. Repetition of this reaction with freshly distilled *t*-BuOH and freshly prepared t-BuOK afforded this unidentified product exclusively. Thus, the structure determination of this substance became of paramount importance.

The ^{1}H NMR spectrum of this compound included three proton signals at δ 6.58, 5.97 and 5.91, all of which are typical for deshielded olefinic protons. However, analysis of a HMQC experiment performed on this material indicated that the proton that corresponded to the singlet at δ 5.97 was in fact not attached to a carbon. Additionally, the IR spectrum of this material displayed a broad O-H stretching absorption at 3402 cm^{-1} and two carbonyl C=O stretching absorptions at 1769 (γ-lactone) and 1674 cm^{-1} (enone). These data suggested that the singlet at δ 5.97 in the ^{1}H NMR spectrum corresponded to the proton of a hydroxyl function and that the γ-lactone moiety was intact. The ^{13}C NMR spectrum of the byproduct exhibited a carbonyl resonance at δ 179.3 (γ-lactone) as well as a second carbonyl resonance at δ 186.3. Thus, in conjunction with the information gathered from analysis of the ^{1}H NMR and IR spectra, it was apparent that the byproduct included an α,β-unsaturated carbonyl and a hydroxyl function. A full suite of spectroscopic experiments (HMBC, HMQC, COSY and APT) were employed to unambiguously determine the structure of this material. Analysis of the results from these experiments identified the structure of the byproduct as that depicted for the enol **132** (Scheme 2.22). The full assignment of proton and carbon resonances for this material is presented in Tables 2.7 and 2.8 (Experimental).
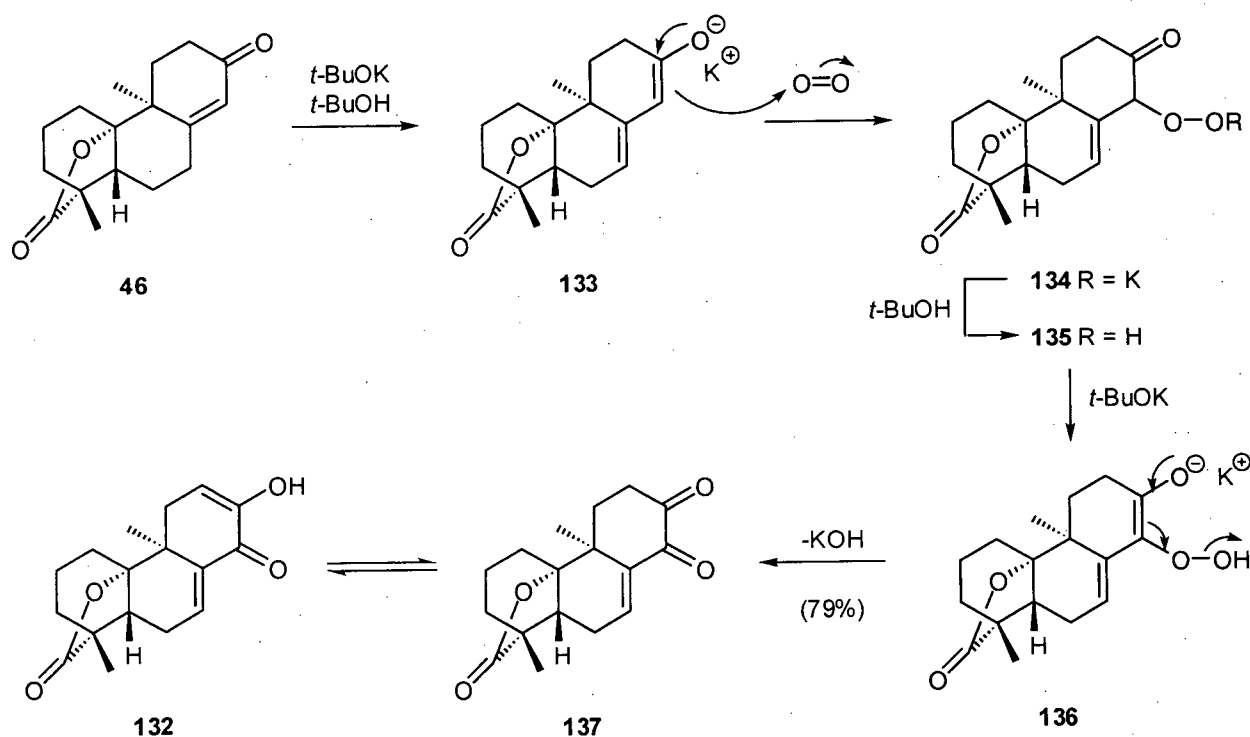
Scheme 2.22. Proposed mechanism for the production
of enol **132** from the tricyclic lactone **46**.

The production of 132 from the tricyclic lactone **46** was indeed surprising and implied

that oxygen had reacted with the enolate **133**, formed by the initial treatment of **46** with base,

producing the potassium peroxide **134**. Abstraction of a proton from solvent, followed by a

second deprotonation event then provides the dienolate **136**. Elimination of potassium hydroxide

from this species affords the α-diketone **137**, a tautomer of the enol **132**. From this proposed

mechanism for the production of 132 from **46**, it was clear that while the generation of the

extended enolate **133** is indeed a facile process, oxygen must be strictly eliminated from the

solvent (*t*-BuOH) to avoid this deleterious result. To this end, the *t*-BuOH was sparged with

argon for 0.5 hours prior to its distillation to ensure that, as much as possible, oxygen had been

eliminated. Applying this procedural modification, treatment of the γ-lactone **46** with *t*-BuOK

under 'oxygen-free' conditions provided, in under three minutes, the desired β,γ-unsaturated

ketone **127** in excellent yield (eq. 22). In fact, analysis of the crude reaction mixture by ^{1}H NMR

showed no trace of the enone **46**. That the deconjugation of **46** under thermodynamic

equilibration conditions provides **127** exclusively, supports the results garnered from molecular

modeling studies, which had indicated a large difference in the relative energies of these species

(*vide supra*). Analysis of spectroscopic data confirmed the formation of the β,γ-unsaturated

ketone **127**. The IR spectrum of **127** included two strong carbonyl stretching absorptions at 1761

and 1717 cm^{-1}, corresponding to the γ-lactone and the ketone, respectively. The ^{1}H NMR

spectrum of **127** displayed an olefinic proton resonance at δ 5.42 and two resonances at δ 3.31

and 2.82 that demonstrated geminal coupling (J = 15.6 Hz) and could be assigned to the α-keto

allylic methylene protons. The ^{13}C NMR spectrum of **127** included two carbonyl resonances at δ

207.3 and 179.8 as well as two olefinic resonances at δ 135.6 and 119.9. Additionally, from an

APT experiment, the correct number of methyl and methine carbons (4) was confirmed.

46   **127**   **(22)**
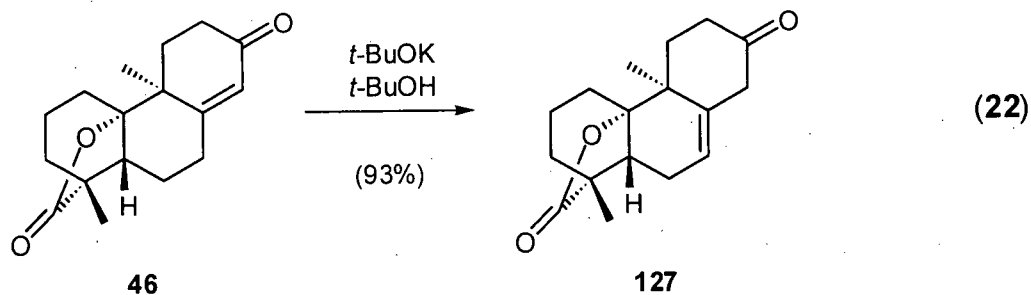
With the desired β,γ-unsaturated ketone **127** in hand, the conversion of this substance into

the vinylstannane **128** was investigated. In this regard, addition of the allyllithium reagent **76** to a

cold solution of **127** in THF, followed by aqueous workup and silica gel chromatography,

provided a 1.5:1 mixture of the α-tertiary alcohol **128** and β-tertiary alcohol **138**, respectively, in

a combined yield of approximately 60% (eq. 23). That the starting material **127** was also

recovered from this reaction, indicated the allyllithium reagent **76** had, to some extent, behaved as a base. As such, **76** may effect the deprotonation of **127**, resulting in the generation of the corresponding lithium dienolate (e.g. Scheme 2.22, **133** Li in place of K) and consequently, upon workup, the recovery of starting material. Therefore, it was desirable to decrease the basicity of the organometallic reagent.[74] To this end, attempts were made to synthesize the organocerium derivative of **76** through the addition of this reagent to anhydrous $CeCl_3$.[47] Unfortunately, efforts to achieve this transmetallation were unsuccessful, resulting exclusively in decomposition of the reagent. However, it could be shown that transmetallation of the allyllithium **76** with magnesium bromide[75] was a facile process. Moreover, treatment of the β,γ-unsaturated ketone **127** with the allylmagnesium reagent **139** resulted in a near quantitative conversion of **127** into the diastereomeric alcohols **128** and **138** (eq. 23). The alcohols **128** and **138** were readily separated by flash chromatography, providing the purified substances in isolated yields of 58 and 40%, respectively. That the major product from this reaction had resulted from addition of the allylmagnesium reagent **139** to the β-face of the ketone could not be deduced from a variety of spectroscopic experiments carried out on the purified diastereomers **128** and **138**. However, both NOE and X-ray crystallographic studies on chemical derivatives of **128** were conclusive in verifying that the relative stereochemistry of this material is as shown (*vide infra*).

The spectral data collected for the diastereomeric alcohols **128** and **138** were consistent with the assigned structures. The IR spectrum of **128** displayed an O-H stretching absorption at 3585 cm^{-1} and a strong C=O stretching absorption at 1756 cm^{-1} for the γ-lactone carbonyl. The ^1H NMR spectrum of **128** included the expected signals for the vinyl trimethylstannyl group: a 9-proton singlet at δ 0.08 and olefinic multiplets at δ 5.63 and 5.32 with satellite peaks due to tin – proton coupling ($^3J_{Sn-H}$ = 152 and 69 Hz, respectively). The ^{13}C NMR spectrum of **128** exhibited a single carbonyl resonance at δ 180.2 and four olefinic carbon resonances at δ 152.1, 138.2, 128.6 and 119.0. Additionally, a resonance characteristic of a tertiary carbinol carbon at δ 73.1 in the

^{13}C NMR spectrum of **128** replaced the ketone carbonyl resonance that appeared in the spectrum

of **127**, the precursor of **128**.

(23)
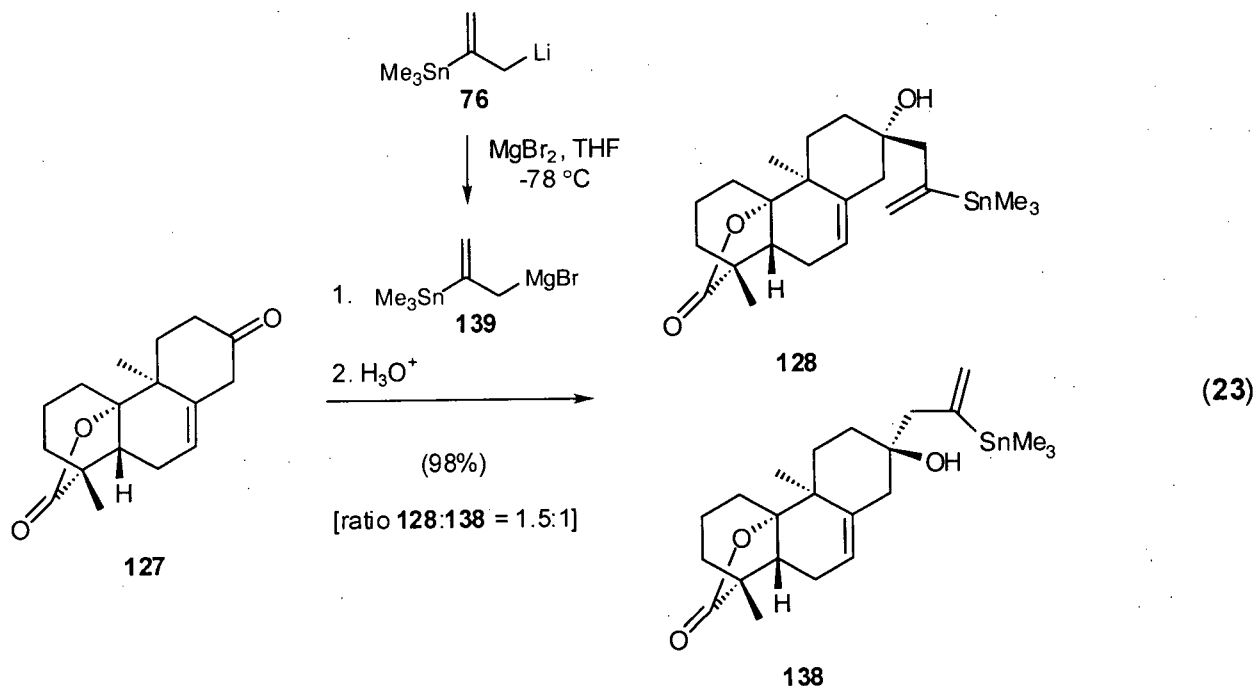
Again, while not definitive in verifying the relative configuration of the tertiary carbinol

center, the spectral data collected for **138** were also consistent with the proposed structure. The

IR spectrum of **138** displayed an O-H stretching absorption at 3606 cm^{-1} and a strong C=O

stretching absorption at 1763 cm^{-1} for the γ-lactone carbonyl. The ^{1}H NMR spectrum included

the expected signals for the vinyl trimethylstannyl group: a 9-proton singlet at δ 0.08 and olefinic

multiplets at δ 5.68 and 5.28, with satellite peaks due to tin - proton coupling ($^3J_{Sn-H}$ = 155 and 70

Hz, respectively). The ^{13}C NMR spectrum of **138** displayed a single carbonyl resonance at δ

180.2 and four olefinic carbon resonances at δ 152.2, 139.0, 128.2 and 119.6. Additionally, a

resonance characteristic of a tertiary carbinol carbon at δ 71.7 in the ^{13}C NMR spectrum of **138**

replaced the ketone carbonyl resonance that was present in **127**, the precursor of **138**. While this

data was not useful for determining the relative configurations of the tertiary carbinol centers in

either **128** or **138**, it had been anticipated that the 1,2-addition of the substituted allylmagnesium reagent **139** would occur, with some preference, from the β-face of the ketone function in **127** (*vide supra*). Thus, it seemed reasonable that the major product from this reaction would be the α-tertiary alcohol **128**. Realizing that the stereochemical assignment of these substances was tentative, we decided to proceed in the manner outlined (*vide supra*) with the major product from the 1,2-addition reaction, compound **128**.

Iododestannylation of the tertiary alcohol **128** was a straightforward process.[41] Treatment of **128** with *N*-iodosuccinimide in methylene chloride provided the alkenyl iodide **129** in excellent yield (eq. 24). The spectral data acquired for **129** was in full accord with the above transformation. The IR spectrum of **129** displayed an O-H stretching absorption at 3467 cm^{-1} and a γ-lactone carbonyl stretching absorption at 1761 cm^{-1}. The ^{1}H NMR spectrum included three olefinic proton resonances at δ 6.13, 5.98 and 5.40. The ^{13}C NMR spectrum of **129** included the γ-lactone carbonyl resonance at δ 180.1 and four olefinic carbon signals at δ 138.2, 131.1, 119.6 and 102.2.
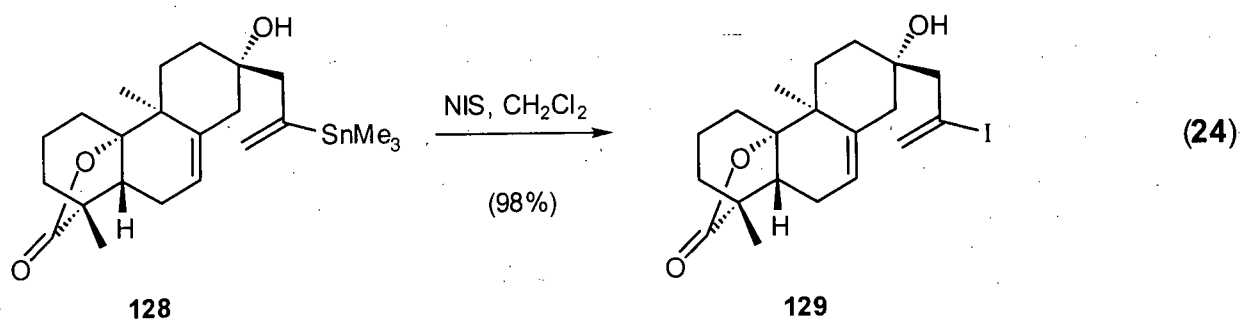
The fortuitous dispersion of proton resonances in the ^{1}H NMR spectrum of the vinyl iodide **129** allowed for the execution of a series of 1D NOESY experiments on this material and, consequently, the determination of the relative stereochemistry at the tertiary carbinol center. The resonances in the ^{1}H NMR spectrum of **129** corresponding to the diastereotopic protons on

the methylene of the 2-iodo-2-propenyl group appear as two doublets at δ 2.79 and 2.58, which

show a geminal coupling constant of 15.0 Hz. Additionally, the terminal olefin proton

resonances occur as two doublets at δ 6.13 and 5.98 that also exhibit geminal coupling ($J = 1.1$

Hz). By elimination, the remaining olefinic proton resonance at δ 5.40 could be assigned to the

endocyclic olefinic methine proton. It was found that irradiation of either of the allylic methylene

protons (e.g. δ 2.79 or 2.58) resulted in the enhancement of the terminal olefin proton resonance

at δ 6.13 and, more importantly, the endocyclic olefinic methine proton resonance at δ 5.40.

These results clearly identify the relative stereochemistry at the tertiary carbinol center as that

depicted for compound **129** in Figure 2.6. Thus, the addition of the substituted allylmagnesium

reagent **139** to the β,γ-unsaturated ketone **127** (eq. 23) had occurred with a slight preference from

the β-face of the ketone. Furthermore, the tentative structural assignment of the two

diastereomeric alcohols **128** and **138** (*vide supra*) had been correct.
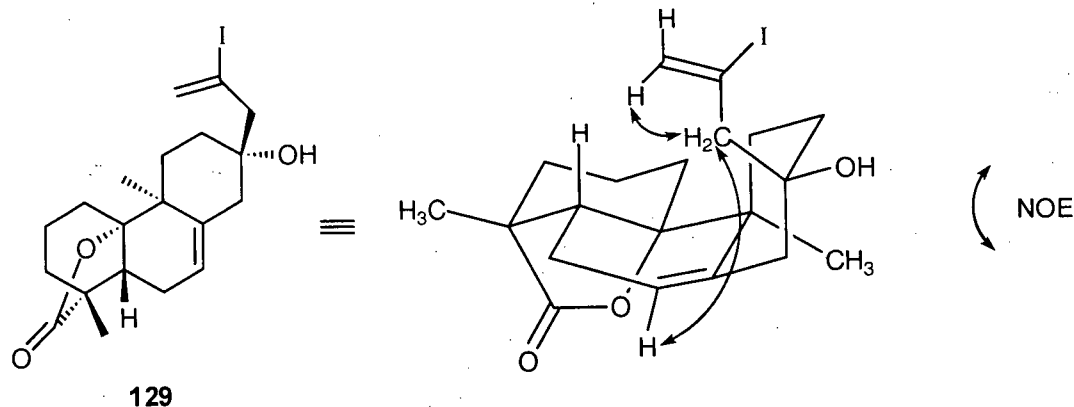
Figure 2.6. Confirmation of the relative stereochemistry of the tertiary carbinol carbon by NOE.

At this point, the stage was set to investigate the intramolecular 5-*exo*-trig radical

cyclization that was intended to complete the construction of the bicyclo[3.2.1]octane portion of

the target compound. Employing Stork's conditions[76] (catalytic AIBN, Bu₃SnH, PhH, irradiation

with a 250-watt sunlamp), the vinyl iodide **129** was consumed in under five minutes, producing,

in quantitative yield, a substance that was initially believed to be the desired tetracyclic lactone

130.

130
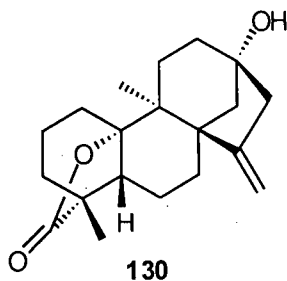
While mass spectrometric analysis indicated the molecular ion for this substance was consistent with the structure **130**, examination of the ^{13}C NMR spectrum of the radical cyclization product raised concerns (*vide infra*). The IR spectrum of this substance included a strong O-H stretching absorption at 3500 cm^{-1} for the tertiary alcohol as well as a strong C=O stretching absorption at 1752 cm^{-1} for the γ-lactone carbonyl. The ^{1}H NMR spectrum displayed two singlets in the olefinic region at δ 4.81 and 4.68, which were expected for the desired tetracyclic lactone **130**. However, analysis of the ^{13}C NMR spectrum and an APT experiment performed on this material indicated the compound in hand possessed a total of five methine and/or methyl carbons. Clearly the structure of this substance could not be that of the desired tetracyclic lactone **130**, which possesses only two methyl carbons and one methine carbon. Thus, while isomeric with the desired tetracyclic lactone **130**, this substance was not the expected 5-*exo*-trig radical cyclization product. A structure that accounted for all of the acquired spectral data (IR, ^{1}H and ^{13}C NMR) is that of **141** (Figure 2.7). A full suite of NMR spectroscopic experiments (HMQC, HMBC, COSY and 1D NOESY) was employed to verify the proposed structure of the radical cyclization product **141**. Analysis of the results from these experiments confirmed the structure of **141** and permitted the assignment of all proton and carbon resonances in the molecule (see Tables 2.9 and 2.10, Experimental). The radical cyclization product **141** is a

crystalline solid (mp 209 °C) that could be recrystallized from ether. Consequently, an X-ray

crystallographic study of this material was undertaken.[64] As anticipated, a single crystal X-ray

analysis of **141** (see Figure 2.7 and Appendix 2.2) provided irrefutable evidence that the

cyclization had in fact resulted in carbon – carbon bond formation in a 6-*endo*-trig and not a 5-

exo-trig manner. While only a minor source of gratification at this point, the X-ray analysis also

provided conclusive evidence that the 1,2-addition of the allylmagnesium bromide reagent **139** to

the ketone function of the β,γ-unsaturated ketone **127** had in fact occurred preferentially from the

β-face of the molecule (eq. 23).
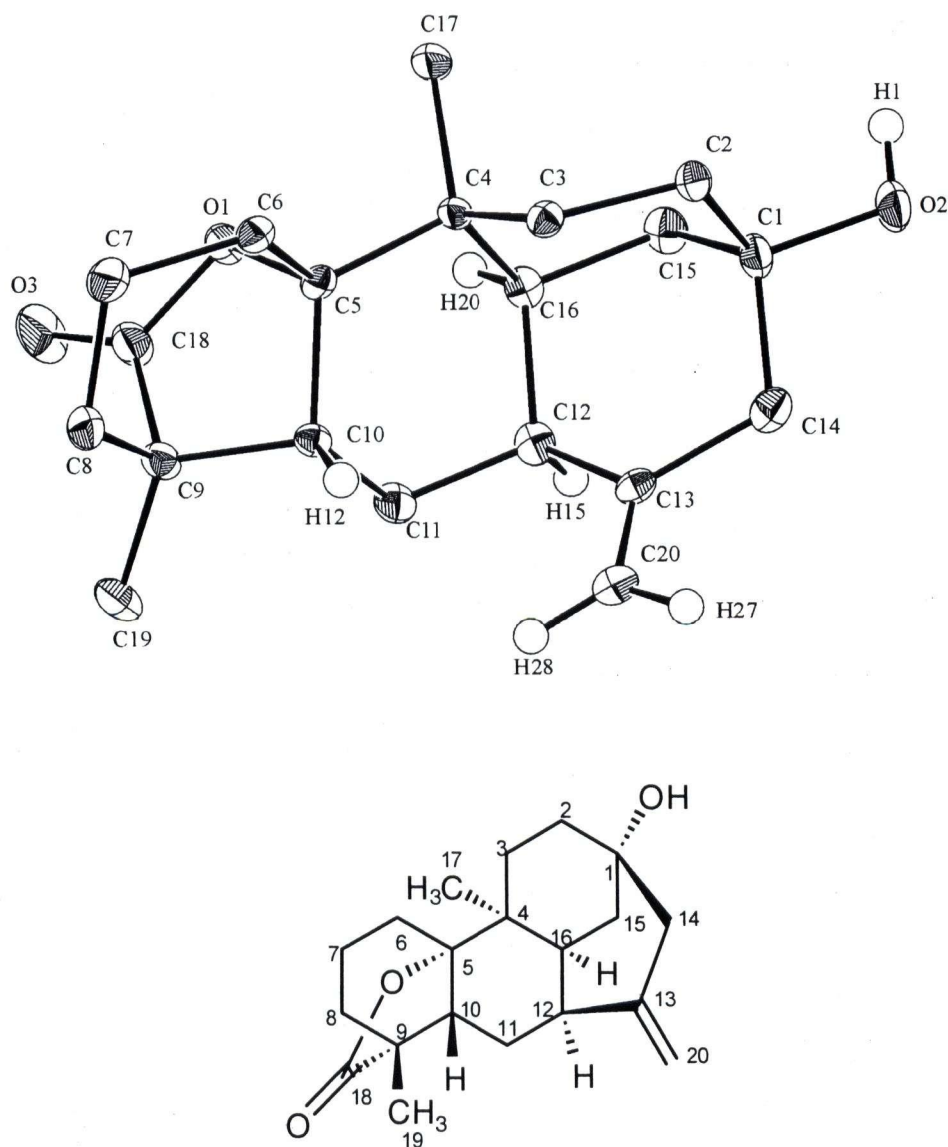
Figure 2.7. X-ray crystal structure of the tetracyclic lactone **141**.

Although formation of **141**, as described above, was unanticipated, it is important to note that 6-*endo*-trig vinyl radical cyclization processes have precedent in the chemical literature.[77,78] An example is shown in Scheme 2.23.[79] Stork and co-workers have proposed that the kinetic product in vinyl radical cyclizations with unactivated olefins involving the possible formation of a five or six membered ring, is typically that resulting from a 5-*exo*-trig cyclization (e.g. **145**, Scheme 2.23).[79] The resulting radical may react with a hydrogen atom donor to provide the methylenecyclopentane derivative **146** or it may rearrange, via the radical intermediate **147**, to the substituted methylenecyclohexyl radical **148**. Thus, at low concentrations of Bu$_3$SnH, distribution of the substituted methylenecyclopentane **146** and methylenecyclohexane **149** products is related to the relative stability of the corresponding radicals **145** and **148**, and the rate by which the rearrangement occurs. Experimentally, this proposal has been supported by the reactions described in Scheme 2.23.[79] Thus, when Bu$_3$SnH was employed as a hydrogen atom donor at a concentration of 0.02 M, the ratio of **146** to **149** was found to be 3:1. However, when the Bu$_3$SnH concentration was increased to 1.7 M, the ratio of these products became >97:1 in favor of the methylenecyclopentane **146**. Therefore, the rearrangement of the substituted methyl radical **145** may be curtailed by increasing the concentration of the hydrogen atom donor.

EtO$_2$C CO$_2$Et

144

Bu$_3$SnH

EtO$_2$C CO$_2$Et

145

Bu$_3$SnH

EtO$_2$C CO$_2$Et

146

EtO$_2$C CO$_2$Et

149

Bu$_3$SnH

EtO$_2$C CO$_2$Et

148

EtO$_2$C CO$_2$Et

147
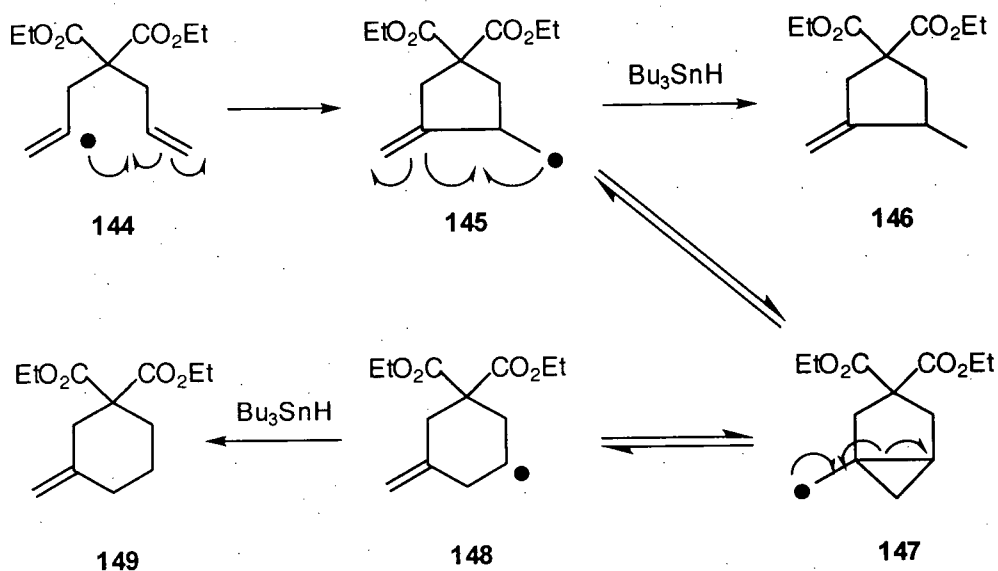
[Bu$_3$SnH]	ratio **146**:**149**
0.02 M	3:1
1.7 M	>97:1

Scheme 2.23. Rearrangement of methyl radical **145**.

In retrospect, it was not surprising that the exclusive product from the vinyl radical cyclization reaction involving **129** was the 'apparent' 6-*endo*-trig product. This result was consistent with molecular modeling calculations that indicated an enormous (> 30 kcal) difference between the relative energies of the 5-*exo*-trig and 6-*endo*-trig products **130** and **141** (Scheme 2.24).[73] That the 6-*endo*-trig product **141** is significantly more stable than the desired 5-*exo*-trig product **130**, and tertiary radicals are generally more stable than secondary radicals,[80] one would expect that of the radical intermediates, **151** would be much less stable than **153**. Nevertheless, an effort was made to 'trap' the proposed radical intermediate **151** through increasing the concentration of Bu$_3$SnH. Unfortunately, it was found that an increase in the concentration of Bu$_3$SnH from 0.02 to 0.1 M resulted in the production of the alkene **154**, which clearly arises from the direct reduction of the vinyl radical **150**. From these results, two possible

mechanistic scenarios exist. Following a sequence of events analogous to those described in Scheme 2.23, the vinyl radical **150** may engage in a 5-*exo*-trig cyclization to provide the cyclohexyl radical **151**, which rapidly rearranges to the more stable tertiary radical **153** prior to reduction by Bu_3SnH. Alternatively, the vinyl radical **150** may react with the endocyclic olefin in a 6-*endo*-trig manner to provide the bridged cyclohexyl radical **153** directly. In line with a synthesis of (±)-13-methoxy-15-oxozoapatlin (**22**), the latter scenario represents a dead end. However, the possibility that this process had in fact proceeded via the former scenario (i.e. a mechanism involving a 5-*exo*-trig radical cyclization) was somewhat encouraging.

The alkene **154**, obtained as a byproduct from the vinyl radical cyclization reaction when high concentrations of Bu_3SnH were employed, provided spectroscopic data consistent with the assigned structure. The IR spectrum of **154** included an O-H stretching absorption at 3467 cm^{-1} and a C=O stretching absorption, for the γ-lactone carbonyl, at 1763 cm^{-1}. The ^1H NMR spectrum of this material displayed four olefinic proton resonances at δ 5.83, 5.38, 5.18 and 5.10. Moreover, the olefinic signal at δ 5.83 exhibited strong coupling with the olefinic proton resonances at δ 5.18 and 5.10, J = 10.3 and 17.2 Hz, respectively, indicating the *cis* and *trans* relationship between these protons and confirming that a hydrodeiodination had occurred. The ^{13}C NMR spectrum of **154** included a carbonyl carbon resonance at δ 186.5 and four olefinic carbon resonances at δ 138.7, 133.3, 119.5 and 118.8. Additionally, mass spectrometric analysis of **154** yielded a molecular ion consistent with the proposed structure.

[Bu₃SnH]	ratio 141:154:130
0.02 M	1:0:0
0.1 M	3:1:0
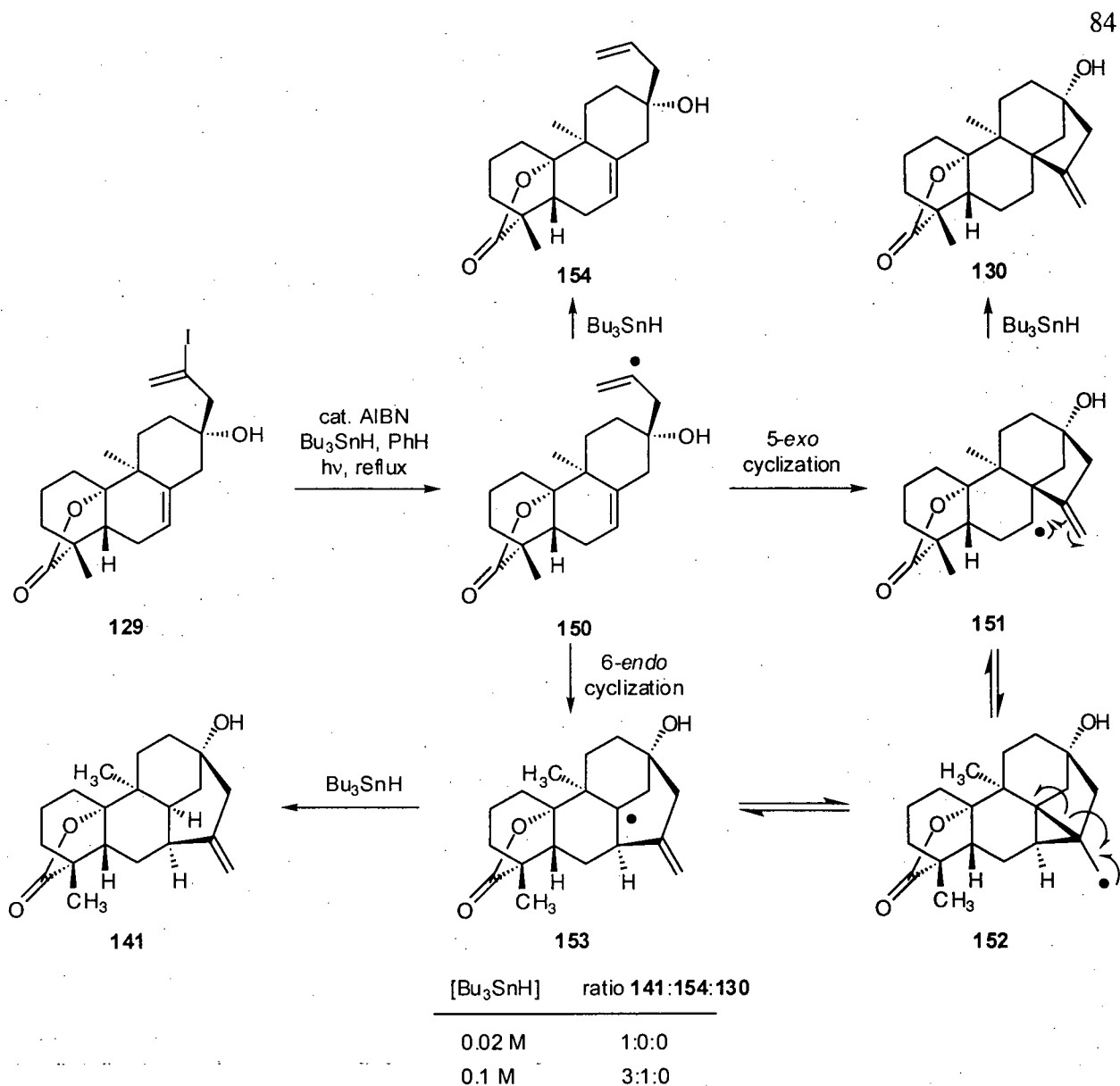
Scheme 2.24. Proposed mechanism for the formation of **141** and **154**.

In order to ascertain whether or not the radical cyclization had in fact proceeded via a rearrangement of the radical resulting from a 5-*exo*-trig cyclization (i.e. **151**), it was necessary to devise a synthetic strategy whereby the initial radical cyclization event would have no avenue for rearrangement. In this regard, it was anticipated that a ketyl radical – olefin coupling reaction promoted by samarium(II) iodide would serve well. Samarium(II) iodide (SmI₂) is an exceptional

reagent for the promotion of intramolecular reductive cyclization reactions and has been the subject of two recent reviews.[81,82] In particular, treatment of aldehydes (e.g. **155**) and ketones with this reagent results in the generation of a ketyl radical anion (e.g. **156**) that is capable of engaging in intramolecular cyclization reactions with nonstabilized alkenes (eq. 25). Additionally, where the choice exists for the formation of a substituted methyl radical or cyclohexenyl radical there is an overwhelming preference for the production of the former (e.g. **157**). In fact, there are only a few known examples of SmI_2 promoted 6-*endo*-trig radical cyclizations.[83,84] It is noteworthy, that the radical intermediate generated by such cyclizations is incapable of rearranging via the mechanisms discussed above. Instead, this species is rapidly reduced by a second equivalent of SmI_2 to an organosamarium species (e.g. **158**), which then abstracts protons from the *t*-BuOH additive to provide a cyclopentanol (e.g. **159**).
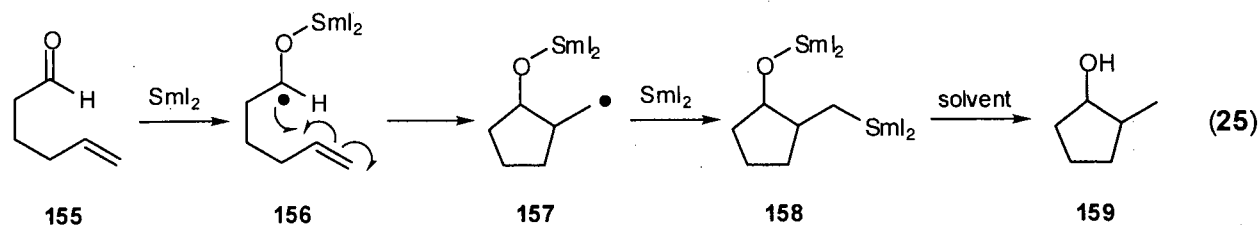
It was anticipated that a SmI_2 promoted cyclization of the tricyclic aldehyde **160** would provide either (or both) of the tetracyclic lactones **161** or (and) **162** and in so doing shed light on the mechanistic quandary at hand (eq. 26). The formation **161**, necessarily through a 5-*exo*-trig process, would have useful implications for the construction of the bicyclo[3.2.1]octane portion of the target molecule (±)-13-methoxy-15-oxozoaptlin (**22**). On the contrary, the production of **162** would indicate that the radical cyclization in fact proceeds via a 6-*endo*-trig mechanism, effectively terminating our approach to **22** via such methods.
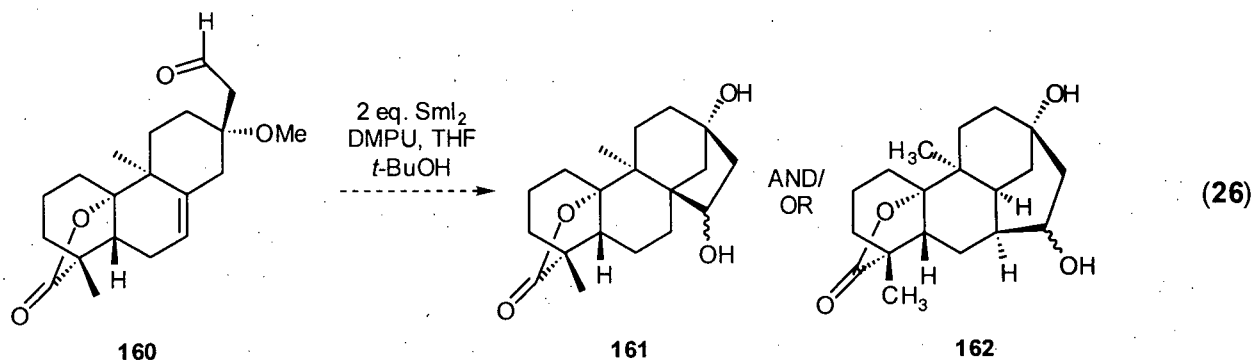
The synthesis of **160** proceeded in a straightforward manner from the tricyclic alkene **154**
(see Scheme 2.24 for the synthesis of **154**). Thus, sequential treatment of **154** with potassium
hydride and methyl iodide smoothly effected the production of the methyl ether **163** (eq. 27).
This material was directly subjected to reactions that would effect the chemoselective oxidative
cleavage of the terminal olefin.[85] Thus, as shown in equation 27, the tricyclic aldehyde **160** was
produced in good yield over three steps from the alkene **154**. While the transformations involved
in this sequence were not optimized, they served to provide the aldehyde **160** in sufficient
quantity to investigate the proposed SmI_2 promoted ketyl radical - olefin coupling reaction.
Spectroscopic evidence was in complete agreement with the formation of the tricyclic aldehyde
160. The IR spectrum of this material exhibited two carbonyl C=O stretching absorptions at 1766
(γ-lactone) and 1719 (aldehyde) cm^{-1}. In addition, the ^1H NMR spectrum of **160** included a
characteristic aldehyde proton resonance at δ 9.79, which appears as a doublet of doublets (J =
2.7 and 3.8 Hz). The ^1H NMR spectrum also displayed a 3-proton singlet at δ 3.30,
corresponding to the methyl ether moiety in **160**, and an olefinic resonance at δ 5.39. The ^{13}C
NMR spectrum of **160** included two carbonyl carbon resonances at δ 202.7 (aldehyde) and 180.0
(γ-lactone) and two olefinic carbon resonances at δ 137.7 and 120.0.

1. OsO$_4$, NMO
   t-BuOH, H$_2$O
2. NaIO$_4$, reflux, (4:2:1)
   H$_2$O:Acetone:t-BuOH

(approx. 50% from 154)

(27)

160

1. KH, THF
2. MeI

154 R = H

163 R = Me
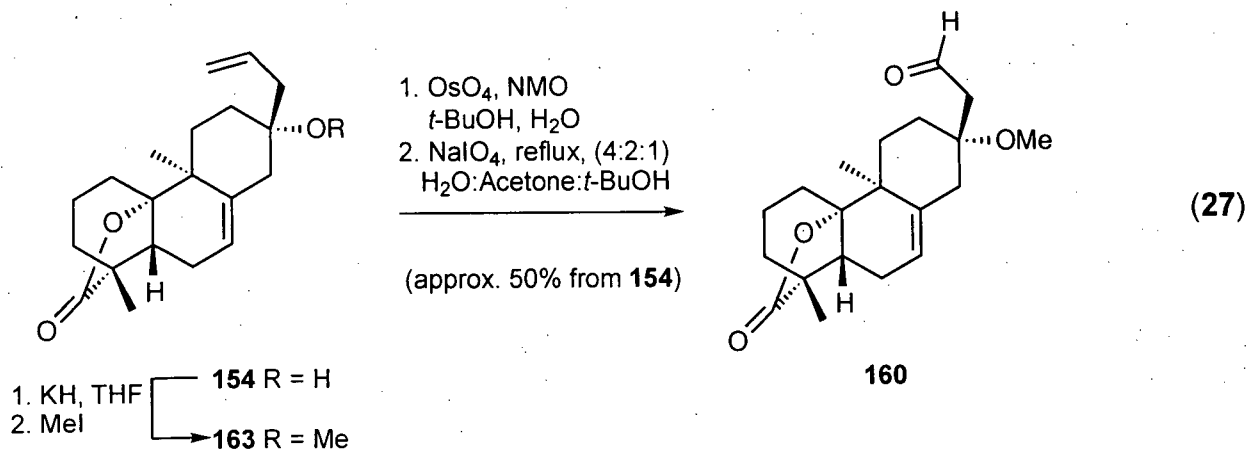
With the tricyclic aldehyde **160** in hand, we were prepared to test the proposed SmI$_2$ promoted ketyl radical – olefin coupling reaction. Treatment of a solution of **160**, DMPU and t-BuOH in THF with a freshly prepared THF solution of SmI$_2$[86] resulted in the rapid consumption of the aldehyde **160**, as indicated by TLC analysis. Standard workup provided an inseparable mixture of the alcohols **167** and **168**, which was oxidized directly using Ley's procedure[65] to provide the readily separable (flash chromatography) aldehyde **160** and the ketone **169** in a ratio of 2:3 (Scheme 2.25). The recovery of the aldehyde **160** from this sequence of transformations indicates that the relative rates of cyclization and reduction of the ketyl radical **164** to the cyclohexyl radical **166** and the organosamarium **165** are similar. It was quite discouraging, however, to discover that the sole ketyl radical – olefin coupling adduct produced by this reaction was that resulting from a 6-$endo$-trig process. From this result, it was clear that a radical cyclization approach to the bicyclo[3.2.1]octane fragment of (±)-13-methoxy-15-oxozoaptlin (**22**) was a fruitless pursuit.
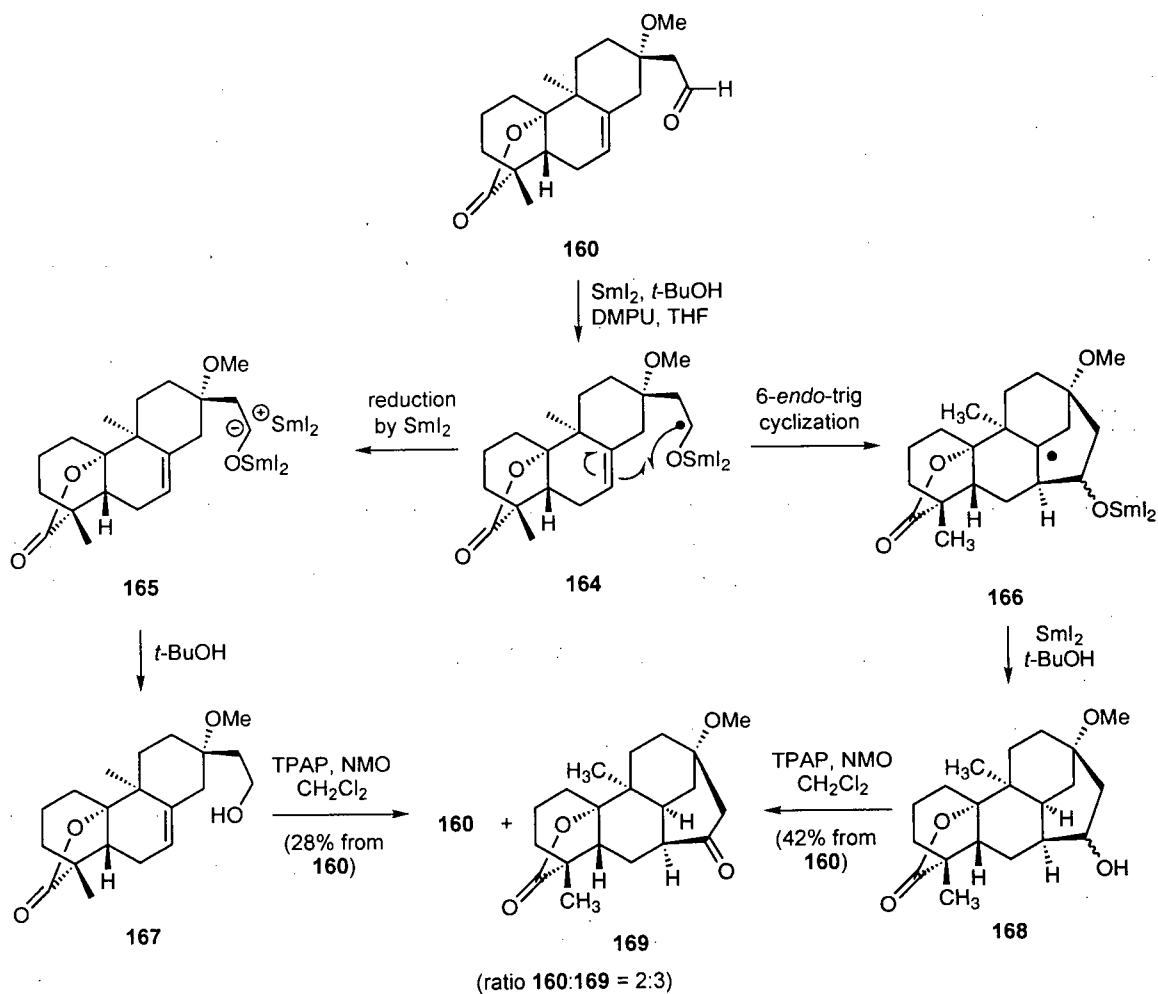
Scheme 2.25. SmI$_2$ promoted ketyl radical – olefin coupling.

Analysis of spectroscopic data collected from the ketyl radical cyclization product was in agreement with the assigned structure. The IR spectrum of **169** included two C=O stretching absorptions at 1766 (γ-lactone) and 1702 (ketone) cm^{-1}. The ^{1}H NMR spectrum of **169** displayed a 3-proton singlet at δ 3.25 and two 1-proton doublets at δ 2.58 and 2.49 corresponding to the methyl ether and the diastereotopic α-keto methylene protons, respectively. The ^{13}C NMR spectrum included two carbonyl resonances at δ 209.9 and 180.5. While this data certainly

agrees with the proposed structure of the tetracyclic ketone 169, it remained to verify the structure of this substance in an unambiguous fashion. To this end, the vinyl radical cyclization product 141, whose structure had been confirmed by X-ray analysis (*vide supra*), was transformed into the tetracyclic ketone 169 in a straightforward manner. Thus, conversion of the tertiary alcohol 141 into the corresponding methyl ether 170 was followed directly by a ruthenium dioxide catalyzed oxidative cleavage of the exocyclic olefin function, providing the ketone 169 in moderate yield (eq. 28). The spectroscopic data acquired from this material was in complete agreement with that reported for the major product from the ketyl radical cyclization – Ley oxidation reaction sequence (Scheme 2.25), confirming the structure of the latter material as that shown.

(28)
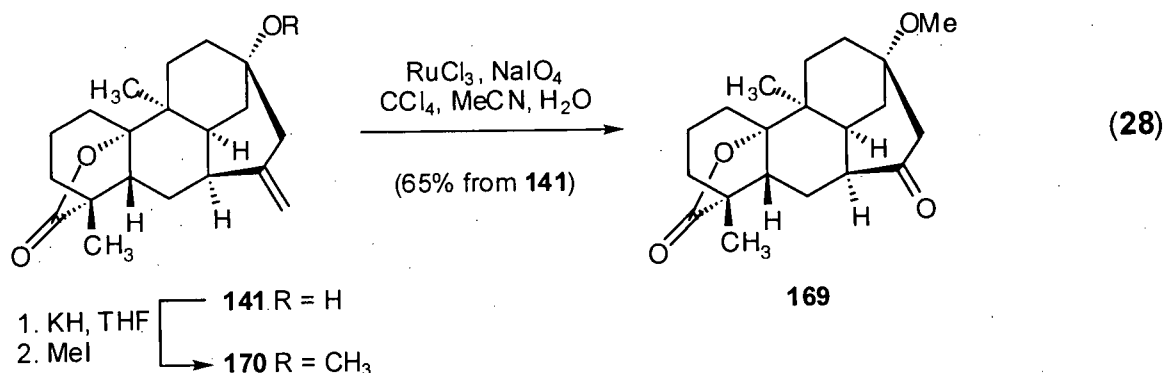
While useless in the context of a synthesis of (±)-13-methoxy-15-oxozoaptlin (22), that the ketyl radical 164 had cyclized exclusively via a 6-*endo*-trig mechanism warrants some explanation. Obviously, from a thermodynamic perspective, the production of the desired tetracyclic lactone 172 is grossly disfavored (*vide supra*). However, the inherent propensity of such cyclizations to yield the kinetic, or 5-*exo*-trig product was anticipated to be the governing factor in this process.[72] Analysis of the relevant 5-*exo*-trig and 6-*endo*-trig transition states for the ketyl radical cyclization was useful in rationalizing the exclusive production of 168.

A pertinent stereoelectronic feature of SmI_2 promoted 5-*exo*-trig ketyl radical - olefin coupling reactions is their inherent preference to proceed via chair-like transition structures that include an anti relationship between the ketyl oxygen and the reacting olefin.[81] Additionally, the trajectory of approach of the carbon-centered radical to the alkene is predicted to be close to 109°.[72] As depicted in Scheme 2.26, two possible transition structures exist that would provide the desired bicyclo[3.2.1]octane fragment. In **171A** the ketyl oxygen adopts an anti relationship to the endocyclic olefin. However, the pseudoaxial orientation of the ketyl oxygen in **171A** leads to severe steric interactions between this function and the axial proton at C-4. Alternatively, in the transition structure **171B** the ketyl oxygen is pseudoequatorially oriented. However, electronic repulsion between this group and the π-system of the olefin destabilizes this transient species. In contrast to **171A** and **171B**, the transition structures **173A** and **173B** that lead to the experimentally observed 6-*endo*-trig product **168** are favorably oriented to react with the endocyclic olefin. In particular, the chair-like transition structure **173A** accommodates the ketyl oxygen in a pseudoequatorial orientation with respect to the developing 6-membered ring, which minimizes non-bonded interactions, and anti to the alkene function, minimizing electronic repulsions. Moreover, while radical reactions proceed via an early transition state with an unusually long forming carbon - carbon bond (> 2.0 Å),[72] the angle strain accompanying a 109° approach vector in the 5-*exo*-trig transition structures **171A** and **171B** is significantly reduced in those of the 6-*endo*-trig process.
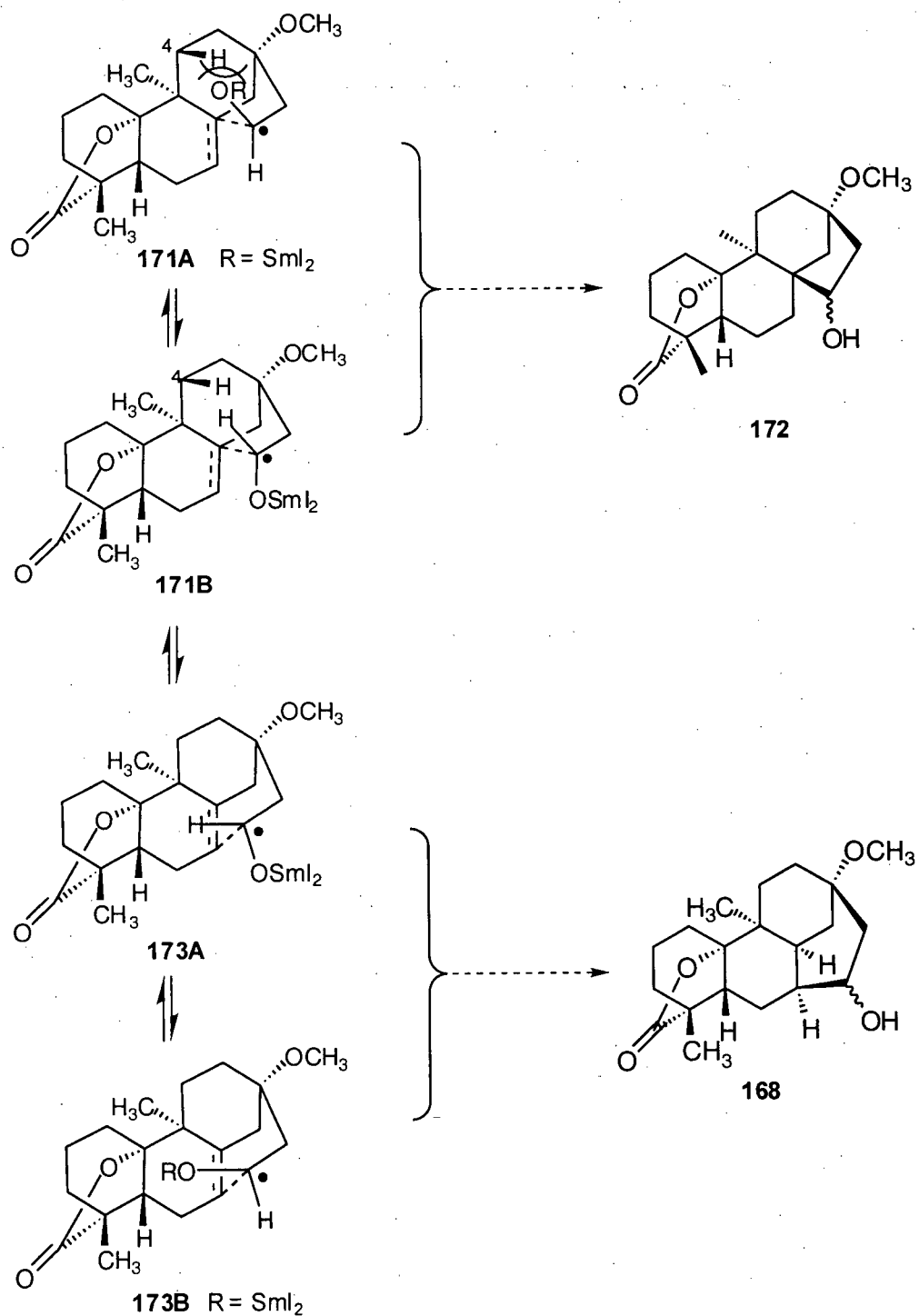
Scheme 2.26. Relevant transition structures for the ketyl radical – olefin coupling.

Having established that the 6-*endo*-trig radical cyclization is indeed a viable process for the ketyl radical cyclization, analysis of the relevant transition structures that led to a similar outcome in the vinyl radical cyclization described in Scheme 2.24 was justified. As portrayed in Scheme 2.27, the transition structure **175** that would provide the desired bicyclo[3.2.1]octane unit suffers from considerable steric interactions between the angular proton at C-8a and the *trans* proton of the terminal olefin. Again, a considerable amount of angle strain in **175** will further serve to retard the 5-*exo*-trig radical cyclization. In contrast, the transition structure **176** that leads to the tetracyclic lactone **141** includes the forming 6-membered ring in a chair-like conformation, minimizing steric interactions.
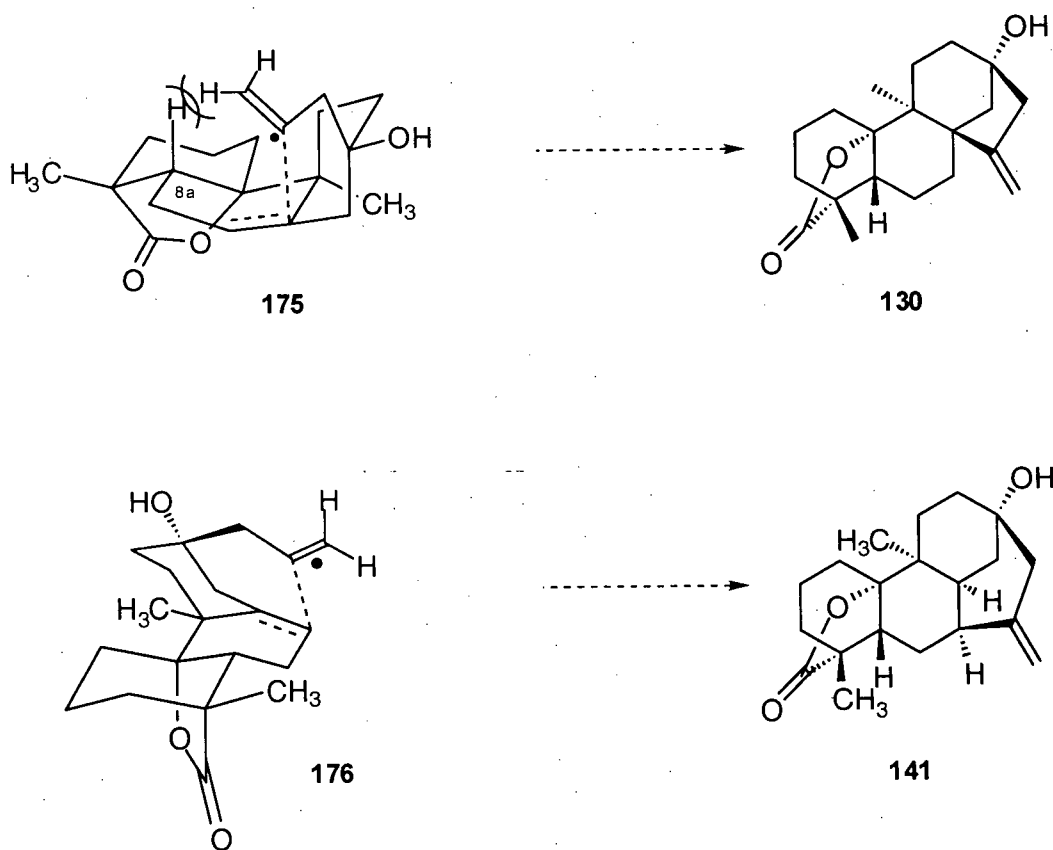
Scheme 2.27. Relevant transition state structures for the vinyl radical cyclization.

It can be surmised then, that in the radical cyclizations involving the tricyclic lactones **129** and **160**, a combination of steric congestion and severe angle strain impede the 5-*exo*-trig process such that the kinetic products from these reactions are those that arise from a 6-*endo*-trig cyclization. Furthermore, while radical cyclizations typically occur via early, reactant-like transition states, a slight pyrimidization of the endocyclic olefinic carbons is expected.[72] Thus, the transition structures leading to the 5-*exo*-trig (**130** and **161**) and 6-*endo*-trig (**141** and **162**) adducts will likely have some sense of the severe energetic disparity that exists between these products, further impeding the 5-*exo*-trig process.

129   **160**
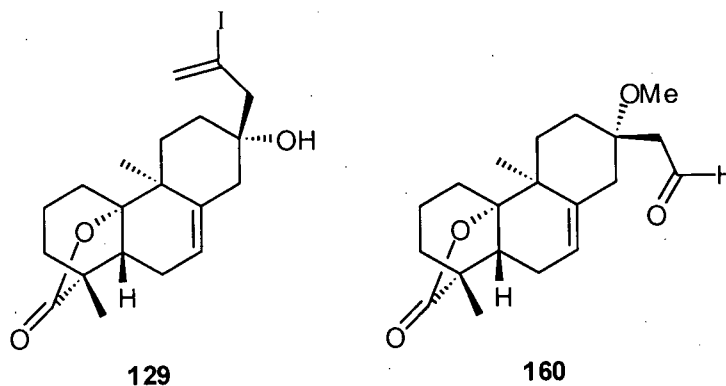
Having secured five of the six requisite stereocenters of (±)-13-methoxy-15-oxozoaptlin (**22**) in a highly efficient manner the disappointment experienced from our failure in the construction of the bicyclo[3.2.1]octane fragment was transient. The formation of carbon - carbon bonds represents a cornerstone in organic synthesis and consequently there are a number of procedures by which the coupling of the vinyl iodide and endocyclic olefin moieties in **129** could be effected in the desired fashion. The following section describes our eventual success in the construction of the bicyclo[3.2.1]octane moiety of **22**.

2.3.7 Application of an intramolecular Heck reaction to the construction of the tetracyclic core of (±)-13-methoxy-15-oxozoapatlin (22)

The Pd(0) catalyzed coupling of alkenyl and arylhalides with alkenes, or the Heck reaction, has become a indispensable method to effect carbon - carbon bond formations in a regio- and stereoselective manner. A number of recent reports have highlighted the utility of this process in regards to the construction of quaternary carbon centers[87,88] and the synthesis of complex natural products.[89,90,91] Although, with respect to an approach towards a synthesis of (±)-13-methoxy-15-oxozoapatlin (22), the 5-*exo*-trig radical cyclization had been a notable failure, it seemed reasonable to propose that a Heck reaction involving the vinyl iodide 129, or a suitable derivative thereof, could yield access to the desired bicyclo[3.2.1]octane portion of the target compound.

The mechanism generally accepted for the Heck coupling process is presented in Scheme 2.28.[91] Thus, the *in situ* generation of a coordinatively unsaturated Pd(0) species, typically from loss of two phosphine ligands from Pd(PPh$_3$)$_4$ or the reduction of palladium(II) salts by the reaction medium, initiates the catalytic cycle. The alkenyl halide 177 then oxidatively adds to this Pd(0) species, generating the *cis*-σ-alkenylpalladium(II) intermediate 178, which rapidly isomerizes to the corresponding *trans*-σ-alkenylpalladium(II) complex 179. Following the elimination of a phosphine ligand, an alkene molecule coordinates to the Pd(II) complex and adopts the necessary *cis* orientation for insertion into the σ-alkenyl carbon - palladium(II) bond (e.g. 180). A migratory *syn* insertion then occurs, presumably via the four-center transition structure 181, providing the σ-alkylpalladium complex 182. An internal rotation then affords the σ-alkylpalladium complex 183, which undergoes reaction-terminating *syn* β-hydride elimination

to afford the diene **184**. Additionally, a reductive elimination of HX from the Pd(II) complex

regenerates the catalytically active Pd(0) species.
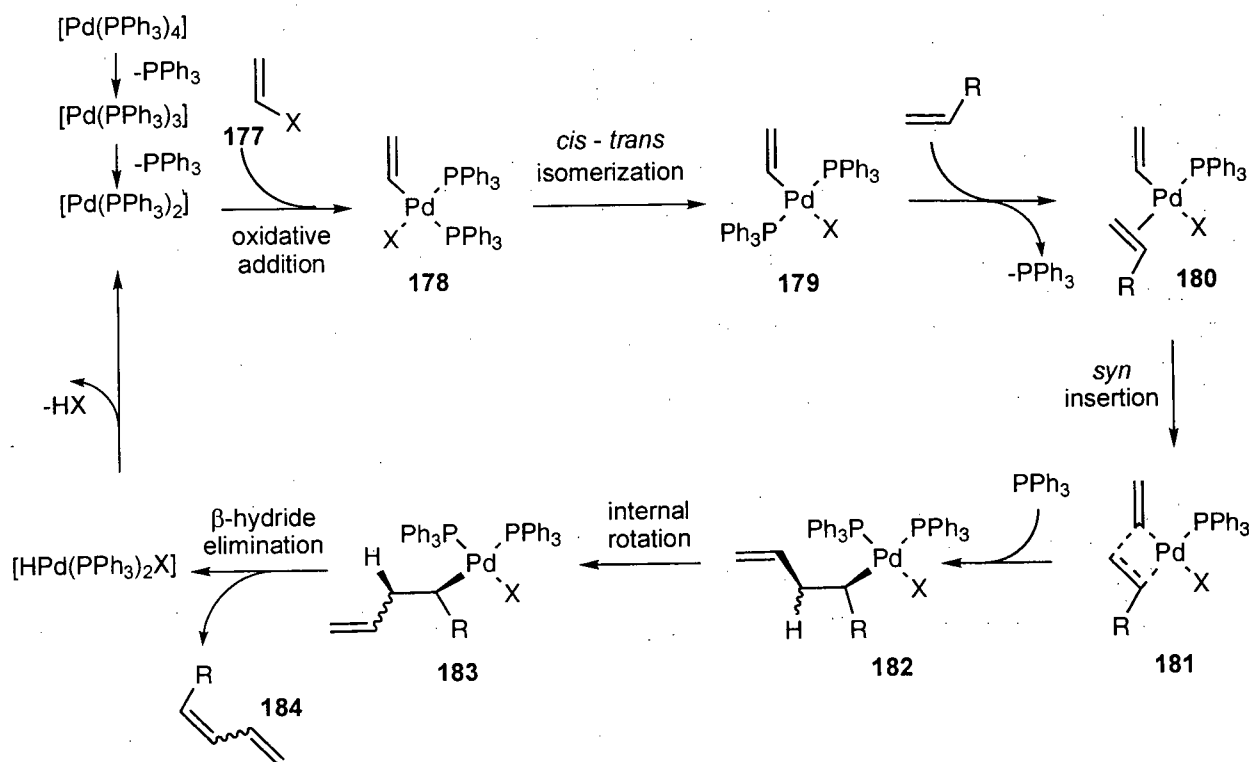
Scheme 2.28. Catalytic cycle for the Pd(0) catalyzed Heck reaction.

Although the events detailed in Scheme 2.28 generally provide the desired dienes in exceptional yield, Negishi and co-workers have reported rearrangements, similar in nature to those discussed above for the vinyl radical cyclizations, in the analogous intramolecular Heck cyclizations.[92] These researchers proposed that a rearrangement involving the (cyclopropyl-carbinyl)palladium intermediate **188** could be responsible for the apparent 6-*endo* mode cyclization of the vinyl iodide **185**. Thus, an initial 5-*exo*-mode carbopalladation provides the cyclopentyl palladium species **187**, which is incapable of undergoing β-hydride elimination and,

consequently, rearranges to **188**. Grigg and co-workers have managed to trap a similar

(cyclopropylcarbinyl)palladium intermediate with hydride, further supporting this proposal.[93]

The cyclopropylcarbinyl to homoallyl rearrangement is a facile process, requiring the *syn-*

coplanar arrangement of the C-Pd bond and the participating cyclopropane C-C bond, that

provides, after β-hydride elimination, the apparent 6-*endo*-trig cyclization product **190**. While a

similar rearrangement was of obvious concern in the vinyl radical cyclization of **129** (*vide*

supra), from molecular models it was clear that this process was not a viable alternative in the

corresponding Heck cyclization.
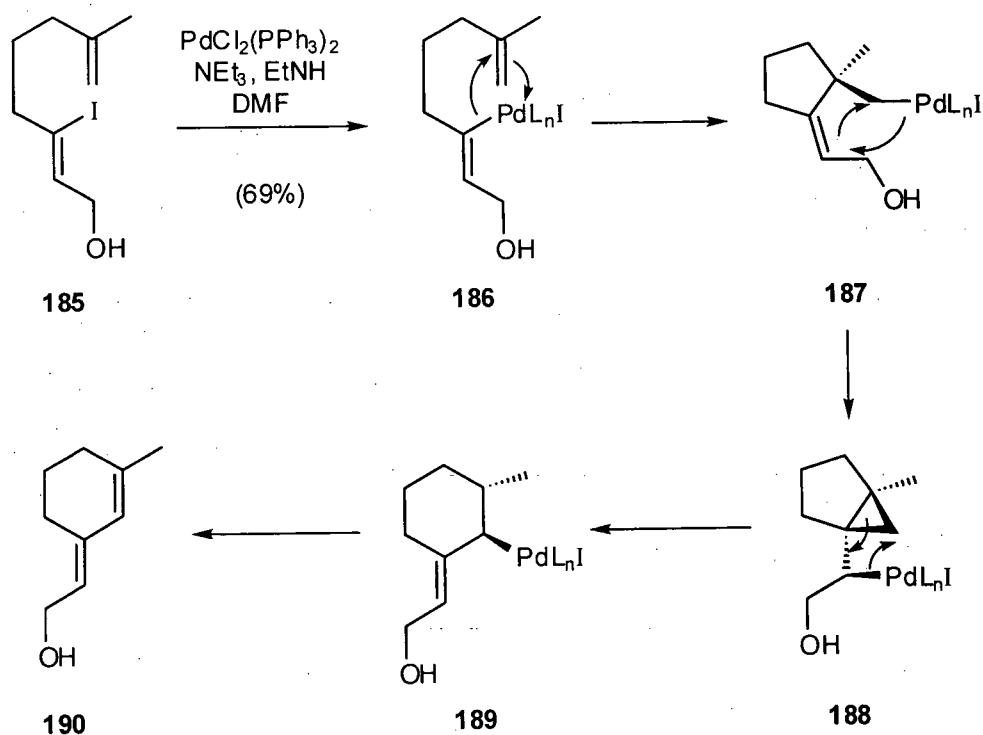
Scheme 2.29. Rearrangements in 5-*exo*-trig Heck cyclizations.

As depicted in Scheme 2.30, the anticipated 5-*exo*-trig Heck reaction involving the vinyl

iodide **129**, while certainly entailing a great deal of ring strain, would not have to contend with

the rearrangements discussed above. Insertion of the catalytically active Pd(0) complex into the

carbon - iodide bond should be followed by an intramolecular carbopalladation, providing the alkyl palladium intermediate **192**. The palladium(II) function in this intermediate is ideally situated to undergo β-hydride elimination to afford the diene **193**. Alternatively, a rearrangement of the alkyl palladium(II) species **192** would provide the (cyclopropylcarbinyl)palladium intermediate **194** and consecutively the corresponding 6-*endo* alkyl palladium(II) intermediate **195**. Fortunately, while the latter intermediate is in principle capable of undergoing a *syn* β-hydride elimination, the resultant bridgehead olefin, while not in violation of Bredt's rule,[50] would certainly entail a tremendous amount of ring strain. Additionally, such gross steric interactions exist between the angular palladium complex and the surrounding elements that the rearrangement process (**192 → 195**) is a highly unlikely event.
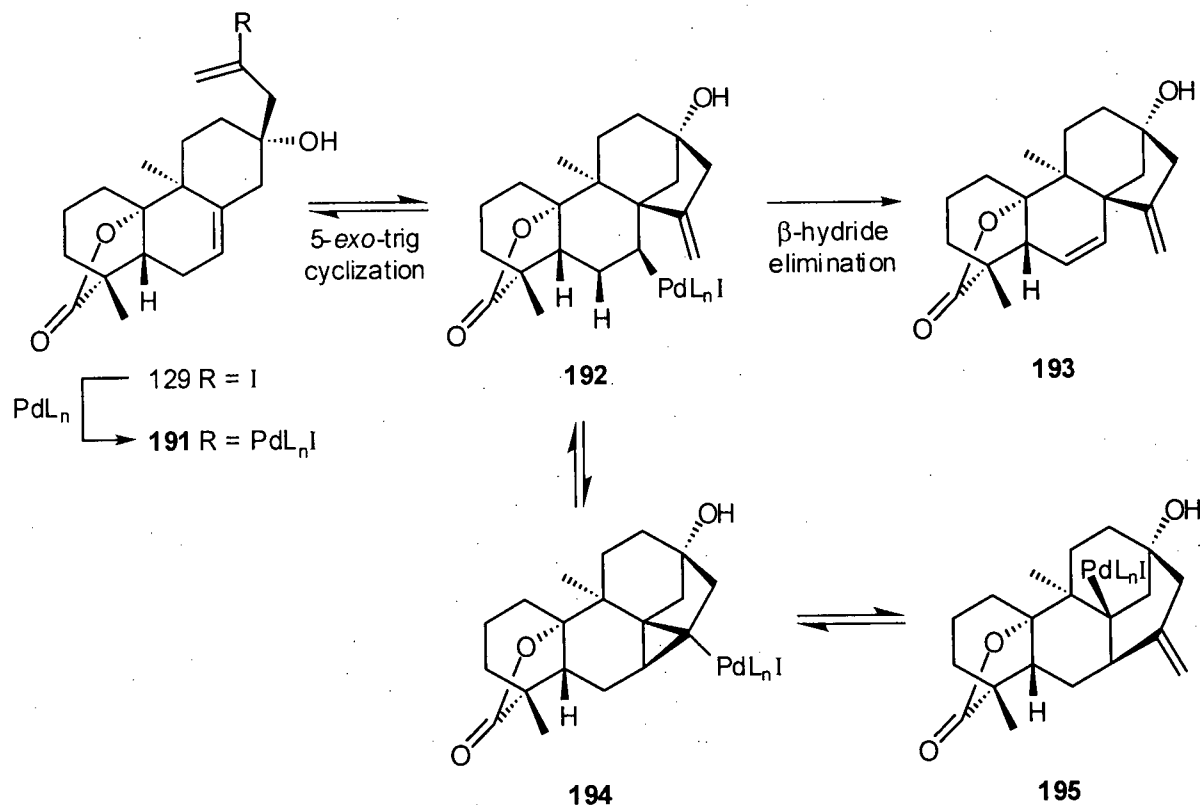
Scheme 2.30. Mechanistic analysis of the proposed Heck cyclization.

Our initial efforts towards the practical application of the Heck cyclization discussed above were fraught with disappointment. Indeed, after much experimentation, the anticipated reaction yielded only complex mixtures of products including insoluble (decomposition) material that was not investigated further. Employing different solvents (THF, MeCN, DMA), bases (Ag_2CO_3, Et_3N) or palladium sources [$Pd(PPh_3)_4$, $Pd(OAc)_2$, $Pd(dppf)_2$, $Pd(dba)_2$] had little effect on these unsatisfactory results. Although purification and consequently full characterization of the individual components of the mixtures recovered from these reactions was not possible, analysis of the spectroscopic data collected on the crude reaction mixtures themselves indicated the presence of monomeric and/or dimeric palladium complexes. That the alcohol function in **191** is ideally situated to form a complex with palladium(II), supports a process whereby the stable alkenylpalladium(II) intermediate **196** interferes with or impedes the progress of the desired cyclization reaction (eq. 29).[94]

(29)
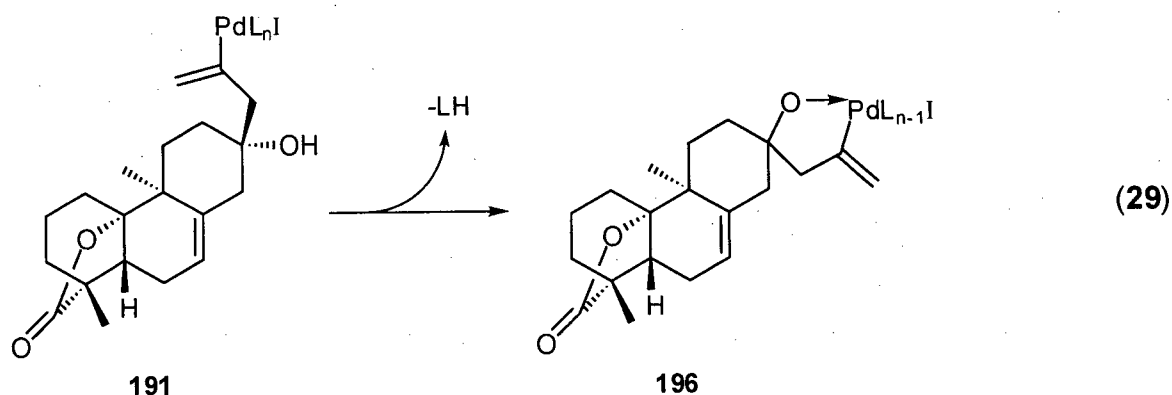
While clearly detrimental to the proposed Heck cyclization, the production of a stabilized Pd(II) complex such as **196** can easily be eliminated through the protection of the tertiary alcohol function in **129**. Conversion of the tertiary alcohol into a methyl ether represents a necessary transformation in the total synthesis of (±)-13-methoxy-15-oxozoapatlin (**22**). However, it was anticipated that a bulky protecting group might serve well in avoiding the formation of stable

alkenyl palladium intermediates. Additionally, it was envisaged that the steric encumberment provided by such a protecting group would, upon insertion of Pd(0) into the alkenyl iodide bond, force the alkenylpalladium moiety into closer proximity with the endocyclic double bond, thus facilitating the desired Heck reaction. To this end, the conversion of the tertiary alcohol **129** into the triethylsilyl (TES) ether **197** was effected smoothly by the addition of TESOTf to a cold solution of **129** and Et_3N in CH_2Cl_2 (eq. 30). The IR spectrum of **197** exhibited a C=O stretching absorption at 1771 cm^{-1} that could be attributed to the γ-lactone carbonyl. The absence of an O-H absorption, observed in the IR spectrum of the tertiary alcohol **129**, indicated that a successful protection of this function had occurred. The ^1H NMR spectrum of **197** included three olefinic proton resonances at δ 6.16, 5.92 and 5.38, which by analysis of coupling constants were assigned to the two terminal olefin protons and the endocyclic olefinic methine proton, respectively. Additionally, the ^1H NMR spectrum displayed a 9-proton triplet at δ 0.95 and a 6-proton quartet at 0.61 characteristic of the triethylsilyl group. The ^{13}C NMR spectrum included a single carbonyl carbon resonance at δ 180.2, which was assigned to the γ-lactone carbonyl, and four olefinic carbon resonances at δ 138.6, 130.3, 119.4 and 103.0. The latter of these olefinic carbon resonances is significantly shielded and is characteristic of an alkenyl iodide carbon. The ^{13}C NMR spectrum also included two carbon resonances at δ 7.2 and 6.9 that, by analysis of an APT experiment performed on this material, corresponded to the methyl and methylene, respectively, of the triethylsilyl group.

(30)
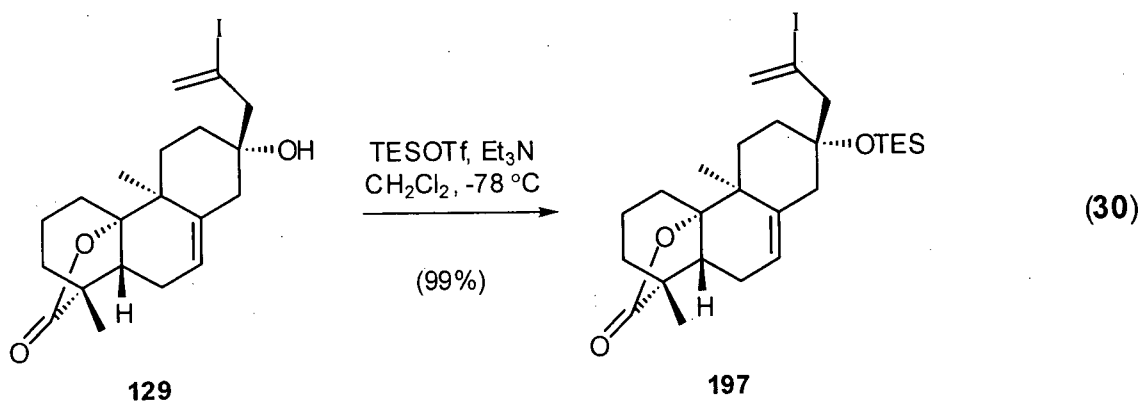
With the triethylsilyl ether **197** in hand, attempts were made to effect the desired Pd(0)

catalyzed 5-*exo*-trig cyclization. Curiously, upon exposure of **197** to standard Heck reaction

conditions[91] (Pd(OAc)$_2$, PPh$_3$, Et$_3$N, MeCN) spectroscopic analysis of the major product, and

indeed the only compound isolated from the reaction mixture, indicated this substance was again

a stable palladium(II) intermediate, ligated with triphenylphosphine. Gratifyingly, after some

experimentation it could be shown that *phosphine free*[95] reaction conditions promoted the desired

5-*exo*-trig cyclization, providing the diene **198**, albeit in low isolated yields (approximately

40%). Analysis of spectroscopic data collected on the two major side products that accompanied

198 identified these substances as the $\Delta^{5,6}$ isomer **200** and the vinyl acetate **199** (eq. 31).

(31)

[ratio **198**:**199**:**200** = 2:1:1]
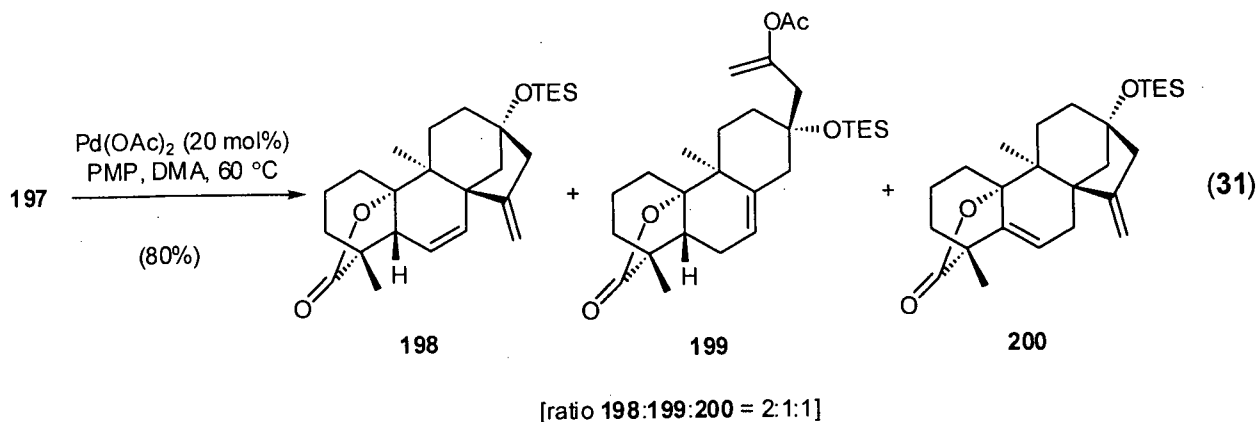
Thin layer chromatographic (TLC) analysis of aliquots removed from the reaction mixture established a direct correlation between the temperature of the reaction and the degree to which the isomerization of **198** into **200** had occurred. Indeed, when the reaction was repeated at 100 °C, these substances were isolated in nearly identical yields. As indicated from molecular models, the isomerization of **198** to the $\Delta^{5,6}$ isomer **200** results in eradication of steric interactions between the angular proton at C-10 and the *cis*-proton of the exocyclic olefin in the former material (Scheme 2.31). Thus, it might be reasoned that upon elimination of HPdI from the intermediate **192**, palladium hydride adds in a non-regioselective manner to the newly formed olefin function in the diene **198**.[89] Such a process would result in the reformation of the alkylpalladium (II) species **192** or the structural isomer **201**. β-Hydride elimination involving **201** would result in overall isomerization of the endocyclic olefin.

The isolation of the vinyl acetate **199** from this process was slightly more peculiar and indicated that, to some extent, acetate is capable of adding to the initially formed alkenylpalladium(II) intermediate and inserting into the σ-alkenyl carbon – palladium(II) bond. While precedent certainly exists for Pd(0) catalyzed carbon – oxygen bond formation,[96,97] and the synthesis of vinyl acetate from ethylene and Pd(OAc)$_2$ in acetic acid is a well known reaction,[98] the competition of this process with the intramolecular Heck reaction was unanticipated. The mere occurrence of the vinyl acetate **199** as a byproduct from this reaction highlights the degree to which ring strain and steric interactions disfavor the desired cyclization.
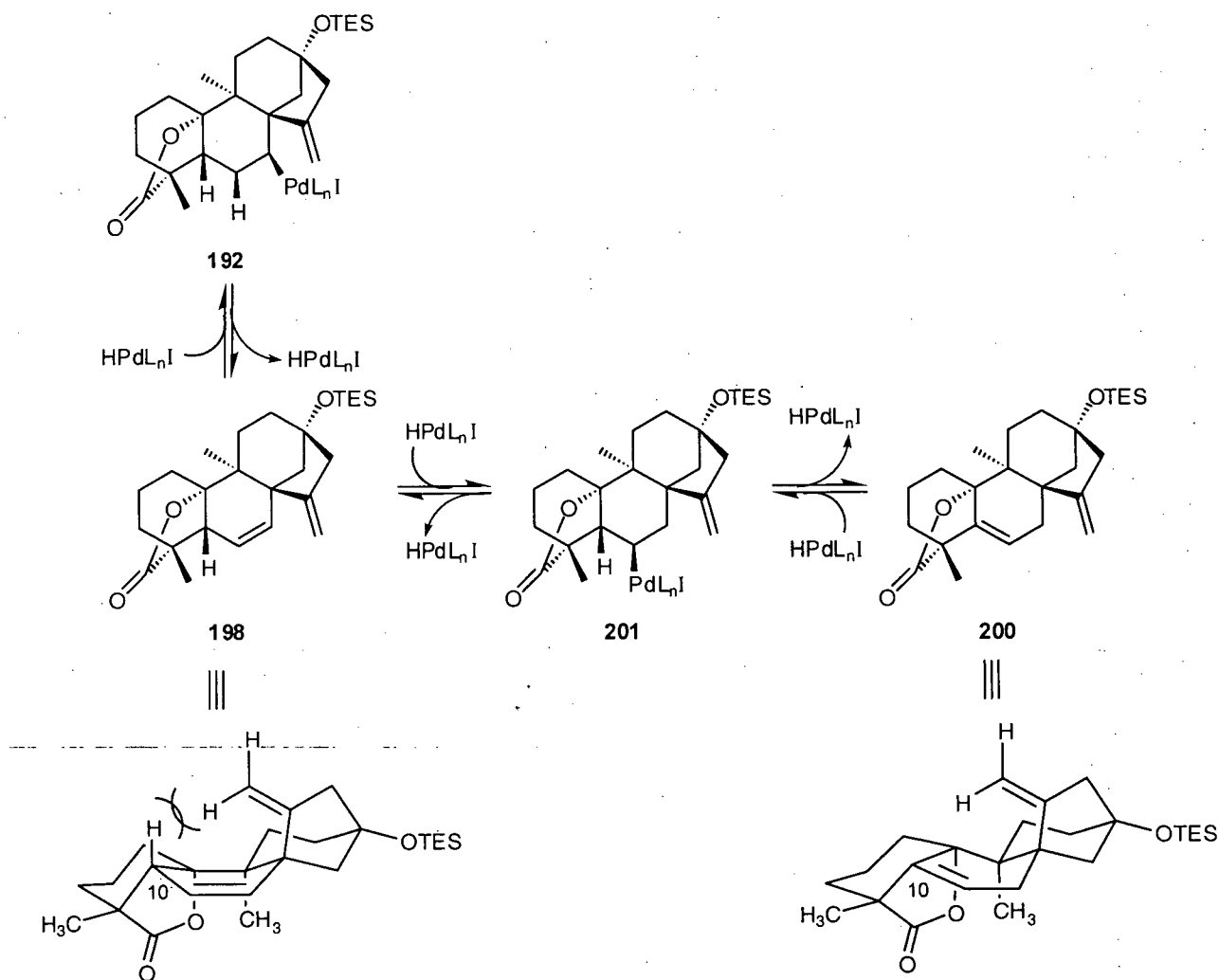
Scheme 2.31. Olefin isomerization in the Heck reaction.

It was fortuitous to discover then, that when the reaction was carried out in refluxing THF, no trace of the byproduct **199**, arising from the acetate coupling process, was observed. Additionally, it could be shown that treatment of the vinyl iodide **197** with a stoichiometric amount of the Pd(0) mediator resulted in rapid consumption of **197**, with little or no isomerization. Thus, although stoichiometric quantities of Pd(OAc)$_2$ were required,[99] these

conditions consistently transformed the vinyl iodide **197** into the diene **198** in good yield (70 –

80%) (eq. 32).

$$(32)$$
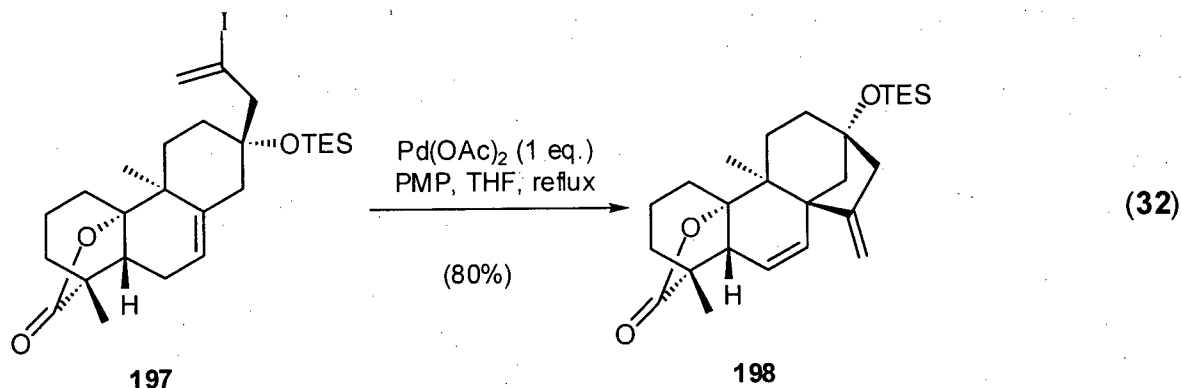
The spectroscopic data exhibited by the diene **198** was consistent with the assigned

structure. The IR spectrum of this material included a single C=O stretching absorption at 1764

cm^{-1}, consistent with the γ-lactone carbonyl. The ^{1}H NMR spectrum of **198** displayed two

doublets of doublets at δ 5.91 and 5.77 corresponding to the olefinic protons at C-11 and C-12

(Figure 2.8). The protons on C-11 and C-12 share a common coupling constant (J = 9.7 Hz), as

well as individual vicinal and allylic couplings with H-10, J = 1.7 and 3.3 Hz, respectively. The

^{1}H NMR spectrum of this material also included two terminal olefinic proton resonances, which

overlap at δ 4.84, and two proton resonances at δ 2.50 and 2.33 that share a geminal coupling

constant (J = 16.3 Hz) and were assigned to the allylic methylene protons (H-15). The ^{13}C NMR

spectrum of **198** displayed a single carbonyl carbon resonance at δ 179.6 and four olefinic carbon

resonances at 148.2, 138.0, 123.4 and 108.7. In order to confirm the structure of the diene in an

unambiguous manner, a suite of spectroscopic experiments (HMQC, HMBC, COSY, APT, 1D

NOESY) was performed on this material. Analysis of the results from these experiments allowed

for the complete assignment of all proton and carbon resonances of **198** (Tables 2.11 and 2.12,

Experimental). Two three-bond H-C correlations in the HMBC spectrum between H-12 and C-

14 and H-17 and C-13 were particularly useful in determining the structure of this material. Additionally, a strong NOE between H-17 and H-10 confirmed the propinquity of these protons (Figure 2.8).
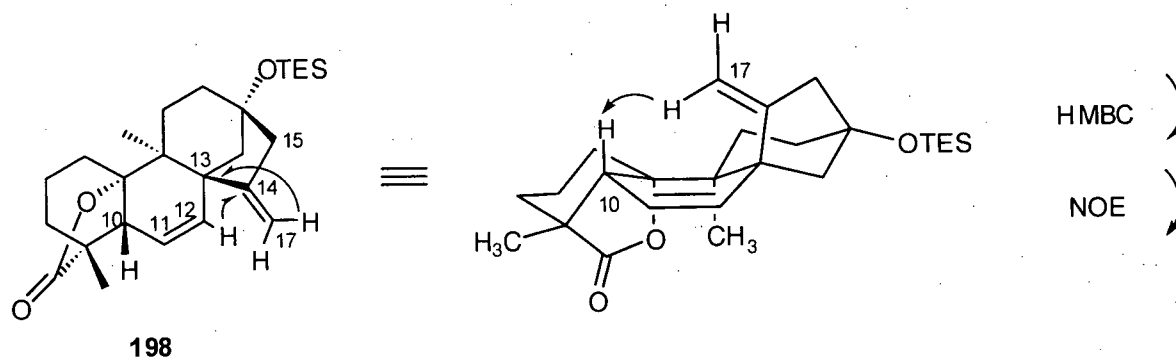
Figure 2.8. Key NOE and HMBC correlations for the diene **198**.

2.3.8 Completion of the synthesis of (±)-13-methoxy-15-oxozoapatlin (22)

With the tetracyclic lactone **198** in hand, it had been anticipated that the exocyclic methylidene function would be easily converted into the requisite ketone function by oxidative cleavage. However, it was soon found that, owing to the strong steric shielding at each π-face, the olefinic functions in **198** were particularly resistant to attack by various OsO$_4$ reagents. As depicted in Figure 2.9, the endocyclic olefin is effectively blocked from reacting on the α-face by the angular methyl at C-4 and the β-face by the exocyclic olefin. Additionally, the α-face of the exocyclic olefin is shielded from approach of OsO$_4$ by the axial protons at C-3 and C-6. While it had been expected that the exocyclic olefin would undergo facile oxidative cleavage from the β-face, structural analysis of the corresponding osmate ester intermediate indicated

severe steric interactions would exist between the methylene protons at C-17 and the axial protons at C-3 and C-6.
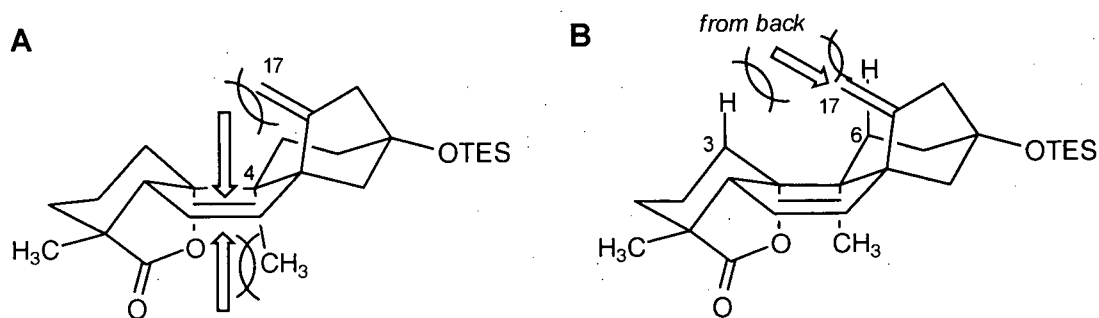
Figure 2.9. Steric hindrance impeding the approach of OsO_4 to the (**A**) endocyclic and (**B**) exocyclic olefin functions in **198**.

While the diene **198** was unreactive towards oxidative cleavage, it could be shown that hydrogenation of this material over palladium-on-carbon proceeded smoothly, providing the tetracyclic olefin **202** (eq. 33). Although the endocyclic alkene was clearly the more reactive of the two olefinic functions in **198** under these reaction conditions, it was necessary to closely monitor the hydrogenation reaction, since a product whose spectral data was consistent with the tetracyclic compound **203** was formed soon after the diene **198** was consumed. Complicating matters further, the diene **198**, the olefin **202** and compound **203** were inseparable on silica gel and, consequently, indistinguishable by TLC analysis. Thus, it was essential to stop the reaction at 15-minute intervals and analyze the crude reaction mixture by ^1H NMR spectroscopy. Due to the fact that the diene **198** and the two hydrogenation products **202** and **203** were chromatographically inseparable (on silica gel), the crude reaction mixture was simply filtered through a plug of silica gel to remove the Pd/C and then was concentrated. The crude material was carried through to the next step without further purification.

$$(33)$$
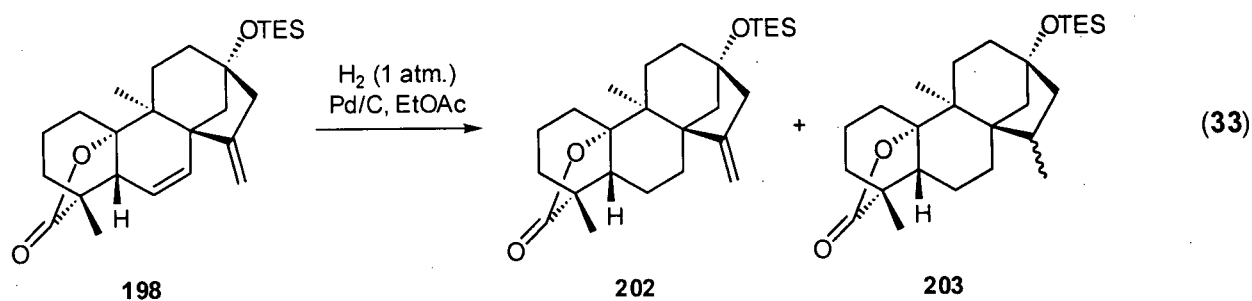
While it was clear from our experience with the diene **198** that the oxidative cleavage of the exocyclic methylene in **202** would prove difficult, chemoselectivity was no longer an issue and, as such, more forcing conditions were applied to effect this transformation. Unfortunately, conditions specifically developed for the oxidative cleavage of hindered olefins[100,101] (OsO_4-pyridine, OsO_4-quinuclidine and OsO_4-DMAP) returned only starting material. Additionally, RuO_4 oxidations[102] led exclusively to an intractable mixture of compounds that were not investigated further. It could be shown, however, that the passage of a mixture of oxygen and ozone through a cold solution of the olefin **202** in CH_2Cl_2 - MeOH,[103] followed by workup with DMS-pyridine, provided a 3:2 mixture of substances, which were readily separated by flash chromatography, in good overall yield from the diene **198** (eq. 34). The spectral data collected from the minor component of the mixture conformed to that expected for the epoxide **204**. Low-resolution mass spectrometric analysis of this material indicated a molecular ion that was consistent with the assigned structure. Additionally, in the ^1H NMR spectrum of **204**, two 1-proton doublets at δ 3.03 and 2.92 (J =3.5 Hz) were diagnostic both in chemical shift and coupling for the expected resonances of the epoxide methylene. The epoxidation of the olefin function in **202** is not surprising as the recovery of epoxides from the ozonolysis of hindered olefins is well documented.[104]

1. O_3, MeOH:CH_2Cl_2 (9:1), -78 °C
2. DMS, pyridine

202 →

(70% from **198**)

204 + **205** + **206**   (34)

[ratio **204:205:206** = 2:0:3]
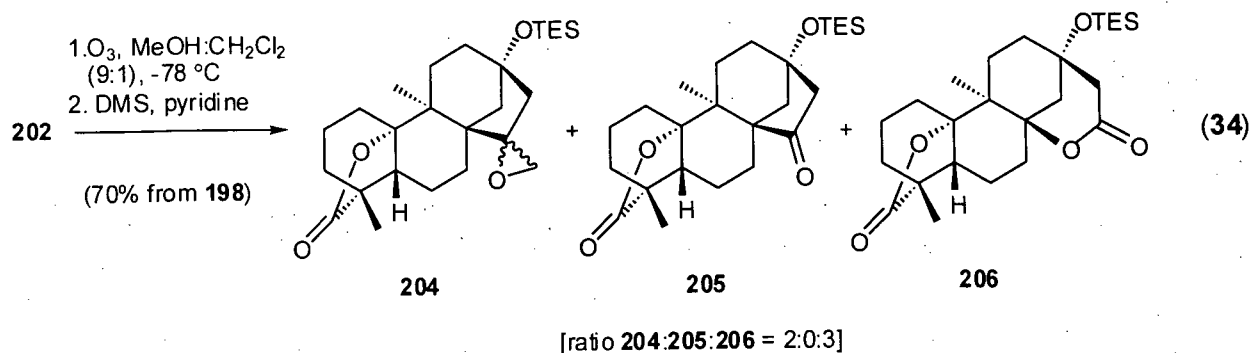
The structure determination of the major product from the reaction was somewhat more difficult. The IR spectrum of this material contained strong C=O absorptions at 1773 and 1728 cm^{-1}. The former C=O stretching absorption could be attributed to the γ-lactone carbonyl and the latter absorption seemed consistent with the ketone carbonyl in **205**. The ^{1}H NMR spectrum of the major product from the ozonolysis was deplete of olefinic proton resonances and included two proton resonances at δ 2.66 and 2.58, characteristic of the α-keto-methylene protons expected for **205**. However, analysis of the ^{13}C NMR spectrum of this material dispelled any notion that the major product from the ozonolysis of **202** was the desired tetracyclic ketone **205**. The ^{13}C NMR spectrum included two carbonyl resonances at δ 180.2 and 170.5, corresponding to the γ-lactone carbonyl carbon and a second lactone or ester carbon. Additionally, the ^{13}C NMR spectrum displayed two resonances typical for acyloxy carbons at δ 87.1 and 86.7 as well as a resonance for the protected tertiary carbinol carbon at δ 69.8. Taken together, this data was suggestive of a structure, such as **206**, that includes both a γ- and δ-lactone. In order to confirm the proposed structure of the bis-lactone **206** in an unambiguous manner, a suite of spectroscopic experiments (HMQC, HMBC, COSY and APT) was performed on this material. Analysis of the results from these experiments allowed for the complete assignment of the proton and carbon resonances in the molecule (Table 2.13, Experimental) and verified that the structure of the major product from the ozonolysis of **202** was in fact **206**.

Although the production of **206** from the ozonolysis of **202** was somewhat surprising,

there is precedent for such rearrangements of ozonides in the literature.[105] A likely scenario for

the production of the bis-lactone **206** involves the rearrangement of a cyclic ozonide intermediate

such as **208**, formed in turn from the fragmentation and recombination of the initially formed

molozonide **207** (eq. 35). That the lactone **206** was isolated as the major product from the

ozonolysis reaction further attests to the ring strain present in the bicyclo[3.2.1]octane portion of

the tetracycle **202** and the thermodynamic incentive to release this strain via a Baeyer-Villiger

type rearrangement.

$$\textbf{202} \xrightarrow{O_3} \textbf{207} \longrightarrow \textbf{208} \longrightarrow \textbf{206} \qquad (35)$$
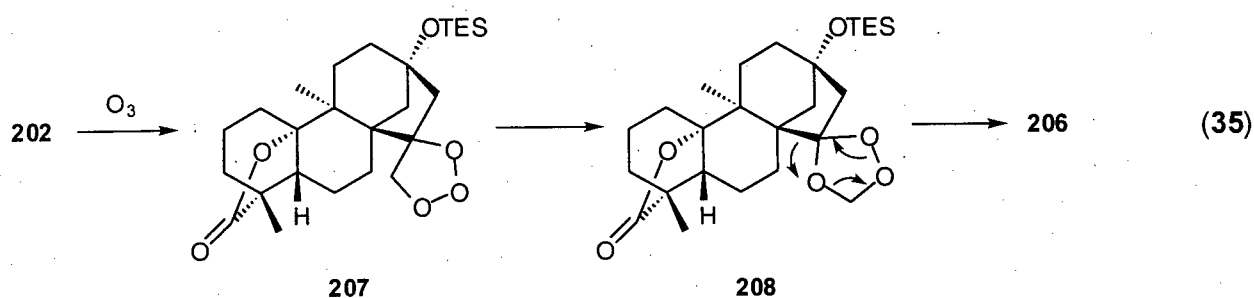
At this point, it was decided to remove the triethylsilyl protecting group and investigate

the oxidative cleavage on the corresponding methyl ether. To this end, treatment of a solution of

the tetracyclic olefin **202** in THF with TBAF smoothly provided the tertiary alcohol **209**. The

hydroxyl function in **209** was then directly converted to the corresponding methyl ether. Thus,

sequential treatment of the crude tetracyclic olefin **209** with KH and MeI provided the methyl

ether **210** in excellent yield (Scheme 2.32). Analysis of the spectroscopic data collected from this

compound was consistent with the assigned structure. The IR spectrum of **210** exhibited a strong

C=O stretching absorption for the γ-lactone carbonyl. The ^{1}H NMR spectrum displayed two

overlapping olefinic proton resonances at δ 4.98 and a 3-proton singlet at δ 3.22 corresponding

to the methyl ether. The ^{13}C NMR spectrum included a carbonyl carbon resonance at δ 180.2,

attributed to the γ-lactone carbonyl, two olefinic carbon resonances at δ 157.3 and 109.4, and a

methoxyl carbon at δ 52.1. Furthermore, an APT experiment performed on this material

confirmed the presence of a total of four methine and methyl carbons.
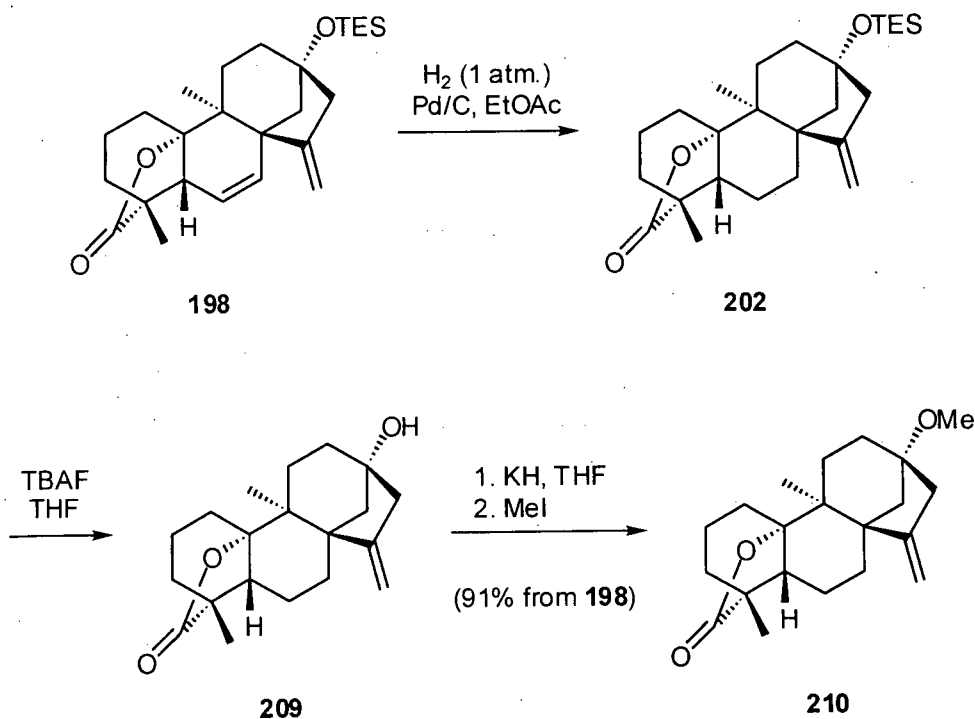
Scheme 2.32. Synthesis of the methyl ether **210**.

With the methyl ether **210** in hand, an investigation of the penultimate step in the total

synthesis of (±)-13-methoxy-15-oxozoapatlin (**22**), that is the oxidative cleavage of the exocyclic

methylidene function, was initiated. Fortunately, treatment of the olefin **210** with a catalytic

amount of $RuCl_3$ and $NaIO_4$ in a mixed solvent system of $MeCN-CCl_4-H_2O^{102}$ provided the

ketone **211** in a high yielding and rapid fashion (eq. 36). Spectroscopic analysis of this material

confirmed the assigned structure. The IR spectrum included two C=O stretching absorptions at

1770 (γ-lactone) and 1733 cm⁻¹ (ketone). The ¹H NMR spectrum of **211** exhibited a 3-proton

singlet for the methyl ether function at δ 3.27. The ¹³C NMR spectrum displayed two carbonyl

carbon resonances at δ 218.8 (ketone) and 180.4 (γ-lactone). Additionally, an APT experiment

carried out on this material verified the correct number of methine and methyl carbon

resonances.

210 → **211** (36)

RuCl₃, NaIO₄
MeCN, CCl₄, H₂O

(78%)
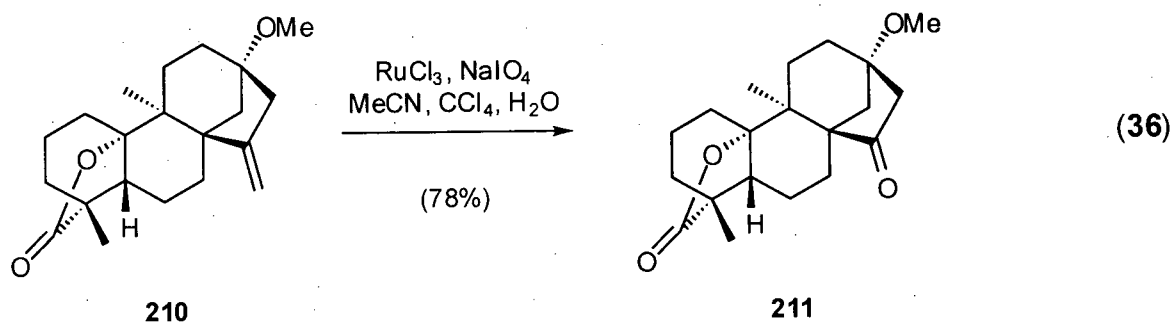
Introduction of the requisite exocyclic methylidene group and, consequently, completion

of the synthesis of (±)-13-methoxy-15-oxozoapatlin (**22**), was achieved in a straightforward

manner.[106] Thus, generation of the potassium enolate of **211** was effected by treatment of this

material with KHMDS. Addition of paraformaldehyde to the enolate thus generated, provided

the primary alcohol **212** which, upon subsequent addition to saturated aqueous NH₄Cl, afforded

(±)-13-methoxy-15-oxozoapatlin (**22**) in moderate yield (eq. 37). The production of **22** was

accompanied by the recovery of a significant amount of starting material. Unfortunately, at this

point, the accessible quantity of the tetracyclic ketone **211** was insufficient to further investigate

and ultimately optimize this final transformation. However, with the recovery of starting material

taken into account the yield for this process was quite acceptable.

The spectral data exhibited by the synthetic material was in complete accordance with

that reported in the literature for (-)-13-methoxy-15-oxozoapatlin (**22**).[20] Additionally, the

spectroscopic data (^{1}H and ^{13}C NMR) acquired from an authentic sample of **22**, isolated from extracts of the South African tree *Parinari curatellifolia* and provided to us by Xin-Hui Huang and Dr. Raymond Andersen, was in agreement with that collected from the synthetic material (Figure 2.10 and 2.11). While the structure of **22** has been unambiguously confirmed by X-ray crystallography,[19] a complete spectroscopic assignment of ^{1}H and ^{13}C NMR resonances for this substance has not been reported. Analysis of HMQC, HMBC and COSY experiments performed on synthetic **22**, allowed for the full assignment of proton and carbon resonances for this molecule (Table 2.14, Experimental).

1. KHMDS, THF
   -78 °C to rt
2. paraformaldehyde

211

212

NH$_4$Cl

22

(37)

(41%, 84% based
on recovered
starting material)
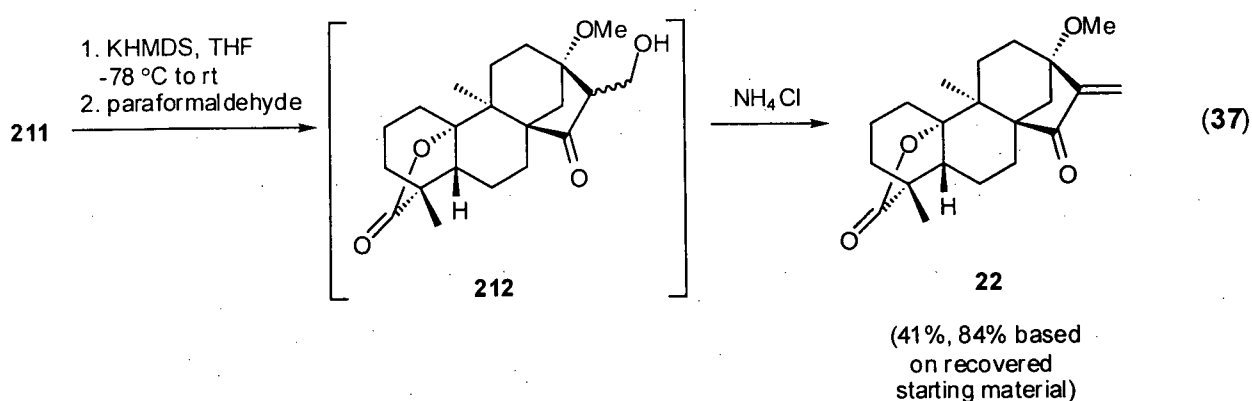
2.4 Conclusions

To the best of our knowledge, the work reported in this chapter constitutes the first total synthesis of the G2 checkpoint inhibitor and antimitotic diterpenoid (±)-13-methoxy-15-oxozoapatlin (**22**) as well as the first synthesis of a structure bearing the zoapatlin (**17**) skeleton. Through the implementation of a linear sequence of 21 consecutive synthetic transformations, a renewable source of this biologically significant compound has ultimately been realized. Additionally, there are a number of points throughout the synthesis where a divergent strategy

could be applied to generate congeners of zoapatlin, thus setting the stage for investigations into the effect of structure on the biological activity of this potentially important family of compounds.

The salient features of this total synthesis of **22** include a Diels-Alder reaction between the diene **93** and methacrolein (**94**), which led to the efficient, diastereoselective construction the A and B rings of **22** and a regioselective iodolactonization that provided the γ-lactone **92** in excellent yield (Scheme 2.33). More prominently, however, was the development of a new annulation sequence for the construction of bicyclo[3.2.1]octanes and the successful application of this methodology to the synthesis of **22**. Thus, addition of the novel bifunctional reagent **139** to the ketone **127** provided the tertiary alcohol **128** as the major diastereomer in good yield. A subsequent intramolecular Heck reaction highlighted the series of transformations that yielded rapid access to the bicyclo[3.2.1]octane portion of the target molecule **22**. This methodology compliments those reported in the literature for the assembly of such structural moieties. The 1,2-addition of the bifunctional reagent **139** to a cyclic ketone permits the inclusion of a bridgehead hydroxyl function in the final bicyclo[3.2.1]octane, a structural necessity in both the zoapatlins and the gibberellins. Furthermore, that this sequence of reactions initiates with the easily accessible β,γ-unsaturated ketone **127** and, through the straightforward transformations described, resulted in construction of the desired *trans*-B-C ring fusion, lends this methodology potentially useful to the synthesis of a great number of biologically significant diterpenoids.
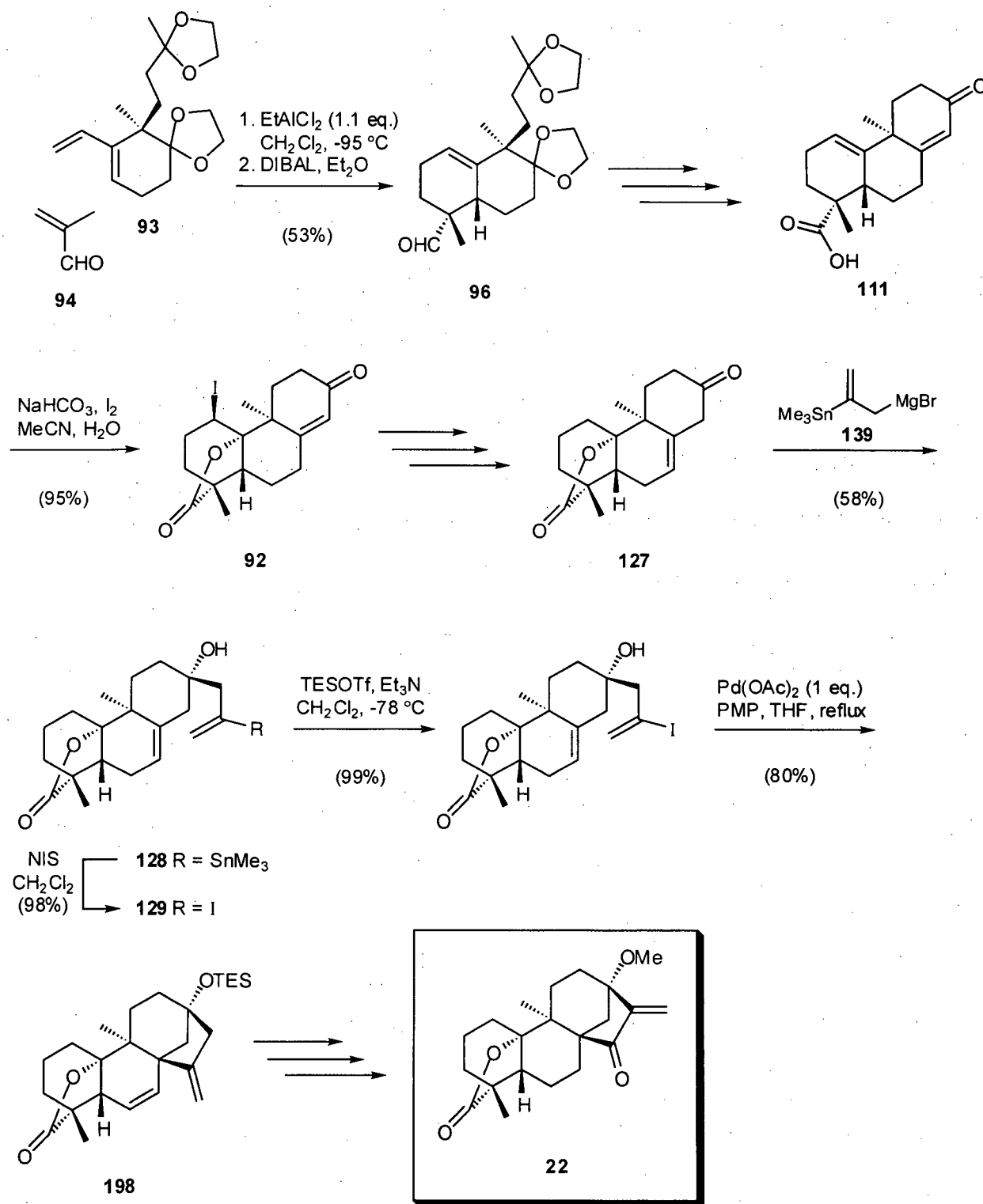
Scheme 2.33. Total synthesis of (±)-13-methoxy-15-oxozoapatlin (**22**).
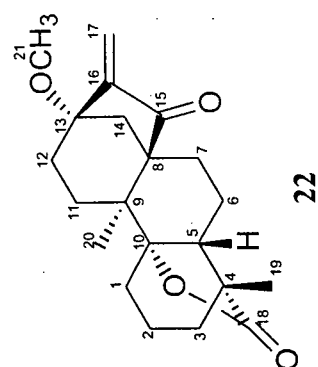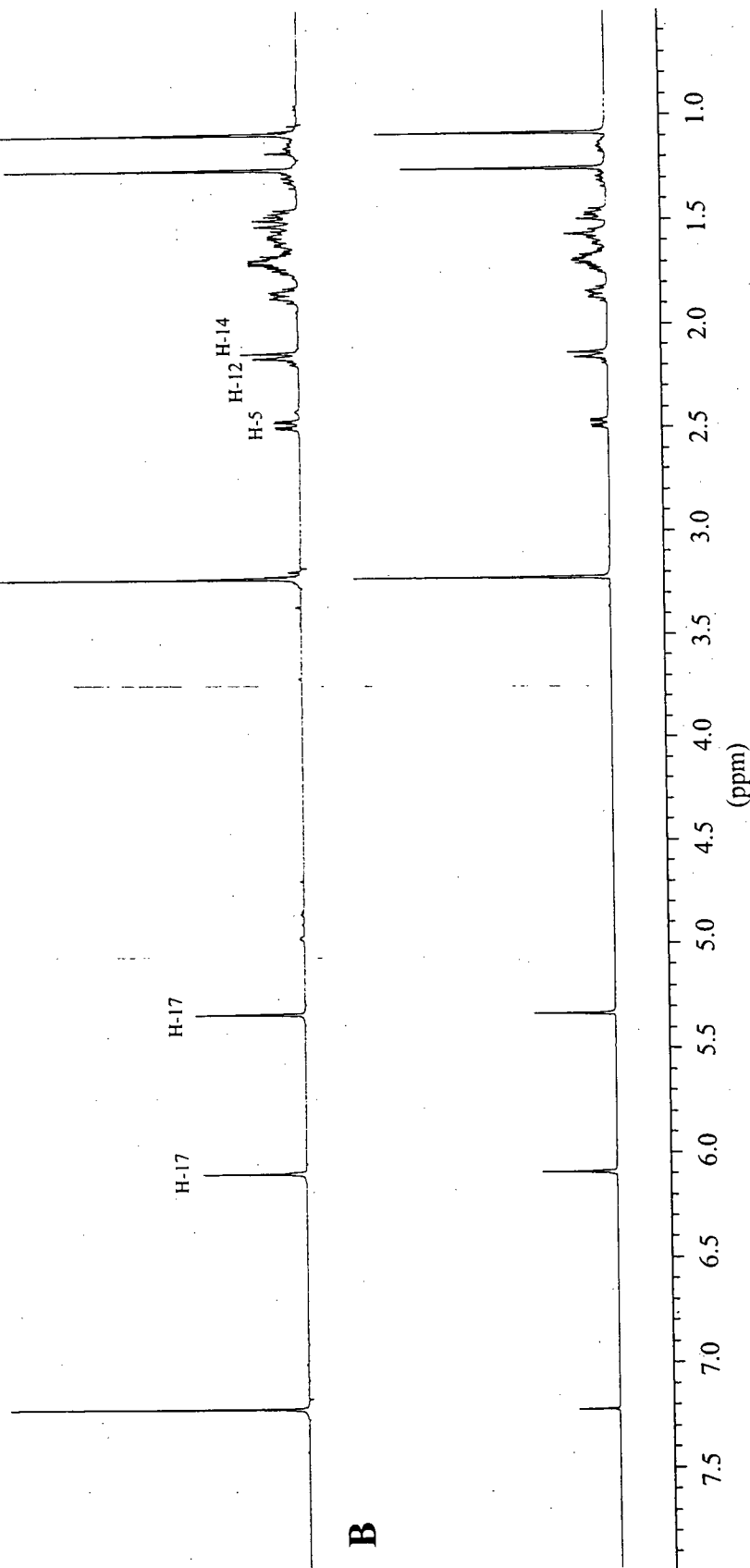
Figure 2.10. ^{1}H NMR spectra of (A) racemic synthetic and (B) natural 13-methoxy-15-oxozoapatlin (**22**) recorded in CDCl$_3$ at 500 MHz.
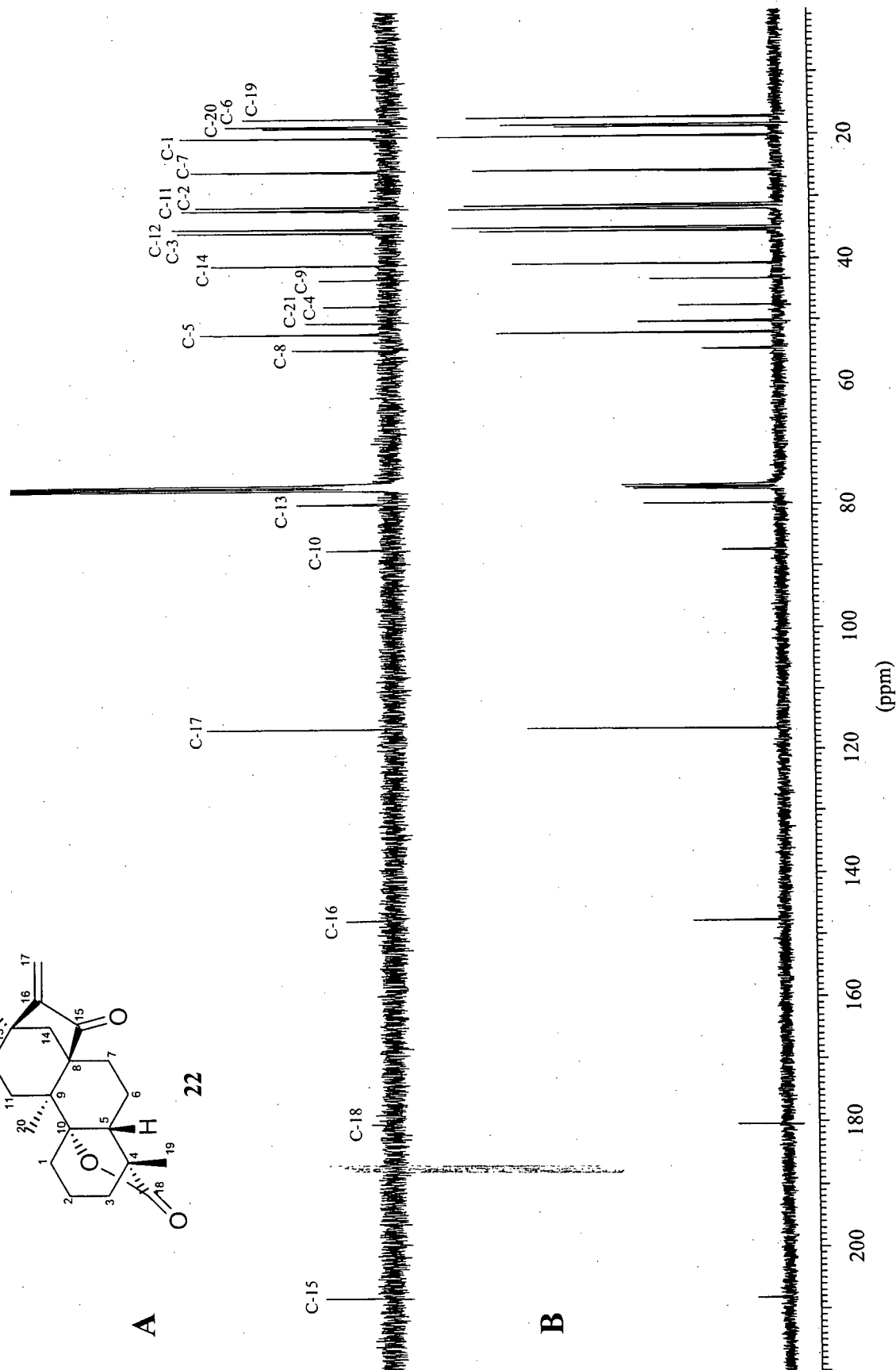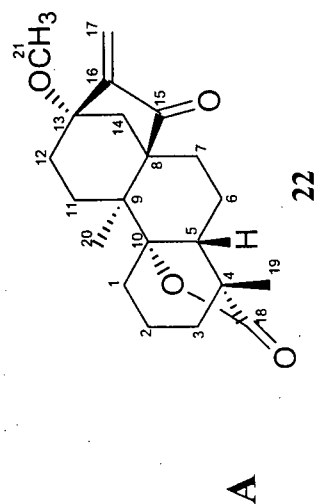
Figure 2.11. ^{13}C NMR spectra of (A) racemic synthetic and (B) natural 13-methoxy-15-oxozoapatlin (**22**) recorded in CDCl$_3$ at 100.5 MHz.

2.5 Experimental

General

All reactions described in this document were performed under an atmosphere of dry argon using glassware that had been thoroughly flame dried or oven (140 °C) dried unless otherwise specified. Glass syringes, stainless steel needles and Teflon® cannulae were used to handle various anhydrous reagents and solvents, and were oven dried and flushed with argon prior to use. For the accurate measurement of sub milliliter volumes of liquid reagents, gas-tight microliter syringes (Hamilton series 1700) were used. Microliter syringes were dried under reduced pressure (vacuum pump) stored in a desiccator and flushed with argon prior to use.

THF was distilled from sodium/benzophenone, Et_2O was distilled from sodium/benzophenone, CH_2Cl_2 was distilled from CaH_2, benzene was distilled from CaH_2, MeOH was distilled from Mg with catalytic I_2 and diisopropylamine was distilled from CaH_2. 'BuOH was sparged with argon for 0.5 h prior to distillation from CaH_2. Commercial EtOH (reagent grade), ethylene glycol (reagent grade), 2,2-dimethyl-1-propanol (reagent grade), Et_3N (anhydrous), DMPU (reagent grade), DMS (reagent grade), 2,2-dimethoxypropane (reagent grade), and pyridine (anhydrous) were used without further purification. MeCN (HPLC grade), acetone (HPLC grade), CCl_4 (HPLC grade), n-propanol (HPLC grade), i-propanol (HPLC grade), n-butanol (HPLC grade), and EtOAc (HPLC grade) were used without further purification. DMSO and DMF were dried sequentially over molecular sieves. Molecular sieves were dried under vacuum with heating (120 °C) for 5 hours prior to use.

Cold temperatures were maintained by the use of the following reaction baths: 0 °C, ice-water; -20 °C, -35 °C, -48 °C, aqueous calcium chloride-dry ice (27, 39, and 47 g $CaCl_2$/100 mL H_2O, respectively)[107]; -78 °C, acetone-dry ice; -98 °C, methanol-liquid nitrogen.

Flash chromatography was carried out with 230-400 mesh silica gel (E. Merck, Silica Gel 60 and Silicycle Silica Gel 230-400 mesh) following the technique described by Still.[108] Gel permeation chromatography was carried out with lipophilic Sephadex LH-20 (Sigma, bead size 25 – 100 μ). High performance liquid chromatography (HPLC) was performed using a Waters 600E Multisolvent Delivery System connected to a Waters 486 tunable Absorbance Detector or a Waters 515 HPLC pump connected to a Waters 2487 Dual λ Absorbance Detector. Thin layer chromatography was carried out on commercial aluminum backed silica gel 60 plates (E. Merck, type 5554, thickness 0.2 mm). Visualization of chromatograms was accomplished using ultraviolet light (254 nm) and/or iodine (iodine which had been adsorbed onto unbound silica gel) followed by heating the plate after staining with one of the following solutions: (a) vanillin in a sufuric acid-EtOH mixture (6% vanillin w/v, 4% sulfuric acid v/v, and 10% water v/v in EtOH); (b) 20% phosphomolybdic acid w/v in EtOH; (c) anisaldehyde in a sulfuric acid-EtOH mixture (5% anisaldehyde v/v and 5% sulfuric acid v/v in EtOH); (d) 20% ceric ammonium molybdate w/v in H_2O; (e) 20% potassium permanganate w/v in H_2O.

Concentration, evaporation or removal of solvent under reduced pressure (water aspirator) refers to solvent removal via a Büchi rotary evaporator at ~15 Torr.

Gas-liquid chromatography (GLC) was performed on Hewlett-Packard models 5880A and 5890 gas chromatographs, both equipped with flame ionization detectors and fused silica columns (Hewlitt-Packard HP-5, ~25 m x 0.20 mm coated with 5% phenylmethylsilicone).

Melting points were measured on a Fisher-Johns melting point apparatus and are uncorrected.

NMR spectra were recorded using deuteriochloroform ($CDCl_3$), hexadeuteriodimethyl sulfoxide (DMSO-d_6) or hexadeutereobenzene (C_6D_6) as the solvent. Signal positions (δ) are given in parts per million from tetramethylsilane (δ 0) and were measured relative to the signal of the solvent in which the sample was analyzed ($CDCl_3$: δ 7.24 ^{1}H NMR; δ 77.0, ^{13}C NMR;

DMSO-d_6: δ 2.49, ^{1}H NMR; δ 39.7, ^{13}C-NMR; C_6D_6: δ 7.15, ^{1}H NMR; δ 128.0, ^{13}C NMR).

Coupling constants (J values) are given in Hertz (Hz) and are reported to the nearest 0.1 Hz. The

tin-proton coupling constants (J_{Sn-H}) are given as an average of the ^{117}Sn and ^{119}Sn values. ^{1}H

NMR spectral data are tabulated in the order: multiplicity (s, singlet; d, doublet; dd, doublet of

doublets; t, triplet; q, quartet; m, multiplet), coupling constant, number of protons and proton

assignment where applicable. Where APT (attached proton test) data is given, signals with

negative phases (methyl and methine carbons) and signals with positive phases (methylene and

quaternary carbons) are indicated in brackets (-ve) or (+ve) respectively, following the ^{13}C NMR

chemical shift. Proton nuclear magnetic resonance (^{1}H NMR) spectra were recorded on Bruker

models WH-400 (400 MHz), Avance-400 (400 MHz) or AMX-500 (500 MHz) spectrometers.

Carbon nuclear magnetic resonance (^{13}C NMR) spectra were recorded on a Bruker AM-400

(100.5 MHz) spectrometer.

Infrared (IR) spectra were recorded on a Perkin Elmer 1710 Fourier transform

spectrophotometer with internal calibration as films between sodium chloride plates (liquid

samples) or as potassium bromide pellets (solid samples). Only selected, characteristic

absorption data are provided for each compound.

Low and high resolution electron impact (EI) mass spectra were recorded on Kratos

MS50 or MS80 mass spectrometers at 70 eV. The molecular ion (M$^+$) masses are reported unless

otherwise stated. Low and high resolution desorption chemical ionization (DCI) mass spectra

were recorded on a Delsi Mermag model R-10-10C mass spectrometer using either ammonia,

isobutane or methane or mixtures of these materials as the ionizing gas. Low and high resolution

fast atom bombardment (FAB) mass spectra were recorded on a Kratos Concept II HQ mass

spectrometer. All compounds subjected to high resolution mass measurements were

homogeneous by GLC and/or TLC analysis. The low and high resolution mass spectrometric

analyses were performed by the UBC Mass Spectrometry Laboratory.

Elemental analyses were performed on a Carlo Erba model 1106 CHN elemental analyzer

or on a Fisons EA model 1108 elemental analyzer using standard micro-analytical techniques.

These analyses were performed by the UBC Microanalytical Laboratory.

Optical rotations of samples were measured with a Jasco P 1010 polarimeter at 589 nm (sodium

'D' line).

Preparation of (2*R**)-1,1-ethylenedioxy-2-(3,3-(ethylenedioxy)butyl)-2-methyl-cyclohexan-3-one (**94**).
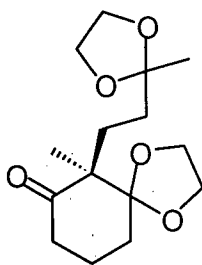
To a cold (-78 °C), stirred solution of 2-(3-oxobutyl)-2-methylcyclohexane-1,3-dione (**95**) (2.80 g, 14.3 mmol) and 1,2-bis(trimethylsilyloxy)ethane (3.50 mL, 14.3 mmol) in dry CH_2Cl_2 (30 mL), was added trimethylsilyl trifluoromethanesulfonate (0.260 mL, 1.43 mmol). After the solution had been stirred at -78 °C for 2 hours, an additional quantity of 1,2-bis(trimethylsilyloxy)ethane (3.50 mL, 14.3 mmol) was added and the reaction mixture was stirred for a further 3 hours at -78 °C. The mixture was treated at -78 °C with saturated aqueous $NaHCO_3$ (20 mL) and the resulting mixture was diluted with Et_2O (40 mL) and allowed to warm to room temperature. The phases were separated and the aqueous phase was extracted with Et_2O (2 x 40 mL). The combined organic phases were washed with brine (25 mL), dried ($MgSO_4$) and concentrated. Purification of the crude product by flash chromatography (200 g of silica gel, 1:1:2 petroleum ether - Et_2O – CH_2Cl_2) and removal of trace amounts of solvent (vacuum pump) from the resulting liquid provided 3.28 g (82%) of **94** as a colorless oil.

^{1}H NMR (400 MHz, $CDCl_3$) δ: 3.85-3.98 (m, 8H), 2.45 (m, 1H), 2.28 (m, 1H), 2.10 (m, 1H), 1.92 (m, 1H), 1.55-1.88 (m, 5H), 1.28 (s, 3H), 1.27 (m, 1H), 0.98 (s, 3H).

^{13}C NMR (100.5 MHz, C_6D_6) δ: 210.1, 114.0, 109.8, 65.2, 65.1, 64.7, 64.6, 58.8, 37.3, 33.9, 29.9, 29.7, 24.0, 19.6, 13.4.

IR (neat): 2957, 2882, 1713, 1460, 1376, 1223, 950, 853 cm^{-1}.

Exact mass calcd for $C_{15}H_{24}O_5$: 284.1624; found: 284.1624.

Preparation of (2R*)-1,1-ethylenedioxy-2-(3,3-(ethylenedioxy)butyl)-2-methyl-3-trifluoro-methanesulfonyloxycyclohex-3-ene (103).
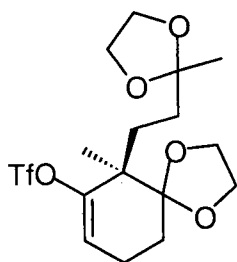
To a cold (0 °C), stirred solution of diisopropylamine (2.00 mL, 14.3 mmol) in dry THF (30 mL) was added a solution of n-BuLi (1.6 M in hexanes, 8.60 mL, 13.8 mmol). After the reaction mixture had been stirred for 20 minutes, it was cooled to -78 °C and (2R*)-1,1-ethylenedioxy-2-(3,3-(ethylenedioxy)butyl)-2-methylcyclohexan-3-one (94) (2.90 g, 10.2 mmol) was added as a solution in dry THF (15 mL). After the mixture had been stirred for 2 hours at -78 °C, N-phenyltrifluoromethanesulfonimide (7.3g, 20.4 mmol) was added as a solid to the yellowish suspension, and the reaction mixture was warmed to room temperature. After the mixture had been stirred at room temperature for 1 hour, it was treated with H$_2$O (20 mL) and the resultant mixture was diluted with Et$_2$O (30 mL). The phases were separated and the aqueous phase was extracted with Et$_2$O (2 x 40 mL). The combined organic phases were washed with brine (25 mL), dried (MgSO$_4$) and concentrated. Purification of the crude product by flash chromatography (200 g of silica gel, 3:2 petroleum ether - Et$_2$O) and removal of trace amounts of solvent (vacuum

pump) from the resulting solid provided 3.4 g (80%) of the triflate **103** as a colorless solid (mp

65 °C).

^{1}H NMR (400 MHz, CDCl$_3$) δ: 5.67 (dd, 1H, J = 4, 4 Hz), 3.80-3.97 (m, 8H), 2.10-2.20 (m, 2H),

1.54-1.76 (m, 6H), 1.22 (s, 3H), 1.07 (s, 3H).

^{13}C NMR (100.5 MHz, CDCl$_3$) δ: 152.1, 118.2 (q, -CF$_3$, J = 319.7 Hz), 115.7, 111.3, 109.7, 65.0,

64.7, 64.5, 64.4, 46.6, 34.4, 30.5, 26.8, 23.6, 20.6, 17.9.

IR (KBr): 2985, 2888, 1412, 1212, 1143, 1031, 987, 883 cm^{-1}.

Exact mass calcd for C$_{16}$H$_{23}$O$_7$F$_3$S: 416.1117; found: 416.1120.

Anal. calcd for C$_{16}$H$_{23}$O$_7$F$_3$S: C 46.15, H 5.57; found C 46.36, H 5.72.

Preparation of (2*R**)-1,1-ethylenedioxy-2-(3,3-(ethylenedioxy)butyl)-2-methyl-3-vinylcyclohex-3-ene (**93**).
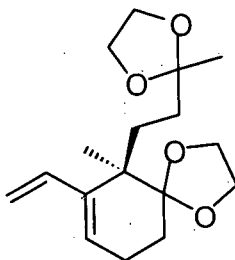
A mixture of the triflate **103** (206 mg, 0.495 mmol), Pd(PPh$_3$)$_4$ (57 mg, 0.049 mmol), LiCl (126 mg, 3.00 mmol), CuCl (250 mg, 2.50 mmol) and tributylvinyltin (0.292 mL, 1.00 mmol) in dry DMSO (5.0 mL) was frozen (-78 °C), allowed to warm to room temperature under vacuum and then purged with Argon. After 2 additional repetitions of the freeze-thaw procedure, the reaction mixture was stirred at room temperature for 1 hour and at 60 °C for 1.5 hours. The reaction mixture was then treated with saturated aqueous NH$_4$Cl-NH$_3$ (pH 8) (10 mL) and the resultant mixture was diluted with Et$_2$O (10 mL). The phases were separated and the aqueous phase was extracted with Et$_2$O (2 x 15 mL). The combined organic phases were washed with brine (4 x 10 mL), dried (MgSO$_4$) and concentrated. Purification of the crude product by flash chromatography (40 g of silica gel, 3:2 petroleum ether - Et$_2$O) and removal of trace amounts of solvent (vacuum pump) from the resulting liquid provided 144 mg (98%) of **93** as a colorless oil.

^{1}H NMR (400 MHz, CDCl$_3$) δ: 6.23 (ddd, 1H, *J* = 0.9, 10.7, 17.1 Hz), 5.78 (dd, 1H, *J* = 3.8, 3.8 Hz), 5.27 (dd, 1H, *J* = 2.0, 17.1 Hz), 4.88 (dd, 1H, *J* = 2.0, 10.7 Hz), 3.82-3.96 (m, 8H), 2.14-2.20 (m, 2H), 1.48-1.77 (m, 6H), 1.23 (s, 3H), 1.04 (s, 3H).

^{13}C NMR (100.5 MHz, CDCl$_3$) δ: 142.9 (+ve), 136.7 (-ve), 122.2 (-ve), 113.6 (+ve), 112.5 (+ve), 110.3 (+ve), 64.7 (+ve), 64.4 (+ve), 64.4 (+ve), 64.4 (+ve), 44.2 (+ve), 34.8 (+ve), 31.4 (+ve), 26.9 (+ve), 23.9 (+ve), 23.7 (-ve), 20.7 (-ve).

IR (neat): 2979, 2878, 1461, 1376, 1202, 1144, 1098, 995, 949, 911, 851 cm^{-1}.

Exact mass calcd for C$_{17}$H$_{26}$O$_4$: 294.1831; found: 294.1829.

Anal. calcd for C$_{17}$H$_{26}$O$_4$: C 69.34, H 8.91; found C 69.17, H 8.89.

Preparation of (1*R**, 4a*S**, 5*R**)-1-(3,3-(ethylenedioxy)butyl)-2,2-ethylenedioxy-1,5-dimethyl-5-hydroxymethyl-1,2,3,4,4a,5,6,7-octahydronaphthalene (**107**) and (1*R**, 4a*R* *, 5*S**)-1-(3,3-(ethylenedioxy)butyl)-2,2-ethylenedioxy-1,5-dimethyl-5-hydroxymethyl-1,2,3,4,4a,5,6,7-octahydronaphthalene (**108**).

96   **106**   **107**   **108**
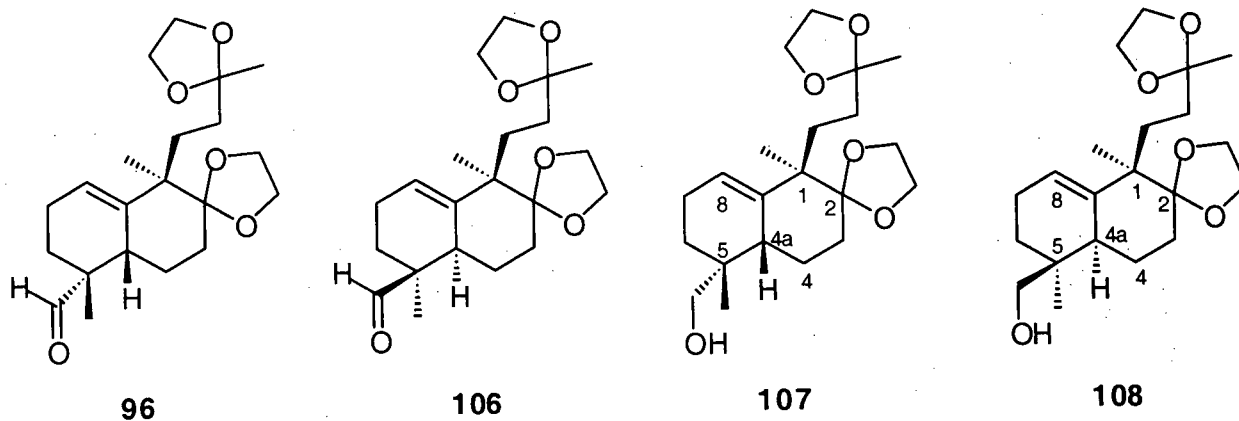
To a cold (-95 °C), stirred solution of the diene **93** (1.30 g, 4.4 mmol) and methacrolein (0.73 mL, 8.8 mmol) in dry CH$_2$Cl$_2$ (43 mL) was added, dropwise, a solution of EtAlCl$_2$ (1.0 M in hexane, 4.8 mL, 4.8 mmol). After the mixture had been stirred for 2 hours at -95 °C, it was

quenched with saturated aqueous $NaHCO_3$ (20 mL) and the resultant mixture was diluted with Et_2O (40 mL) and allowed to warm to room temperature. The phases were separated and the aqueous phase was extracted with Et_2O (2 x 40 mL). The combined organic phases were washed with brine (25 mL), dried ($MgSO_4$) and concentrated under reduced pressure to yield an inseparable mixture (silica gel chromatography) of the aldehydes **96** and **106** (2:1 by ^{1}H NMR spectroscopic analysis) as a crude oil which was used without further purification.

To a cold (0 °C), stirred solution of the aldehydes **96** and **106** in Et_2O (40 mL) was added a solution of DIBAL (1.0 M in hexane, 4.8 mL, 4.8 mmol). After 1 hour, $Na_2SO_4 \cdot 10\ H_2O$ (5.0 g, 15.5 mmol) was added and the reaction mixture was warmed to room temperature and stirred for an additional 30 minutes. The mixture was filtered, the collected material was washed with Et_2O (100 mL) and the solvent was removed from the filtrate under reduced pressure. The crude product was purified by flash chromatography (150 g of silica gel, 3:2 CH_2Cl_2 - Et_2O) and the appropriate fractions were combined and concentrated to provide 0.442 g (27%) of **108** ($R_F = 0.3$, 3:2 CH_2Cl_2 - Et_2O) and 0.846 g (53%) of **107** ($R_F = 0.2$, 3:2 CH_2Cl_2 - Et_2O), both as colorless solids. Recrystallization of **108** from pentane - Et_2O afforded the alcohol **108** as colorless needles (mp 94 °C). Similarly, recrystallization of **107** from pentane - Et_2O afforded the desired alcohol **107** as colorless needles (mp 105 °C).

(1R*,4aR*,5S*)-1-(3,3-(ethylenedioxy)butyl)-2,2-ethylenedioxy-1,5-dimethyl-5-hydroxymethyl -1,2,3,4,4a,5,6,7-octahydronaphthalene (**108**):

^{1}H NMR (400 MHz, $CDCl_3$) δ: 5.50 (m, 1H), 3.85-3.95 (m, 8H), 3.47 (dd, 1H, $J = 5.5$, 10.7 Hz), 3.29 (dd, 1H, $J = 4.9$, 10.7 Hz), 2.03-2.14 (m, 2H), 1.95 (bd, 1H, $J = 12.5$ Hz), 1.86 (ddd, 1H, $J = 5.3$, 14, 14 Hz), 1.79 (m, 1H), 1.48-1.75 (m, 4H), 1.36 (m, 1H), 1.32 (s, 3H), 1.28 (m, 1H), 1.10-1.22 (m, 2H), 1.07 (s, 3H), 1.03 (m, 1H), 0.90 (s, 3H).

^{13}C NMR (100.5 MHz, CDCl$_3$) δ: 141.1, 118.3, 113.5, 110.4, 69.8, 64.8, 64.7, 64.3, 64.3, 47.3, 39.0, 35.6, 33.0, 31.0, 25.5, 25.4, 24.5, 23.6, 21.9, 21.0, 20.6.

IR (KBr): 3505, 2931, 1459, 1377, 1263, 1192, 1138, 951, 909, 861 cm^{-1}.

Exact mass calcd for C$_{21}$H$_{34}$O$_5$: 366.2406; found: 366.2406.

Anal. calcd for C$_{21}$H$_{34}$O$_5$: C 68.82, H 9.35; found C 68.67, H 9.32.

(1R*,4aS*,5R*)-1-(3,3-(ethylenedioxy)butyl)-2,2-ethylenedioxy-1,5-dimethyl-5-hydroxymethyl -1,2,3,4,4a,5,6,7-octahydronaphthalene (**107**):

^{1}H NMR (400 MHz, CDCl$_3$) δ: 5.42 (m, 1H), 3.85-95 (m, 8H), 3.48 (dd, 1H, J = 6.1, 10.7 Hz), 3.33 (dd, 1H, J = 5.5, 10.7 Hz), 1.84-2.14 (m, 5H), 1.64-1.78 (m, 2H), 1.18-1.54 (m, 6H), 1.28 (s, 3H), 1.06 (m, 1H), 0.94 (s, 3H), 0.93 (s, 3H).

^{13}C NMR (100.5 MHz, CDCl$_3$) δ: 141.3, 120.5, 113.4, 110.3, 70.4, 65.2, 65.1, 64.6, 64.6, 49.0, 39.7, 36.1, 33.3, 30.9, 29.1, 26.3, 25.4, 23.8, 22.3, 21.9, 15.9.

IR (KBr): 3506, 2877, 1474, 1446, 1376, 1277, 1207, 1078, 951, 868 cm^{-1}.

Exact mass calcd for C$_{21}$H$_{34}$O$_5$: 366.2406; found: 366.2409.

Anal. calcd for C$_{21}$H$_{34}$O$_5$: C 68.82, H 9.35; found C 69.04, H 9.36.

Preparation of (1*R**, 4a*S**, 5*R**)-1,5-dimethyl-5-hydroxymethyl-1-(3-oxobutyl)-1,2,3,4,4a,5,6,7-octahydronaphthalen-2-one (**109**).

O

O

8

1 2

5 4a

H 4

OH
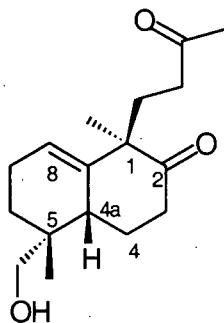
To a stirred solution of the alcohol **107** (272 mg, 0.75 mmol) in acetone (5.0 mL) and H_2O (2.0 mL) was added *p*-TsOH (142 mg, 0.75 mmol) and the resulting solution was heated to reflux for 1.5 hours. The reaction was cooled to room temperature and concentrated under reduced pressure. The residual mixture was treated with saturated aqueous $NaHCO_3$ (15 mL) and the resultant mixture was diluted with Et_2O (25 mL). The phases were separated and the aqueous phase was extracted with Et_2O (2 x 20 mL). The combined organic phases were washed with brine (25 mL), dried ($MgSO_4$) and concentrated under reduced pressure to yield 209 mg (100%) of the dione **109** as colorless needles (mp 109 °C) which required no further purification.

^{1}H NMR (400 MHz, $CDCl_3$) δ: 5.54 (dd, 1H, *J* = 4, 4 Hz), 3.49 (dd, 1H, *J* = 6.1, 10.7 Hz), 3.37 (dd, 1H, *J* = 5.2, 10.7 Hz), 2.60 (ddd, 1H, *J* = 7.2, 11.8, 15.6 Hz), 2.41 (ddd, 1H, *J* = 3.1, 6.1, 15.6 Hz), 2.27 (dd, 2H, *J* = 8, 8 Hz), 2.20 (dd, 1H, *J* = 4.3, 12.8 Hz), 1.98-2.13 (m, 3H), 2.10 (s, 3H), 1.79 (ddd, 1H, *J* = 8.2, 8.2, 14.3 Hz), 1.41 (ddd, 1H, *J* = 6.1, 11.8, 12.2 Hz), 1.28-1.35 (m, 2H), 1.14 (m, 1H), 1.11 (s, 3H), 0.98 (s, 3H).

^{13}C NMR (100.5 MHz, CDCl$_3$) δ: 213.8 (+ve), 208.1 (+ve), 140.8 (+ve), 121.6 (-ve), 69.4 (+ve), 55.0 (+ve), 39.8 (-ve), 38.0 (+ve), 37.7 (+ve), 36.3 (+ve), 31.1 (+ve), 30.0 (-ve), 26.6 (+ve), 26.0 (+ve), 22.3 (+ve), 21.6 (-ve), 18.9 (-ve).

IR (KBr): 3414, 2971, 1697, 1422, 1372, 1176, 1057, 923 cm^{-1}.

Exact mass calcd for C$_{17}$H$_{26}$O$_3$: 278.1882; found: 278.1879.

Anal. calcd for C$_{17}$H$_{26}$O$_3$: C 73.35, H 9.41; found C 73.15, H 9.38.

X-Ray crystallographic data: see Appendix 2.1

Preparation of (4a*S* *, 8*R**, 8a*S**)-4a,8-dimethyl-8-hydroxymethyl-2,3,4,4a,6,7,8,8a,9,10-decahydrophenanthren-2-one (**110**).

A solution of the dione **109** (300 mg, 1.08 mmol) and NaOH (432 mg, 10.8 mmol) in dry MeOH (10.8 mL) was stirred for 9 hours at room temperature. The resulting orange solution was acidified to pH 2 with 1N aqueous HCl and the resultant mixture was diluted with Et_2O (50 mL). The phases were separated and the aqueous phase was extracted with Et_2O (2 x 50 mL). The combined organic phases were washed with brine (25 mL), dried ($MgSO_4$) and concentrated. Purification of the crude product by flash chromatography (150 g of silica gel, 3:2 hexanes - EtOAc) and removal of trace amounts of solvent (vacuum pump) from the resulting solid provided 252 mg (90%) of the enone **110** as a colorless solid (mp 112 °C).

^{1}H NMR (400 MHz, $CDCl_3$) δ: 5.78 (bs, 1H), 5.58 (dd, 1H, *J* = 4, 4 Hz), 3.41 (d, 1H, *J* = 11.0 Hz), 3.25 (d, 1H, *J* = 11.0 Hz), 2.49 (ddd, 1H, *J* = 5.7, 14.5, 17.9 Hz), 2.34 (dd, 1H, *J* = 5.0, 17.9 Hz), 2.14-2.25 (m, 2H), 1.99-2.10 (m, 3H), 1.70-1.91 (m, 3H), 1.57 (ddd, 1H, *J* = 1.5, 5.4, 13.0 Hz), 1.52 (m, 1H), 1.31 (s, 3H), 1.23 (m, 1H), 1.09 (dd, 1H, *J* = 5.0, 12.9 Hz), 0.87 (s, 3H).

^{13}C NMR (100.5 MHz, $CDCl_3$) δ: 199.1 (+ve), 174.3 (+ve), 145.5 (+ve), 125.1 (-ve), 119.0 (-ve), 69.7 (+ve), 42.9 (+ve), 38.3 (-ve), 35.7 (+ve), 35.4 (+ve), 34.2 (+ve), 29.6 (+ve), 26.9 (+ve), 25.0 (+ve), 21.8 (+ve), 21.5 (-ve), 20.6 (-ve).

IR (KBr): 3413, 2909, 1651, 1445, 1359, 1229, 1047, 940 cm^{-1}.

Exact mass calcd for $C_{17}H_{24}O_2$: 260.1776; found: 260.1777.

Anal. calcd for $C_{17}H_{24}O_2$: C 78.42, H 9.29; found C 77.85, H 9.30.

Preparation of (4a*S**, 8*R**, 8a*S**)-4a,8-dimethyl-8-formyl-2,3,4,4a,6,7,8,8a,9,10-decahydro-phenanthren-2-one (**91**).
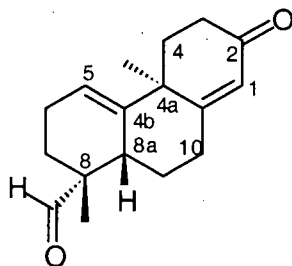
To a stirred solution of the enone **110** (36 mg, 0.14 mmol) and 4-methylmorpholine *N*-oxide (19 mg, 0.16 mmol) in CH_2Cl_2 (1.5 mL) at room temperature, was added a catalytic amount of tetrapropylammonium perruthenate. After 30 minutes, the crude reaction mixture was passed through a plug of silica gel (50 g) and the product was eluted with Et_2O - petroleum ether (2:1). Concentration of the filtrate and removal of trace amounts of solvent (vacuum pump) from the resulting solid provided 31 mg (87%) of the aldehyde **91** as a white solid (mp 113 °C).

^{1}H NMR (400 MHz, CDCl$_3$) δ: 9.53 (s, 1H), 5.80 (s, 1H), 5.65 (d, 1H, *J* = 4.2 Hz), 2.53 (ddd, 1H, *J* = 5.3, 14.5, 17.9 Hz), 2.38 (dddd, 1H, *J* = 0.8, 1.9, 5.3 17.9 Hz), 1.96-2.28 (m, 6H), 1.67-1.80 (m, 2H), 1.64 (ddd, 1H, *J* = 1.9, 5.7, 11.5 Hz), 1.50 (ddd, 1H, *J* = 3.8, 8.8, 11.8 Hz), 1.43 (m, 1H), 1.34 (s, 3H), 1.01 (s, 3H).

^{13}C NMR (100.5 MHz, CDCl$_3$) δ: 205.7 (-ve), 198.6 (+ve), 172.5 (+ve), 143.6 (+ve), 125.5 (-ve), 119.7 (-ve), 46.9 (+ve), 42.8 (+ve), 37.6 (-ve), 35.5 (+ve), 34.2 (+ve), 29.4 (+ve), 27.7 (+ve), 22.4 (+ve), 21.7 (-ve), 21.2 (+ve), 18.7 (-ve).

IR (KBr): 2933, 1718, 1662, 1623, 1460, 1212, 917, 886 cm^{-1}.

Exact mass calcd for $C_{17}H_{22}O_2$: 258.1620; found: 258.1624.

Anal. calcd for $C_{17}H_{22}O_2$: C 79.03, H 8.58; found C 78.87, H 8.66.

Preparation of (4aS*, 8R*, 8aS*)-4a,8-dimethyl-8-carboxy-2,3,4,4a,6,7,8,8a,9,10-decahydro-phenanthren-2-one (111) and (4aS*, 4bS*, 5R*, 8R*, 8aR*)-4a,8-dimethyl-5-iodo-2,3,4,4a,4b,5,6,7,8,8a,9,10-dodecahydrophenanthren-2-one-8,4b-carbolactone (92).

111   **92**
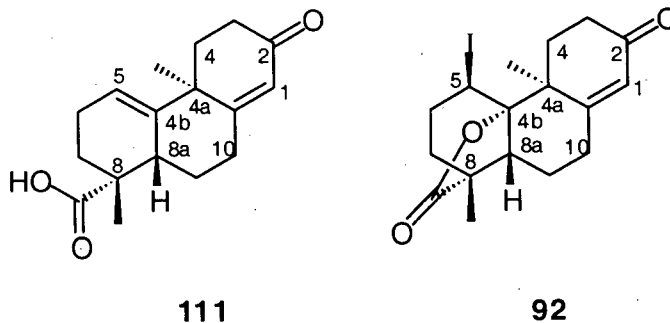
To a stirred solution of the aldehyde **91** (120 mg, 0.465 mmol) in t-BuOH (6.0 mL) and 2-methyl-2-butene (1.0 mL) at room temperature, was added a solution of $NaClO_2$ (376 mg, 4.15 mmol) and $NaH_2PO_4\cdot H_2O$ (446 mg, 3.23 mmol) in H_2O (3.0 mL). After 1.5 hours, the reaction mixture was acidified to pH 2 with 1N aqueous HCl and the resultant mixture was diluted with Et_2O (25 mL). The phases were separated and the aqueous phase was extracted with Et_2O (2 x 20 mL). The combined organic phases were washed with brine (25 mL), dried ($MgSO_4$) and concentrated. The crude acid **111** was used in the next transformation without further purification.

To a stirred solution of the crude acid **111** in MeCN (5.0 mL) and H$_2$O (2.0 mL) at room temperature was added NaHCO$_3$ (156 mg, 1.83 mmol) and the resulting suspension was stirred for 5 minutes. After this time, I$_2$ (236 mg, 0.929 mmol) was added and the reaction mixture was stirred for a further 1.5 hours at room temperature. Saturated aqueous NaHCO$_3$ (10 mL) was added and the resultant mixture was diluted with Et$_2$O (20 mL). The phases were separated and the aqueous phase was extracted with Et$_2$O (2 x 20 mL). The combined organic phases were washed with Na$_2$SO$_3$ (10% aqueous solution, 10 mL), brine (25 mL), dried (MgSO$_4$) and concentrated. Purification of the crude product by flash chromatography (50 g of silica gel, 10:1 CH$_2$Cl$_2$ - Et$_2$O) and removal of trace amounts of solvent (vacuum pump) from the resulting solid provided 168 mg (90%) of the iodo lactone **92** as a colorless solid (mp 125-128 °C - decomposition).

^{1}H NMR (500 MHz, CDCl$_3$) δ: 5.82 (s, 1H, H-1), 4.45 (d, 1H, H-5, J = 5.0 Hz), 3.03 (dd, 1H, H-8a, J = 4.4, 14.0 Hz), 2.78 (m, 1H, H-10α), 2.75 (m, 1H, H-4β), 2.64 (ddd, 1H, H-3α, J = 4.9, 15, 15 Hz), 2.58 (m, 1H, H-10β), 2.46 (m, 1H, H-3β), 2.41 (dd, 1H, H-6β, J = 6, 6, 16.1 Hz), 2.21 (dd, 1H, H-6α, J = 5.5, 16.1 Hz), 1.99 (ddd, 1H, H-4α, J = 2.5, 4.9, 12.6 Hz), 1.84 (ddd, 1H, H-7β, J = 6, 6, 13.1 Hz), 1.75 (m, 1H, H-9β), 1.62 (dd, 1H, H-7α, J = 6.0, 13.1 Hz), 1.56 (m, 1H, H-9α), 1.43 (s, 3H, H-13), 1.17 (s, 3H, H-12).

^{13}C NMR (100.5 MHz, CDCl$_3$) δ: 196.5 (+ve, C-2), 178.7 (+ve, C-11), 165.7 (+ve, C-10a), 126.6 (-ve, C-1), 85.8 (+ve, C-4b), 51.5 (-ve, C-8a), 48.0 (+ve, C-8), 41.6 (+ve, C-4a), 33.8 (+ve, C-6), 33.7 (+ve, C-3), 32.6 (+ve, C-7), 31.4 (-ve, C-5), 31.0 (+ve, C-4), 28.4 (+ve, C-10), 23.8 (-ve, C-13), 18.5 (+ve, C-9), 16.4 (-ve, C-12).

IR (KBr): 2951, 1773, 1661, 1611, 1452, 1265, 1202, 1125, 1085, 922, 946 771 cm^{-1}.

Exact mass calcd for $C_{17}H_{21}O_3I$: 400.0536; found: 400.0538.

Anal. calcd for $C_{17}H_{21}O_3I$: C 51.01, H 5.29; found C 50.93, H 5.28.

The assignment of proton and carbon resonances observed in the ^1H and ^{13}C NMR spectra of the iodo lactone **92** are summarized in Tables 2.3 and 2.4. These assignments are based on analysis of HMQC (Table 2.3), HMBC (Table 2.3), COSY (Table 2.4), and 1D NOESY (Table 2.4) data.

Table 2.3. NMR data for (4a*S**, 4b*S**, 5*R**, 8*R**, 8a*R**)-4a,8-dimethyl-5-iodo-2,3,4,4a,4b,5,6,7,8,8a,9,10-dodecahydrophenanthren-2-one-8,4b-carbolactone (**92**) (recorded in CDCl₃).
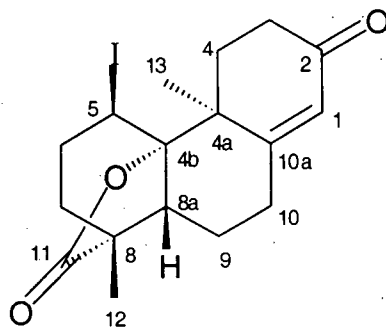
Carbon No.	^{13}C δ (ppm)[a]	^{1}H δ (ppm) (mult, J (Hz))[b,c]	HMBC[b]
1	126.6	H 5.82 (s)	H-10α, H-10β
2	196.5		H-3α, H-3β, H-4α
3	33.7	Hα 2.64 (ddd, J = 4.9, 15, 15 Hz) Hβ 2.46 (m)	H-1, H-4β, H-4α
4	31.0	Hα 1.99 (ddd, J = 2.5, 4.9, 12.6 Hz) Hβ 2.75 (m)	H-3α, H-3β, H-13
4a	41.6		H-1, H-3β, H-4α, H-5, H-10β, H-13
4b	85.8		H-6α, H-9β, H-13
5	31.4	4.45 (d, J = 5.0 Hz)	H-6α, H-7α
6	33.8	Hα 2.21 (dd, J = 5.5, 16.1 Hz) Hβ 2.41 (ddd, J = 6, 6, 16.1 Hz)	H-7α, H-7β
7	32.6	Hα 1.62 (dd, J = 6.0, 13.1 Hz) Hβ 1.84 (ddd, J = 6, 6, 13.1 Hz)	H-5, H-6α, H-6β, H-8a, H-12
8	48.0		H-6α, H-7α, H-7β, H-8a, H-12
8a	51.5	H 3.03 (dd, J = 4.4, 14.0 Hz)	H-5, H-7α, H-7β, H-9α, H-10α, H-12
9	18.5	Hα 1.56 (m) Hβ 1.75 (m)	H-8a, H-10α, H-10β
10	28.4	Hα 2.78 (m) Hβ 2.58 (m)	H-8a, H-9α, H-9β, H-1
10a	165.7		H-4α, H-9β, H-10α, H-10β, H-13
11	178.7		H-7β, H-8a, H-12
12	16.4	H 1.17 (s)	H-7α, H-7β,
13	23.8	H 1.43 (s)	H-4α, H-4β

[a] Recorded at 100.5 MHz. [b] Recorded at 500 MHz. [c] Assignments based on HMQC data.

Table 2.4. NMR data for (4aS*, 4bS*, 5R*, 8R*, 8aR*)-4a,8-dimethyl-5-iodo-2,3,4,4a,4b,5,6,7,8,8a,9,10-dodecahydrophenanthren-2-one-8,4b-carbolactone (**92**) (recorded in CDCl$_3$).

Proton No.	^{1}H δ (ppm) (mult, J (Hz))^a	COSY^a	NOE^b
1	5.82 (s)	H-10α	
3α	2.64 (ddd, J = 4.9, 15, 15 Hz)	H-3β, H-4α, H-4β	
3β	2.46 (m)	H-3α, H-4α, H-4β	
4α	1.99 (ddd, J = 2.5, 4.9, 12.6 Hz)	H-3α, H-3β, H-4β	
4β	2.75 (m)	H-3α, H-3β, H-4α	
5	4.45 (d, J = 5.0 Hz)	H-6α, H-6β	H-4α, H-4β, H-6α, H-6β
6α	2.21 (dd, J = 5.5, 16.1 Hz)	H-5, H-6β, H-7α, H-7β	
6β	2.41 (ddd, J = 6, 6, 16.1 Hz)	H-5, H-6α, H-7α, H-7β	
7α	1.62 (dd, J = 6.0, 13.1 Hz)	H-6α, H-6β, H-7β	
7β	1.84 (ddd, J = 6, 6, 13.1 Hz)	H-6α, H-6β, H-7α	
8a	3.03 (dd, J = 4.4, 14.0 Hz)	H-9α, H-9β	H-7β, H-10β, H-12
9α	1.56 (m)	H-8a, H-9β, H-10α, H-10β	
9β	1.75 (m)	H-8a, H-9α, H-10β	
10α	2.78 (m)	H-9α, H-10β	
10β	2.58 (m)	H-9α, H-9β, H-10α	
12	1.17 (s)		H-7α, H-7β, H-8a, H-9β
13	1.43 (s)		H-4α, H-3α, H-9α

^{a} Recorded at 500 MHz. ^{b} Recorded as NOE difference at 400 MHz using 1D selective NOE experiments.

Preparation of (4a*S**, 4b*S**, 8*R**, 8a*R**)-4a,8-dimethyl-2,3,4,4a,4b,5,6,7,8,8a,9,10-dodecahydro-phenanthren-2-one-8,4b-carbolactone (**46**) and (4a*R**, 4b*S**, 5*S**, 8*R**, 8a*S**)-4a,8-dimethyl-2,3,4,4a,4b,5,6,7,8,8a,9,10-dodecahydrophenanthren-2-one-8,5-carbolactone (**113**).
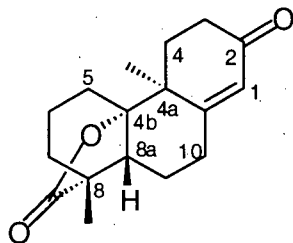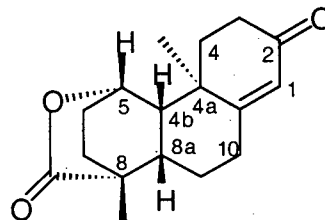
46   **113**

Procedure A. To a stirred solution of the iodo lactone **92** (296 mg, 0.74 mmol) in dry benzene (6.0 mL) was added tri-*n*-butyltin hydride (0.40 mL, 1.5 mmol) and a catalytic amount of AIBN and the mixture was heated at reflux for 0.5 hours. The reaction mixture was then cooled to room temperature and concentrated to approximately 2 mL under reduced pressure. The crude product was purified by flash chromatography (50 g of silica gel, 2:1 Et_2O - petroleum ether, then 4:1 CH_2Cl_2 - Et_2O). Combination and concentration of the appropriate fractions and removal of trace amounts of solvent (vacuum pump) provided 180 mg (89%) of the lactone **46** (R_F = 0.4, 10:1 CH_2Cl_2 - Et_2O) as a colorless solid (mp 122-123 °C).

Procedure B. To a stirred solution of the iodo lactone **92** (48 mg, 0.12 mmol) in dry benzene (2.5 mL) was added tri-*n*-butyltin hydride (0.036 mL, 0.13 mmol) and a catalytic amount of AIBN and the mixture was heated at reflux for 0.5 hours. The reaction mixture was then cooled to room temperature and concentrated to approximately 1 mL under reduced pressure. The crude mixture of products were separated by flash chromatography (50 g of silica gel, 2:1 Et_2O - petroleum ether, then 4:1 CH_2Cl_2 - Et_2O). Combination and concentration of the appropriate fractions and removal of trace amounts of solvent (vacuum pump) from the resulting products

provided 20 mg (61%) of the γ-lactone **46** (R$_F$ = 0.4, 10:1 CH$_2$Cl$_2$ - Et$_2$O) as a colorless solid (mp 122-123 °C) and 10 mg (30%) of the δ-lactone **113** as a colorless oil.

(4aS*, 4bS*, 8R*, 8aR*)-4a,8-dimethyl-2,3,4,4a,4b,5,6,7,8,8a,9,10-dodecahydrophenanthren-2-one-8,4b-carbolactone (**46**):

^{1}H NMR (400 MHz, CDCl$_3$) δ: 5.77 (d, 1H, J = 1.5 Hz), 2.65 (dddd, 1H, J = 1.9, 6.5, 8.8, 14.5 Hz), 2.52 (ddd, 1H, 5.7, 10.3. 17.9 Hz), 2.40 (ddd, 1H, 5.3, 5.3, 18.3 Hz), 2.20 (m, 1H), 2.07 (m, 1H), 1.80-2.01 (m, 5H), 1.47-1.73 (m, 5H), 1.31 (s, 3H), 1.16 (s, 3H).

^{13}C NMR (100.5 MHz, CDCl$_3$) δ: 197.9 (+ve), 179.4 (+ve), 170.4 (+ve), 124.6 (-ve), 88.6 (+ve), 49.9 (-ve), 48.4 (+ve), 41.0 (+ve), 35.7 (+ve), 33.9 (+ve), 31.8 (+ve), 30.5 (+ve), 29.6 (+ve), 22.4 (+ve), 21.2 (-ve), 19.8 (+ve), 17.5 (-ve).

IR (KBr): 2947, 1770, 1667, 1452, 1126, 963, 921 cm^{-1}.

Exact mass calcd for C$_{17}$H$_{22}$O$_3$: 274.1569; found: 274.1573.

Anal. calcd for C$_{17}$H$_{22}$O$_3$: C 74.41, H 8.09; found C 74.22, H 8.23.

(4aR*,4bS*,5S*,8R*,8aS*)-4a,8-dimethyl-2,3,4,4a,4b,5,6,7,8,8a,9,10-dodecahydrophenanthren-2-one-8,5-carbolactone (**113**):

^{1}H NMR (500 MHz, CDCl$_3$) δ: 5.77 (bs, 1H, H-1), 4.75 (d, 1H, J = 2.6 Hz, H-5), 2.72 (dd, 1H, J = 6.2, 19.5 Hz, H-10α), 2.45 (ddd, 1H, J = 5.1, 12.6, 17.5 Hz, H-3α), 2.40 (dddd, 1H, J = 1.5, 6.7, 6.7, 19.5 Hz, H-10β), 2.30 (ddd, 1H, J = 4.8, 4.8, 17.5 Hz, H-3β), 1.96-2.09 (m, 3H, H-4α, H-6, H-8a), 1.89 (d, 1H, J = 11.2 Hz, H-4b), 1.68-1.84 (m, 5H, H-4β, H-6, H-7, H-7, H-9β), 1.46 (m, 1H, H-9α), 1.28 (s, 3H, H-13), 1.14 (s, 3H, H-12).

^{13}C NMR (100.5 MHz, CDCl$_3$) δ: 197.6 (C-2), 176.8 (C-11), 168.2 (C-10a), 125.5 (C-1), 75.0 (C-5), 45.9 (C-4b), 43.6 (C-8a), 42.2 (C-8), 37.6 (C-4), 36.7 (C-4a), 33.4 (C-3), 30.9 (C-7), 28.8 (C-10), 27.9 (C-6), 22.9 (C-13), 21.1 (C-9), 18.6 (C-12).

IR (neat): 2947, 1746, 1666, 1379, 1112, 980 cm^{-1}.

Mass calcd for C$_{17}$H$_{22}$O$_3$: 274; found: 274.

The assignment of proton and carbon resonances observed in the ^{1}H and ^{13}C NMR spectra of the δ-lactone **113** are summarized in Tables 2.5 and 2.6. These assignments are based on analysis of HMQC (Table 2.5), HMBC (Table 2.5), COSY (Table 2.6), and 1D NOESY (Table 2.6) data.

Table 2.5. NMR data for (4a*R**, 4b*S**, 5*S**, 8*R**, 8a*S**)-4a,8-dimethyl-2,3,4,4a,4b,-5,6,7,8,8a,9,10-dodecahydrophenanthren-2-one-8,5-carbolactone (**113**) (recorded in CDCl$_3$).
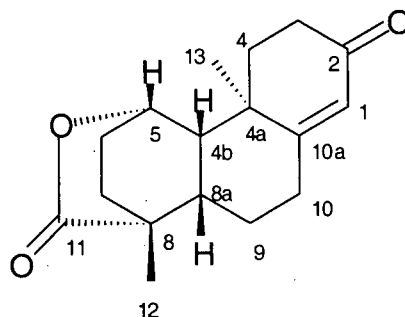
Carbon No.	^{13}C δ (ppm)^a	^{1}H δ (ppm) (mult, J (Hz))^{b,c}	HMBC^b
1	125.5	5.77 (bs)	H-3β, H-10α, H-10β
2	197.6		H-3α, H-3β, H-4α, H-4β
3	33.4	Hα 2.45 (ddd, 5.6, 12.6, 17.5) Hβ 2.30 (ddd, 4.8, 4.8, 17.5)	H-1, H-4α, H-4β
4	37.6	Hα 2.04 (m) Hβ 1.74 (m)	H-4b, H-13
4a	36.7		H-1, H-3β, H-4α, H-4b, H-5
4b	45.9	1.89 (d, 11.2)	H-4α, H-8a, H-13
5	75.0	4.75 (d, 2.6)	H-6, H-7
6	27.9	2.03 (m) 1.71 (m)	H-4b, H-5
7	30.9	1.82 (m) 1.74 (m)	H-5, H-6, H-12
8	42.2		H-4b, H-8a, H-9α, H-12
8a	43.6	1.98 (m)	H-4b, H-5, H-9α, H-12
9	21.1	Hα 1.46 (m) Hβ 1.80 (m)	H-4b, H-8a, H-10α, H-10β
10	28.8	Hα 2.72 (dd, 6.2, 19.5) Hβ 2.40 (dddd, 1.5, 6.7, 6.7, 19.5)	H-1, H-8a, H-9α, H-9β
10a	168.2		H-4α, H-4β, H-10α, H-10β, H-13
11	176.8		H-7, H-8a, H-12
12	18.6	1.14 (s)	
13	22.9	1.28 (s)	H-4α, H-4β, H-4b

^{a} Recorded at 100.5 MHz. ^{b} Recorded at 500 MHz. ^{c} Assignments based on HMQC data.

Table 2.6. NMR data for (4aR*, 4bS*, 5S*, 8R*, 8aS*)-4a,8-dimethyl-2,3,4,4a,4b,-5,6,7,8,8a,9,10-dodecahydrophenanthren-2-one-8,5-carbolactone (**113**) (recorded in CDCl$_3$).
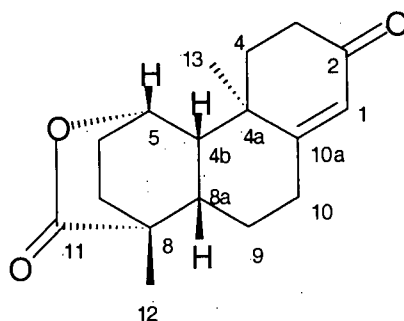
Proton No.	^{1}H δ (ppm) (mult, J (Hz))^a	COSY^a	NOE^b
1	5.77 (bs)	H-10α, H-10β	
3α	2.45 (ddd, 5.6, 12.6, 17.5)	H-3β, H-4α, H-4β	
3β	2.30 (ddd, 4.8, 4.8, 17.5)	H-3α, H-4α, H-4β	
4α	2.04 (m)	H-3α, H-3β, H-4β	
4β	1.74 (m)	H-3α, H-3β, H-4α	
4b	1.89 (d, 11.2)	H-8a	H-5, H-8a
5	4.75 (d, 2.6)	H-6	H-4b, H-4α, H-13
6	2.03 (m)	H-6, H-7	
6	1.71 (m)	H-6, H-7	
7	1.82 (m)	H-6, H-7	
7	1.74 (m)	H-6, H-7	
8a	1.98 (m)	H-4b, H-9α, H-9β	
9α	1.46 (m)	H-8a, H-9β, H-10α, H-10β	
9β	1.80 (m)	H-8a, H-9α, H-10α, H-10β	
10α	2.72 (dd, 6.2, 19.5)	H-1, H-9α, H-9β, H-10β	H-1, H-9α, H-10β
10β	2.40 (dddd, 1.5, 6.7, 6.7, 19.5)	H-1, H-9α, H-9β, H-10α	
12	1.14 (s		H-7, H-8a
13	1.28 (s)		H-3α, H-5, H-9α

^{a} Recorded at 500 MHz. ^{b} Recorded as NOE difference at 400 MHz using 1D selective NOE experiments.

Preparation of (4a*S**, 4b*S**, 8*R**, 8a*R**)-4a,8-dimethyl-1,2,3,4,4a,4b,5,6,7,8,8a,9-dodecahydro-phenanthren-2-one-8,4b-carbolactone (**127**) and (4a*S**, 4b*S**, 8*R**, 8a*R**)-4a,8-dimethyl-2-hydroxy-1,4,4a,4b,5,6,7,8,8a,9-decahydrophenanthren-1-one-8,4b-carbolactone (**132**).

127   **132**
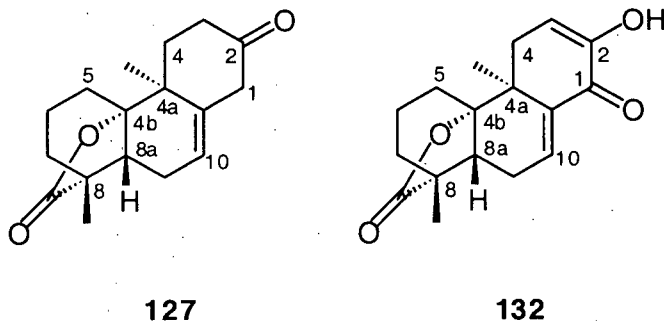
Method A: To a stirred solution of the lactone **46** (160 mg, 0.58 mmol) in dry, oxygen-free *t*-BuOH (see General experimental) (12.0 mL) at room temperature, was added *t*-BuOK (390 mg, 3.48 mmol). The reaction mixture was stirred for 4 minutes, was treated with saturated aqueous NH_4Cl (10 mL), and the resultant mixture was diluted with Et_2O (20 mL). The phases were separated and the aqueous phase was extracted with Et_2O (2 x 20 mL). The combined organic phases were washed with brine (10 mL), dried ($MgSO_4$) and concentrated. Purification of the crude product by flash chromatography (50 g of silica gel, 10:1 $CH_2Cl_2 - Et_2O$) and removal of trace amounts of solvent (vacuum pump) from the resulting solid provided 148 mg (93%) of the β,γ-unsaturated ketone **127** as a colorless solid (mp 148-152 °C).

Method B: To a stirred solution of the lactone **46** (14 mg, 0.051 mmol) in dry *t*-BuOH (2.0 mL) at room temperature, was added *t*-BuOK (60 mg, 0.53 mmol). The reaction mixture was stirred for 40 minutes, was treated with saturated aqueous NH_4Cl (5 mL), and the resultant mixture was diluted with Et_2O (10 mL). The phases were separated and the aqueous phase was extracted with Et_2O (2 x 10 mL). The combined organic phases were washed with brine (10 mL), dried ($MgSO_4$) and concentrated. Purification of the crude product by flash chromatography (20 g of

silica gel, 10:1 CH_2Cl_2 – Et_2O) and removal of trace amounts of solvent (vacuum pump) from the resulting solid provided 12 mg (79%) of the α-hydroxy enone **132** as a colorless oil.

(4a*S**, 4b*S**, 8*R**, 8a*R**)-4a,8-dimethyl-1,2,3,4,4a,4b,5,6,7,8,8a,9-dodecahydrophenanthren-2-one-8,4b-carbolactone (**127**):

^{1}H NMR (400 MHz, CDCl$_3$) δ: 5.42 (m, 1H), 3.31 (ddd, 1H, J = 1.9, 2.2, 15.6 Hz), 2.82 (dd, 1H, J = 2.2, 15.6 Hz), 2.58 (ddd, 1H, J = 7.3, 12.6, 16.4 Hz), 2.40 (dddd, 1H, J = 2.2, 2.2, 5.7, 16.4 Hz), 2.06-2.16 (m, 2H), 1.93 (dd, 1H, J = 7.3, 9.5 Hz), 1.72-1.87 (m, 3H), 1.60-1.69 (m, 2H), 1.44-1.58 (m, 3H), 1.36 (s, 3H), 1.13 (s, 3H).

^{13}C NMR (100.5 MHz, CDCl$_3$) δ: 207.3 (+ve), 179.8 (+ve), 135.6 (+ve), 119.9 (-ve), 86.5 (+ve), 50.7 (+ve), 49.2 (+ve), 44.9 (-ve), 39.4 (+ve), 37.6 (+ve), 34.3 (+ve), 34.0 (+ve), 29.8 (+ve), 24.5 (+ve), 20.0 (+ve), 17.4 (-ve), 15.9 (-ve).

IR (KBr): 2942, 1761, 1717, 1385, 1203, 1115, 936, 912 cm^{-1}.

Exact mass calcd for C$_{17}$H$_{22}$O$_3$: 274.1569; found: 274.1567.

(4a*S**,4b*S**,8*R**,8a*R**)-4a,8-dimethyl-2-hydroxy-1,4,4a,4b,5,6,7,8,8a,9-decahydrophenanthren-1-one-8,4b-carbolactone (**132**):

^{1}H NMR (500 MHz, CDCl$_3$) δ: 6.58 (dd, 1H, J = 2.1, 6.6 Hz, H-10), 5.97 (s, 1H, OH), 5.91 (dd, 1H, J = 3.7, 5.8 Hz, H-3), 2.41 (ddd, 1H, J = 6.6, 6.6, 18.4 Hz, H-9β), 2.36 (m, 2H, H-4, H-4),

2.14 (m, 1H, H-5α), 1.97 (dd, 1H, J = 6.6, 9.8 Hz, H-8a), 1.88 (ddd, 1H, J = 2.1, 9.8, 18.4 Hz, H-9α), 1.85 (m, 1H, H-6), 1.70 (m, 2H, H-6, H-7), 1.58 (m, 1H, H-7), 1.54 (m, 1H, H-5β), 1.29 (s, 3H, H-13), 1.18 (s, 3H, H-12).

^{13}C NMR (100.5 MHz, CDCl$_3$) δ: 186.3 (C-1), 179.3 (C-11), 147.0 (C-2), 140.2 (C-10a), 130.4 (C-10), 113.4 (C-3), 85.8 (C-4b), 50.5 (C-8), 46.2 (C-8a), 40.7 (C-4a), 35.2 (C-4), 33.9 (C-7), 29.0 (C-5), 24.4 (C-9), 19.8 (C-6), 18.5 (C-13), 17.5 (C-12).

IR (neat): 3402, 2940, 1769, 1674, 1637, 1402, 1238, 951 cm^{-1}.

Mass calcd for C$_{17}$H$_{20}$O$_4$: 288.1362; found: 288.1360.

The assignment of proton and carbon resonances observed in the ^{1}H and ^{13}C NMR spectra of the α-hydroxy enone **132** are summarized in Tables 2.7 and 2.8. These assignments are based on analysis of HMQC (Table 2.7), HMBC (Table 2.7), COSY (Table 2.8), and 1D NOESY (Table 2.8) data.

Table 2.7. NMR data for (4aS*, 4bS*, 8R*, 8aR*)-4a,8-dimethyl-2-hydroxy-1,4,4a,4b,-5,6,7,8,8a,9-decahydrophenanthren-1-one-8,4b-carbolactone (**132**) (recorded in CDCl$_3$).
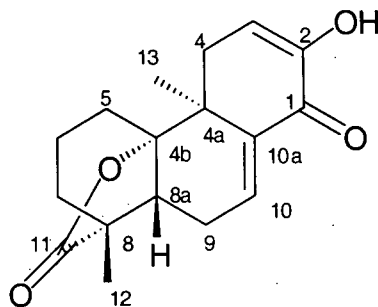
Carbon No.	^{13}C δ (ppm)^a	^{1}H δ (ppm) (mult, J (Hz))^{b,c}	HMBC^b
1	186.3		OH, H-3, H-10
2	147.0	OH 5.97 (s)	OH, H-3, H-4
3	113.4	5.91 (dd, 3.7, 5.8)	OH, H-4
4	35.2	2.36 (m)	H-13
		2.36 (m)	
4a	40.7		H-3, H-4, H-10, H-13
4b	85.8		H-5α, H-9α, H-9β, H-13
5	29.0	Hα 2.14 (m)	H-6
		Hβ 1.54 (m)	
6	19.8	1.85 (m)	H-5α, H-7
		1.70 (m)	
7	33.9	1.70 (m)	H-5α, H-6, H-8a, H-12
		1.58 (m)	
8	50.5		H-7, H-9α, H-12
8a	46.2	1.97 (dd, 6.6, 9.8)	H-5α, H-7, H-9α, H-12
9	24.4	Hα 1.88 (ddd, 2.1, 9.8, 18.4)	H-8a, H-10
		Hβ 2.41 (ddd, 6.6, 6.6, 18.4)	
10	130.4	6.58 (dd, 2.1, 6.6)	H-9β, H-9α
10a	140.2		H-9α, H-9β, H-13
11	179.3		H-7, H-8a, H-12
12	17.5	1.18 (s)	
13	18.5	1.29 (s)	H-4

^{a} Recorded at 100.5 MHz. ^{b} Recorded at 500 MHz. ^{c} Assignments based on HMQC data.

Table 2.8. NMR data for (4a*S**, 4b*S**, 8*R**, 8a*R**)-4a,8-dimethyl-2-hydroxy-1,4,4a,4b,-5,6,7,8,8a,9-decahydrophenanthren-1-one-8,4b-carbolactone (**132**) (recorded in CDCl$_3$).

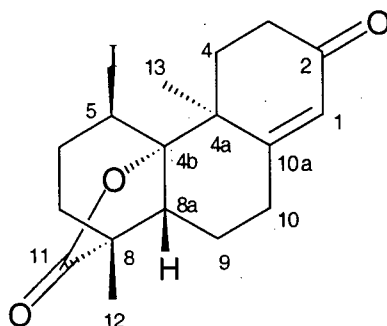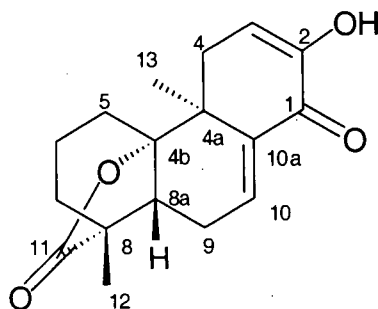| Proton No.	^{1}H δ (ppm) (mult, J (Hz))[a]	COSY[a]	NOE[b]
2	OH 5.97 (s)		
3	5.91 (dd, 3.7, 5.8)	H-4	H-4
4	2.36 (m)	H-3, H-4	
4	2.36 (m)	H-3, H-4	
5α	2.14 (m)	H-5β, H-6	
5β	1.54 (m)	H-5α, H-6	
6	1.85 (m)	H-5, H-6, H-7	
	1.70 (m)	H-5, H-6, H-7	
7	1.70 (m)	H-6, H-7	
	1.58 (m)	H-6, H-7	
8a	1.97 (dd, 6.6, 9.8)	H-9α, H-9β	
9α	1.88 (ddd, 2.1, 9.8, 18.4)	H-8a, H-9β, H-10	
9β	2.41 (ddd, 6.6, 6.6, 18.4)	H-8a, H-9α, H-10	
10	6.58 (dd, 2.1, 6.6)	H-9α, H-9β	H-9α, H-9β
12	1.18 (s)		H-8a, H-9α, H-9β
13	1.29 (s)		H-4, H-5α

[a] Recorded at 500 MHz. [b] Recorded as NOE difference at 400 MHz using 1D selective NOE experiments.

Preparation of (2S*, 4aS*, 4bS*, 8R*, 8aR *)-4a,8-dimethyl-2-(2-(trimethylstannyl)allyl)-1,2,3,4,4a,4b,5,6,7,8,8a,9-dodecahydrophenanthren-2-ol-8,4b-carbolactone (**128**) and (2R *, 4aS*, 4bS*, 8R *, 8aR *)-4a,8-dimethyl-2-(2-(trimethylstannyl)allyl)-1,2,3,4,4a,4b,5,6,7,8,8a,9-dodecahydrophenanthren-2-ol-8,4b-carbolactone (**138**).
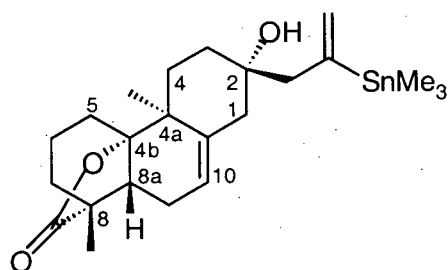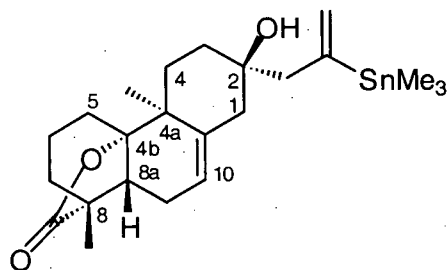
128   **138**

To a cold (-78 °C), stirred solution of freshly distilled 2,3-bis(trimethylstannyl)propene (**75**) (436 mg, 1.18 mmol) in dry THF (8.0 mL) was added a solution of MeLi (1.4 M in Et_2O, 0.68 mL, 0.95 mmol). After the light yellow solution had stirred for 30 minutes, $MgBr_2 \cdot OEt_2$ (304 mg, 1.18 mmol) was added as a solid, and the resulting milky solution was stirred for a further 30 minutes at -78 °C. A solution of the β,γ-unsaturated ketone **127** (145 mg, 0.53 mmol) in dry THF (3.0 mL) was added and the reaction mixture was stirred for 20 minutes at -78 °C. The mixture was treated with saturated aqueous NH_4Cl (10 mL) and the resultant mixture was diluted with Et_2O (30 mL). The phases were separated and the aqueous phase was extracted with Et_2O (2 x 30 mL). The combined organic phases were washed with brine (25 mL), dried ($MgSO_4$) and concentrated. The crude products were purified by flash chromatography (150 g of silica gel, 3:2 CH_2Cl_2 - Et_2O) and the appropriate fractions were combined and concentrated to provide 144 mg (58%) of **128** (R_F = 0.5, 10:1 CH_2Cl_2 - Et_2O) as a colorless solid (mp 195 °C) and 100 mg (40%) of **138** (R_F = 0.8, 10:1 CH_2Cl_2 - Et_2O), as a colorless oil.

(2*S**,4a*S**,4b*S**,8*R**,8a*R**)-4a,8-dimethyl-2-(2-(trimethylstannyl)allyl)-1,2,3,4,4a,4b,-

5,6,7,8,8a,9-dodecahydrophenanthren-2-ol-8,4b-carbolactone (**128**):

^{1}H NMR (400 MHz, CDCl$_3$) δ: 5.63 (m, 1H, $^{3}J_{Sn-H}$ = 152 Hz), 5.35 (bd, 1H, J = 6.1 Hz), 5.32 (d,

1H, J = 3.2 Hz, $^{3}J_{Sn-H}$ = 69 Hz), 2.41 (bd, 1H, J = 13.9 Hz), 2.33 (bd, 1H, J = 13.9 Hz), 2.31 (m,

1H), 2.00-2.15 (m, 3H), 1.92 (dd, 1H, J = 7.0, 9.9 Hz), 1.60-1.85 (m, 6H), 1.40-1.58 (m, 4H),

1.21 (s, 3H), 1.16 (m, 1H), 1.13 (s, 3H), 0.08 (s, 9H).

^{13}C NMR (100.5 MHz, CDCl$_3$) δ: 180.2, 152.1, 138.2, 128.6, 119.0, 87.3, 73.1, 50.7, 47.1, 46.9,

45.9, 45.3, 39.5, 34.3, 33.9, 32.7, 29.6, 24.5, 20.1, 17.5, 16.4, -8.0.

IR (KBr): 3585, 2932, 1756, 1438, 1381, 1123, 914, 763 cm^{-1}.

Exact mass calcd for C$_{23}$H$_{37}$O$_3$Sn (+CI, M+H): 481.1765; found: 481.1758.

(2*R**,4a*S**,4b*S**,8*R**,8a*R**)-4a,8-dimethyl-2-(2-(trimethylstannyl)allyl)-1,2,3,4,4a,4b,5,6,7,8,8a,-

9-dodecahydrophenanthren-2-ol-8,4b-carbolactone (**138**):

^{1}H NMR (400 MHz, CDCl$_3$) δ: 5.68 (m, 1H, $^{3}J_{Sn-H}$ = 155 Hz), 5.40 (bd, 1H, J = 6.1 Hz), 5.28 (d,

1H, J = 3.4 Hz, $^{3}J_{Sn-H}$ = 70 Hz), 2.50 (d, 1H, J = 13.4 Hz), 2.33 (d, 1H, J = 13.4 Hz), 2.33 (m,

1H), 2.15 (ddd, 1H, J = 6.5, 6.5, 17.9 Hz), 2.04 (m, 1H), 1.95 (dd, 1H, J = 7.3, 9.9 Hz), 1.90 (s,

1H), 1.72-1.83 (m, 2H), 1.43-1.70 (m, 8H), 1.32 (ddd, 1H, J = 5.0, 13.4, 13.4 Hz), 1.16 (s, 3H),

1.13 (s, 3H), 0.08 (s, 9H).

^{13}C NMR (100.5 MHz, CDCl$_3$) δ: 180.2 (+ve), 152.0 (+ve), 139.0 (+ve), 128.2 (+ve), 119.6 (-ve), 87.0 (+ve), 71.7 (+ve), 53.1 (+ve), 50.7 (+ve), 45.2 (-ve), 44.5 (+ve), 39.9 (+ve), 34.0 (+ve), 33.8 (+ve), 32.4 (+ve), 29.3 (+ve), 24.5 (+ve), 20.0 (+ve), 17.4 (-ve), 15.3 (-ve), -8.0 (-ve).

IR (neat): 3606, 2931, 1763, 1437, 1381, 1121, 930 cm^{-1}.

Exact mass calcd for C$_{23}$H$_{37}$O$_3$Sn (+CI, M+H): 481.1765; found: 481.1758.

Preparation of (2S*,4aS*,4bS*,8R*,8aR*)-4a,8-dimethyl-2-(2-iodoallyl)-1,2,3,4,4a,4b,-5,6,7,8,8a,9-dodecahydrophenanthren-2-ol-8,4b-carbolactone (129).
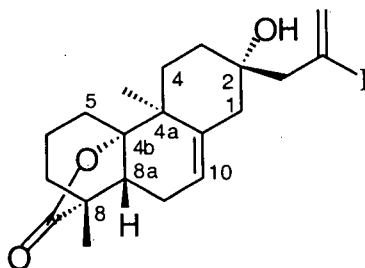
To a stirred solution of the alcohol 128 (51 mg, 0.11 mmol) in dry CH$_2$Cl$_2$ (3.0 mL) at room temperature was added N-iodosuccinimide (50 mg, 0.22 mmol). The pink reaction mixture was stirred for 10 minutes, after which it was filtered through a short plug of silica gel (15 g of silica gel) and the product was eluted with CH$_2$Cl$_2$ - Et$_2$O (20:1). Concentration of the filtrate and removal of trace amounts of solvent (vacuum pump) from the resulting solid provided 47 mg (98%) of the vinyl iodide 129 as a colorless solid (mp 132 °C).

^{1}H NMR (400 MHz, CDCl$_3$) δ: 6.13 (d, 1H, J = 0.8 Hz), 5.98 (d, 1H, J = 1.1 Hz), 5.40 (bd, 1H, J = 6.1 Hz), 2.79 (bd, 1H, J = 15.0 Hz), 2.58 (bd, 1H, J = 15.0 Hz), 2.47 (dd, 1H, J = 3.2, 12.6 Hz),

2.00-2.15 (m, 4H), 1.40-1.98 (m, 10H), 1.24 (s, 3H), 1.20 (ddd, 1H, J = 4.3, 13.4, 13.4 Hz), 1.13 (s, 3H).

^{13}C NMR (100.5 MHz, CDCl$_3$) δ: 180.1 (+ve), 138.2 (+ve), 131.1, (+ve), 119.6 (-ve), 102.2 (+ve), 87.1 (+ve), 73.0 (+ve), 50.7 (+ve), 50.1 (+ve), 45.7 (+ve), 45.3 (-ve), 39.5 (+ve), 33.9 (+ve), 33.2 (+ve), 33.0 (+ve), 29.6 (+ve), 24.5 (+ve), 20.1 (+ve), 17.4 (-ve), 16.6 (-ve).

IR (KBr): 3467, 2936, 1761, 1438, 1381, 1260, 1125, 909, 731 cm^{-1}.

Exact mass calcd for C$_{20}$H$_{28}$O$_3$I (+CI, M+H): 443.1083; found: 443.1079.

Preparation of (1S*, 4S*, 5S*, 9R*, 10R*, 12S*, 16S*)-4,9-dimethyl-13-methylidene-[10,2,2,0^{4,16},0^{5,10}]-tetracyclotetradecan-1-ol-9,5-carbolactone (141) and (2R*, 4aS*, 4bS*, 8R*, 8aR*)-2-allyl-4a,8-dimethyl-1,2,3,4,4a,4b,5,6,7,8,8a,9-dodecahydrophenanthren-2-ol-8,4b-carbolactone (154).
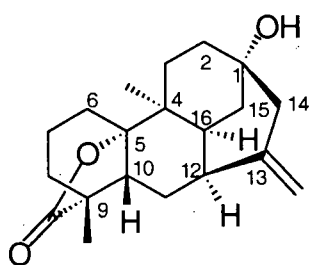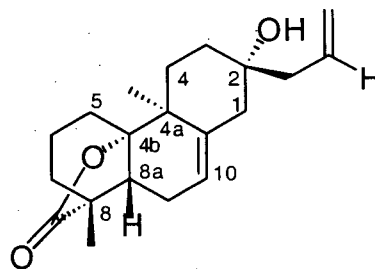
141   **154**

Procedure A. A stirred solution of the vinyl iodide **129** (47 mg, 0.11 mmol), tri-n-butyltin hydride (57 μL, 0.21 mmol) and a catalytic amount of AIBN in dry benzene (11.0 mL) was irradiated with a 275 watt sun lamp for 5 minutes. The refluxing solution was then cooled to room temperature and was concentrated to approximately 1 mL. Purification of the crude product by flash chromatography (25 g of silica gel, 5:2 CH$_2$Cl$_2$ - Et$_2$O) and removal of trace amounts of solvent (vacuum pump) from the resulting solid provided 33 mg (99%) of the pentacycle **141** as a colorless solid (mp 209 °C).

Procedure B. A stirred solution of the vinyl iodide **129** (5.0 mg, 0.011 mmol), tri-n-butyltin hydride (55 μL, 0.20 mmol) and a catalytic amount of AIBN in dry benzene (2.0 mL) was irradiated with a 275 watt sun lamp for 5 minutes. The refluxing solution was cooled to room temperature and was concentrated to approximately 1 mL. The crude products were purified by flash chromatography (150 g of silica gel, 5:2 CH$_2$Cl$_2$ - Et$_2$O) and the appropriate fractions were combined and concentrated to provide 2.8 mg (75%) of the pentacycle **141** (R$_F$ 0.4, 10:1 CH$_2$Cl$_2$ -

Et$_2$O) as a colorless solid (mp 209 °C) and approximately 1.0 mg (23%) of the olefin **154** (R$_F$ 0.3,

10:1 CH$_2$Cl$_2$ - Et$_2$O) as a colorless oil.

(1R*, 4S*, 5S*, 9R*, 10R*, 12S*, 16S*)-4,9-dimethyl-13-methylidene-[10,2,2,0^{4,16},0^{5,10}]-tetracyclotetradecan-1-ol-9,5-carbolactone (**141**):

^{1}H NMR (400 MHz, CDCl$_3$) δ: 4.81 (s, 1H, H-17$_a$), 4.68 (s, 1H, H-17$_b$), 2.49 (dd, 1H, J = 2.6,

14.0 Hz, H-14β), 2.34 (ddd, 1H, 2.2, 2.2, 14.0 Hz, H-14α), 2.31 (m, 1H, H-12), 2.15 (ddd, 1H, J

= 2.3, 5.7, 14.1 Hz, H-11β), 2.08 (dd, 1H, J = 5.7, 12.4 Hz, H-10), 2.03 (m, 1H, H-15β), 2.01 (m,

1H, H-16), 1.94 (m, 1H, H-6α), 1.84 (ddd, 1H, J = 5.9, 13.2, 13.2 Hz, H-3β), 1.76 (m, 1H, H-7),

1.75 (m, 1H, H-2), 1.66 (m, 1H, H-2), 1.63 (m, 1H, H-8), 1.50-1.60 (m, 3H, H-7, H-15α, OH),

1.49 (m, 1H, H-8), 1.32 (m, 1H, H-11α), 1.30 (m, 1H, H-6β), 1.12 (s, 3H, H-19), 1.10 (m, 1H,

H-3α), 1.09 (s, 3H, H-20).

^{13}C NMR (100.5 MHz, CDCl$_3$) δ: 180.6 (+ve, C-18), 147.5 (+ve, C-13), 107.2 (+ve, C-17), 88.6

(+ve, C-5), 69.6 (+ve, C-1), 50.3 (+ve, C-9), 49.2 (+ve, C-14), 44.9 (-ve, C-10), 40.2 (-ve, C-16),

39.5 (+ve, C-15), 38.4 (-ve, C-12), 37.8 (+ve, C-4), 36.1 (+ve, C-2), 34.6 (+ve, C-8), 28.9 (+ve,

C-3), 28.6 (+ve, C-6), 26.0 (+ve, C-11), 19.9 (+ve, C-7), 18.9 (-ve, C-20), 17.0 (-ve, C-19).

IR (KBr): 3500, 2942, 1752, 1378, 1204, 1136 cm^{-1}.

Exact mass calcd for C$_{20}$H$_{29}$O$_3$ (+CI, M+H): 317.2117; found: 317.2118.

X-Ray crystallographic data: see Apendix 2.2

(2*R**, 4a*S* *, 4b*S* *, 8*R**, 8a*R* *)-2-allyl-4a,8-dimethyl-1,2,3,4,4a,4b,5,6,7,8,8a,9-dodecahydro-phenanthren-2-ol-8,4b-carbolactone (**154**):

^{1}H NMR (400 MHz, CDCl$_3$) δ: 5.83 (dddd, 1H, *J* = 7.2, 7.6, 10.3, 17.2 Hz), 5.38 (bd, 1H, *J* = 6.1 Hz), 5.18 (dd, 1H, *J* = 2.3, 10.3 Hz), 5.10 (dddd, 1H, *J* = 1.1, 1.2, 2.3, 17.2 Hz), 2.44 (dd, 1H, *J* = 2.7, 12.2 Hz), 2.24 (m, 1H), 2.19 (dd, 1H, *J* = 7.2, 15.6 Hz), 2.01-2.15 (m, 3H), 1.91 (dd, 1H, *J* = 6.7, 9.8 Hz), 1.84 (dd, 1H, *J* = 4.9, 13.7 Hz), 1.62-1.80 (m, 4H), 1.44-1.60 (m, 5H), 1.24 (s, 3H), 1.13 (s, 3H), 0.85 (m, 1H).

^{13}C NMR (100.5 MHz, CDCl$_3$) δ: 186.5, 138.7, 133.3, 119.5, 118.8, 87.2, 72.4, 50.7, 45.4, 45.0, 40.9, 39.7, 34.1, 34.0, 32.9, 29.7, 24.5, 20.1, 17.5, 16.4.

IR (neat): 3467, 2932, 1763, 1438, 1122, 929 cm^{-1}.

Exact mass calcd for C$_{20}$H$_{28}$O$_3$: 316.2038; found: 316.2040.

The assignment of proton and carbon resonances observed in the ^{1}H and ^{13}C NMR spectra of the olefin **141** are summarized in Tables 2.9 and 2.10. These assignments are based on analysis of HMQC (Table 2.9), HMBC (Table 2.9), COSY (Table 2.10), and 1D NOESY (Table 2.10) data.

Table 2.9. NMR data for (1*R**, 4*S**, 5*S**, 9*R**, 10*R**, 12*S**, 16*S**)-4,9-dimethyl-13-methylidene-[10,2,2,0^{4,16},0^{5,10}]-tetracyclotetradecan-1-ol-9,5-carbolactone (**141**) (recorded in CDCl$_3$).
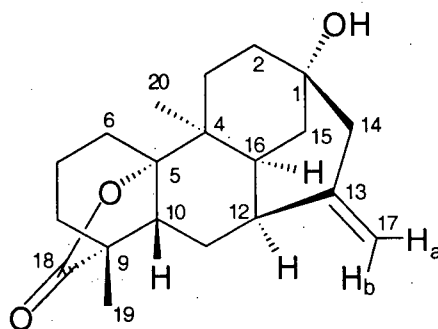
Carbon No.	^{13}C δ (ppm)^a	^{1}H δ (ppm) (mult, J (Hz))^{b,c}	HMBC^d
1	69.6	OH 1.50 (s)	H-2, H-14α, H-14β, H-15α, H-15β
2	36.1	1.75 (m), 1.66 (m)	H-15β
3	28.9	Hα 1.10 (m)	
		Hβ 1.84 (ddd, J = 5.9, 13.2, 13.2)	
4	37.8		H-3β
5	88.6		H-3β, H-6β, H-7, H-11β
6	28.6	Hα 1.94 (m)	H-7
		Hβ 1.30 (m)	
7	19.9	1.76 (m), 1.50 (m)	
8	34.6	1.49 (m), 1.63 (m)	H-6α, H-7, H-10, H-19
9	50.3		H-7, H-10, H-11β, H-19
10	44.9	2.08 (dd, J = 5.7, 12.41)	H-6α, H-8, H-11β, H-12
11	26.0	Hα 1.32 (m)	H-10
		Hβ 2.15 (ddd, J = 2.3, 5.7, 14.1)	
12	38.4	2.31 (m)	H-11β, H-14β, H-16, H-17$_a$, H-17$_b$
13	147.5		H-11α, H-11β, H-14α, H-14β, H-16
14	49.2	Hα 2.34 (ddd, J = 2.2, 2.2, 14.0)	H-2, H-15α, H-15β, H-17$_a$, H-17$_b$
		Hβ 2.49 (dd, J =2.6, 14.0)	
15	39.5	Hα 1.50 (m)	H-2, H-14β
		Hβ 2.03 (m)	
16	40.2	2.01 (m)	H-11β, H-20
17	107.2	H$_a$ 4.81 (m)	H-14α, H-14β
		H$_b$ 4.68 (m)	
18	180.6		H-8, H-10, H-19
19	17.0	1.12 (s)	
20	18.9	1.09 (s)	H-3β

^{a} Recorded at 100.5 MHz. ^{b} Recorded at 400 MHz. ^{c} Assignments based on HMQC data recorded at 500 MHz.

Table 2.10. NMR data for ($1R*$, $4S*$, $5S*$, $9R*$, $10R*$, $12S*$, $16S*$)-4,9-dimethyl-13-methylidene-[10,2,2,0^{4,16},0^{5,10}]-tetracyclotetradecan-1-ol-9,5-carbolactone (**141**) (recorded in CDCl$_3$).

Proton No.	^{1}H δ (ppm) (mult, J (Hz))^a	COSY^a	NOE^b
2	1.75 (m)		
2	1.66 (m)		
3α	Hα 1.10 (m)	H-2, H-3β	
3β	Hβ 1.84 (ddd, J = 5.9, 13.2, 13.2)	H-2, H-3α	H-3α, H-10. H-14β
6α	Hα 1.94 (m)	H-6β, H-7	
6β	Hβ 1.30 (m)		
7	1.76 (m)		
7	1.50 (m)		
8	1.49 (m)		
8	1.63 (m)		
10	2.08 (dd, J = 5.7, 12.41)	H-11α, H-11β	H-6β, H-17$_b$, H-19
11α	Hα 1.32 (m)	H-10, H-11β, H-12	
11β	Hβ 2.15 (ddd, J = 2.3, 5.7, 14.1)	H-10, H-11α, H-12	H-11α, H-17$_b$, H-19
12	2.31 (m)	H-11α, H-11β, H-16	
14α	Hα 2.34 (ddd, J = 2.2, 2.2, 14.0)	H-14β, H-17$_a$, H-17$_b$	H-14β, H-17$_a$, OH
14β	Hβ 2.49 (dd, J =2.6, 14.0)	H-14α, H-15α	H-14α, H-17$_a$, OH
15α	Hα 1.50 (m)	H-15β, H-16	
15β	Hβ 2.03 (m)	H-15α, H-16	
16	2.01 (m)	H-12, H-15α, H-15β	
17$_a$	4.81 (m)	H-14α, H-17$_b$	H-14α, H-14β, H-17$_b$
17$_b$	4.68 (m)	H-14α, H-17$_a$	H-10, H-11β, H-17$_a$
19	1.12 (s)		
20	1.09 (s)		

^{a} Recorded at 400 MHz. ^{b} Recorded as NOE difference at 400 MHz using 1D selective NOE experiments.

Preparation of (2S*, 4aS*, 4bS*, 8R *, 8aR *)-4a,8-dimethyl-2-(formylmethyl)-2-methoxy-1,2,3,4,4a,4b,5,6,7,8,8a,9-dodecahydrophenanthren-8,4b-carbolactone (**160**).

163   **160**
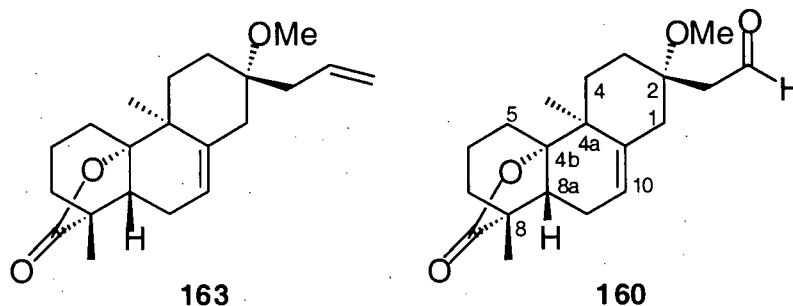
To a stirred solution of the olefin **154** (10 mg, 0.030 mmol) in dry THF (2.0 mL) at room temperature, was added MeI (20 μL, 0.32 mmol) and KH (6.0 mg, 0.15 mmol). After the mixture had been stirred for 30 minutes, it was treated with saturated aqueous NH_4Cl (10 mL) and the resultant mixture was diluted with Et_2O (20 mL). The phases were separated and the aqueous phase was extracted with Et_2O (2 x 20 mL). The combined organic phases were washed with brine (10 mL), dried ($MgSO_4$) and concentrated to provide the methyl ether **163** as a crude oil which was used without further purification.

To a stirred solution of the methyl ether **163** in *t*-BuOH (1.0 mL) and H_2O (1.0 mL) at room temperature, was added 4-methylmorpholine *N*-oxide (6.0 mg, 0.051 mmol) and a catalytic amount of OsO_4. After the mixture had been stirred for 2 hours, H_2O (5 mL) was added and the resultant mixture was diluted with CH_2Cl_2 (10 mL). The phases were separated and the aqueous phase was extracted with CH_2Cl_2 (2 x 10 mL). The combined organic phases were washed with brine (10 mL), dried ($MgSO_4$) and concentrated to provide a mixture of diols as a crude oil, which was used without further purification.

A stirred solution of the crude diols and $NaIO_4$ (13 mg, 0.060 mmol) in H_2O (2 mL), acetone (1 mL) and *t*-BuOH (0.5 mL) was heated at reflux for 10 minutes. The mixture was cooled to room temperature and diluted with H_2O (5 mL) and Et_2O (10 mL). The phases were separated and the

aqueous phase was extracted with Et$_2$O (2 x 10 mL). The combined organic phases were washed with brine (10 mL), dried (MgSO$_4$) and concentrated. Purification of the crude product by flash chromatography (10 g of silica gel, 3:2 CH$_2$Cl$_2$ - Et$_2$O) and removal of trace amounts of solvent (vacuum pump) from the resulting solid provided 5 mg (50%) of aldehyde **160** as a colorless solid (mp 138-139 °C).

^{1}H NMR (400 MHz, CDCl$_3$) δ: 9.79 (dd, 1H, J = 2.7, 3.8 Hz), 5.39 (bd, 1H, J = 6.1 Hz), 3.30 (s, 3H), 2.57 (m, 2H), 2.45 (dd, 1H, J = 3.8, 15.6 Hz), 2.14 (dd, 1H, J = 3.1, 9.9 Hz), 2.08 (dd, 1H, J = 6.9, 13.7 Hz), 2.01 (m, 1H), 1.98 (ddd, 1H, J = 1.1, 4.6, 14.1 Hz), 1.91 (dd, 1H, J = 6.9, 9.9 Hz), 1.41-1.84 (m, 8H), 1.23 (s, 3H), 1.18 (m, 1H), 1.13 (s, 3H).

^{13}C NMR (100.5 MHz, CDCl$_3$) δ: 202.7, 180.0, 137.7, 120.0, 86.9, 77.2, 50.7, 49.1, 45.5, 45.3, 41.8, 39.6, 34.0, 32.5, 30.8, 29.6, 24.5, 20.0, 17.4, 16.4.

IR (KBr): 2937, 1766, 1719, 1465, 1260, 1121, 931 cm^{-1}.

Exact mass calcd for C$_{20}$H$_{28}$O$_4$: 332.1988; found: 332.1987.

Preparation of (1S*,4S*,5S*,9R*,10R*,12S*,16S*)-4,9-dimethyl-1-methoxy-[10.2.2.0^{4,16}.0^{5,10}]-tetracyclotetradecan-13-one-9,5-carbolactone (**169**).
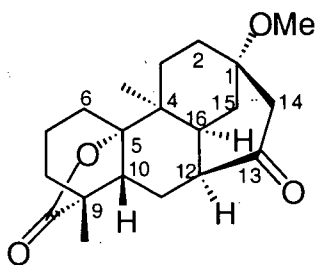
Procedure A (from the aldehyde **160**). To a stirred solution of the aldehyde **160** (5 mg, 0.015 mmol) in dry THF (5.0 mL) at room temperature was added t-BuOH (5 µL), DMPU (15 µL, 0.12 mmol) and a freshly prepared solution of SmI$_2$ (0.065 M in THF, 0.56 mL, 0.036 mmol). After 20 minutes the reaction mixture was treated with saturated aqueous NH$_4$Cl (10 mL) and the resultant mixture was diluted with Et$_2$O (10 mL). The phases were separated and the aqueous phase was extracted with Et$_2$O (2 x 5 mL). The combined organic phases were washed with brine (10 mL), dried (MgSO$_4$) and concentrated to provide a crude mixture of alcohols as an oil which was used without further purification.

To a stirred solution of the crude alcohols and 4-methylmorpholine-N-oxide (5 mg, 0.04 mmol) in CH$_2$Cl$_2$ (1.5 mL) at room temperature was added a catalytic amount of tetrapropylammonium perruthenate. After 30 minutes, the crude reaction mixture was placed directly on a column of silica gel (50 g). The products were eluted with CH$_2$Cl$_2$ - Et$_2$O (3:2) and the appropriate fractions were combined and concentrated to provide 2.1 mg (42%) of the ketone **169** (R$_F$ = 0.6, 1:1 CH$_2$Cl$_2$- Et$_2$O) as a colorless film and 1.4 mg (28%) of the aldehyde **160** (R$_F$ = 0.9, 1:1 CH$_2$Cl$_2$-Et$_2$O), as a colorless oil.

Procedure B (from the pentacycle **141**). To a stirred solution of the pentacycle **141** (11 mg, 0.035 mmol) in dry THF at room temperature was added KH (4.0 mg, 0.10 mmol). After 30 minutes, MeI (21 µL, 0.34 mmol) was added and the reaction mixture was stirred for a further 30

minutes at room temperature. The reaction mixture was then treated with saturated aqueous

NH_4Cl (10 mL) and the resultant mixture was diluted with Et_2O (10 mL). The phases were

separated and the aqueous phase was extracted with Et_2O (2 x 5 mL). The combined organic

phases were washed with brine (10 mL), dried ($MgSO_4$) and concentrated to provide the methyl

ether **170** as a crude oil which was used without further purification.

To a stirred solution of the methyl ether **170** and $NaIO_4$ (22 mg, 0.10 mmol) in CCl_4 (1.0 mL)

CH_3CN (1.0 mL) and H_2O (1.5 mL) at room temperature was added a catalytic amount of $RuCl_3 \cdot$

H_2O. After 30 minutes, the reaction mixture was treated with saturated aqueous NH_4Cl (10 mL)

and the resultant mixture was diluted with Et_2O (10 mL). The phases were separated and the

aqueous phase was extracted with Et_2O (2 x 5 mL). The combined organic phases were washed

with brine (10 mL), dried ($MgSO_4$) and concentrated. Purification of the crude product by flash

chromatography (10 g of silica gel, 3:1 CH_2Cl_2 – Et_2O) and removal of trace amounts of solvent

(vacuum pump) from the resulting liquid provided 7.5 mg (65%) of the ketone **169** as a colorless

film.

($1S^*,4S^*,5S^*,9R^*,10R^*,12S^*,16S^*$)-4,9-dimethyl-1-methoxy-$[10,2,2,0^{4,16},0^{5,10}]$-tetracyclotetra-

decan-13-one-9,5-carbolactone (**169**):

^1H NMR (400 MHz, $CDCl_3$) δ: 3.25 (s, 3H), 2.58 (dd, 1H, J = 2.7, 15.3 Hz), 2.51 (bd, 1H, J =

15.3 Hz), 2.25-2.40 (m, 3H), 2.16 (ddd, 1H, J = 2.7, 3.1, 12.6 Hz), 2.02 (dd, 1H, J = 6.1, 12.6

Hz), 1.94 (m, 1H), 1.85 (ddd, 1H, J = 3.1, 3.4, 13.0 Hz), 1.68-1.81 (m, 2H), 1.45-1.63 (m, 3H),

1.18-1.35 (m, 4H), 1.15 (s, 3H), 1.13 (s, 3H), 1.05 (ddd, 1H, J = 5.0, 12.2, 12.2 Hz).

^{13}C NMR (100.5 MHz, $CDCl_3$) δ: 209.9, 180.5, 87.6, 75.1, 50.6, 50.5, 48.8. 47.6, 45.0, 38.5,

38.0, 34.7, 34.4, 31.9, 28.6, 27.3, 23.2, 19.8, 18.4, 16.9.

IR (film): 2944, 1766, 1702, 1460, 1379, 1131 1101 cm⁻¹.

Exact mass calcd for $C_{20}H_{28}O_4$: 332.1988; found: 332.1990.

(2S*,4aS*,4bS*,8R*,8aR*)-4a,8-dimethyl-2-(2-formylethyl)-3,4,4a,4b,5,6,7,8,8a,9-decahydro-1H-phenanthren-2-ol-8,4b-carbolactone (160) isolated from the reaction described above in Procedure A was identical with the compound prepared previously.

Preparation of (2S*,4aS*,4bS*,8R*,8aR*)-4a,8-dimethyl-2-(2-iodoallyl)-2-triethylsiloxy-1,2,3,4,4a,4b,5,6,7,8,8a,9-dodecahydrophenanthren-8,4b-carbolactone (197).
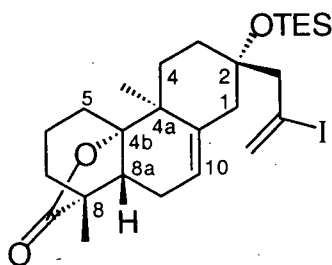
To a cold (-78 °C), stirred solution of the vinyl iodide 129 (46 mg, 0.10 mmol) and triethylamine (0.22 mL, 1.6 mmol) in dry CH_2Cl_2 (3.0 mL) was added triethylsilyl trifluoromethanesulfonate (0.19 mL, 8.4 mmol). After 40 minutes, the reaction mixture was treated with saturated aqueous $NaHCO_3$ (10 mL) and the resultant mixture was diluted with Et_2O (20 mL). The phases were separated and the aqueous phase was extracted with Et_2O (2 x 10 mL). The combined organic phases were washed with brine (1 x 10 mL), dried ($MgSO_4$) and concentrated. Purification of the crude product by flash chromatography (25 g of silica gel, 5:1 petroleum ether - Et_2O) and

removal of trace amounts of solvent (vacuum pump) from the resulting liquid provided 57 mg

(99%) of the vinyl iodide **197** as a colorless oil.

^{1}H NMR (400 MHz, CDCl$_3$) δ: 6.16 (d, 1H, J = 0.9 Hz), 5.92 (d, 1H, J = 0.9 Hz), 5.38 (d, 1H, J

= 6.1 Hz), 2.71 (d, 1H, J = 15.3 Hz), 2.52 (d, 1H, J = 15.3 Hz), 2.46 (dd, 1H, J = 3.4, 12.5 Hz),

1.95-2.15 (m, 4H), 1.90 (dd, 1H, J = 7.0, 9.8 Hz), 1.60-1.85 (m, 5H), 1.43-1.57 (m, 3H), 1.23

(ddd, 1H, J = 4.3, 13.7, 13.7 Hz), 1.22 (s, 3H), 1.13 (s, 3H), 0.95 (t, 9H, J = 7.9 Hz), 0.61 (q, 6H,

J = 7.9 Hz).

^{13}C NMR (100.5 MHz, CDCl$_3$) δ: 180.2 (+ve), 138.6 (+ve), 130.3 (+ve), 119.4 (-ve), 103.0

(+ve), 87.2 (+ve), 76.7 (+ve), 51.1 (+ve), 50.7 (+ve), 46.6 (+ve), 45.3 (-ve), 39.5 (+ve), 33.9

(+ve), 33.4 (+ve), 33.4 (+ve), 29.6 (+ve), 24.5 (+ve), 20.1 (+ve), 17.5 (-ve), 16.8 (-ve), 7.2 (-ve),

6.9 (+ve).

IR (neat): 2952, 1771, 1458, 1121, 741 cm^{-1}.

Exact mass calcd for C$_{24}$H$_{36}$O$_3$SiI (EI, M-CH$_2$CH$_3$): 527.1479; found: 527.1477.

Preparation of (1R*,4S*,5S*,9R*,10R*,13R*)-4,9-dimethyl-14-methylidene-1-triethylsiloxy-[11,2,1.0^{4,13}.0^{5,10}]-tetracyclopentadec-11-ene-9,5-carbolactone (**198**).
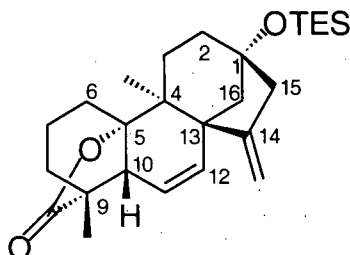
A stirred solution of the vinyl iodide (**197**) (17.4 mg, 0.031 mmol), 1,2,2,6,6-pentamethyl-piperidine (17 μL, 0.094 mmol) and Pd(OAc)$_2$ (7.0 mg, 0.031 mmol) in dry THF (1.5 mL) was heated to reflux. After the mixture had been stirred for 2 hours at reflux, it was cooled to room temperature and concentrated under reduced pressure. Purification of the crude product by flash chromatography (25 g of silica gel, 5:1 petroleum ether - Et$_2$O) and removal of trace amounts of solvent (vacuum pump) from the resulting solid provided 10.7 mg (80%) of the diene **198** as a colorless solid (mp 111-113 °C).

^{1}H NMR (400 MHz, CDCl$_3$) δ: 5.91 (dd, 1H, J = 1.7, 9.7 Hz, H-11), 5.77 (dd, 1H, J = 3.3, 9.7 Hz, H-12), 4.84 (bs, 1H, H-17), 4.83 (bs, 1H, H-17), 2.53 (m, 1H, H-10), 2.50 (dd, 1H, J = 2.1, 16.3 Hz, H-15), 2.33 (dd, 1H, J = 1.7, 16.3 Hz, H-15), 2.22 (dd, 1H, J = 2.4, 11.3 Hz, H-16β), 2.06 (dd, 1H, J = 5.8, 13.4 Hz, H-6α), 1.97 (m, 1H, H-2), 1.77 (dd, 1H, J = 4.8, 12.3 Hz, H-8β), 1.70 (m, 1H, H-2), 1.68 (m, 1H, H-3), 1.66 (m, 1H, H-7), 1.65 (m, 1H, H-8α), 1.64 (m, 1H, H-16α), 1.56 (m, 1H, H-6β), 1.53 (m, 1H, H-3), 1.48 (m, 1H, H-7), 1.24 (s, 3H, H-19), 1.09 (s, 3H, H-20), 0.93 (t, 9H, J = 7.9 Hz, SiCH$_2$CH$_3$), 0.57 (q, 6H, J = 7.9 Hz, SiCH$_2$CH$_3$).

^{13}C NMR (100.5 MHz, CDCl$_3$) δ: 179.6 (+ve, C-18), 148.2 (+ve, C-14), 138.0 (-ve, C-12), 123.4 (-ve, C-11), 108.7 (+ve, C-17), 89.6 (+ve, C-5), 77.2 (+ve, C-1), 55.4 (+ve, C-13), 54.2 (-ve, C-

10), 48.6 (+ve, C-16), 46.5 (+ve, C-9), 45.4 (+ve, C-4), 44.4 (+ve, C-15), 36.8 (+ve, C-7), 36.6 (+ve, C-2), 32.8 (+ve, C-6), 31.1 (+ve, C-3), 19.9 (+ve, C-8), 19.9 (-ve, C-20), 16.9 (-ve, C-19), 7.0 (-ve, SiCH$_2$C̲H$_3$), 6.5 (+ve, SiC̲H$_2$CH$_3$).

IR (KBr): 2957, 1764, 1459, 1143, 1116, 938, 743 cm^{-1}.

Exact mass calcd for C$_{26}$H$_{40}$O$_3$Si: 428.2747; found: 428.2746.

The assignment of proton and carbon resonances observed in the ^{1}H and ^{13}C NMR spectra of the tetracyclic olefin **198** are summarized in Tables 2.11 and 2.12. These assignments are based on analysis of HMQC (Table 2.11), HMBC (Table 2.11), COSY (Table 2.12), and 1D NOESY (Table 2.12) data.
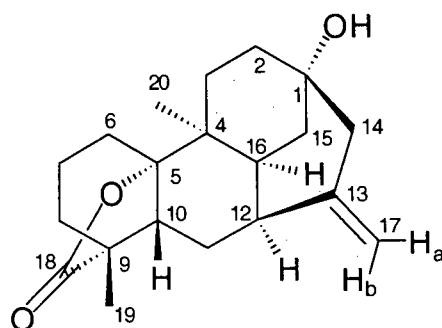
Table 2.11. NMR data for (1R*, 4S*, 5S*, 9R*, 10R*, 13S*)-4,9-dimethyl-14-methylidene-1-triethylsiloxy-[11,2,1,0^{4,13},0^{5,10}]-tetracyclopentadec-11-ene-9,5-carbolactone (**198**) (recorded in CDCl$_3$).
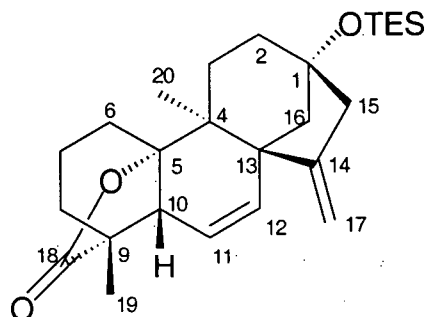
Carbon No.	^{13}C δ (ppm)^a	^{1}H δ (ppm) (mult, J (Hz))^{b,c}	HMBC^d
1	77.2		H-2, H-15, H-16β
2	36.6	1.97 (m), 1.70 (m)	H-3, H-15
3	31.1	1.68 (m), 1.53 (m)	H-20
4	45.4		H-3, H-20
5	89.6		H-6α, H-11, H-20
6	32.8	Hα 2.06 (dd, 13.4, 5.8) Hβ 1.56 (m)	H-7
7	36.8	1.66 (m), 1.48 (m)	H-6, H-8
8	19.9	Hα 1.65 (m) Hβ 1.77 (dd, 4.8, 12.3)	H-6, H-7
9	46.5		H-7, H-8, H-10, H-11, H-19
10	54.2	2.53 (m)	H-6α, H-6β, H-12, H-19
11	123.4	5.91 (dd, 1.7, 9.7)	H-10
12	138.0	5.77 (dd, 3.3, 9.7)	H-10, H-11, H-16α
13	55.4		H-3, H-11, H-17, H-20
14	148.2		H-15, H-16β, H-17
15	44.4	2.50 (dd, 2.1, 16.3) 2.33 (dd, 1.7, 16.3)	H-2, H-16β, H-17
16	48.6	Hα 1.64 (m) Hβ 2.22 (dd, 2.4, 11.3)	H-12, H-15
17	108.7	4.84 (bs), 4.83 (bs)	H-15
18	179.6		H-8, H-10, H-19
19	16.9	1.24 (s)	
20	19.9	1.09 (s)	H-3

^{a} Recorded at 100.5 MHz. ^{b} Recorded at 400 MHz. ^{c} Assignments based on HMQC data recorded at 400 MHz.

Table 2.12. NMR data for (1*R**, 4*S**, 5*S**, 9*R**, 10*R**, 13*S**)-4,9-dimethyl-14-methylidene-1-triethylsiloxy-[11,2,1,0^{4,13},0^{5,10}]-tetracyclopentadec-11-ene-9,5-carbolactone (**198**) (recorded in CDCl$_3$).
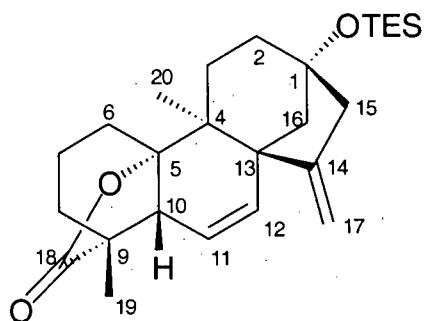
Proton No.	^{1}H δ (ppm) (mult, J (Hz))[a]	COSY[a]	NOE[b]
2	1.97 (m)	H-2, H-3	
2	1.70 (m)	H-2, H-3	
3	1.68 (m)	H-2, H-3	
3	1.53 (m)	H-2, H-3	
6α	2.06 (5.8, 13.4)	H-6β, H-7	
6β	1.56 (m)	H-6α, H-7	
7	1.66 (m)		
7	1.48 (m)		
8α	1.65 (m)	H-7, H-8β	
8β	1.77 (dd, 12.3, 4.8)	H-7, H-8α	
10	2.53 (m)	H-11, H-12	
11	5.91 (dd, 1.7, 9.7)	H-10, H-12	
12	5.77 (dd, 3.3, 9.7)	H-10, H-11	
15	2.50 (dd, 2.1, 16.3)	H-15, H-17	
15	2.33 (dd, 1.7, 16.3)	H-15, H-17	
16α	1.64 (m)	H-16β	
16β	2.22 (dd, 2.4, 11.3)	H-2, H-16α	
17	4.84 (bs)	H-15, H-17	H-10, H-15
17	4.83 (bs)	H-15, H-17	
19	1.24 (s)		
20	1.09 (s)		

[a] Recorded at 400 MHz. [b] Recorded as NOE difference at 400 MHz using 1D selective NOE experiments

Preparation of (2S*, 4aS*, 4bS*, 8R*, 8aR*, 10aR*)-4a,8-dimethyl-10a-hydroxy-2-triethylsiloxy-perhydrophenanthrene-8,4b-carbolactone-2-ethanoic acid δ-lactone (206) and (1S*, 4S*, 5S*, 9R*, 10R *, 13R*, 14S*)-4,9-dimethyl-14,17-epoxy-1-triethylsiloxy-[11,2,1,0^{4,13},0^{5,10}]-tetracyclopentadecane-9,5-carbolactone (204).
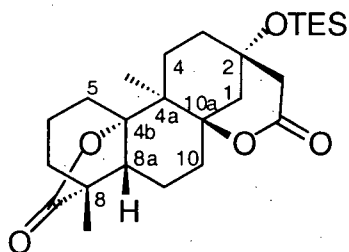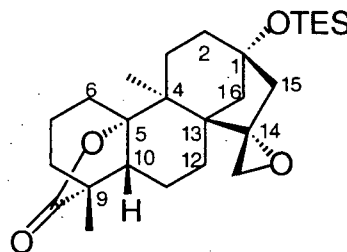
206   204

To a stirred solution of the diene 198 (8.6 mg, 0.020 mmol) in EtOAc (2.0 mL) at room temperature was added a catalytic amount of palladium on carbon (10% Pd-on-carbon) and the resulting black suspension was stirred under an atmosphere (balloon) of H_2. After 25 minutes, the crude reaction mixture was placed directly on a plug of silica gel (5 g of silica gel) and the product was eluted with CH_2Cl_2 - Et_2O (5:1). The filtrate was concentrated and the crude hydrogenation product was used without further purification.

Through a cold (-78 °C) solution of the crude hydrogenation product and Sudan III (approx. 0.1 mg) in MeOH-CH_2Cl_2 (1:9, 3.0 mL) was passed a stream of ozone. After the red color of the dye disappeared (5 minutes), the stream of ozone was replaced by a stream of argon, which was passed through the solution for 5 minutes. After this time, pyridine (10 µL, 0.12 mmol) and DMS (40 µL, 0.54 mmol) were added and the reaction mixture was stirred overnight, with gradual warming to room temperature. The mixture was then concentrated under reduced pressure and the crude products were purified by flash chromatography (25 g of silica gel, 30:1 CH_2Cl_2 - Et_2O). The appropriate fractions were combined and concentrated to provide 3.7 mg

(42%) of the bislactone **206** (R_F = 0.4, 1:1 petroleum ether - Et_2O) as a colorless oil and 2.5 mg

(28%) of the epoxide **204** (R_F = 0.5, 1:1 petroleum ether - Et_2O) as a colorless oil.

(2*S**, 4a*S**, 4b*S**, 8*R**, 8a*R**, 10a*R**)-4a,8-dimethyl-10a-hydroxy-2-triethylsiloxy-perhydro-phenanthrene-8,4b-carbolactone-2-ethanoic acid δ-lactone (**206**):

^{1}H NMR (500 MHz, $CDCl_3$) δ: 2.66 (dd, 1H, J = 2.3, 17.9 Hz, H-11), 2.58 (dd, 1H, J = 1.5, 17.9 Hz, H-11), 2.40 (dd, 1H, J = 4.9, 14.5 Hz, H-8a), 2.11 (dd, 1H, J = 2.7, 13.7 Hz, H-1), 1.94 (m, 1H, H-7), 1.92 (m, 2H, H-5, H-5), 1.88 (m, 2H, H-10, H-10), 1.80 (m, 1H, H-6), 1.52-1.76 (m, 8H, H-1, H-3, H-3, H-4, H-4, H-6, H-7, H-9), 1.37 (m, 1H, H-9), 1.15 (s, 3H, H-15), 1.06 (s, 3H, H-14), 0.92 (t, 9H, J = 8.0 Hz, SiCH$_2$**CH$_3$**), 0.57 (q, 6H, J = 8.0 Hz, Si**CH$_2$**CH$_3$).

^{13}C NMR (100.5 MHz, $CDCl_3$) δ: 180.2 (+ve, C-13), 170.5 (+ve, C-12), 87.1 (+ve, C-4b), 86.7 (+ve, C-10a), 69.8 (+ve, C-2), 51.0 (-ve, C-8a), 47.4 (+ve, C-8), 45.3 (+ve, C-11), 43.0 (+ve, C-1), 42.9 (+ve, C-4a), 35.8 (+ve, C-7), 35.3 (+ve, C-3), 32.2 (+ve, C-10), 31.2 (+ve, C-5), 29.9 (+ve, C-4), 20.0 (+ve, C-6), 19.0 (-ve, C-15), 17.6 (+ve, C-9), 16.8 (-ve, C-14), 6.9 (-ve, SiCH$_2$**C**H$_3$), 6.7 (+ve, Si**C**H$_2$CH$_3$).

IR (KBr): 2953, 1773, 1728, 1214, 934 cm^{-1}.

Exact mass calcd for $C_{25}H_{41}O_5Si$ (+CI, M+H): 449.2723; found: 449.2725.

The assignment of proton and carbon resonances observed in the ^{1}H and ^{13}C NMR spectra of the bislactone **206** are summarized in Table 2.13. These assignments are based on analysis of HMQC and HMBC data.

(1*S* *, 4*S* *, 5*S* *, 9*R**, 10*R* *, 13*S**, 14*S**)-4,9-dimethyl-14,17-epoxy-1-triethylsiloxy-[11,2,1,0^{4,13},0^{5,10}]-tetracyclopentadecane-9,5-carbolactone (**204**):

^{1}H NMR (400 MHz, CDCl$_3$) δ: 3.03 (d, 1H, *J* = 3.5 Hz), 2.92 (d, 1H, *J* = 3.5 Hz), 2.15 (dd, 1H, *J* = 2.1, 16.5 Hz), 2.10 (m, 1H), 2.05 (dd, 1H, *J* = 2.8, 11.6 Hz), 1.30-1.90 (m, 16H), 1.21 (s, 3H), 1.03 (s, 3H), 0.92 (t, 9H, *J* = 7.9 Hz), 0.55 (q, 6H, *J* = 7.9 Hz).

Exact mass calcd for C$_{26}$H$_{42}$O$_4$Si: 446.2852; found: 446.2853.

Table 2.13. NMR data for (2*S**, 4a*S**, 4b*S**, 8*R**, 8a*R**, 10a*R**)-4a,8-dimethyl-10a-hydroxy-2-triethylsiloxy-perhydrophenanthren-8,4b-carbolactone-2-ethanoic acid δ-lactone (**206**) (recorded in CDCl₃).
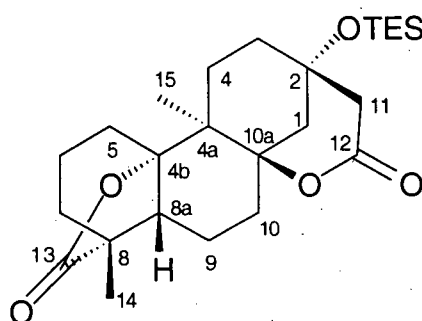
Carbon No.	¹³C δ (ppm)[a]	¹H δ (ppm) (mult, J (Hz))[b,c]	HMBC[b]
1	43.0	2.11 (dd, 2.7, 13.7) 1.74 (m)	H-11
2	69.8		H-1, H-11
3	35.3	1.60 (m) 1.62 (m)	H-11
4	29.9	1.56 (m) 1.56 (m)	H-3, H-15
4a	42.9		H-15
4b	87.1		H-5
5	31.2	1.92 (m) 1.92 (m)	H-6, H-8a
6	20.0	1.80 (m) 1.56 (m)	H-5
7	35.8	1.94 (m) 1.72 (m)	H-14
8	47.4		H-14
8a	51.0	2.40 (dd, 4.9, 14.5)	H-5, H-14
9	17.6	1.72 (m) 1.37 (m)	H-8a, H-10
10	32.2	1.88 (m) 1.88 (m)	H-9
10a	86.7		H-10, H-15
11	45.3	2.66 (dd, 2.3, 17.9) 2.58 (dd, 1.5, 17.9)	H-1
12	170.5		H-11
13	180.2		H-8a, H-14
14	16.8	1.06 (s)	
15	19.0	1.15 (s)	

[a] Recorded at 100.5 MHz. [b] Recorded at 500 MHz. [c] Assignments based on HMQC data.

Preparation of (1R*, 4S*, 5S*, 9R*, 10R*, 13S*)-4,9-dimethyl-1-methoxy-14-methylene-[11.2.1.0^{4,13}.0^{5,10}]-tetracyclopentadecane-9,5-carbolactone (210).
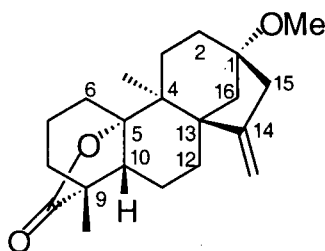
To a stirred solution of the diene **198** (19.0 mg, 0.044 mmol) in EtOAc (2.0 mL) at room temperature was added palladium-on-carbon (10% Pd, 4.7 mg, 0.0044 mmol Pd) and the resulting black suspension was stirred under an atmosphere (balloon) of H_2. After 25 minutes, the reaction mixture was placed directly on a plug of silica gel (5 g of silica gel) and the product was eluted with CH_2Cl_2 - Et_2O (5:1). The combined eluate was concentrated and the crude hydrogenation product **202** was used without further purification.

To a stirred solution of the crude hydrogenation product in dry THF (1.5 mL) at room temperature was added a solution of TBAF (1.0 M in THF, 88 μL, 0.088 mmol). The mixture was stirred for 20 minutes and then treated with saturated aqueous NH_4Cl (5 mL) and the resultant mixture was diluted with Et_2O (10 mL). The phases were separated and the aqueous phase was extracted with Et_2O (2 x 10 mL). The combined organic phases were washed with brine (1 x 10 mL), dried ($MgSO_4$) and concentrated to provide the crude tertiary alcohol **209**, which was used without further purification.

To a stirred solution of the crude tertiary alcohol **209** in dry THF (1.5 mL) at room temperature was added KH (3.5 mg, 0.88 mmol) and the mixture was stirred for 30 minutes. After this time, MeI (14 μL, 0.22 mmol) was added and the mixture was stirred for a further 30 minutes. Saturated aqueous NH_4Cl (5 mL) was added and the resultant mixture was diluted with Et_2O (10 mL). The phases were separated and the aqueous phase was extracted with Et_2O (2 x 10 mL).

The combined organic phases were washed with brine (1 x 10 mL), dried (MgSO$_4$) and concentrated. Purification of the crude product by flash chromatography (15 g of silica gel, 20:1 CH$_2$Cl$_2$ - Et$_2$O) and removal of trace amounts of solvent (vacuum pump) from the resulting solid provided 13.1 mg (91%) of the methyl ether **210** as a colorless solid (mp 128 °C).

^{1}H NMR (400 MHz, CDCl$_3$) δ: 4.98 (m, 2H), 3.22 (s, 3H), 2.42 (m, 2H), 2.11 (dd, 1H, J = 4.6, 14.9 Hz), 2.00 (dd, 1H, J = 5.3, 13.4 Hz), 1.95 (dd, 1H, J = 1.5, 11.5 Hz), 1.55-1.90 (m, 8H), 1.32-1.53 (m, 6H), 1.17 (s, 3H), 1.07 (s, 3H).

^{13}C NMR (100.5 MHz, CDCl$_3$) δ: 180.2 (+ve), 157.3 (+ve), 109.4 (+ve), 88.0 (+ve), 78.8 (+ve), 52.1 (-ve), 50.7 (-ve), 50.7 (+ve), 47.6 (+ve), 46.8 (+ve), 42.9 (+ve), 41.4 (+ve), 36.0 (+ve), 31.9 (+ve), 31.5 (+ve), 30.9 (+ve), 28.2 (+ve), 20.0 (+ve), 19.0 (-ve), 18.4 (+ve), 16.9 (-ve).

IR (KBr): 2932, 1766, 1445, 1142, 933 cm^{-1}.

Exact mass calcd for C$_{21}$H$_{30}$O$_3$: 330.2195; found: 330.2195.

Preparation of (±)-13-methoxy-15-oxo-17-norzoapatlin (**211**).
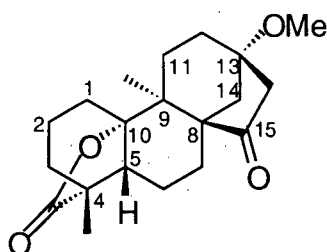
To a cold (0 °C), stirred solution of the methyl ether **210** (11.1 mg, 0.033 mmol) and $NaIO_4$ (29 mg, 0.14 mmol) in MeCN (0.5 mL), CCl_4 (0.5 mL) and H_2O (0.75 mL) was added a catalytic amount of $RuCl_3 \cdot H_2O$. After 40 minutes, H_2O (5 mL) was added to the dark brown mixture and the resultant mixture was diluted with CH_2Cl_2 (10 mL). The phases were separated and the aqueous phase was extracted with CH_2Cl_2 (2 x 10 mL). The combined organic phases were washed with brine (1 x 10 mL), dried ($MgSO_4$) and concentrated. Purification of the crude product by flash chromatography (15 g of silica gel, 15:1 CH_2Cl_2 - Et_2O) and removal of trace amounts of solvent (vacuum pump) from the resulting solid provided 8.7 mg (78%) of the ketone **211** as a colorless solid (mp 156-157 °C).

^1H NMR (400 MHz, $CDCl_3$) δ: 3.27 (s, 3H), 2.41 (dd, 1H, J = 4.2, 14.5 Hz), 2.33 (m, 2H), 2.24 (dd, 1H, J = 3.1, 11.8 Hz), 1.97 (ddd, 1H, J = 5.7, 12.2, 12.6 Hz), 1.85-1.95 (m, 3H), 1.71-1.82 (m, 2H), 1.54-1.70 (m, 7H), 1.45 (dd, 1H, J = 8.8, 14.9 Hz), 1.23 (m, 1H), 1.22 (s, 3H), 1.07 (s, 3H).

^{13}C NMR (100.5 MHz, $CDCl_3$) δ: 218.8 (+ve), 180.4 (+ve), 87.1 (+ve), 76.6 (+ve), 56.7 (+ve), 51.9 (-ve), 50.8 (-ve), 47.5 (+ve), 47.5 (+ve), 44.7 (+ve), 42.2 (+ve), 35.2 (+ve), 31.4 (+ve), 31.1 (+ve), 30.0 (+ve), 25.2 (+ve), 20.0 (+ve), 18.1 (+ve), 17.9 (-ve), 17.0 (-ve).

IR (KBr): 2943, 1770, 1733, 1458, 1281, 1141, 1124, 939 cm^{-1}.

Exact mass calcd for C$_{20}$H$_{28}$O$_4$: 332.1988; found: 332.1985.

Preparation of (±)-13-methoxy-15-oxozoapatlin (22).
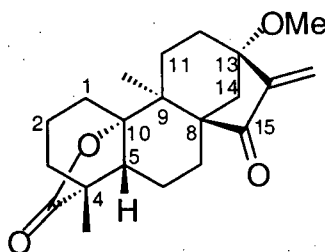
To a cold (-78 °C), stirred solution of the ketone 211 (6.0 mg, 0.018 mmol) in dry THF (1.0 mL) was added a solution of KHMDS (0.30 M in toluene, 120 µL, 0.036 mmol). After the mixture had been stirred for 15 minutes, it warmed to 0 °C and stirred for a further 45 minutes. Paraformaldehyde (5 mg, 0.17 mmol) was added and the mixture was stirred for 15 minutes at 0 °C and a further 1 hour at room temperature. The mixture was treated with saturated aqueous NH$_4$Cl (5 mL), stirred for 10 minutes and then diluted with Et$_2$O (10 mL). The phases were separated and the aqueous phase was extracted with Et$_2$O (2 x 10 mL). The combined organic phases were washed with brine (1 x 10 mL), dried (MgSO$_4$) and concentrated. The crude products were purified by flash chromatography (10 g of silica gel, 15:1 CH$_2$Cl$_2$ - Et$_2$O) and the appropriate fractions were combined and concentrated to provide 3.0 mg (51%) of recovered starting material (R$_F$ = 0.5, 4:1 CH$_2$Cl$_2$ - Et$_2$O) as a white solid and 2.5 mg (41%) of 13-methoxy-15-oxozoapatlin (22) (R$_F$ = 0.6, 4:1 CH$_2$Cl$_2$ - Et$_2$O) as a colorless solid (mp 134 °C).

^{1}H NMR (500 MHz, CDCl$_3$) δ: 6.12 (s, 1H, H-17), 5.35 (s, 1H, H-17), 3.24 (s, 3H, -OC$\underline{H}_3$), 2.49 (dd, 1H, J = 4.3, 14.4 Hz, H-5), 2.17 (dd, 1H, J = 7.5, 11.5 Hz, H-12), 2.15 (d, 1H, J = 11.8 Hz, H-14), 1.82-1.90 (m, 2H, H-2, H-7), 1.63-1.76 (m, 5H, H-1, H-6, H-11, H-12, H-14), 1.52-1.62 (m, 2H, H-3, H-3), 1.44-1.50 (m, 3H, H-1, H-7, H-11), 1.29 (m, 1H, H-6), 1.26 (s, 3H, H-20), 1.15 (m, 1H, H-2), 1.09 (s, 3H, H-19).

^{13}C NMR (100.5 MHz, CDCl$_3$) δ: 208.2 (+ve, C-15), 180.4 (+ve, C-18), 147.6 (+ve, C-16), 116.5 (+ve, C-17), 87.3 (+ve, C-10), 79.8 (+ve, C-13), 54.4 (+ve, C-8), 51.9 (-ve, C-5), 50.1 (-ve, C-O$\underline{C}$H$_3$), 47.5 (+ve, C-4), 43.1 (+ve, C-9), 40.6 (+ve, C-14), 35.3 (+ve, C-3), 34.7 (+ve, C-12), 31.7 (+ve, C-11), 31.2 (+ve, C-2), 25.5 (+ve, C-7), 20.0 (+ve, C-1), 18.6 (-ve, C-20), 18.2 (+ve, C-6), 17.1 (-ve, C-19).

IR (KBr): 2938, 1765, 1720, 1644, 1275, 1212, 1140, 1110 cm^{-1}.

Exact mass calcd for C$_{21}$H$_{28}$O$_4$: 344.1988; found: 344.1988.

The assignment of proton and carbon resonances observed in the ^{1}H and ^{13}C NMR spectra of (±)-13-methoxy-15-oxozoapatlin (**22**) are summarized in Tables 2.14. These assignments are based on analysis of HMQC and HMBC data.

Table 2.14. NMR data for (±)-13-methoxy-15-oxozoapatlin (**22**) (recorded in CDCl$_3$).
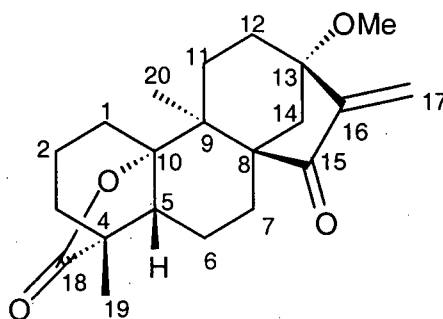
Carbon No.	^{13}C δ (ppm)^a	^{1}H δ (ppm) (mult, J (Hz))^{b,c}	HMBC^b
1	20.0	1.79 (m), 1.49 (m)	H-2, H-3
2	31.2	1.87 (m), 1.15 (m)	H-3
3	35.3	1.57 (m), 1.55 (m)	H-2, H-5, H-19
4	47.5		H-3, H-5, H-19
5	51.9	2.49 (dd, 4.3, 14.4)	H-1, H-6, H-7, H-19
6	18.2	1.66 (m), 1.29 (m)	H-5, H-7,
7	25.5	1.85 (m), 1.46 (m)	H-5, H-6
8	54.4		H-6, H-7, H-14, H-17
9	43.1		H-7, H-11, H-12, H-14, H-20
10	87.3		H-20
11	31.7	1.48 (m), 1.68 (m)	H-12, H-20
12	34.7	2.17 (dd, 7.5, 11.5) 1.68 (m)	H-11, H-14, H-17
13	79.8		H-11, H-12, H-14, H-17, H-21
14	40.6	2.15 (d, 11.8) 1.71 (m)	H-17
15	208.2		H-7, H-14, H-17
16	147.6		H-12, H-14, H-17
17	116.5	6.12 (s) 5.35 (s)	
18	180.4		H-3, H-5, H-19
19	17.1	1.09 (s)	
20	18.6	1.26 (s)	H-11
OMe	50.1	3.24 (s)	

^{a} Recorded at 100.5 MHz. ^{b} Recorded at 500 MHz. ^{c} Assignments based on HMQC data.

Appendix 2.1. X-Ray crystallographic data for the dione **109**.
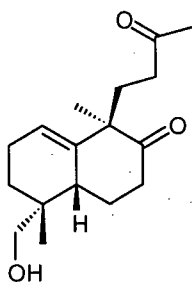
Compound	**109**
Formula	$C_{17}H_{26}O_3$
Formula Weight	278.39
Crystal Color, Habit	clear, block
Crystal dimensions	0.35 x 0.20 x 0.10 mm
Crystal System	orthorhombic
Space Group	Pccn (#56)
Lattice Parameters	
a (Å)	22.1223 (9)
b (Å)	15.4374 (6)
c (Å)	9.0417 (4)
V (Å^3)	3087.8 (2)
Z Value	8
D_{calc} (g/cm^3)	1.198
No. of reflections Measured	
Unique (R_{int} = 0.061)	3722
Total	27135

Appendix 2.2. X-Ray crystallographic data for the olefin 141.
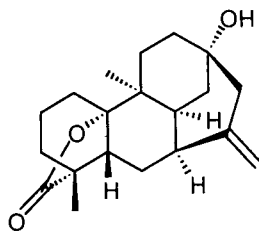
Compound	**141**
Formula	$C_{20}H_{28}O_3$
Formula Weight	316.44
Crystal Color, Habit	clear, chip
Crystal dimensions	0.40 x 0.20 x 0.20 mm
Crystal System	orthorhombic
Space Group	Pbca (#61)
Lattice Parameters	
a (Å)	17.3240 (9)
b (Å)	10.9278 (7)
c (Å)	17.0861 (8)
V (Å³)	3234.6 (5)
Z Value	8
D_{calc} (g/cm³)	1.299
No. of reflections Measured	
Unique (R_{int} = 0.047)	4213
Total	29928

2.6 References

(1)   Hanson, J. R. *Nat. Prod. Rep.* **2002**, *19*, 125 (and references cited therein).

(2)   Wani, M. C.; Taylor, H. L.; Wall, M. E.; Coggin, P.; Mcphail, A. T. *J. Am. Chem. Soc.* **1971**, *93*, 2325.

(3)   Schiff, P. B.; Fant, J.; Horwitz, S. B. *Nature* **1979**, *277*, 665.

(4)   Dewick, P. M. *Medicinal Natural Products*; John Wiley & Sons Ltd.: West Sussex, 1997.

(5)   Crimmins, M. T.; Pace, J. M.; Nantermet, P. G.; Kim-Meade, A. S.; Thomas, J. B.; Watterson, S. H.; Wagman, A. S. *J. Am. Chem. Soc.* **2000**, *122*, 8453. (and references cited therein).

(6)   Nakanishi, K. *Pure Appl. Chem.* **1967**, *14*, 89.

(7)   Braquet, P. *Drugs Future* **1987**, *12*, 643.

(8)   Crimmins, M. T.; Pace, J. M.; Nantermet, P. G.; Kim-Meade, A. S.; Thomas, J. B.; Watterson, S. H.; Wagman, A. S. *J. Am. Chem. Soc.* **2000**, *122*, 8453.

(9)   Bearder, J. R. *The Biochemistry and Physiology of Gibberellins*; Praeger: New York, **1983**; Vol. 1.

(10)   Graebe, J.; Dennis, D. T.; Upper, C. D.; West, C. A. *J. Biol. Chem.* **1965**, *240*, 1847.

(11)   For a review on the chemistry of gibberellins see: Mander, L. N. *Chem. Rev.* **1992**, *92*, 573.

(12)   Paleg, L. G. *A. Rev. Pl. Physiol.* **1965**, *16*, 291.

(13)   Delgado, G.; Romo de Vivar, A. *Chem. Lett.* **1984**, 1237.

(14)   Caballero, Y.; Walls, F. *Bol. Inst. Quim. Univ. Nac. Auton. Mex.* **1970**, *22*, 79.

(15)   The abstract in *Chem. Abstr.*, **74**, 136398w (**1971**), erroneously refered to zoapatlin (**14**) as a sesquiterpene lactone.

(16)   Ohno, N.; Mabry, T. J.; Zabel, V.; Watson, W. H. *Phytochemistry* **1979**, *18*, 1687.

(17)   Herz, W.; Govindan, S. V.; Blount, J. F. *J. Org. Chem.* **1979**, *44*, 2999.

(18)   Delgado, G.; Alvarez, L.; Romo de Vivar, A. *Phytochemistry* **1984**, *23*, 2674.

(19)   Garo, E.; Maillard, M.; Hostettmann, K.; StoeckliEvans, H.; Mavi, S. *Helv. Chim. Acta* **1997**, *80*, 538.

(20)   Lee, I. S.; Shamon, L. A.; Chai, H. B.; Chagwedera, T. E.; Besterman, J. M.; Farnsworth, N. R.; Cordell, G. A.; Pezzuto, J. M.; Kinghorn, A. D. *Chem.-Biol. Interact.* **1996**, *99*, 193.

(21) Rundle, N. T.; Xu, L.; Andersen, R. J.; Roberge, M. *J. Biol. Chem.* **2001**, *276*, 48231.

(22) See reference 11.

(23) Goldsmith, D. In *The Total Synthesis of Natural Products*; ApSimon, J., Ed.; Wiley-Interscience: New York, 1991; Vol. VIII, pp 1-243.

(24) Filippini, M.-H.; Rodriguez, J. *Chem. Rev.* **1999**, *99*, 27.

(25) Komppa, G.; Hirn, T. *Chem. Ber.* **1903**, *36*, 3610.

(26) Bell, R. A.; Ireland, R. E.; Partyka, R. A. *J. Org. Chem.* **1962**, *27*, 3741.

(27) Mori, K.; Nakahara, Y.; Matsui, M. *Tetrahedron* **1972**, *28*, 2411.

(28) Corey, E. J.; Carney, R. L. *J. Am. Chem. Soc.* **1971**, *93*, 7318.

(29) Marinovic, N. N.; Ramanathan, H. *Tetrahedron Lett.* **1983**, *24*, 1871.

(30) Duc, D. K.; Fetizon, M.; Lazare, S. *J. Chem. Soc., Chem. Commun.* **1975**, 282.

(31) Corey, E. J.; Liu, K. *Tetrahedron Lett.* **1997**, *38*, 7491.

(32) See for example: (a) Posner, G. H. *An Introduction to Synthesis Using Organocopper Reagents*; John Wiley & Sons: New York, **1980**. (b) Lipshutz, B. H.; Sengupta, S. *Org. React.* **1992**, *41*, 135.

(33) Vellekoop, A. S.; Smith, R. A. J. *Tetrahedron* **1998**, *54*, 11971.

(34) Paquette, L. A. *Angew. Chem. Int. Ed. Engl.* **1990**, *29*, 609.

(35) Evans, D. A.; Golob, A. M. *J. Am. Chem. Soc.* **1975**, *97*, 4765.

(36) Paquette, L. A. *Tetrahedron* **1997**, *53*, 13971.

(37) Evans, D. A.; Baillargeon, D. J.; Nelson, G. V. *J. Am. Chem. Soc.* **1978**, *100*, 2242.

(38) Chu, Y.; Colclough, D.; Hotchkin, D.; Tuazon, M.; White, J. B. *Tetrahedron* **1997**, *53*, 14235.

(39) For example see: (a) Piers, E.; Renaud, J. *J. Org. Chem.* **1993**, *58*, 11. (b) Piers, E.; Renaud, J.; Rettig, S. J. *Synthesis* **1998**, 590.

(40) For the synthesis of 2,3-bis(trimethylstannyl)propene see: Mitchell, T. N.; Kwekat, K.; Rutschow, D.; Schneider, U. *Tetrahedron* **1989**, *45*, 969. For synthetic applications of 2,3-bis(trimethylstannyl)propene see: Piers, E.; Kaller, A. M. *Synlett* **1996**, 549.

(41) Kaller, A. M., Ph. D. Thesis, Department of Chemistry, University of British Columbia, Vancouver, B.C., **1997**.

(42) Takai, K.; Tagashira, M.; Kuroda, T.; Oshima, K.; Utimoto, K.; Nozaki, H. *J. Am. Chem. Soc.* **1986**, *108*, 6048.

(43) Jin, H.; Uenishi, J.; Christ, W. J.; Kishi, Y. *J. Am. Chem. Soc.* **1986**, *108*, 5644.

(44) Nielson, A. T.; Houlihan, W. J. *Org. React.* **1968**, *16*, 1.

(45) Cardillo, G.; Orena, M. *Tetrahedron* **1990**, *46*, 3321.

(46) Takahashi, M.; Dodo, K.; Hashimoto, Y.; Shirai, R. *Tetrahedron Lett.* **2000**, *41*, 2111.

(47) Boukouvalas, J.; Cheng, Y.-X.; Robichaud, J. *J. Org. Chem.* **1998**, *63*, 228.

(48) Magnuson, S. R.; Sepp-Lorenzino, L.; Rosen, N.; Danishefsky, S. J. *J. Am. Chem. Soc.* **1998**, *120*, 1615.

(49) Corey, E. J.; Desai, M. C.; Engler, T. A. *J. Am. Chem. Soc.* **1985**, *107*, 4339.

(50) Lowry, T. H.; Richardson, K. S. *Mechansim and Theory in Organic Chemistry*; Harper & Row: New York, **1987**; Vol. 3.

(51) Ramachandran, S.; Newman, M. S. *Org. Synth.* **1961**, *41*, 38.

(52) Kagechika, K.; Oshima, T.; Shibasaki, M. *Tetrahedron* **1993**, *49*, 1773.

(53) Tsuda, T.; Suzuki, M.; Noyori, R. *Tetrahedron Lett.* **1980**, *21*, 1357.

(54) Oshima, T.; Kagechika, K.; Adachi, M.; Sodeoka, M.; Shibasaki, M. *J. Am. Chem. Soc.* **1996**, *118*, 7108.

(55) Wendler, N. L.; Slates, H. L.; Tishler, M. *J. Am. Chem. Soc.* **1951**, *73*, 3816.

(56) McMurry, J. E.; Scott, W. *Tetrahedron Lett.* **1983**, *24*, 979.

(57) Scott, W. J.; Stille, J. K. *J. Am. Chem. Soc.* **1986**, *108*, 3033.

(58) McMurry, J. E.; Scott, W. J. *Tetrahedron Lett.* **1980**, *21*, 4313.

(59) For development of the cuprous chloride accelerated Stille reaction see: (a) Farina, V.; Kapadia, S.; Krishnan, B.; Wang, C.; Liebeskind, L. S. *J. Org. Chem.* **1994**, *59*, 5905. (b) Liebeskind, L. S.; Fengl, R. *J. Org. Chem.* **1990**, *55*, 5459. For the application of this reaction to the coupling of sterically congested substrates see: (c) Han, X.; Stoltz, B. M.; Corey, E. J. *J. Am. Chem. Soc.* **1999**, *121*, 7600.

(60) Hunt, I.; Rogers, C.; Woo, S.; Rauk, B.; Keay, B. *J. Am. Chem. Soc.* **1995**, *117*, 1049.

(61) Snider, B. *J. Am. Chem. Soc.* **1979**, *101*, 5283.

(62) Winterfeldt, E. *Synthesis* **1975**, 617.

(63) Hagiwara, H.; Uda, H. *J. Chem. Soc., Chem. Commun.* **1987**, 1351.

(64) We thank Dr. Brian Patrick (of the X-ray Crystallographic Laboratory in the Department of Chemistry at UBC) for performing the X-ray structure determinations. All X-ray structure determinations were performed on racemic materials.

(65)   Griffith, W. P.; Ley, S. V. *Aldrichim. Acta.* **1990**, *23*, 1.

(66)   Kraus, G. A.; Roth, B. *J. Org. Chem.* **1980**, *45*, 4825.

(67)   Bartlett, P. A.; Richardson, D. P.; Myerson, J. *Tetrahedron* **1984**, *40*, 2317.

(68)   Furber, M.; Kraft-Klaunzer, P.; Mander, L. N.; Pour, M.; Yamaguchi, T.; Murofushi, N.; Yamane, H.; Schraudolf, H. *Aust. J. Chem.* **1995**, *48*, 427.

(69)   Crich, D.; Beckwith, A. L. J.; Filzen, G. F.; Longmore, R. W. *J. Am. Chem. Soc.* **1996**, *118*, 7422.

(70)   Jasperse, C. P.; Curran, D. P.; Fevig, T. L. *Chem. Rev.* **1991**, *91*, 1237.

(71)   Curran, D. P. In *Comprehensive Organic Synthesis: Additions to and Substitutions at C=C π Bonds*; Trost, B. M., Flemming, I., Semmelhack, M. F., Eds.; Permagon Press: New York, 1991; Vol. 4.

(72)   Curran, D. P.; Porter, N. A.; Giese, B. *Stereochemistry of Radical Reactions*; VCH Verlagsgesellschaft mbH: Wienheim, 1996.

(73)   The molecular modeling software: Hyperchem release 4 for Windows (**1994**) was used to determine the relative energies of structural isomers. All geometry optimizations were executed using molecular mechanics (MM+) calculations.

(74)   Carey, F. A.; Sundberg, R. J. *Advanced Organic Chemistry, Part B: Reactions and Synthesis*; Plenum Press: New York, 1993; Vol. 3.

(75)   Flemming, F. F., Ph. D. Thesis, Department of Chemistry, University of British Columbia, Vancouver, B.C., **1990**.

(76)   Stork, G. E.; Baine, N. H. *Tetrahedron Lett.* **1985**, *26*, 5927.

(77)   Toyota, M.; Yokota, M.; Ihara, M. *Tetrahedron Lett.* **1999**, *40*, 1551.

(78)   Toyota, M.; Yokota, M.; Ihara, M. *J. Am. Chem. Soc.* **2001**, *123*, 1856.

(79)   Stork, G. E.; Mook, R. *Tetrahedron Lett.* **1986**, *27*, 4529.

(80)   *CRC Handbook of Chemistry and Physics*; 70th ed.; CRC: Boca Raton, 1990.

(81)   Molander, G. A.; Harris, C. R. *Chem. Rev.* **1996**, *96*, 307.

(82)   Molander, G. A.; Harris, C. R. *Tetrahedron* **1998**, *54*, 3321.

(83)   Sono, M.; Nakashiba, Y.; Nakashima, K.; Tori, M. *J. Org. Chem.* **2000**, *65*, 3099.

(84)   Sono, M.; Hashimoto, A.; Nakashima, K.; Tori, M. *Tetrahedron Lett.* **2000**, *41*, 5115.

(85)   Snider, B.; Vo, N. H.; O'Niel, S. V. *J. Org. Chem.* **1998**, *63*, 4732.

(86)   Molander, G. A.; Hahn, G. *J. Am. Chem. Soc.* **1986**, *51*, 1135.

(87)   Ashimori, A.; Bachand, B.; Overman, L. E.; Poon, D. J. *J. Am. Chem. Soc.* **1998**, *120*, 6477.

(88)   Ashimori, A.; Bachand, B.; Calter, M. A.; Govek, S. P.; Overman, L. E.; Poon, D. J. *J. Am. Chem. Soc.* **1998**, *120*, 6488.

(89)   Beletskaya, I. P.; Cheprakov, A. V. *Chem. Rev.* **2000**, *100*, 3009.

(90)   Negishi, E.-I.; Coperet, C.; Ma, S.; Liou, S.-Y.; Liu, F. *Chem. Rev.* **1996**, *96*, 365.

(91)   de Meijere, A.; Meyer, F. E. *Angew. Chem. Int. Ed. Engl.* **1994**, *33*, 2379.

(92)   Owczarczyk, Z.; Lamaty, F.; Vawter, E. J.; Negishi, E.-I. *J. Am. Chem. Soc.* **1992**, *114*, 10091.

(93)   Grigg, R.; Sridharan, V.; Sukirthalingham, S. *Tetrahedron Lett.* **1991**, *32*, 3855.

(94)   For examples in which stable palladium containing products have been isolated from intramolecular Pd(0) catalyzed cyclizations see: (a) Eichberg, M. J.; Dorta, R. L.; Grotjahn, D. B.; Lamottke, K.; Schmidt, M.; Vollhardt, P. C. *J. Am. Chem. Soc.* **2001**, *123*, 9324. (b) Danishefsky, S. J.; Masters, J. J.; Young, W. B.; Link, J. T.; Snyder, L. B.; Magee, T. V.; Jung, D. K.; Isaacs, R. C. A.; Bornmann, W. G.; Alaimo, C. A.; Coburn, C. A.; Di Grandi, M. J. *J. Am. Chem. Soc.* **1996**, *118*, 2843.

(95)   Hegedus, L. S. In *Organometallics in Synthesis*; Schlosser, M., Ed.; John Wiley & Sons: New York, 1995; pp 420-423.

(96)   Marcoux, J.-F.; Doye, S.; Buchwald, S. L. *J. Am. Chem. Soc.* **1997**, *119*, 10539.

(97)   Hartwig, J. F. *Angew. Chem. Int. Ed. Engl.* **1998**, *37*, 2046.

(98)   For the original reports regarding the synthesis of vinyl acetate from ethylene and Pd(OAc)$_2$ in acetic acid see: (a) Moiseev, I. I.; Vargaftic, M. N.; Syrkin, Y. K. *Dolk. Akad. Nauk. SSSR* **1960**, *133*, 377. (b) Smidt, J.; Hafner, W.; Jira, R.; Sedlmeier, J.; Sieber, R.; Ruttinger, R.; Kojer, H. *Angew. Chem.* **1962**, *74*, 93.

(99)   For an example of an intramolecular Heck reaction requiring stoichiometric quantities of Pd(OAc)$_2$ see reference 94 (b).

(100) Corey, E. J.; Sarshar, S.; Azimioara, M. D.; Newbold, R. C.; Noe, M. C. *J. Am. Chem. Soc.* **1996**, *118*, 7851.

(101) He, F.; Bo, Y.; Altom, J. D.; Corey, E. J. *J. Am. Chem. Soc.* **1999**, *121*, 6771.

(102) Carlsen, H. J.; Katsuki, T.; Martin, V. S.; Sharpless, K. B. *J. Org. Chem.* **1981**, *46*, 3936.

(103) Ward, D. *Can. J. Chem.* **1987**, 2380.

(104) Bailey, P.; Lane, A. G. *J. Am. Chem. Soc.* **1967**, *89*, 4473.

(105) Barrero, A. J.; Alvarez-Manzaneda, E. J.; Chahboun, R.; Cuerva, J. M.; Segovia, A. *Synlett* **2000**, *9*, 1269.

(106) Skupinska, K., Ph. D. Thesis, Chemistry Department, University of British Columbia, Vancouver, B.C., **2000**.

(107) Bryan, W. P.; Byrne, R. H. *J. Chem. Educ.* **1970**, *47*, 361.

(108) Still, W. C.; Kahn, M.; Mitra, A. *J. Org. Chem.* **1978**, *43*, 2923.

3. Isolation, Structure Elucidation, Total Synthesis and Biological Evaluation of Granulatimide Alkaloids

3.1 Introduction

There has been tremendous success in the discovery of unique compounds from marine organisms since 1950, generally considered the birth-date of marine natural product chemistry.[1] Traditionally these discoveries have resulted from chemical investigations on invertebrates such as sponges, soft corals, and molluscs. However, as screening for biological activity and specimen collection techniques have become more sophisticated, the realm of organisms studied by marine natural product chemists has expanded. Recently, numerous reports have cited sessile, filter feeding ascidians as a new source of biologically active and structurally novel compounds.[2]

Ascidians belong to the phylum Chordata, owing to the presence of a primitive spinal chord during their larval stage of development.[3] The larval spinal chord, first reported in 1866, placed ascidians in the same phylum as mammals and was an important factor in bringing about the acceptance of Darwin's evolutionary theory.[3] Members of the class Ascidiacea (ascidians), along with two other classes included in the subphylum Urochordata, have a sac-like body which is enclosed in an outer sheath or tunic. Consequently, these organisms are most commonly referred to as tunicates.[3]

Typically bright in color, ascidians attracted interest from scientists as early as 1847. An observation by a German physiologist that, upon exposure to air, ascidian blood changed in color from yellow-green to deep blue, led eventually to the discovery of the hydroquinoid tunichromes (e.g. tunichrome An-1 (1)).[4,5] These blood pigments are apparently involved in the sequestration of vanadium by ascidians, providing concentrations of the metal 10 million times greater than

that found in seawater. More recently, attention has focused on biologically active metabolites produced by ascidians. The first of these was the cytotoxic metabolite geranyl hydroquinone (**2**) isolated by Fenical and co-workers from an *Aplidium sp.* (Figure 3.1).[6]

3 R$_1$ = OH, R$_2$ = H
4 R$_1$ = R$_2$ = O
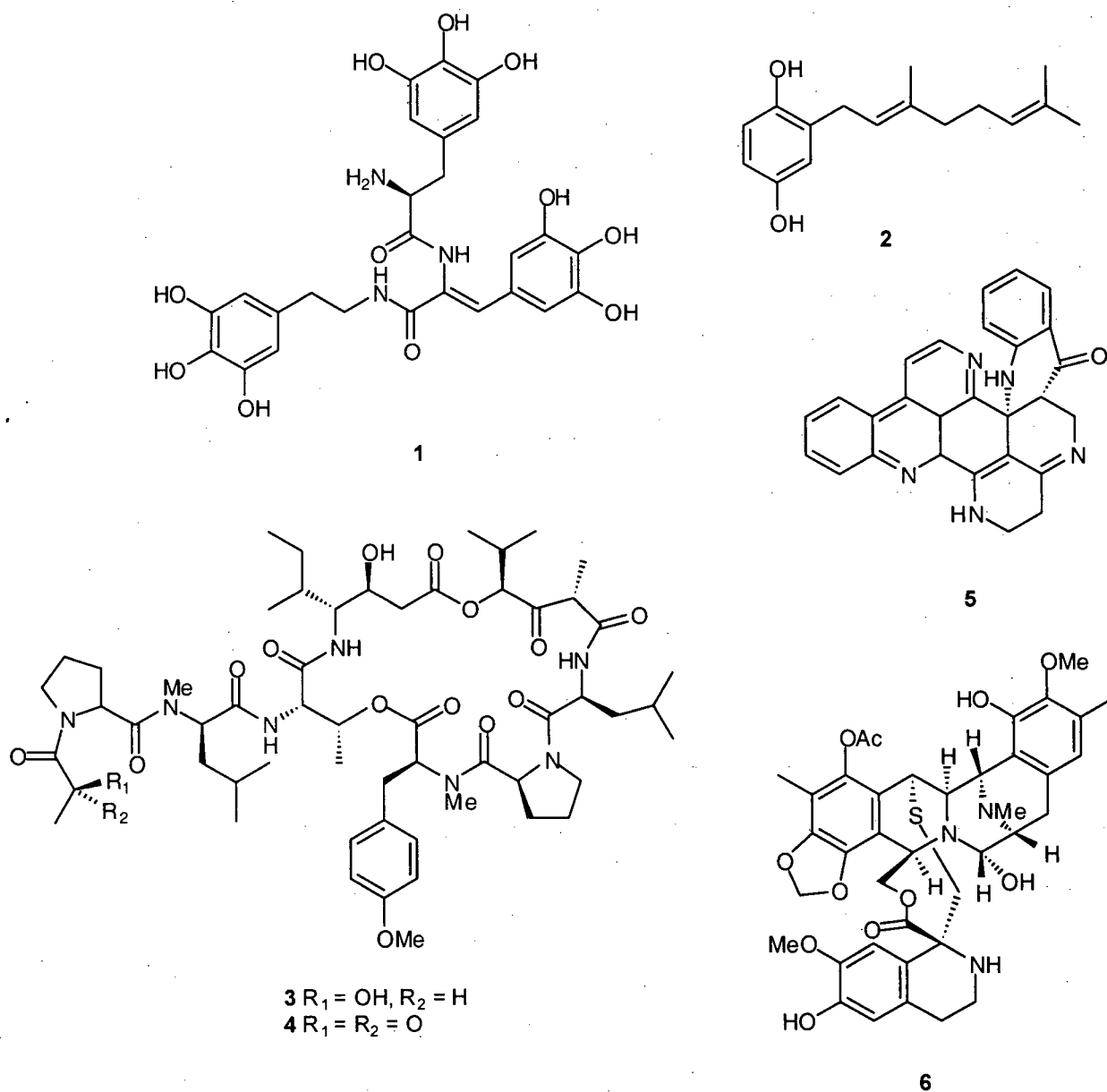
Figure 3.1. Natural products isolated from ascidians.

Over the last three decades, the metabolites isolated from ascidians have predominantly been nitrogenous compounds, with peptides representing the majority of ascidian natural

products reported to date. Included among the ascidian peptides is didemnin B (**3**), a cyclodepsipeptide isolated from the Caribbean ascidian *Trididemnum solidum*.[7] An oxidized derivative of **3**, dehydrodidemnum B (**4**), is presently in clinical trials as an antitumor agent.[8] Although structurally unique peptides continue to be isolated from ascidians, the fastest growing class of ascidian secondary metabolites reported in the literature are the polycyclic aromatic alkaloids, which include eudistone A (**5**), isolated from an ascidian of the genus *Eudistoma*.[9] Because members of this class of compounds are highly unsaturated, few protons exist for spectroscopic proton-proton correlation experiments (e.g. COSY, TOCSY, NOE) and, consequently, the structure determination of alkaloids such as **5** continue to challenge natural product chemists. However, aided by the increasing sophistication of spectroscopic techniques, which now include long-range heteronuclear coupling experiments, the structure determination of these complex natural products has become routine. For example, the water-soluble alkaloid ecteinascidin (**6**), first isolated from the ascidian *Ecteinascidia turbinata* in 1969,[10] has recently succumbed to structural identification and is currently in clinical trials as an anticancer agent.[8]

Ongoing interest in the origin of these complex alkaloids has led to numerous reports regarding the biosynthesis of ascidian metabolites. A common biogenesis has been proposed for the alkaloids polycitone A (**7**) and polycitrin A (**8**), both isolated from the Indo Pacific ascidian *Polycitor sp.* (Scheme 3.1).[11] An oxidative dimerization of 4-hydroxyphenyl pyruvic acid (**9**), derived from tryrosine, and condensation of the resulting dimer with tyramine yields the dicarboxylic acid **10**, a plausible intermediate in the biosynthesis of both **7** and **8**. *Ortho*-bromination of the pyrrolyl hydroxyphenyl functions in **10** would then provide the bromo phenol **11**. Polycitone A (**7**) could be accessed from **11** via activation of the two carboxylic acid moieties and subsequent addition of two substituted phenyl units. Alternatively, oxidative decarboxylation of **11** would provide polycitrin A (**8**). This proposed biogenesis has been supported by a short, biomimetic synthesis of **8**.[12] Additionally, the isolation of lycogalic acid

(12) and arcyriarubin A (13) from the slime mould *Lycogala epidendrum* lends credence to this biosynthetic proposal (Figure 3.2).[13]
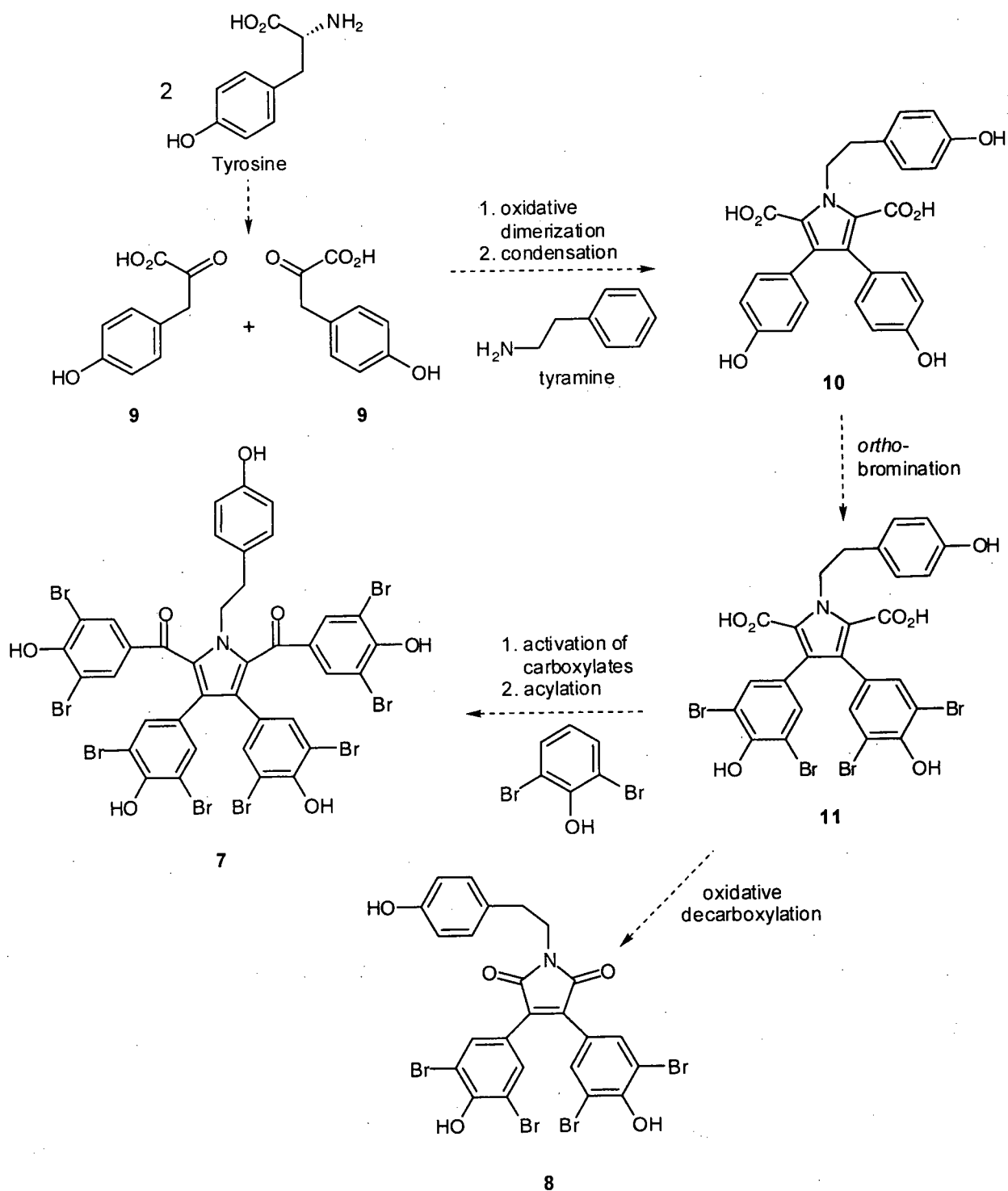
Scheme 3.1. Proposed biosynthesis polycitone A (7) and polycitrin A (8).

Figure 3.2. Lycogalic acid (**12**) and arcyriarubin A (**13**).

In addition to the polycitrins (e.g. **8**), various other substituted maleimides have been isolated from ascidians. The didemnimides A-D (**14-17**), isolated from the Caribbean mangrove ascidian *Didemnum conchyliatum*,[14] and the dihydro maleimide **18**, recently isolated from the ascidian *Eudistoma toealensis*,[15] are members of this growing family of alkaloids (Figure 3.3). Biosynthetically, the didemnimides could be derived from the oxidative decarboxylation of the dicarboxylic acid **19** as outlined in Scheme 3.2. The dicarboxylic acid **19** should, in turn, be formed in an analogous fashion to **10** (Scheme 3.1), through the oxidative coupling of indole pyruvic acid (**20**) with imidazole pyruvic acid (**21**) and a subsequent condensation with ammonia.

14 R₁ = R₂ = H
15 R₁ = Br, R₂ = H
16 R₁ = H, R₂ = CH₃
17 R₁ = Br, R₂ = CH₃

18

Figure 3.3. Substituted maleimides isolated from ascidians.

Scheme 3.2. Proposed biosynthesis of didemnimide A (**14**).

The structure elucidation of ascidian secondary metabolites continually forces natural product chemists to draw on new spectroscopic tools and a thorough understanding of alkaloid biosynthesis. However, the biological evaluation of many of these metabolites has provided valuable leads in the ongoing pursuit for new, more selective cancer chemotherapeutics. The following sections discuss the isolation, structure elucidation, total synthesis and biological activity of a new class of alkaloids produced by the Brazilian ascidian *Didemnum granulatum*. Chromatographic acquisition, spectroscopic analysis and proposal of candidate structures for the natural product were carried out by Dr. Roberto Berlinck while on sabbatical at UBC (Instituto de Quimica de Sao Carlos, Universidade de Sao Paulo, Brazil).

3.2 Isolation of a G2 checkpoint inhibitor from *Didemnum granulatum*

Until recently, the marine organisms inhabiting the coastline of Brazil were unexplored as a potential source of novel, biologically active natural products. Traditionally, chemists have concentrated on natural products produced by terrestrial plants, abundant in Brazil's rich

rainforests. However, collaboration between our research group and Brazilian scientists has focused on the investigation of secondary metabolites produced by marine organisms that inhabit the coastal waters of Brazil. This collaboration resulted in collection of the ascidian *Didemnum granulatum,* whose ethanolic extract displayed promising activity in a screen for G2 checkpoint inhibitors.
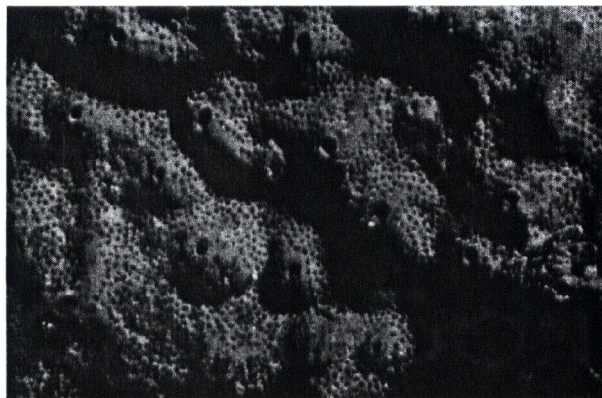
Figure 3.4. Photograph of *Didemnum granulatum.*[16]

The ascidian *D. granulatum* (Figure 3.4) occurs in rocky, shallow water marine habitats along the coastline of southern Brazil. Specimens of *D. granulatum* were collected by hand using SCUBA at Araca Beach, São Sebastião in August of 1995 and at Arquipelago do Arvoredo and the São Sebastião Channel in November of 1997 (Figure 3.5), and were immediately immersed in EtOH. Further work up involved decanting the EtOH followed by blending the ascidian tissue with MeOH and exhaustively extracting the solid residue with fresh MeOH. Concentration of the organic extract and further fractionation, via Sephadex LH20 chromatography, provided a number of deep red and orange colored fractions, one of which demonstrated G2 checkpoint inhibition activity. The major compound in the active fraction was further purified by reversed phase HPLC to yield a red amorphous solid, which in its pure form, exhibited G2 checkpoint inhibition activity. Further fractionation of the inactive, colored fractions by reversed phase

HPLC yielded didemnimides A (**14**), B (**15**) and D (**17**) (Figure 3.3) which were identified by comparison of their spectroscopic data with that reported in the literature.[14]
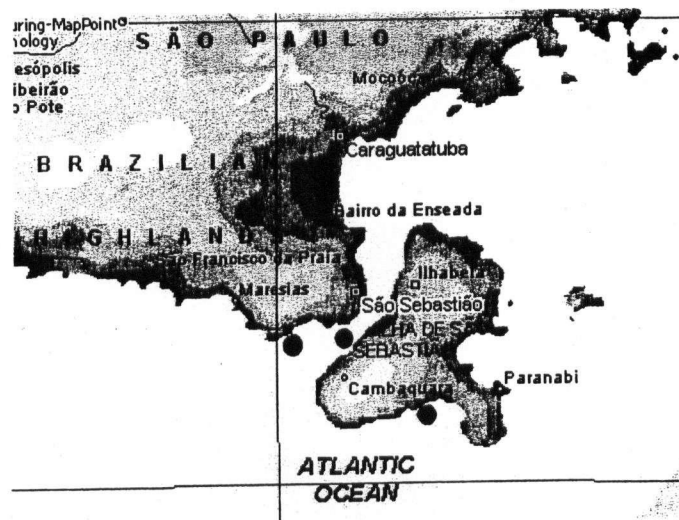
Figure 3.5. Map of collection sites (●) for *Didemnum granulatum.*

The G2 checkpoint inhibitor gave an (M+H)$^+$ ion in high resolution FAB mass spectrum (HRFABMS) at *m/z* 277.0714, which was accounted for by the molecular formula $C_{15}H_8N_4O_2$. The HRFABMS differed from that of didemnimide A (**14**) by two mass units, corresponding to an additional degree of unsaturation. Comparison of ^{1}H NMR spectra recorded on **14** (*vide infra*) and the checkpoint inhibitor (Figure 3.6) confirmed the absence of two aromatic proton signals. This data led to the proposal of two candidate structures for the checkpoint inhibitor (Scheme 3.3), both of which are cyclized didemnimides, termed granulatimide (**22**) and isogranulatimide (**23**). Biogenetically, granulatimide (**22**) could arise through a 6π-electrocyclization of didemnimide A (**14**), thus forming a new bond between the indole C-2 and imidazole C-14. Oxidation of the dihydro intermediate **24** would give rise to the planar aromatic alkaloid, granulatimide (**22**). Alternatively, an intramolecular 1,6 addition of **14B**, a tautomer of

Candidate structures
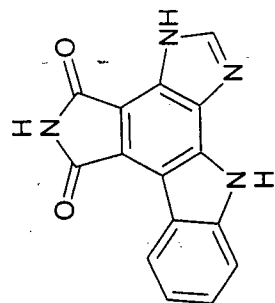
22
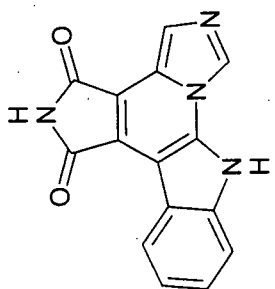
23
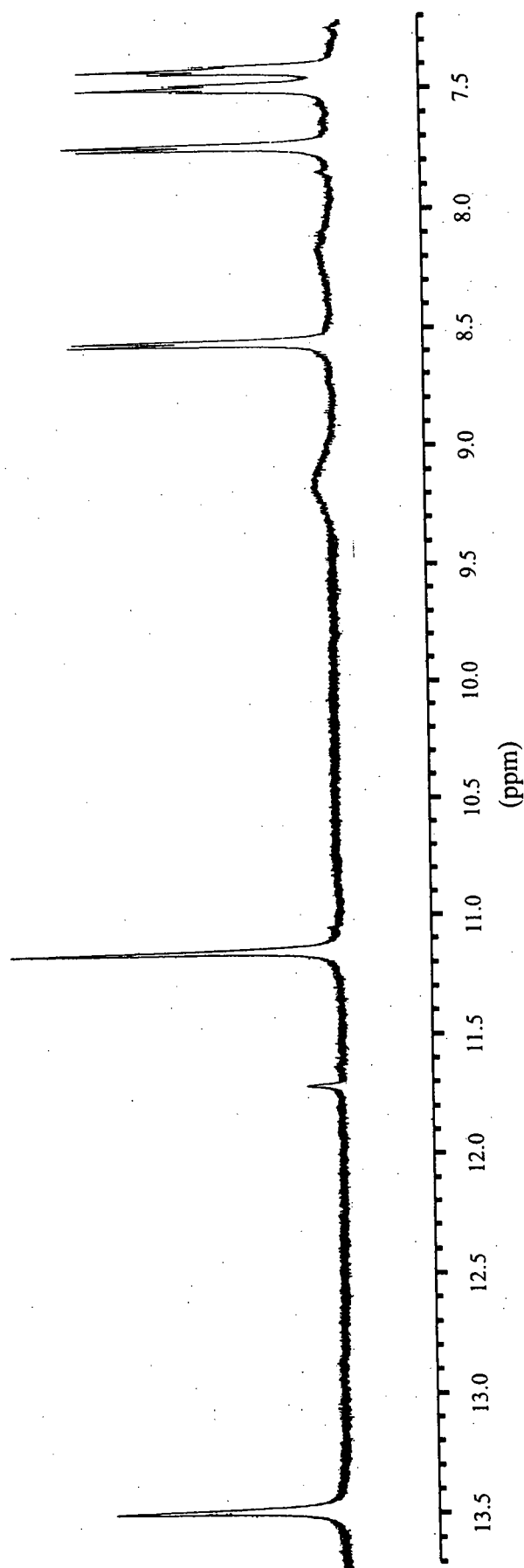
Figure 3.6. ^{1}H NMR spectra of the G2 checkpoint inhibitor (recorded in DMSO-d_6, 500 MHz)

didemnimide A (14), would generate the intermediate 26. Oxidation of the latter species (or of a structurally related intermediate derived from 26) would regenerate the indole system, thus providing isogranulatimide (23).
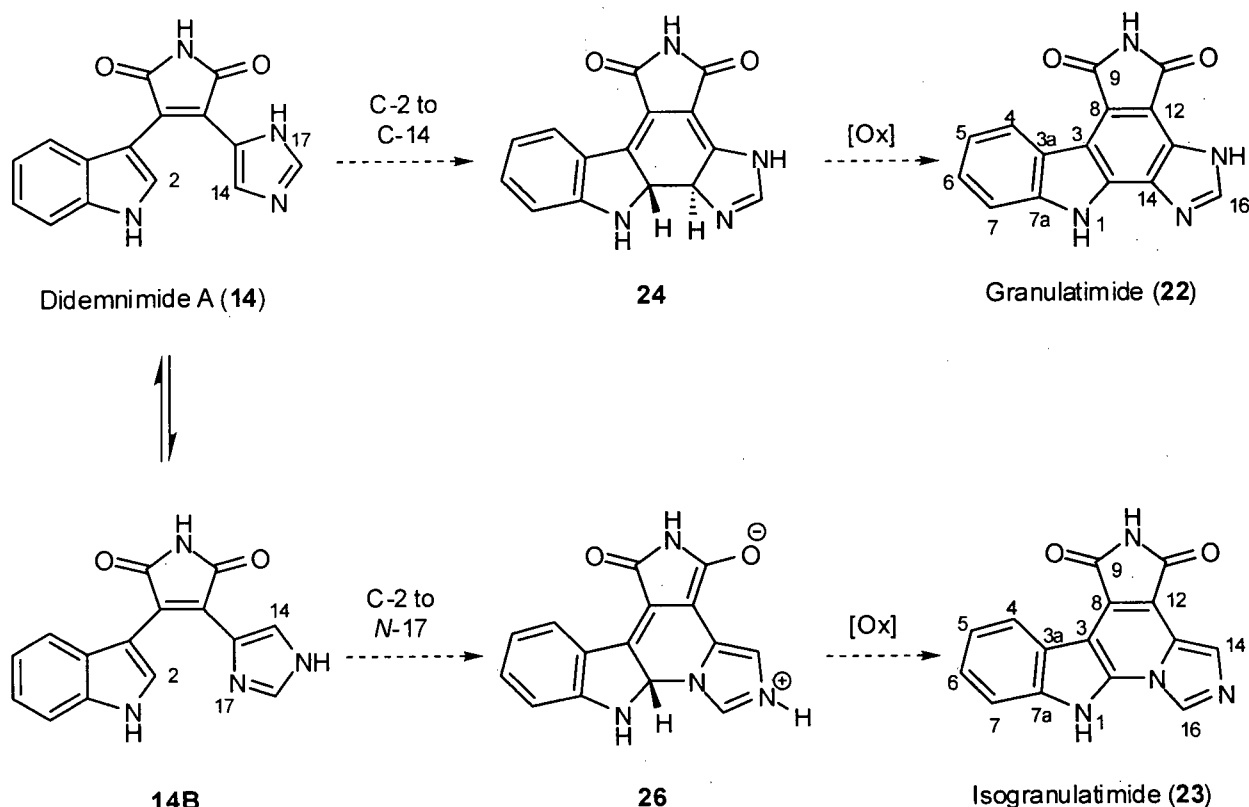
Scheme 3.3. Proposed biosynthesis of granulatimide (22)
and isogranulatimide (23) from didemnimide A (14).

Evidence in support of a planar, polycyclic aromatic structure for the G2 checkpoint inhibitor could be found in the ^{1}H NMR spectroscopic data. The large chemical shift observed for the H-4 resonance (δ 8.51) in the G2 checkpoint inhibitor (see Figure 3.6) relative to the chemical shift observed for the H-4 resonance in didemnimide A (14) (δ 7.07)[14] can be attributed to a deshielding effect from the neighboring C-9 maleimide carbonyl in either candidate structure 2 2 or 23. A similar diamagnetic anisotropic effect deshields the H-4 resonance in staurosporinone (27) (DMSO-d_6 δ 9.36)[17] and arcyriaflavin A (28) (DMSO-d_6 δ 9.15)[18] relative

to the H-4 resonance in arcyriarubin A (13) (DMSO-d_6 δ 7.33)[18] (Figure 3.7). The deshielding effect of the maleimide carbonyl on H-4 in the ^{1}H NMR of the checkpoint inhibitor and not in didemnimide A (14) was consistent with the proposed planar aromatic structures 22 and 23 (Scheme 3.3).

13
δ 7.33 (H-4)

27
δ 9.26 (H-4)

28
δ 9.15 (H-4)
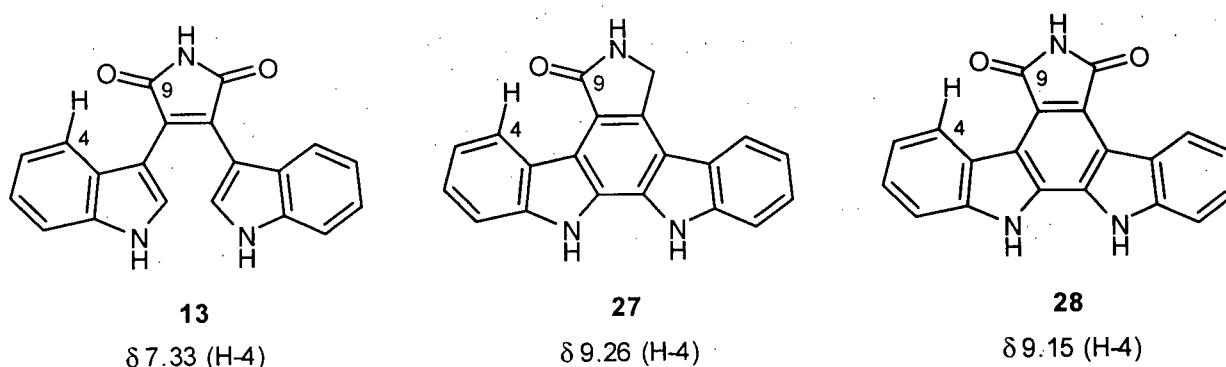
Figure 3.7. Bis-indolyl maleimide and indolocarbazole natural products and the ^{1}H NMR chemical shift of H-4 (DMSO-d_6).

In principle, a variety of different NMR spectroscopic experiments should readily distinguish between the candidate structures 22 and 23. However, the two key resonances at δ 8.10 and δ 9.12 in the ^{1}H NMR spectrum of the G2 checkpoint inhibitor (Figure 3.6), that could be assigned to the imidazole fragment, gave very broad signals that failed to show any HMBC or HMQC correlations or nuclear Overhauser enhancements (NOEs), precluding a clear spectroscopic resolution of the structural problem. The broadness of the imidazole resonances in the NMR spectra of the checkpoint inhibitor was attributed to a tautomeric equilibrium involving the imidazole NH proton. Similar broadening of the imidazole CH and NH proton resonances was also observed in the ^{1}H NMR spectrum of didemnimide A (14) and the related analogues which do not have a methyl substituent on one of the imidazole nitrogens. In contrast, didemnimide C (16), which has methyl substitution on one of the imidazole ring nitrogens, gives sharp, well-resolved NMR spectra.[14] By analogy with the didemnimides, only one of the

candidate structures for the checkpoint inhibitor, granulatimide (**22**), would be expected to undergo tautomeric equilibrium involving an imidazole *N*H. Therefore, the observed broadening of the ^{1}H NMR signals assigned to the imidazole fragment of the inhibitor appeared to be most consistent with candidate structure **22**. From a biogenetic perspective, it seemed reasonable that the co-occurring alkaloid didemnimide A (**14**) represented a logical precursor to either candidate structure **22** or **23** (Scheme 3.3). Structure **22** is related to staurosporinone (**27**),[17] arcyriaflavin (**28**)[18] and other polycyclic naturally occurring bisindole maleimides, whereas structure **23** was apparently without precedent among natural products. Therefore, from a biogenetic perspective, **22** was also deemed to be the most probable structure for the G2 checkpoint inhibitor.

Since it was not possible to distinguish between candidate structures **22** and **23** using the available spectroscopic data, it was decided to resolve the issue through total synthesis. The synthesis was also required to generate sufficient material for complete biological evaluation. Based on the combination of chemical and biogenetic arguments presented above, granulatimide (**22**) was believed to be the most probable structure for the checkpoint inhibitor and was therefore chosen as the initial synthetic target. The following sections describe the development of methodology generally useful for the synthesis of substituted maleimides and the application of these methods to the synthesis of granulatimide (**22**).

3.3 Syntheses of substituted maleimides

A growing number of substituted maleimides and indolocarbazoles have shown pronounced biological activity and hence their syntheses have garnered much interest. The arcyriarubins (e.g. **13**) (Figure 3.2), a family of bis-indolyl maleimide pigments produced by slime moulds, represent the simplest members of this family.[18] These slime mould compounds have recently become a scaffold for the creation of highly selective inhibitors of protein kinase C

(PKC), a family of phosphorylating enzymes which play a crucial role in cellular processes such as signal tansduction and cell growth. This new generation of PKC inhibitors includes the bis-indolyl maleimides GF 109203X (29), Ro 32-0432 (30) and LY333531 (31) (Figure 3.8).[19] Perhaps of greater interest to pharmaceutical chemists, however, is the potential intermediacy of bis-indolyl maleimides in the synthesis of indolocarbazole alkaloids such as staurosporine (32),[20] one of the most potent inhibitors of PKC, and the antitumor antibiotic rebeccamycin (33).[21]
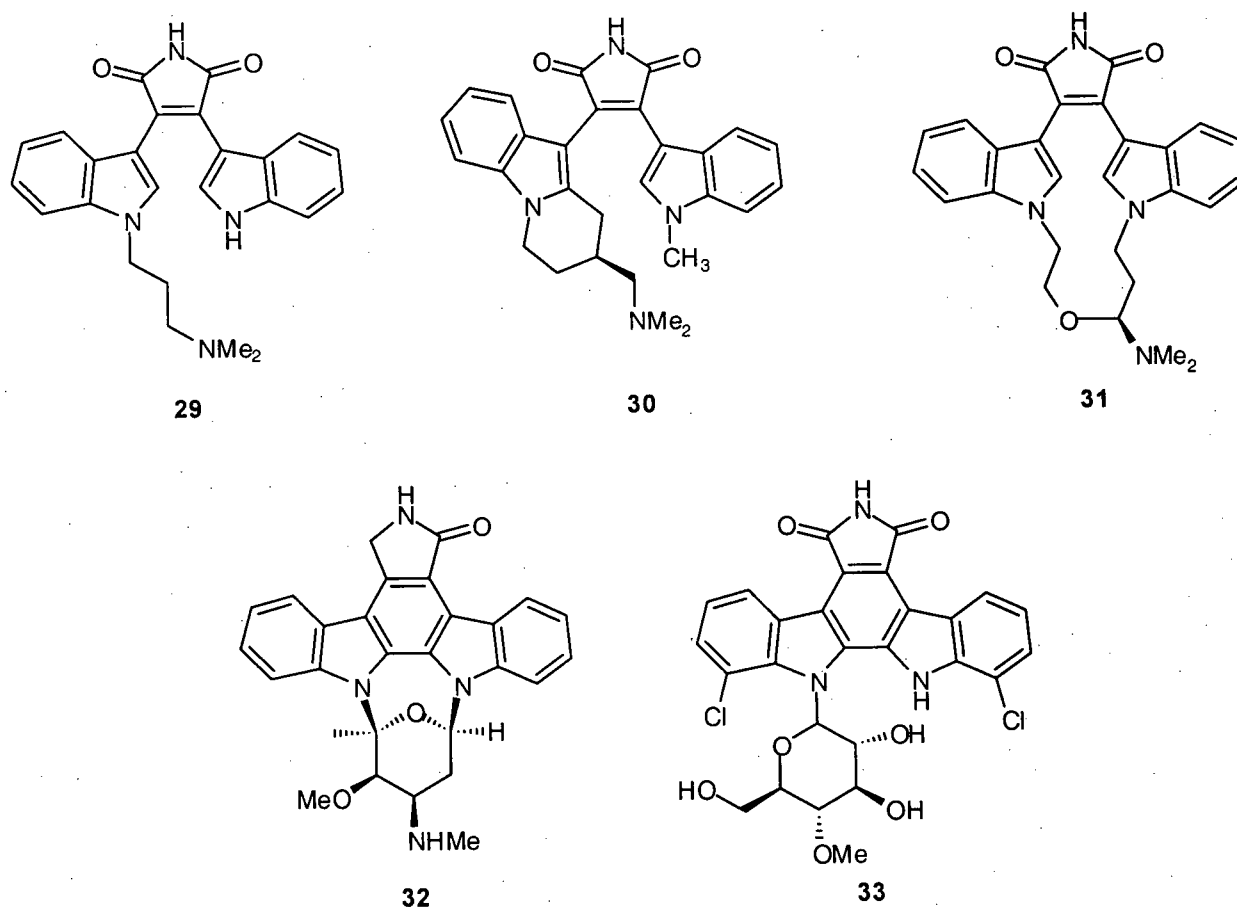
Figure 3.8. Biologically active bis-indolyl maleimide and indolocarbazoles.

The most common method for the preparation of bis-indolyl maleimides involves the addition of indolylmagnesium bromide (34) to a 2,3-dihalomaleimide (e.g. 35). Steglich and co-workers were the first to demonstrate the potential of this reaction in the synthesis of

arcyriarubin A (13).[18] The key step in a synthesis of 13 involved the addition of four equivalents

of indolylmagnesium bromide (34) to 2,3-dibromo-*N*-methylmaleimide (35), which afforded the

bis-indolyl maleimide 36 in high yield (Scheme 3.4). Although this reaction provided rapid

access to bis-indolyl maleimides, the use of two additional equivalents of indolylmagnesium

bromide (34) was deemed necessary, as the product of the reaction, compound 36, is a stronger

acid than indole itself and thus consumes an equivalent of 34. Further limitations to this process

included the restriction of target molecules to symmetrical bis-indolyl maleimides and the

necessary protection of the relatively acidic maleimide *N*H.
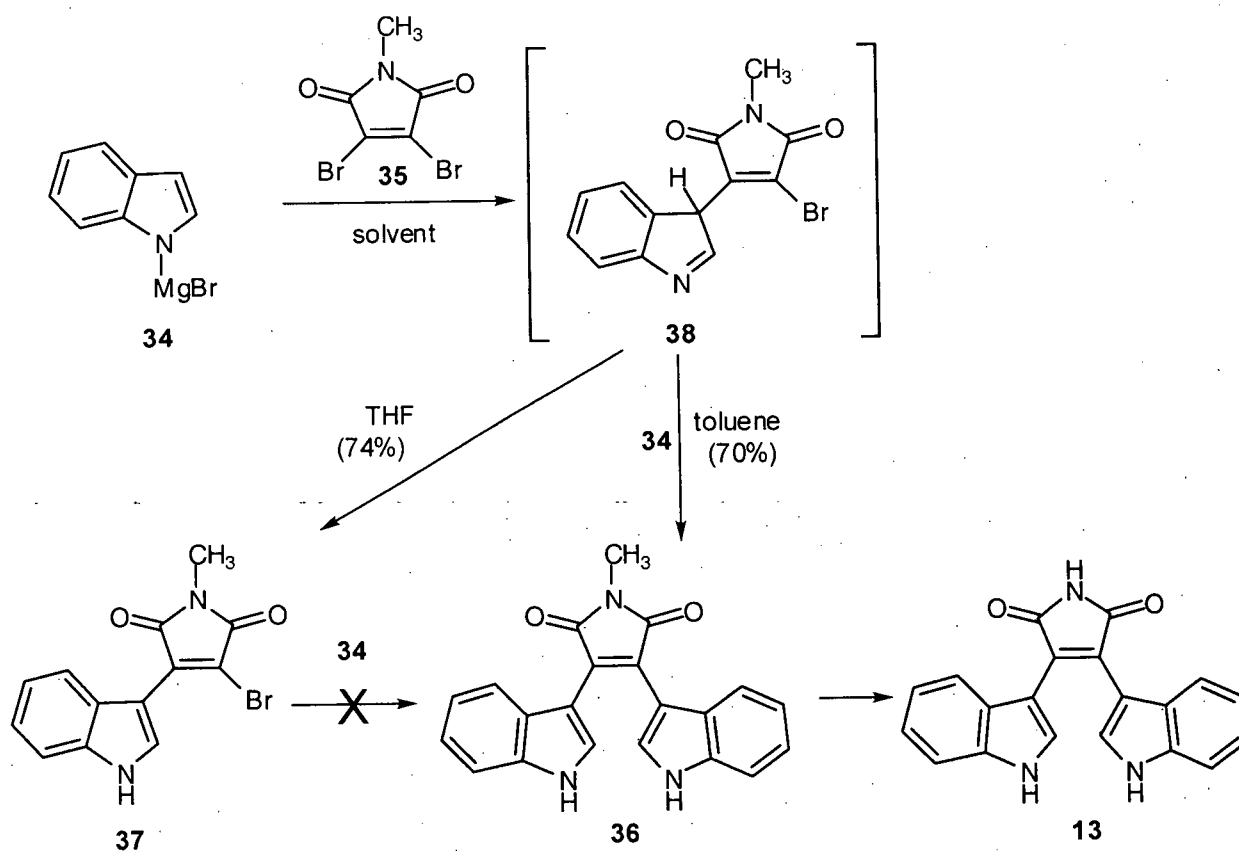
Scheme 3.4. Synthesis of indolyl maleimides.

It was later shown, however, that through judicious choice of reaction solvent and

equivalents of indolylmagnesium bromide (34), the outcome of the reaction may be altered.[22] In

toluene, the symmetric bis-indolyl maleimide **36** was isolated in good yield when 4 equivalents

of **34** were added to the dibromomaleimide **35**. Alternatively, in THF, the monosubstitution

product **37** was obtained in 74% yield from the reaction of 2 equivalents of **34** with **35** (Scheme

3.4). The production of **36** or **37** is rationalized by the difference between the rate of

isomerization of **38** to the monosubstitution product **37** and the rate of reaction of the

intermediate **38** with a second equivalent of indolylmagnesium bromide in the two solvents. The

mono-substitution product **37** has found use in the synthesis of unsymmetric bis-indolyl

maleimides. Thus, through protection of the indole NH and subsequent addition of a second,

structurally different indolylmagnesium bromide reagent, a variety of unsymmetric bis-indolyl

and bis-aryl maleimides have been generated.[23] This methodology has been applied successfully

in the syntheses of staurosporine (**32**)[24] and rebeccamycin (**33**).[25]
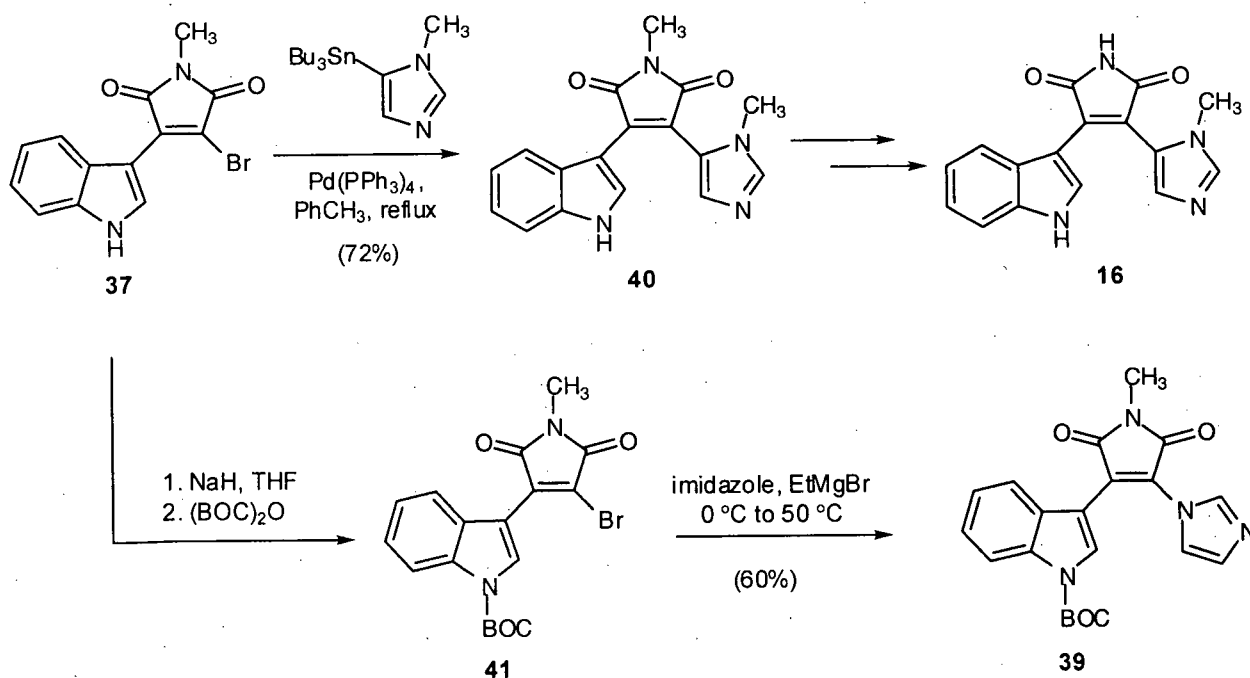
Scheme 3.5. Synthesis of didemnimide C (**16**) and the imidazol-1-yl analogue (**39**).

The bromomaleimide **37** has also been employed in the synthesis of the alkaloid

didemnimide C (**16**) and the imidazol-1-yl analogue **39**.[26] Steglich and co-workers reported that a

Stille coupling between **37** and 5-tributylstannyl-1-methylimidazole, provided, after subsequent

manipulations, didemnimide C (**16**) in 27% overall yield. Additionally, the imidazol-1-yl isomer

39 was accessed through treatment of the maleimide **41** with the bromomagnesium salt of

imidazole in hot THF (Scheme 3.5).
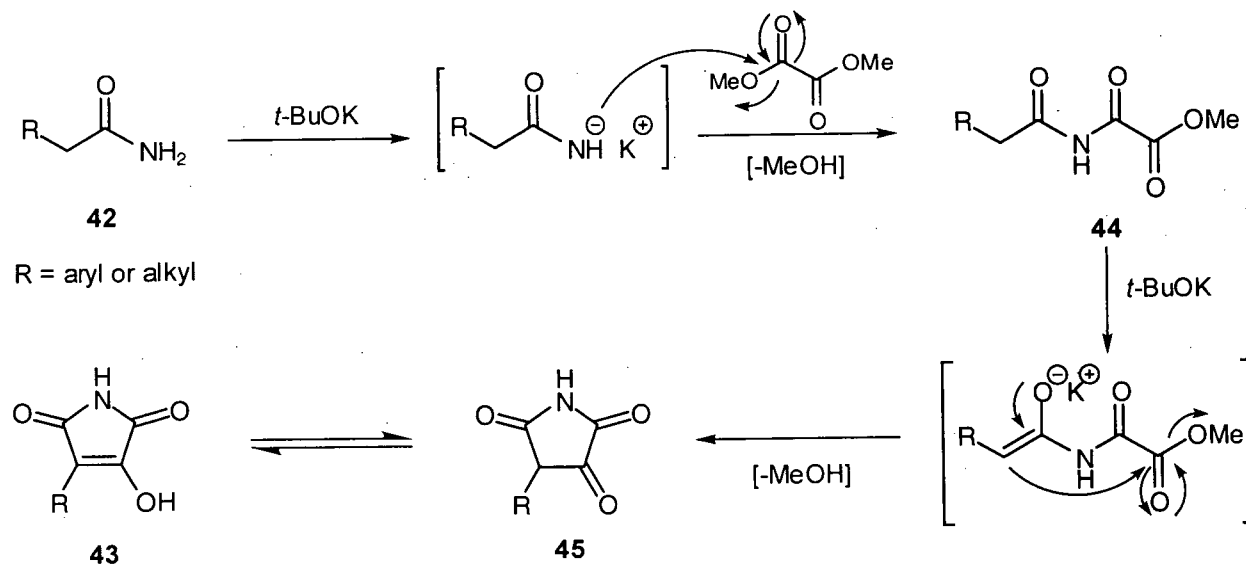
Scheme 3.6. Synthesis of substituted hydroxy maleimides.

Recently, a number of new methods for the synthesis of substituted maleimides[19,27-29] and

maleic anhydrides[30,31] have been reported. Of particular note, Rooney and co-workers have

developed a versatile approach to 4-substituted 3-hydroxy maleimides (Scheme 3.6).[32] These

researchers found that treatment of a substituted acetamide derivative (e.g. **42**) with dimethyl

oxalate and two equivalents of base in DMF, EtOH or benzene, afforded hydroxy maleimides

(e.g. **43**) in moderate yield. Presumably, the first step in this transformation involves

deprotonation of an acetamide *N*H, followed by attack of the nitrogen anion thus generated onto

either carbonyl of the dialkyl oxalate. Removal of a proton from the acetamide methylene in **44**,

followed by an intramolecular Claisen type condensation, provides the ketone **45**, a tautomer of

the hydroxy maleimide **43**.

3.3.1 Synthesis of arcyriarubin A (13)

Perhaps due to the low isolated yields reported for the monosubstituted hydroxy maleimides produced by the condensation sequence described above (Scheme 3.6), this methodology has not been extended to the synthesis of bis-indolyl maleimides.[33] However, we were encouraged by the economy of this reaction and believed a similar condensation sequence, involving α-keto esters and substituted acetamides, would provide expedient access to bis-indolyl maleimides and perhaps unsymmetrical didemnimide type alkaloids. Thus, it was envisaged that the anion derived from the treatment of indole-3-acetamide (46) with base, would react with either the ester carbonyl (pathway A) or the ketone carbonyl (pathway B) of an α-keto ester such as 47 (Scheme 3.7). While both pathways are reversible, the use of a MeOH trap (i.e. 4 Å molecular sieves) should drive the formation of the acetamide 49 via pathway A. Removal of a proton from the acetamide methylene function in 49, followed by an intramolecular Perkin type condensation, would then furnish the hydroxy succinimide 50, presumably as a mixture of diastereomers. Finally, dehydration of the hydroxy succinimide 50 would yield the desired unsymmetric maleimide 51. This process would offer advantages over traditional approaches to bis-indolyl maleimides in that the formation of unsymmetric maleimides would be accomplished in "one-pot" and, additionally, no prior protections of the amine or amide functions on the acetamide starting material would be required.
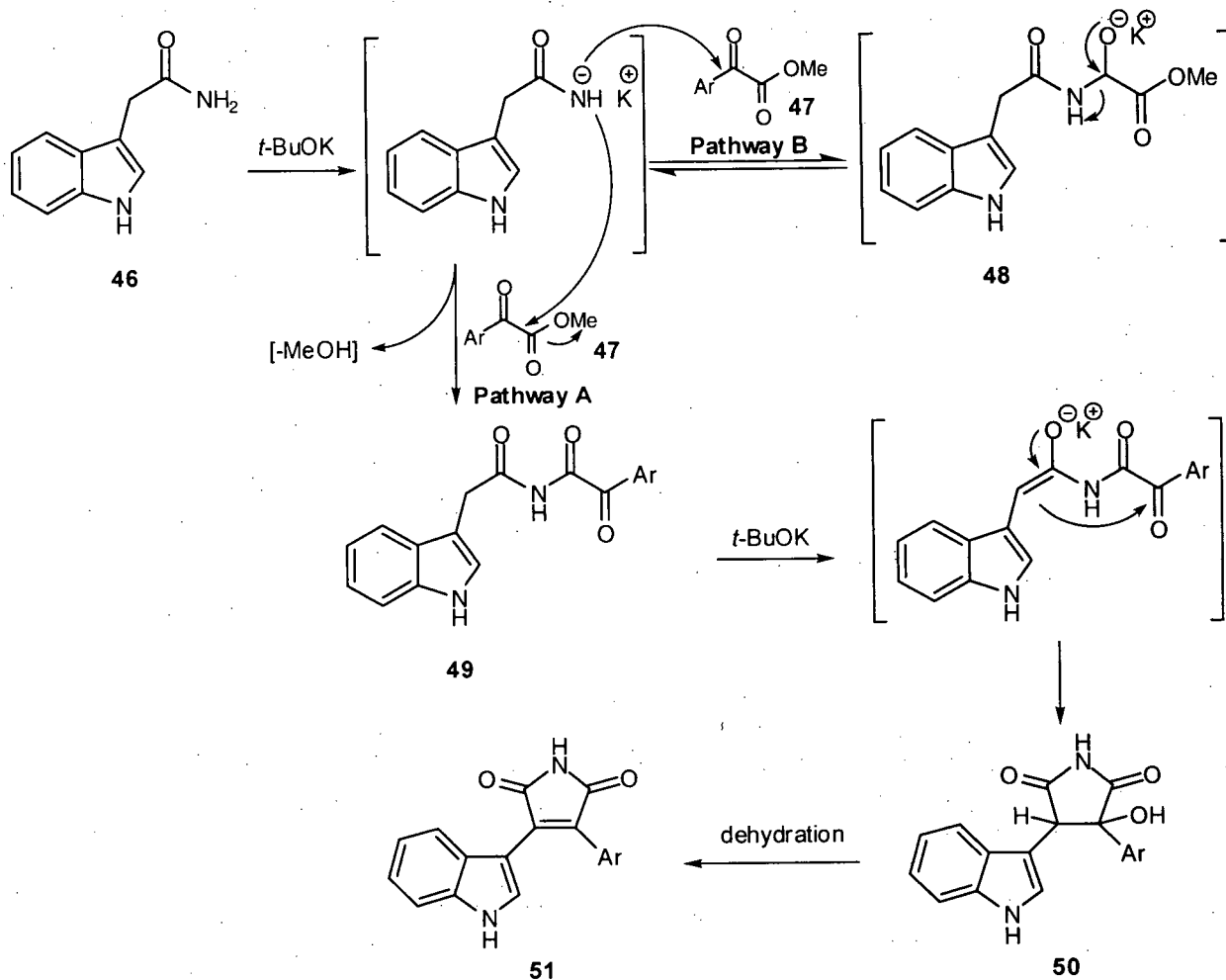
Scheme 3.7. Proposed synthesis of unsymmetric maleimides.

As a model system, we chose to explore the potential of this condensation reaction in the synthesis of arcyriarubin A (**13**) (eq. 1). It was anticipated that a condensation involving the commercially available materials indole-3-acetamide (**46**) and methyl indolyl-3-glyoxylate (**52**) would provide **13** in one step. Gratifyingly, upon warming of a solution of **46** and **52** in DMF with excess *t*-BuOK,[32] a red color that indicated the formation of **13**, appeared almost immediately. After stirring overnight, workup of the reaction and purification of the colored product by flash chromatography, arcyriarubin A (**13**) was isolated in 14% yield. The data (^{1}H NMR, ^{13}C NMR, IR, HRMS, MP) recorded for the synthetic product was consistent with that

reported in the literature[34] (see Table 3.1). Although the optimization of this condensation reaction was not pursued, this work represented the most efficient synthesis of arcyriarubin A (13) and supported further investigations into the syntheses of didemnimide A (14) and related alkaloids through a similar condensation sequence (vide infra).[33]

(1)
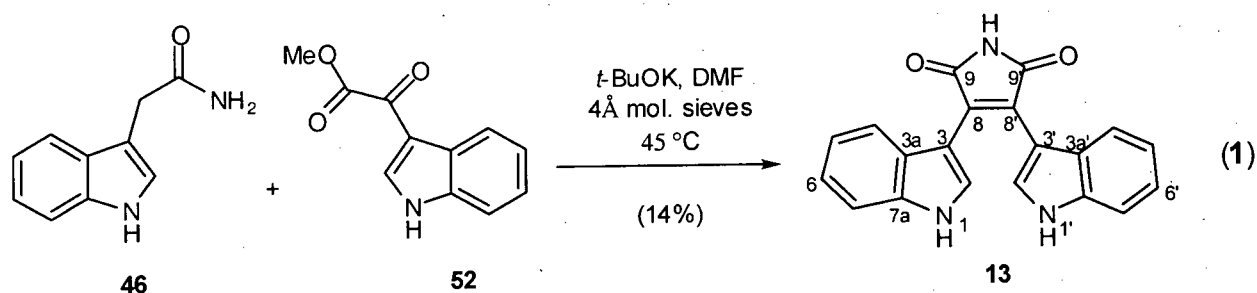
Table 3.1. ^{1}H and ^{13}C NMR data for natural[34] and synthetic arcyriarubin A (13) (recorded in DMSO-d_6).

| Atom No. | Natural arcyriarubin A | | Synthetic arcyriarubin A | |
	[13]C δ (ppm)[a]	[1]H δ (ppm) (mult, J (Hz))[b]	[13]C δ (ppm)[c]	[1]H δ (ppm) (mult, J (Hz))[d]
1 (1')		10.9 (s)		10.87 (bs)
2 (2')	128.7	7.70 (s), 7.69 (s)[e]	129.0	7.72 (d, 2.7)
3 (3')	105.2		105.5	
3a (3a')	125.1		125.4	
4 (4')	121.2	7.33 (d, 8.1)	121.5	7.35 (d, 8.1)
5 (5')	120.5	6.94 (t, 7.3)	120.8	6.96 (dd, 8, 8)
6 (6')	118.9	6.59 (t, 7.72)	119.2	6.61 (dd, 8, 8)
7 (7')	111.3	6.77 (d, 8.0)	111.6	6.79 (d, 8.0)
7a (7a')	135.6		135.9	
8 (8')	127.4		127.7	
9 (9')	172.6		172.9	
10 (10')		11.6 (s)		11.64 (bs)

[a] Recorded at 75 MHz. [b] Recorded at 300 MHz. [c] Recorded at 100.5 MHz. [d] Recorded at 300 MHz. [e] The doublet attributed to H-2 in the ^{1}H NMR spectrum was incorrectly assigned as two singlets (δ 7.70 and 7.69 ppm).

3.4 Syntheses of didemnimide A (14) and the proposed G2 checkpoint inhibitor, granulatimide (22)

The highly convergent total synthesis of granulatimide (22) that was envisaged, as outlined in general terms in Scheme 3.9, was to include two key steps. The first of these was the condensation of the α-keto ester 53 with indole-3-acetamide (46), which was expected (*vide supra*) to furnish the maleimide 54. The second key transformation was envisioned to be a photochemically induced, 6π-electrocyclization, resulting in bond formation between the indole C-2 carbon and the imidazole C-4 carbon (C-14) of the natural product didemnimide A (14) to afford granulatimide (22). The results gathered from this pursuit are summarized in the following sections.
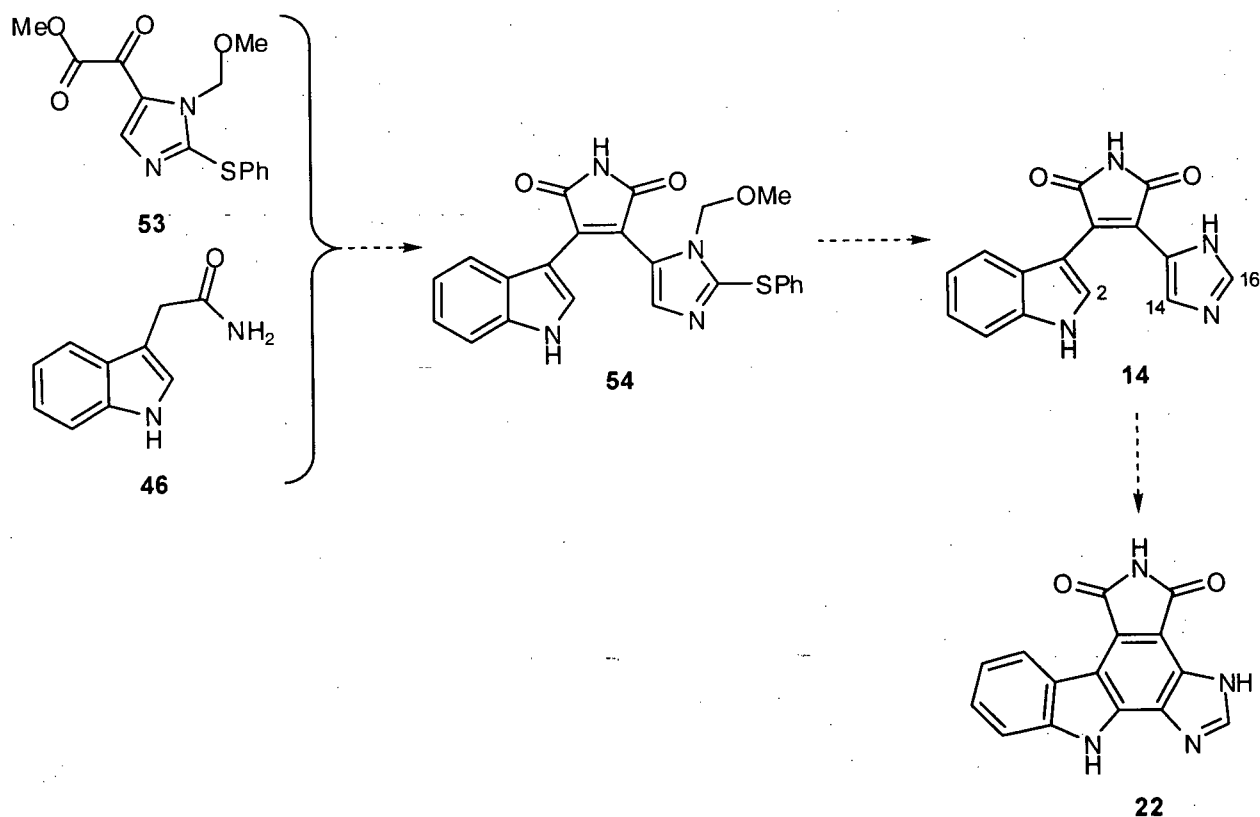
Scheme 3.9. Synthetic proposal for the syntheses of didemnimide A (14) and granulatimide (22).

3.4.1 Background on 6π-Photocyclizations

As outlined in the proposed synthesis of granulatimide (**22**) a key transformation was to involve the 6π-photocyclization of didemnimide A (**14**). Historically, this reaction has received much use in the syntheses of a number of polyaromatic hydrocarbons and alkaloids. The first example of a photoinduced 6π-electrocyclization dates back to 1934, when irradiation of stilbene (**55**) produced a compound that had a λ_{max} at 247 nm and was later identified as phenanthrene (**56**) (Scheme 3.10).[35,36] Hence, 6π-photocyclizations are typically referred to as stilbene type cyclizations.
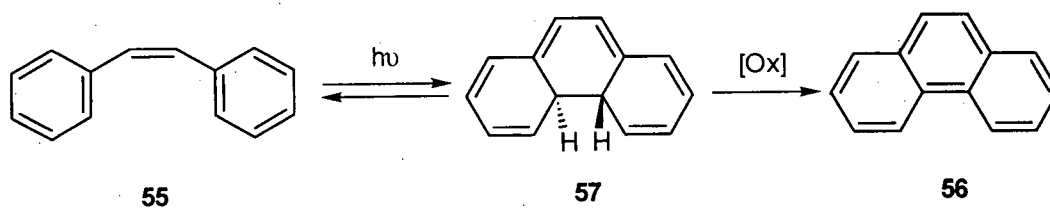
Scheme 3.10. Photocyclization of stilbene.

The 6π-photocyclization is considered to arise from the electronic excited state of a triene (e.g. **55**) and proceed in a symmetry-allowed conrotatory fashion to yield a *trans*-dihydro species (e.g. **57**).[37] The reversibility of this reaction has been demonstrated by the ring opening of **57**, which provides stilbene (**55**) (Scheme 3.10). The stability of the *trans*-dihydro species is highly dependent on the structural features of the parent triene and the half-life of these intermediates may vary from microseconds to days. Typically, dehydrogenation of the *trans*-dihydro intermediates by oxidants such as O_2 and I_2 or π-electron acceptors such as tetracyanoethylene provide the aromatic phenanthrene (e.g. **56**) in good yield.[38] Cava and co-workers have demonstrated that improved yields in the photochemical cyclization of heterocyclic analogues of

stilbene can be realized through the use of catalytic amounts of Pd/C, which effects a mild dehydrogenation of the *trans*-dihydro intermediate (e.g. **61**) (Scheme 3.11).[39] Prior to this report, the general practicality of heterocyclic 6π-photocyclizations had suffered from the competitive destruction of the indole-like products by the oxidant additives.
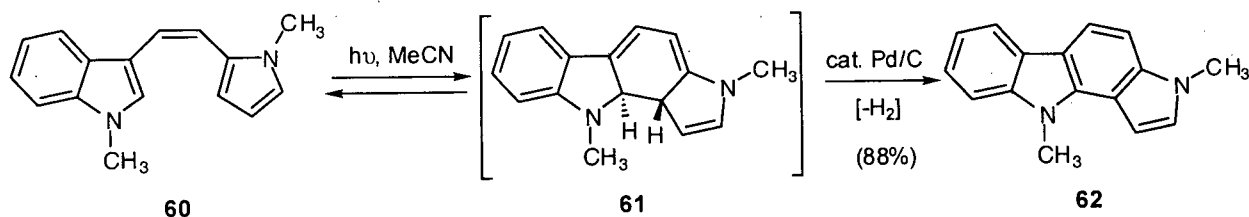
Scheme 3.11. Palladium catalysed dehydrogenation in the stilbene reaction.

3.4.2 Synthesis of selectively substituted imidazoles

As delineated in the retrosynthetic analysis of granulatimide (**22**) (Scheme 3.9), our initial goal in this pursuit was the synthesis of the imidazole glyoxylate **53**. Two reports that focus on the synthesis of substituted imidazoles were invaluable in this regard.[40,41] The most acidic proton of imidazole is the NH (pK$_A$ 17) and thus, the protection of N-1 is antecedent to regioselective deprotonation reactions involving the imidazole ring. A survey of protecting groups used for this purpose include benzyl,[40] TMS,[42] SEM,[43] EtOCH$_2$ (EOM),[44] MeOCH$_2$ (MOM),[45] trityl[46] and SO$_2$NMe$_2$,[45] all of which may be removed under mild conditions.

The deprotonation of N-1 protected imidazole (e.g. **64**), by strong base, proceeds exclusively on C-2 (Scheme 3.12),[40] providing the C-2 lithio derivative in good yield. A number of electrophiles, including brominating agents, alkylating agents, aldehydes, ketones, and nitriles, have been shown to react with 2-lithio imidazoles (e.g. **65**).[40] It is noteworthy, however, that reaction of 2-lithio imidazoles with acylating agents, such as acid halides or anhydrides, has been largely unsuccessful.[43]

Where the synthesis of C-5 substituted imidazoles is desired, the C-2 position is generally

blocked by a thiophenyl protecting group.[47] Such C-2 protected imidazoles are accessed in

excellent yield by the reaction of 2-lithio imidazoles (e.g. **65**) with phenyl disulfide. The ease

with which the sulfide blocking group is removed[48] has made this an attractive sequence for

producing variably substituted imidazoles.
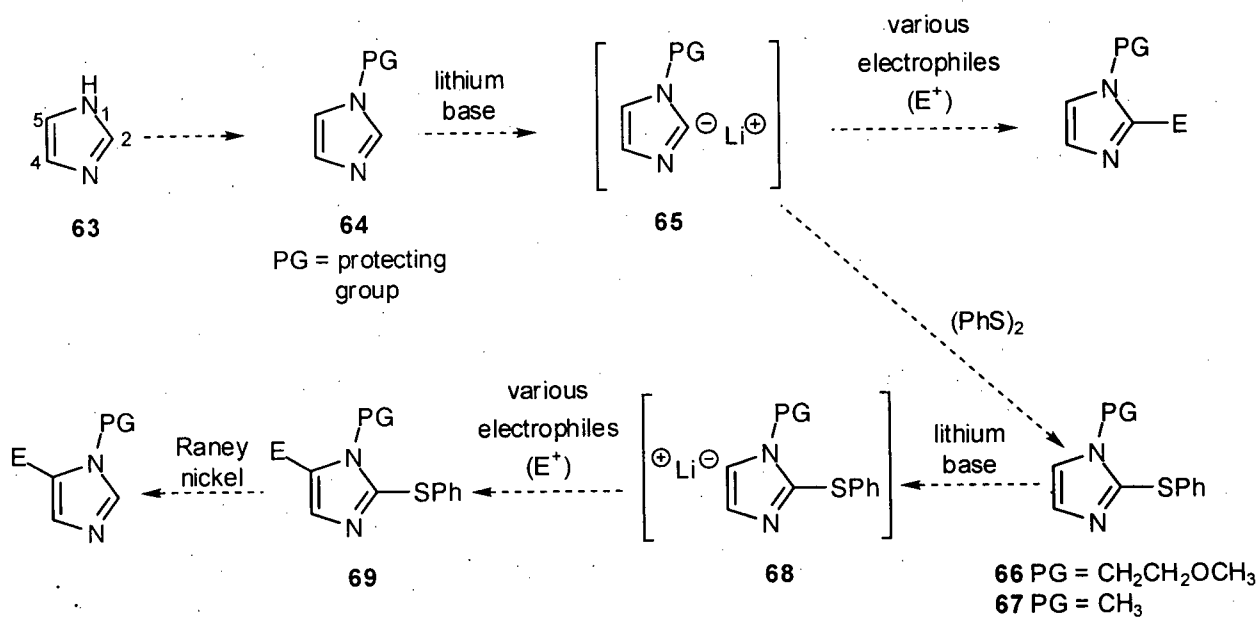
Scheme 3.12. Functionalization of imidazole.

Deprotonation of C-2 blocked *N*-1 protected imidazoles (e.g. **66**), generally effected by *n*-

BuLi, removes the C-5 proton.[49,50] Not suprisingly, the degree of efficiency of this reaction is

highly dependent on the nature of the *N*-1 protecting group. Thus, the reaction of the *N*-methyl

imidazole **67** with alkyl lithium, followed by treatment with various electrophiles (e.g.

alkylhalides, esters, ketones and aldehydes) typically provides the desired 5-substituted

imidazole in yields no greater than 50%.[48] However, the use of protecting groups such as MOM,

EOM and SEM, which are capable of complexing the alkyl lithium base and facilitating the

metallation at C-5, produce the desired 5-substituted imidazoles in consistently high yield.

3.4.3 Total synthesis of didemnimide A (14) and granulatimide (22)

The total syntheses of didemnimide A (**14**) and granulatimide (**22**) are summarized in Scheme 3.13. Treatment of the substituted imidazole **70**[47] with n-BuLi in THF at -78 °C, followed by reaction of the resultant 5-lithio imidazole intermediate with dimethyl oxalate, provided the required α-keto ester **53** in 66% yield. The structural assignment of **53** was in full accord with its spectral data. The α-keto ester moiety showed stretching absorptions in the IR spectrum at 1729 (ester C=O) and 1657 cm^{-1} (ketone C=O). The ^{13}C NMR spectrum included two carbonyl resonances (δ 172.2 and 161.6) and two resonances which could be assigned to the methyl ester and methyl ether carbons of **53** (δ 56.5 and 53.0, respectively). The ^{1}H NMR spectrum of **53** displayed, in addition to six aromatic proton resonances, two 3-proton singlets (δ 3.91 and 3.36) corresponding to the methyl ester and methyl ether protons, respectively.

The condensation of **53** with indole-3-acetamide (**46**) was effected efficiently by treatment of a solution of the two reactants with t-BuOK in warm DMF in the presence of molecular sieves. The use of molecular sieves was crucial to the success of this reaction, since, in the absence of this material, a second major product resulting from the displacement of the phenylthio group by a methoxyl function was formed (i.e. **54**, OMe in place of SPh). Presumably, the byproduct arises through the reaction of **54** with methoxide ion, which is generated during the condensation of **53** and **46**. It is likely that, to a large degree, the sieves adsorb the MeOH produced during the reaction and thus are effective in significantly reducing the amount of byproduct. As expected, the spectral data acquired on the desired product, compound **54**, was similar to that reported by Fenical and co-workers for the didemnimides.[14] The IR spectrum of **54** included two carbonyl C=O stretching absorptions (1765 and 1708 cm^{-1}) which resembled those reported for didemnimide A (**14**) (1755 and 1702 cm^{-1}). In the ^{1}H NMR spectrum, two broad NH resonances (δ 12.11 and 11.25) were observed and assigned to the

indole *N*H and the maleimide *N*H, respectively. In addition, the ^{13}C NMR spectrum contained 17

aromatic carbon resonances and two characteristic maleimide carbonyl resonances (δ 171.7 and

171.6). As anticipated, the protected didemnimide **54** was isolated as an orange solid, resembling

in appearance the didemnimides A-D (Figure 3.3), which all exist as orange to red solids.[14]
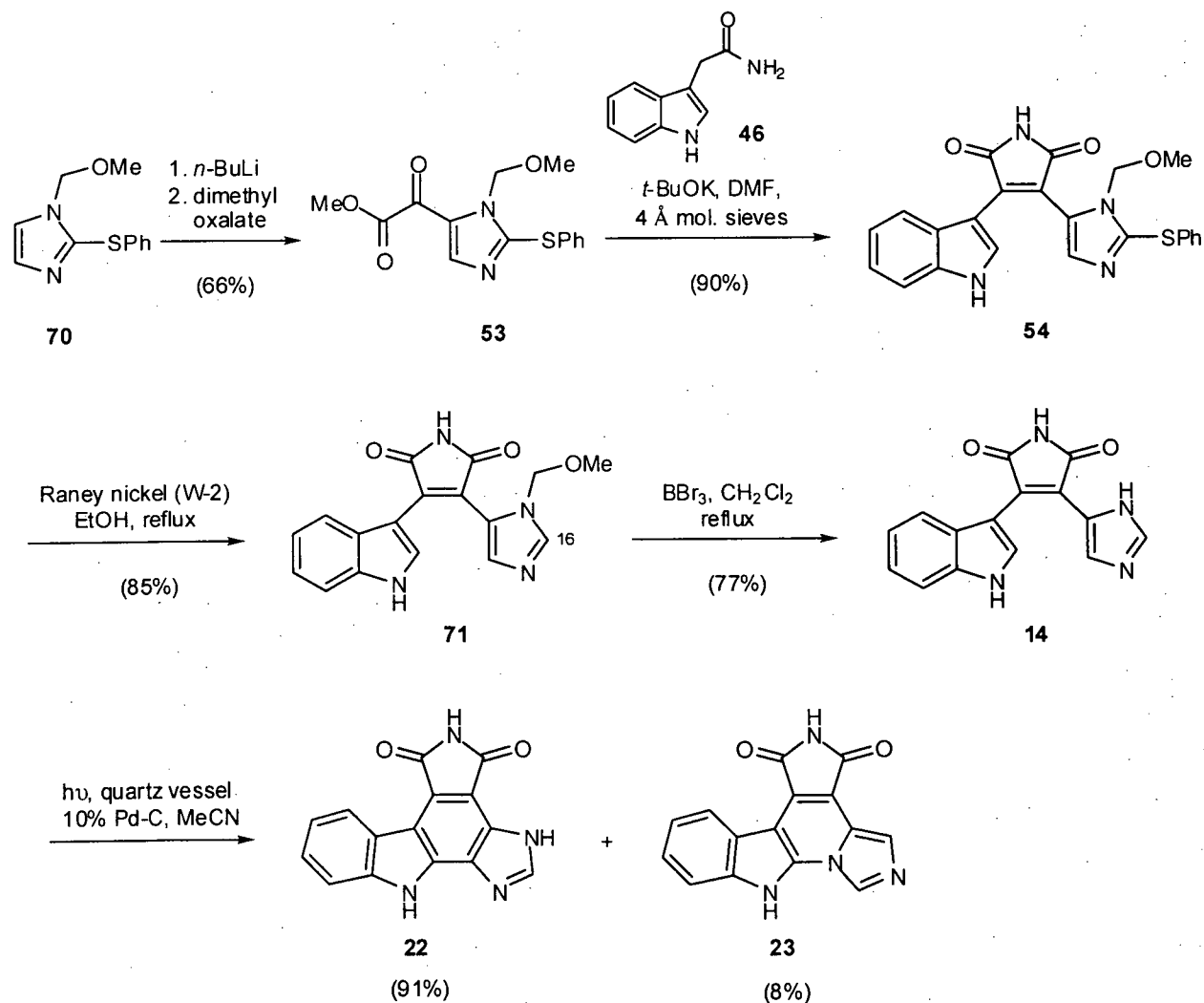
Scheme 3.13. Total syntheses of didemnimide A (**14**),
granulatimide (**22**) and isogranulatimide (**23**).

Treatment of the tetracycle **54** with W-2 Raney nickel in refluxing EtOH[48] furnished the

desulfurized product **71** in excellent yield. The ^{1}H NMR spectrum of **71** included seven aromatic

proton resonances, which supported the removal of the thiophenyl protecting group from **54**.

Additionally, a singlet (δ 7.95) in the ^{1}H NMR spectrum of **71** could be assigned to the imidazole H-16, consistent with the replacement of the phenylthio group with a proton. The ^{13}C NMR and IR spectral data compared well with those reported for the didemnimides and the molecular formula of **71** was confirmed by a high-resolution mass spectrometric measurement on the molecular ion.

Removal of the methoxymethyl group was accomplished by reaction of the didemnimide **71** with 10 equivalents of boron tribromide (BBr$_3$) in refluxing CH$_2$Cl$_2$. Reaction at room temperature and (or) use of lesser amounts of the reagent resulted in the recovery of considerable amounts of starting material. The product of this reaction, didemnimide A (**14**), exhibited spectral data in accordance with that reported in the literature for the natural product (Table 3.2).[14] However, the interpretation of the NMR spectra of didemnimide A (**14**) in DMSO-d_6 was complicated by the existence of both tautomers **14** and **14B** (Figure 3.9). Also, given that the pK_A of the conjugate acid of imidazole is approximately 7, both the protonated and non-protonated forms of didemnimide A (**14**) were likely to be present.[14] These factors led to the broadening of proton resonances in the ^{1}H NMR spectrum of **14**, the degree of which was found to be dependent on concentration, making comparison of NMR spectral data difficult. However, this problem could be resolved through the addition of trifluoroacetic acid (TFA) to the NMR sample prior to analysis, providing the TFA salt of didemnimide A **72**, which yielded consistent NMR spectra (Figure 3.9).
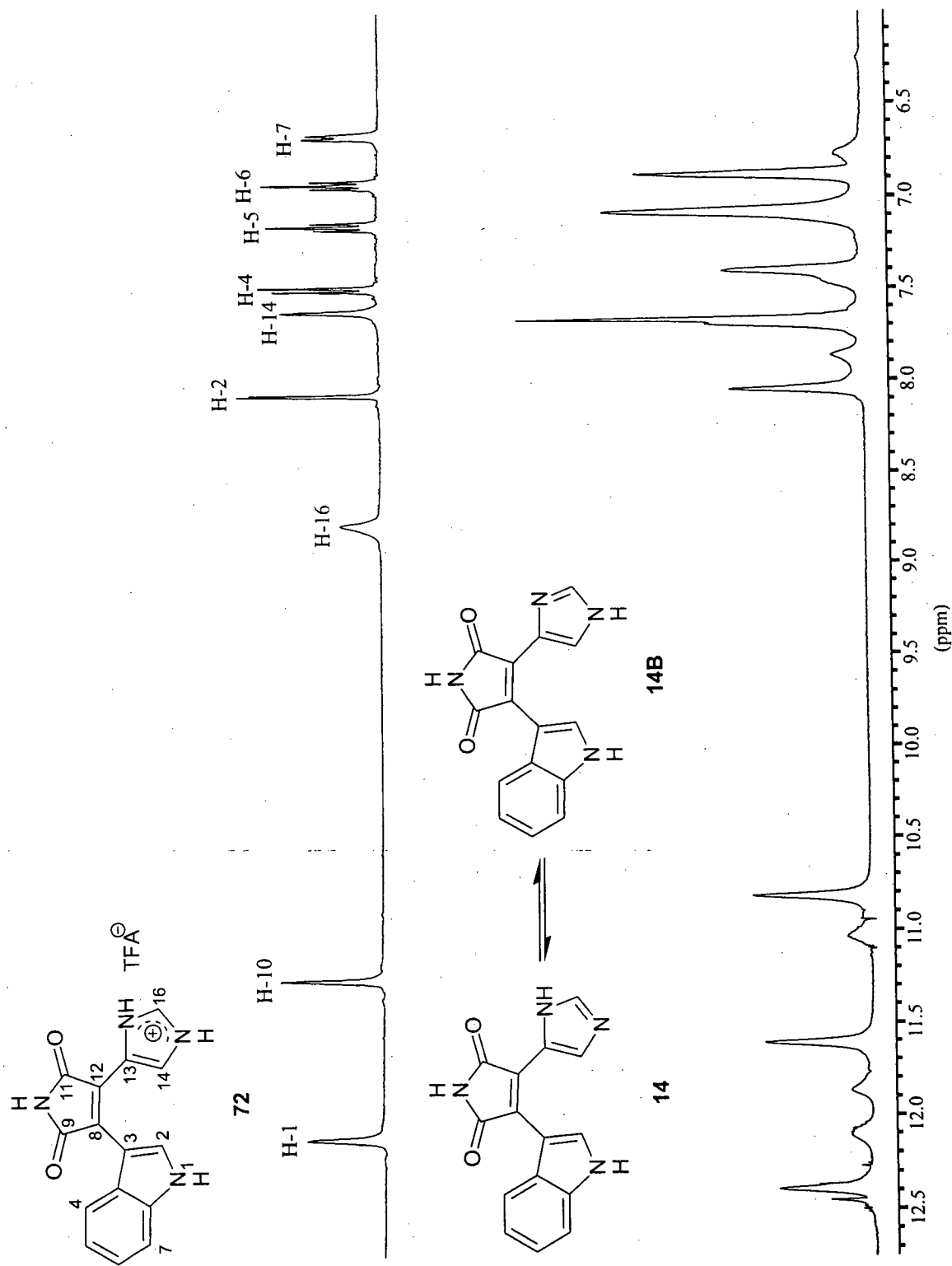
Figure 3.9. ^{1}H NMR spectra of didemnimide A (**14** and **14B**) and the TFA salt of didemnimide A **72** (recorded in DMSO-d_6, 500 MHz).

Table 3.2. ^{1}H and ^{13}C NMR data for natural[14] and synthetic didemnimide A (**14**) (recorded in DMSO-d_6).
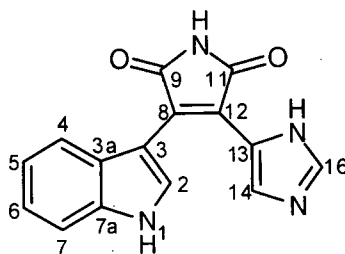
	Natural didemnimide A		Synthetic didemnimide A	
Atom No.	^{13}C δ (ppm)[a]	^{1}H δ (ppm) (mult, J (Hz))[b]	^{13}C δ (ppm)[a]	^{1}H δ (ppm) (mult, J (Hz))[c]
1		12.45 (bs)		12.45 (bs)
2	130.7	8.05 (bs)	130.9	8.05 (bs)
3	104.7		105.0	
3a	125.6		126.0	
4	121.7	7.07 (m)	121.7	7.07 (m)
5	119.6	6.87 (m)	119.7	6.87 (m)
6	121.7	7.07 (m)	121.3	7.07 (m)
7	112.0	7.39 (d, 7.8)	112.2	7.39 (d, 7.8)
7a	136.5		136.1	
8	n.o.		130.5[e]	
9	172.9[d]		172.8[d]	
10		11.66 (bs)		11.66 (bs)
11	172.8[d]		172.6[d]	
12	n.o.		111.5[e]	
13	125.7		126.0	
14	119.6	7.71 (bs)	119.2	7.71 (bs)
15				
16	136.5	7.68 (bs)	135.9	7.68 (bs)
17		10.87 (bs)		10.87 (bs)

[a] Recorded at 100.5 MHz. [b] Recorded at 500 MHz. [c] Recorded at 400 MHz. [d,e] May be interchanged.

Finally, photolysis of a solution of didemnimide A (**14**) in acetonitrile containing a small amount of palladium-on-carbon[39] produced granulatimide (**22**) in 91% yield and isgranulatimide (**23**) in 8% yield (Scheme 3.13). The spectroscopic data obtained for granulatimide (**22**) were in full accord with the assigned structure and ^{1}H and ^{13}C NMR resonances could be assigned by HMBC, HMQC and COSY experiments (see Experimental). A series of NOE difference

experiments were particularly instrumental in assigning the ¹H NMR spectrum and confirming

the structure (Figure 3.10). Irradiation of a broad singlet at δ 12.58 induced a NOE in a doublet

at δ 7.61, thereby assigning the broad singlet to the indole N*H* and the doublet to H-7. Similarly,

irradiation of a broad singlet at δ 13.57 induced a NOE in a sharp singlet at δ 8.50, which led to

the assignment of the downfield singlet to the imidazole N*H* and the upfield singlet to H-16. It

was interesting to note that contrary to our expectations, granulatimide (**22**) gives sharp, well-

resolved ¹H NMR spectroscopic resonances for all of the protons in the molecule. The imidazole

N*H* in granulatimide (**22**) is strongly deshielded (δ 13.57), and it does not show a NOE to the

indole N*H*, suggesting it participates in a strong intramolecular hydrogen bond to the maleimide

C-11 carbonyl (Figure 3.10). Thus, the stabilization of the H*N*-17 tautomer **22** is likely

responsible for the suppression of imidazole *N*H tautomerization in granulatimide (**22**).
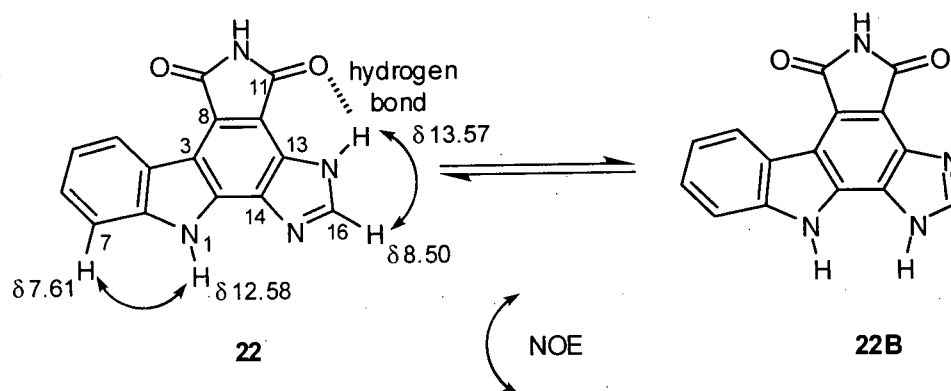
Figure 3.10. NOE's observed for granulatimide (**22**).

Comparison of the NMR data for synthetic granulatimide (**22**) with the data for the

checkpoint inhibitor isolated from the EtOH extract of *D. granulatum* clearly revealed that the

two molecules were different (Figure 3.11). Therefore, we concluded that the G2 checkpoint

inhibitor must be isogranulatimide (**23**), the only alternate candidate structure consistent with the

spectroscopic data and a biogenesis from didemnimide A (**14**) (*vide supra*). A minor product

from the photochemical conversion of didemnimide A (**14**) to granulatimide (**22**) had TLC properties identical with those of a sample of natural isogranulatimide (**23**). Their ^{1}H NMR spectra were also nearly identical (Figure 3.11). However, the synthetic product gave sharp, well-resolved singlets at δ 7.88 and 8.93 for H-14 and H-16, respectively, while the natural sample gave broad resonances for these protons at δ 8.10 and 9.12. These spectroscopic discrepancies were attributed to the different chromatographic procedures employed to purify the two samples, resulting in different protonation states for the natural and synthetic isogranulatimides. Therefore, both the natural and synthetic samples were repurified using identical reversed phase HPLC conditions (1:1 CH$_3$CN - 0.05% TFA) resulting in them having identical HPLC retention times and ^{1}H NMR spectra. The formation of isogranulatimide (**23**) via the photolysis of didemnimide A (**14**), while unanticipated, confirmed the structure of the natural product.

I

II

III
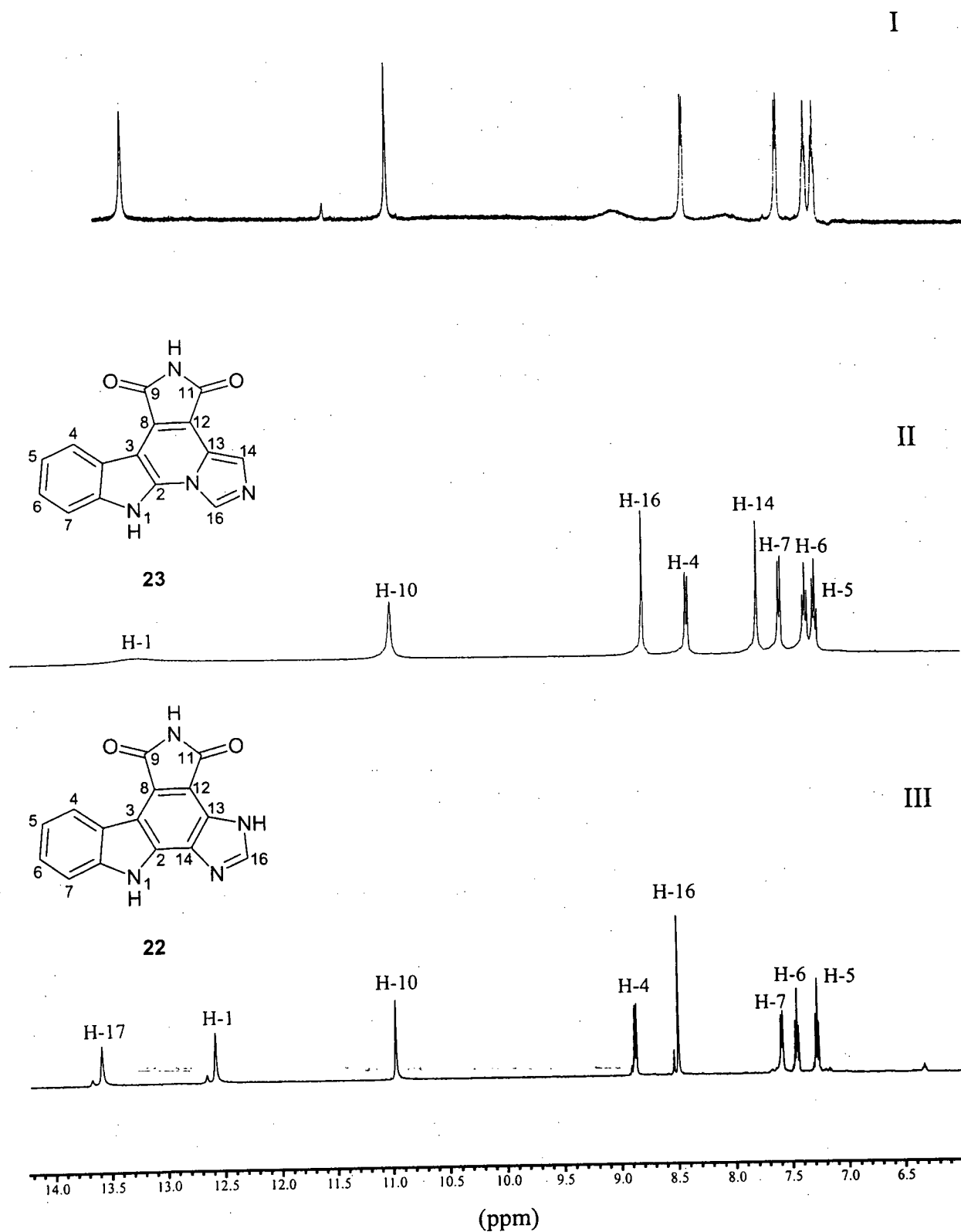
Figure 3.11. ¹H NMR spectra of (I) the G2 checkpoint inhibitor from *Didemnum granulatum*, (II) synthetic isogranulatimide (23) and (III) synthetic granulatimide (22) (recorded in DMSO-d_6, 500 MHz).

3.5 Improved synthesis of isogranulatimide (23)

As part of the investigations leading to the structural elucidation of isogranulatimide (23), a short, efficient synthesis of granulatimide (22) was developed. The final step in this synthesis also generated isogranulatimide (23), albeit in very low yield (Scheme 3.13). With a highly convergent synthesis of granulatimide (22) established, our primary objective became the development of an alternative protocol that would result in an efficient conversion of 14 into 23.

Repetition of the reaction shown in Scheme 3.13 revealed that the amount of isogranulatimide (23) generated through this process was variable. Indeed, the yields of 23 were typically even lower than indicated, and in some experiments this substance was not present in the crude reaction mixture at all. During the photolysis of 14 in MeCN, the reaction mixture heated quite significantly, which led to the proposal that the conversion of 14 into 23 might in fact be a thermally induced process. To gain further insight into this transformation, a number of high-temperature ^{1}H NMR experiments were performed on 14, using DMSO-d_6 as the solvent (Figure 3.12). Fortuitously, the spectrum obtained when a solution of 14 was heated to 140 °C showed, in addition to signals due to starting material, resonances that revealed the presence of isogranulatimide (23). The latter material became the major compound in solution when the mixture was heated to 160 °C (Figure 3.12, IV).

14   22   23
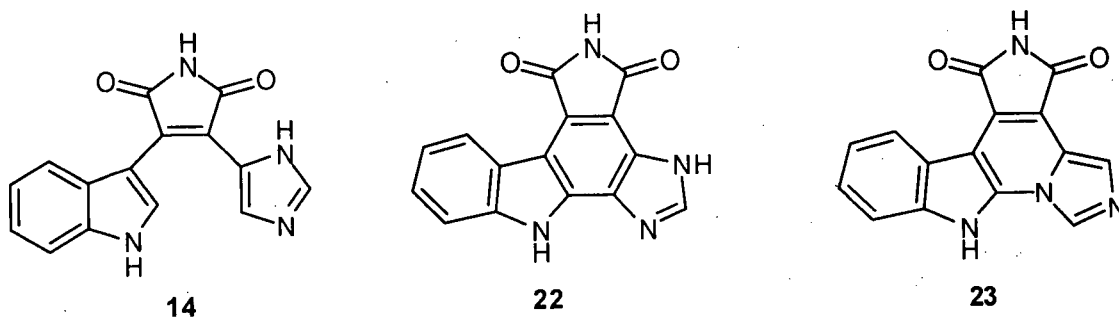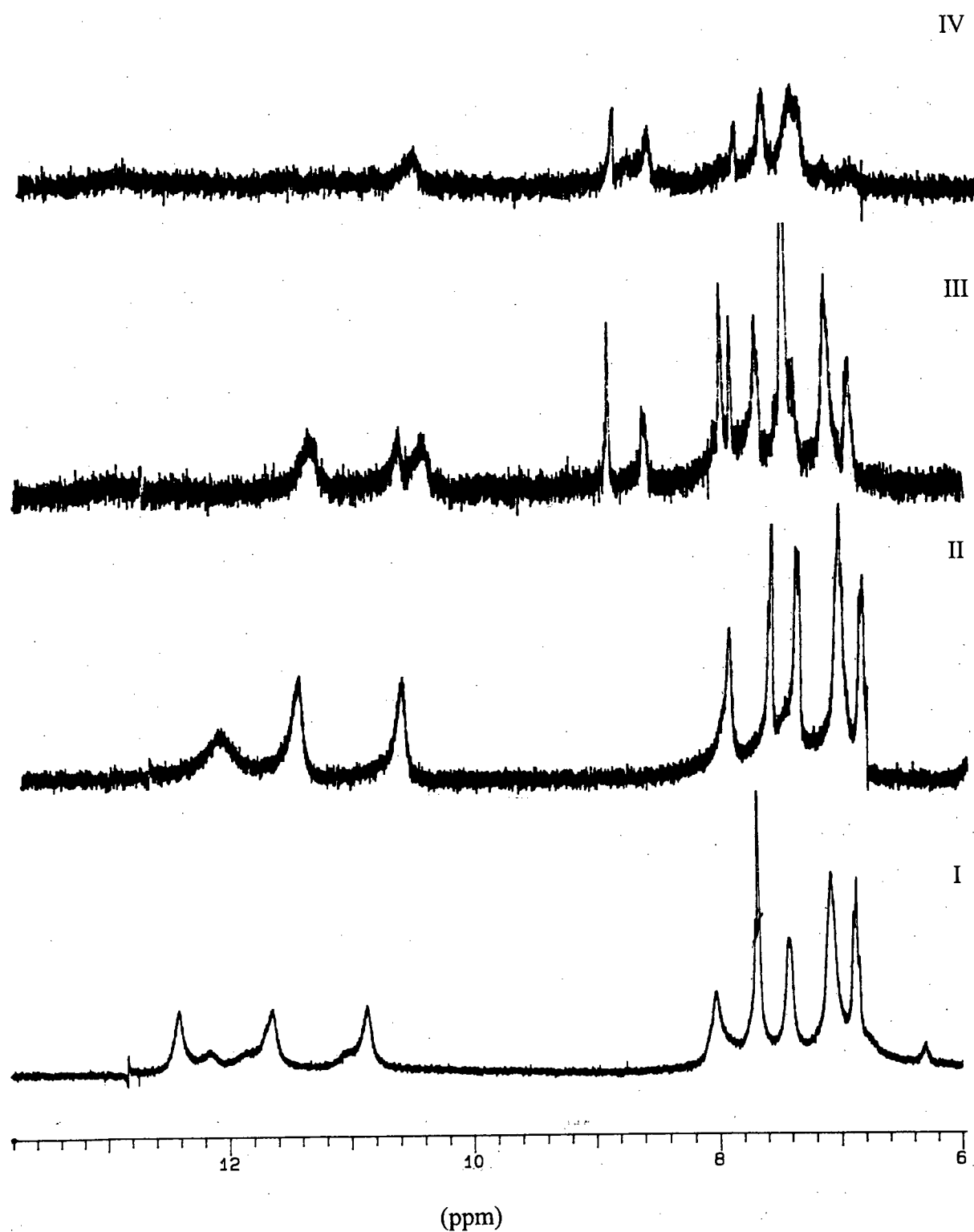
Figure 3.12. Selected variable temperature ¹H NMR spectra of didemnimide A (**14**)
(I) room temperature, (II) 80 °C, (III) 140 °C (IV) 160 °C (recorded in DMSO-d_6, 300 MHz).
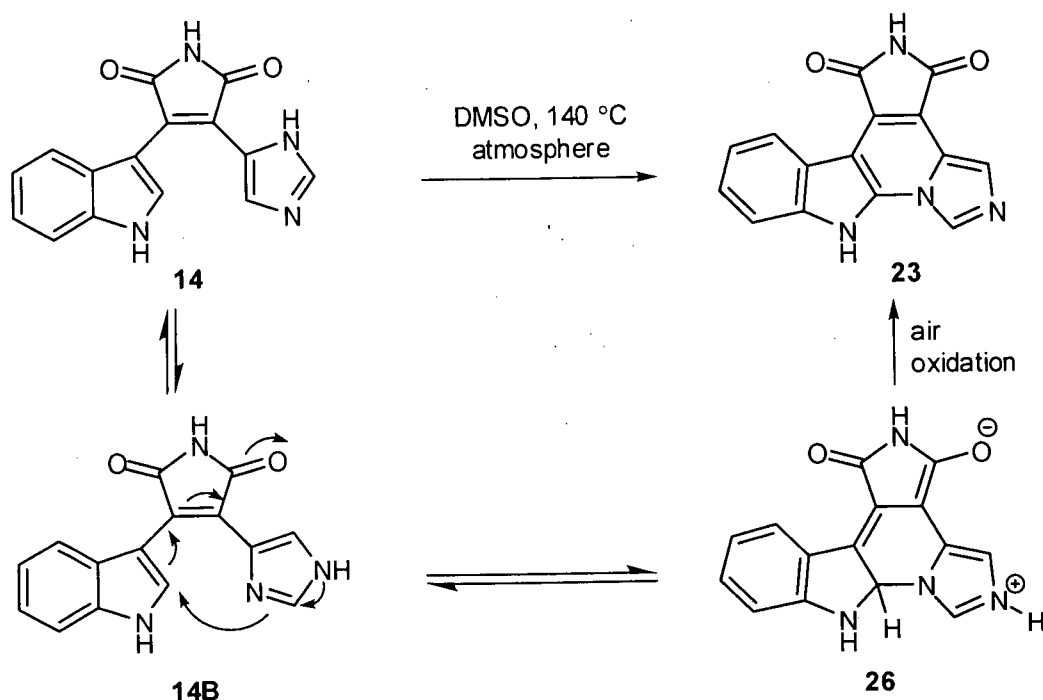
Scheme 3.14. Proposed mechanism for the thermal production of isogranulatimide (**23**).

These observations led to the preparative-scale experiments summarized in Table 3.3. It was found that heating of a solution of didemnimide A (**14**) in DMSO (140 °C, open to the atmosphere) provided isogranulatimide (**23**) in a maximum yield of about 50%. In addition, starting material was recovered in amounts varying from 0 to 20%, depending on reaction times (see, for example, Table 3.3, entry 1). Presumably, the transformation of **14** into **23** proceeds via (reversible) intramolecular 1,6-addition of **14B** (a tautomer of **14**) to generate the intermediate **26**, as shown in Scheme 3.14. Air oxidation of the latter species (or of a structurally related intermediate derived from **26**) would regenerate the indole system and thus provide isogranulatimide (**23**). Unfortunately, further experimentation employing DMSO as solvent failed to identify conditions that would provide yields of **23** in excess of about 50%. The reactions consistently produced, in addition to **23**, insoluble (decomposition) material that was not investigated further. It could be shown, however, that after heating a solution of

isogranulatimide (**23**) in DMSO (150 °C, open to the atmosphere) for two hours, no decomposition products were observed. Consequently, the generation of byproducts, encountered in the transformation of didemnimide A (**14**) into **23** in DMSO, must result from decomposition of **14** and/or an intermediate generated during this process (e.g. **26**).

In an effort to increase the efficiency of this transformation (i.e. **14** → **23**), a variety of reaction conditions were investigated. Unfortunately, the addition of oxidants such as DDQ, CuCl$_2$ or MnO$_2$ to hot solutions of didemnimide A (**14**) in DMSO, MeCN or *N*-methyl pyrrolidinone (NMP) failed to identify conditions superior to those described above. In fact, the isolated yield of isogranulatimide (**23**) from these reactions was typically less than 15%. Undaunted by these poor results, we explored the use of dehydrogenation catalysts, which had proved successful in the conversion of **14** into granulatimide (**22**) (*vide supra*). Thus, when a hot solution of didemnimide A (**14**) in di(ethylene glycol) ethyl ether containing a catalytic amount of Pd/C, as a hydrogen transfer agent, was stirred for sixteen hours, **23** was produced in moderate yield (Table 3.3, entry 2). Repetition of this reaction with excess Pd/C was fruitless and resulted in the production of a substantial amount of insoluble (decomposition) materials. A report by Cava and co-workers indicated that the addition of hydrogen acceptors in heterocyclic photocyclizations that involve dehydrogenation of the dihydro intermediates by palladium catalysts was beneficial to these processes. In this manner, the deleterious hydrogenation of reactants and products, also catalysed by Pd/C, is avoided.[51]

Nitrobenzene is a well-known hydrogen acceptor in hydrogen transfer reactions.[52] It could be shown that isogranulatimide (**23**) is quite stable for extended periods of time in refluxing nitrobenzene and, therefore, a number of experiments involving this solvent were performed. When a solution of **14** in hot (200 °C) nitrobenzene, containing 10% Pd/C as a hydrogen transfer catalyst, was stirred for 3 hours, **23** was produced in 46% yield, accompanied by recovered starting material (Table 3.3, entry 3). The relatively low material balance from this

reaction can probably be attributed to adsorption of **14** and **23** onto the carbon support. Replacement of the Pd/C with Pd/CaCO$_3$ and an increase in the reaction time to 7 hours resulted in complete consumption of the starting material but produced the product **23** in only moderate yield (entry 4). The rather "dirty" reaction mixture indicated that partial decomposition of the organic substances present had occurred. Additional experimentation showed that a satisfactory result could be obtained by using Pd black as the hydrogen transfer agent (entries 5 and 6). Indeed, although extended reaction times were required, the conditions summarized in entry 6 consistently transformed **14** into **23** in very good yields (~75%). Thus, an experimentally straightforward and efficient synthesis of isogranulatimide (**23**) had been developed, allowing the production of quantities sufficient for biological activity evaluations (*vide infra*).

Table 3.3. Conversion of didemnimide A (**14**) into isogranulatimide (**23**)
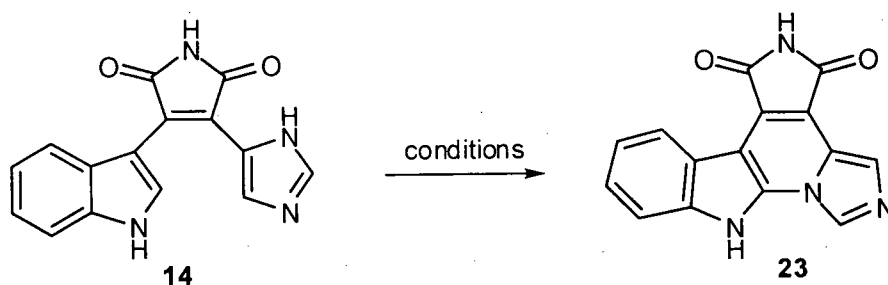
entry	solvent	T (°C)	time (h)	conditions or additive	recovered 14 (%)	yield of 23 (%)
1	DMSO	140	2	open to atmosphere	22	51
2	DEGEE[a]	202	16	Pd/C[b]	27	50
3	C$_6$H$_5$NO$_2$	200	3	Pd/C[c]	22	46
4	C$_6$H$_5$NO$_2$	200	7	Pd/CaCO$_3$[d]	0	46
5	C$_6$H$_5$NO$_2$	200	8	Pd black[e]	28	62
6	C$_6$H$_5$NO$_2$	200	20	Pd black[e]	0	75

[a] Di(ethylene glycol) ethyl ether. [b] Approximately 0.04 g of 10% Pd/C per mmol of **14**. [c] Approximately 0.2 g of 10% Pd/C per mmol of **14**. [d] Approximately 0.4 g of 5% Pd/CaCO$_3$ per mmol **14**. [e] Approximately 0.1 g of Pd black per mmol of **14**.

3.6 Syntheses of structural analogues of didemnimide A (14), granulatimide (22) and isogranulatimide (23)

Having developed an efficient synthetic sequence which provided access to both granulatimide (22) and isogranulatimide (23), we next sought the syntheses of analogues of these alkaloids and didemnimide A (14). Our primary objectives in this study were the exploration of the generality of condensation-cyclization routes developed in the previous work and the preparation of structural analogues of 22 and 23, including 17-methylgranulatimide (74) and substances 75-77 (Figure 3.13), in which the imidazole unit is incorporated into the final products in structural ways different from those present in 22 and 23. For the sake of convenience, substances 75-77 have been dubbed isogranulatimide A, isogranulatimide B and isogranulatimide C, respectively. Additionally, we wished to investigate the syntheses of *N*-alkylated analogues of 22 and 23 (substances 78-81) and extend the condensation-cyclization sequence to include the syntheses of the phenylmaleimide 82 and the 3-azaindole 83. Successful completion of these goals would set the stage for investigations into the effect of structure on the biological activity of this potentially important family of compounds.

14

22

23

74

75

76

77

78 R₁ = H, R₂ = *n*-hexyl
80 R₁ = CH₃, R₂ = H
81 R₁ = *n*-hexyl, R₂ = H

79

82

83
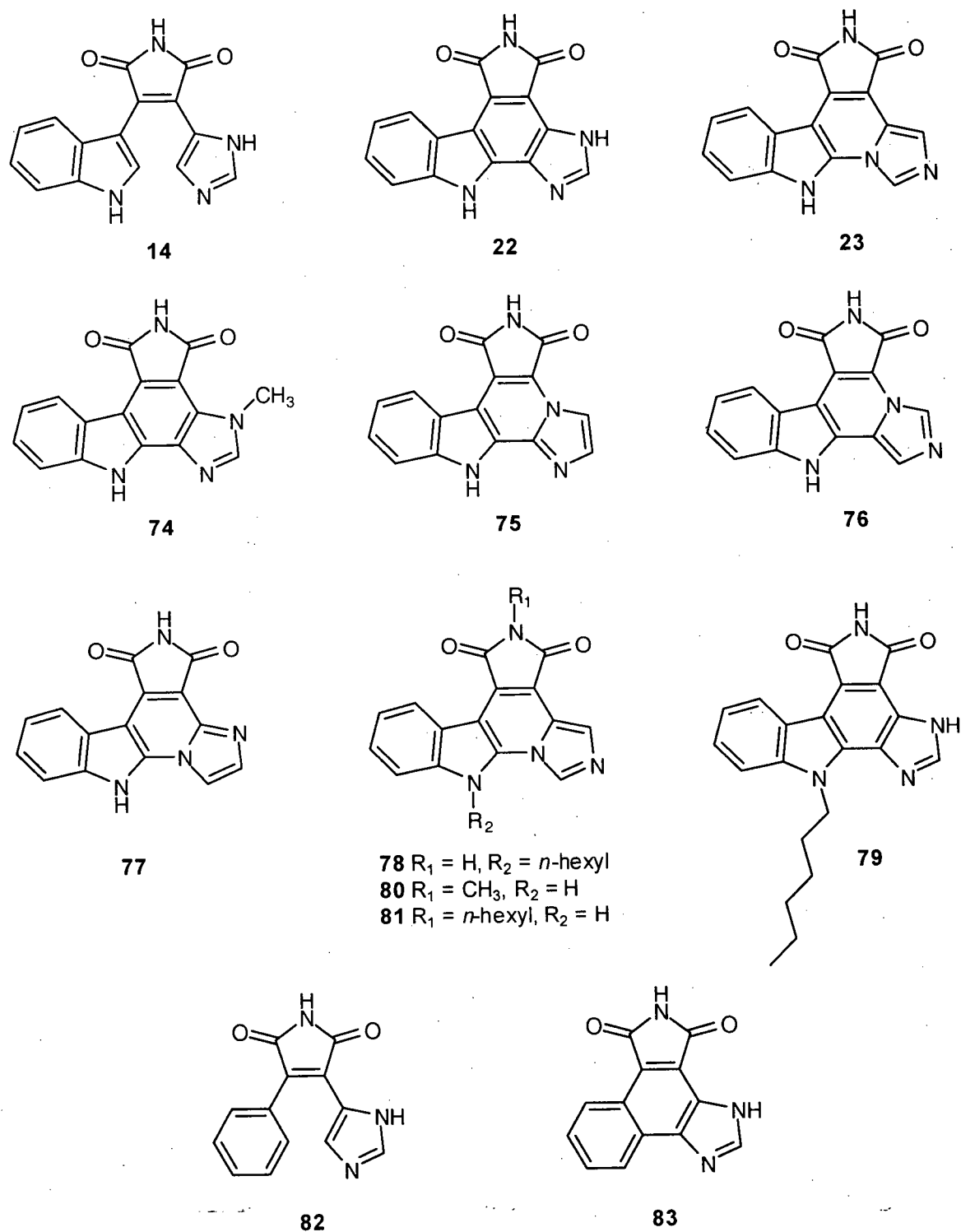
Figure 3.13. Targeted synthetic analogues of granulatimide (**22**) and isogranulatimide (**23**).

3.6.1 Syntheses of didemnimide C (16) and 17-methylgranulatimide (74)

As mentioned above, one of the objectives of the current study was to carry out the syntheses of a number of substances (Figure 3.13) structurally related to granulatimide (**22**) and isogranulatimide (**23**). On the basis of our earlier work, it was expected that one of the proposed targets, 17-methylgranulatimide (**74**), should be readily produced by the photocyclization of didemnimide C (**16**).[14] Although a total synthesis of **16** had been achieved by Steglich and co-workers (Scheme 3.5),[26] it seemed likely that a shorter synthesis, involving use of the methodology devised for the synthesis of didemnimide A (**14**), could be developed. The results derived from the pursuit of this approach are summarized in Scheme 3.15.

Sequential treatment of 1-methyl-2-phenylthioimidazole (**67**)[48] with LDA and dimethyl oxalate provided the required α-keto ester **84** as the major product, accompanied by a number of minor unidentified byproducts. Pure **84**, readily obtained by flash chromatography of the crude product mixture on silica gel, was obtained in 41% yield. Efforts to increase the moderate yield of **84** involved the use of alternative lithium bases (e.g. *n*-BuLi and LiTMP) and solvent systems (Et$_2$O, THF-DME). Unfortunately, no conditions were identified that offered improvments to this process. The structural assignment of **84** was in full accord with its spectral data. The α-keto ester moiety displayed stretching absorptions in the IR spectrum at 1736 (ester C=O) and 1651 cm^{-1} (ketone C=O). The ^{13}C NMR spectrum included two carbonyl resonances (δ 172.9 and 162.2) and two resonances which could be assigned to the methyl ester and *N*-methyl carbons of **84** (δ 53.3 and 34.3, respectively). The ^{1}H NMR spectrum of **84** displayed, in addition to six aromatic proton resonances, two singlets corresponding to the methyl ester (δ 3.93) and *N*-methyl (δ 3.92) protons.
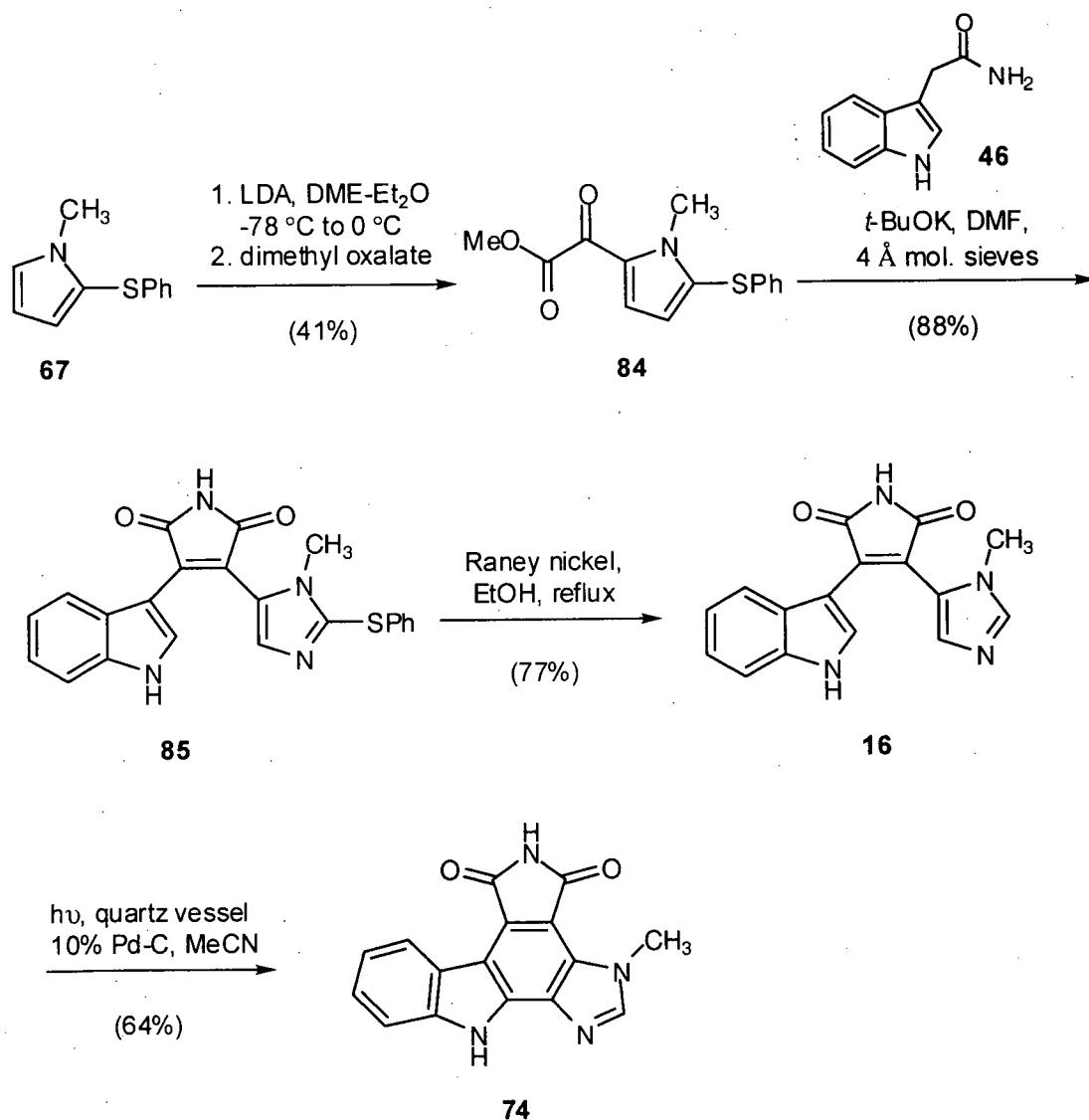
Scheme 3.15. Total syntheses of didemnimide C (**16**) and 17-methylgranulatimide (**74**).

Condensation of **84** with indole-3-acetamide (**46**) in the presence of 4 Å molecular sieves

gave an excellent yield of the substituted maleimide **85**. As expected, the spectral data acquired

from **85** was similar to that reported by Fenical and co-workers for didemnimide C (**16**).[14] The IR

spectrum of **85** included two carbonyl C=O stretching absorptions (1760 and 1713 cm⁻¹) which

corresponded well to those reported for **16** (1766 and 1700 cm⁻¹).[14] In the ¹H NMR spectrum, two

broad NH resonances (δ 12.06 and 11.19) were assigned to the indole NH and the maleimide NH,

respectively, by comparison of their chemical shifts to those reported for **16** (δ 12.02 and 11.13).

In addition, the ^{13}C NMR spectrum contained 17 aromatic carbon resonances and two characteristic maleimide carbonyl resonances at δ 171.6 and 171.4. As expected, the didemnimide **85** was isolated as a red solid, which resembled in color the structurally related didemnimides A-D (Figure 3.3).

Employing conditions used in the synthesis of didemnimide A (**14**) (*vide supra*), desulfurization of the substituted maleimide **85** with W-2 Raney nickel in refluxing EtOH, provided didemnimide C (**16**). The ^{1}H and ^{13}C NMR spectral data (Table 3.5) derived from this material agreed with those reported by Steglich and co-workers for their synthetic material.[26]

The photocyclization of didemnimide C (**16**) in the presence of Pd/C provided 17-methylgranulatimide (**74**) in 64% yield. The relatively low efficiency of this transformation is likely due to very low solubility of the latter compound in organic solvents. As expected, the ^{1}H NMR spectrum of **74** was similar to that of granulatimide (**22**), except that the resonance due to the imidazole N-Me function in **74** (δ 4.31) replaced the corresponding NH signal (δ 13.57) of **22**. Interestingly, as observed in the ^{1}H NMR spectrum of **22**, the resonance of the indole C-4 proton in **74** appeared at δ 8.94. Furthermore, the imidazole N-Me groups of didemnimide C (**16**) and **74** gave rise to singlets at δ 3.17 and 4.31, respectively. These data clearly demonstrated the deshielding effects of the neighbouring maleimide carbonyl groups on the indole C-4 proton and the imidazole N-Me protons in the planar structure **74**. The IR spectrum of **74** showed two strong maleimide C=O stretching absorptions (1734 and 1703 cm^{-1}). Additionally, high-resolution mass spectrometric analysis yielded a molecular ion at m/z 290.0804, which was accounted for by the formula $C_{16}H_{10}N_4O_2$. Complete assignment of all resonances in the ^{1}H and ^{13}C NMR spectra (see Experimental) by HMBC, HMQC and COSY experiments confirmed the structure of **74**.

Table 3.4. ^{1}H and ^{13}C NMR spectral data for didemnimide C (**16**) (recorded in DMSO-d_6).
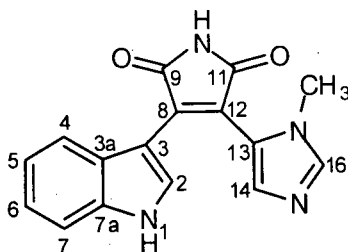
Atom No.	Literature values[26]		Synthetic Didemnimide C	
	^{13}C δ (ppm)[a]	^{1}H δ (ppm) (mult., J (Hz))[b]	^{13}C δ (ppm)[a]	^{1}H δ (ppm) (mult, J (Hz))[c]
1		12.02 (bs)		11.97 (bs)
2	131.8	8.07 (bs)	132.0	8.06 (d, 2.6)
3	105.2		105.0	
3a	125.0		124.7	
4	119.9	6.38 (d, 8.0)	119.7	6.40 (d, 8.1)
5	120.8	6.77 (dd, 8, 8)	120.5	6.78 (dd, 8, 8)
6	122.6	7.10 (dd, 8, 8)	122.3	7.10 (dd, 8, 8)
7	112.5	7.44 (d, (8.0))	112.2	7.44 (d, 8.1)
7a	136.6		136.4	
8	134.1		133.9	
9	172.0[d]		171.9[d]	
10		11.13 (bs)		11.09 (bs)
11	171.8[d]		171.7[d]	
12	134.1		118.6	
13	122.6		122.3	
14	131.8	7.07 (s)	131.5	7.07 (bs)
16	140.4	7.70 (s)	140.3	7.69 (s)
N-Me	32.3	3.15 (s)	32.0	3.17 (s)

[a] Recorded at 100.5 MHz. [b] Recorded at 500 MHz. [c] Recorded at 400 MHz. [d] May be interchanged.

3.6.2 Syntheses of isodidemnimide A (86), isogranulatimide A (75) and B (76)

Substance **86** (Scheme 3.17) is isomeric with didemnimide A (**14**) and, consequently, we have named the former compound isodidemnimide A. On the basis of earlier studies, it seemed probable that **86** could be conveniently prepared by a base promoted condensation of the amide **87** with methyl glyoxyate **88**. It also seemed likely that **86**, or suitable derivatives thereof, would serve as convenient synthetic precursors to isogranulatimides A (**75**) and B (**76**).

The syntheses of the known compounds **87** and **88** are summarized in Scheme 3.16. Thus, conversion of imidazole into the required amide **87** was effected via modification of a procedure reported by Sundberg and co-workers.[54] It was found that generation of the acetamide **87** by the sequential treatment of a solution of imidazole in DMF with NaH and iodoacetamide was superior to conditions (KOH, DMSO, iodoacetamide) reported by Sundberg for this transformation and consistently provided higher yields of imidazole-1-acetamide (**87**). The spectral and physical data obtained from **87** agreed with that reported in the literature.[54]
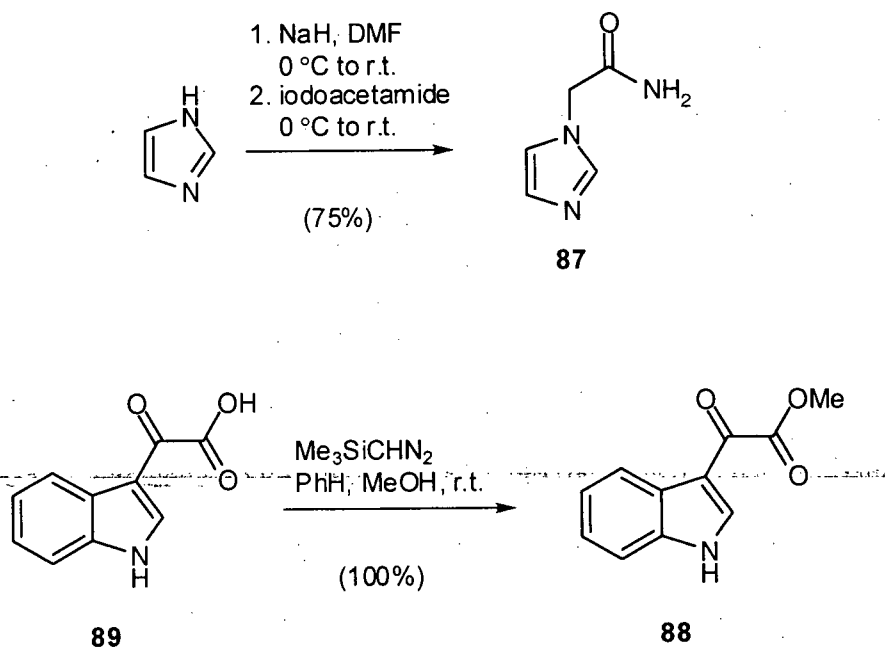
Scheme 3.16. Syntheses of imidazole-1-acetamide (**87**) and methyl indolyl-3-glyoxylate (**88**).

Esterification of 3-indoleglyoxylic acid (89) with MeOH in the presence of an ion-exchange resin has been reported to provide 88 in good yield.[34] However, it could be shown that the conversion of 89 into 88 can be accomplished conveniently and quantitatively by treatment of a solution of 89 in MeOH and benzene with trimethylsilyldiazomethane (TMSCHN$_2$)[55] (Scheme 3.16). Upon reaction with MeOH, TMSCHN$_2$ generates diazomethane and methoxytrimethylsilane *in situ*, avoiding the need to prepare and handle the former reagent, which is both highly toxic and explosive. The spectral and physical data obtained from 88 was in agreement with that reported in the literature.[34]

Scheme 3.17 outlines the use of substances 87 and 88 for the synthesis of isodidemnimide A (86). Initially, potassium *tert*-butoxide-mediated condensation of 87 and 88 in warm (~45 °C) DMF gave modest yields (~30%) of the expected product isodidemnimide A (86). Examination of the reaction mixture revealed that a significant amount of *N*,*N*-dimethyl-3-indoleglyoxylamide (90) was also produced. Presumably, this material resulted from reaction of 88 with KNMe$_2$, which in turn had been produced by the reaction of solvent (DMF) with *t*-BuOK. This unsatisfactory result was ameliorated by carrying out the initial steps of the condensation process at room temperature. Under these conditions, the starting materials 87 and 88 were consumed, but the expected product 86 was not generated. It was thus assumed, that the desired condensation reactions (87 + 88 → 91 → 92) had taken place but that the final (dehydration) step (92 → 86) of the overall transformation had not yet occurred. Fortunately, when the reaction mixture was subsequently warmed to 45 °C to promote the dehydration step, isodidemnimide A (86) was produced in very good yield (Scheme 3.17). The IR spectrum of 86 exhibited strong maleimide carbonyl stretching absorptions at 1767 and 1719 cm^{-1}. The ^{1}H NMR spectrum of 86 included three singlets (δ 7.78, 7.29 and 7.04) which corresponded to the three imidazole protons. Further proof of a successful condensation between 87 and 88 was seen in the

^{13}C NMR spectrum, which contained the expected 13 aromatic carbon signals as well as two maleimide carbonyl resonances (δ 170.4 and 168.4).
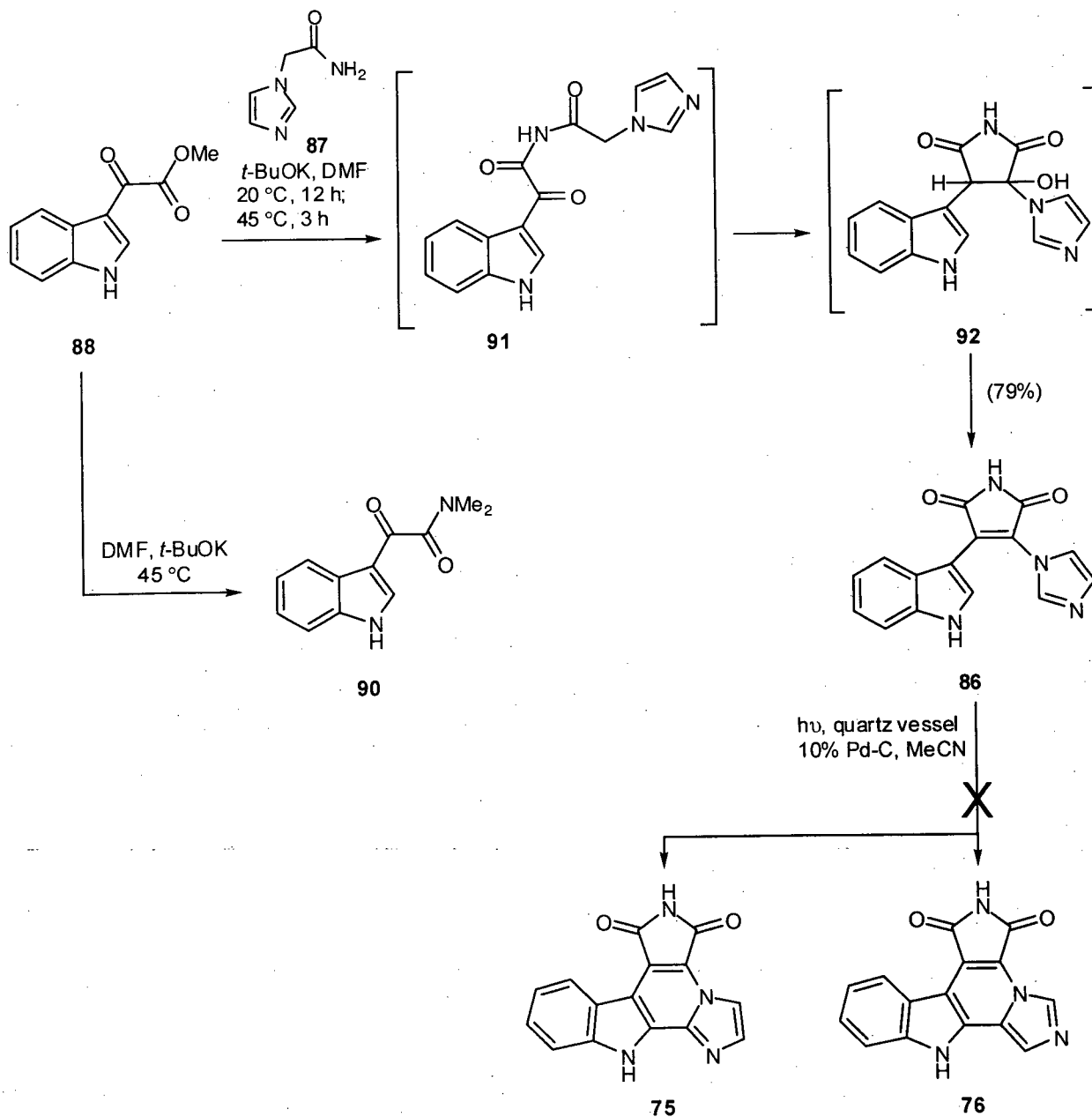
Scheme 3.17. Synthesis of isodidemnimide A (**86**).

Attempts to convert **86** into isogranulatimides A (**75**) and/or B (**76**) (Figure 3.17) via the previously employed photocyclization-oxidation protocol were notably unsuccessful. Both the starting material **86** and the products **75** and **76** are sparingly soluble in acetonitrile, and various

attempts to effect the photocyclization reaction consistently produced intractable material that was very difficult to cope with experimentally. Consequently, attention was directed toward the preparation and cyclization of suitable derivatives of **86**. To that end, treatment of **88** with NaH in THF, followed by reaction of the resultant anion with (2-trimethylsilylexthoxy)methyl chloride (SEM-Cl), furnished the SEM derivative **93** (Scheme 3.18). The spectral data obtained from **93** was in full accord with the assigned structure. The IR spectrum of **93** showed two strong C=O stretching absorptions (1733 and 1637 cm^{-1}). The ^{1}H NMR spectrum of **93** was similar to that obtained for the starting material **88**, however, a resonance attributed to the indole NH (δ 12.40) in **88** was replaced by a series of resonances assigned to the SEM function in **93** (see Experimental).

Condensation of the oxalate **93** with the amide **87**, in the presence of 4 Å molecular sieves, produced the desired 1-(SEM)-isodidemnimide A (**94**) in high yield, accompanied by a minor amounts (14%) of the methoxy derivative **95**. Presumably, **95** was produced by reaction (conjugate addition-β-elimination) of the maleimide **94** with methoxide ion, which is produced during the condensation of **93** with **87**. It is noteworthy, that when the reaction was carried out in the absence of 4 Å molecular sieves, **95** was the major product. Spectral data acquired for **94** supported the structural assignment, and was in close agreement with that reported for isodidemnimide A (**86**) (Scheme 3.17). The IR spectrum of **94** exhibited two strong stretching absorptions (1769 and 1723 cm^{-1}) corresponding to the two maleimide carbonyls. The ^{1}H NMR spectrum displayed resonances for the 1-(SEM)-indole as well as three 1-proton singlets (δ 7.97, 7.24 and 7.15) which were attributed to the three imidazole protons.
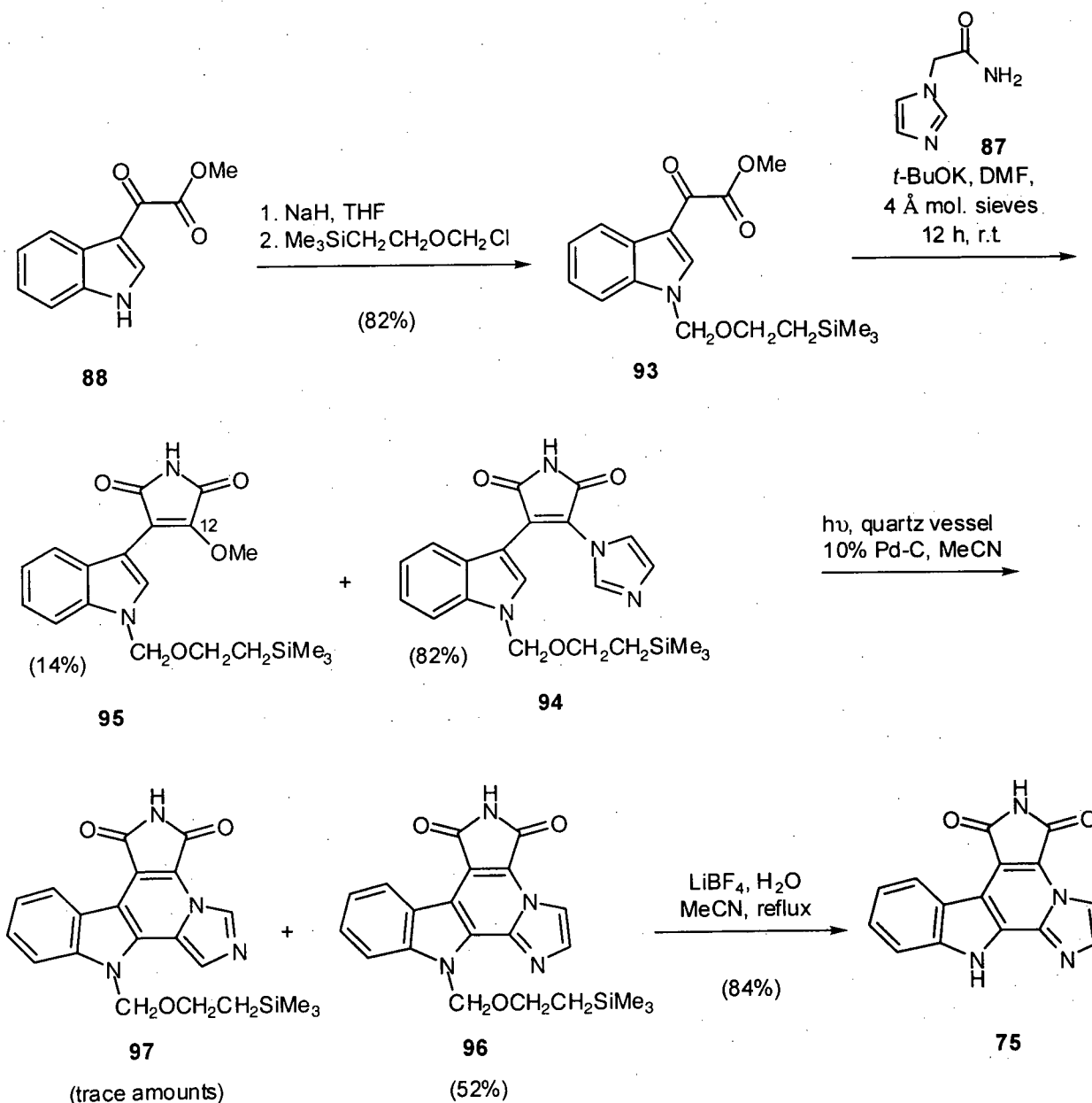
Scheme 3.18. Synthesis of isogranulatimide A (**75**).

The structure of the byproduct **95** was determined through analysis of spectral data acquired on this substance. Low resolution mass spectrometric analysis of **95**, presented a molecular ion peak at m/z 372 which was accounted for by the formula $C_{19}H_{24}N_2O_4Si$, consistent with the proposed structure. Comparison of ^1H NMR spectra recorded from 1-(SEM)-isodidemnimide A (**94**) and the byproduct **95** supported the displacement of the imidazole

function in the byproduct, as the three imidazole CH resonances (δ 7.97, 7.24 and 7.15) observed in the spectrum of **94**, were absent in that of **95**. The ^{1}H NMR spectrum of **95** also displayed an additional 3-proton singlet at δ 4.27, which corresponded to the C-12 methoxyl function. The IR spectrum included two strong maleimide C=O stretching absorptions at 1761 and 1713 cm^{-1}.

The SEM derivative of isodidemnimide A, compound **94**, is considerably more soluble in organic solvents than the parent substance, isodidemnimide A (**86**). Irradiation of a solution of **94** in MeCN in the presence of 10% Pd-C produced, after chromatographic purification of the crude product, 1-(SEM)-isogranulatimide A (**96**) in 52% yield, accompanied by a trace amount of the isomeric 1-(SEM)-isogranulatimide B (**97**). Although the reaction was not particularly clean (a number of unidentified byproducts were produced), the chromatographic acquisition of pure **96** was straightforward. The fact that the major mode of cyclization had involved C-2 of the imidazole ring was shown clearly by performing suitable ^{1}H NMR NOE difference experiments on the product **96**. In the ^{1}H NMR spectrum of **96**, the imidazole protons resonated at δ 7.87 and 8.49. Irradiation of the signal at δ 7.87 caused enhancement of the signal at δ 8.49 and vice versa (Figure 3.14). Again, the planarity of **96** was evidenced in the ^{1}H NMR spectrum by the large chemical shift of the indole H-4 proton (δ 8.78), which results from the deshielding effect of the neighbouring maleimide C-9 carbonyl. The IR spectrum of **96** showed two strong maleimide C=O stretching absorptions (1757 and 1721 cm^{-1}). Additionally, high-resolution mass spectrometric analysis yielded a molecular ion at m/z 406.1461, which was accounted for by the formula $C_{21}H_{22}N_4O_2Si$.
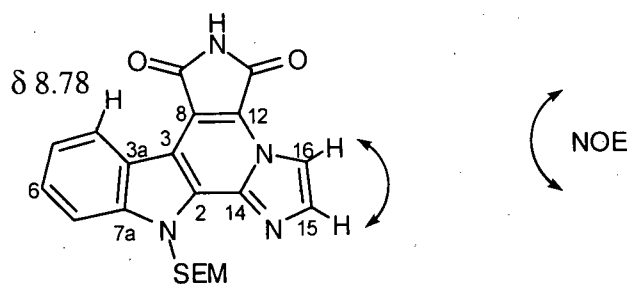
Figure 3.14. Spectroscopic evidence for the planar
structure of 1-SEM-isogranulatimide A (**96**).

Finally, reaction of **96** with LiBF$_4$ in MeCN containing a small amount of water[53] furnished isogranulatimide A (**75**) in excellent yield (Scheme 3.18). As expected, the ^{1}H NMR spectrum of **75** is very similar to that of 1-(SEM)-isogranulatimide A (**96**), except that the resonance due to the indole NH function in **75** (δ 13.14) replaced the corresponding N-SEM resonances observed in that of **96**. The ^{13}C NMR spectrum of **75** included the 13 expected aromatic carbon signals in addition to the two maleimide carbonyl resonances (δ 168.5 and 165.3). Complete assignment of both ^{1}H and ^{13}C NMR resonances (see Experimental) using HMBC, HMQC and COSY experiments, further supported the structural assignment of **75**.

The original goal of this study, however, was the syntheses of both isogranulatimide A (**75**) and B (**76**). Consequently, attention was focused on the synthesis of a suitably solubilized analogue of isodidemnimide A (**86**) whose photocyclization might lend access to both isomers **75** *and* **76**. Steglich and co-workers have reported success in a similar cyclization, in which the indole NH was protected by a t-butoxycarbonyl (BOC) function,[26] hence, 1-(BOC)-isodidemnimide A (**98**) (Scheme 3.19) was selected as a potential precursor to both **75** and **76**.
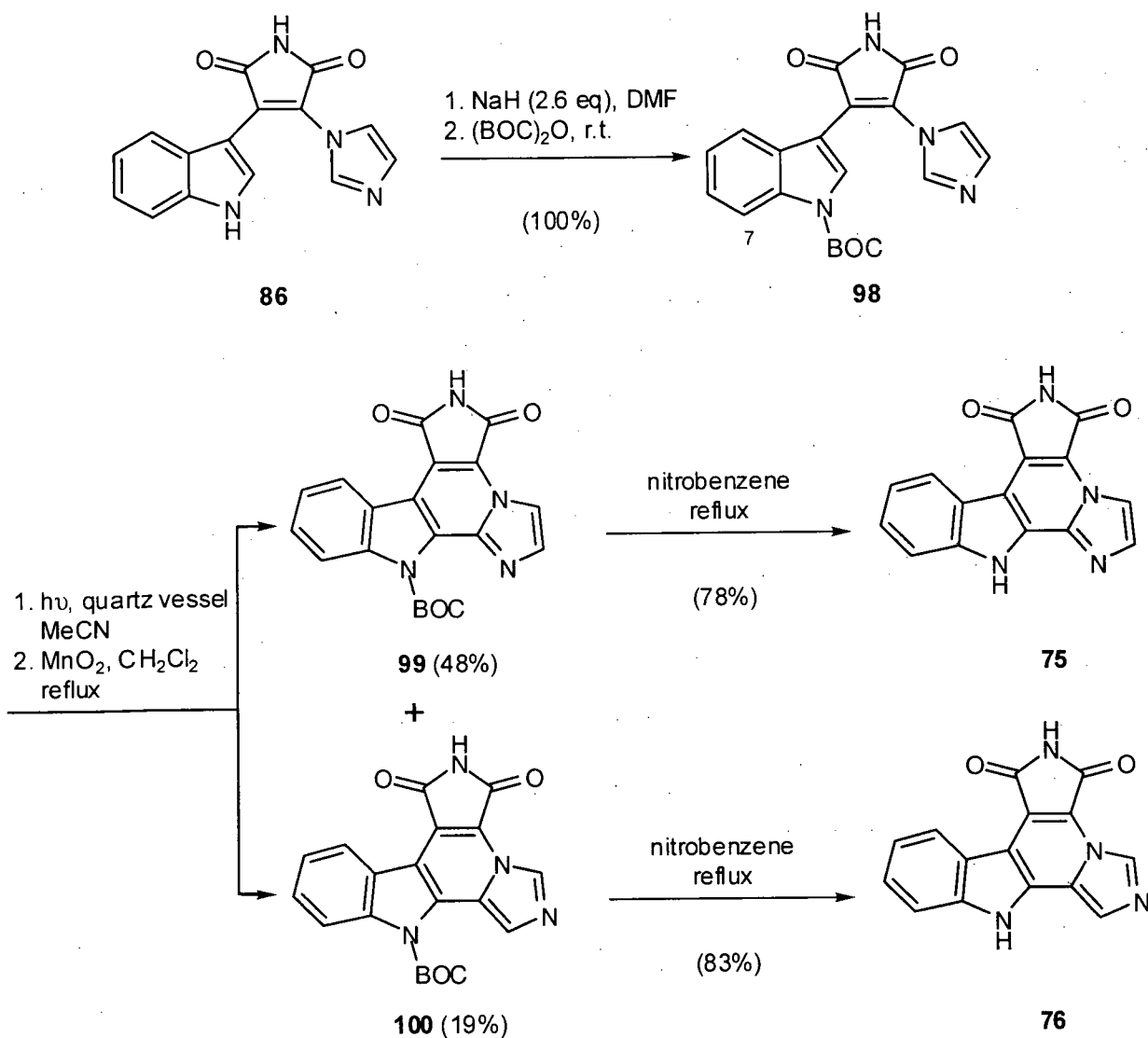
Scheme 3.19. Syntheses of isogranulatimide A (**75**) and isogranulatimide B (**76**).

Scheme 3.19 summarizes the use of 1-(BOC)-isodidemnimide A (**98**) as an intermediate

for the syntheses of both isogranulatimides A (**75**) and B (**76**). Sequential treatment of

isodidemnimide A (**86**) with sodium hydride (2.6 equivalents) and di-*tert*-butyl dicarbonate

resulted in the production of **98** in quantitative yield. Spectral data acquired from **98** confirmed

the structural assignment. In particular, the ¹H NMR spectrum displayed, in addition to

resonances similar to those of the parent compound isodidemnimide A (**86**), a 9-proton singlet at

δ 1.66 for the *t*-butyl moiety. Further evidence for the assigned structure came from the

deshielding of the indole H-7 in the ^{1}H NMR spectrum of **98** (δ 8.10) relative to that in 1-(SEM)-isodidemnimide A (**94**) (δ 7.50). This data supported the propinquity of the di-*tert*-butyl carbonate carbonyl and the adjacent indole C-7 proton.

After some preliminary experimentation, it was found that irradiation of a solution of **98** in MeCN with a 275 Watt light bulb for one hour, followed by treatment of the resultant crude product with manganese dioxide in refluxing dichloromethane,[26] afforded a mixture of products. Flash chromatography of this material on silica gel provided 1-(BOC)-isogranulatimide A (**99**) and 1-(BOC)-isogranulatimide B (**100**) in yields of 48 and 19% respectively. Mechanistically, the cyclization that leads, after oxidation, to both **99** and **100** can be viewed as an electrocyclic (10 e⁻) ring closure.[56] Consequently, the cyclization should proceed in a conrotatory fashion, via a photochemically excited state. In this manner, a carbon-carbon bond is formed between the indole C-2 and the imidazole C-14 or C-17 (Pathway A or B, respectively, Scheme 3.20). This ring closure yields either the zwitterionic species **101** or **102**. In pathway A, a five-electron anionic [1,4]-hydrogen shift, a suprafacial process, would provide the resonance-stabilized zwitterion **103**. A subsequent five-electron anionic [1,4]-hydrogen shift should then yield the zwitterionic succinimide **104**, a resonance form of the succinimide **105**. Enolization of a maleimide carbonyl in the highly unstable *trans*-succinimide **105** would then provide the *cis*-succinimide **106**, a derivative of which has been isolated and fully characterized by Steglich and co-workers.[26] In pathway B, a similar sequence of events leads to the *cis*-succinimide **110**. Oxidation of the stable dihydro intermediates **106** and **110** by MnO_2 affords the pentacyclic alkaloids **99** and **100**.
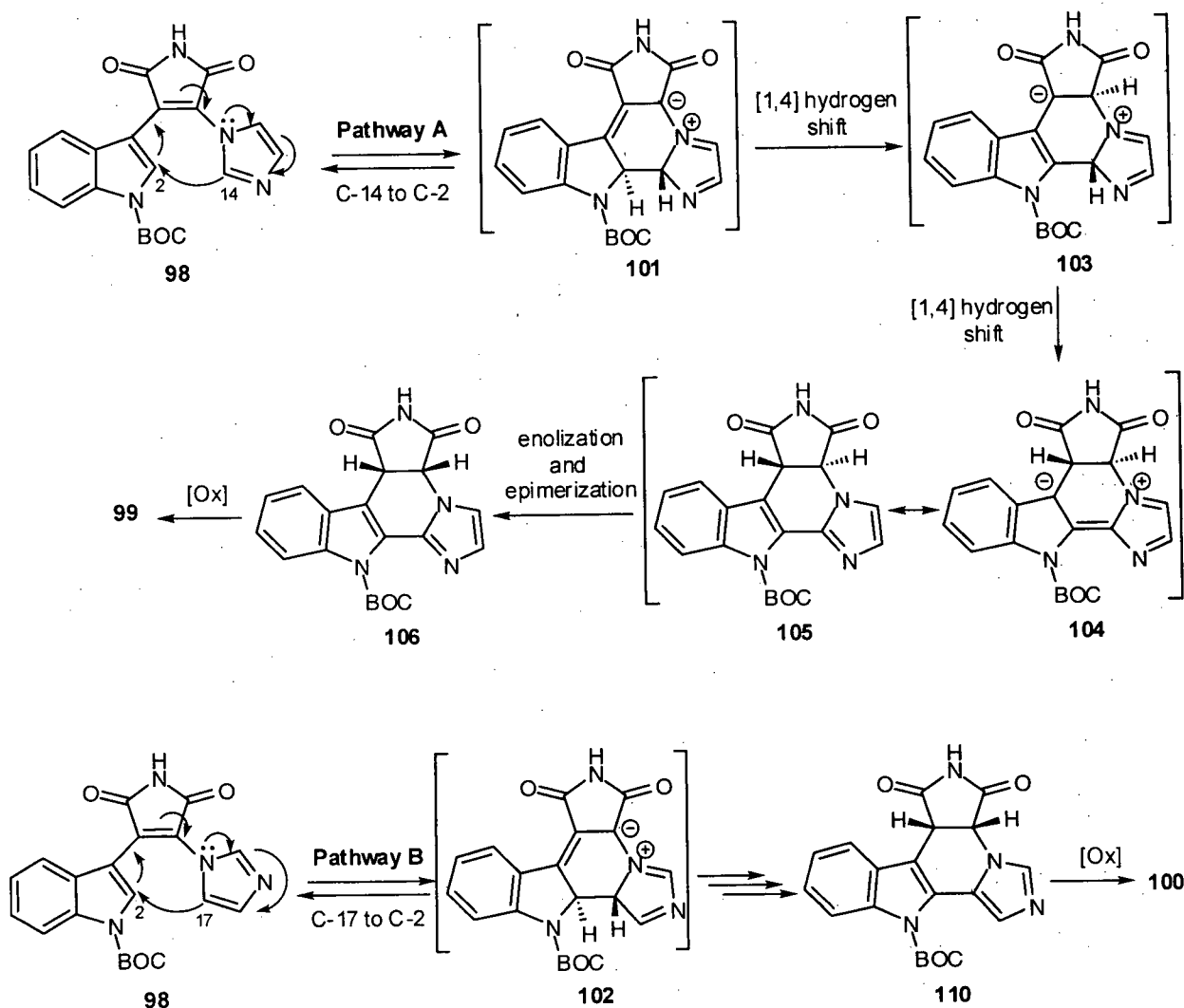
Scheme 3.20. Proposed mechanism for the photochemical conversion of 1-BOC-isodidemnimide A (**98**) into 1-BOC-isogranulatimide A (**99**) and 1-BOC-isogranulatimide B (**100**).

Thermolytic removal of the BOC function from **99** and **100** was conveniently achieved[57] by refluxing nitrobenzene solutions of each of these substances for one hour (Scheme 3.19). The corresponding products, isogranulatimide A (**75**) and B (**76**) were obtained in yields of 78 and 83%, respectively. The ¹H NMR spectrum of the former compound was identical with that of the same substance obtained as described above (Scheme 3.18). On the other hand, the NMR spectra of **76** clearly showed that this material is isomeric with **75**. In the ¹H NMR spectrum of **76**, the two imidazole protons gave rise to singlets at δ 8.87 (C-14 proton) and 7.94 (C-16 proton)

(Figure 3.15). In key NOE difference experiments, irradiation at δ 7.94 increased the intensity of the indole NH resonance (δ 12.99) and vice versa (Figure 3.15). Additionally, no NOE was observed between the protons at C-14 and C-16. The planarity of **76** was evidenced in the ¹H NMR spectrum by the large chemical shift of H-4 (δ 8.53), which results from the deshielding effect of the neighbouring maleimide C-9 carbonyl. The ¹³C NMR spectrum of **76** contained the 13 expected aromatic carbon signals in addition to the two maleimide carbonyl resonances (δ 169.1 and 165.9). The IR spectrum of **76** exhibited two key stretching absorptions (1761 and 1719 cm⁻¹), which were attributed to the maleimide carbonyls. Complete assignment of all resonances in the ¹H and ¹³C NMR spectra (see Experimental) through analysis of HMBC, HMQC and COSY spectral data, confirmed the structural assignment of **76**.
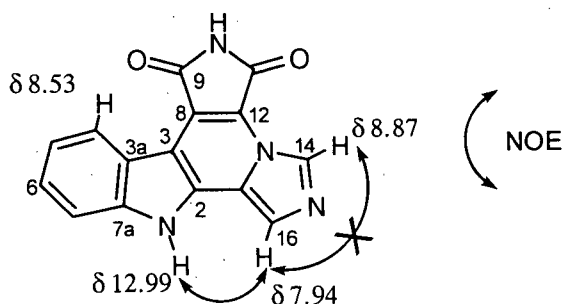
Figure 3.15. Spectroscopic evidence for the planar structure of isogranulatimide B (**76**).

3.6.3 Syntheses of neodidemnimide A (111) and isogranulatimide C (77)

The syntheses of substances **111** and **77** (which we have named neodidemnimide A and isogranulatimide C, respectively) are summarized in Scheme 3.21. A review of the chemical literature relating to the metallation of imidazoles shows that there exists a disparity in the efficiency of acylation of C-2 lithio derivatives of *N*-substituted imidazoles. Although some success has been realised through the use of tertiary amides[58] or the sterically bulky pivaloyl chloride,[45] the use of less hindered acid chlorides or anhydrides[43] has generally provided low yields of the desired 2-acyl adducts. Consequently, it was not surprising to find that reaction of 1-methoxymethylimidazole (**112**)[59] with *n*-BuLi in THF followed by addition of dimethyl oxalate, provided a mixture of products. Nevertheless, column chromatography of the mixture allowed the ready isolation of the required oxalate **113** in 49% yield. The major byproduct isolated from this reaction was the symmetrical diketone **114**, produced by reaction of **113** with a second equivalent of the anion derived from **112**. The structural assignment of **113** was in full accord with its spectral data. The α-keto ester moiety showed stretching absorptions, in the IR spectrum, at 1744 (ester C=O) and 1679 cm^{-1} (imidazolyl ketone C=O). The ^{13}C NMR spectrum included two carbonyl resonances (δ 177.9 and 164.3) and two resonances which could be assigned to the methyl ester and methyl ether carbons of **113** (δ 55.5 and 53.4). The ^{1}H NMR spectrum of **113** displayed two imidazole CH resonances (δ 7.38 and 7.33). In addition, two 3-proton singlets at δ 3.96 and 3.33, corresponding to the methyl ester and methyl ether protons, respectively, and one 2-proton singlet (δ 5.71), assigned to the methylene function of the methoxymethyl protecting group, completed the spectrum.
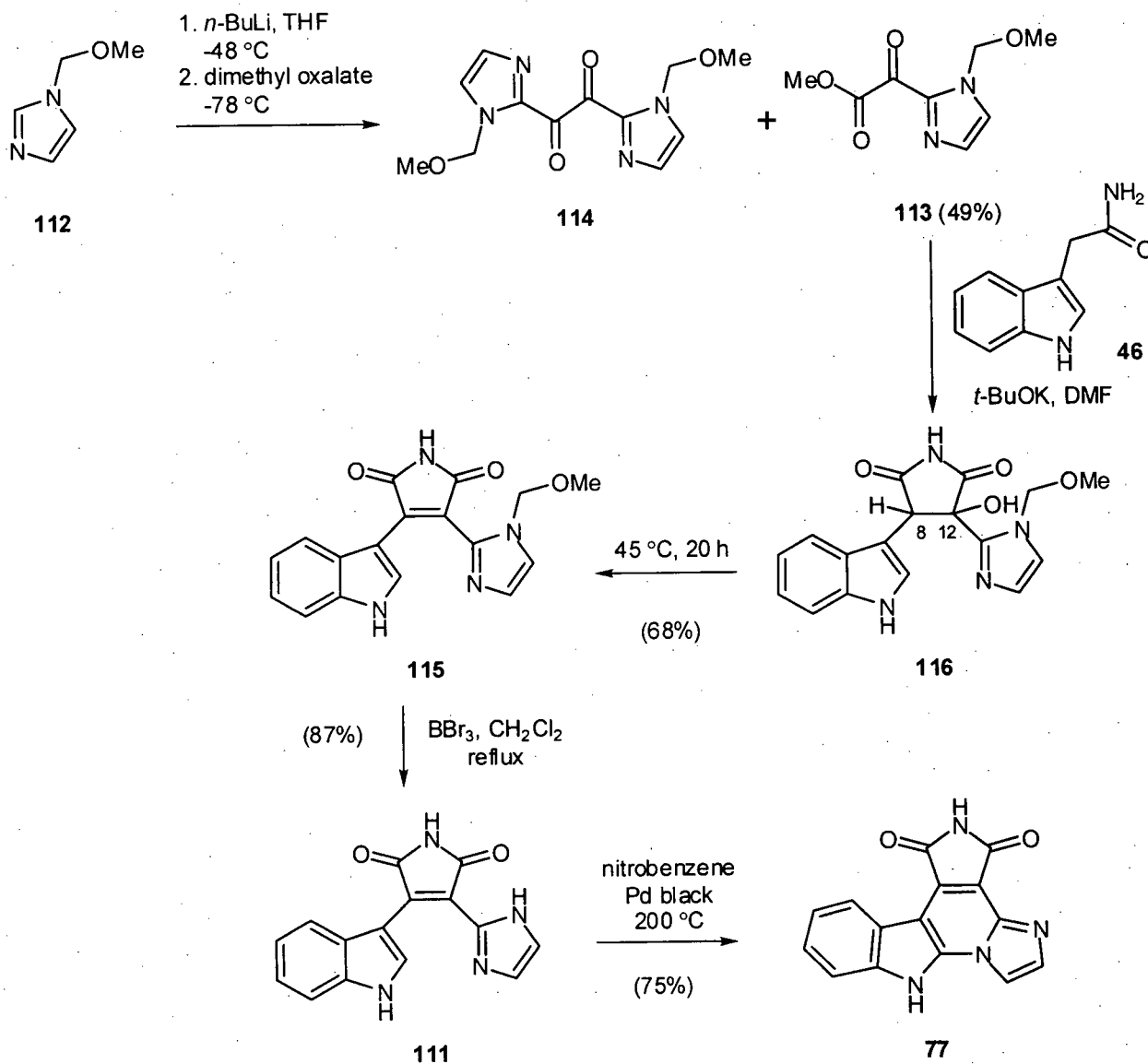
Scheme 3.21. Syntheses of neodidemnimide A (**111**) and isogranulatimide C (**77**).

The structure of the byproduct **114** was determined by analysis of spectral data collected from this substance. Low resolution mass spectrometric analysis of **114** presented a molecular ion peak at m/z 278, which was accounted for by the formula $C_{12}H_{14}N_4O_4$, consistent with the proposed structure. Comparison of ^1H NMR spectra recorded on the α-keto ester **113** and the byproduct **114** differed mainly by the absence of a signal attributed to the methyl ester function in **113** (δ 3.33). The ^{13}C NMR spectrum displayed six carbon resonances, including only one

carbonyl resonance (δ 183.7), indicating the byproduct was indeed symmetric. Analysis of the IR spectrum of **114** confirmed the symmetric nature of the byproduct, as only one C=O stretching absorption, at 1674 cm^{-1}, was observed.

Interestingly, base-mediated condensation of **113** with indole-3-acetamide (**46**) in DMF required extended reaction times at 45 °C to effect efficient formation of the neodidemnimide derivative **115**. For example, when a DMF solution of **113**, indole-3-acetamide (**46**) and *t*-BuOK was stirred at room temperature overnight and then heated at 45 °C for about four hours, little of the product **115** was formed. A spectroscopic examination of the components of the reaction mixture indicated that the major product at this stage was the hydroxy succinimide **116** and that therefore, the required dehydration step (**116** → **115**) had not yet taken place. Spectral data collected from the succinimide **116** confirmed the assigned structure of this intermediate. Low resolution mass spectrometric analysis of **116** presented a molecular ion peak at *m/z* 340, which was accounted for by the formula $C_{17}H_{16}N_4O_4$, consistent with the proposed structure. The ^{1}H NMR spectrum displayed two 1-proton doublets (δ 5.68 and 5.40) which could be assigned to the diastereotopic methylene protons of the methoxymethyl (MOM) protecting group in **116**. In addition, the ^{1}H NMR spectrum showed resonances for both the maleimide and indole *N*H protons (δ 11.64 and 11.05), as well as the expected indole and imidazole CH signals. The ^{13}C NMR spectrum included two carbonyl resonances (δ 177.0 and 176.9) and only 11 aromatic carbon signals. Two additional signals in the ^{13}C NMR spectrum of **116**, which were attributed to C-8 and C-12, resonated at 50.3 and 77.5, respectively. Presumably, the elimination of water from the hydroxy succinimide **116** is impeded by the electron-withdrawing nature of the α-carboxamidine function (i.e. N-C=N of imidazole). Faul and co-workers[60] have reported a similar result in the condensation of indole-3-acetamide (**46**) with 2-thienyl oxalates (e.g. **117**, Scheme 3.22). In fact, it was necessary to isolate the hydroxy succinimide intermediate **118** and perform an additional dehydration step to complete the condensation of these substrates.[60]
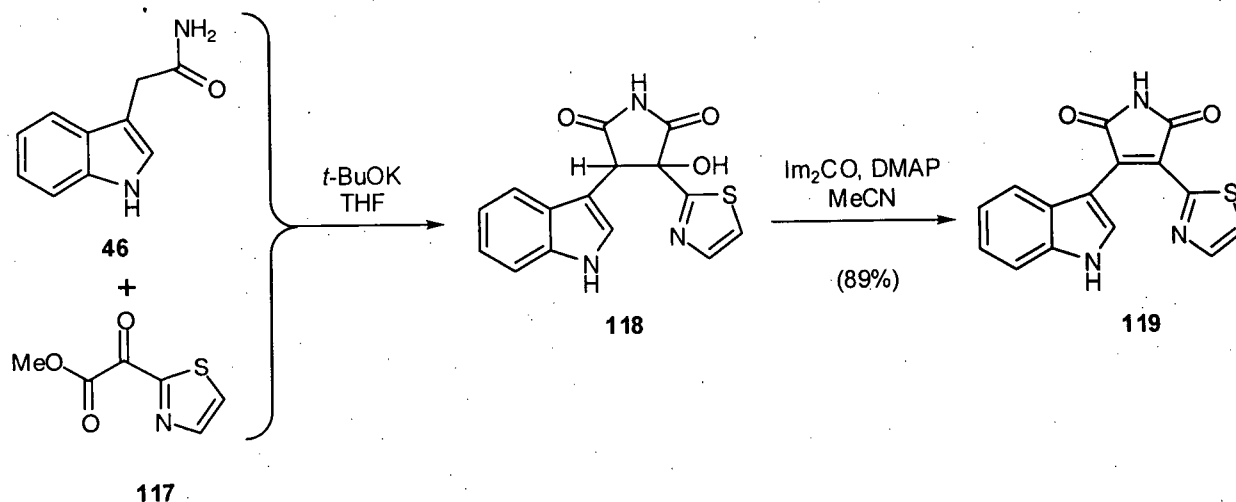
Scheme 3.22. Synthesis of indolyl thienyl maleimides.

Fortunately, when a mixture of indole-3-acetamide (**46**) and the α-keto ester **113** were stirred at 45 °C for twenty hours, 14-methoxymethylneodidemnimide A (**115**) was obtained in 68% yield (Scheme 3.21). The IR spectrum of **115** exhibited two maleimide C=O stretching absorptions at 1759 and 1713 cm^{-1}. The ^{1}H NMR displayed, in addition to the five expected indole CH signals, two imidazole CH resonances (δ 7.46 and 7.11) and two singlets (δ 5.06 and 3.08) which corresponded to the methylene and methyl protons, respectively, of the methoxymethyl (MOM) protecting group. Further evidence that a successful condensation had occurred came from the ^{13}C NMR spectrum, which contained the expected 13 aromatic carbon signals in addition to two resonances (δ 171.6 and 171.4) characteristic of maleimide carbonyls and two resonances at δ 76.8 and 55.7, which were attributed to the methylene and methyl carbons, respectively, of the MOM protecting group.

The conversion of **115** into neodidemnimide A (**111**) by the agency of BBr$_3$ in refluxing CH$_2$Cl$_2$ was clean and efficient. As was observed with didemnimide A (**14**) (*vide supra*), the ^{1}H NMR spectrum recorded for **111** in DMSO-d_6 was complicated by both tautomerization and protonation. This led to the broadening of proton resonances in the ^{1}H NMR spectrum of **111**, the

degree of which was dependent on concentration, making analysis of NMR spectral data difficult. However, this problem could be resolved through the addition of trifluoroacetic acid (TFA) to the NMR sample prior to analysis, providing the neodidemnimide A TFA salt (**120**) (Figure 3.16), which yielded consistent NMR spectra. The ^{1}H NMR spectrum of **120** displayed resonances for both the indole *N*H and maleimide *N*H (δ 12.45 and 11.61, respectively). Additionally, the symmetric nature of the imidazole function in **120** was confirmed by the existence of a 2-proton singlet at δ 7.83, which was attributed to the protons on C-15 and C-16 of the imidazole function. The ^{13}C NMR spectrum of **120** contained, in addition to two maleimide carbonyl signals (δ 170.8 and 170.2), only twelve aromatic carbon resonances, as the imidazole carbons C-15 and C-16 are equivalent in **120**. The IR spectrum of **111** exhibited two strong stretching absorptions for the maleimide carbonyls at 1759 and 1709 cm^{-1}.

120
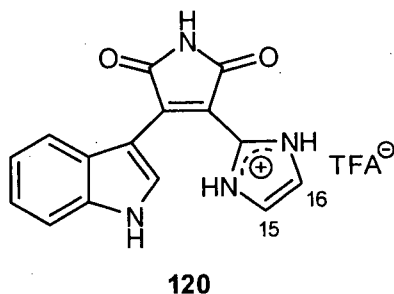
Figure 3.16. Neodidemnimide A TFA salt (**120**).

When a solution-suspension of **111** and Pd black in nitrobenzene was heated at 200 °C under an atmosphere of argon, isogranulatimide C (**77**) was produced in good yield (Scheme 3.21). The spectroscopic data derived from **77** fully supported the structural assignment. The ^{1}H NMR spectrum displayed signals for the two imidazole protons at δ 7.93 (C-16 hydrogen) and δ 8.40 (C-15 hydrogen). In key NOE difference experiments, irradiation at δ 7.93 increased the intensity of the signal at δ 8.40, while irradiation at δ 8.40 enhanced the signals at 7.93 and 13.36

(indole *N*H) (Figure 3.17). The planarity of isogranulatimide C (**77**) was also evidenced in the ^{1}H NMR spectrum, where the large chemical shift of the signal corresponding to H-4 (δ 8.63) indicated the propinquity of this proton to the neighbouring maleimide (C-9) carbonyl. The IR spectrum of **77** showed two strong maleimide C=O stretching absorptions (1755 and 1717 cm^{-1}). Additionally, high-resolution mass spectrometric analysis on **77** yielded a molecular ion at *m/z* 276.0639, which was accounted for by the formula $C_{15}H_8N_4O_2$. Complete assignment of all ^{1}H and ^{13}C NMR resonances (see Experimental) using HMBC, HMQC and COSY experiments confirmed the structure of **77**. It is noteworthy, that the transformation of neodidemnimide A (**111**) into **77** could also be effected, in 75% yield, by simply heating a solution of **111** in DMSO (120 °C, open to the atmosphere) for eight hours.
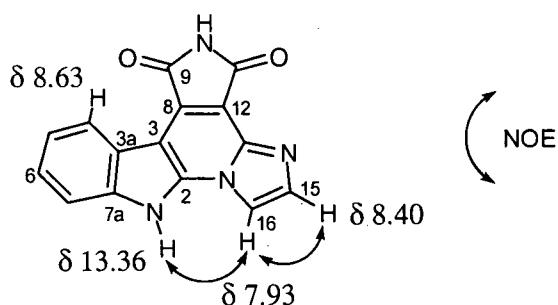
Figure 3.17. Spectroscopic evidence for the planar structure of isogranulatimide C (**77**).

3.6.4 Syntheses of the phenylmaleimide (82) and the 3-aza-indolocarbazole 83

82   83
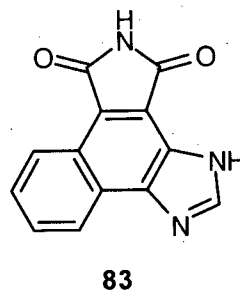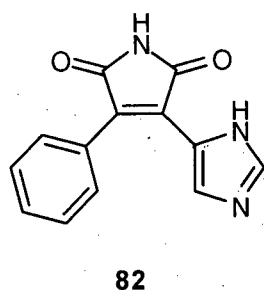
The syntheses of substances **82** and **83** are summarized in Schemes 3.23 and 3.24, respectively, and follow a sequence of reactions similar to that used to synthesize granulatimide (**22**). Thus, base-mediated condensation of the oxalate **53** and phenylacetamide (**121**) effected formation of the phenylmaleimide **122** in excellent yield. The spectral data obtained from **122** was in full accord with the assigned structure. The IR spectrum showed, for the maleimide function, two strong C=O stretching absorptions at 1767 and 1723 cm^{-1}. The ^{1}H and ^{13}C NMR spectra included the expected signals for the maleimide, phenyl and imidazole fragments and the molecular formula of **122** was confirmed by a high-resolution mass spectrometric analysis on the molecular ion.

At this point, it was found that the order chosen for the deprotection and photocyclization events, required to access **83**, was crucial to the success of this sequence. Thus, attempts to effect desulfurization of **122** using Raney nickel in refluxing EtOH provided **123** in very low yield (typically less than 30%). Furthermore, while the removal of the methoxymethyl protecting group proceeded smoothly, irradiation (MeCN, medium pressure mercury vapour lamp) of **124** in the presence of 10% Pd-C yielded a complex mixture of compounds, which was inseparable by standard chromatographic techniques.
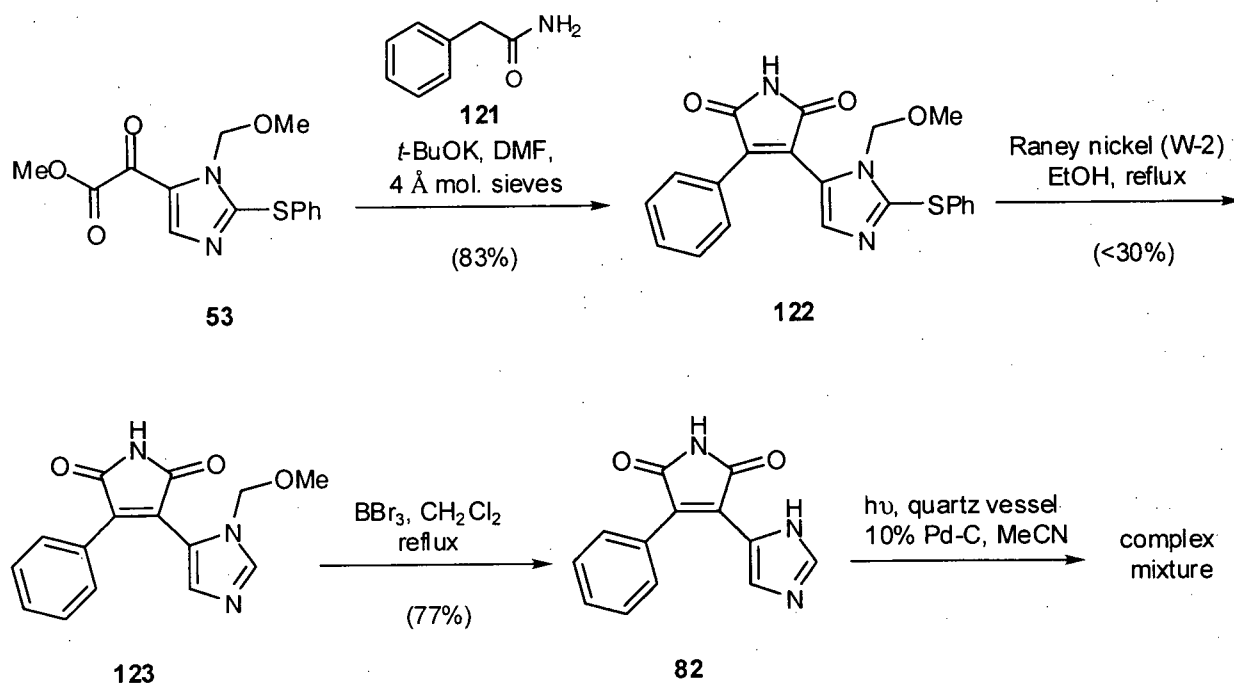
Scheme 3.23. Synthesis of the phenylmaleimide **82**.

The experimental difficulty encountered in the production of **82**, as described in Scheme 3.23, could be avoided through the sequence of reactions described in Scheme 3.24. Thus, photolysis of the phenyl maleimide **122** afforded the 3-azainodole **126**, which could be isolated in good yield from the crude reaction mixture by flash chromatography. The spectral data obtained from **126** were in full accord with the assigned structure. The IR spectrum showed two maleimide carbonyl stretching absorptions at 1762 and 1718 cm^{-1}. In the ^{1}H NMR spectrum of the carbazole **126**, a one-proton doublet that was attributed to the phenyl H-4" resonated at δ 8.95. The downfield chemical shift of this resonance in the ^{1}H NMR spectrum clearly demonstrated the deshielding effect of the neighbouring maleimide carbonyl group on the phenyl C-4" proton in the planar structure **126**. The ^{13}C NMR spectrum contained the 19 expected resonances and the molecular formula of **126** was confirmed by a high-resolution mass spectrometric analysis on the molecular ion.

Treatment of **126** with BBr_3 in refluxing CH_2Cl_2 effected the removal of the MOM

protecting group and the crude product from this reaction was directly subjected to conditions

(refluxing EtOH, W-2 Raney nickel) to effect desulfurization, affording the 3-azaindole **83** in

good yield. The spectral data obtained for **83** were similar to those of granulatimide (**22**) and

isogranulatimide (**23**). The IR spectrum of **83** exhibited two maleimide C=O stretching

absorptions at 1759 and 1719 cm^{-1}, which compared well with those observed for **23** (1758 and

1719 cm^{-1}). As well, the ^1H NMR spectrum of **83** was similar to that of **22**, except that there was

no resonance corresponding to the indole NH. Again, the deshielding effects of the neighbouring

maleimide carbonyl on the phenyl C-4" proton (δ 8.92) in the ^1H NMR spectrum corroborated

the planarity of **83**.
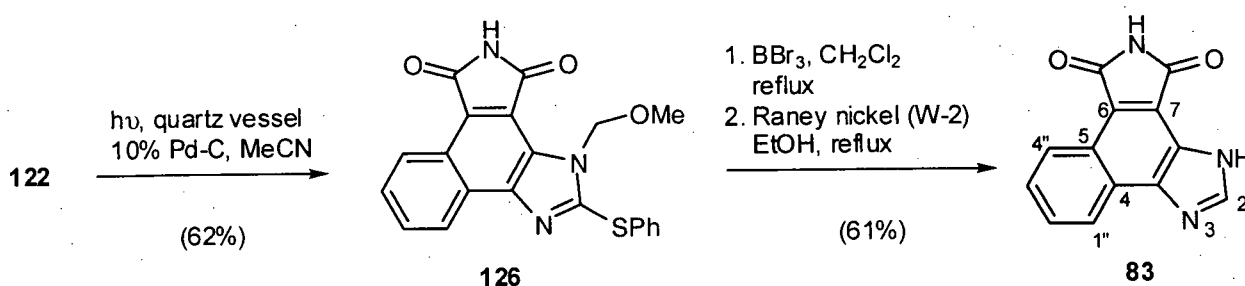
Scheme 3.24. Synthesis of the 3-azaindole **83**.

3.6.5 Syntheses of 1-hexylisogranulatimide (78), 1-hexylgranulatimide (79), 10-methylisogranulatimide (80) and 10-hexylisogranulatimide (81)

Our last objective was the synthesis of alkylated versions of granulatimide (**22**) and isogranulatimide (**23**). The successful completion of this task would provide new analogues of **22** and **23** with different solubility characteristics than the parent compounds, thus expanding the scope of our library of synthetic G2 checkpoint inhibitors. The sequence of synthetic transformations, which led to the successful completion of our objectives are summarized in Schemes 3.25 and 3.26. Thus, treatment of a solution of isogranulatimide (**23**) in DMF with NaH followed by iodomethane provided 10-methylisogranulatimide (**80**) in moderate yield. Similarly, 10-hexyl-isogranulatimide (**81**) was produced by the sequential treatment of **23** with NaH and 1-iodohexane. From the spectroscopic data collected for both **80** and **81**, it was clear that alklyation had occurred on N-10, and not N-1. In the ^{1}H NMR spectra of **80** and **81**, the indole NH appeared at δ 13.22 and 13.35, respectively. These resonances corresponded well to the indole NH resonance observed for isogranulatimide (**23**) (δ 13.48). Additionally, both the ^{1}H NMR spectra of **80** and **81** were without a resonance that could be attributed to the maleimide NH, which appeared at δ 11.11 in that of **23**. In key NOE difference experiments carried out on 10-methylisogranulatimide (**80**), irradiation at δ 13.22 (indole NH) increased the intensities of the signals at 8.65 (imidazole H-16) and 7.52 (indole H-7). Furthermore, irradiation of the 3-proton singlet at 2.94 (N-10 methyl) resulted in no signal enhancements, supporting our structural assignment of **80**, and consequently **81**. Additionally, both the IR spectra of **80** and **81** included two maleimide C=O stretching absorptions at 1758 and 1706 cm^{-1}, and 1761 and 1703 cm^{-1}, respectively.
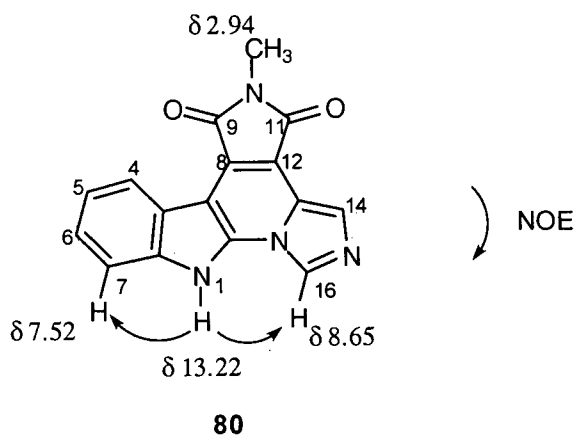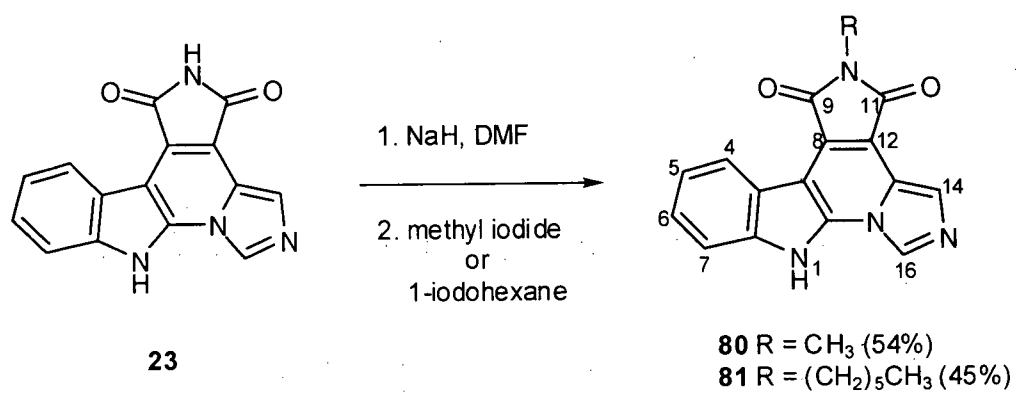
Scheme 3.25. Syntheses of 10-methylisogranulatimide (**80**) and 10-hexylisogranulatimide (**81**).
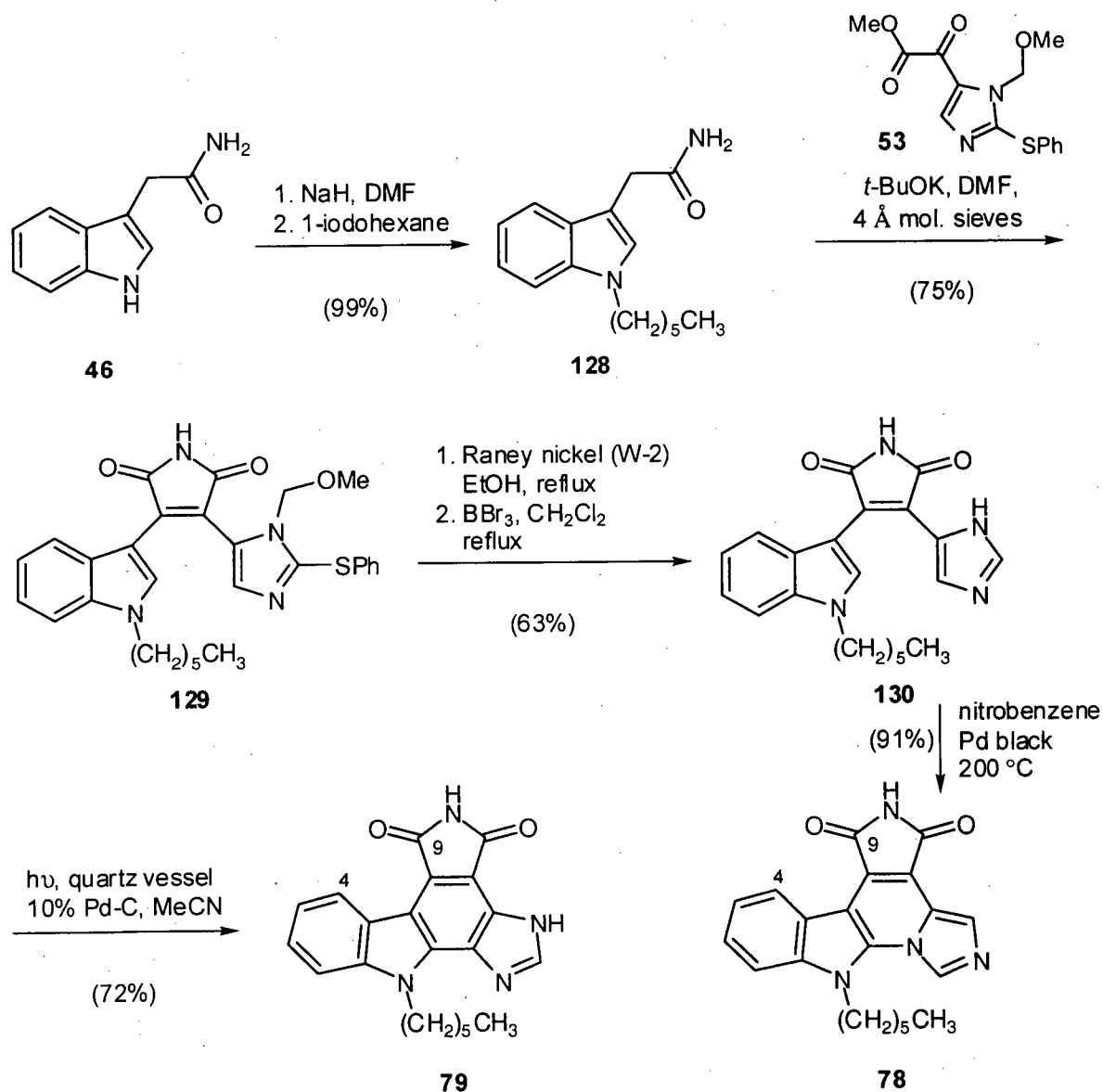
Scheme 3.26. Syntheses of 1-hexylisogranulatimide (**78**) and 1-hexylgranulatimide (**79**).

The syntheses of 1-hexylisogranulatimide (**78**) and 1-hexylgranulatimide (**79**) follow a sequence of reactions analogous to those used to prepare the parent compounds granulatimide (**22**) and isogranulatimide (**23**). *N*-Hexylindole-3-acetamide (**128**), which was required for this sequence, was available in excellent yield through the treatment of indole-3-acetamide (**46**) with two equivalents of NaH, followed by reaction of the resulting dianion with one equivalent of 1-iodohexane. The spectral data obtained from **128** were in accordance with the above

transformation. The IR spectrum showed a C=O stretching absorption at 1651 cm^{-1}. The ^{1}H

NMR indicated, in addition to the expected indole-3-acetamide CH resonances, the presence of

an *n*-hexyl group (13 aliphatic proton signals) and a primary amide, which exhibited two broad

*N*H resonances at δ 6.57 and 5.87.

Condensation of **128** with the oxalate **53**, in the presence of *t*-BuOK and 4 Å molecular

sieves, furnished the substituted maleimide **129**. The spectroscopic data derived from **129** fully

supported the structural assignment. The ^{1}H NMR spectrum displayed two singlets (δ 5.11 and

3.02) for the methoxymethyl (MOM) protecting group and a series of aliphatic resonances (13

protons total) for the *N*-hexyl function. The aromatic resonances in the ^{1}H NMR spectrum

included signals that related to the indole, imidazole and thiophenyl functions of **129**. The IR

spectrum of **129** showed two strong maleimide C=O stretching absorptions at 1760 and 1713

cm^{-1}. Additionally, high-resolution mass spectrometric analysis on **129** yielded a molecular ion at

m/z 514.2043, which was accounted for by the formula $C_{29}H_{30}N_4O_3S$.

Desulfurization of **129** with Raney nickel in EtOH, followed by direct removal of the

methoxymethyl protecting group using BBr$_3$ in refluxing CH$_2$Cl$_2$ afforded 1-hexyldidemnimide

A (**130**) in good yield. It is noteworthy that the reactions and chromatographic purifications

which led to the production of **130** were much easier to cope with experimentally than those

involved in the sequence of reactions that produced didemnimide A (**14**) (*vide supra*). The hexyl

moiety, present in the former sequence, increases the solubility of the parent alkaloid, which

translated to shortened reaction times and simplified chromatographic purifications. As expected,

the ^{1}H NMR spectrum of **130** was similar to that of didemnimide A (**14**), except that the

resonances due to the indole *N*-hexyl function in **130** replaced the corresponding *N*H signal (δ

12.45) of **14**. The ^{13}C NMR spectrum of **130** contained the expected 21 carbon resonances. The

IR spectrum of **130** showed two strong maleimide C=O stretching absorptions (1753 and 1713

cm^{-1}).

The conversion of 1-hexyldidemnimide A (**130**) into 1-hexylisogranulatimide (**78**) was effected by heating a solution of **130** in nitrobenzene at 200 °C with one equivalent of Pd black for eight hours (Scheme 3.26). As expected, the ^{1}H NMR spectrum of **78** was very similar to that of isogranulatimide (**23**), except that the resonances attributed to the indole *N*-hexyl function in **78** (see Experimental) replaced the corresponding indole *N*H signal (δ 13.48) of **23**. The resonance attributed to the indole C-4 proton in **78** appeared at δ 8.49. The large chemical shift for this resonance results from the deshielding effect of the neighbouring maleimide C-9 carbonyl on the C-4 proton, corroborating the planarity of **78**. The IR spectrum showed two strong maleimide C=O stretching absorptions at 1753 and 1713 cm^{-1} and the ^{13}C NMR spectrum included the expected 21 carbon resonances. Additionally, high-resolution mass spectrometric analysis on **78** yielded a molecular ion at *m/z* 360.1585, which was accounted for by the formula $C_{21}H_{20}N_4O_2$.

The synthesis of 1-hexylgranulatimide (**79**), from 1-hexyldidemnimide A (**130**), was accomplished in good yield through the irradiation (MeCN, medium-pressure mercury vapour lamp) of **130** (Scheme 3.26). As expected, the ^{1}H NMR spectrum of **79** is very similar to that of granulatimide (**22**), except that the resonances due to the indole *N*-hexyl function in **79** (see Experimental) replaced the corresponding indole *N*H signal (δ 12.58) of **22**. The resonance attributed to the indole C-4 proton in **79** appeared at δ 8.95. The large chemical shift for this resonance results from the deshielding effect of the neighbouring maleimide C-9 carbonyl on the C-4 proton, corroborating the planarity of **79**. The IR spectrum of **79** showed two maleimide C=O stretching absorptions at 1752 and 1698 cm^{-1} and the ^{13}C NMR spectrum included the expected 21 resonances. Additionally, high-resolution mass spectrometric analysis on **79** yielded a molecular ion at *m/z* 360.1592, which was accounted for by the formula $C_{21}H_{20}N_4O_2$.

3.7 Isolation of granulatimide (22) and 6-bromogranulatimide (131) from *Didemnum granulatum*

During the investigation of the photochemical transformation of didemnimide A (**14**) to granulatimide (**22**), it was discovered that this conversion occurs upon standing in DMSO under natural sunlight.[61] The ascidian *D. granulatum* grows in very shallow water where it is exposed to intense sunlight and didemnimide A (**14**) is a constituent of *D. granulatum* extracts, so it seemed reasonable to expect that granulatimide (**22**) might be a co-occurring metabolite. Granulatimide (**22**) is insoluble in most common organic solvents including methanol and ethanol, and can only be effectively solubilized with DMF or DMSO. Therefore, in hindsight it was apparent that the extraction of *D. granulatum* with EtOH or MeOH, standard solvents for this purpose, would yield only small amounts of **22**. Nevertheless, with synthetic granulatimide (**22**) as a TLC reference, it was possible to identify **22** in chromatography fractions generated during purification *D. granulatum* alkaloids. Unfortunately, the extracted ascidian tissue had been discarded by the time the solubility and chromatographic properties of synthetic granulatimide (**22**) were discovered. Therefore, the true concentration of granulatimide (**22**) in *D. granulatum* remained to be resolved.

With our knowledge of the solubility of granulatimide (**22**), an alternative extraction procedure was envisaged whereby the ascidian *D. granulatum* would first be extracted with MeOH, then with DMF (see Experimental). Accordingly, a fresh sample of *D. granulatum* was extracted sequentially with MeOH and DMF by Dr. Roberto Berlinck and co-workers in Brazil and the latter extract was concentrated and transported to UBC for further fractionation. Normal phase TLC analysis of the residue indicated the presence of yellow bands with similar chromatographic characteristics to those observed for an authentic sample of synthetic granulatimide (**22**) ($R_F = 0.3$, 10:1 CH_2Cl_2 - MeOH).

Flash chromatography and normal phase HPLC led, eventually, to the isolation of pure granulatimide (**22**) as a yellow solid (see Experimental). The natural sample of granulatimide (**22**) exhibited spectroscopic data identical to that of the synthetic compound. A second, co-occurring metabolite, 6-bromogranulatimide (**131**), was also isolated during the normal phase HPLC purification of granulatimide as a yellow solid. The HREIMS of **131** presented molecular ion peaks at m/z 355.9738 and 353.9792, which were accounted for by the formulae $C_{15}H_7O_2N_4{}^{81}Br$ and $C_{15}H_7O_2N_4{}^{79}Br$, respectively. Comparison of ^1H NMR spectra recorded on granulatimide (**22**) and 6-bromogranulatimide (**131**) verified the absence of a resonance (δ 7.48) assigned to H-6 in **22**. Again, the large chemical shift of H-4 (δ 8.80) in the ^1H NMR spectrum of **131** (Figure 3.18), which results from a deshielding interaction with the neighbouring C-9 maleimide carbonyl, verified the planar nature of **131**. Both ^1H and ^{13}C NMR spectral data of **131** are presented in Table 3.5 and were assigned by analysis of HMQC (Figure 3.19) and HMBC spectra. With the exception of H-6, the proton resonances observed for 6-bromogranulatimide (**131**) were similar to those of granulatimide (**22**). Due to the small amount of available material, however, the carbon resonances of 6-bromogranulatimide (**131**) were necessarily attributed by analysis of HMQC and HMBC spectra. The structure of 6-bromogranulatimide (**131**) is also supported by the co-occurrence of the alkaloid didemnimide B (**15**), a 6-bromo analogue of didemnimide A (**14**), in extracts of *D. granulatum*.

Table 3.5. ^{1}H and ^{13}C NMR data for granulatimide (**22**) and 6-bromogranulatimide (**131**) (recorded in DMSO-d_6).

	Granulatimide		6-Bromogranulatimide	
Atom No.	^{1}H δ (ppm) (mult, J (Hz))[a]	^{13}C δ (ppm)[b]	^{1}H δ (ppm) (mult, J (Hz))[a]	^{13}C δ (ppm)[b,c]
1	12.58 (s)		12.74 (s)	
2		135.4		n.o.
3		113.0		112.0
3a		121.4		118.5
4	8.89 (d, 7.0)	123.8	8.80 (d, 8.6)	125.1
5	7.30 (dd, 7, 7)	120.0	7.47 (dd, 8.6, 1.5)	122.6
6	7.48 (dd, 7, 7)	126.1		120.6
7	7.61 (d, 7.0)	111.6	7.75 (d, 1.5)	114.1
7a		140.4		141.1
8		122.7		122.5
9		169.8		169.3
10	10.96 (s)		11.06 (s)	
11		171.0		171.4
12		109.5		109.9
13		125.7		n.o.
14		133.4		n.o.
15				
16	8.50 (s)	144.5	8.56 (s)	144.7
17	13.57 (bs)		13.68 (bs)	

[a] Recorded at 500 MHz. [b] Recorded at 100.5 MHz. [c] Assignments by inverse detection at 500 MHz (HMQC and HMBC). n.o. (not observed)

131
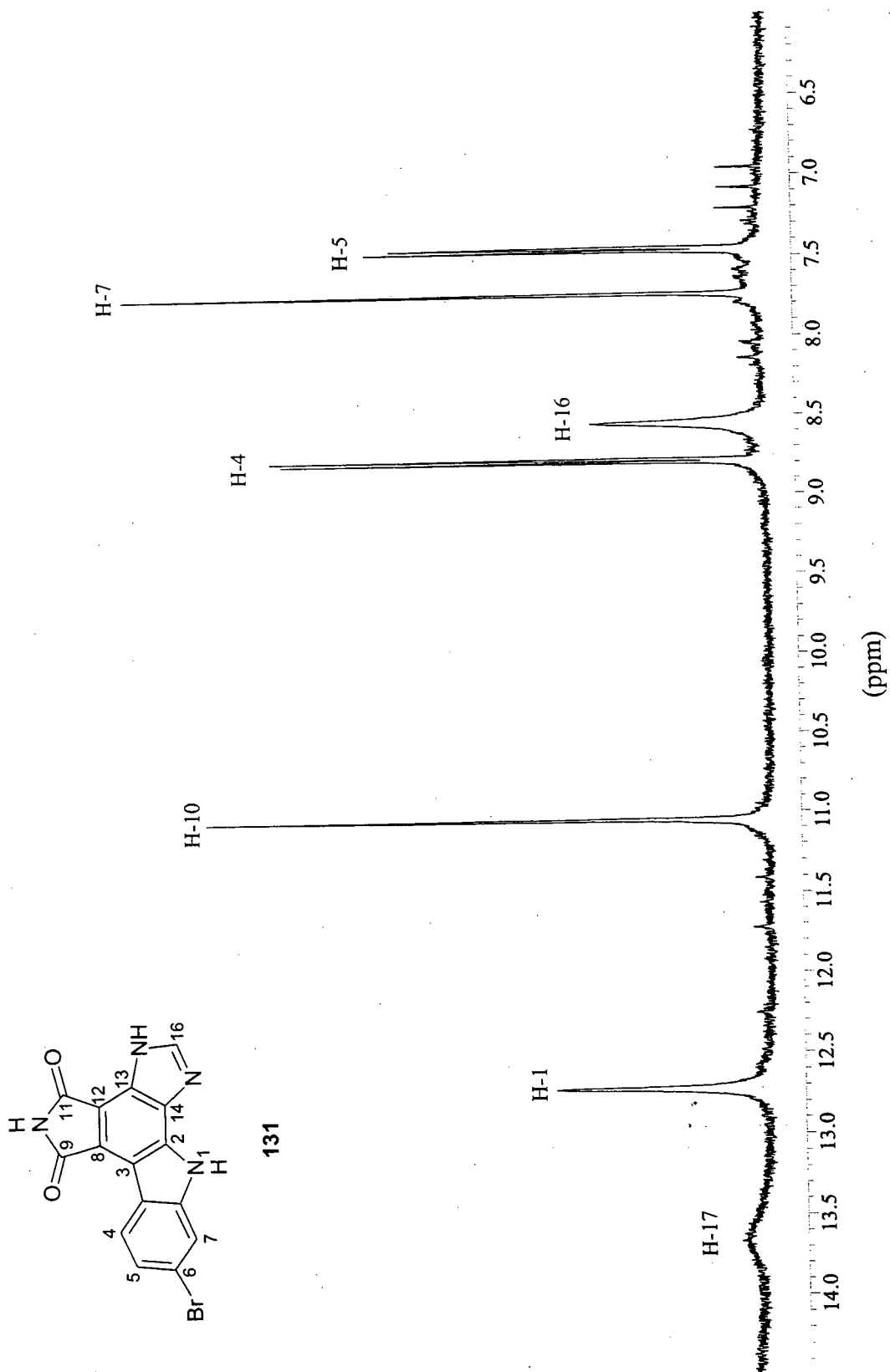
Figure 3.18. ^{1}H NMR spectrum of 6-bromogranulatimide (**131**) (recorded in DMSO-d_6, 500 MHz).
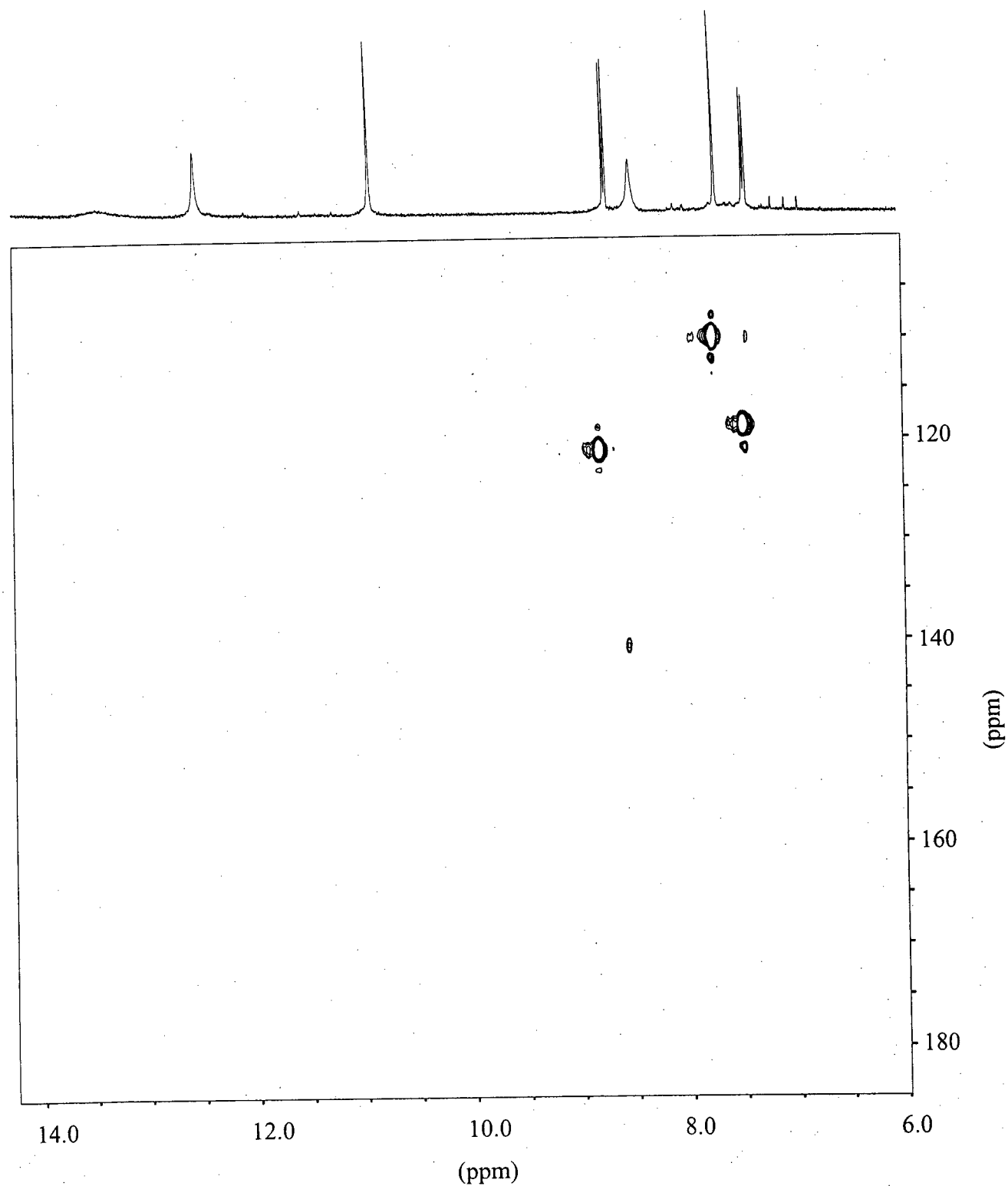
Figure 3.19. HMQC spectrum of 6-bromogranulatimide **(131)** (recorded in DMSO-d_6, 500 MHz).

The isolation of granulatimide (**22**), isogranulatimide (**23**) and 6-bromogranulatimide (**131**), along with a number of didemnimides from *D. granulatum* points to a common biogenetic pathway for this family of alkaloids. Biosynthetically, **22** and **131** represent an alternative mode of cyclization of the putative precursors didemnimide A (**14**) and didemnimide B (**15**),[14] respectively, than is observed with isogranulatimide (**23**) (Scheme 3.27). The structures of granulatimide (**22**) and 6-bromogranulatimide (**131**) are without precedent in natural products and further investigations are warranted to determine whether additional granulatimides, derived from didemnimides C, D and E are present in extracts of *D. granulatum*.

14 $R_1 = R_2 = H$
15 $R_1 = Br$, $R_2 = H$
16 $R_1 = H$, $R_2 = CH_3$
17 $R_1 = Br$, $R_2 = CH_3$

C-2 to C-14 then [O]

22 $R_1 = H$
131 $R_1 = Br$

C-2 to *N*-17 then [O]

23
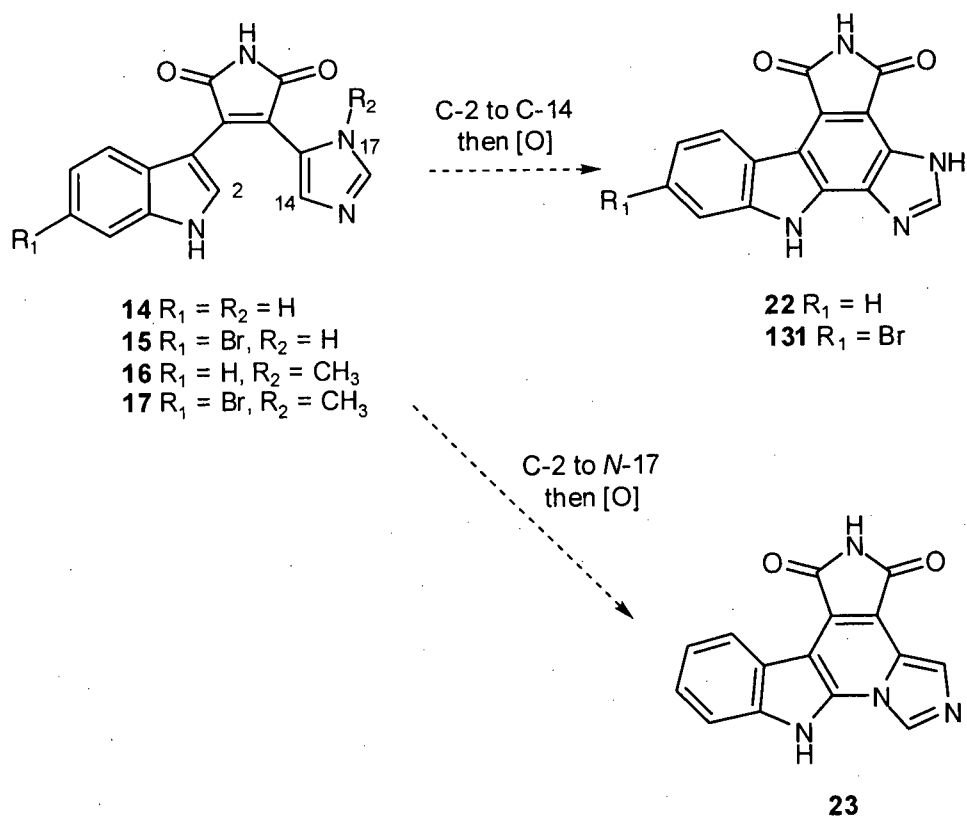
Scheme 3.27. Alternative cyclization modes for the didemnimide alkaloids.
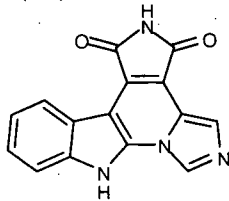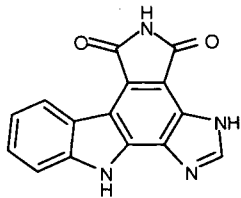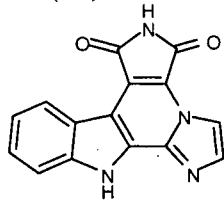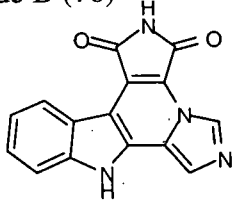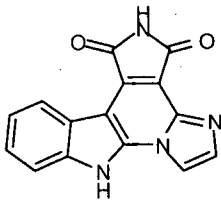
3.8 Biological activity

The biological testing of granulatimide (**22**), isogranulatimide (**23**), the congeners and analogues described above as well as the didemnimide type alkaloids (**14, 16, 86** and **111**) were carried out by collaborators at the University of British Columbia (UBC), Kinetek Pharmaceuticals and the University of Calgary (U of C). Information relating to G2 checkpoint inhibition, investigations into the mechanism of action of isogranulatimide and *in vivo* inhibition of GSK-3β was provided by Professor Michel Roberge and co-workers in the Department of Biochemistry and Molecular Biology at UBC. The *in vitro* inhibition of selected mammalian kinases and Chk1 was performed at Kinetek Pharmaceuticals in Vancouver B.C. by Dr. Jeffery Wheeler and co-workers. The *in vitro* inhibition of Chk2 by isogranulatimide and granulatimide was studied in the Department of Biological Sciences at the U of C by Dr. Susan Lees-Miller and co-workers.

3.8.1 G2 checkpoint inhibition results
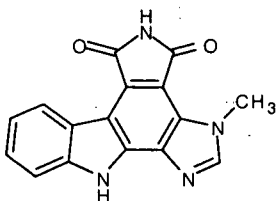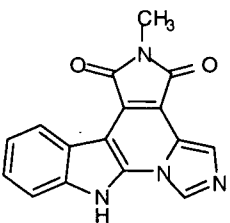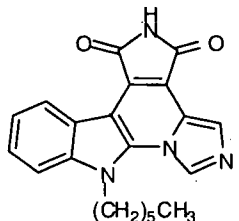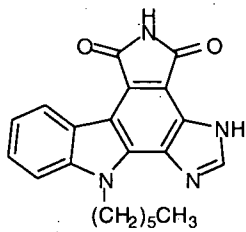
The G2 checkpoint inhibition results obtained for granulatimide (**22**), isogranulatimide (**23**) and congeners and analogues thereof are presented in Tables 3.6 and 3.7 and were obtained following procedures described in Section 1.3. As the biological analysis of these substances is an ongoing pursuit, the results from the biological testing of analogues not presented in this section will be reported in due course. The peak inhibitory concentrations (see Tables 3.6 and 3.7) refer to the concentration of the added alkaloid that induced a maximum number of cells arrested in G2 to enter mitosis, thus overcoming the G2 checkpoint.

Table 3.6. G2 checkpoint inhibition by isogranulatimide (**23**), granulatimide (**22**), isogranulatimide A (**75**), isogranulatimide B (**76**) and isogranulatimide C (**77**).

Compound name and structure	Peak inhibitory Concentration (μM)
Isogranulatimide (**23**)	10
Granulatimide (**22**)	3
Isogranulatimide A (**75**)	Inactive[a]
Isogranulatimide B (**76**)	0.3
Isogranulatimide C (**77**)	30

[a] Inactive at all concentrations tested (from 0.01 to 500 μM).

Table 3.7. G2 checkpoint inhibition by alkylated analogues
of granulatimide (**22**) and isogranulatimide (**23**).

Compound name and structure	Peak inhibitory Concentration (μM)
17-methylgranulatimide (**74**)	Inactive[a]
10-methylisogranulatimide (**80**)	180
1-hexylisogranulatimide (**78**)	60
1-hexylgranulatimide (**79**)	Inactive

[a] Inactive at all concentrations tested (from 0.01 to 500 μM).

The biological data presented in Tables 3.6 and 3.7 indicate that, indeed, this new family of alkaloids possess the ability to override the G2 checkpoint and send cells arrested in G2 prematurely into mitosis. The natural products isogranulatimide (**23**) and granulatimide (**22**) demonstrated maximal G2 checkpoint inhibition activity at concentrations of 10 and 3 μM, respectively. However, the IC_{50} values, or the concentration required for half maximal activity, for **22** and **23** were in the range of 1 to 1.8 μM. Interestingly, while the synthetic isomers isogranulatimide B (**76**) and isogranulatimide C (**77**) were G2 checkpoint inhibitors, cells treated with isogranulatimide A (**75**) were incapable of overcoming the G2 checkpoint and entering mitosis.

From the data presented in Table 3.7, it is likely that the additional steric bulk and/or increased hydrophobicity of the alkylated analogues of granulatimide (**22**) and isogranulatimide (**23**) deters from their activity as G2 checkpoint inhibitors. Both 1-hexylisogranulatimide (**78**) and 1-hexylgranulatimide (**79**) showed a decrease in activity when compared to the parent alkaloids **23** and **22**. Additionally, cells treated with 17-methylgranulatimide (**74**) were unable to overcome the G2 checkpoint at the concentrations tested. Although not presented in either table, the synthetic precursors to the granulatimide type alkaloids, namely didemnimide A (**14**), didemnimide C (**16**), isodidemnimide A (**86**) and neodidemnimide A (**111**), were inactive in the G2 checkpoint inhibition assay. This data suggests a planar structure, adopted by the granulatimide type alkaloids, is essential for G2 checkpoint abrogation.

The concentration dependence of G2 checkpoint inhibition by both isogranulatimide (**23**) and granulatimide (**22**) is depicted in Figure 3.20. The percentage of mitotic cells was determined by microscopy and represents the number of cells that overcame the G2 checkpoint and entered mitosis divided by the total number of cells counted. As indicated in both figures, at concentrations greater than that required for the maximum G2 checkpoint inhibition activity, a dramatic decrease in the number of mitotic cells was observed. This decrease in G2 checkpoint

inhibition activity is largely the result of drug toxicity, which was observed visually by the

appearance of apoptotic nuclei. Indeed, in cytotoxicity studies, isogranulatimide (**23**) was shown

to be a mild cytotoxin (IC_{50} = 40 μM) to MCF-7 breast cancer cells.
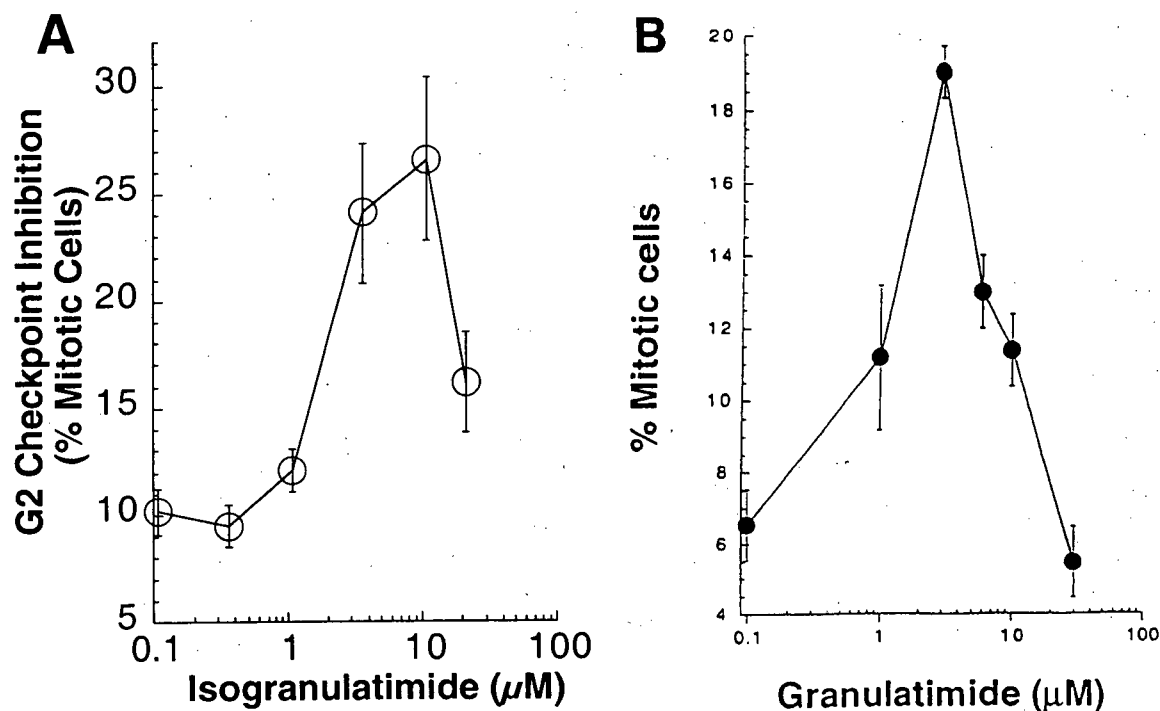
Figure 3.20. Graph of G2 checkpoint inhibition by
A) isogranulatimide (**23**) and B) granulatimide (**22**).

3.8.2 Isogranulatimide (23) selectively potentiates the killing of mp53 MCF-7 cells by γ-irradiation

Having established that isogranulatimide (**23**) is an effective G2 checkpoint inhibitor, it

remained to test the hypothesis outlined in Section 1.3, namely, that inhibition of the G2

checkpoint in concert with a DNA damaging agent would enhance the killing of cells lacking

p53 function.[62] Figure 3.21 summarizes the results of this pursuit. When MCF-7 cells with p53

function (wtp53) were exposed to 2, 4 or 6 Grays of DNA damaging γ-irradiation in the absence

of isogranulatimide (**23**) little cell death was observed. As the concentration of **23** added to the

cells was increased, a moderate increase in cell death was observed. The increase in cell death at higher concentrations of **23** (i.e. 35 μM) is largely the result of the cytotoxic nature of isogranulatimide (**23**) at these concentrations (*vide supra*). However, when MCF-7 cells that lack p53 function (mp53) were treated in the same manner, the cells died in much higher numbers as the concentration of **23** was increased. In fact, the combination of isogranulatimide (**23**) applied at a concentration of 35 μM with 6 Grays of γ-irradiation (♦) resulted in a doubling of cell death when compared to cells treated with **23** alone (O). These data suggest that isogranulatimide (**23**) acts in a synergistic fashion with DNA-damaging γ-irradiation to potentiate the killing of MCF-7 cells lacking p53 function. These findings were further supported by studies with lung andenocarcinoma A549 cells, where a combination of γ-irradiation and isogranulatimide (**23**) killed A549 cells without p53 function but not those with p53 function.
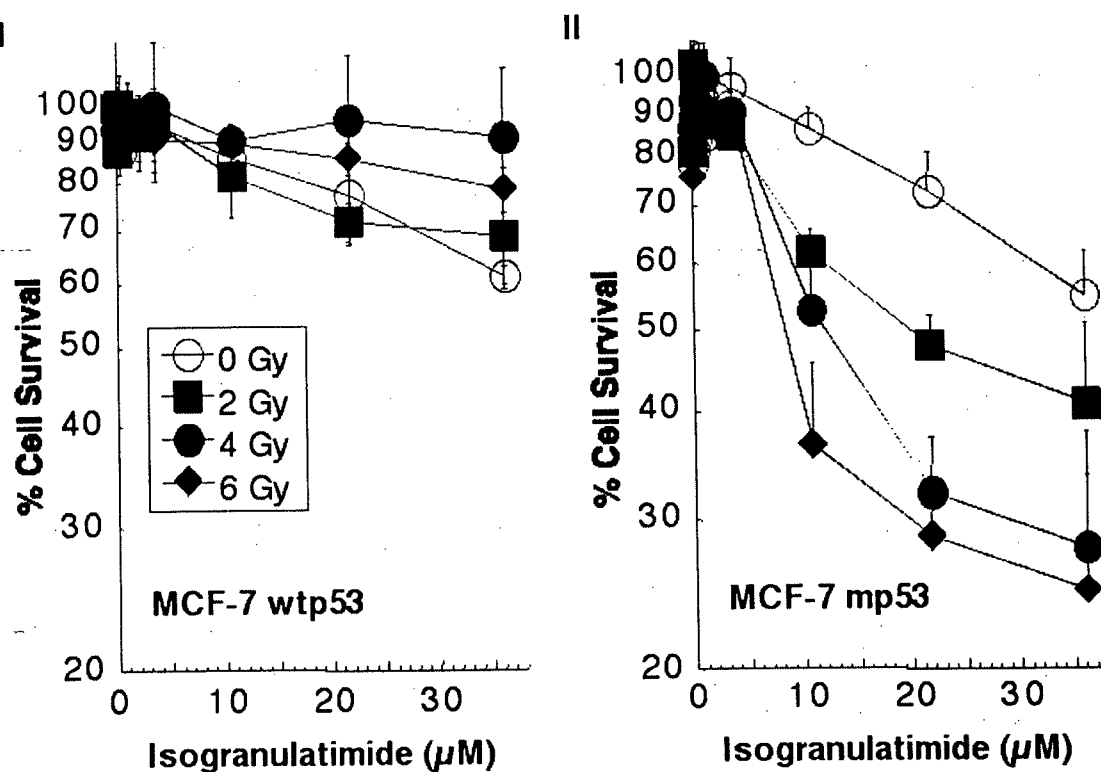
Figure 3.21. Cytotoxicity of isogranulatimide (**23**) in combination with γ-irradiation to MCF-7 cells with p53 function (I) or without p53 function (II).

3.8.3 Investigation of the mechanism of action of isogranulatimide (23)

Having established that isogranulatimide (23) is in fact a G2 checkpoint inhibitor, and is capable of potentiating the killing of certain cancerous cells by γ-irradiation *in vitro*, it was of interest to elucidate the mechanism by which this G2 checkpoint inhibitor operates. A key regulator for the entry of a cell into mitosis is the Cdc2 kinase. When the ATP binding site of Cdc2 is phosphorylated, cell cycle arrest in G2 occurs. The phosphorylation of Cdc2 occurs at Thr14 and Tyr15 by the kinases Myt1 and Wee1, respectively. For the cell to enter mitosis these residues (i.e. Thr14 and Tyr15) must be dephosphorylated, an action carried out by Cdc25 protein phosphatase. Thus, the effect of isogranulatimide (23) on Cdc2 was investigated.[63]

Western blot is a technique that can be used to identify the phophorylation state of various proteins. When proteins are added to a glass slide covered in a nitrocellulose gel and a voltage is applied along the length of the slide, these proteins travel at different rates in the direction of the applied charge depending on the level of phosphorylation. When MCF-7 mp53 cells were exposed to an antimitotic agent, which arrests cells in mitosis (see Section 1.2), and the phosphoryation of Cdc2 was analyzed by Western blots (Figure 3.22), only one band corresponding to unphosphorylated Cdc2 was observed, indicating the cells had entered mitosis.[64] However, when the same cells were exposed to DNA-damaging γ-irradiation, an increase in both doubly and singly phosphorylated Cdc2 was found, indicating the cells are arrested in G2 phase. As evidenced in Figure 3.22, cells that were arrested in G2 by exposure to γ-irradiation and then treated with isogranulatimide (23) showed a time dependant dephosphorylation of Cdc2. Thus, when cells were incubated with 23 for 2, 4 or 6 hours, a decrease in doubly phosphorylated Cdc2 and an increase in unphosphorylated Cdc2 was observed. These results indicate that isogranulatimide overcomes G2 arrest by interfering with the inhibitory phosphorylation of Cdc2 kinase.

I   II

Control   IGR

+ γ   2 4 6   Time (hours)

← doubly phosphorylated
← singly phosphorylated
← unphosphorylated
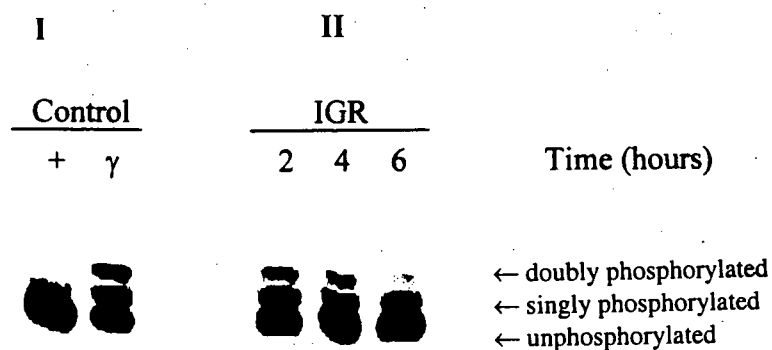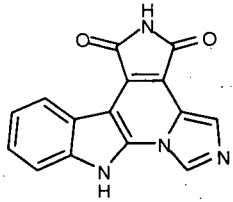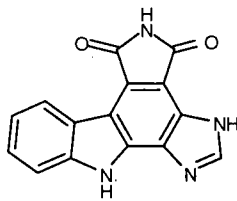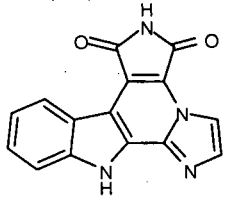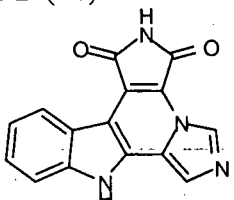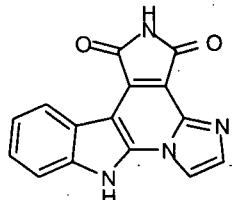
Figure 3.22. Effect of isogranulatimide (**23**) on the phosphorylation level of Cdc2 kinase in MCF-7 mp53 cells. I) The control (+) indicates cell was treated with an antimitotic agent (nocodoazole) and the control (γ) indicates cell was irradiated with 6.5 Grays of γ-irradiation. II) The cells were irradiated with 6.5 Grays of γ-irradiation and, after 16 hours, isogranulatimide (**23**) (10 μM) was added and the cells were incubated for the indicated times. Western blots were performed using anti-p34^{cdc2} antibody.

As an activator of the Cdc2 kinase, there are a number of known upstream targets which isogranulatimide (**23**) might interact with to elicit this response.[64] However, a detailed analysis of the effect of isogranulatimide (**23**) on the abundance and distribution of cell regulatory proteins provided no clear indication of the nature of these targets.[64] As such, it seemed likely that the activation of Cdc2 kinase by isogranulatimide (**23**) occurs either further upstream or by an, as of yet, unknown mechanism. To gain insight into this matter, isogranulatimide (**23**), granulatimide (**22**) and the congeners **75, 76** and **77** were screened against a panel of 14 common mammalian kinases. Interestingly, these alkaloids demonstrated pronounced activity against only one of the kinases in the screen, the glycogen synthase kinase-3β (GSK-3β). Moreover, the *in vitro* inhibition of GSK-3β mirrored, to a large extent, the G2 checkpoint inhibition activity of these substances (Table 3.8). GSK-3β is known to phosphorylate and inhibit glycogen synthase, which is a key cellular enzyme that catalyzes the incorporation of glucosyl residues into glycogen. The selective inhibition of GSK-3β by the G2 checkpoint inhibitors, while unanticipated, presented the possibility that this enzyme might also play a role in cell cycle regulation.

Table 3.8. Inhibition of GSK-3β and the G2 checkpoint by isogranulatimide (**23**), granulatimide (**22**), isogranulatimide A (**75**), isogranulatimide B (**76**) and isogranulatimide C (**77**).

Compound name and structure	*In vitro* GSK-3β inhibition (μM)	G2 checkpoint inhibition (peak inhibitory concentration in μM)
Isogranulatimide (**23**)	5	10
Granulatimide (**22**)	2	3
Isogranulatimide A (**75**)	25	Inactive[a]
Isogranulatimide B (**76**)	0.1	0.3
Isogranulatimide C (**77**)	5	30

[a] Inactive at all concentrations tested (from 0.01 to 500 μM).

A series of elegant experiments carried out by Michel Roberge and co-workers,[64] demonstrated that isogranulatimide (**23**) was also able to inhibit GSK-3β *in vivo*. This result supported the possibility of a new cellular regulation pathway in which GSK-3β plays a key role. Unfortunately, it was discovered that the didemnimide type alkaloids, which were inactive in the G2 checkpoint inhibition assay, were also potent inhibitors of GSK-3β. Thus, didemnimide A (**14**) (0.6 μM) and didemnimide C (**16**) (1.0 μM) inhibited GSK-3β at concentrations equal to or lower than those demonstrated by the granulatimide type G2 checkpoint inhibitors. Although this result did not exclude the possibility of GSK-3β involvement in the G2 checkpoint, it suggested that the activation of Cdc2 kinase by isogranulatimide (**23**) might involve a signaling pathway further upstream from those initially investigated.

Current understanding of the G2 checkpoint suggests that DNA damage results in the activation of certain members of the phosphoinositide kinase family.[63] When activated, members of this family of kinases transmit a signal via the protein kinases Chk1 and Chk2, which phosphorylate Cdc25 protein phosphatatase (Figure 3.23).[63] The phosphorylation of Cdc25 protein phosphatase is believed to result in the inability of Cdc25 to activate Cdc2 protein kinase. Additionally, Chk1 and Chk2 are known to phosphorylate and activate Wee1, a kinase responsible for the inhibitory phosphorylation of Cdc2.[63] Thus, a key function of Chk1 and Chk2, in response to DNA damage, is the inactivation of Cdc2 and, consequently, the inhibition of cell cycle progress from G2 phase into mitosis.[63]

It could be shown that isogranulatimide (**23**) inhibits Chk1 ($IC_{50} = 0.1$ μM) and Chk2 ($IC_{50} = 8.8$ μM) protein kinases at concentrations roughly equal to that in which **23** inhibits the G2 checkpoint. Additionally, it was found that granulatimide (**22**) also inhibits Chk1 ($IC_{50} = 0.3$ μM) and Chk2 ($IC_{50} = 9.8$ μM). Consequently, it may be supposed that the inhibition of Chk1 and Chk2 by these compounds results in a breakdown in the signal pathway described in Figure 3.23. Namely, the inhibition of Chk1 and Chk2 impedes their ability to deactivate Cdc2, which,

consequently remains in its active or unphosphorylated state and promotes premature transition from G2 phase to mitosis.

(P) = phosphorylated

deactivated
Wee-1 (P)   (P)

Chk1 or Chk2 ◄— activated by DNA damage

Chk1 or Chk2

activated
Wee-1 —(P)

(P)

G2 arrest | deactivated Cdc2 kinase ◄— activated Cdc2 kinase | Progress into mitosis

activated
Cdc25 (P)   (P)

Chk1 or Chk2 ◄— activated by DNA damage

Chk1 or Chk2

deactivated
Cdc25 —(P)
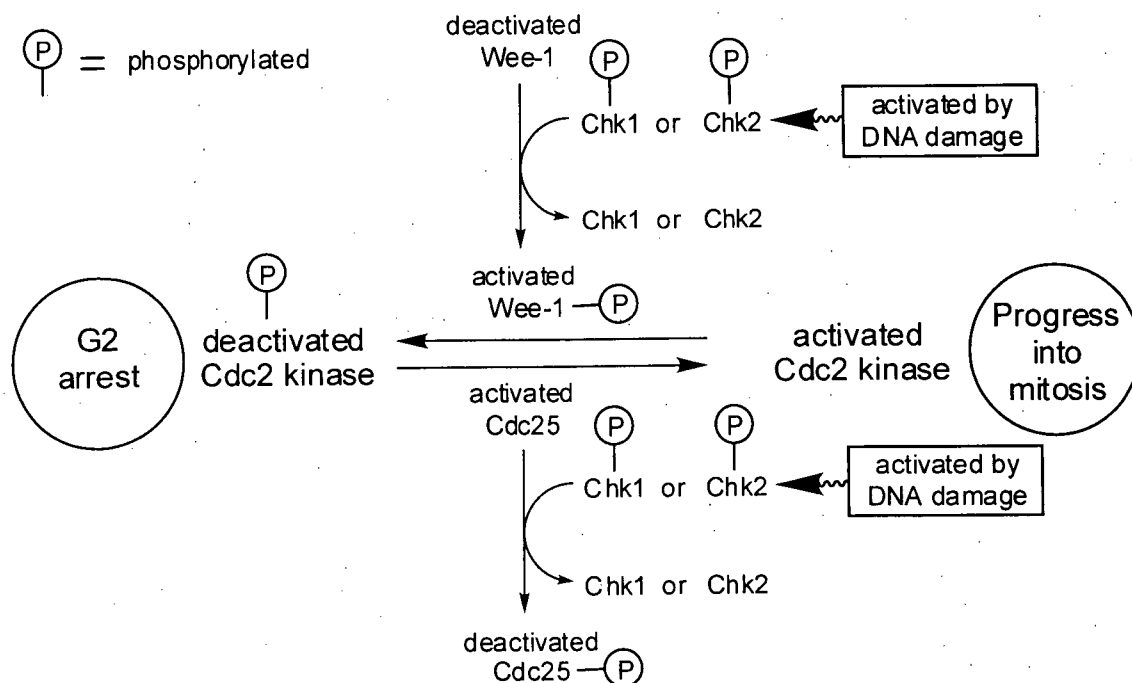
Figure 3.23. Involvement of Chk1 and Chk2 in the G2 checkpoint signal transduction pathway.

3.9 Conclusions

Isogranulatimide (**23**)[61] and granulatimide (**22**)[65] are novel ascidian alkaloids that possess heterocyclic aromatic skeletons without precedent in natural products. Biogenetically, they represent alternative modes of cyclization of the putative precursor didemnimide A (**14**),[14] also isolated from the ascidian *Didemnum granulatum*. Due to a lack of protons for proton-proton or heteronuclear correlation experiments, spectroscopic analysis, and consequently a confident structure determination of these alkaloids, was unfeasible by standard spectroscopic methods. However, a short and highly efficient synthesis generated both granulatimide (**22**) and

isogranulatimide (**23**) from didemnimide A (**14**) and aided in unambiguously establishing the

structures of these novel alkaloids.
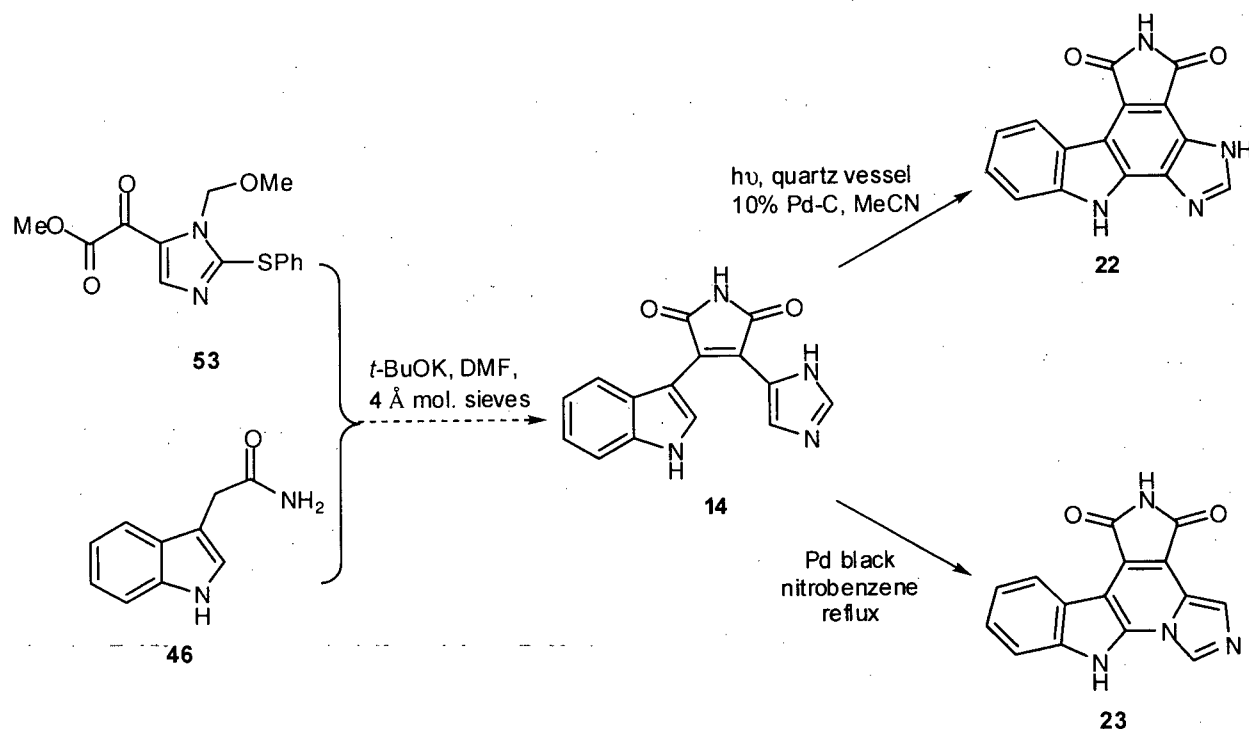
Scheme 3.28. Rapid construction of didemnimide and granulatimide alkaloids
through a novel condensation-cyclization sequence of reactions.

The synthesis of didemnimide A (**14**) involved the development and application of new

methodology useful for the synthesis of substituted maleimides (Scheme 3.28). In general terms,

the condensation of an α-keto ester (e.g. **53**) and a substituted acetamide (e.g. **46**) was shown to

provide unsymmetrical maleimides, including didemnimide type molecules (e.g. didemnimide A

(**14**)), in excellent yield. Subsequently, the production of either isogranulatimide (**23**) via a novel,

thermally induced cyclization of didemnimide A' (**14**), or granulatimide (**22**) via a

photocyclization of **14** provided expedient access to these alkaloids. The methodology devised

for the synthesis of substituted maleimides was further extended to include arcyriarubin A (**13**), a

bis-indolyl maleimide, didemnimide C (**16**), and the didemnimide A (**14**) isomers:

isodidemnimide A (86) and neodidemnimide A (111). Subjection of the isomers and analogues of didemnimide A (14) to conditions initially devised to produce isogranulatimide (23) (i.e. thermal cyclization) or granulatimide (22) (i.e. photocyclization) showcased the efficiency of these transformations.[66] Furthermore, through exploration of the generality of the condensation-cyclization routes developed for the synthesis of 22 and 23, a number of analogues of these alkaloids were created. The successful synthesis of these substances set the stage for investigations into the effect of structure on the biological activity of this important family of compounds.

From the G2 checkpoint inhibition results obtained for isogranulatimide (23), granulatimide (22) and analogues and congeners thereof, several observations can be made. By comparison with the didemnimide type alkaloids, it is clear that a prerequisite for G2 checkpoint inhibition is a rigid planar structure, as didemnimide A (14),[14] inactive as a G2 checkpoint inhibitor, differs from 22 and 23 primarily in this regard. The decrease in activity observed for the series of alkylated analogues of granulatimide (22) and isogranulatimide (23) (Table 3.7) indicates the parent compounds are superior G2 checkpoint inhibitors. This observation is likely the result of either detrimental interactions posed by the steric bulk of the additional alkyl groups or a decrease in cellular solubility or mobility imparted by these appendages.

From a structure activity relationship perspective, the inability of isogranulatimide A (75) and 17-methylgranulatimide (74) to inhibit the G2 checkpoint is of particular interest (Tables 3.6 and 3.7). The key difference between these substances and isogranulatimide (23) or granulatimide (22) is the positioning of the basic nitrogen in the imidazole ring. The term basic nitrogen refers to the imidazolyl nitrogen whose lone pair of electrons is not involved in the π bonds that contribute to the aromaticity of these molecules. Thus, this 'free' lone pair of electrons is capable of engaging in hydrogen bonds with acidic residues in enzyme active sites, an action essential for the binding of substrates to enzymes. Isogranulatimide (23) has a basic

nitrogen at position B, as depicted in Figure 3.24, while the tautomer of granulatimide **132** has a basic nitrogen at position C. The other congeners of these compounds, which inhibit the G2 checkpoint, namely isogranulatimide B (**76**) and isogranulatimide C (**77**), have basic nitrogens at positions B and C, respectively. Interestingly, the basic nitrogen in both 17-methylgranulatimide (**74**) and isogranulatimide A (**75**) resides at position A. Since neither **74** or **75** demonstrated activity as G2 checkpoint inhibitors it is proposed that the positioning of the basic nitrogen in these structures, plays a pivotal role in determining their biological activity.

132 N-15 tautomer
of granulatimide (3.0)

Position C

77 isogranulatimide C (30)

23 isogranulatimide (10)

Position B

76 isogranulatimide B (0.3)

74 17-methylgranulatimide
(inactive)

Position A

75 isogranulatimide A
(inactive)
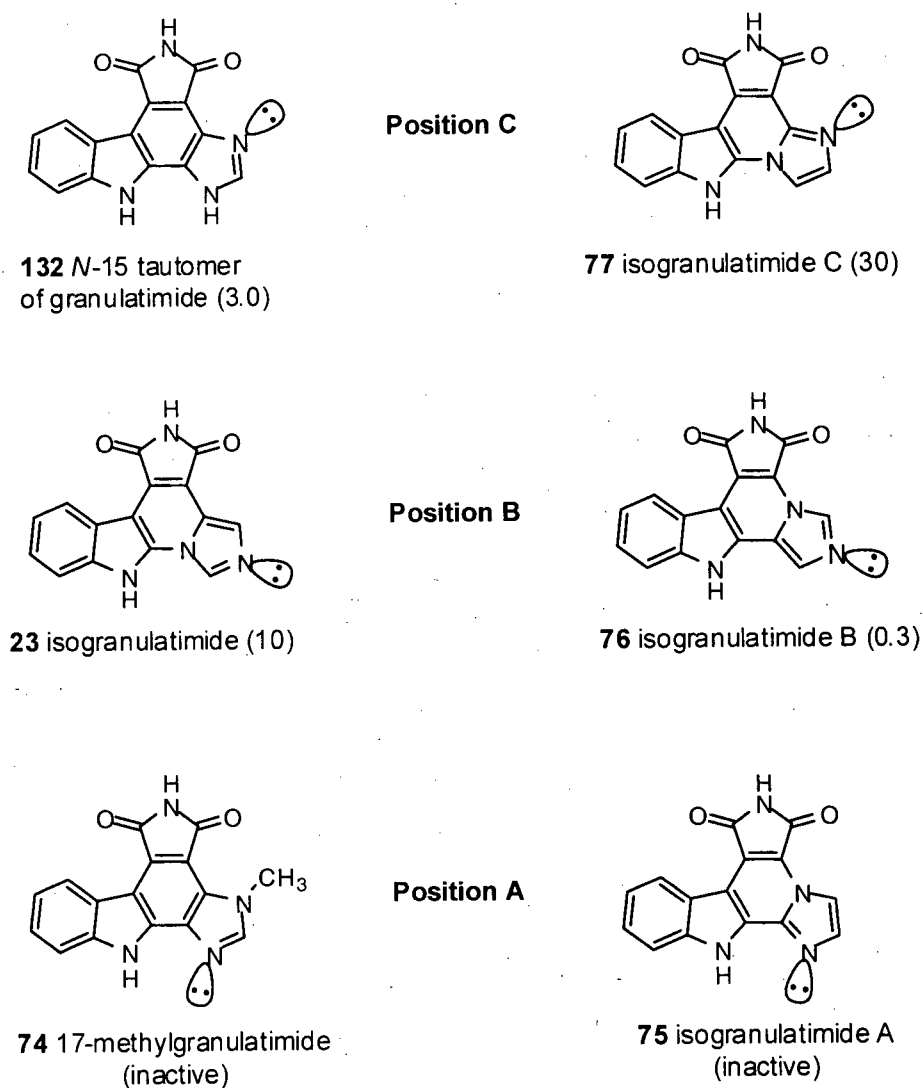
Figure 3.24. Positioning of basic nitrogen and G2 checkpoint inhibition activity.
The numbers in parentheses refer to the concentration in μM required to elicit maximum inhibition of the G2 checkpoint.

Both isogranulatimide (**23**) and granulatimide (**22**) are mildly cytotoxic alkaloids that display G2 checkpoint inhibition. Preliminary data indicates that the effective dose of these alkaloids necessary to inhibit the G2 checkpoint is approximately an order of magnitude lower than the toxic dose. The inhibition of the G2 checkpoint by isogranulatimide (**23**), is believed to involve interactions between this substance and the protein kinases Chk1 and Chk2. The downstream result of this action is the dephosphorylation of Cdc2 protein kinase and, consequently, the abrogation of the G2 checkpoint and the premature transition from G2 phase to mitosis. The selective enhancement of γ-irradiation-induced killing of cancerous cells lacking p53 function by isogranulatimide (**23**), warrant its consideration as a lead compound for experimental cancer therapy.

3.10 Experimental

For General Experimental see Section 2.5.

Isolation Procedure.

Samples of *Didemnum granulatum* (1 kg wet weight) were collected in São Sebastião channel and around São Sebastião Island (Ilhabela), Brazil in September of 1997 and November of 1998 using SCUBA at depths of 1 meter. The samples were immediately immersed in MeOH (500 mL) and stored at -20 °C for one month. The MeOH was decanted and the ascidian was then immersed in DMF (500 mL). After 1 week, the DMF was decanted and diluted with EtOAc (500 mL) and brine (1 L). The phases were separated and the aqueous phase was washed with EtOAc (2 x 500 mL). The organic phases were combined and concentrated to provide a brownish gum (1.2 g).

The brown gum was placed on a column of silica gel (50 g) and the least polar compounds in the mixture were eluted with CH_2Cl_2. An increasing gradient of CH_2Cl_2 - MeOH provided 5 fractions; DMF-1 (31 mg), DMF-2 (9.2 mg), DMF-3 (17 mg), DMF-4 (40 mg) and DMF-5 (11 mg) which contained compounds of increasing polarity. The fractions were concentrated and transported to the University of British Columbia.

Spectroscopic analysis (^{1}H NMR, 400 MHz, DMSO-d_6) of the fractions indicated fractions DMF-3 and DMF-4 contained NMR signals corresponding to didemnimide and granulatimide type molecules. Combination of these fractions (57 mg), and purification of the crude residue by flash chromatography (20 g of silica gel, 15:1 CH_2Cl_2 - MeOH) provided a series of fractions with TLC characteristics (R_F = 0.3, 10:1 CH_2Cl_2 - MeOH) similar to granulatimide. Concentration of these fractions, provided a brown residue which was dissolved in DMSO (0.2

mL) diluted with CH_2Cl_2 - MeOH - TFA (25:1:0.001, 1 mL) and purified by NP HPLC (radial pac column, 25:1:0.001 CH_2Cl_2 - MeOH – TFA, 2.0 mL/minute, monitor at 254 nm) to provide 0.8 mg (0.00008% wet weight) of 6-bromogranulatimide (**131**) (retention time: 10 minutes) as a yellow solid and 0.5 mg (0.00005% wet weight) of granulatimide (**22**) (retention time: 12 minutes) as a yellow solid.

6-bromogranulatimide (**131**): for a summary of the assignments of ^{1}H and ^{13}C NMR resonances based on HMQC and HMBC data see Table 3.9.

UV λ_{max} (MeOH): 236, 282, 308, 386 nm.

^{1}H NMR (400 MHz, DMSO-d_6) δ 13.68 (s, 1H, H-17), 12.74 (s, 1H, H-1), 11.06 (s, 1H, H-10), 8.80 (d, 1H, J = 8.6 Hz, H-4), 8.56 (s, 1H, H-16), 7.75 (d, 1H, J = 1.5 Hz, H-7), 7.47 (dd, 1H, J = 1.5, 8.6 Hz, H-6).

^{13}C NMR (100.5 MHz, DMSO-d_6) δ 171.4 (C-11), 169.3 (C-9), 144.7 (C-16), 141.1 (C-7a), 125.1 (C-4), 122.6 (C-5), 122.5 (C-8), 120.6 (C-6), 118.5 (C-3a), 114.1 (C-7), 112.0 (C-3), 109.9 (C-12).

Exact mass calcd for $C_{15}H_7N_4O_2{}^{81}Br$: 355.9732; found: 355.9738.

Exact mass calcd for $C_{15}H_7N_4O_2{}^{79}Br$: 353.9752; found: 353.9755.

granulatimide (**22**): spectral data was in accord with that reported for the synthetic material (*vide infra*).

Table 3.9. NMR data for 6-bromogranulatimide (**131**) (recorded in DMSO-d_6).
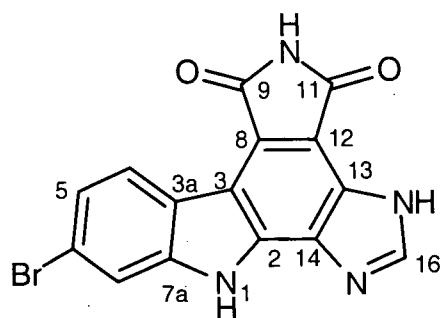
Carbon No.	^{13}C δ (ppm)[a]	^1H δ (ppm) (mult, J (Hz))[b,c]	HMBC[b]
1		12.74 (bs)	
2	n.o.		
3	112.0		H-4
3a	118.5		H-7, H-5
4	125.1	8.80 (d, 8.6)	
5	122.6	7.47 (dd, 1.5, 8.6)	H-7
6	120.6		H-5, H-7
7	114.1	7.75 (d, 1.5)	
7a	141.1		H-4
8	122.5		H-10
9	169.3		H-10
10		11.06 (s)	
11	171.4		H-10
12	109.9		H-10
13	n.o.		
14	n.o.		
15			
16	144.7	8.56 (s)	
17		13.68 (s)	

[a] Recorded at 100.5 MHz. [b] Recorded at 500 MHz. [c] Assignments based on HMQC data.

Preparation of arcyriarubin A (**13**).
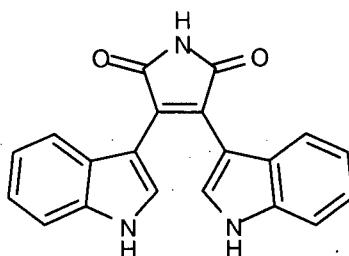
To a stirred solution of methyl-3-indoleglyoxylate (**88**) (57 mg, 0.28 mmol) and indole-3-acetamide (**46**) (59 mg, 0.34 mmol) in dry DMF (3.0 mL) at room temperature was added sequentially 4 Å molecular sieves (approximately 300 mg) and a solution of *t*-BuOK (78 mg, 0.70 mmol) in dry DMF (2.0 mL). The resulting solution was heated at 60 °C for 12 hours. The reaction mixture was then cooled to room temperature and treated with saturated aqueous NH_4Cl (5 mL) and the resulting mixture was diluted with EtOAc (20 mL). The phases were separated and the aqueous phase was extracted with EtOAc (2 x 20 mL). The combined organic phases were washed with brine (4 x 10 mL), dried ($MgSO_4$) and concentrated. Purification of the crude material by flash chromatography (40 g of silica gel, 1:1 petroleum ether - EtOAc) and removal of trace amounts of solvent (vacuum pump) from the resulting solid, afforded 14.0 mg (15%) of arcyriarubin A (**13**) as a red solid (mp 175 °C) which exhibited spectral data that was in accordance with that reported for the natural product.[34]

^{1}H NMR (400 MHz, DMSO-d_6) δ 11.64 (bs), 10.87 (bs), 7.72 (d, 1H, J = 2.7 Hz), 7.35 (d, 1H, J = 8.1 Hz), 6.96 (dd, 1H, J = 8.0, 8.0 Hz), 6.79 (d, 1H, J = 8.0 Hz), 6.61 (dd,1H, J = 8.0, 8.0 Hz).

^{13}C NMR (100.5 MHz, DMSO-d_6) δ 172.9, 135.9, 129.0, 127.7, 125.4, 121.5, 120.8, 119.2, 111.6, 105.5.

IR (KBr): 3395, 3218, 1733, 1698, 1617, 1423, 1231, 1118 cm^{-1}.

Exact mass calcd for $C_{20}H_{13}N_3O_2$: 327.1008; found: 327.1013.

Preparation of Methyl 2-(1-methoxymethyl-2-phenylthioimidazol-5-yl)-glyoxylate (53).
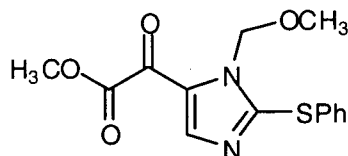
To a cold (-78 °C), stirred solution of 1-methoxymethyl-2-phenylthioimidazole (70) (340 mg, 1.55 mmol) in dry THF (8.0 mL), was added a solution of *n*-BuLi (1.47 M in hexanes, 1.26 mL, 1.85 mmol) and the reaction mixture was stirred for 1 hour. A solution of dimethyl oxalate (540 mg, 4.58 mmol) in dry THF (2.0 mL) was then added, and the reaction mixture was stirred for an additional 1.25 hours at -78 °C. The reaction mixture was then treated with saturated aqueous NH_4Cl (5 mL) and the resulting mixture was diluted with Et_2O (20 mL). The phases were separated and the aqueous phase was extracted with Et_2O (2 x 25 mL). The combined organic phases were washed with brine (10 mL), dried ($MgSO_4$) and concentrated. Purification of the crude material by flash chromatography (35 g of silica gel, 1:1 petroleum ether - Et_2O) and removal of trace amounts of solvent (vacuum pump) from the resulting solid, afforded 305 mg (66%) of the ester 53 as a beige solid (mp 59-60 °C).

^{1}H NMR (400 MHz, CDCl$_3$) δ 8.23 (s, 1H), 7.52-7.54 (m, 2H), 7.37-7.38 (m, 3H), 5.81 (s, 2H), 3.91 (s, 3H), 3.36 (s, 3H).

^{13}C NMR (100.5 MHz, CDCl$_3$) δ: 172.2, 161.6, 154.1, 145.4, 145.3, 133.2, 129.5, 129.2, 128.7, 75.8, 56.5, 53.0.

IR (KBr): 1729, 1657, 1305, 1273, 1167, 1114, 748 cm^{-1}.

Exact mass calcd for C$_{14}$H$_{14}$N$_2$O$_4$S: 306.0674; found: 306.0674.

Anal. calcd for C$_{14}$H$_{14}$N$_2$O$_4$S: C 54.89, H 4.61, N 9.15; found: C 55.00, H 4.66, N 8.94.

Preparation of 17-methoxymethyl-16-phenylthiodidemnimide A (**54**).
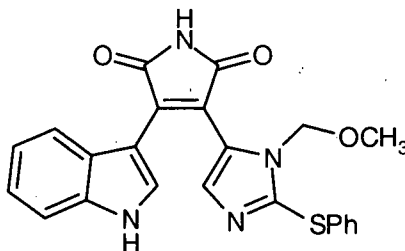
To a stirred solution of *t*-BuOK (150 mg, 1.34 mmol) in dry DMF (3.0 mL) at room temperature, was added sequentially 4 Å molecular sieves (~500 mg), a solution of the ester **53** (167 mg, 0.54 mmol) and indole-3-acetamide (**46**) (114 mg, 0.66 mmol) in dry DMF (4.0 mL). The deep red reaction mixture was heated at 45 °C for 12 hours. The resulting dark purple solution was then treated with hydrochloric acid (1 N, 3.0 mL) and the resulting mixture was diluted with EtOAc (30 mL). The phases were separated and the aqueous phase was extracted with EtOAc (2 x 10 mL). The combined organic phases were washed with brine (4 x 15 mL), dried (MgSO$_4$) and concentrated. Purification of the crude material by flash chromatography (25 g of silica gel, 30:1

CH$_2$Cl$_2$ - MeOH) and removal of trace amounts of solvent (vacuum pump) from the resulting solid, afforded 208 mg (90%) of the maleimide **54** as an orange solid (mp 243 °C).

^{1}H NMR (400 MHz, DMSO-d_6) δ 12.11 (br s, 1H), 11.25 (br s, 1H), 8.14 (s, 1H), 7.46 (d, 1H, J = 7.9 Hz), 7.18-7.33 (m, 6H), 7.14 (dd, 1H, J = 8.0, 8.0 Hz), 6.77 (dd, 1H, J = 8.0, 8.0 Hz), 6.51 (d, 1H, J = 8.0), 5.00 (s, 2H), 2.97 (s, 3H).

^{13}C NMR (100.5 MHz, DMSO-d_6) δ 171.7, 171.6, 140.3, 136.7, 135.3, 133.8, 133.5, 132.5, 129.5, 128.4, 127.2, 125.7, 124.3, 122.7, 120.8, 120.2, 117.4, 112.6, 104.6, 75.8, 55.9.

IR (KBr): 3400-2600, 1765, 1708, 1537, 1341, 741 cm^{-1}.

Exact mass calcd for C$_{23}$H$_{18}$N$_4$O$_3$S: 430.1100; found: 430.1094.

Preparation of 17-methoxymethyldidemnimide A (71).
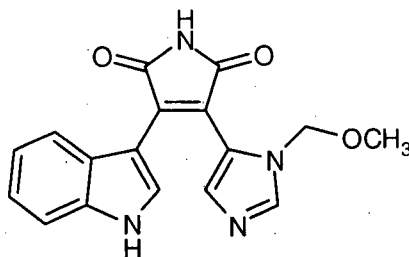
To a refluxing solution of maleimide **54** (52 mg, 0.12 mmol) in EtOH (5.0 mL), was added Raney Ni (W-2, 50% slurry in water, ~150 mg) and the resulting suspension was refluxed for 1 hour. After this time, an additional amount of Raney Ni (W-2, 50% slurry in water, ~100 mg) was added and the mixture was refluxed for an additional 3 hours. The reaction mixture was then

cooled to room temperature and filtered through Celite®. The Celite® was washed with CH_2Cl_2 -

MeOH (1:1, 75 mL) and the combined organic washes were concentrated. Purification of the

crude material by flash chromatography (14 g of silica gel, 20:1 CH_2Cl_2 - MeOH) and removal of

trace amounts of solvent (vacuum pump) from the resulting solid, afforded 33 mg (85%) of the

maleimide **71** as an orange solid (m.p. > 235 °C, dec).

^{1}H NMR (400 MHz, DMSO-d_6) δ 12.03 (br s, 1H), 11.18 (br s, 1H), 8.07 (s, 1H), 7.95 (s, 1H),

7.44 (d, 1H, J = 8.5 Hz), 7.09 (dd, 1H, J = 7.0, 7.0 Hz), 7.01 (s, 1H), 6.79 (dd, 1H, J = 7.0, 7.0

Hz), 6.45 (d, 1H, J = 8.0 Hz), 5.02 (s, 2H), 3.07 (s, 3H).

^{13}C NMR (100.5 MHz, DMSO-d_6) δ 171.8, 171.7, 140.5, 136.5, 134.3, 132.9, 131.8, 124.3,

122.4, 121.7, 120.5, 120.3, 118.4, 112.3, 104.7, 76.4, 55.6.

IR (KBr): 3400-2600, 1765, 1703, 1537, 1440, 1342, 1113 cm^{-1}.

Exact mass calcd for $C_{17}H_{14}N_4O_3$: 322.1066; found: 322.1066.

Preparation of didemnimide A (**14**).
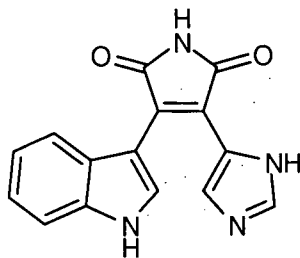
To a stirred suspension of the didemnimide **71** (67.4 mg, 0.209 mmol) in dry CH_2Cl_2 (15.0 mL) at room temperature, was added a solution of BBr_3 in CH_2Cl_2 (1.0 M, 2.1 mL, 2.1 mmol) and the deep blue solution was heated at reflux for 5 hours. The reaction mixture was then cooled to room temperature and was treated with saturated aqueous $NaHCO_3$ (10 mL) and the resulting mixture was diluted with EtOAc (20 mL) and stirred for 15 minutes at room temperature. The phases were separated and the aqueous phase was extracted with EtOAc (2 x 15 mL). The combined organic phases were washed with brine (10 mL), dried ($MgSO_4$) and concentrated. Purification of the crude product by flash chromatography (20 g of silica gel, 15:1 CH_2Cl_2-MeOH) and removal of trace amount of solvent (vacuum pump) from the resulting solid, afforded 15.8 mg of recovered **71** as well as 45.0 mg (77%, 100% based on recovered starting material) of didemnimide A (**14**) as an orange solid.

UV λ_{max} (MeOH): 275, 332, 431 nm.

^{1}H NMR (400 MHz, major tautomer , DMSO-d_6) δ 12.45 (br s, 1H), 11.66 (br s, 1H), 10.87 (br s, 1H), 8.05 (s, 1H), 7.71 (br s, 1H), 7.68 (br s, 1H), 7.39 (br d, 1H, J = 7.8 Hz), 7.07 (br m, 2H), 6.87 (br m, 1H).

¹H NMR (400 MHz, with excess TFA, DMSO-d_6) δ 12.13 (s, 1H), 11.27 (s, 1H), 8.80 (s, 1H), 8.08 (d, 1H, J = 2.7 Hz), 7.63 (s, 1H), 7.50 (d, 1H, J = 7.9 Hz), 7.15 (dd, 1H, J = 8.0, 8.0 Hz), 6.93 (dd, 1H, J = 8.0, 8.0 Hz), 6.67 (d, 1H, J = 7.8 Hz).

¹³C NMR (100.5 MHz, DMSO-d_6) δ 172.8, 172.6, 136.1, 135.9, 130.9, 130.5, 126.0, 126.0, 121.7, 121.3, 119.7, 119.2, 112.2, 111.5, 105.0.

IR (KBr): 3247, 1760, 1708, 1557, 1423, 1345, 1240, 747 cm⁻¹.

Exact mass calcd for $C_{15}H_{10}N_4O_2$: 278.0804; found: 278.0799.

Preparation of granulatimide (**22**) and isogranulatimide (**23**).
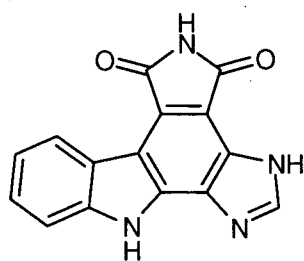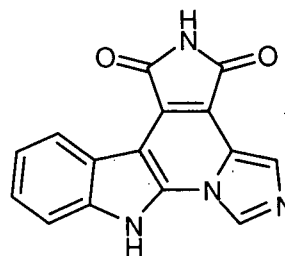
22   **23**

To a stirred solution of didemnimide A (**14**) (12.9 mg, 0.046 mmol) in MeCN (5.0 mL), was added a catalytic amount of Pd/C (10% Pd) and the resulting mixture was sparged with argon for 30 minutes. The mixture was then irradiated (450 Watt Hanovia medium pressure mercury vapor lamp, quartz reaction vessel) for 6.5 hours. After this time, the reaction mixture was filtered through Celite®, the Celite® was washed with DMF (10 mL), and the combined filtrate was concentrated. The remaining material was taken up in EtOAc (30 mL) and the resultant solution

was washed with brine (4 x 20 mL), dried (MgSO$_4$) and concentrated. Purification of the crude material by flash chromatography (20 g of silica gel, 10:1 CH$_2$Cl$_2$ - MeOH) and removal of trace amounts of solvent from the resulting solids afforded 11.7 mg (91%) of granulatimide (**22**) as a yellow solid and 1.0 mg (8%) of isogranulatimide (**23**) as a purple solid.

Granulatimide (**22**): for a summary of the assignments of ^{1}H and ^{13}C NMR resonances based on HMQC and HMBC data see Table 3.10, and COSY and NOE data see Table 3.11.

UV λ_{max} (MeOH): 204, 277, 301, 385 nm.

^{1}H NMR (400 MHz, DMSO-d_6) δ 13.57 (s, 1H, H-17), 12.58 (bs, 1H, H-1), 10.96 (s, 1H, H-10), 8.89 (d, 1H, $J = 7.0$ Hz, H-4), 8.50 (s, 1H, H-16), 7.61 (d, 1H, $J = 7.0$ Hz, H-7), 7.48 (dd, 1H, $J = 7.0, 7.0$ Hz, H-6), 7.30 (dd, 1H, $J = 7.0, 7.0$ Hz, H-5).

^{13}C NMR (100.5 MHz, DMSO-d_6) δ 171.0 (C-11), 169.8 (C-9), 144.5 (C-16), 140.4 (C-7a), 135.4 (C-2), 133.4 (C-14), 126.1 (C-6), 125.7 (C-13), 123.8 (C-4), 122.7 (C-8), 121.4 (C-3a), 120.0 (C-5), 113.0 (C-3), 111.6 (C-7), 109.5 (C-12).

IR (KBr): 3246, 2925, 1743, 1698, 1328, 1227, 743 cm^{-1}.

Exact mass calcd for C$_{15}$H$_8$N$_4$O$_2$: 276.0647; found: 276.0652.

Isogranulatimide (**23**):spectral data was in accord with that reported for the synthetic material (*vide infra*)

Table 3.10. NMR data for granulatimide (**22**) (recorded in DMSO-d_6).
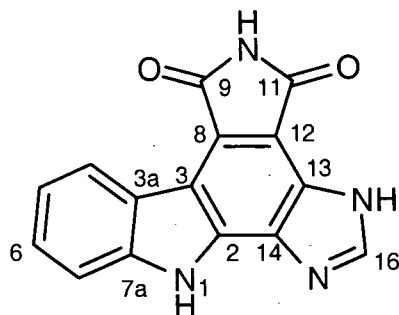
Carbon No.	^{13}C δ (ppm)[a]	^1H δ (ppm) (mult, J (Hz))[b,c]	HMBC[b]
1		12.58 (bs)	
2	135.4		H-1
3	113.0		H-1, H-4
3a	121.4		H-1, H-5, H-7
4	123.8	8.89 (d, 7.0)	H-6
5	120.0	7.30 (dd, 7.0, 7.0)	H-7, H-6
6	126.1	7.48 (dd, 7.0, 7.0)	H-4, H-7, H-5
7	111.6	7.61 (d, 7.0 Hz)	H-7
7a	140.4		H-1, H-4, H-7
8[d]	122.7		H-10
9[e]	169.8		H-10
10		10.96 (s)	
11[e]	171.0		H-10
12[d]	109.5		H-10
13[f]	125.7		H-16, H-17
14[f]	133.4		H-17
15			
16	144.5	8.50 (s)	H-17
17		13.57 (s)	

[a] Recorded at 100.5 MHz. [b] Recorded at 500 MHz. [c] Assignments based on HMQC data.
[d,e,f] Assignments may be interchanged.

Table 3.11. NMR data for granulatimide (**22**) (recorded in DMSO-d_6).
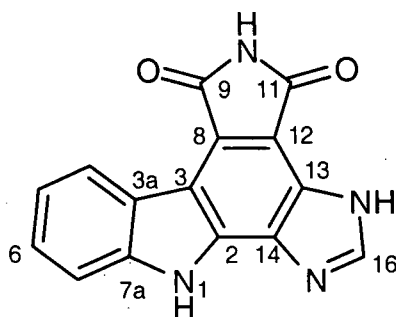
Proton No.	^{1}H δ (ppm) (mult, J (Hz))[a]	COSY[a]	NOE[b]
1	12.58 (bs)		H-7
4	8.89 (d, 7.0)	H-5	H-5
5	7.30 (dd, 7.0, 7.0)	H-4, H-6	H-4, H-6
6	7.48 (dd, 7.0, 7.0)	H-5, H-7	H-5, H-7
7	7.61 (d, 7.0 Hz)	H-6	H-6
10	10.96 (s)		
16	8.50 (s)		
17	13.57 (s)		H-16

[a] Recorded at 500 MHz. [b] Recorded at 400 MHz.

Preparation of isogranulatimide (23).
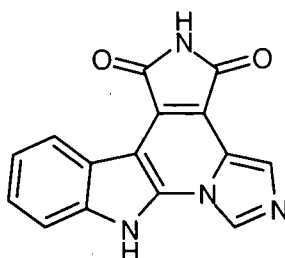
Procedure A. A stirred solution of didemnimide A (**14**) (27.6 mg, 0.099 mmol) in dry DMSO (5.0 mL) was heated open to the atmosphere at 140 °C for 2 hours. The reaction mixture was then cooled to room temperature, diluted with EtOAc (30 mL) and treated with an aqueous solution of NaOH (10% NaOH, 5 mL). The phases were separated and the organic phase was washed with brine (3 x 10 mL), dried (MgSO$_4$), and concentrated. Purification of the crude

material by flash chromatography (20 g of silica gel, 10:1 CH_2Cl_2 - MeOH) and removal of trace amounts of solvent (vacuum pump) from the resulting solid, afforded 6.0 mg of recovered didemnimide A (**14**) and 14.0 mg (51%, 65% based on recovered starting material) of isogranulatimide (**23**) as a purple solid.

Procedure B. To a stirred solution of didemnimide A (**14**) (31.3 mg, 0.113 mmol) in dry nitrobenzene (4.0 mL) was added Pd black (12.0 mg, 0.113 mmol) and the resulting suspension was heated at reflux for 20 hours. The reaction mixture was then cooled to room temperature, diluted with CH_2Cl_2 (10 mL) and placed on a short plug of silica gel (5 g). The nitrobenzene was eluted using CH_2Cl_2 and the crude product was eluted with CH_2Cl_2 - MeOH (5:1) and the filtrate was concentrated. Purification of the crude product by flash chromatography (25 g of silica gel, 10:1 CH_2Cl_2 - MeOH) and removal of trace amounts of solvent (vacuum pump) from the resulting solid, afforded 23.3 mg (75%) of isogranulatimide (**23**) as a purple solid which exhibited spectral data that was in accordance with that reported for the natural product.

UV λ_{max} (MeOH): 280, 304, 377, 466 nm.

^{1}H NMR (400 MHz, DMSO-d_6)[67] δ 13.49 (bs, 1H, H1), 11.12 (bs, 1H, H-10), 8.91 (s, 1H, H-16), 8.54 (d, 1H, J = 7.6 Hz, H-4), 7.88 (s, 1H, H-14), 7.70 (d, 1H, J = 8.0 Hz, H-7), 7.45 (dd, 1H, J = 8.0, 8.0 Hz, H-6), 7.37 (dd, 1H, J = 8.0, 8.0 Hz, H-5).

^{13}C NMR (100.5 MHz, DMSO-d_6)[67] δ 169.9 (C-9), 169.0 (C-11), 135.6 (C-7a), 134.9 (C-2), 126.9 (C-14), 126.0 (C-8), 124.7 (C-6), 123.1 (C-13), 122.3 (C-4), 121.8 (C-5), 121.3 (C-3a), 121.0 (C-16), 113.9 (C-12), 112.3 (C-7), 97.6 (C-3).

IR (KBr): 2732, 1758, 1719, 1586, 1568, 1368, 1234, 1109, 744 cm^{-1}.

Exact mass calcd for $C_{15}H_8N_4O_2$: 276.0647; found: 276.0644.

Preparation of methyl 2-(1-methyl-1*H*-2-phenylthioimidazol-5-yl)-glyoxylate (**84**).
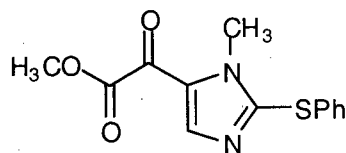
To a cold (-78 °C), stirred solution of diisopropylamine (175 µL, 1.25 mmol) in dry Et$_2$O (2.0 mL) and dry DME (2.0 mL) was added a solution of *n*-BuLi (1.60 M in hexanes, 0.74 mL, 1.18 mmol) and the reaction mixture was stirred for 30 minutes. A solution of 1-methyl-2-phenylthioimidazole (**67**) (140 mg, 0.737 mmol) in dry Et$_2$O (3.0 mL) was then added and the resulting solution was stirred at -78 °C for 15 minutes and then warmed to 0 °C for an additional 1 hour. Dimethyl oxalate (520 mg, 4.40 mmol) was added in one portion and the mixture was allowed to warm to room temperature and stir for an additional 3 hours. The reaction mixture was then treated with saturated aqueous NH$_4$Cl (5 mL) and the resulting mixture was diluted with EtOAc (20 mL). The phases were separated and the aqueous phase was extracted with EtOAc (2 x 20 mL). The combined organic phases were washed with brine (10 mL), dried (MgSO$_4$) and concentrated. Purification of the crude material by flash chromatography (35 g of silica gel, 70:1 CH$_2$Cl$_2$ - MeOH) and removal of trace amounts of solvent (vacuum pump) from the resulting solid provided 84.5 mg (41%) of the ester **84** as a beige solid (mp 98-99 °C).

^{1}H NMR (400 MHz, CDCl$_3$) δ 8.22 (s, 1H), 7.42-7.44 (m, 2H), 7.34-7.37 (m, 3H), 3.93 (s, 3H), 3.92 (s, 3H).

^{13}C NMR (100.5 MHz, CDCl$_3$) δ 172.9, 162.2, 151.8, 144.7, 132.4, 130.2, 129.9, 129.8, 129.1, 53.3, 34.3.

IR (KBr): 1736, 1651, 1437, 1277, 1216, 1013 cm^{-1}.

Exact mass calcd for C$_{13}$H$_{12}$N$_2$O$_3$S: 276.0569; found: 276.0564.

Preparation of 16-phenylthiodidemnimide C (85).
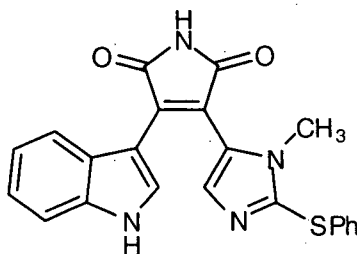
To a stirred solution of t-BuOK (28 mg, 0.25 mmol) in dry DMF (1.0 mL) at room temperature was added sequentially 4 Å molecular sieves (~50 mg), a solution of ester **84** (28 mg, 0.10 mmol) and indole-3-acetamide (22 mg, 0.13 mmol) in dry DMF (1.5 mL). The deep red solution was then heated to 40 °C and stirred for 48 hours. The resulting dark purple solution was treated with aqueous hydrochloric acid (1N, 1.0 mL) and the resulting mixture was diluted with EtOAc (20 mL). The phases were separated and the aqueous phase was extracted with EtOAc (2 x 20 mL). The combined organic phases were washed with brine (4 x 10 mL), dried (MgSO$_4$), and concentrated. Purification of the crude material by flash chromatography (20 g of silica gel, 30:1 CH$_2$Cl$_2$ - MeOH) and removal of trace amounts of solvent (vacuum pump) from the resulting solid, afforded 35 mg (88%) of the didemnimide **85** as a red solid (mp >240 °C, decomp).

^{1}H NMR (400 MHz, DMSO-d_6) δ 12.06 (bs, 1H), 11.19 (bs, 1H), 8.09 (d, 1H, J = 2.1 Hz), 7.46 (d, 1H, J = 8.0 Hz), 7.14-7.31 (m, 6H), 7.03 (d, 1H, J = 7.6 Hz), 6.81 (dd, 1H, J = 8.0, 8.0 Hz), 6.47 (d, 1H, J = 8.1 Hz), 3.07 (s, 3H).

^{13}C NMR (100.5 MHz, DMSO-d_6) δ 171.6, 171.4, 138.6, 136.4, 134.6, 133.7, 132.7, 131.8, 129.4, 127.4, 126.7, 126.6, 124.5, 122.5, 120.8, 119.5, 117.9, 112.4, 104.8, 32.4.

IR (KBr): 2500-3600, 1760, 1713, 1631, 1581, 1441, 1339, 744 cm^{-1}.

Exact mass calcd for $C_{22}H_{16}N_4O_2S$: 400.0994; found: 400.0985.

Preparation of didemnimide C (**16**).
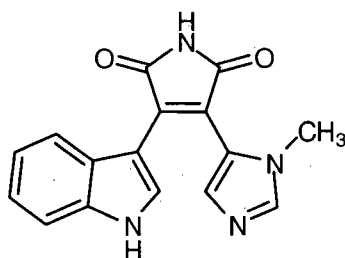
To a refluxing solution of the didemnimide **85** (46.7 mg, 0.117 mmol) in EtOH (10.0 mL), was added Raney Ni (W-2, 50% slurry in water, ~120 mg) and the resulting suspension was refluxed for 1 hour. The reaction mixture was then cooled to room temperature and filtered through Celite®. The Celite® was washed with DMF (6 mL) followed by MeOH - TFA (100:1, 30 mL), and the combined organic washes were concentrated. The residue was dissolved in EtOAc (40 mL) and the solution was washed with aqueous NaHCO$_3$ (4 x 10 mL), brine (3 x 20 mL), dried (MgSO$_4$) and concentrated. Purification of the crude material by flash chromatography (25 g of

silica gel, 10:1 CH_2Cl_2 - MeOH) and removal of trace amounts of solvent (vacuum pump) from the resulting solid, afforded 26.4 mg (77%) of didemnimide C (**16**) as an orange solid which exhibited spectral data that was in accordance with that reported for the natural product.[14]

^{1}H NMR (400 MHz, DMSO-d_6) δ 11.97 (bs, 1H), 11.09 (bs, 1H), 8.06 (d, 1H, J = 2.6 Hz), 7.69 (bs, 1H), 7.44 (d, 1H, J = 8.1 Hz), 7.10 (dd, 1H, J = 8.0, 8.0 Hz), 7.07 (bs, 1H), 6.78 (dd, 1H, J = 8.0, 8.0 Hz), 6.40 (d, 1H, J = 8.1 Hz), 3.17 (s, 3H).

^{13}C NMR (100.5 MHz, DMSO-d_6)[53] δ 171.9, 171.7, 140.3, 136.4, 133.9, 132.0, 131.5, 124.7, 122.3, 122.3, 120.5, 119.7, 118.6, 112.2, 105.0, 32.0.

IR (KBr): 3163, 3041, 1766, 1702, 1538, 1345, 1236, 1221, 748 cm^{-1}.

Exact mass calcd for $C_{16}H_{12}N_4O_2$: 292.0960; found: 292.0957.

Preparation of 17-methylgranulatimide (**74**).
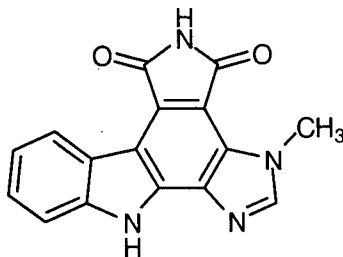
To a solution of didemnimide C (**16**) (20.5 mg, 0.070 mmol) in MeCN (30.0 mL) was added a catalytic amount of Pd/C (10% Pd), and the resulting suspension was sparged with argon for 30 minutes. The reaction mixture was then irradiated (450-watt Hanovia medium pressure mercury

vapor lamp, quartz reaction vessel) for 3.5 hours. The reaction mixture was then filtered through Celite® and the Celite® was washed with MeOH (30 mL) and DMF (40 mL). The MeOH washings were combined with the initial filtrate, while the DMF washings were collected separately. The MeCN - MeOH solution was concentrated and the resulting organic residue was triturated with MeOH (3 x 10 mL) to afford 2.4 mg of 17-methylgranulatimide (**74**) as a yellow solid. The DMF washings were concentrated to provide 10.1 mg (total of 12.5 mg, 64%) of 17-methylgranulatimide (**74**) as a yellow solid (mp >300 °C).

^{1}H NMR (400 MHz, DMSO-d_6) δ 12.58 (bs, 1H, H-1), 11.04 (bs, 1H, H-10), 8.94 (d, 1H, J = 7.7 Hz, H-4), 8.48 (s, 1H, H-16), 7.60 (d, 1H, J = 8.1 Hz, H-7), 7.48 (dd, 1H, J = 8.0, 8.0 Hz, H-6), 7.30 (dd, 1H, J = 8.0, 8.0 Hz, H-5), 4.31 (s, 3H, H-18).

^{13}C NMR (100.5 MHz, DMSO-d_6) δ 170.7 (C-9), 169.1 (C-11), 147.1 (C-16), 140.6 (C-7a), 135.6 (C-14), 133.8 (C-2), 128.5 (C-13), 126.2 (C-6), 124.0 (C-4), 123.6 (C-8), 121.3 (C-3a), 120.1 (C-5), 113.0 (C-3), 111.6 C-7), 109.8 (C-12), 35.1 (C-18).

IR (KBr): 3257, 2951, 2726, 1734, 1703, 1650, 1505, 1479, 1461, 1393, 1326, 1225, 1068, 761, 744 cm^{-1}.

Exact mass calcd for $C_{16}H_{10}N_4O_2$: 290.0804; found: 290.0800.

A summary of the assignments of ^{1}H and ^{13}C NMR resonances for 17-methylgranulatimide (**74**), based on HMQC and HMBC data, is presented in Table 3.12.

Table 3.12. NMR data for 17-methylgranulatimide (**74**) (recorded in DMSO-d_6).
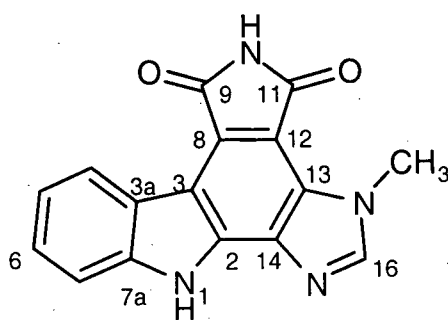
Atom No.	^{13}C δ (ppm)[a]	^{1}H δ (ppm) (mult, J (Hz))[b,c]	HMBC[b]
1		12.58 (bs)	
2	133.8		H-7, H-16
3	113.0		H-1, H-7
3a	121.3		H-1, H-5, H-7
4	124.0	8.94 (d, 7.7)	H-6
5	120.1	7.30 (dd, 8.0, 8.0)	H-7
6	126.2	7.48 (dd, 8.0, 8.0)	H-4, H-5
7	111.6	7.60 (d, 8.1 Hz)	H-4, H-5
7a	140.6		H-4, H-6, H-7
8	123.6		H-10
9[d]	169.1		H-10
10		11.04 (bs)	
11[d]	170.7		H-10
12	109.8		H-10
13	128.5		H-16, H-18
14	135.6		H-1
15			
16	147.1	8.48 (s)	H-18
17			
18	35.1	4.31 (s)	

[a] Recorded at 100.5 MHz. [b] Recorded at 500 MHz. [c] Assignments based on HMQC data.
[d] Assignments may be interchanged.

Preparation of imidazol-1*H*-1-acetamide (**87**).
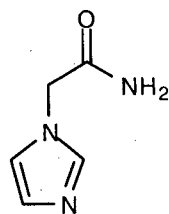
To a cold (0 °C) stirred suspension of NaH (60% dispersion in oil, 352 mg, 8.80 mmol) in dry DMF (5.0 mL) was added a solution of imidazole (536 mg, 8.00 mmol) in dry DMF (10.0 mL). The reaction mixture was then warmed to room temperature and stirred for 30 minutes. The mixture was then cooled to 0 °C, and iodoacetamide (1.63 g, 8.81 mmol) was added in one portion and the resulting solution was warmed to room temperature and stirred for an additional 1.5 hours. The reaction mixture was then diluted with CH_2Cl_2 (20 mL) and the NaI crystals, which precipitated, were removed by filtration. The filtrate was concentrated and the residue was placed on a column of basic alumina (40 g). The crude product was eluted with CH_2Cl_2 - MeOH (6:1) and the eluate was concentrated. Purification of the crude concentrate by flash chromatography (60 g of silica gel, 7:1 CH_2Cl_2 - MeOH) and removal trace amounts of solvent (vacuum pump) from the resulting solid, afforded 747 mg (75%) of the amide **87** as a white solid (mp 185-186 °C, lit. 182-183 °C) which exhibited spectral data that was in accordance with that reported in the literature.[54]

^{1}H NMR (400 MHz, DMSO-d_6) δ 7.54 (s, 1H), 7.51 (bs, 1H), 7.20 (bs, 1H), 7.06 (s, 1H), 6.84 (s, 1H), 4.61 (s, 2H).

^{13}C NMR (100.5 MHz, DMSO-d_6) δ: 168.5, 138.0, 127.5, 120.4, 48.4.

IR (KBr): 3349, 3116, 1685, 1516, 1408, 1312, 1236, 1080, 750, 663 cm^{-1}.

Exact mass calcd for $C_5H_7N_3O$: 125.0589; found: 125.0585.

Preparation of methyl indolyl-3-glyoxylate (88).
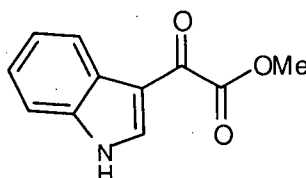
To a cold (0 °C), solution of 3-indoleglyoxylic acid (89) (305 mg, 1.61 mmol) in dry MeOH (3.0 mL) and dry benzene (12.0 mL) was added (trimethylsilyl)diazomethane (2.0 M in hexanes, 1.60 mL, 3.20 mmol) and the reaction mixture was warmed to room temperature and stirred for 4 hours. The reaction mixture was then concentrated to provide the crude product as a beige solid. Purification of the crude product by flash chromatography (40 g of silica gel, 25:1 then 10:1 CH_2Cl_2 - MeOH) and removal of trace amounts of solvent (vacuum pump) from the resulting solid, afforded 327 mg (100%) of the ester 88 as a beige solid (mp 227-228 °C, lit. 227-230 °C) which exhibited spectral data that was in accordance with that reported in the literature.[68]

^{1}H NMR (400 MHz, DMSO-d_6) δ 12.40 (bs, 1H), 8.44 (d, 1H, J = 3.0 Hz), 8.15 (d, 1H, J = 7.0 Hz), 7.54 (d, 1H, J = 7.6 Hz), 7.24-7.31 (m, 2H), 3.88 (s, 3H).

^{13}C NMR (100.5 MHz, DMSO-d_6) δ 178.7, 163.9, 138.3, 136.7, 125.4, 123.8, 122.8, 121.1, 112.7, 112.4, 52.5.

Exact mass calcd for $C_{11}H_9NO_3$: 203.0582; found: 203.0587.

Anal. calcd for $C_{11}H_9NO_3$: C 65.01, H 4.47, N 6.90; found: C 65.16; H 4.34, N 6.77.

Preparation of isodidemnimide A (**86**).
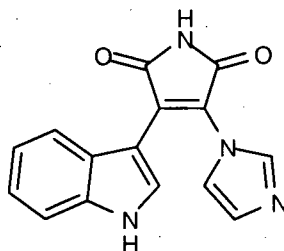
To a cold (0 °C), stirred solution of *t*-BuOK (140 mg, 1.25 mmol) in dry DMF (2.0 mL) was added a solution of the amide **87** (31.1 mg, 0.249 mmol) and methyl indolyl-3-glyoxylate (**88**) (101 mg, 0.498 mmol) in dry DMF (3.0 mL). The orange reaction mixture was stirred for 12 hours at room temperature and then heated to 45 °C for 3 hours. The reaction mixture was then cooled to room temperature and treated with saturated aqueous NH_4Cl (5 mL) and the resulting mixture was diluted with EtOAc (20 mL). The phases were separated and the aqueous phase was extracted with EtOAc (2 x 20 mL). The combined organic phases were washed with brine (4 x 10 mL), dried ($MgSO_4$) and concentrated. Purification of the crude material by flash chromatography (25 g of silica gel, 10:1 then 6:1 CH_2Cl_2 - MeOH) and removal of trace amounts of solvent (vacuum pump) from the resulting solid, afforded 54.5 mg (79%) of the maleimide **86** as a red solid (mp >300 °C).

^{1}H NMR (400 MHz, DMSO-d_6) δ 12.04 (bs, 1H), 11.28 (bs, 1H), 8.03 (d, 1H, J = 3.1 Hz), 7.78 (s, 1H), 7.45 (d, 1H, J = 8.2 Hz), 7.29 (s, 1H), 7.11 (dd, 1H, J = 8.0, 8.0 Hz), 7.04 (s, 1H), 6.80 (dd, 1H, J = 8.0, 8.0 Hz), 6.21 (d, 1H, J = 7.6 Hz).

^{13}C NMR (100.5 MHz, DMSO-d_6) δ 170.4, 168.4, 137.8, 136.4, 131.6, 128.8, 125.8, 124.3, 124.1, 122.5, 120.6, 120.1, 119.6, 112.3, 102.3.

IR (KBr): 3121, 2729, 1767, 1719, 1651, 1495, 1340, 1239, 746 cm^{-1}.

Exact mass calcd for $C_{15}H_{10}N_4O_2$: 278.0804; found: 278.0798.

Preparation of methyl [N-(2-trimethylsilylethoxy)methyl]indole-3-glyoxylate (**93**).
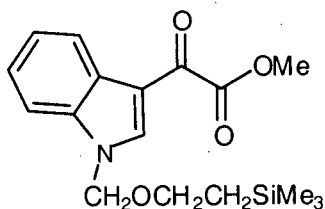
To a cold (0 °C), stirred suspension of NaH (60% dispersion in mineral oil, 123 mg, 3.08 mmol) in dry THF (5.0 mL) was added a solution of the ester **88** (500 mg, 2.46 mmol) in dry THF (20.0 mL) and the reaction mixture was stirred for 10 minutes at 0 °C and 50 minutes at room temperature. The resulting yellow solution was then cooled to 0 °C, SEM-Cl (0.61 mL, 3.44 mmol) was added and the reaction mixture was warmed to room temperature. After 1.5 hours the mixture was treated with saturated aqueous NH$_4$Cl (10 mL) and the resulting mixture was diluted with EtOAc (30 mL). The phases were separated and the aqueous phase was extracted with

EtOAc (2 x 25 mL). The combined organic phases were washed with brine (20 mL), dried (MgSO$_4$) and concentrated. Purification of the crude material by flash chromatography (50 g of silica gel, 3:2 petroleum ether - Et$_2$O) and removal of trace amounts of solvent (vacuum pump) from the resulting solid, afforded 667 mg (82%) of the ester **93** as a colorless solid (mp 96-97 °C).

^{1}H NMR (400 MHz, CDCl$_3$) δ 8.41-8.44 (m, 2H), 7.52-7.54 (m, 1H), 7.33-7.38 (m, 2H), 5.52 (s, 2H), 3.94 (s, 3H), 3.51 (t, 2H, J = 8.1 Hz), 0.89 (t, 2H, J = 8.1 Hz), -0.07 (s, 9H).

^{13}C NMR (100.5 MHz, CDCl$_3$) δ 177.3, 163.0, 139.3, 136.5, 127.2, 124.5, 123.9, 122.8, 113.6, 110.8, 76.7, 66.6, 52.7, 17.6, -1.5.

IR (KBr): 3122, 1733, 1637, 1519, 1398, 1198, 1086, 752 cm^{-1}.

Exact mass calcd for C$_{17}$H$_{23}$NO$_4$Si: 333.1397; found: 333.1395.

Preparation of 1-[(2-trimethylsilylethoxy)methyl]isodidemnimide A (**94**) and 3-[3-methoxy-2,5-dioxo-2,5-dihydro-1*H*-pyrrol-4-yl]-*N*-[(2-trimethylsilylethoxy)methyl]indole (**95**).
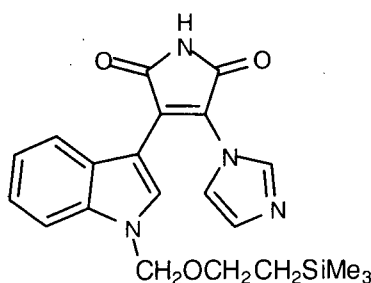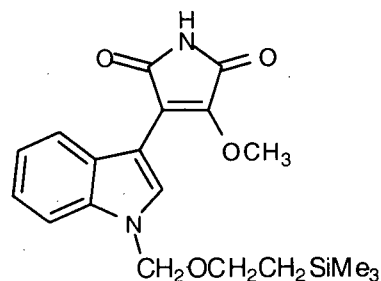
94   **95**

To a cold (0 °C), stirred suspension of the amide **87** (12 mg, 0.096 mmol), the ester **93** (40 mg, 0.12 mmol) and 4 Å molecular sieves (~100 mg) in dry DMF (3.0 mL) was added a solution of *t*-BuOK (27 mg, 0.24 mmol) in dry DMF (2.0 mL) and the reaction mixture was stirred for 12 hours at room temperature. The mixture was then treated with saturated aqueous NH_4Cl (5 mL) and the resulting mixture was diluted with EtOAc (20 mL). The phases were separated and the aqueous phase was extracted with EtOAc (2 x 20 mL). The combined organic phases were washed with brine (4 x 10 mL), dried ($MgSO_4$) and concentrated. Purification of the crude material by flash chromatography (25 g of silica gel, 30:1 CH_2Cl_2 - MeOH) and removal of trace amounts of solvent (vacuum pump) from the resulting solid, afforded 5.0 mg (14%) of the maleimide **95** as a yellow solid and 32.0 mg (82%) of the maleimide **95** as a yellow solid (mp >168 °C, decomp).

Maleimide **95**:

^{1}H NMR (400 MHz, $CDCl_3$) δ 7.97 (d, 1H, *J* = 8.0 Hz), 7.85 (s, 1H), 7.48 (d, 1H, *J* = 8.0 Hz), 7.20-7.32 (m, 2H), 5.50 (s, 2H), 4.27 (s, 3H), 3.49 (t, 2H, *J* = 8.1 Hz), 0.88 (t, 2H, *J* = 8.1 Hz), -0.08 (s, 9H).

IR (KBr): 3222, 2953, 1761, 1713, 1641, 1518, 1299, 1087, 836 cm^{-1}.

Mass calcd for $C_{19}H_{24}N_2O_4Si$: 372; low resolution EIMS found: 372.

Maleimide **94**:

^{1}H NMR (400 MHz, CDCl$_3$) δ 8.95 (bs, 1H), 7.99 (s, 1H), 7.97 (bs, 1H), 7.50 (d, 1H, J = 8.1 Hz), 7.24 (bs, 1H), 7.24 (dd, 1H, J = 8.0, 8.0 Hz), 7.15 (bs, 1H), 6.98 (dd, 1H, J = 8.0, 8.0 Hz), 6.37 (d, 1H, J = 8.1 Hz), 5.53 (s, 2H), 3.55 (t, 2H, J = 8.1 Hz), 0.90 (t, 2H, J = 8.1 Hz), -0.07 (s, 9H).

^{13}C NMR (100.5 MHz, CDCl$_3$) δ 169.3, 167.0, 137.8, 136.7, 133.9, 129.4, 125.4, 124.7, 124.3, 123.9, 122.4, 120.7, 119.6, 111.0, 102.9, 76.3, 66.6, 17.7, -1.5.

IR (KBr): 2953, 2719, 1769, 1723, 1656, 1519, 1337, 1235, 1083, 837, 741 cm^{-1}.

Exact mass calcd for $C_{21}H_{24}N_4O_3Si$: 408.1618; found: 408.1620.

Preparation of 1-[(2-trimethylsilylethoxy)methyl]isogranulatimide A (**96**).
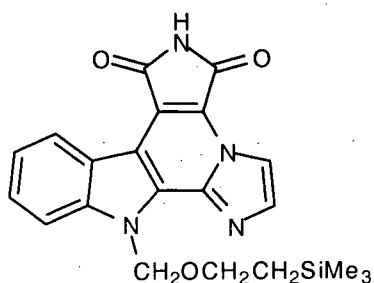
To a stirred solution of 1-[2-trimethylsilylethoxy)methyl]isodidemnimide A (**94**) (60.0 mg, 0.147 mmol) in dry MeCN (20.0 mL) was added Pd/C (8 mg, 10% Pd) and the resulting mixture was sparged with Ar for 30 minutes. The reaction mixture was irradiated (450-watt Hanovia medium pressure mercury vapor lamp, quartz reaction vessel) for 2 hours. The solvent was then removed under reduced pressure to provide a yellow residue. Purification of the yellow residue by flash chromatography (25 g of silica gel, 40:1 CH_2Cl_2 - MeOH) and removal of trace amounts of solvent (vacuum pump) from the resulting solids, afforded trace amounts (less than 1 mg) of 1-(SEM)-isogranulatimide B and 30.8 mg (52%) of 1-(SEM)-isogranulatimide A (**96**) as a yellow solid.

^{1}H NMR (400 MHz, CDCl$_3$) δ 8.78 (d, 1H, J = 8.0 Hz), 8.49 (s, 1H), 7.87 (s, 1H), 7.72 (d, 1H, J = 8.0 Hz), 7.56 (dd, 1H, J = 8.0, 8.0 Hz), 7.52 (bs, 1H), 7.43 (dd, 1H, J = 8.0, 8.0 Hz), 6.50 (s, 2H), 3.63 (t, 2H, J = 8.2 Hz), 0.91 (t, 2H, J = 8.2 Hz), -0.16 (s, 9H).

^{13}C NMR (100.5 MHz, CDCl$_3$) δ 166.6, 163.6, 140.3, 137.8, 135.2, 131.0, 127.1, 125.5, 124.3, 122.8, 121.6, 118.0, 112.8, 111.4, 110.6, 74.0, 66.1, 17.9, -1.5.

IR (KBr): 3108, 2707, 1757, 1721, 1650, 1364, 1291, 1080, 732 cm^{-1}.

Exact mass calcd for $C_{21}H_{22}N_4O_3Si$: 406.1461; found: 406.1456.

Table 3.13. NMR data for 1-[(2-trimethylsilylethoxy)methyl]-isogranulatimide A (**96**) (recorded in $CDCl_3$).
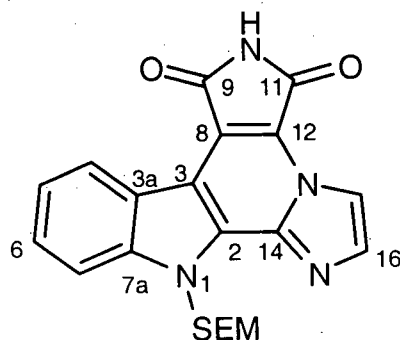
Proton No.	^1H δ (ppm) (mult, J (Hz))[a]	NOE[b]
4	8.78 (d, 8.0)	H-5
5	7.43 (dd, 8.0, 8.0)	H-4
6	7.56 (dd, 8.0, 8.0)	
7	7.72 (d, 8.0)	
10	7.52 (bs)	
16	8.49 (s)	H-17
17	7.87 (s)	H-16
2'	6.50 (s)	H-7, H-4'
4'	3.63 (t, 8.2)	
5'	0.91 (t, 8.2)	
7'	-0.16 (s)	

[a] Recorded at 400 MHz. [b] Recorded at 400 MHz.

Preparation of 1-*tert*-butoxycarbonylisodidemnimide A (**98**).
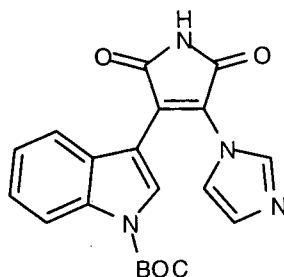
To a cold (0 °C), suspension of NaH (60% dispersion in mineral oil, 23 mg, 0.58 mmol) in dry DMF (2.0 mL) was added a solution of isodidemnimde A (**86**) (62 mg, 0.22 mmol) in dry DMF (2.0 mL) and the deep red reaction mixture was allowed to gradually warm to room temperature and stir for 1.5 hours. A solution of di-*tert*-butyl dicarbonate (58 mg, 0.27 mmol) in dry DMF (2.0 mL) was then added and the reaction mixture was stirred for a further 30 minutes at room temperature. The mixture was then treated with saturated aqueous NH$_4$Cl (5 mL) and the resulting mixture was diluted with and EtOAc (30 mL). The phases were separated and the aqueous phase was extracted with EtOAc (10 mL). The combined organic phases were washed with brine (5 x 10 mL), dried (MgSO$_4$) and concentrated. Purification of the crude material by flash chromatography (40 g of silica gel, 30:1 CH$_2$Cl$_2$ - MeOH) and removal of trace amounts of solvent (vacuum pump) from the resulting solid, afforded 84 mg (100%) of the didemnimide **98** as a yellow solid (mp 133 °C).

^{1}H NMR (400 MHz, CDCl$_3$) δ 11.52 (s, 1H), 8.10 (d, 1H, J = 8.4 Hz), 8.06 (s, 1H), 7.85 (s, 1H), 7.34 (dd, 1H, J = 8.0, 8.0 Hz), 7.28 (s, 1H), 7.03 (dd, 1H, J = 8.0, 8.0 Hz), 7.00 (s, 1H), 6.55 (d, 1H, J = 8.0 Hz), 1.66 (s, 9H).

^{13}C NMR (100.5 MHz, CDCl$_3$) δ 168.7, 166.6, 148.8, 137.7, 135.4, 130.3, 129.8, 128.7, 126.4, 125.6, 123.8, 121.2, 120.1, 119.1, 115.6, 106.6, 85.3, 28.1.

IR (KBr): 3400-2800, 1778, 1728, 1665, 1454, 1358, 1311, 1231, 1153, 1100, 736 cm^{-1}.

Exact mass calcd for C$_{20}$H$_{18}$N$_4$O$_4$: 378.1328; found: 378.1329.

Preparation of 1-*tert*-butoxycarbonylisogranulatimide A (**99**) and 1-*tert*-butoxycarbonyl-isogranulatimide B (**100**).
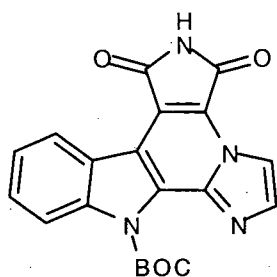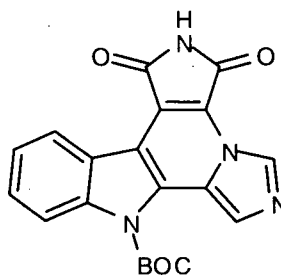
99   **100**

A stirred solution of the didemnimde **98** (42.5 mg, 0.112 mmol) in dry MeCN (4.0 mL) was irradiated (275-watt light bulb) for 1 hour at room temperature. The solvent was removed under reduced pressure and the orange residue was dissolved in CH$_2$Cl$_2$ (6.0 mL). MnO$_2$ (58 mg, 0.67 mmol) was added and the stirred mixture was refluxed overnight. The mixture was then cooled to room temperature, filtered through a short plug of silica gel (10 g of silica gel), and the reaction products were eluted with CH$_2$Cl$_2$ - MeOH (5:1). Concentration of the filtrate provided the crude products as a residue, which was separated by flash chromatography (30 g of silica gel, 25:1 CH$_2$Cl$_2$ - MeOH). Concentration of the appropriate fractions and removal of trace amounts

of solvent (vacuum pump) from the resulting solids, afforded 20.2 mg (48%) of **99** as a yellow solid (mp >200 °C, decomp) and 7.8 mg (19%) of **100** as a purple solid (mp >200 °C, decomp).[69]

1-*tert*-butoxycarbonyl-isogranulatimide A (**99**):

^{1}H NMR (400 MHz, DMSO-d_6) δ 11.46 (s, 1H), 8.66 (d, 1H, J = 8.1 Hz), 8.46 (d, 1H, J = 1.1 Hz), 8.01 (d, 1H, J = 8.4 Hz), 7.92 (d, 1H, J = 1.1 Hz), 7.56 (dd, 1H, J = 8.0, 8.0 Hz), 7.43 (dd, 1H, J = 8.0, 8.0 Hz), 1.69 (s, 9H).

^{13}C NMR (100.5 MHz, DMSO-d_6) δ 167.9, 164.8, 148.6, 138.4, 137.2, 135.3, 127.9, 127.7, 126.3, 123.8, 123.5, 121.8, 115.6, 113.4, 113.3, 112.6, 85.7, 27.3.

IR (KBr): 3226, 1776, 1724, 1649, 1380, 1310, 1287, 1157, 750, 729 cm^{-1}.

Exact mass calcd for $C_{20}H_{16}N_4O_4$: 376.1172; found: 376.1176.

1-*tert*-butoxycarbonyl-isogranulatimide B (**100**):

IR (KBr): 2980, 1729, 1654, 1526, 1370, 1299, 1150, 1130, 740 cm^{-1}.

Exact mass calcd for $C_{20}H_{16}N_4O_4$: 376.1172; found: 376.1177.

Preparation of isogranulatimide A (75).
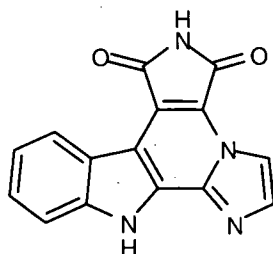
Procedure A. To a stirred solution of the isogranulatimde A **96** (16 mg, 0.040 mmol) in MeCN (5.0 mL) and H_2O (0.2 mL) was added $LiBF_4$ (37 mg, 0.40 mmol) and the reaction mixture was heated at reflux overnight. The solvent was removed under reduced pressure and the yellow residue was dissolved in DMF (4 mL). The resulting solution was diluted with EtOAc (30 mL), washed with brine (4 x 15 mL), dried ($MgSO_4$) and concentrated. Trituration of the residue with Et_2O gave 9.2 mg (84%) of isogranulatimde A **(75)** as a yellow solid.

Procedure B. A suspension of the isogranulatimide **99** (21 mg, 0.056 mmol) in nitrobenzene (1.5 mL) was heated to reflux for 1 hour. The mixture was then cooled to room temperature, diluted with CH_2Cl_2 (5 mL) and placed on a short plug of silica gel (10 g of silica gel). The nitrobenzene was eluted with CH_2Cl_2 (40 mL) followed by CH_2Cl_2 - MeOH (10:1, 40 mL) and isogranulatimide A **(75)** was eluted with CH_2Cl_2 - MeOH - TFA (200:40:1, 100 mL). The CH_2Cl_2 - MeOH - TFA eluate was concentrated under reduced pressure to provide a yellow residue that was dissolved in EtOAc (50 mL). The solution was washed with water (2 x 25 mL), saturated aqueous $NaHCO_3$ (2 x 15 mL), brine (15 mL), dried ($MgSO_4$) and concentrated to provide 12 mg (78%) of isogranulatimide A **(75)** as a yellow solid (mp > 300 °C) which required no further purification.

^{1}H NMR (400 MHz, DMSO-d_6)^{67} δ 13.14 (bs, 1H, H-1), 11.27 (bs, 1H, H-10), 8.63 (d, 1H, $J =$ 8.1 Hz, H-4), 8.46 (s, 1H, H-16), 7.90 (s, 1H, H-17), 7.66 (d, 1H, $J =$ 8.0 Hz, H-7), 7.50 (dd, 1H, $J =$ 8.0, 8.0 Hz, H-6), 7.36 (dd, 1H, $J =$ 8.0, 8.0 Hz, H-5).

^{13}C NMR (100.5 MHz, DMSO-d_6)^{67} δ 168.5 (C-11), 165.3 (C-9), 139.6 (C-7a), 137.6 (C-14), 134.0 (C-17), 129.7 (C-2), 126.5 (C-6), 123.1 (C-4), 121.9 (C-12), 121.4 (C-5), 120.9 (C-3a), 117.8 (C-8), 112.8 (C-16), 112.5 (C-7), 109.7 (C-3).

IR (KBr): 3184, 2931, 2692, 1756, 1718, 1656, 1365, 1309, 1134, 730 cm^{-1}.

Exact mass calcd for $C_{15}H_8N_4O_2$: 276.0647; found: 276.0638.

UV λ_{max} (MeOH): 224, 278, 305, 420 nm.

A summary of the assignments of ^{1}H and ^{13}C NMR resonances for isogranulatimide A (**75**), based on HMQC and HMBC data, is presented in Table 3.14.

Table 3.14. NMR data for isogranulatimide A (**75**) (recorded in DMSO-d_6).

Atom No.	^{13}C δ (ppm)[a]	^{1}H δ (ppm) (mult, J (Hz))[b,c]	HMBC[b]
1		13.14 (bs)	
2	129.7		H-1
3	109.7		H-1, H-4
3a	120.9		H-1, H-5
4	123.1	8.63 (d, 8.1)	H-6
5	121.4	7.36 (dd, 8.0, 8.0)	H-7
6	126.5	7.50 (dd, 8.0, 8.0)	H-4
7	112.5	7.66 (d, 8.0)	H-5
7a	139.6		H-1, H-4, H-6
8[d]	117.8		H-10
9[e]	165.3		H-10
10		11.27 (bs)	
11[e]	168.5		
12[d]	121.9		H-10
13			
14	137.6		H-16
15			
16	112.8	8.46 (s)	H-17
17	134.0	7.90 (s)	H-16

[a] Recorded at 100.5 MHz. [b] Recorded at 500 MHz. [c] Assignments based on HMQC data. [d,e] Assignments may be interchanged.

Preparation of isogranulatimide B (76).
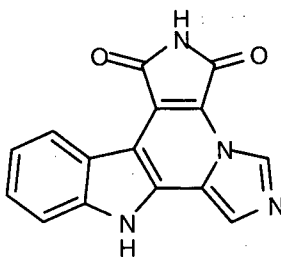
A stirred suspension of the isogranulatimide B **100** (14 mg, 0.037 mmol) in nitrobenzene (1.5 mL) was heated at reflux for 1 hour. The reaction mixture was then cooled to room temperature, diluted with CH_2Cl_2 (5 mL) and filtered through a short plug of silica gel (10 g of silica gel). The nitrobenzene was eluted with CH_2Cl_2 (30 mL), while CH_2Cl_2 - MeOH (5:1, 50 mL) was used to elute isogranulatimide B (**76**). Removal of solvent from the latter eluate provided 8.5 mg (83%) of isogranulatimide B (**76**) as a deep red solid (mp >300 °C) that required no further purification.

^{1}H NMR (400 MHz, DMSO-d_6)[67] δ 12.99 (s, 1H, H-1), 11.23 (s, 1H, H-10), 8.87 (bs, 1H, H-17), 8.53 (d, 1H, J = 7.9 Hz, H-4), 7.94 (bs, 1H, H-15), 7.66 (d, 1H, J = 8.0 Hz, H-7), 7.43 (dd, 1H, J = 8.0, 8.0 Hz, H-6), 7.34 (dd, 1H, J = 8.0, 8.0 Hz, H-5).

^{13}C NMR (100.5 MHz, DMSO-d_6)[67] δ 169.1 (C-9), 165.9 (C-11), 138.7 (C-7a), 132.0 (C-2), 128.4 (C-17), 125.0 (C-6), 122.4 (C-14), 122.3 (C-4), 121.3 (C-5), 121.2 (C-3a), 119.8 (C-8), 119.6 (C-12), 119.3 (C-15), 112.0 (C-7), 104.4 (C-3).

IR (KBr): 3400, 3180, 1761, 1719, 1651, 1556, 1519, 1504, 1365, 1313, 1011, 964, 740 cm^{-1}.

Exact mass calcd for $C_{15}H_8N_4O_2$: 276.0647; found: 276.0649.

UV λ_{max} (MeOH): 228, 304, 472 nm.

Table 3.15. NMR data for isogranulatimide B (**76**) (recorded in DMSO-d_6).
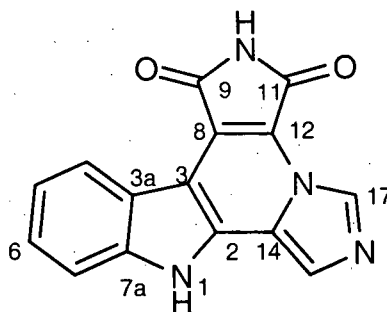
Atom No.	^{13}C δ (ppm)[a]	^{1}H δ (ppm) (mult, J (Hz))[b,c]	HMBC[b]
1		12.99 (s)	
2	132.0		H-1
3	104.4		H-1, H-4, H-7, H-5
3a	121.2		H-1
4	122.3	8.53 (d, 7.9)	H-5
5	121.3	7.34 (dd, 8.0, 8.0)	H-7, H-6
6	125.0	7.43 (dd, 8.0, 8.0)	H-4
7	112.0	7.66 (d, 8.0)	H-5, H-6
7a	138.7		H-1, H-4, H-5
8[d]	119.8		H-10
9[e]	169.1		H-10
10		11.23 (s)	
11[e]	165.9		H-10
12[d]	119.6		
13			
14	122.4		H-15, H-17
15	119.3	7.94 (s)	H-17
16			
17	128.4	8.87 (bs)	H-15

[a] Recorded at 100.5 MHz. [b] Recorded at 500 MHz [c] Assignments based on HMQC data. [d,e] Assignments may be interchanged.

Table 3.16. NMR data for isogranulatimide B (76) (recorded in DMSO-d_6).
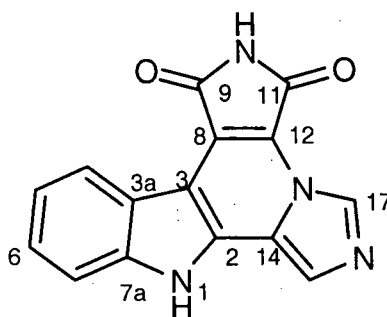
Proton No.	^{1}H δ (ppm) (mult, J (Hz))^a	NOE^b
1	12.99 (s)	H-7, H-15
4	8.53 (d, 7.9)	
5	7.34 (dd, 8.0, 8.0)	
6	7.43 (dd, 8.0, 8.0)	
7	7.66 (d, 8.0)	
10	11.23 (s)	
15	7.94 (s)	H-1
17	8.87 (bs)	no NOE

^{a} Recorded at 400 MHz. ^{b} Recorded at 400 MHz.

Preparation of methyl (1-methoxymethyl-1*H*-imidazol-2-yl)glyoxylate (113).
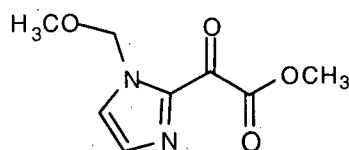
To a cold (-48 °C), stirred solution of 1-methoxymethyl-1*H*-imidazole (112) (335 mg, 2.99 mmol) in dry THF (15.0 mL) was added a solution of *n*-BuLi (1.50 M in hexanes, 2.30 mL, 3.45 mmol) and the resultant mixture was stirred for 1 hour. The mixture was then cooled to -78 °C and added to a solution of dimethyl oxalate (1.17 g, 9.92 mmol) in dry THF (10.0 mL) at -78 °C and the resulting mixture was stirred for an additional 20 minutes. The mixture was then treated with saturated aqueous NH$_4$Cl (5 mL) and the resulting mixture was diluted with EtOAc (15 mL)

and allowed to warm to room temperature. The phases were separated and the aqueous phase was extracted with EtOAc (2 x 20 mL). The combined organic phases were washed with brine (10 mL), dried (MgSO$_4$), and concentrated. Purification of the crude material by flash chromatography (50 g of silica gel, 50:1 CH$_2$Cl$_2$ - MeOH) and removal of trace amounts of solvent (vacuum pump) from the resulting liquid, afforded 290 mg (49%) of the oxalate **113** as an oil.

^{1}H NMR (400 MHz, CDCl$_3$) δ 7.38 (s, 1H), 7.33 (s, 1H), 5.71 (s, 2H), 3.96 (s, 3H), 3.33 (s, 3H).

^{13}C NMR (100.5 MHz, CDCl$_3$) δ 177.9, 164.3, 140.6, 132.9, 126.9, 78.8, 57.5, 53.4.

IR (KBr): 2957, 1744, 1679, 1412, 1276, 1215, 1109, 1005 cm^{-1}.

Exact mass calcd for C$_8$H$_{10}$N$_2$O$_4$: 198.0641; found: 198.0646.

Preparation of 14-methoxymethylneodidemnimide A (**115**).
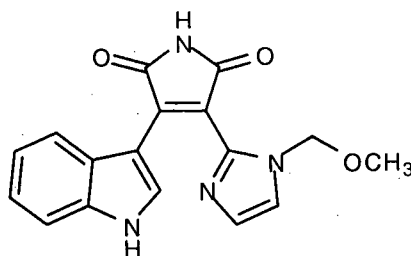
To a stirred solution of the oxalate **113** (142 mg, 0.717 mmol) and indole 3-acetamide (62.7 mg, 0.360 mmol) in dry DMF (5.0 mL) was added a solution of *t*-BuOK (101 mg, 0.902 mmol) in dry DMF (5.0 mL) at room temperature. The reaction mixture was stirred overnight at room

temperature and was then heated to 45 °C and stirred for an additional 20 hours. The mixture was then cooled to room temperature and treated with saturated aqueous NH_4Cl (5 mL) and the resulting mixture was diluted with EtOAc (20 mL). The phases were separated and the aqueous phase was extracted with EtOAc (2 x 20 mL). The combined organic phases were washed with brine (4 x 10 mL), dried ($MgSO_4$) and concentrated. Purification of the crude material by flash chromatography (40 g of silica gel, 40:1 CH_2Cl_2 - MeOH) and removal of trace amounts of solvent (vacuum pump) from the resulting solid, afforded 79.1 mg (68%) of the neodidemnimide **115** as a red solid (mp >240 °C, decomp).

^{1}H NMR (400 MHz, DMSO-d_6) δ 12.06 (bs, 1H), 11.17 (bs, 1H), 8.22 (d, 1H, J = 3.0 Hz), 7.46 (s, 1H), 7.41 (d, 1H, J = 7.9 Hz), 7.11 (s, 1H), 7.08 (dd, 1H, J = 8.0, 8.0 Hz), 6.77 (dd, 1H, J = 8.0, 8.0 Hz), 6.22 (d, 1H, J = 8.1 Hz), 5.06 (s, 2H), 3.08 (s, 3H).

^{13}C NMR (100.5 MHz, DMSO-d_6) δ 171.6, 171.4, 138.0, 137.7, 136.6, 132.7, 129.2, 124.8, 122.4, 122.0, 120.7, 120.2, 118.1, 112.1, 105.1, 76.8, 55.7.

IR (KBr): 2500-3400, 1759, 1713, 1626, 1531, 1341, 1025, 745 cm^{-1}.

Exact mass calcd for $C_{17}H_{14}N_4O_4$: 322.1066; found: 322.1058.

Preparation of neodidemnimide A (**111**).
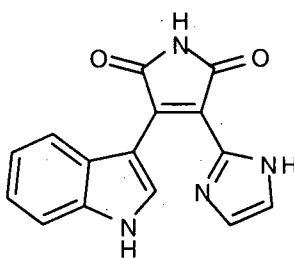
To a stirred suspension of the neodidemnimide A **115** (18 mg, 0.056 mmol) in dry CH_2Cl_2 (5.0 mL) at room temperature was added a solution of BBr_3 (1.0 M in CH_2Cl_2, 0.56 mL, 0.56 mmol) and the resulting blue mixture was heated at reflux for 5 hours. The reaction mixture was then cooled to room temperature, treated with saturated aqueous $NaHCO_3$ (5 mL) and the resulting mixture was diluted with EtOAc (10 mL) and stirred for 30 minutes. The phases were separated and the aqueous phase was extracted with EtOAc (3 x 10 mL). The combined organic phases were washed with brine (10 mL), dried ($MgSO_4$) and concentrated. Purification of the crude material by flash chromatography (25 g of silica gel, 20:1 CH_2Cl_2 - MeOH) and removal of trace amounts of solvent (vacuum pump) from the resulting solid, afforded 13.5 mg (87%) of neodidemnimide A (**111**) as an orange solid (mp 265 °C, decomp).

^{1}H NMR (400 MHz, with excess TFA, DMSO-d_6) δ 12.45 (s, 1H), 11.61 (s, 1H), 8.37 (d, 1H, J = 2.7 Hz), 7.83 (s, 2H), 7.55 (d, 1H, J = 7.8 Hz), 7.20 (dd, 1H, J = 8.0, 8.0 Hz), 6.93 (dd, 1H, J = 8.0, 8.0 Hz), 6.13 (d, 1H, J = 7.6 Hz).

^{13}C NMR (100.5 MHz, with excess TFA, DMSO-d_6) δ 170.8, 170.2, 137.5, 137.1, 135.3, 134.6, 124.4, 122.9, 121.8, 121.3, 119.7, 112.9, 111.4, 104.5.

IR (KBr): 3385, 3140, 1759, 1709, 1630, 1494, 1431, 1346, 1025, 1002, 747 cm^{-1}.

Exact mass calcd for $C_{15}H_{10}N_4O_2$: 278.0804; found: 278.0797.

Preparation of isogranulatimide C (**77**).
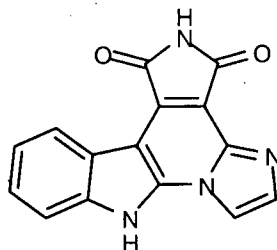
A stirred suspension of neodidemnimide A (**111**) (27 mg, 0.097 mmol) and Pd black (10 mg, 0.097 mmol) in nitrobenzene (4.0 mL) was heated at reflux for 8 hours. The reaction mixture was then cooled to room temperature, diluted with CH_2Cl_2 (10 mL) and placed on a short plug of silica gel (5 g). The nitrobenzene was eluted using CH_2Cl_2 (10 mL) and the reaction product was eluted with CH_2Cl_2 - MeOH - TFA (10:1:0.05, 50 mL). The latter eluate was concentrated to provide a yellow residue that was dissolved in EtOAc (50 mL). The solution was washed with saturated aqueous $NaHCO_3$ (3 x 25 mL), water (20 mL), brine (20 mL), dried ($MgSO_4$) and concentrated to afford 20.1 mg (75%) of isogranulatimide C (**77**) as an orange solid (mp >300 °C) which required no further purification.

^{1}H NMR (400 MHz, DMSO-d_6)[67] δ 13.36 (bs, 1H, H-1), 11.13 (bs, 1H, H-10), 8.63 (d, 1H, J = 7.7 Hz, H-4), 8.40 (s, 1H, H-15), 7.93 (s, 1H, H-16), 7.69 (d, 1H, J = 8.2 Hz, H-7), 7.48 (dd, 1H, J = 8.0, 8.0 Hz, H-6), 7.38 (dd, 1H, J = 8.0, 8.0 Hz, H-5).
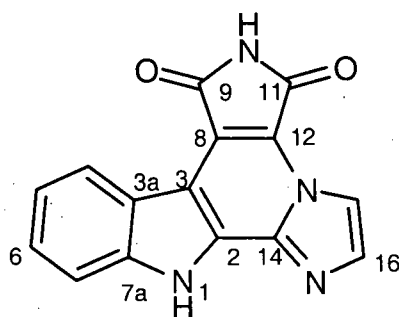
^{13}C NMR (100.5 MHz, DMSO-d_6)[67] δ 169.9 (C-9), 168.2 (C-11), 138.5 (C-13), 138.3 (C-2), 136.9 (C-7a), 135.5 (C-16), 128.9 (C-8), 125.4 (C-6), 122.8 (C-4), 121.7 (C-5), 120.8 (C-3a), 112.5 (C-7), 111.2 (C-15), 109.5 (C-12), 99.0 (C-3).

IR (KBr): 2600-3400, 1755, 1717, 1631, 1591, 1575, 1464, 1376, 1336, 1232, 751 cm^{-1}.

Exact mass calcd for $C_{15}H_8N_4O_2$: 276.0647; found: 276.0639.

A summary of the assignments of ^{1}H and ^{13}C NMR resonances for isogranulatimide C (**77**), based on HMQC and HMBC data, is presented in Table 3.17 and NOE correlations are presented in Table 3.18.

Table 3.17. NMR data for isogranulatimide C (**77**) (recorded in DMSO-d_6).
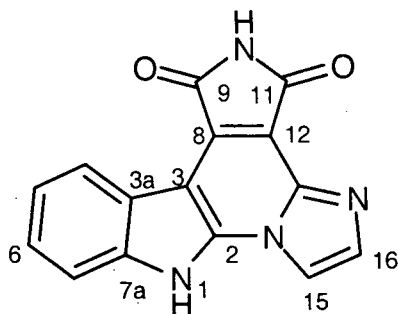
Atom No.	^{13}C δ (ppm)[a]	^1H δ (ppm) (mult, J (Hz))[b,c]	HMBC[b]
1		13.36 (bs)	
2	138.3		
3	99.0		H-4
3a	120.8		H-7, H-5
4	122.8	8.63 (d, 7.7)	H-7, H-6
5	121.7	7.38 (dd, 8.0, 8.0)	
6	125.4	7.48 (dd, 8.0, 8.0)	H-4
7	112.5	7.69 (d, 8.2)	H-5
7a	136.9		H-, H-6
8[d]	128.9		H-10
9[e]	169.9		H-10
10		11.13 (bs)	
11[e]	168.2		H-10
12[d]	109.5		H-10,
13	138.5		H-15, H-16
14			
15	111.2	8.40 (s)	H-16
16	135.5	7.93 (s)	H-15

[a] Recorded at 100.5 MHz. [b] Recorded at 500 MHz. [c] Assignments based on HMQC data.
[d,e] Assignments may be interchanged.

Table 3.18. NMR data for isogranulatimide C (**77**) (recorded in DMSO-d_6).
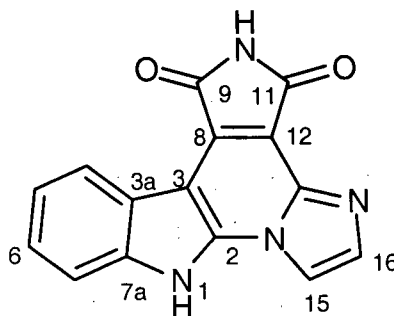
Proton No.	^{1}H δ (ppm) (mult, J (Hz))^a	NOE^b
1	13.36 (bs)	H-7, H-15
4	8.63 (d, 7.7)	H-5
5	7.38 (dd, 8.0, 8.0)	
6	7.48 (dd, 8.0, 8.0)	
7	7.69 (d, 8.2)	
10	11.13 (bs)	
15	8.40 (s)	H-1, H-16
16	7.93 (s)	H-15

^{a} Recorded at 400 MHz. ^{b} Recorded at 400 MHz.

Preparation of the maleimide 122.
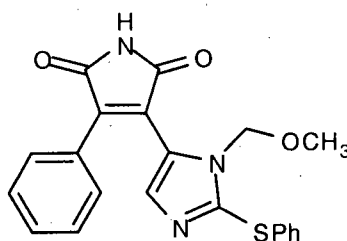
To a stirred solution of phenyl acetamide (29.0 mg, 0.21 mmol) and the oxalate **53** (60 mg, 0.20 mmol) in dry DMF (3.0 mL) at room temperature, was added was added sequentially 4 Å molecular sieves (~200 mg) and a solution of t-BuOK (53 mg, 0.47 mmol) in dry DMF (2.0 mL). The resulting solution was then heated at 45 °C for 12 hours. The reaction mixture was then cooled to room temperature and treated with saturated aqueous NH_4Cl (5 mL) and the resulting

mixture was diluted with EtOAc (20 mL). The phases were separated and the aqueous phase was extracted with EtOAc (2 x 20 mL). The combined organic phases were washed with brine (4 x 10 mL), dried (MgSO$_4$) and concentrated. Purification of the crude material by flash chromatography (40 g of silica gel, 50:1 CH$_2$Cl$_2$ - MeOH) and removal of trace amounts of solvent (vacuum pump) from the resulting solid, afforded 61.3 mg (83%) of the maleimide **122** as a yellow solid (mp 175 °C, decomp).

^{1}H NMR (400 MHz, CDCl$_3$) δ 8.18 (bs, 1H), 7.46 (d, 2H, J = 7.0 Hz), 7.29-7.38 (m, 8H), 5.06 (s, 2H), 3.01 (s, 3H).

^{13}C NMR (100.5 MHz, CDCl$_3$) δ 169.6, 168.9, 144.3, 137.8, 134.6, 132.9, 130.7, 129.7, 129.4, 129.4, 128.9, 128.2, 127.6, 127.1, 123.2, 76.9, 56.2.

IR (KBr): 3019, 2745, 1767, 1723, 1336, 1114, 1024, 737 cm^{-1}.

Exact mass calcd for C$_{21}$H$_{17}$N$_3$O$_3$S: 391.0991; found: 391.0987.

Preparation of the 3-azaindole **126.**
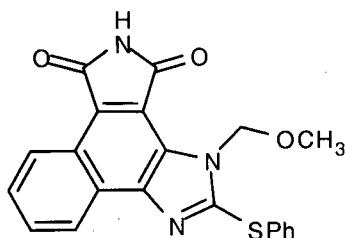
To a solution of the maleimide **122** (14.6 mg, 0.037 mmol) in dry MeCN (5.0 mL), was added a catalytic amount of Pd/C (10% Pd) and the resulting suspension was sparged with argon for 30 minutes. The mixture was then irradiated (450-watt Hanovia medium pressure mercury vapor lamp, quartz reaction vessel) for 10 hours. The reaction mixture was filtered through Celite®, the Celite® was washed with MeOH (30 mL) and the filtrate was concentrated under reduced pressure. Purification of the crude material by flash chromatography (40 g of silica gel, 45:1 CH_2Cl_2 - MeOH) and removal of trace amounts of solvent (vacuum pump) from the resulting solid, afforded 8.9 mg (62%) of the maleimide **126** as a yellow solid (mp 240 °C).

^{1}H NMR (400 MHz, DMSO-d_6) δ 11.38 (bs, 1H), 8.95 (d, 1H, J = 7.9 Hz), 8.42 (d, 1H, J = 7.9 Hz), 7.69-7.78 (m, 2H), 7.62-7.67 (m, 2H), 7.41-7.50 (m, 3H), 6.24 (s, 2H), 3.28 (s, 3H).

^{13}C NMR (100.5 MHz, DMSO-d_6, acquired at 55 °C) δ 170.2, 168.1, 152.1, 143.7, 131.6, 130.0, 129.2, 128.7, 128.4, 127.6, 127.4, 126.2, 124.5, 124.2, 123.2, 122.0, 118.8, 76.8, 55.1.

IR (KBr): 3438, 3219, 1762, 1718, 1402, 1328, 1114, 764 cm^{-1}.

Exact mass calcd for $C_{21}H_{15}N_3O_3S$: 389.0834; found: 389.0830.

Preparation of the 3-azaindole **83**.
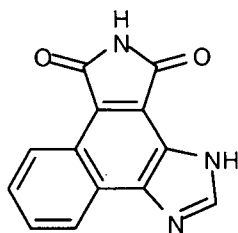
To a stirred solution of the maleimide **126** (10.0 mg, 0.025 mmol) in dry CH_2Cl_2 (3.0 mL) at room temperature, was added a solution of BBr_3 (1.0 M solution in CH_2Cl_2, 0.25 mL, 0.25 mmol) and the reaction mixture was heated at reflux for 3 hours. The reaction mixture was then cooled to room temperature, treated with saturated aqueous $NaHCO_3$ (5 mL) and the resulting mixture was diluted with EtOAc (10 mL) and stirred for an additional 30 minutes. The phases were separated and the aqueous phase was extracted with EtOAc (3 x 10 mL). The combined organic phases were washed with brine (10 mL), dried ($MgSO_4$) and concentrated to provide a crude yellow solid which was used in the next transformation without further purification.

To a stirred, refluxing solution of the crude yellow solid in EtOH (2.5 mL) was added Raney Ni (W-2, 50% slurry in water, ~50 mg) and the suspension was refluxed for 8 hours. The reaction mixture was then cooled to room temperature and filtered through Celite®. The Celite® was washed with CH_2Cl_2 - MeOH (1:1, 75 mL) and the combined organic washes were concentrated. Purification of the crude material by flash chromatography (14 g of silica gel, 20:1 CH_2Cl_2 - MeOH) and removal of trace amounts of solvent (vacuum pump) from the resulting solid, afforded 3.6 mg (61%) of the maleimide **83** as a yellow solid (mp >300 °C).

^{1}H NMR (400 MHz, 0.05% v/v TFA in DMSO-d_6) δ 11.22 (bs, 1H), 8.92 (d, 1H, J = 7.9 Hz), 8.72 (bs, 1H), 8.57 (d, 1H, J = 8.4 Hz), 7.80 (dd, 1H, J = 8.0, 8.0 Hz), 7.73 (dd, 1H, J = 8.0, 8.0 Hz).

^{13}C NMR (100.5 MHz, 0.05% v/v TFA in DMSO-d_6) δ 171.2, 168.6, 144.5, 128.6, 127.2, 126.9, 124.9, 124.3, 122.3, 122.3, 121.2.

IR (KBr): 3435, 2924, 1759, 1719, 1630, 1344, 779 cm^{-1}.

Exact mass calcd for $C_{17}H_7N_3O_2$: 237.0538; found: 237.0532.

Preparation of 10-methylisogranulatimide (80).
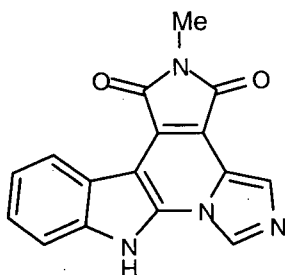
To a solution of isogranulatimide (23) (13.1 mg, 0.047 mmol) in dry DMF (2.0 mL) at room temperature was added NaH (60% dispersion in mineral oil, 3.8 mg, 0.095 mmol) and the reaction mixture was stirred for 1 hour. After this time, iodomethane (6 µL, 0.096 mmol) was added and the resulting solution was stirred for 30 minutes at room temperature. The reaction mixture was then treated with saturated aqueous NH$_4$Cl (5 mL) and the resulting mixture was diluted with EtOAc (15 mL). The phases were separated and the organic phase was washed with brine (4 x 10 mL), dried (MgSO$_4$) and concentrated. Purification of the crude product by flash chromatography (20 g of silica gel, 20:1 CH$_2$Cl$_2$ - MeOH) and removal of trace amount of solvent (vacuum pump) from the resulting solid, afforded 7.3 mg (54%) of 10-methylisogranulatimide (80) as a purple solid (mp >300 °C).

^{1}H NMR (400 MHz, DMSO-d_6) δ 13.22 (bs, 1H), 8.65 (s, 1H), 8.25 (d, 1H, J = 8.0 Hz), 7.69 (s, 1H), 7.52 (d, 1H, J = 8.0 Hz), 7.34 (dd, 1H, J = 8.0, 8.0 Hz), 7.22 (dd, 1H, J = 8.0, 8.0 Hz), 2.94 (s, 3H).

^{13}C NMR (100.5 MHz, DMSO-d_6) δ 168.3, 167.5, 135.6, 134.7, 126.7, 125.1, 124.8, 122.1, 121.8, 121.1, 120.8, 112.8, 112.3, 97.6, 23.1.

IR (KBr): 3124, 2925, 1758, 1706, 1622, 1586, 1436, 1110, 989 cm^{-1}.

Exact mass calcd for $C_{16}H_{10}N_4O_2$: 290.0804; found: 290.0799.

Preparation of 10-hexylisogranulatimide (81).
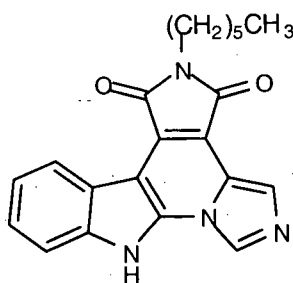
To a solution of isogranulatimide (23) (11.2 mg, 0.041 mmol) in dry DMF (2.0 mL) at room temperature was added NaH (60% dispersion in mineral oil, 3.2 mg, 0.08 mmol) and the reaction mixture was stirred for 1 hour. After this time, 1-iodohexane (12 μL, 0.082 mmol) was added and the resulting solution was stirred for 30 minutes at room temperature. The reaction mixture was then treated with saturated aqueous NH$_4$Cl (5 mL) and the resulting mixture was diluted with EtOAc (15 mL). The phases were separated and the organic phase was washed with brine (4 x 10 mL), dried (MgSO$_4$) and concentrated. Purification of the crude product by flash

chromatography (20 g of silica gel, 20:1 CH_2Cl_2 - MeOH) and removal of trace amount of solvent (vacuum pump) from the resulting solid, afforded 6.6 mg (45%) of 10-hexylisogranulatimide (**81**) as a purple solid (mp >300 °C).

^{1}H NMR (400 MHz, DMSO-d_6) δ 13.35 (bs, 1H), 8.79 (s, 1H), 8.40 (d, 1H, J = 8.0 Hz), 7.80 (s, 1H), 7.59 (d, 1H, J = 8.0 Hz), 7.38 (dd, 1H, J = 8.0, 8.0 Hz), 7.29 (dd, 1H, J = 8.0, 8.0 Hz), 3.53 (m, 2H), 1.61 (m, 2H), 1.28 (m, 6H), 0.84 (t, 3H, J = 7.0 Hz).

^{13}C NMR (100.5 MHz, DMSO-d_6) δ 168.3, 167.5, 135.6, 134.8, 126.8, 125.0, 124.8, 123.0, 122.1, 121.8, 121.2, 120.8, 112.7, 112.3, 97.6, 37.3, 30.7, 28.0, 25.8, 21.8, 13.8.

IR (KBr): 3449, 2927, 1761, 1703, 1586, 1568, 1393, 1236 cm^{-1}.

Exact mass calcd for $C_{21}H_{20}N_4O_2$: 360.1586; found: 360.1577.

Preparation of 1-hexyl-indole-3-acetamide (**128**).
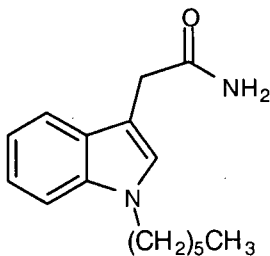
To a stirred suspension of NaH (70 mg, 60% dispersion in oil, 1.75 mmol) in dry DMF (2.0 mL) at room temperature, was added a solution of indole acetamide (300 mg, 1.72 mmol) in dry DMF (4.0 mL) and the mixture was stirred for 1.5 hours. After this time, 1-iodohexane (0.26 mL, 1.76

mmol) was added and the reaction mixture was stirred for an additional 1 hour at room temperature. The reaction mixture was then treated with saturated aqueous NH_4Cl (10 mL) and the resulting mixture was diluted with EtOAc (25 mL). The phases were separated and the aqueous phase was extracted with EtOAc (2 x 25 mL). The combined organic phases were washed with brine (4 x 20 mL), dried ($MgSO_4$) and concentrated to provide 438 mg of the acetamide **128** (99%) as a white solid (mp 74 °C) which required no further purification.

^{1}H NMR (400 MHz, $CDCl_3$) δ 7.56 (d, 1H, J = 8.1 Hz), 7.32 (d, 1H, J = 8.0 Hz), 7.21 (dd, 1H, J = 7.0, 7.0 Hz), 7.10 (dd, 1H, J = 7.0, 7.0 Hz), 7.00 (s, 1H), 6.57 (bs, 1H), 5.87 (bs, 1H), 4.04 (t, 2H, J = 7.3 Hz), 3.65 (s, 2H), 1.78-1.82 (m, 2H), 1.29-1.33 (m, 6H), 0.89 (t, 3H, J = 6.6 Hz).

^{13}C NMR (100.5 MHz, $CDCl_3$) δ 174.6, 136.2, 127.3, 126.9, 121.6, 119.1, 118.6, 109.3, 107.4, 46.0, 32.6, 31.1, 29.9, 26.4, 22.2, 13.7.

IR (KBr): 3386, 3200, 2932, 1651, 1470, 1368, 1284, 1014, 735 cm^{-1}.

Exact mass calcd for $C_{16}H_{22}N_2O$: 258.1732; found: 258.1730.

Preparation of 1-hexyl-17-methoxymethyl-16-thiophenyldidemnimide A (**129**).
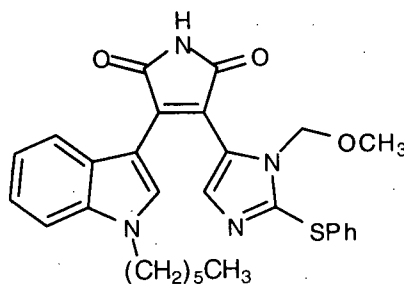
To a stirred solution of *t*-BuOK (135 mg, 1.20 mmol) in dry DMF (2.0 mL) at room temperature

was added sequentially 4 Å molecular sieves (~500 mg), a solution of the oxalate **53** (147 mg,

0.0.48 mmol) and 1-hexylindole-3-acetamide (**128**) (137 mg, 0.53 mmol) in dry DMF (4.0 mL).

The reaction mixture was heated at 45 °C for 12 hours. The dark purple reaction mixture was

then treated with saturated aqueous NH_4Cl (10 mL) and the resulting mixture was diluted with

EtOAc (50 mL). The phases were separated and the aqueous phase was extracted with EtOAc (2

x 10 mL). The combined organic phases were washed with brine (4 x 15 mL), dried ($MgSO_4$)

and concentrated. Purification of the crude material by flash chromatography (25 g of silica gel,

40:1 CH_2Cl_2 - MeOH) and removal of trace amounts of solvent (vacuum pump) from the

resulting solid, afforded 286 mg (75%) of the maleimide **129** as an orange solid which required

no further purification.

^{1}H NMR (400 MHz, $CDCl_3$) δ 8.07 (s, 1H), 7.78 (s, 1H), 7.37 (s, 1H), 7.32 (d, 1H, $J = 8.2$ Hz),

7.15-7.30 (m, 6H), 6.84 (dd, 1H, $J = 8.0, 8.0$ Hz), 6.59 (d, 1H, $J = 8.1$ Hz), 5.11 (s, 2H), 4.15 (t,

2H, $J = 7.2$ Hz), 3.02 (s, 3H), 1.82-1.92 (m, 2H), 1.23-1.38 (m, 6H), 0.86 (t, 3H, $J = 6.7$ Hz).

^{13}C NMR (100.5 MHz, CDCl$_3$) δ 170.6, 170.1, 142.2, 136.8, 134.7, 134.5, 129.3, 129.2, 127.2, 125.3, 125.2, 123.2, 121.7, 121.5, 121.4, 117.7, 117.1, 110.3, 104.8, 76.5, 56.3, 47.2, 31.2, 29.8, 26.5, 22.4, 13.9.

IR (KBr): 3271, 2929, 1760, 1713, 1629, 1541, 1333, 1115, 913, 743 cm^{-1}.

Exact mass calcd for C$_{29}$H$_{30}$N$_4$O$_3$S: 514.2039; found: 514.2034.

Preparation of 1-hexyl-17-methoxymethyldidemnimide A (**132**) and 1-hexyldidemnimide A (**130**).

132   **130**
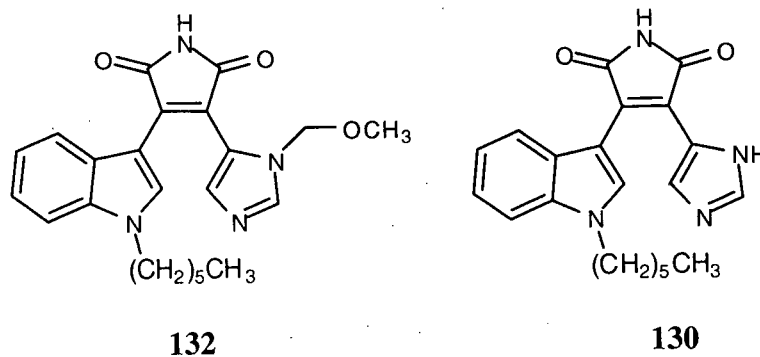
To a stirred, refluxing solution of the didemnimide **129** (57 mg, 0.11 mmol) in EtOH (3.0 mL) was added Raney Ni (W-2, 50% slurry in water, ~150 mg) and the resulting suspension was heated at reflux for 1 hour. An additional amount of Raney Ni (W-2, 50% slurry in water, ~100 mg) was then added and the mixture was heated at reflux for an additional 3 hours. The reaction mixture was cooled to room temperature and filtered through Celite®. The Celite® was washed with CH$_2$Cl$_2$ - MeOH (1:1, 75 mL) and the combined organic washes were concentrated to provide the didemnimide **132** as an orange solid which was used without further purification.

To a stirred suspension of the didemnimide **132** in dry CH_2Cl_2 (3.0 mL) at room temperature was added a solution of BBr_3 in CH_2Cl_2 (1.0 M, 0.9 mL, 0.90 mmol) and the resulting deep blue solution was heated at reflux for 1.5 hours. The reaction mixture was then cooled to room temperature, treated with saturated aqueous $NaHCO_3$ (10 mL) and the resulting mixture was diluted with EtOAc (10 mL) and stirred for 15 minutes. The phases were separated and the aqueous phase was extracted with EtOAc (2 x 15 mL). The combined organic phases were washed with brine (10 mL), dried ($MgSO_4$) and concentrated. Purification of the crude product by flash chromatography (20 g of silica gel, 30:1 CH_2Cl_2 - MeOH) and removal of trace amount of solvent (vacuum pump) from the resulting solid, afforded 25 mg (63% over 2 steps) of 1-hexyldidemnimide A (**130**) as an orange solid (mp 188 °C).

^{1}H NMR (400 MHz, DMSO-d_6) δ 11.36 (s, 1H), 9.00 (s, 1H), 8.15 (s, 1H), 7.66 (s, 1H), 7.62 (d, 1H, J = 8.3 Hz), 7.21 (dd, 1H, J = 8.0, 8.0 Hz), 6.97 (dd, 1H, J = 8.0, 8.0 Hz), 6.65 (d, 1H, J = 8.0 Hz), 4.30 (dd, 1H, J = 7.3 Hz), 1.70-1.81 (m, 2H), 1.18-1.32 (m, 6H), 0.84 (t, 3H, J = 6.9 Hz).

^{13}C NMR (100.5 MHz, DMSO-d_6) δ 171.4, 171.0, 136.6, 135.5, 134.8, 133.2, 124.7, 123.1, 122.4, 121.2, 120.9, 120.7, 116.5, 111.0, 103.1, 46.1, 30.7, 29.5, 25.7, 21.9, 13.8.

IR (KBr): 3392, 2930, 2709, 1753, 1713, 1550, 1509, 1339, 1098, 738 cm^{-1}.

Exact mass calcd for $C_{21}H_{22}N_4O_2$: 362.1743; found: 362.1741.

Preparation of 1-hexylgranulatimide (**79**).
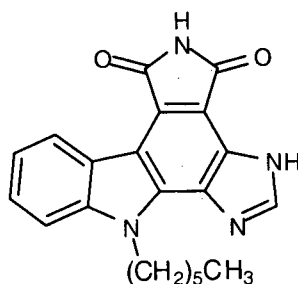
To a solution of 1-hexyldidemnimide A (**130**) (12.1 mg, 0.033 mmol) in dry MeCN (4.0 mL) was added a catalytic amount of Pd/C (10% Pd) and the resulting suspension was sparged with argon for 30 minutes. The mixture was then irradiated (450 Watt Hanovia medium pressure mercury vapor lamp, quartz reaction vessel) for 4 hours. The reaction mixture was filtered through Celite®, the Celite® was washed with MeOH - CH_2Cl_2 - TFA (1:10:0.5, 20 mL), and the combined filtrates were concentrated. The crude product was purified by flash chromatography (20 g of silica gel, 20:1:0.01 CH_2Cl_2 - MeOH - TFA) and the yellow fractions, containing **79**, were combined and concentrated. The resulting yellow residue was dissolved in EtOAc (30 mL) and washed successively with saturated aqueous $NaHCO_3$ (2 x 10 mL) and H_2O (10 mL), dried ($MgSO_4$) and concentrated to afford 8.5 mg (72%) of 1-hexylgranulatimide (**79**) as a yellow solid (mp >300 °C) which required no further purification.

^{1}H NMR (400 MHz, DMSO-d_6) δ 13.62 (bs, 1H), 10.99 (s, 1H), 8.95 (d, 1H, J = 7.8 Hz), 8.54 (s, 1H), 7.73 (d, 1H, J = 8.1 Hz), 7.54 (dd, 1H, J = 8.0, 8.0 Hz), 7.34 (dd, 1H, J = 8.0, 8.0 Hz), 4.98 (m, 2H), 1.80-1.92 (m, 2H), 1.10-1.35 (m, 6H), 0.76 (t, 3H, J = 6.6 Hz).

^{13}C NMR (100.5 MHz, DMSO-d_6) δ 170.1, 169.2, 144.4, 140.4, 135.1, 133.1, 126.1, 124.0, 122.7, 121.1, 120.2, 112.3, 109.8, 109.3, 44.2, 30.8, 29.0, 25.7, 21.8, 13.6.

IR (KBr): 3255, 2928, 1752, 1698, 1592, 1477, 1331, 1237, 741 cm^{-1}.

Exact mass calcd for $C_{21}H_2N_4O_2$: 360.1586; found: 360.1592.

Preparation of 1-hexylisogranulatimide (78).
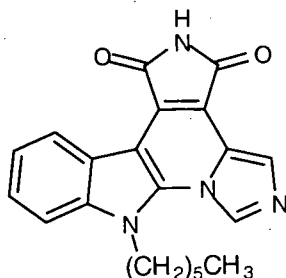
A stirred suspension of **130** (7.0 mg, 0.019 mmol) and Pd black (2 mg, 0.019 mmol) in nitrobenzene (1.5 mL) was heated at reflux for 8 hours. The reaction mixture was cooled to room temperature, diluted with CH_2Cl_2 (5 mL) and placed on a short plug of silica gel (5 g). The nitrobenzene was eluted with CH_2Cl_2 (10 mL) and the reaction product was eluted with CH_2Cl_2 - MeOH (10:1, 25 mL). The latter eluate was concentrated to provide the crude product as a purple residue. Purification of the crude product by flash chromatography (20 g of silica gel, 35:1 CH_2Cl_2 - MeOH) and removal of trace amount of solvent (vacuum pump) from the resulting solid, afforded 6.3 mg (91%) of 1-hexylisogranulatimide (**78**) as a purple solid (mp >300 °C).

^{1}H NMR (400 MHz, DMSO-d_6) δ 11.09 (s, 1H), 9.06 (s, 1H), 8.49 (d, 1H, J = 7.8 Hz), 7.85 (s, 1H), 7.73 (d, 1H, J = 8.3 Hz), 7.41 (dd, 1H, J = 8.0, 8.0 Hz), 7.28 (dd, 1H, J = 8.0, 8.0 Hz), 4.72 (m, 2H), 1.65-1.76 (m, 2H), 1.12-1.40 (m, 6H), 0.77 (t, 3H, J = 6.8 Hz).

^{13}C NMR (100.5 MHz, DMSO-d_6) δ 169.5, 168.6, 136.4, 134.7, 127.6, 125.3, 124.7, 124.3, 122.4, 122.0, 121.0, 120.0, 114.4, 110.7, 98.6, 44.4, 30.7, 30.5, 25.3, 21.6, 13.7.

IR (KBr): 3151, 2930, 2739, 1726, 1567, 1473, 1384, 1319, 1125, 743 cm^{-1}.

Exact mass calcd for $C_{21}H_{20}N_4O_2$: 360.1586; found: 360.1585.

3.11 References

(1)   Bergmann, W.; Feeney, R. J. *J. Am. Chem. Soc.* **1950**, *72*, 2809.

(2)   Davidson, B. S. *Chem. Rev.* **1993**, *1993*, 1771.

(3)   Miner, R. W. *Field Book of Seashore Life*; G. P. Putnam's Sons: New York, 1950.

(4)   Harless *Mueller's Arch* **1847**, 148.

(5)   Bruening, R. C.; Oltz, E. M.; Furukawa, J.; Nakanishi, K.; Kustin, K. *J. Nat. Prod.* **1986**, *49*, 193.

(6)   Fenical, W. *Proc. Food-Drugs Sea* **1976**, *1974*, 388.

(7)   Rinehart, K. L.; Gloer, J. B.; Cook, J. C.; Mizsak, S. A.; Scahill, T. A. *J. Am. Chem. Soc.* **1981**, *103*, 1857.

(8)   Jaspars, M. In *Advances in Drug Discovery Techniques*; Harvey, A. L., Ed.; John Wiley & Sons: New York, 1999; p 65.

(9)   He, H.-H.; Faulkner, D. J. *J. Org. Chem.* **1991**, *56*, 5369.

(10)   Sigel, M. M.; Wellham, L. L.; Lichter, W.; Dudeck, L. E.; Gargus, J. L.; Lucas, A. H. *Food-Drugs Sea Proc.* **1970**, *1969*, 281.

(11)   Rudi, A.; Goldberg, I.; Stein, Z.; Frolow, F.; Benayuhu, Y.; Schleyer, M.; Kashman, Y. *J. Org. Chem.* **1994**, *59*, 999.

(12)   Terpin, A.; Polborn, K.; Steglich, W. *Tetrahedron* **1995**, *51*, 9941.

(13)   Frode, R.; Hinze, C.; Josten, I.; Schmidt, B.; Steffan, R.; Steglich, W. *Tetrahedron Lett.* **1994**, *35*, 1689.

(14)   Vervoort, H. C.; RichardsGross, S. E.; Fenical, W.; Lee, A. Y.; Clardy, J. *J. Org. Chem.* **1997**, *62*, 1486-1490.

(15)   Schupp, P.; Eder, C.; Proksch, V.; Wray, B.; Schneider, B.; Herderich, M.; Paul, V. *J. Nat. Prod.* **1999**, *62*, 959.

(16)   Photograph taken by Rosana Moreira da Rocha: Departamento de Zoologia, Setor de Ciencias Biologicas, Universidade Federal do Parana, Curitiba, Parana, Brazil.

(17)   Furusaki, A.; Hashida, T.; Matsumoto, T. *J. Chem. Soc. Chem. Commun.* **1978**, 800.

(18)   Steglich, W.; Steffan, R.; Kopanski, L.; Eckhardt, G. *Angew. Chem. Int. Ed. Engl.* **1980**, *19*, 459.

(19) Neel, D. A.; Jirousek, M. R.; McDonald III, J. H. *Bioorg. Med. Chem. Lett.* **1998**, *8*, 47.

(20) Omura, S.; Iwai, Y.; Nakayawa, A.; Awaya, J.; Tsuchiya, T.; Takahashi, Y.; Masuma, R. *J. Antibiot.* **1977**, *30*, 275.

(21) Nettleton, D. E.; Doyle, T. W.; Krishnan, B.; Matsumoto, G. K.; Clardy, J. *Tetrahedron Lett.* **1985**, *26*, 4011.

(22) Brenner, M.; Rexhausen, H.; Steffan, B.; Steglich, W. *Tetrahedron* **1988**, *44*, 2887-2892.

(23) Ohkubo, M.; Nishimura, T.; Jona, H.; MHonma, T.; Ito, S.; Morishima, H. *Tetrahedron* **1997**, *53*, 5937.

(24) Link, J. T.; Raghaven, S.; Gallant, M.; Danishefsky, S. J.; Chou, T. C.; Ballas, L. M. *J. Am. Chem. Soc.* **1996**, *118*, 2825.

(25) Gallant, M.; Link, J. T.; Danishefsky, S. J. *J. Org. Chem.* **1993**, *58*, 343.

(26) Terpin, A.; Winklhofer, C.; Schumann, S.; Steglich, W. *Tetrahedron* **1998**, *54*, 1745.

(27) McCort, G.; Duclos, O.; Cadilhac, C.; Guilpain, E. *Tetrahedron Lett.* **1999**, *40*, 6211.

(28) Smith, P.; Friar, J. J.; Resemann, W.; Watson, A. C. *J. Org. Chem.* **1990**, *55*, 3351.

(29) Davis, P. D.; Bit, R. A. *Tetrahedron Lett.* **1990**, *31*, 5201.

(30) Davis, P. D.; Bit, R. A.; Hurst, S. A. *Tetrahedron Lett.* **1990**, *31*, 2353.

(31) Bergman, J.; Pelcman, B. *Tetrahedron Lett.* **1987**, *28*, 4441.

(32) Rooney, C. S.; Randall, W. C.; Streeter, K. B.; Ziegler, C.; Cragoe Jr., E. J.; Schwam, H.; Michelson, S. R.; Williams, H. W. R.; Eichler, E.; Duggan, D. E.; Ulm, E. H.; Noll, R. M. *J. Med. Chem.* **1983**, *26*, 700.

(33) After the work reported herein had been completed and accepted for publication, a paper describing condensations similar to those disclosed in this work was published: Faul, M. M.; Wineneroski, L. L.; Krumrich, C. A. *J. Org. Chem.* **1998**, *63*, 6053.

(34) Faul, M. M.; Winneroski, L. L.; Krumrich, C. A. *J. Org. Chem.* **1998**, *63*, 6053.

(35) Smakula, A. *Z. Phys. Chem.* **1934**, *B25*, 90.

(36) Buckles, R. E. *J. Am. Chem. Soc.* **1955**, *77*, 1040.

(37) Gilbert, A. In *CRC Handbook of Photochemistry and Photobiology*; Harspool, W. M., Ed.; CRC Press: New York, 1995; p 513.

(38) Muszkat, K. A. *Top. Curr. Chem.* **1980**, *88*, 89.

(39)   Cava, M. P.; Edie, D. L.; Saa, J. M. *J. Org. Chem.* **1975**, *40*, 3601.

(40)   Iddon, B.; Ngochindo, R. I. *Heterocycles* **1994**, *38*, 2487.

(41)   Katritzky, A. R.; Slawinski, J. J.; Brunner, F. *J. chem. Soc. Perkin Trans. I* **1989**, 1139.

(42)   Chadwick, D. J.; Hodgson, S. T. *J. Chem. Soc. Perkin Trans. I* **1982**, 1833.

(43)   Lipshutz, B. H.; Vaccaro, W.; Huff, B. *Tetrahedron Lett.* **1986**, *27*, 4095.

(44)   Tang, C. C.; Davalian, D.; Huang, P.; Breslow, R. *J. Am. Chem. Soc.* **1978**, *100*, 3918.

(45)   Chadwick, D. J.; Ngochindo, R. I. *J. Chem. Soc. Perkin Trans. I* **1984**, 481.

(46)   Kirk, K. L. *J. Org. Chem.* **1978**, *43*, 4381.

(47)   Achab, S.; Guyot, M.; Potier, P. *J. Am. Chem. Soc.* **1978**, *100*, 3918.

(48)   Ohta, S.; Yamamoto, T.; Kawasaki, I.; Yamashita, M.; Katsuma, H.; Nasako, R.; Kobayashi, K.; Ogawa, K. *Chem. Pharm. Bull.* **1992**, *40*, 2681.

(49)   Lipshutz, B. H.; Huff, B.; Hagan, W. *Tetrahedron Lett.* **1988**, *29*, 3411.

(50)   Philips, B. T.; Claremon, D. A.; Varga, S. L. *Synthesis* **1990**, 761.

(51)   Rawal, V. H.; Jones, R. J.; Cava, M. P. *Tetrahedron Lett.* **1985**, *26*, 2423.

(52)   Brieger, G.; Nestrick, T. *J. Chem. Rev.* **1974**, *74*, 567.

(53)   Ireland, R. E.; Varney, M. D.; *J. Org. Chem.* **1986**, *51*, 635.

(54)   Sundberg, R. J.; Mente, D. C.; Yilmaz, I.; Gupta, G. J. *J. Heterocycl. Chem.* **1977**, *14*, 1279.

(55)   Hashimoto, N.; Aoyama, T.; Shioiri, T. *Chem. Pharm. Bull.* **1981**, *29*, 1475.

(56)   For a mechanistic analysis of a similar photocyclization see: Blache, Y.; Sinibaldi-Troin, M.-E.; Hichour, M.; Benezech, V.; Chavignon, O.; Gramain, J.-C.; Teulade, J.-C.; Chapat, J.-P. *Tetrahedron,* **1999**, *55*, 1959 (and references cited therein).

(57)   Rawal, V. H.; Cava, M. P. *Tetrahedron Lett.* **1985**, *26*, 6141.

(58)   Ohta, S.; Hayakawa, S.; Moriwaki, H.; Tsuboi, S.; Okamoto, M. *Heterocycles* **1985**, *23*, 1759.

(59)   Roe, A. M. *J. Chem. Soc.* **1963**, 2195.

(60)   Faul, M. M.; Winneroski, L. L.; Krumrich, C. A. *Tetrahedron Lett.* **1999**, *40*, 1109.

(61) Berlinck, R. G. S.; Britton, R.; Piers, E.; Lim, L.; Roberge, M.; da Rocha, R. M.; Andersen, R. J. *J. Org. Chem.* **1998**, *63*, 9850.

(62) Roberge, M.; Berlinck, R. G. S.; Xu, L.; Anderson, H.; Lim, L.; Curman, D.; Stringer, C. M.; Friend, S. H.; Davies, P.; Vincent, I.; Haggarty, S. J.; Kelly, M. T.; Britton, R.; Piers, E.; Andersen, R. J. *Cancer Res.* **1998**, *58*, 5701.

(63) For a similar study on the marine sponge alkaloid debromohymenialdisine see: Curman, D.; Cinel, B.; Williams, D. E.; Rundle, N.; Block, W. D.; Goodarzi, A. A.; Hutchins, J. R.; Clarke, R. P.; Zhou, B.-B.; Lees-Miller, S. P.; Andersen, R. J.; Roberge, M. *J. Biol. Chem.* **2001**, *276*, 21, 17914.

(64) Curman, D., M. Sc. Thesis, Department of Biochemistry and Molecular Biology, University of British Columbia, Vancouver, B.C., **1999**.

(65) Britton, R.; de Oliveira, J. H. H. L.; Andersen, R. J.; Berlinck, R. G. S. *J. Nat. Prod.* **2001**, *64*, 254.

(66) Piers, E.; Britton, R.; Andersen, R. J. *J. Org. Chem.* **2000**, *65*, 530.

(67) The ^{1}H and ^{13}C NMR signals shift depending on the concentration of the NMR sample. Thus, for consistency, the ^{1}H NMR spectrum was acquired at a concentration of 1 mg/mL and the ^{13}C NMR spectrum was acquired at a concentration of 5 mg/mL.

(68) The literature melting point is that reported in the Aldrich Handbook of Fine Chemicals and Laboratory Equipment, 2000-2001, page 1126.

(69) 1-*tert*-Butoxycarbonyl-Isogranulatimide B (**100**) was insufficiently soluble in DMSO-d_6, or other standard NMR solvents, for complete spectroscopic characterization.

4. Isolation, Structure Determination and Synthetic Transformations of Antimitotic Diterpenes from *Erythropodium Caribaeorum*

4.1 Introduction

Sessile marine invertebrates rely on a spectacular array of secondary metabolites to thwart predators and competitors for desirable living space. The investigation of chemicals produced by these invertebrates has demonstrated that they are a particularly rich source of structurally unique and biologically active compounds. In fact, the diversity in both structure and biological function of marine natural products rivals that of those produced by terrestrial organisms.[1] In particular, members of the marine phylum Coelenterata continue to yield a wealth of novel diterpenoids.[2]

The phylum Coelenterata, also known as Cnidaria, includes the jellyfish, hydras, sea anemones, and corals.[3] While these invertebrates are quite distinct, similarities within this phylum include a single opening for ingestion and expulsion of food, radial symmetry, and tentacles armed with stinging nematocysts for both defense and the capture of prey. The anthozoans represent the largest and most diverse class within the phylum Coelenterata and, based on the presence of six or eight unbranched tentacles, are classified as Hexacorallia or Octacorallia, respectively. The colonial Octacorallia, or octacorals, are in turn divided into four primary groups; namely the stoliniferans, the alcyonaceans, the penatulaceans, and the gorgonians.

Gorgonians are particularly abundant in tropical and subtropical waters and have been found in densities as high as 25 colonies per square meter on some Caribbean reefs.[4] It is noteworthy, however, that while these organisms may represent close to 40% of the fauna in

certain locales, only a few species of reef predators are known to prey upon them.[5] Thus, the predator deterrent and potential cytotoxic nature of the secondary metabolites produced by gorgonians has fueled a long-standing interest in the isolation and structure determination of these substances.

The study of gorgonian natural products was initiated in 1950, when Burkholder and co-workers documented the occurrence of antibiotic substances in gorgonian corals collected off the coast of Puerto Rico.[6] Since then, the prolificity with which these organisms produce diterpenoids has been well documented. In fact, it has recently been reported that approximately 75% of the secondary metabolites isolated from West Indian gorgonians are diterpenoid in origin.[2] Moreover, almost one third of these diterpenes were shown to possess a cembranoid carbon skeleton. This is not surprising, as cembranoids, such as crassin acetate (1) isolated from the gorgonian *Eunicea calyculata*,[7] are the simplest cyclic diterpenes and further serve as intermediates in the biosynthesis of various polycyclic diterpenoids (Figure 4.1). Thus, through subsequent transannular cyclization events, the cembranoids provide access to more complex carbocyclic skeletons, including those of the eunicellin and briarane diterpenoids.

The first example of a compound bearing the eunicellin skeleton was reported in 1968, when eunicellin (2) was isolated from the gorgonian *Eunicella stricta*.[8] While less than 3% of the diterpenoids considered in the survey of West Indian gorgonian secondary metabolites possessed this carbon skeleton,[6] the biological activity attributed to certain eunicellanes has attracted considerable interest to this relatively small family of natural products.[9] Alternatively, the discovery of numerous briarane diterpenes as soft-coral metabolites attests to their ecological significance.[2] Fenical and co-workers have reported the isolation of the structurally unique substance erythrolide B (3) from the Caribbean gorgonian *Erythropodium caribaeorum*.[10] Subsequently, these researchers disclosed that 3 plays an important role as a feeding deterrent, protecting *E. caribaeorum* from a variety of predatory reef fish.[5,11]
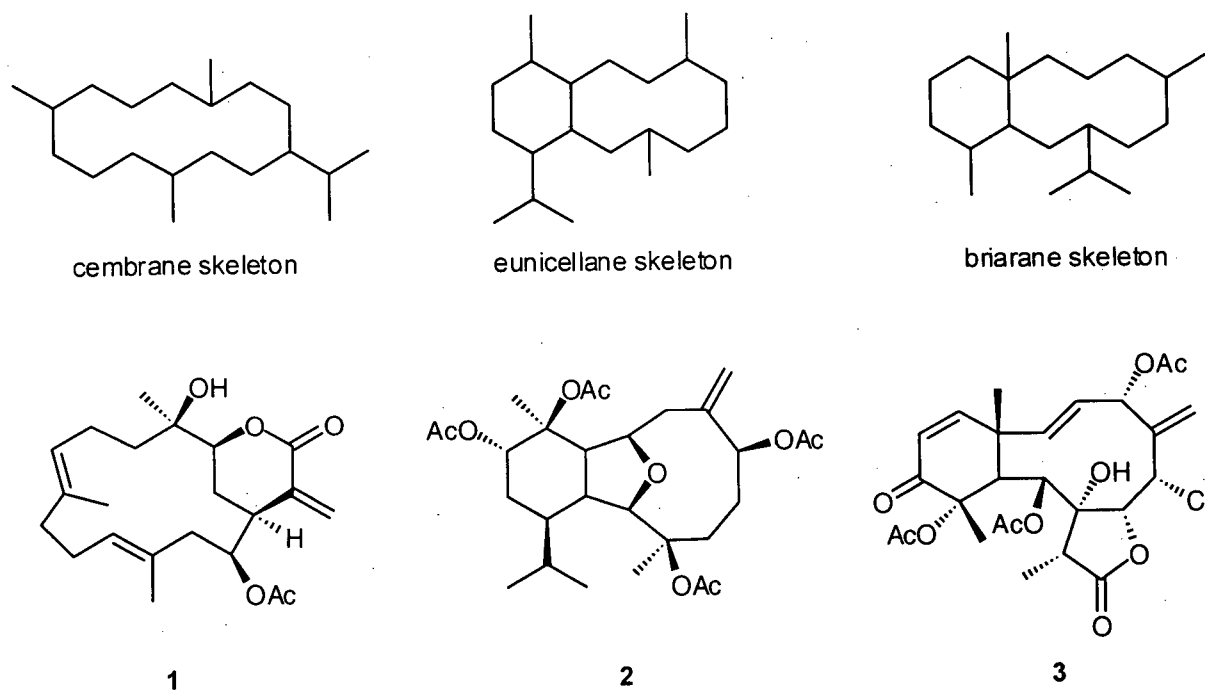
Figure 4.1. Typical carbon skeletons of gorgonian diterpenes.

Recently, a new family of eunicellane diterpenes, namely the sarcodictyins (i.e. **4** and **5**, Figure 4.2), was reported by Peitra and co-workers from the Mediterranean stoliniferan coral *Sarcodictyon roseum*.[12,13] The methyl ester, sarcodictyin A (**4**) has also been isolated, along with the structurally related eunicellanes, eleuthosides A (**6**) and B (**7**), from the South African soft-coral *Eleutherobia aurea* by two separate groups (Figure 4.2).[14,15] While no biological activity was attributed to these compounds, a patent issued in December of 1995 disclosed the potent cyctotoxic activity of the closely related diterpene eleutherobin (**8**).[16] Motivated by a unique biological activity profile imputed to eleutherobin (**8**) in a subsequent report by Fenical and co-workers,[17] considerable interest has been generated for the isolation and total synthesis of both the sarcodictyins and eleuthosides.

4 (R = Me) Sarcodictyin A
5 (R = Et) Sarcodictyin B

6 R₁ = H, R₂ = R₃ = Ac, R₄ = H
7 R₁ = H, R₂ = Ac, R₃ = H, R₄ =Ac
8 R₁ = Me, R₂ = Ac, R₃ = R₄ = H
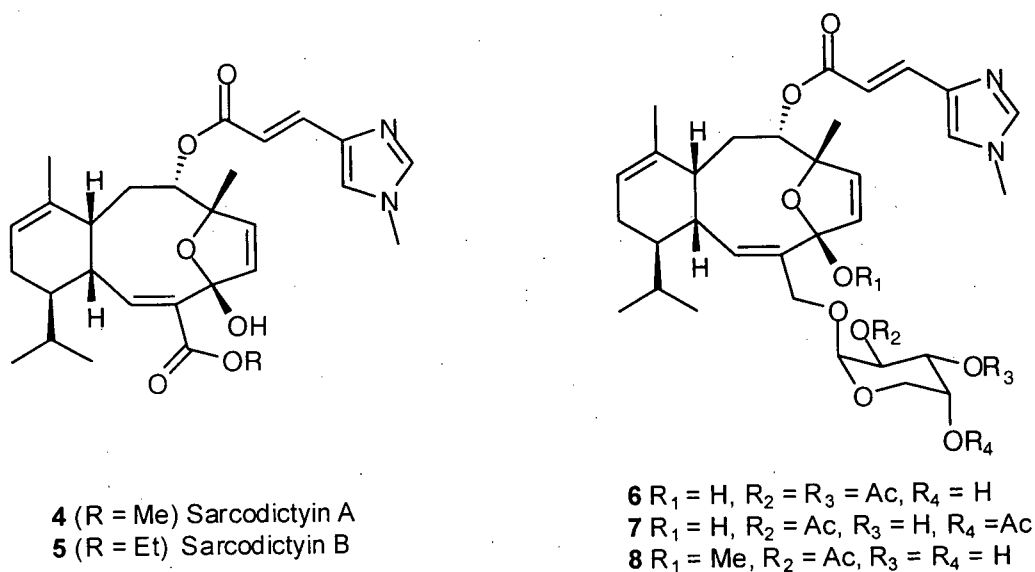
Figure 4.2. Antimitotic eunicellanes.

4.1.2 Eleutherobin: isolation, biological activity and total synthesis

With the clinical success of the antimitotic agent taxol (9) (Figure 4.3) against ovarian and breast cancer well established,[18] the search for new cytotoxins that target mitosis, or cell division, has become an important pursuit for natural product chemists. Considering the anticancer potential of such substances, it is not surprising that the original disclosure regarding the structure elucidation and biological activity of eleutherobin (8) came in the form of a patent application, filed in November of 1994.[19] Eleutherobin (8), isolated from a rare *Eleutherobia sp.* soft-coral collected off Bennett's Shoal in Western Australia, was shown to be a potent cytotoxic agent with an *in vitro* IC$_{50}$ range of 10 - 15 nM against a panel of cancer cell lines.[17] Moreover, when the cellular mechanism by which 8 operates was investigated, it was discovered that eleutherobin (8) is in fact an antimitotic agent, affecting cell division in the same manner as taxol (9).[20] Namely, eleutherobin (8) inhibits mitosis by interacting with the taxol binding site on

tubulin, thus stabilizing microtubules, an action that ultimately leads to cell death. Furthermore, in studies carried out at the US National Cancer Institute, eleutherobin (**8**) displayed an approximate 100-fold increase in potency, when compared to mean toxicity, towards breast, renal, ovarian and lung cancer cell lines.[17] At the time of this discovery, eleutherobin (**8**) and taxol (**9**) were the only compounds known to stabilize microtubules. However, in the years preceding publication of these results in the chemical literature, both discodermolide (**10**)[21] and epothilone A (**11**)[22] (Figure 4.3) were also reported to posses similar microtubule stabilizing properties. Additionally, the antimitotic properties of the sarcodictyins (i.e. **4**, Figure 4.2) were investigated and it was found that these compounds also inhibit mitosis at nM concentrations.[23]
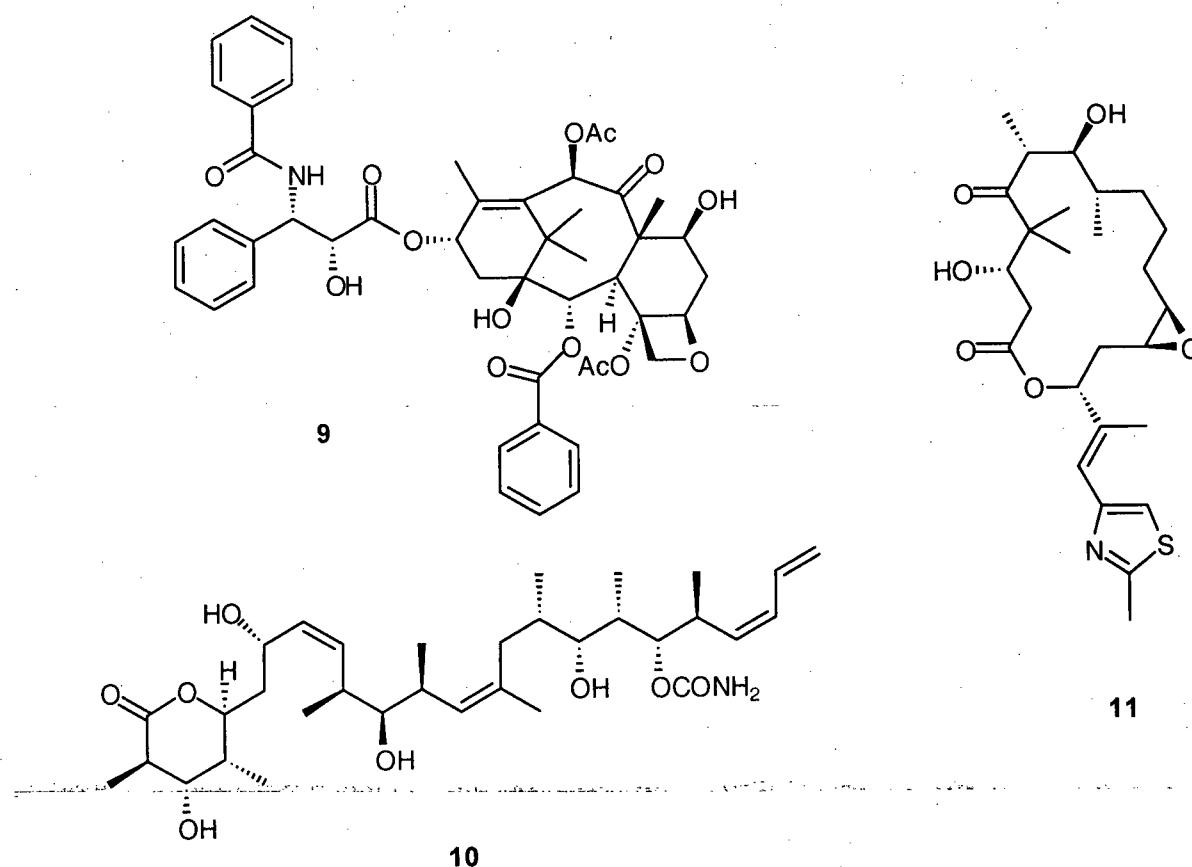
Figure 4.3. Microtubule stabilizing antimitotic agents.

Unfortunately, while eleutherobin (**8**) possessed obvious potential as an anticancer drug lead, the lack of material generated through the isolation of this substance from the *Eleutherobia sp.* soft-coral thwarted its progress into preclinical trials.[24] Further complicating matters, the Australian government banned foreign scientists from collecting marine invertebrates in their coastal waters. Thus, the development of eleutherobin (**8**) as a chemotherapeutic agent would clearly rely on the generation of a renewable source of this substance.

Shortly following the disclosure regarding the antimitotic activity of eleutherobin (**8**), two separate total syntheses of this compound were reported.[25-29] The key step in a synthesis of **8** by Nicolaou and co-workers involved generation of the acetylide anion of **12** and a subsequent intramolecular addition of this reactive function onto the aldehyde carbonyl (Scheme 4.1).[27] Deprotection of the tertiary alcohol in **13** was followed by the hydrogenation of the alkyne function in the resultant eneyneone **14** over Lindlar's catalyst. Generation of the *cis* olefin in this manner led directly to the formation of the hemiketal **16**, thus furnishing the eleuthoside skeleton. Further manipulations included a second chemoselective deprotection event and subsequent treatment of the alcohol **17** with the mixed anhydride **18**, to furnish the eleuthoside **19**. The eventual transformation of the latter substance into eleutherobin (**8**), and comparison of the spectroscopic and physical data recorded for both the natural and synthetic material, confirmed the relative stereochemical relationship between the appended glycon and the diterpenoid core. Following a similar sequence of events, treatment of the enal **20** with LiHMDS provided the bicyclo[4.8.0]tetradecane **21**, which proved to be a key intermediate in the synthesis of sarcodictyin A (**4**).[25]
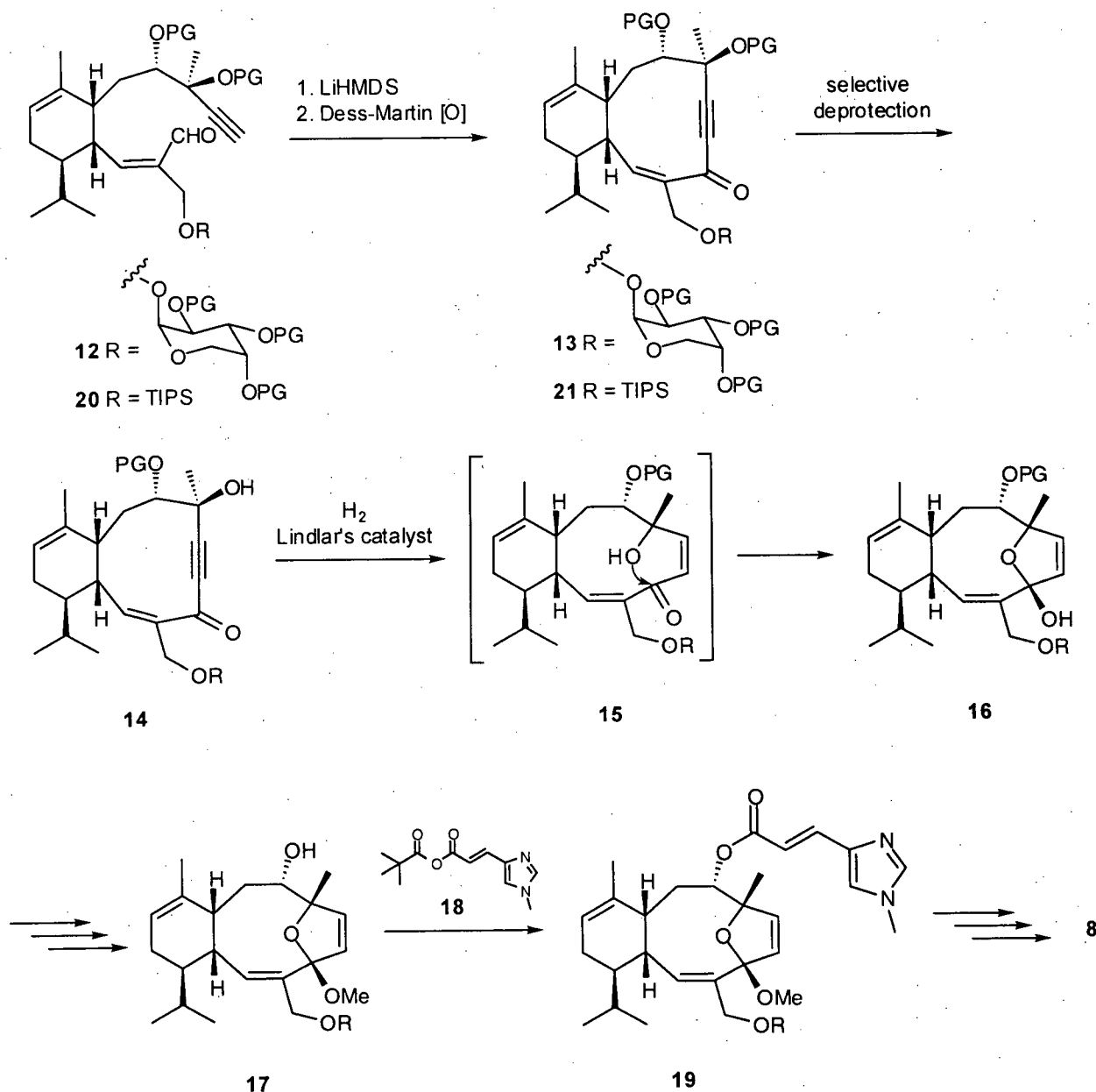
Scheme 4.1. Key transformations in Nicolaou's synthesis of eleutherobin (**8**) (PG = suitable protecting groups).

Danishefsky and co-workers have disclosed an alternative approach to this molecule.[29] The key step in their synthesis of **8** involved a $CrCl_2$-$NiCl_2$ mediated (Nozaki-Kishi) reductive cyclization of the bromoaldehyde **22** (eq. 1). While both total syntheses of eleutherobin (**8**) provided milligram amounts of this substance, these quantities were insufficient to facilitate thorough preclinical studies. Furthermore, the syntheses of **8** by Nicolaou and Danishefsky

required the application of 35 and 25 consecutive transformations, respectively, affording

eleutherobin (8) in under 1% overall yield. Consequently, the failure to provide a viable source

of eleutherobin (8) resulted in the relinquishment of all rights to this material by the

pharmaceutical firm that had licensed the original patent for eleutherobin (8).[24]

$$CrCl_2, NiCl_2$$
$$DMF$$

(1)

22   **23**

While unable to procure a supply of eleutherobin (8) sufficient to warrant its preclinical

evaluation, both total syntheses of 8 were amenable to modifications, such that a library of

congeners of this substance could be generated. In this manner, the effect of structure on the

biological activity of both the sarcodictyins and the eleuthosides was evaluated. From these

studies, a number of significant correlations were established. Nicolaou and co-workers

demonstrated that the N-methylurocanic ester appendage at C-8 plays a crucial role in the

biological activity of these compounds.[30] Additionally, these researchers found that various ketal

substitutions at C-4 of sarcodictyin A (4) were well tolerated and that the interconversion of

aliphatic and aromatic esters at C-15 had little effect on the *in vitro* antimitotic activity of these

substances (Figure 4.4).[30] With regard to the diterpenoid core of sarcodictyin A (4), the

importance of the $\Delta^{5,6}$ olefin was evaluated through the synthesis of the 5,6-dihydrosarcodictyin

A derivative 24, which was found to retain the antimitotic activity of the parent compound. It is

noteworthy that the alcohol 25, which resulted from reduction of the C-15 ester functionality in

sarcodictyin A (4), was completely inactive in tubulin polymerization assays.

4 (240 nM)   24 (45 nM)   25 (inactive)

Figure 4.4. Sarcodictyin A (**4**) and structural analogues generated for biological evaluation. Concentrations in parentheses indicate the IC_{50} values for these compounds when screened against 1A9 ovarian cancer cells.

Likewise, Danishefsky and co-workers have demonstrated that the C-8 N-methylurocanic ester function in eleutherobin (**8**) plays a crucial role in determining its cytotoxic activity.[31] Thus, the desurocanate analogue **26** was found to be inactive in a series of cell-based assays for cytotoxins (Figure 4.5). Interestingly, both neoeleutherobin (**27**), in which the arabinose unit possesses the opposite absolute stereochemistry to that found in eleutherobin (**8**), and the C-15 acetate **28**, demonstrated activity in the range of 100 - 200 nM, only an order of magnitude less than that reported for **8**. Additionally, the sarcodictyin A (**4**) analogue **29**, in which the C-15 ester function is replaced by a proton, was also found to be active at nM concentrations.

In the hope of generating a detailed understanding of the structural requirements for antimitotic activity and thus provide a venue for the rational design of new antimitotic drugs, a number of pharmacophore models have evolved from these studies.[32-34] Unfortunately, the inability to establish a concrete relationship between biological activity and salient structural features of the eleuthoside diterpenoid core has stalled the progression of these models. In fact, only through comparison of computer generated conformational models of eleutherobin (**8**) to those of the other antimitotic agents (e.g. taxol (**9**)), was a set of structural parameters required

for eleuthoside antimitotic activity proposed.[33] Thus, the accuracy of these pharmacophore models remains to be rigorously evaluated.
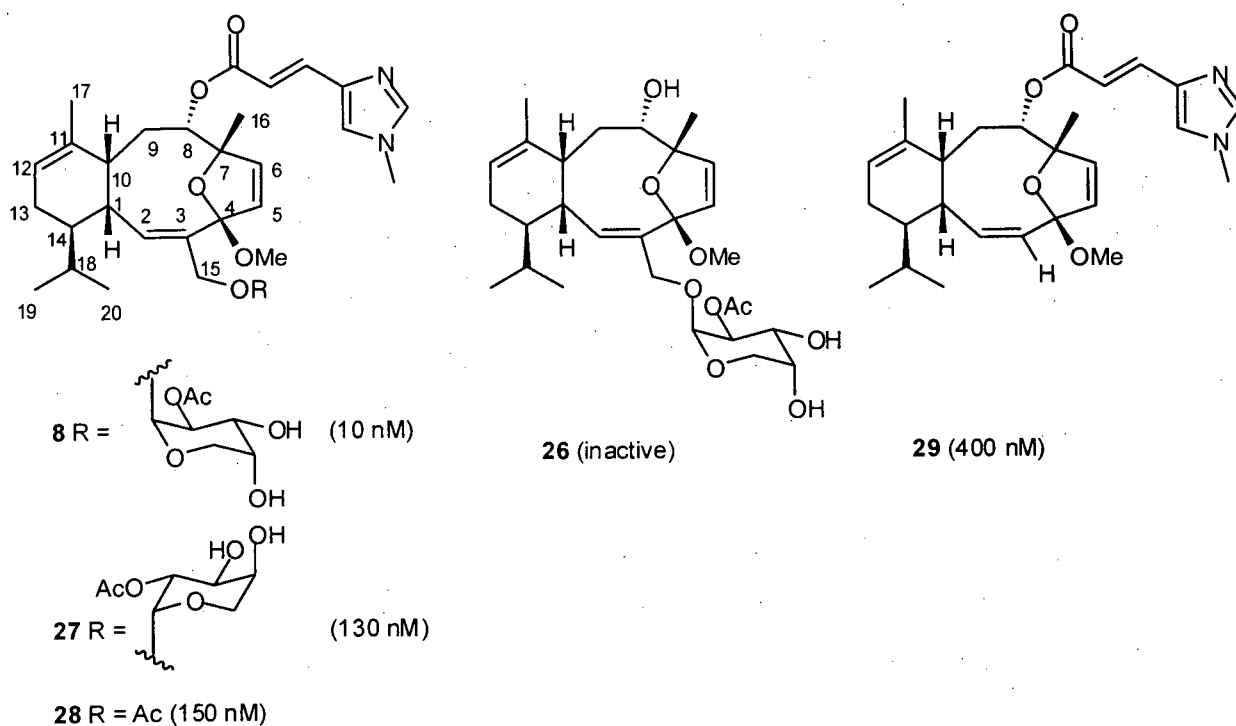
Figure 4.5. Eleutherobin (**8**) and structural analogues generated for biological evaluation. Concentrations in parentheses indicate the IC_{50} values for these compounds when screened against A549 lung cancer cells.

Recently, members of our research group have reported that the relatively abundant Caribbean gorgonian *Erythropodium caribaeorum* is a good source of eleutherobin (**8**) and a number of analogues of this substance.[35,36] Through the isolation of a new series of eleuthosides, namely caribaeoside (**30**), Z-eleutherobin (**31**), and desmethyleleutherobin (**32**) (Figure 4.6), the predictive power of the pharmacophore models was assessed.[35] Additionally, both the solid state and solution conformations of **8**, obtained from X-ray diffraction analysis and solution NOE data, provided further refinements for these models.[37] From a practical perspective, owing to the relative abundance of gorgonian *E. caribaeorum*, this organism might potentially provide

adequate quantities of eleutherobin (**8**) for preclinical evaluation and possibly clinical trials should this compound progress that far.

8 R$_1$ = Me, R$_2$ = Ac, R$_3$ = R$_4$ = H (30 nM)
32 R$_1$ = H, R$_2$ = Ac, R$_3$ = R$_4$ = H (20 nM)

30 (20,000 nM)

31 (250 nM)
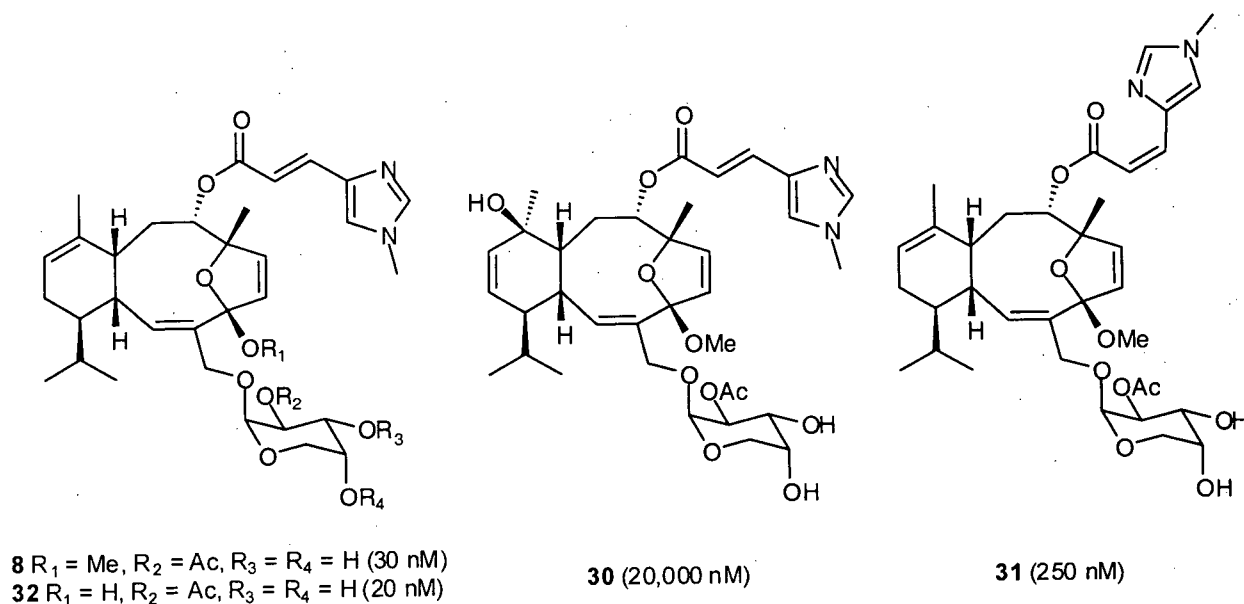
Figure 4.6. Eleutherobin (**8**) and structural analogues isolated from *E. caribaeorum*. Concentrations in parentheses indicate the IC$_{50}$ values for these compounds when screened against MCF-7 breast cancer cells.

While the isolation of eleutherobin (**8**) from *E. caribaeorum* for preclinical studies is well warranted, it was our contention that synthetic transformations involving the diterpenoid core of this substance would further the development of the eleuthosides as potential cancer chemotherapeutics. In this manner, a concrete relationship between structure and antimitotic activity in this series of compounds would be established. Furthermore, the predictive power of the eleuthoside pharmacophore models could be accurately assessed or refined, thus facilitating the generation of structurally simplified antimitotic substances, more amenable to total synthesis than **8**. In this regard, a project involving the isolation of eleutherobin (**8**) from *E. caribaeorum* in quantities sufficient to explore this avenue of studies was initiated. The results gathered from this pursuit are presented in the following sections.

4.2 The isolation and structure determination of antimitotic diterpenes from *Erythropodium caribaeorum*

The octacoral *E. caribaeorum* (Figure 4.7) is unique among gorgonians in that rather than developing in a typical upright fashion, it grows over substrates as an encrusting sheet.[5] By virtue of this unusual growth pattern, *E. caribaeorum* may persist on unstable terrain and is thus a dominant component of the gorgonian fauna in many Caribbean locations. Samples of *E. caribaeorum* (total 6 kg) were collected by hand using SCUBA at depths of 3-5 meters off Prince Rupert Point, Dominica in September of 2000 (Figure 4.8). The samples were frozen and subsequently transported to the University of British Columbia, where they were immediately immersed in MeOH. Concentration of the organic extract and partitioning of the resulting residue as described in the Experimental section, yielded a brown gum which was fractionated by normal phase silica gel flash chromatography. In this manner, the major secondary metabolites produced by this organism, namely the erythrolides[10] (i.e. erythrolide B (**3**), Figure 4.1), were separated from the fractions containing the sarcodictyin and eleuthoside diterpenes.
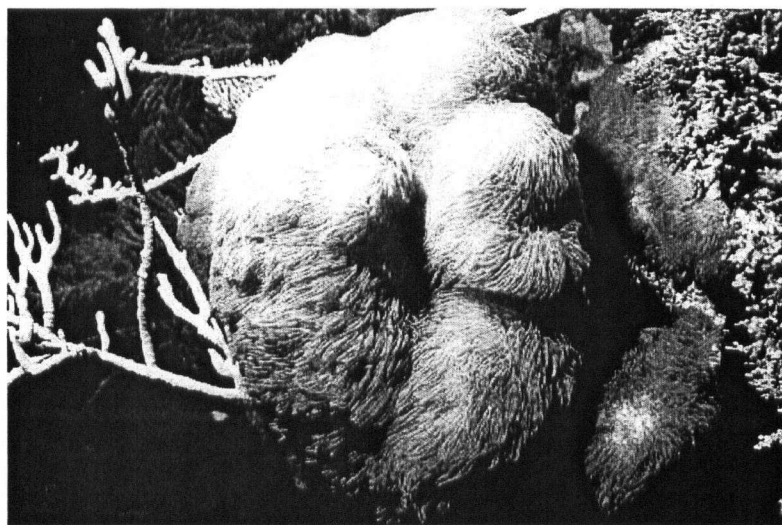
Figure 4.7. Photograph of *Erythropodium caribaeorum.*[38]
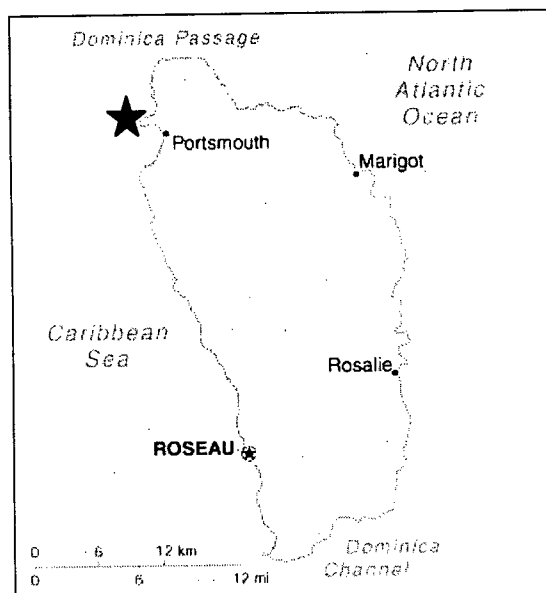
Figure 4.8. Map of collection site (★) for *Erythropodium caribaeorum.*

During the course of routine ¹H NMR spectroscopic analysis of the non-polar sarcodictyin containing fractions, two substances that displayed resonances in their ¹H NMR spectra atypical for sarcodictyins were discovered. Further purification of these compounds by flash chromatography and normal phase HPLC provided the eleutherobin aglycon **34** and methylcaribaeorane (**35**) (Figure 4.9). The structural assignment of these novel diterpenoids was confirmed through analysis of their spectroscopic data (*vide infra*). Additionally, purification of the eleuthoside containing fractions yielded 50 mg of eleutherobin (**8**), 40 mg of desmethyleleutherobin (**32**) and 7 mg of Z-eleutherobin (**31**). The spectral data exhibited by the eleuthosides were in complete agreement with that reported in the literature for these substances.[17,35]
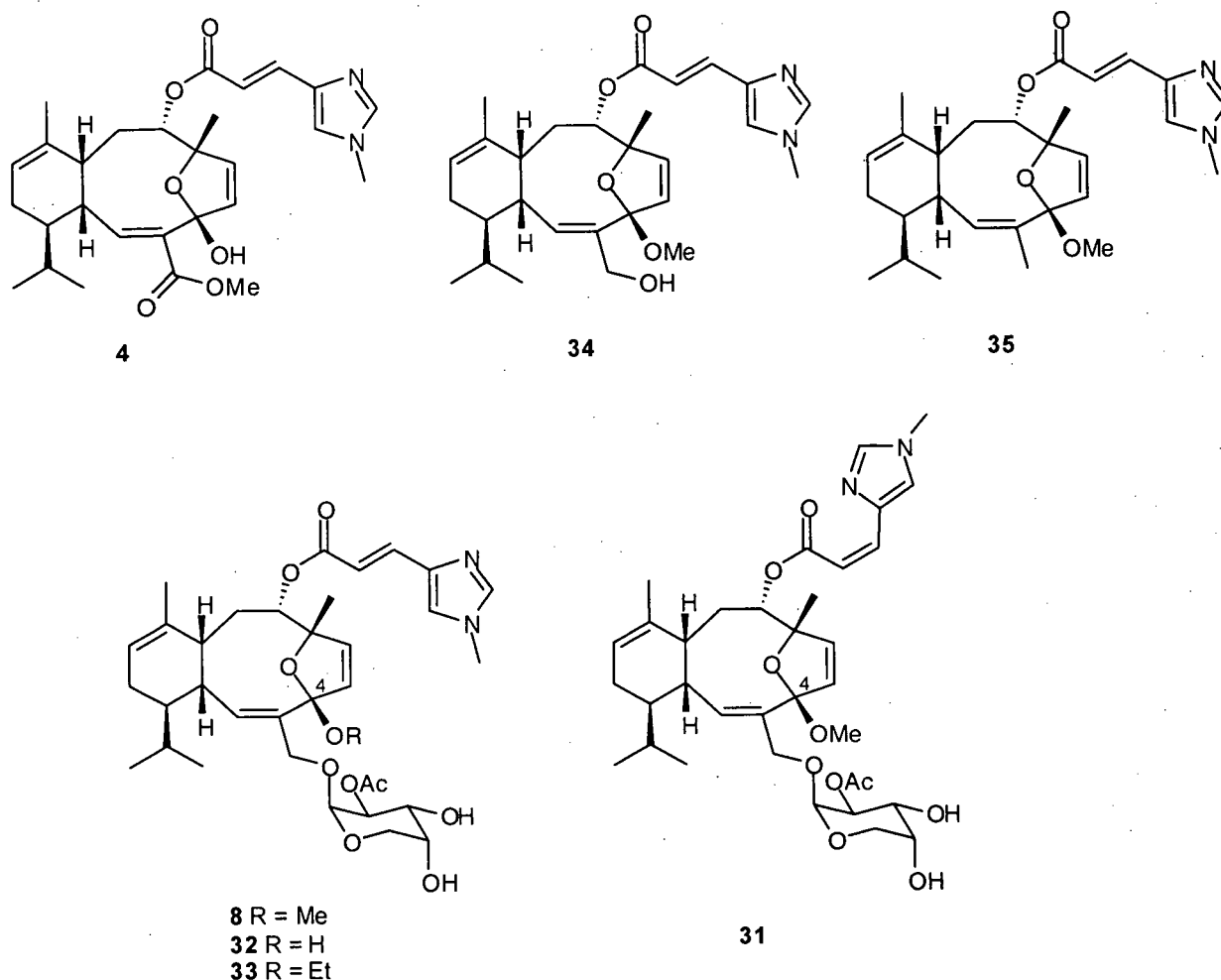
Figure 4.9. Antimitotic diterpenes isolated from *Erythropodium caribaeorum.*

It is noteworthy that comparison of the isolated yields of eleutherobin (**8**) and desmethyleleutherobin (**32**) obtained from the initial collections of *E. caribaeorum* examined by our laboratory[35] and that disclosed above, indicated the ratio of these materials was highly variable. Kashman and co-workers have reported the isolation of C-4 hemiketal eleuthosides (i.e. **6** and **7**, Figure 4.2) from *Eleutherobia aurea* by extraction of this organism with non-alcohol solvents such as EtOAc.[14] These observations fueled a hypothesis that eleutherobin (**8**) was actually an artifact, resulting from ketalization of desmethyleleutherobin (**32**) during the isolation procedure. This proposal gained further support from the fact that Fenical and co-workers also

employed a methanolic extraction in their isolation of eleutherobin (**8**) from the soft-coral

Eleutherobia sp.[17] To resolve this issue, a fresh sample of *E. caribaeorum* was extracted with

EtOH. Not surprisingly, this extract yielded the C-4 ethyl ketal of eleutherobin **33** along with

sarcodictyin A (**4**) and desmethyleleutherobin (**32**) (Figure 4.9). Furthermore, eleutherobin (**8**)

was not detected by analytical HPLC or ^{1}H NMR analysis of the chromatography fractions

generated from this extract. These results indicate that the C-4 methyl ketal in eleutherobin (**8**)

and likely that in the corresponding analogues of this substance isolated from *E. caribaeorum*,

are indeed artifacts of the hemiketal natural products, generated during the methanolic extraction

procedure. The spectroscopic data exhibited by the ethyl ketal of eleutherobin **33**, was consistent

with the structure assigned for this material. The ^{1}H NMR spectrum of **33** included a 2-proton

multiplet at δ 3.44 that corresponded to the diastereotopic methylene protons of the ethyl ketal

function. Additionally, the diagnostic 3-proton methyl ketal singlet at δ 3.22 in the ^{1}H NMR

spectrum of **8**,[17] was noticeably absent in that of **33**. The ^{13}C NMR spectrum of **33** displayed

resonances at δ 57.7 and 15.5 for the methylene and methyl carbons, respectively, of the ethyl

ketal function. Aside from these discrepancies, however, the ^{1}H and ^{13}C NMR spectra of **8** and

33 were very similar. Furthermore, high resolution mass spectrometric analysis of **33** confirmed

the molecular formula of this substance.

4.2.1 Isolation of the eleutherobin aglycon 34
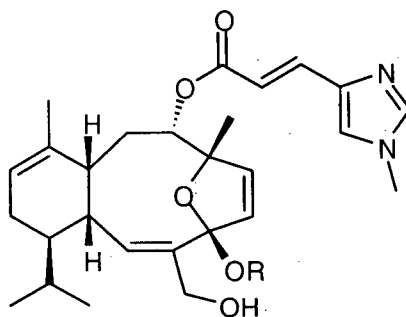
34 R = OMe
36 R = OH

The eleutherobin aglycon **34** was detected as a minor component of the non-polar, sarcodictyin containing fractions that were eluted from silica gel with CH_2Cl_2 - MeOH (95:5). Further purification of this material by normal phase flash chromatography, eluting with EtOAc - MeOH (97:3), provided **34** as a colorless solid. Although this substance was not known as a natural product, the eleutherobin aglycon **34** has previously been reported as an intermediate in the total synthesis of eleutherobin (**8**).[25] Comparison of the spectral data collected for the material isolated from *E. caribaeorum* (see Table 4.1 and Experimental section) with that in the literature for the synthetic material confirmed that these compounds were indeed identical. Additionally, when assayed against MCF-7 breast cancer cells, the eleutherobin aglycon **34** was inactive below concentrations of 1 μM.[39] The biological activity expressed by the natural product was in accordance with that reported by Danishefsky and co-workers for the synthetic eleutherobin algycon **34**, which displayed an IC_{50} value of 1 μM when screened against lung carcinoma cells.[31] The eleutherobin aglycon **34** is presumed to be an artifact formed from the corresponding hemiketal natural product 15-hydroxycaribaeorane (**36**) during the MeOH extraction of *E. caribaeorum.*

Table 4.1. Selected ^{1}H NMR spectral data for both natural and synthetic eleutherobin aglycon **34** (recorded in CDCl$_3$).
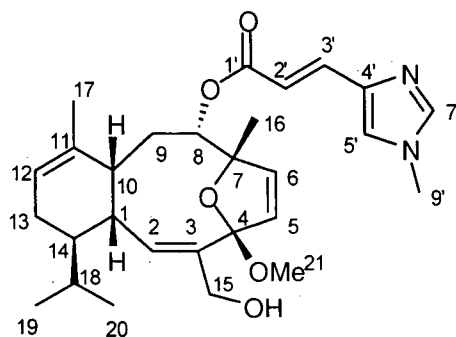
Carbon No.	Natural **34** ^{1}H δ (ppm) (mult., J (Hz))^a	Synthetic **34** ^{1}H δ (ppm) (mult., J (Hz))^b
5	6.02 (d, 6.0)	6.01 (d, 6.1)
6	6.21 (d, 6.0)	6.20 (d, 6.1)
8	4.80 (d, 7.4)	4.79 (d, 7.4)
12	5.25 (m)	5.24 (m)
15	4.16 (d, 12.0)	4.14 (d, 12.0)
	3.88 (d, 12.0)	3.88 (d, 12.0)
16	1.45 (s)	1.43 (s)
17	1.50 (s)	1.49 (s)
19	0.97 (d, 6.5)	0.96 (d, 6.5)
20	0.91 (d, 6.5)	0.90 (d, 6.5)
21	3.23 (s)	3.22 (s)
2'	6.54 (d, 15.4)	6.54 (d, 15.6)
3'	7.52 (d, 15.4)	7.51 (d, 15.6)
5'	7.08 (s)	7.08 (s)
7'	7.45 (s)	7.42 (s)
9'	3.69 (s)	3.68 (s)

^{a} Recorded at 400 MHz. ^{b} Recorded at 600 MHz.

Having demonstrated the ease with which methyl ketal formation occurs in the MeOH extraction medium, it seemed possible that the eleutherobin aglycon **34** was also an isolation artifact, formed by the hydrolysis or methanolysis of the glycosidic linkage in eleutherobin (**8**). Thus, an investigation geared towards resolving this issue was initiated. In this regard, it was found that desmethyleleutherobin (**32**) could be transformed into eleutherobin (**8**) in a near quantitative manner, through the treatment of the former substance with a catalytic amount of pyridinium p-toluenesulfonate (PPTS) in MeOH at room temperature (eq. 2).[25] The reverse

transformation, that is the conversion of **8** into **32**, was also effected by simply adding PPTS and H_2O to a solution of eleutherobin (**8**) in CH_2Cl_2. That neither of these transformations resulted in glycoside hydrolysis was clear from analysis of the ^1H NMR spectra recorded on the crude reaction products. Furthermore, employing conditions identical to those that convert **32** into **8**, sarcodictyin A (**4**) was smoothly transformed into the corresponding C-4 methyl ketal.[30]

The isolation of methylcaribaeorane (**35**), eleutherobin aglycon (**34**) and eleutherobin (**8**) from *E. caribaeorum* (Figure 4.9), indicates the MeOH extraction conditions are sufficiently acidic to promote the conversion of the eleuthoside C-4 hemiketal into a methyl ketal when there is a proton (i.e. **35**), hydroxyl (i.e. **34**) or glycosidic function (i.e. **8**) at C-15. Notably, the more forcing action of PPTS in MeOH or PPTS in H_2O readily interconvert all C-4 hemiketals and methylketals, including those of sarcodictyin A (**4**), yet is unable to effect glycoside hydrolysis or methanolysis in the eleuthosides. Taken together, it is apparent that the milder MeOH extraction conditions, in which the conversion of sarcodictyin A (**4**) into the corresponding methyl ketal does not occur, would be unable cleave the glycosidic linkage in eleutherobin (**8**). These data support the consideration of 15-hydroxycaribaeorane (**36**) as natural product.

(2)
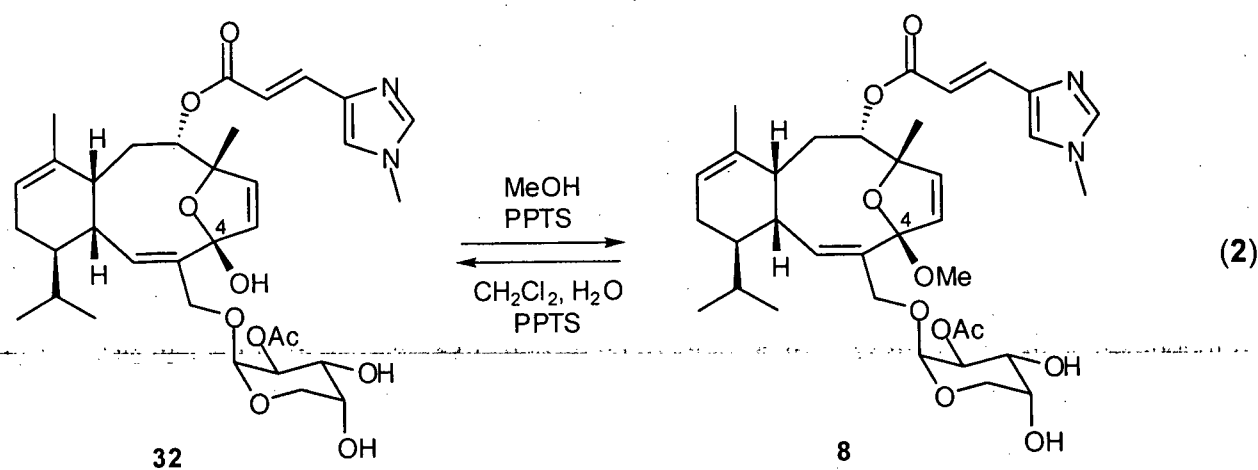
4.2.2 Isolation of methylcaribaeorane (35)

Methylcaribaeorane (**35**) was detected as a minor component of the non-polar, sarcodictyin containing fractions that were eluted from silica gel with CH_2Cl_2 - MeOH (95:5). Further purification of this material by normal phase flash chromatography using EtOAc - MeOH (97:3) provided **35** as a colorless solid. High resolution FAB mass spectrometric analysis of **35** yielded an $[M+H]^+$ ion at m/z 467.2912, appropriate for a molecular formula of $C_{28}H_{38}N_2O_4$, which differed from that of the eleutherobin aglycon **34** by the loss of one oxygen atom. Examination of the ^{1}H NMR spectral data obtained for methylcaribaeorane (**35**) revealed the presence of two 3-proton singlets that corresponded to olefinic methyl groups, at δ 1.65 and 1.80. Additionally, it was noted that the proton resonances at δ 4.16 and 3.88, assigned to the hydroxymethyl fragment in the ^{1}H NMR spectrum of **34**, were absent in that of **35** (Figure 4.10). These observations indicated that methylcaribaeorane (**35**) was simply missing the C-15 allylic hydroxyl function found in the eleutherobin aglycon **34**. HMBC correlations observed between the methyl ketal proton resonance at δ 3.18 and a carbon resonance at δ 117.4, aided in assigning the carbon resonance to C-4 (see Figure 4.11). The olefinic methyl resonance at δ 1.80 displayed HMBC correlations to the C-4 ketal carbon resonance at δ 117.4 and to the C-2 and C-3 olefinic carbon resonances at δ 131.3 and 134.0, respectively. This data confirmed the presence of an allylic methyl group at C-15. The remaining NMR data for methylcaribaeorane (**35**) was completely consistent with the assigned structure (see Table 4.3 and 4.4, Experimental). It is noteworthy that methylcaribaeorane (**35**) is presumed to be an isolation artifact, formed from the corresponding hemiketal natural product caribaeorane (**37**) (Figure 4.10). Interestingly, while Danishefsky and co-workers found 15-normethylcaribaeorane (**29**) (Figure 4.5) to be active at a concentration of 400 nM against lung cancer cells,[31] methylcaribaeorane (**35**) was inactive below concentrations of 10,000 nM in an assay against MCF-7 breast cancer cells.[39]
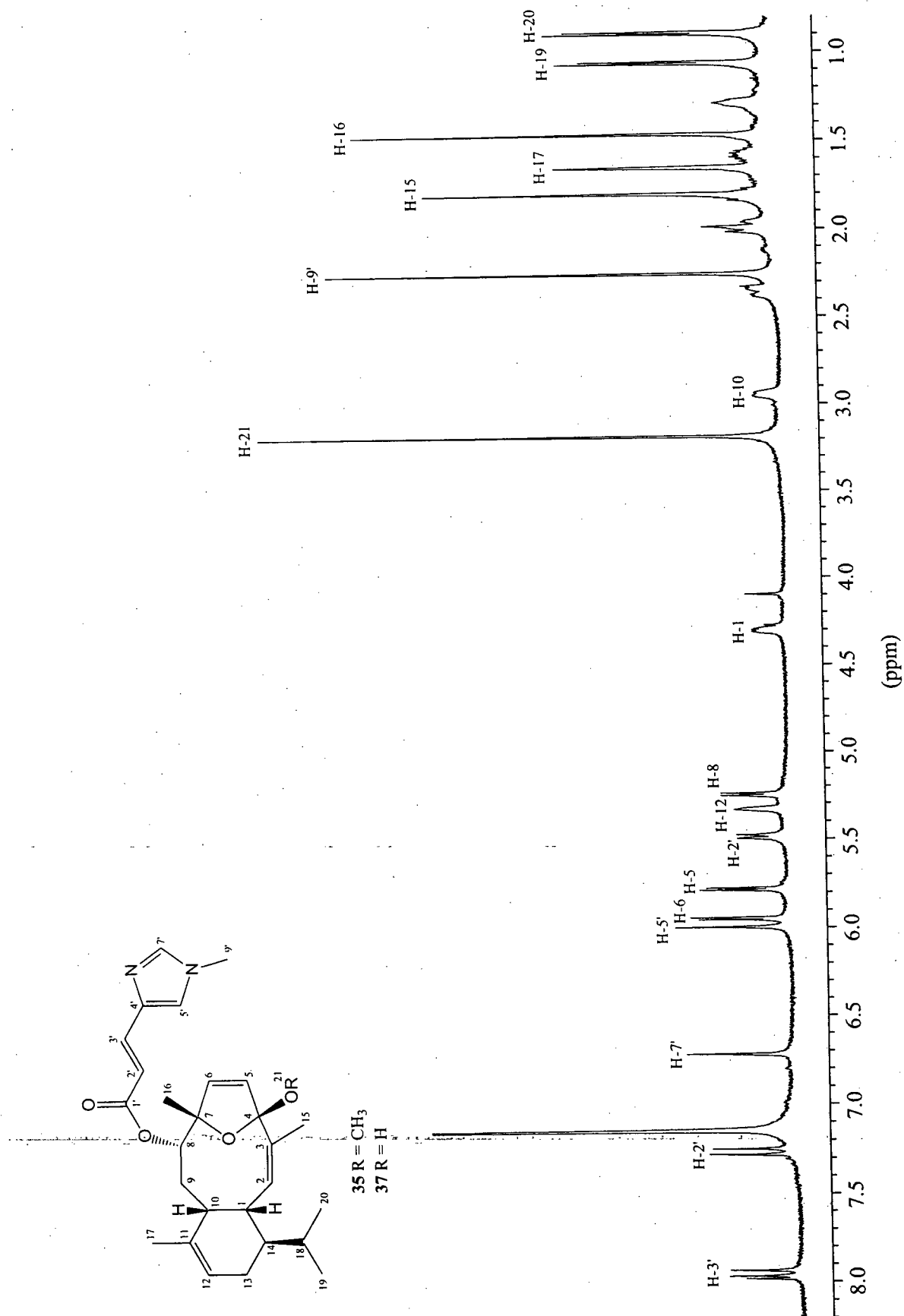
Figure 4.10. ^{1}H NMR spectrum of methylcaribaeorane (**35**) recorded in C_6D_6 at 500 MHz.
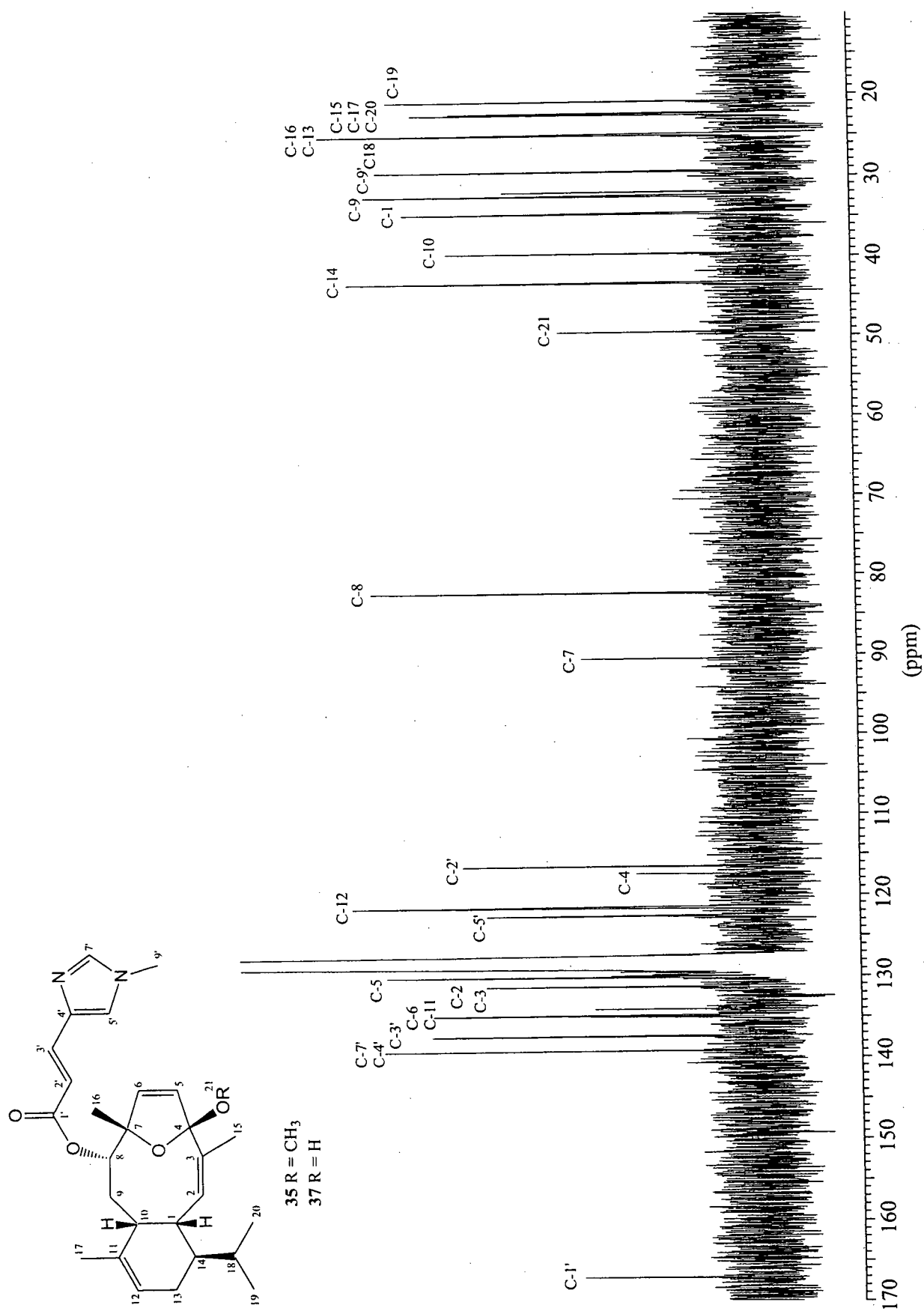
Figure 4.11. ^{13}C NMR spectrum of methylcaribaeorane (**35**) recorded in C_6D_6 at 100.5 MHz.

35 R = CH$_3$
37 R = H

4.2.3 Proposal for the biosynthesis of eleutherobin (8)

The discovery of methylcaribaeorane (35) and the eleutherobin aglycon 34 as minor

constituents in the MeOH extracts of *E. caribaeorum* along with the previously reported

eleuthosides and sarcodictyins, led to the biosynthetic proposal outlined in Scheme 4.2. Thus, it

may be conjectured that geranylgeranyl pyrophosphate undergoes cyclization and oxidative

functionalization to yield the eleuthoside diterpenoid core. Esterification of the C-8 hydroxyl

function with *N*-methylurocanic acid affords caribaeorane (37), the first known intermediate in

the biosynthetic pathway. An allylic oxidation at C-15 of caribaeorane (37) would then furnish

15-hydroxycaribaeorane (36). Subsequent glycosylation appends the arabinose unit to the

diterpenoid core and affords desacetyldesmethyleleutherobin (38), the methyl ketal artifact of

which has also been isolated from *E. caribaeorum*.[35] A monoacetylation event at C-2" or C-3" of

38 would provide desmethyleleutherobin (32) or desmethylisoeleutherobin (39), respectively.

Further acetylation of either 32 or 39 would then yield eleuthoside A (6), while acetylation of

desmethyleleutherobin (32) at C-4" would give eleuthoside B (7). In this proposal, sarcodictyin

A (4) represents a shunt metabolite formed by the oxidation of 15-hydroxycaribaeorane (36) and

subsequent methylation of the resulting carboxylic acid by *S*-adenosylmethionine (SAM). It

should be noted that while there is no evidence for the occurrence of either 6 or 7 in the *E.*

caribaeorum extract, their biosynthesis in *Eleutherobia aurea* would presumably follow a similar

pathway.
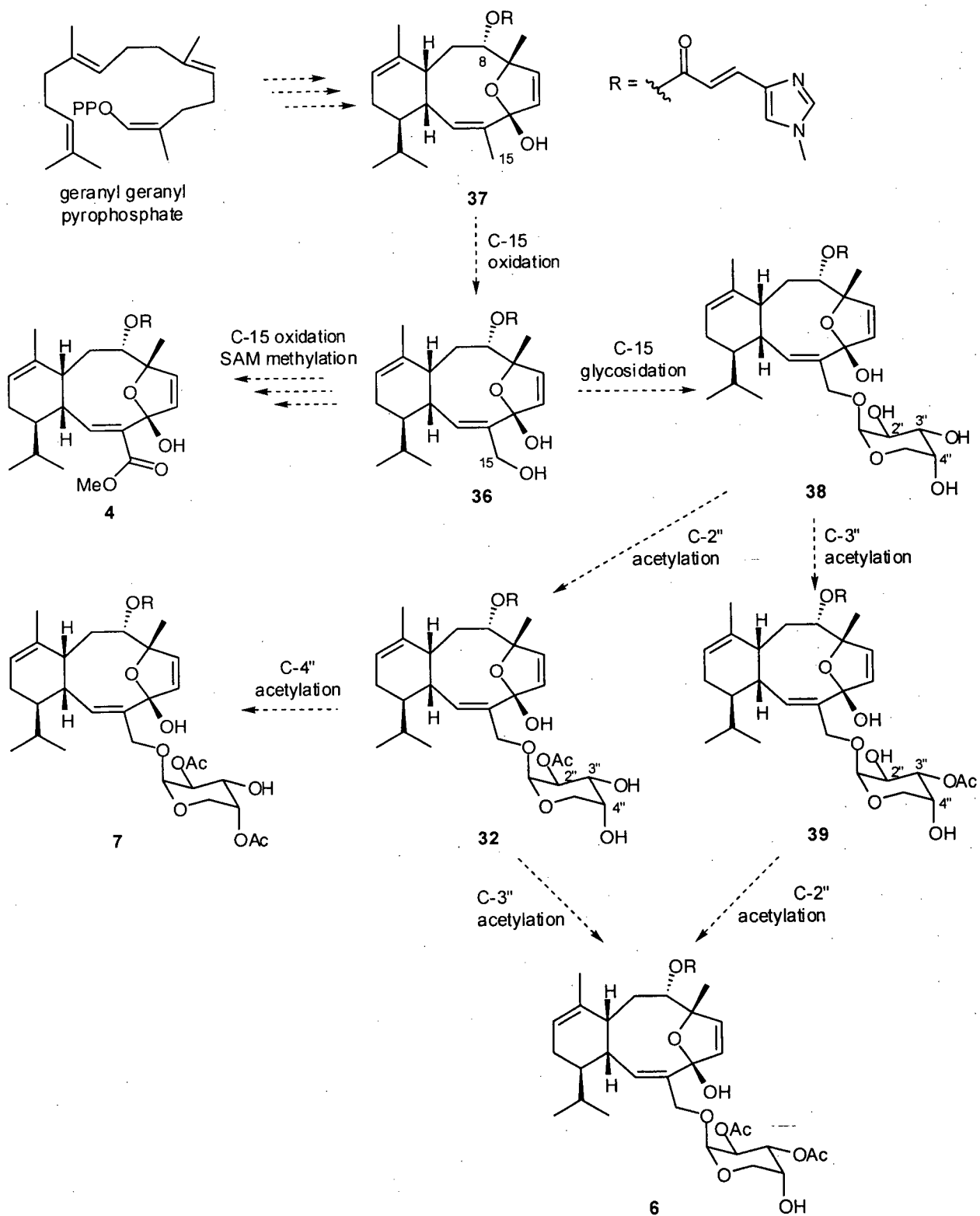
Scheme 4.2. Proposed biosynthesis of the caribaeoranes, eleuthosides and sarcodictyin A (**4**).

The premise that the *N*-methylurocanic ester residue is added to the eleuthoside diterpenoid core prior to the introduction of the C-15 alcohol function is a significant aspect of the biosynthetic events detailed in Scheme 4.2. In an attempt to lend credence to this suggestion, the *N*-methylurocanic ester residue was hydrolyzed from methylcaribaeorane (**35**) and 15-hydroxymethylcaribaeorane (**34**) and, using the corresponding hydrolysis products as analytical standards, the MeOH extracts of *E. Caribaeorum* were analyzed for these substances. In this regard, a solution of **35** in MeOH was treated with 5N NaOH, affording the desurocanate methylcaribaeorane **40** in excellent yield (eq. 3). This substance represents the C-4 methyl ketal analogue of the desurocanate caribaeorane **41**, a potential biosynthetic precursor to caribaeorane (**37**). Unfortunately, using **40** as a reference, examination of the fractions generated during the chromatographic acquisition of the erythrolides, sarcodictyins and eleuthosides by ¹H NMR spectroscopy, TLC and GLC analysis failed to provide any evidence for **40** in the MeOH extract of *E. caribaeorum*. The spectral data acquired for the desurocanate methylcaribaeorane **40** was consistent with the assigned structure. The signals that were assigned to the *N*-methylurocanic ester moiety in the ¹H and ¹³C NMR spectra of methyl caribaeorane (**35**) were noticeably absent in that of **40**. Additionally, in the ¹H NMR spectrum of **35**, the proton resonance at δ 5.25 assigned to H-8 was replaced in that of the hydrolysis product **40** by a resonance at δ 3.47. This data confirmed that the C-8 urocanate function, which deshields the proximal proton in the former substance, had been removed. While certainly the hydrolysis product **40** has the potential to undergo furanose to pyranose isomerization, providing **42**, analysis of the coupling constant between the protons at C-5 and C-6 in the hydrolysis product supported the proposed structure. The proton resonances corresponding to H-5 and H-6 occurred at δ 5.74 and 5.99, respectively, and shared a common coupling constant of 5.9 Hz. Had an isomerization (i.e. **40** → **42**) transpired, the vicinal coupling constant for these protons would be on the order of 10 Hz.[40]

Additionally, ^{13}C NMR spectroscopic analysis and a high resolution mass spectrometric measurement of the molecular ion supported the assigned structure for the hydrolysis product **40**.

35 R = Me   40 R = Me   42
37 R = H   41 R = H

(3)
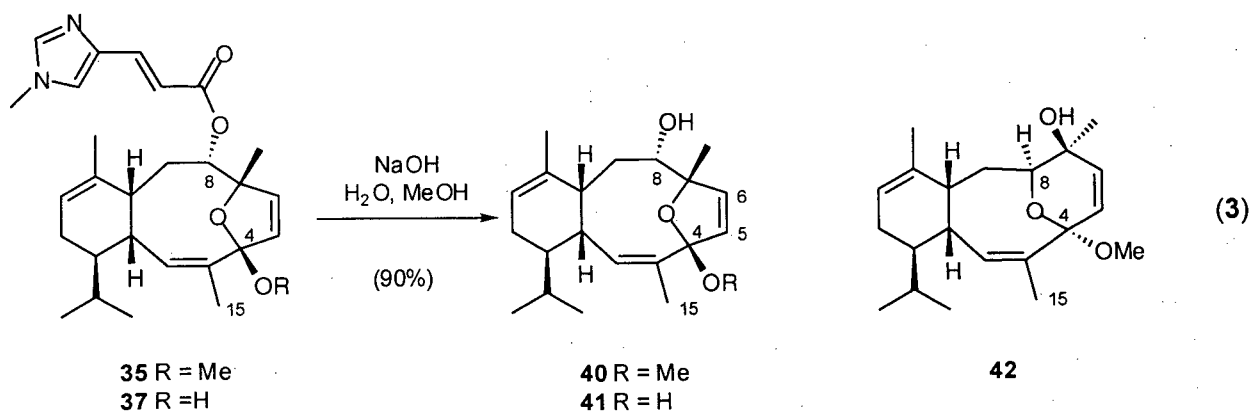
The corresponding hydrolysis product of the eleutherobin aglycon **34** was prepared in a similar fashion (eq. 4). Again, ^{1}H NMR, TLC and GLC analysis failed to provide any evidence to support the presence of this substance in the MeOH extracts of *E. caribaeorum*. While these results do not eliminate **41** or **44** as the immediate biosynthetic precursors to caribaeorane (**37**) (eq. 3) or 15-hydroxycaribaeorane (**36**) (eq. 4), they are suggestive that esterification of the diterpenoid core with *N*-methylurocanic acid occurs at an earlier stage in the biosynthesis of the eleuthosides. The structure of the desurocanate eleutherobin aglycon **44** was assigned in the same manner as that described above for desurocanate methylcaribaeorane (**40**). Notably, the ^{1}H and ^{13}C NMR spectra of this material were deplete of resonances that could be ascribed to the *N*-methylurocanic ester function and the signal that corresponded to H-8 in the ^{1}H NMR spectrum of this material resonated at δ 3.44. Additionally, a high resolution mass spectrometric measurement of the molecular ion confirmed the molecular formula of the hydrolysis product (**43**).

34 R = Me
36 R = H

43 R = Me
44 R = H

$$\text{(4)}$$
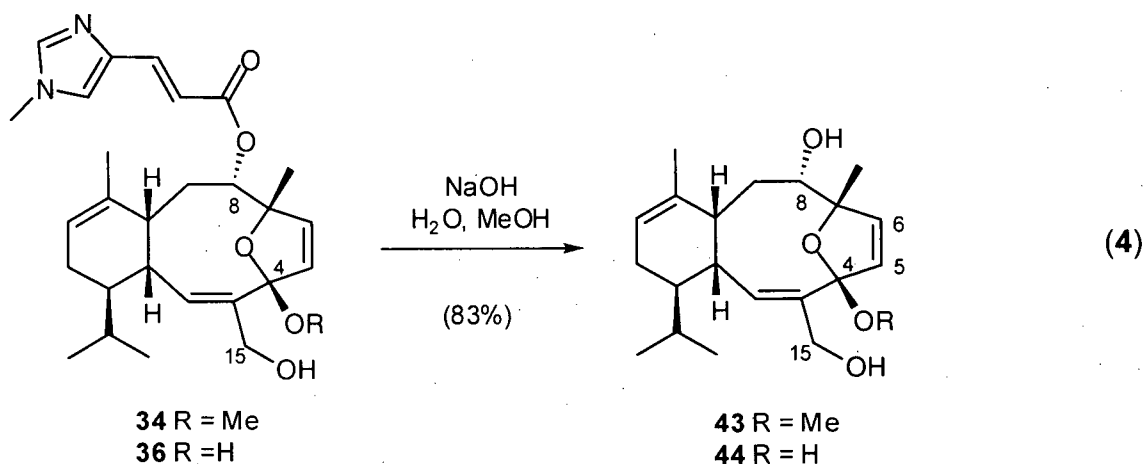
At this juncture, unable to identify biosynthetic precursors for either caribaeorane (**37**) or 15-hydroxy caribaeorane (**36**) in the MeOH extracts of *E. caribaeorum*, our focus returned to the original objective. Thus, an investigation into the effect structural modifications to eleutherobin (**8**) have on its antimitotic activity was initiated. The results gathered from this pursuit are summarized in the following section.

4.3 Synthetic transformations of eleutherobin (8) reveal new features of its microtubule-stabilizing pharmacophore

While the methodology employed in the total syntheses of the sarcodictyins and eleuthosides (*vide supra*) was amenable to the construction of a library of congeners of these substances, the majority of the analogues thus fashioned resulted from modifications at C-15. Nevertheless, based solely on structural overlays of eleutherobin (**8**) and taxol (**9**), the eleuthoside pharmacophore models suggest that the cyclohexene ring and its appended substituents (i.e. the C-14 isopropyl residue) are key determinants of antimitotic activity.[32-34] Additionally, it is generally agreed that both the *N*-methylurocanic ester function and the C-4/C-7 ether bridge (i.e. the dihydrofuran oxygen) are crucial for biological activity. The significance

of the cyclohexene ring has been supported by the observation that caribaeoside (**30**) (Figure 4.6), which bears a β-hydroxyl function at C-11 and a $\Delta^{12,13}$ olefin, is roughly 1000-fold less potent as a cytotoxin than eleutherobin (**8**).[35] However, with regard to the eleuthosides, the accuracy of the latter statements remained to be substantiated. Thus, prompted by the lack of data in the literature relating the structural features and antimitotic agency of the eleuthosides, synthetic modifications of eleutherobin (**8**), geared towards the production of novel derivatives of this substance, were explored.
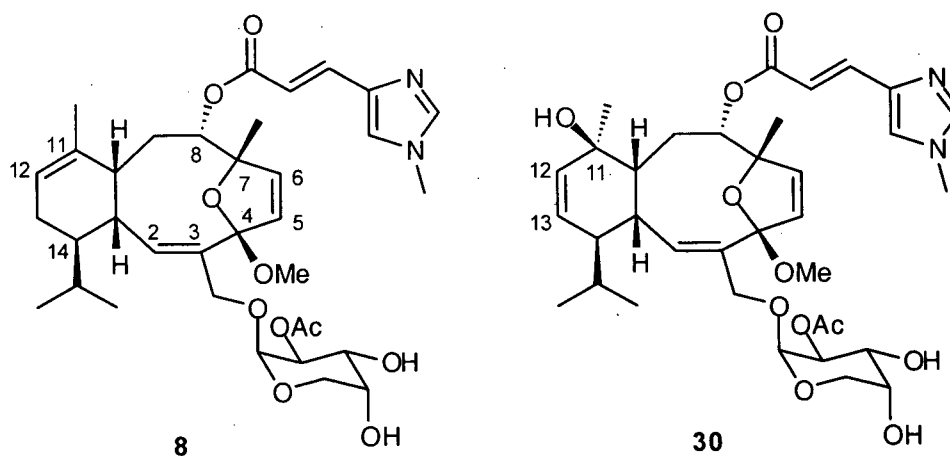
4.3.1 Synthetic transformations involving the C-4 ketal function of eleutherobin (8)
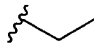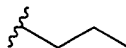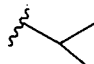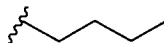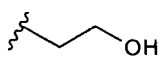
Our first objective in this regard was to investigate the importance of the C-4 methyl or hemiketal function in mediating the biological activity of the eleuthosides. From the biological assessment of a library of synthetic congeners of sarcodictyin A (**4**),[30] it was anticipated that modifications of the C-4 ketal would have a minimal effect on the ability of these substances to promote tubulin polymerization. However, this hypothesis remained to be validated in the eleuthoside series. Additionally, the isolation of eleutherobin (**8**) as an artifact from the MeOH extraction of *E. caribaeorum* (*vide supra*) indicated that construction of various ketals of

desmethyleleutherobin (32) would be a facile process. Thus, in order to provide information relating the effect of various substituents at C-4 to eleuthoside biological activity, a series of C-4 ketals were generated and assayed against MCF-7 breast cancer cells for antimitotic activity.[39]

Employing conditions described in Table 4.2, the ethyl, propyl, isopropyl, butyl, 2-hydroxyethyl and 2,2-dimethyl-3-hydroxyprpoyl eleuthoside ketals were produced in good to excellent yield from desmethyleleutherobin (32). The structures of these substances were assigned by analysis of their spectroscopic data. For instance, the ^{1}H NMR spectrum of the propyl ketal of eleutherobin 46 included a 3-proton triplet at δ 0.89 for the terminal methyl of the appended propyl group. Additionally, a 2-proton multiplet at δ 3.33 in the ^{1}H NMR spectrum of this material was assigned to the methylene protons of the propyl function. Similarly, the butyl ketal of eleutherobin 48 displayed a 3-proton triplet at δ 0.89 and a 2-proton multiplet at δ 3.37, indicative of the terminal methyl and methylene protons, respectively, of the butyl moiety. The ^{1}H NMR spectrum of the isopropyl ketal of eleutherobin 47 included two 3-proton doublets at δ 1.16 and 1.13 for the methyl groups of the isopropyl function. Through similar analysis of ^{1}H NMR spectral data (see Experimental), the structures of the 2-hydroxyethyl ketal 49 and 2,2-dimethyl-3-hydroxypropyl ketal of eleutherobin 50 were confirmed. It should be noted that aside from the discrepancies resulting from the various substituents at C-4, the ^{1}H and ^{13}C NMR spectra of all these substances agreed well with that reported for eleutherobin (8).[17] Moreover, the molecular formula of 33 and 46-50 were confirmed by high resolution mass spectrometric measurements on their molecular ions.

Table 4.2. Transformation of desmethyleleutherobin (**32**) into the
C-4 ketal analogues **33** and **46-47**.

(**5**)
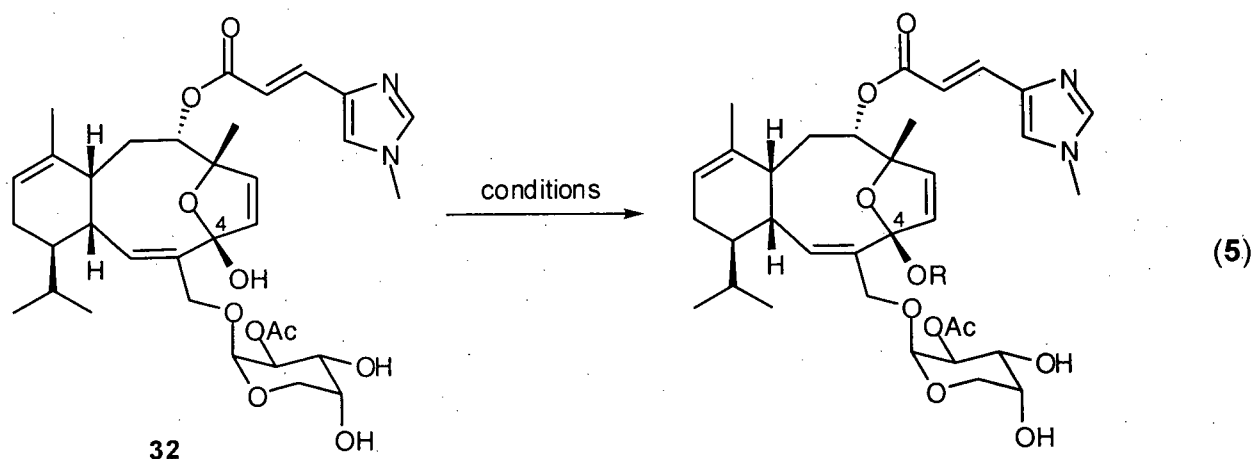
entry	conditions [a,b]	alcohol	product	yield (%)	IC_{50}[c] (nM)
1	N/A	N/A	**32** R = H	N/A	20
2	N/A	N/A	**8** R = Me	N/A	20
3	A	ethanol	**33**, R =	88	50
4	A	n-propanol	**46**, R =	91	50
5	A	i-propanol	**47**, R =	84	30
6	B	n-butanol	**48**, R =	60	30
7	B	ethylene glycol	**49**, R = OH	60	20
8	C	neopentyl glycol	**50**, R = OH	60	80

[a] A: alcohol, PPTS (5 eq.); B: alcohol (1.0 mL), CH_2Cl_2 (1.0 mL), PPTS (5 eq.); C: neopentyl glycol (1.0 mL), CH_2Cl_2 (1.0 mL), PPTS (5 eq.), 4 Å mol. sieves. [b] All reactions were complete in 3 hours at room temperature. [c] Biological assays were performed on MCF-7 breast cancer cells.[39]

As outlined in Table 4.2, the C-4 ketal analogues of eleutherobin (**8**) possessed biological activity comparable to that of the parent compound when assayed against MCF-7 breast cancer cells.[39] While these results may reflect a broad tolerance for substitutions at C-4 of the eleuthosides with regards to antimitotic activity, it is also possible that upon entering the cell, the ketal function is hydrolyzed, thus generating the biologically active hemiketal, desmethyleleutherobin (**32**). In this manner, the minor differences in biological activity

expressed by the series of C-4 ketal analogues may be rationalized by the difference in solubility or cell permeability of these compounds. Fortunately, as the available quantity of eleutherobin (**8**) and desmethyleleutherobin (**32**) was indeed limited, these C-4 ketal analogues (i.e. **33** and **46-50**) could be converted into eleutherobin (**8**) in good yield by their treatment with MeOH and PPTS as previously described.

4.3.2 Allylic oxidation of eleutherobin (8)

The allylic oxidation of olefinic functions is a well-established reaction in organic synthesis.[41] Standard conditions for this reaction involve the treatment of an alkene (e.g. **51**, eq. 6) with SeO_2, upon which an electrophilic "ene" reaction occurs. A sigmatropic rearrangement restores the original position of the olefin[42] and is followed by breakdown of the resulting selenium ester **53**, which provides the allylic alcohol **54**. It is noteworthy that the reaction of trisubstituted olefins with SeO_2 in EtOH displays a marked preference for oxidation in the order $CH_2 > CH_3 > CH$.[41] However, the practicality of this reaction is often precluded by further oxidation of the allylic alcohol (e.g. **54**) generated by this process to a carbonyl function.[42]

$$(6)$$
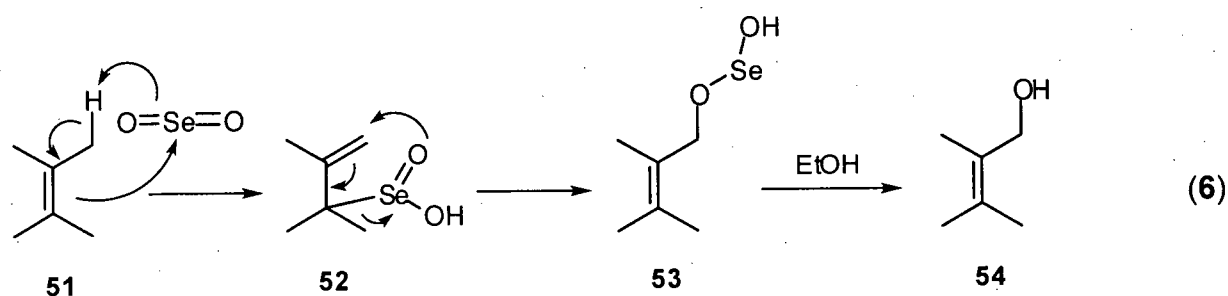
Analysis of the X-ray and solution structures reported for **8**,[37] indicated that steric hindrance of the $\Delta^{2,3}$ olefin would impede the allylic oxidation of this function. Additionally, neither the $\Delta^{5,6}$ or $\Delta^{2',3'}$ olefin functions in eleutherobin (**8**) bear allylic protons. Thus, it was our contention that the reaction of **8** with SeO_2 would proceed chemoselectively at the $\Delta^{11,12}$ olefin.

Furthermore, based on the regioselectivity typified by such processes, it was expected that oxidation would occur primarily on the methylene adjacent to the $\Delta^{11,12}$ olefin. Thus, it was anticipated that treatment of eleutherobin (8) with SeO_2 in refluxing EtOH would result in oxidation at C-13, affording the secondary allylic alcohol 55. In the event, it was discovered that close monitoring of the reaction progress was indeed necessary, as byproducts, presumed to arise from the over oxidation of the formed allylic alcohol function, were also generated. However, after considerable experimentation, it was found that an oxidation product could be isolated from the crude reaction mixture in moderate yield, purified by normal phase HPLC and characterized as the primary allylic alcohol 56 (eq. 7). Clearly, the non-bonded interactions associated with a reaction between C-11 and SeO_2 impedes the archetypical, and indeed anticipated, formation of the secondary alcohol 55. Additionally, that the oxidation product 56 was isolated as its ethyl ketal was not surprising, as transketalization of the eleuthosides in alcohol solvents is a facile process (vide supra).
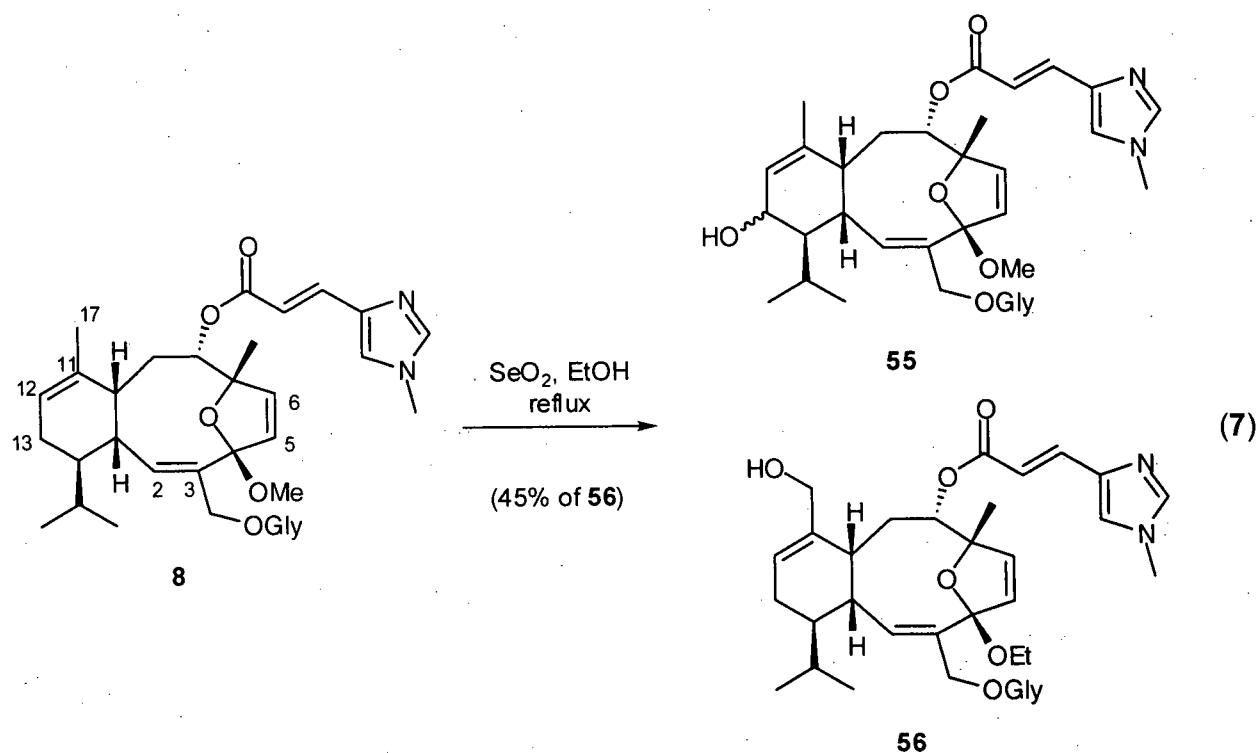
The spectral data exhibited by **56** was in complete accord with the assigned structure. When compared to that of eleutherobin **8**, the ^{1}H NMR spectrum of this material included an additional 2-proton multiplet at δ 3.33 and two one-proton multiplets at δ 3.71 and 3.61, which corresponded to the protons on the methylene of the ethyl ketal and the hydroxymethylene at C-17, respectively. In addition, the 3-proton singlet, which appears in the ^{1}H NMR spectrum of eleutherobin (**8**) at δ 1.52 and is attributed to the C-17 methyl group, was noticeably absent in that of **56**. In order to confirm the structure of this material in an unambiguous manner, both HMQC and COSY spectroscopic experiments were performed. Analysis of the results from these experiments allowed for the complete assignment of all proton and carbon resonances in the spectra of **56** (see Table 4.7, Experimental). In particular, HMQC correlations between the proton resonances at δ 3.71 and 3.61 and a carbon resonance at δ 63.1 allowed the assignment of the latter resonance to C-17. That this carbon was attached to two protons confirmed the structural assignment of the oxidation product as that depicted for the primary allylic alcohol **56**, and *not* the secondary alcohol **55**.

Owing to the relative inability of caribaeoside (**30**) to inhibit mitosis,[35] it was anticipated that the 17-hydroxyeleuthoside **56** would also show a marked decrease in antimitotic activity due to the presence of a polar hydroxymethyl function on the cyclohexene ring. It was surprising then, that this substance demonstrated activity (IC_{50} = 20 nM)[39] equivalent to that of eleutherobin (**8**) (IC_{50} = 20 nM)[17] and the corresponding ethyl ketal of eleutherobin **33** (IC_{50} = 50 nM) when assayed against MCF-7 breast cancer cells (Figure 4.12). From this result, it was apparent that the structural features of caribaeoside (**30**) that detract from its antimitotic agency are more subtle than originally thought. Thus, simply increasing the polarity of the hydrophobic cyclohexene region of eleutherobin (**8**) is not sufficient to alter the biological activity of the eleuthosides.

8 R = Me (20 nM)
33 R = Et (50 nM)

56 (20 nM)

30 (20,000 nM)
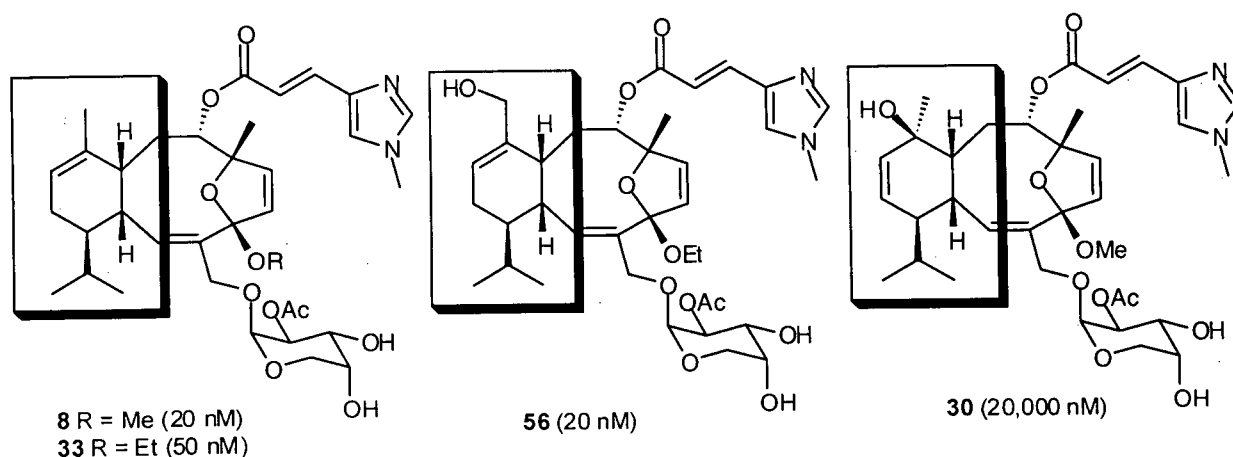
Figure 4.12. Eleutherobin (**8**), the ethyl ketal of eleutherobin **33**, the ethyl ketal of 17-hydroxyeleuthoside **56** and caribaeoside (**30**). Concentrations in parentheses indicate the IC_{50} values for these compounds when screened against MCF-7 breast cancer cells.

4.3.3 Hydrogenation of eleutherobin (8)

While allylic oxidation of eleutherobin (**8**) highlighted the reactivity of the $\Delta^{11,12}$ olefin, this transformation had failed to modify the eleuthoside diterpenoid core. It was our contention, however, that hydrogenation would necessarily result in the formation of one or more new eleuthosides, in which the diterpenoid core differs from that of **8**. Nicolaou and co-workers have reported that hydrogenation of the eunicellane **57** over Pd/BaSO$_4$ resulted in a chemoselective reduction of the alkyne function and, subsequently, the $\Delta^{5,6}$ olefin (eq. 8).[25] From this, it was anticipated that under similar conditions, the $\Delta^{5,6}$ olefin in eleutherobin (**8**) could be selectively hydrogenated. Based on analysis of the X-ray and solution structures reported for **8**,[37] a subsequent hydrogenation event should result in the selective reduction of the $\Delta^{11,12}$ olefin, as the $\Delta^{2,3}$ olefin suffers from notable steric congestion. In this manner, a series of hydrogenated eleuthosides would be generated for biological testing. The results of this pursuit would certainly aid in the refining the known pharmacophore models for these substances.

(8)
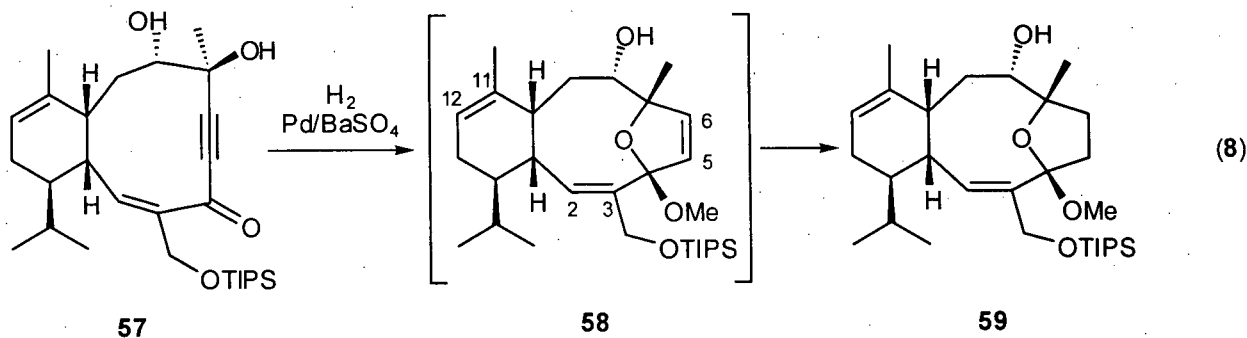
To this end, a solution of eleutherobin (**8**) in EtOAc, containing a catalytic amount of Pd on BaSO₄ was stirred at room temperature for one hour under an atmosphere of hydrogen. After this time, a single product, 5,6,11,12,2',3'-hexahydroeleutherobin (**60**) was isolated from the crude reaction mixture in excellent yield (eq. 9). The ¹H NMR spectrum of the hydrogenation product included only one olefinic proton resonance at δ 5.78 (doublet, *J* = 9.3 Hz), which, compared well to that reported for the olefinic proton resonance at C-2 (δ 5.56) of eleutherobin (**8**).[17] Surprisingly, in subsequent hydrogenations where reaction times were shortened, only complex mixtures of compounds were recovered. The results from these experiments indicated that under the conditions described above, the $\Delta^{5,6}$, $\Delta^{11,12}$ and $\Delta^{2',3'}$ alkene functions in **8** are reduced at similar rates.

(9)
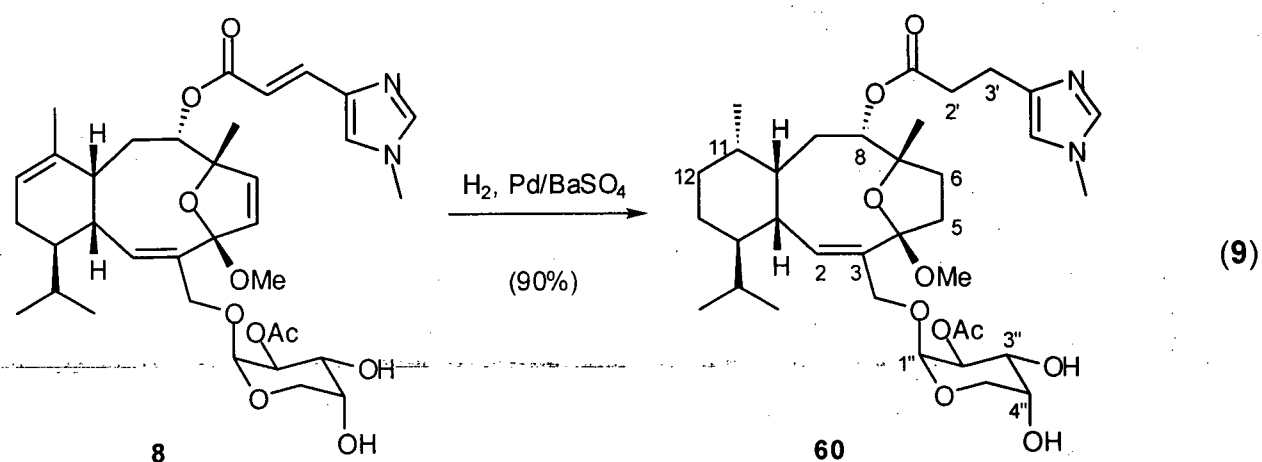
Analysis of the spectral data obtained for **60** confirmed the structural assignment of this material. The ¹H NMR spectrum included a resonance at δ 5.78 that corresponded to the olefinic

proton at C-2 and demonstrated coupling to a proton resonance diagnostic for H-1 at δ 3.76.[17]

That the arabinose function had been unaffected by this reaction, was supported by the observation of resonances characteristic for the anomeric proton (H-1") at δ 5.02 and the methyl function of the C-2" acetate at δ 2.08 in the ¹H NMR spectrum of **60**. Additionally, the *N*-methylimidazole moiety exhibited three typical resonances at δ 7.35 (H-7'), 6.63 (H-5') and 3.60 (*N*-Me) confirming its inclusion in the hydrogenated product. Comparison of the ¹³C NMR spectra of **60** to that of eleutherobin (**8**) verified the reduction of three olefinic functions, as six alkene resonances, that appeared in the spectrum of the latter compound at δ 136.4, 134.2, 133.7, 131.0, 121.3, 115.9, were noticeably absent in that of **60**. Moreover, six additional aliphatic carbon resonances (δ 41.0, 34.1, 34.0, 30.4, 28.3, 23.6) in the ¹³C NMR spectrum of the hydrogenation product **60** supported the assigned structure. However, unambiguous structural determination of this material relied on the execution of a suite of spectroscopic experiments (HMQC, HMBC, 2D NOESY and COSY). Analysis of the results from these experiments allowed for the complete assignment of all proton and carbon resonances in the spectra of **60** (see Tables 4.9 and 4.10, Experimental). It remained then to identify the relative configuration at C-11, the stereogenicity of which had resulted from the hydrogenation of the $\Delta^{11,12}$ olefin.
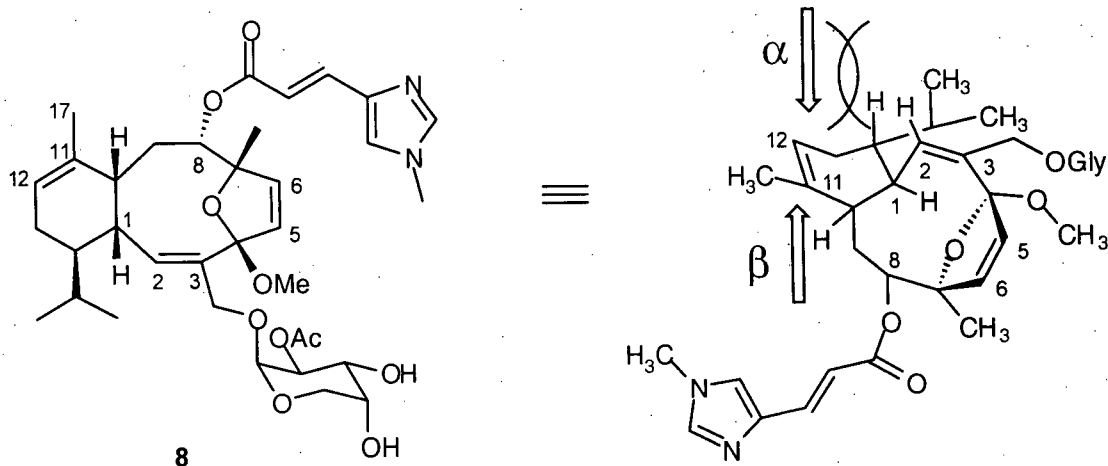
Figure 4.13. Steric shielding of the α-face of the $\Delta^{11,12}$ olefin in eleutherobin (**8**). For clarity, the conformational representation of eleutherobin (**8**) is rotated.

From consideration of molecular models and the known solid state and solution conformations of eleutherobin (**8**),[37] it was anticipated that hydrogenation of the α-face of the $\Delta^{11,12}$ olefin would be hindered by the propinquity of the pseudoaxial substituent at C-1, resulting in reduction of the $\Delta^{11,12}$ olefin from the β-face, as depicted in Figure 4.13. However, analysis of the spectral data gathered from **60** was required to confirm the relative stereochemistry of the newly formed carbon chirality center. From HMQC, HMBC and COSY experiments, a doublet ($J = 7.0$ Hz) at δ 0.76 in the ^{1}H NMR spectrum of **60** could be assigned to the protons of the C-17 methyl group. It is noteworthy that the small chemical shift of this resonance indicated that the C-17 methyl group was shielded by the $\Delta^{2,3}$ olefin function. This shielding effect was suggestive of a structure where both the C-17 methyl group and $\Delta^{2,3}$ olefin bear a *cis* relationship with respect to the eleuthoside topography. Analysis of the results from a 2D NOESY experiment supported this qualitative observation. Thus, a correlation between the C-2 olefinic proton resonance and the proton resonances corresponding to H-14 and H-17, unambiguously confirmed the stereochemical assignment at C-11 as that depicted in Figure 4.14.
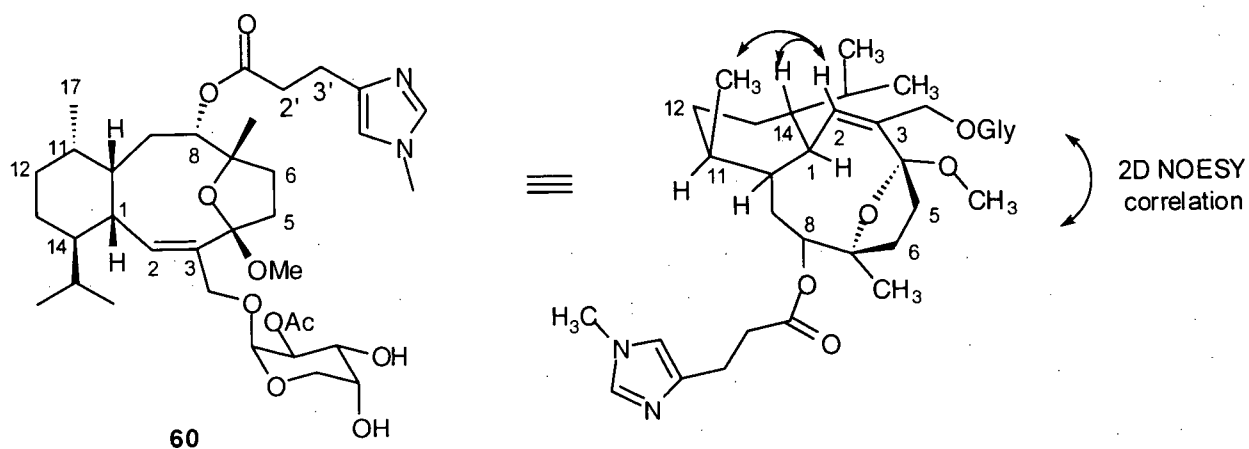
Figure 4.14. Key 2D NOESY correlations for 5,6,11,12,2',3'-hexahydroeleutherobin (**60**). For clarity, the conformational representation this substance is rotated.

Having successfully elucidated the structure of 5,6,11,12,2',3'-hexahydroeleutherobin (**60**), the biological evaluation of this substance was undertaken.[39] Interestingly, in an assay against MCF-7 breast cancer cells, **60** ($IC_{50} > 100,000$ nM) was found to be more that 5000-fold less active than eleutherobin (**8**) ($IC_{50} = 20$ nM)[17] (Figure 4.15). This data indicated that one or more of the reduced double bonds is crucial for the binding of eleuthosides to tubulin. From the synthesis and biological evaluation of the 17-hydroxyeleuthoside **56**, it was noted that the simple introduction of a polar substituent onto the hydrophobic cyclohexene ring did not greatly affect its ability to inhibit mitosis (*vide supra*). Thus, the inactivity of caribaeoside (**30**) and the hexahydroeleuthoside **60**, as antimitotic agents, was tentatively attributed to the stereogenicity at C-11 and, consequently, detrimental interactions between the appended methyl group at C-11 and residues in the taxol binding site on tubulin. Evaluation of this hypothesis, however, would rely on the construction of eleuthosides in which the olefinic functions were selectively reduced. In this manner, the necessity of the $\Delta^{11,12}$ olefin could be directly assessed.
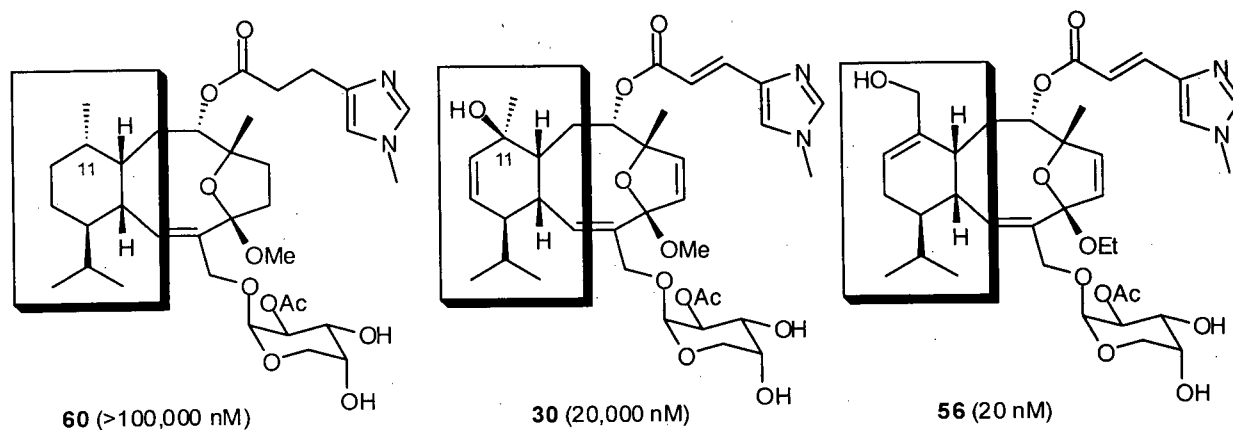
Figure 4.15. 5,6,11,12,2',3'-hexahydroeleutherobin (**60**), caribaeoside (**30**) and the 17-hydroxyeleuthoside **56**. Concentrations in parentheses indicate the IC_{50} values for these compounds when screened against MCF-7 breast cancer cells.

4.3.4 Synthesis of selectively hydrogenated congeners of eleutherobin (8)

While cognizant of literature procedures designed to effect the chemoselective reduction of enoates or olefins,[42] at this stage, a sequence of reactions with proven success in the synthesis eleutherobin or sarcodictyin type substances would be required to realize our current objective with the material that remained. Fortunately, biological evaluation of synthetic congeners of sarcodictyin A (**4**) suggested that reduction of the $\Delta^{5,6}$ olefin has a minimal effect on the antimitotic potency of these compounds.[25] Therefore, our quandary was somewhat simplified, as only the reduction of the $\Delta^{2',3'}$ and $\Delta^{11,12}$ olefins required independent deliberation. Thus, two target molecules were selected to evaluate the biological significance of these functions, namely 5,6,11,12-tetrahydroeleutherobin (**61**) and 2',3'-dihydroeleutherobin (**62**).

61   62
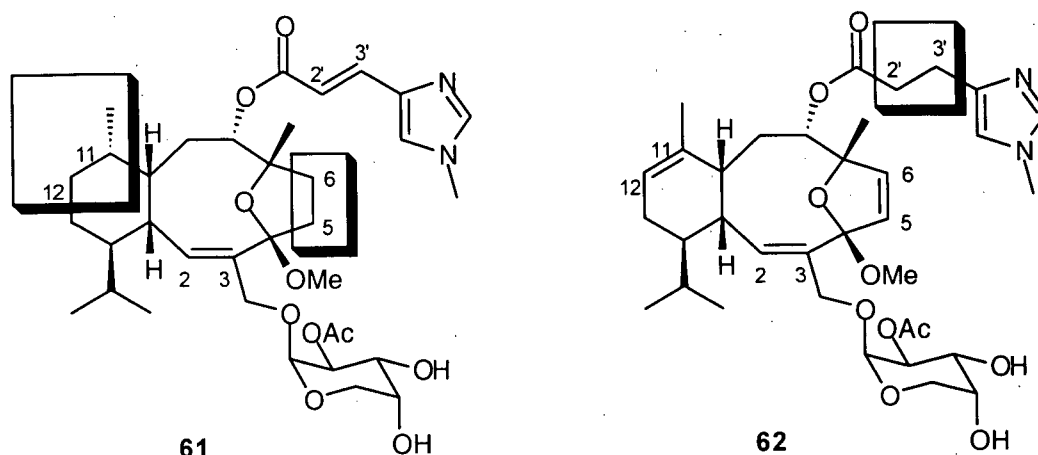
With a waning supply of eleutherobin (**8**), it was expected that a synthesis of both **61** and

62 would necessarily diverge from a common intermediate. As such, the eleuthoside **63**, in

which the alcohol functions on the arabinose fragment are selectively protected, represented a

logical precursor for both of these substances (Scheme 4.3). Selection of isopropylidene and *t*-

butyldimethylsilyl protecting groups for this purpose was founded on their successful service in a

total synthesis of eleutherobin (**8**) reported by Danishefsky and co-workers.[29] Based on the facile

reduction of **8** (*vide supra*), hydrogenation of **63** was expected to provide the corresponding

hexahydroeleuthoside **64**. Hydrolysis of the ester function in **64** and subsequent coupling of the

unveiled secondary alcohol with the mixed anhydride **18** would then yield access to the

tetrahydroeleuthoside **65**. The latter reaction, namely the coupling of **18** with the diterpenoid

core of eleutherobin (**8**), has precedent in the synthesis of **8** by Nicolaou and co-workers (see

Scheme 4.1).[27] A series of well established transformations,[29] that included deprotection of the

arabinose alcohol moieties and introduction of the C-2" acetate, would then provide 5,6,11,12-

tetrahydroeleutherobin (**61**). Alternatively, the synthesis of **62** would involve direct hydrolysis of

the *N*-methylurocanic ester appendage from the eleuthoside **63** and a subsequent coupling of the

revealed secondary alcohol at C-8 with the mixed anhydride **66**. A deprotection and acetylation

sequence, similar to that proposed for the synthesis of **61**, would then afford 2',3'-

dihydroeleutherobin (**62**).
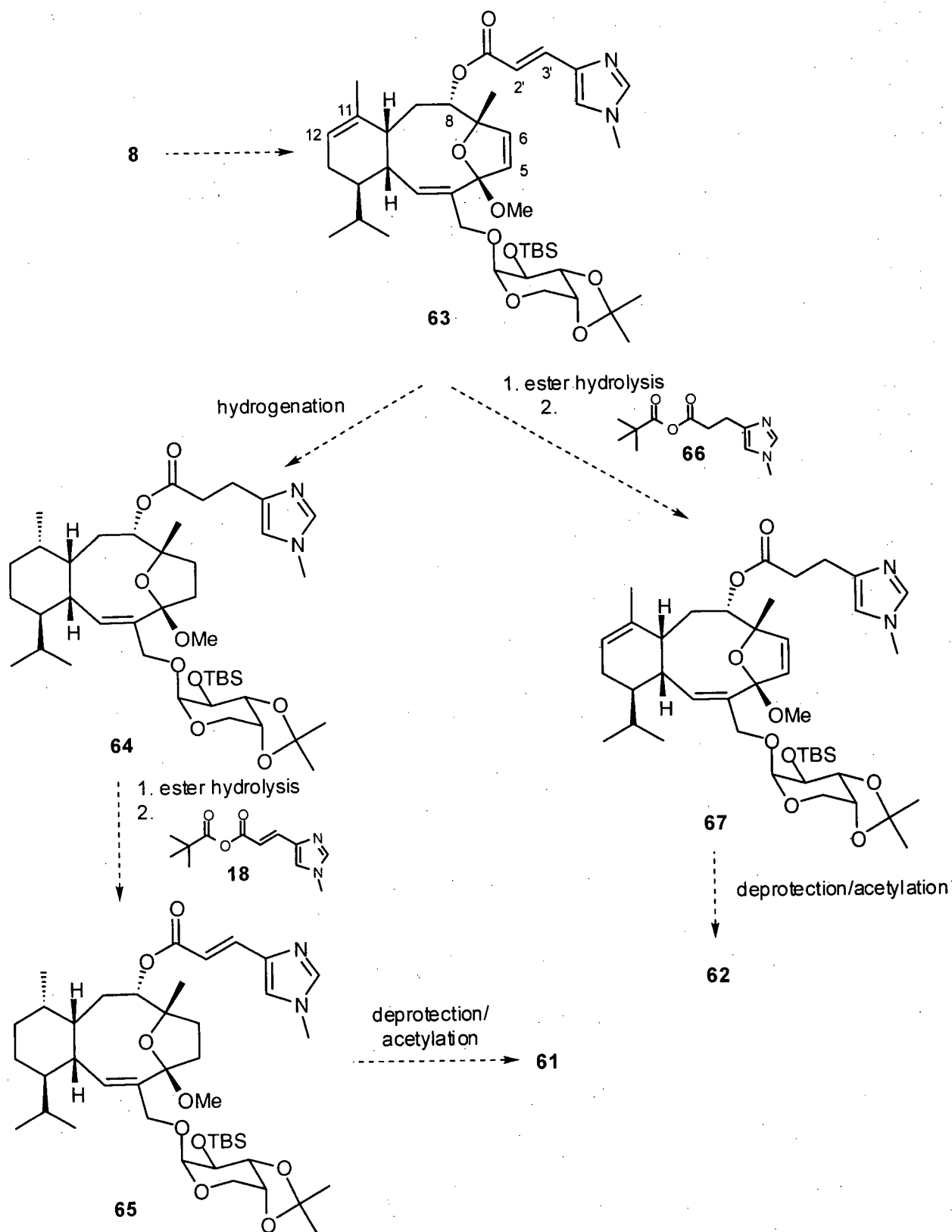
Scheme 4.3. Proposal for the synthesis of 5,6,11,12-tetrahydroeleutherobin (**61**) and 2',3'-dihydroeleutherobin (**62**).

As delineated in the synthetic proposal for both **61** and **62**, the eleuthoside **63**, in which the glycon portion of the molecule is selectively protected, represented a pivotal intermediate in both syntheses. Thus, the transformation of eleutherobin (**8**) into the dihydro and tetrahydroeleuthosides **61** and **62** commenced with the protection of the 3",4"-*cis*-diol in eleutherobin (**8**). In this regard, treatment of **8** with a catalytic amount of PPTS in 2,2-dimethoxypropane[29] resulted in a transketalization that afforded the acetonide of eleutherobin **68** in good yield (eq. 10). Analysis of spectroscopic data recorded for **68** confirmed the structural assignment of this material. The ¹H NMR spectrum of **68** included two 3-proton singlets for the isopropylidene methyl groups at δ 1.50 and 1.33. The similarity between resonances observed in the ¹H NMR spectra of **68** and **8** revealed the diterpenoid core and *N*-methylurocanic ester function in the former material were unchanged by the above transformation. The ¹³C NMR spectrum of **68** displayed a resonance at δ 115.8, in addition to resonances at δ 115.9 and 92.8 that could be assigned to the ketal and anomeric carbons at C-4 and C-1", respectively. The former resonance was thus assigned to the O-C-O carbon of the acetonide function. In addition to this spectral data, the molecular formula of **68** was confirmed by a high resolution mass spectrometric measurement on the molecular ion.

(10)
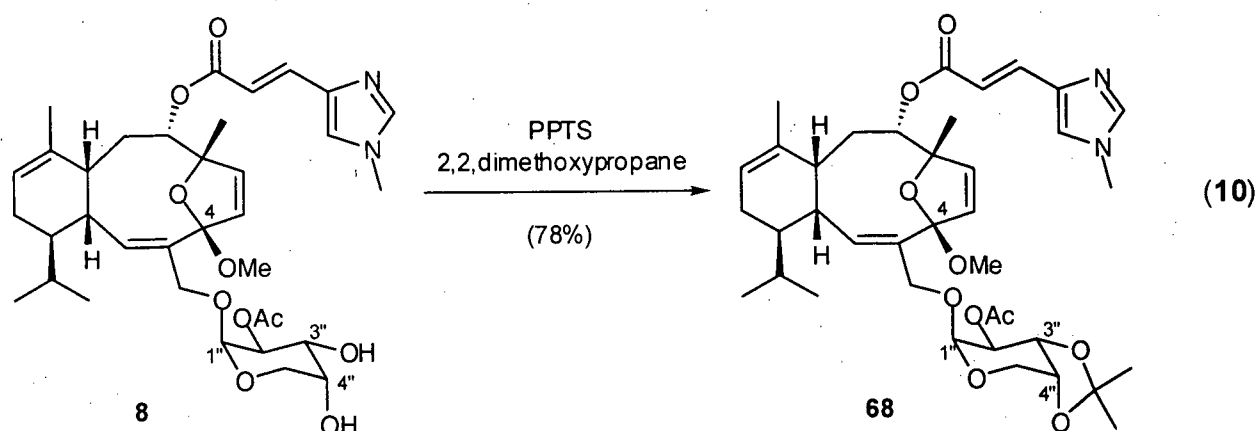
With the acetonide **68** in hand, the projected functional group manipulations would involve hydrolysis of the C-2" acetate and protection of the resulting secondary alcohol as its *t*-butyldimethylsilyl ether. To this end, a solution of the acetonide **68** in MeOH was treated with NaOMe. While the potential for concomitant hydrolysis of the *N*-methylurocanic ester function was a cause for concern, the desired alcohol **69** was the only material isolated from this reaction. The crude hydrolysis product **69** was then directly transformed into the corresponding *t*-butyldimethylsilyl ether **63** in good yield, through the treatment of a solution of the former substance in CH_2Cl_2 with TBSCl and imidazole (eq. 11).[29] The spectral data displayed by the silyl ether **63** was in accordance with the assigned structure. The ^1H NMR spectrum of this material included a 9-proton singlet at δ 0.85 and two 3-proton singlets at δ 0.08 and 0.02, corresponding to the *t*-butyl and methyl groups of the silyl ether, respectively. That the desired series of transformations had occurred was further evidenced by the upfield shift of H-2" from δ 4.89 to δ 3.72 in the ^1H NMR spectra of **68** and **63**, respectively. This difference between the ^1H NMR spectra of these substances highlighted the deshielding effect on the C-2" proton by the proximal acetate moiety in the ^1H NMR spectrum of **68** and, consequently, the absence of the acetate function in **63**. Additionally, the ^{13}C NMR spectrum of **63** included the urocanic ester carbonyl resonance at δ 166.8, and two highly shielded carbon resonances at δ -3.6 and -4.5 that could be assigned to the two diastereotopic silylmethyl groups.
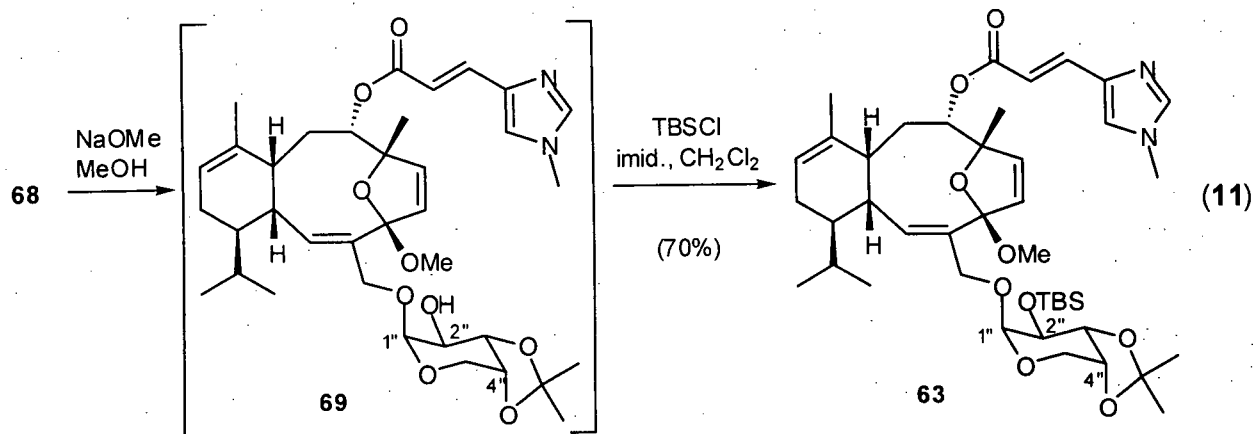
Having gained access to this key intermediate, the transformation of **63** into 5,6,11,12-tetrahydroeleutherobin (**61**) was investigated. As outlined in the proposed synthesis of **61** (Scheme 4.3), of initial importance was the reduction of the $\Delta^{5,6}$, $\Delta^{11,12}$ and $\Delta^{2',3'}$ olefin functions in this material. To this end, a solution of **63** in EtOAc was treated with Pd on $BaSO_4$ and stirred under an atmosphere of hydrogen for one hour (eq. 12).[25] Spectroscopic data exhibited by the crude hydrogenation product indicated the presence of minor byproducts, which, TLC analysis suggested, would be difficult to separate from the desired hexahydroeleuthoside by standard chromatographic procedures. As such, it was anticipated that the direct hydrolysis of the ester function and concomitant coupling of the resultant alcohol with the mixed anhydride **18** would yield a product more amenable to purification. In this regard, treatment of the crude hydrogenation product with NaOH afforded, upon workup, the alcohol **70**. Subsequent treatment of this material with triethylamine, DMAP and a solution of the mixed anhydride **18** in CH_2Cl_2[27] provided the tetrahydroeleuthoside **65**, which was readily obtained in pure form by flash chromatography (eq. 12). Analysis of the spectroscopic data recorded for **65** confirmed the structural assignment of this material. The ^1H NMR spectrum included two 1-proton doublets at δ 7.49 and 6.53, which displayed a *trans* olefinic coupling ($J = 15.6$ Hz) to one another and were thus assigned to the protons at C-3' and C-2', respectively, of the *N*-methylurocanic ester appendage. Additionally, a doublet at δ 5.83 in the ^1H NMR spectrum of **65** was attributed to the

olefinic proton at C-2. The alkene proton resonances that had appeared in the spectrum of the

acetonide **63** at δ 6.10 (H-5), 6.08 (H-6) and 5.24 (H-12), were noticeably absent in that of the

tetrahydroeleuthoside **65**. Moreover, a 3-proton doublet at δ 0.75 in the ^{1}H NMR spectrum of **65**,

replaced the C-17 methyl resonance, which had appeared as a singlet (δ 1.49) in that of **63**. The

^{1}H NMR chemical shift of the C-17 methyl group (δ 0.75) was in accordance with that of

5,6,11,12,2',3'-hexahydroeleutherobin **(60)** (δ 0.76), clearly indicating the shielding effect and,

consequently, *cis* relationship between the $\Delta^{2,3}$ olefin and C-17. The ^{13}C NMR spectrum of **65**

included the urocanate carbonyl carbon resonance at δ 167.0 and carbon resonances for the

highly shielded diastereotopic silyl methyl groups at δ -4.4 and -4.7. In addition to this spectral

data, the molecular formula of **65** was confirmed by a high resolution mass spectrometric

measurement on the molecular ion.
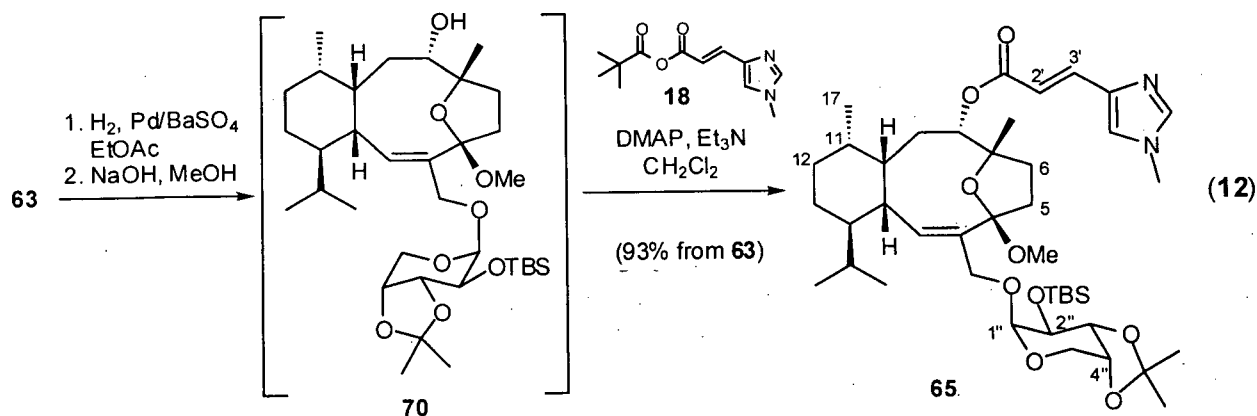
With the tetrahydroeleuthoside **65** in hand, it remained to deprotect and subsequently

acetylate the C-2" hydroxyl function of the arabinose unit. Treatment of **65** with TBAF in THF

resulted in the facile removal of the *t*-butyldimethylsilyl protecting group.[29] The resulting alcohol

71 was then directly acetylated through the action of acetic anhydride in pyridine to provide the

acetonide of 5,6,11,12-tetrahydroeleutherobin **72** in excellent yield. Spectroscopic data collected

from this substance was in accord with the assigned structure. The ^{1}H NMR spectrum of **72**

included a 3-proton singlet at δ 2.08 that could be attributed to the methyl group of the C-2"

acetate function. Additionally, a proton resonance at δ 4.89, which was coupled (J = 3.4 Hz) to

the anomeric proton (H-1", δ 4.96) could thus be assigned to H-2". The deshielding of the former

proton by the appended acyl group provided evidence that a successful acetylation of the C-2"

hydroxyl group had occurred.
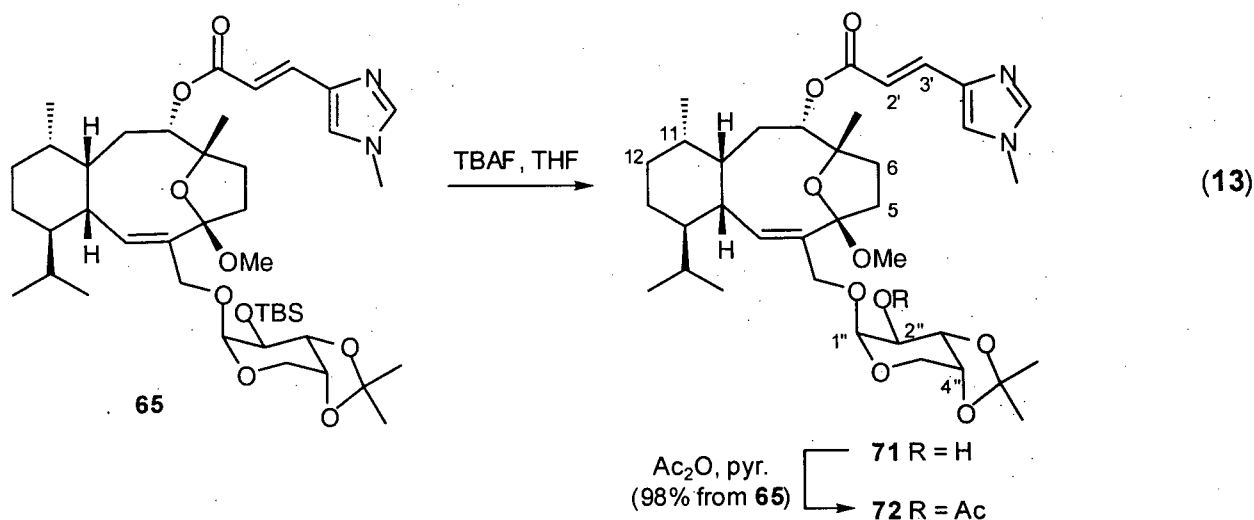
$$\text{(13)}$$

Removal of the acetonide protecting group and, consequently, completion of the

synthesis of 5,6,11,12-tetrahydroeleutherobin (61) was smoothly effected by heating a solution

of 72 in MeOH with a catalytic amount of PPTS (eq. 14).[29] In this manner, a quantity of 61

sufficient to analyze the role of the $\Delta^{11,12}$ olefin in potentiating the biological activity of the

eleuthosides was obtained. Surprisingly, in assays against MCF-7 breast cancer cells,[39] 61 (IC_{50} >

200 nM) was found to be only 10-fold less active than eleutherobin (IC_{50} = 20 nM)[17] and

consequently greater than 500-fold more active than 5,6,11,12,2',3'-hexahydroeleutherobin (60)

(IC_{50} >100,000 nM). Clearly, our hypothesis regarding the biological significance of the C-17

methyl group in determining antimitotic activity was incorrect. Moreover, this data suggested

that the dramatic decrease in biological activity observed for the hexahydroeleuthoside 60 was

due primarily to the reduction of the $\Delta^{2',3'}$ olefin. While other researchers have highlighted the

importance of the urocanate function,[30,31] the stringent requirement of the $\Delta^{2',3'}$ olefin for eleuthoside biological activity was unfounded. Confirmation of this remarkable result, however, would necessarily rely on the successful synthesis and biological evaluation of the dihydroeleuthoside **62** (Scheme 4.3).
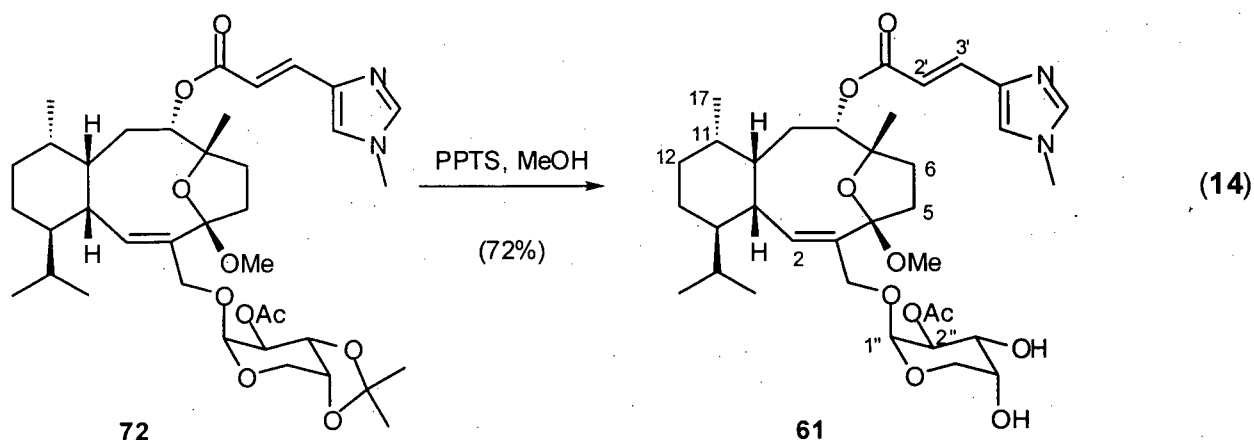
The spectroscopic data exhibited by **61** was in complete accord with the assigned structure. The ^{1}H NMR spectrum of **61** displayed resonances for the $\Delta^{2',3'}$ olefin at δ 7.49 and 6.53. Additionally, two broad singlets at δ 2.62 and 2.39 could be assigned to the hydroxyl protons on the arabinose unit. The ^{13}C NMR spectrum of **61** included two carbonyl carbon resonances at δ 171.7 and 166.9, which corresponded to the acetate and urocanate carbonyls, respectively. Comparison of the ^{1}H NMR spectra of **61** to that of eleutherobin (**8**) (Figure 4.17) confirmation that the diterpenoid core and the *N*-methyl urocanic ester were unaffected by the transformation of **72** into **61**. However, in order to confirm the structure of **61** in an unambiguous manner, a suite of spectroscopic experiments (HMQC, HMBC, 1D NOESY and COSY) was performed on this material. Analysis of the results from these experiments allowed for the complete assignment of all proton and carbon resonances (see Tables 4.6 and 4.7, Experimental). Furthermore, a series of 1D NOESY experiments proved crucial in unambiguously determining the relative configuration at C-11. Thus, in an analogous fashion to the stereochemical

assignment of the hexahydroeleuthoside **60** (Figure 4.14), irradiation of the proton resonance at δ

5.80 (H-2) resulted in enhancement of a 3-proton singlet at δ 0.78 (H-17) and visa versa.

Figure 4.16. Eleutherobin (**8**), 5,6,11,12,2',3'-hexahydroeleutherobin (**60**) and 5,6,11,12-tetrahydroeleutherobin (**61**). Concentrations in parentheses indicate the IC_{50} values for these compounds when screened against MCF-7 breast cancer cells.
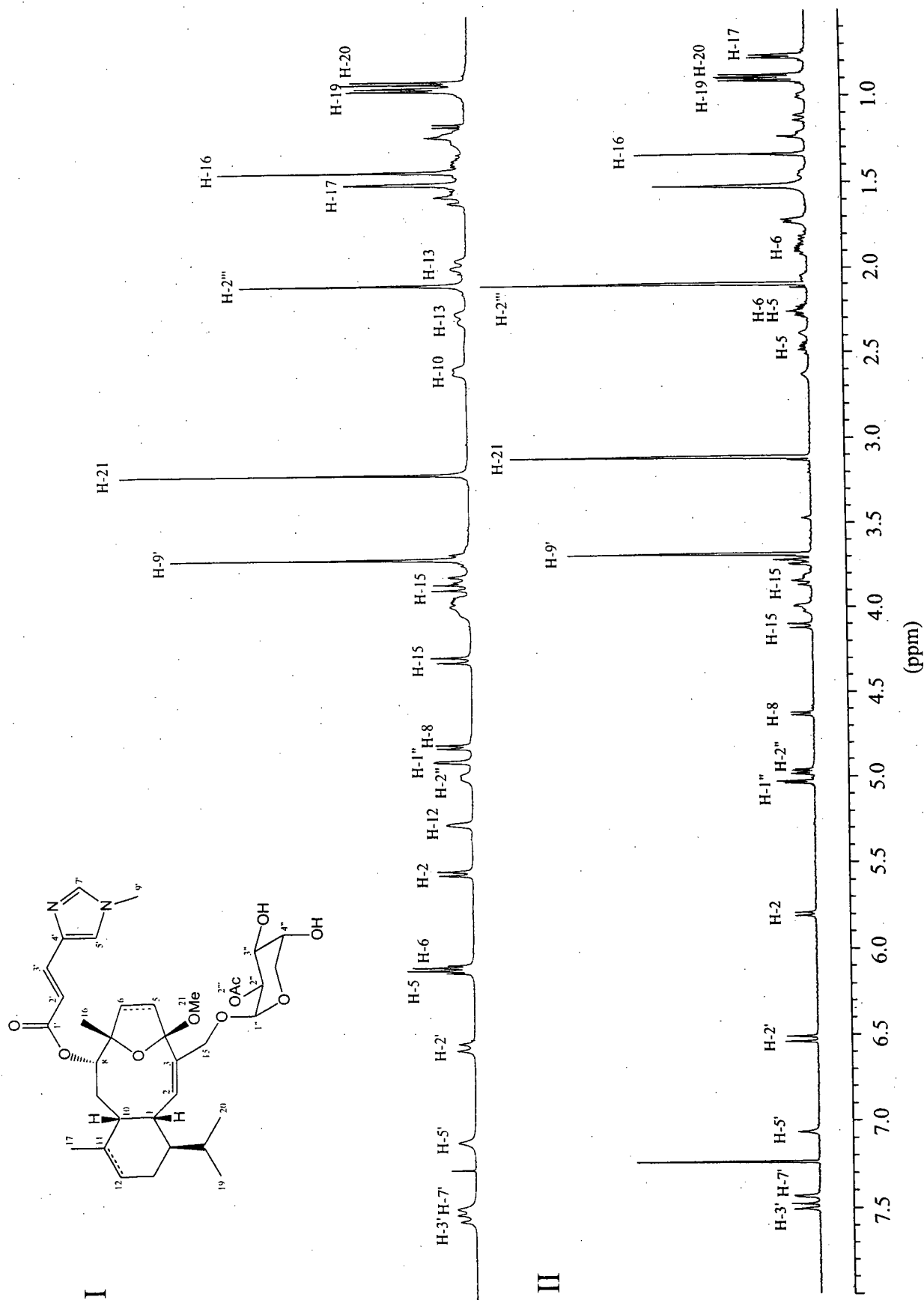
Figure 4.17. ^{1}H NMR spectra of (I) eleutherobin (**8**) recorded in CDCl$_3$ at 400 MHz and (II) 5,6,11,12-tetrahydroeleutherobin (**61**) recorded in CDCl$_3$ at 500 MHz.

62
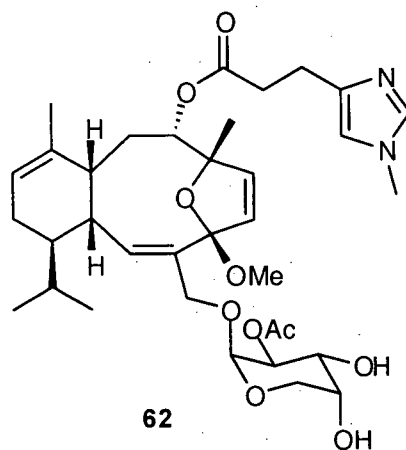
The synthesis of 2',3'-dihydroeleutherobin (**62**) followed closely the sequence of events outlined in Scheme 4.3. Therefore, it was necessary to synthesize the mixed anhydride **66**, which would eventually couple to the diterpenoid core of eleutherobin (**8**). To this end, a solution of *N*-methylurocanic acid ethyl ester (**73**)[43] in EtOAc was treated with Pd on $BaSO_4$ and stirred under an atmosphere of hydrogen (eq. 15).[27] Filtration of the crude reaction product through a plug of Celite®, concentration of the filtrate and purification of the material thus obtained by flash chromatography, afforded the dihydrourocanic ester **74**. The spectral data exhibited by this substance was in complete accord with the assigned structure. The IR spectrum displayed a strong stretching absorption at 1729 cm^{-1} for the ester carbonyl. The ^1H NMR spectrum included two aromatic proton resonances at δ 7.15 and 6.48, which corresponded to the imidazole protons at C-7 and C-5, respectively. Additionally, two 2-proton triplets in the ^1H NMR spectrum of **74** at δ 2.70 and 2.49 could be assigned to the protons at C-2 and C-3. The ^{13}C NMR spectrum included a carbonyl carbon resonance at δ 172.9 and three aromatic carbon resonances at 141.1, 136.8 and 116.1 for the imidazole fragment.

Unfortunately, although hydrolysis of the ester function in **74** provided the corresponding acid **75** in good yield, this substance was very difficult to cope with experimentally. Furthermore, owing to the sparingly soluble nature of **75** in organic solvents, all attempts to construct the desired mixed anhydride from this material were fraught with difficulty.

Danishefsky and co-workers have demonstrated that N-methylurocanic acid also couples efficiently to the C-8 hydroxyl function on the diterpenoid core of eleutherobin (**8**) through the agency of dicyclohexylcarbodiimide (DCC) and DMAP in $CHCl_3$.[29] Motivated by this report, it was anticipated that a similar reaction involving 2,3-dihydro-N-methylurocanic acid (**75**) would yield access to the desired dihydroeleuthoside **67**. Thus, treatment of the ethyl ester **74** with 1.1 equivalents of LiOH in THF and H_2O followed by careful neutralization of the reaction mixture with 1N HCl provided the carboxylic acid **75** (eq. 15). Removal of solvents under reduced pressure afforded a mixture of the desired urocanic acid **75** and LiCl, which was used in the coupling reaction (*vide infra*) without further purification.
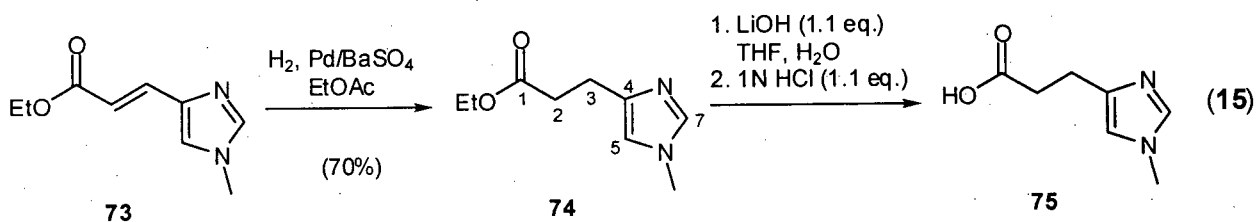
With the requisite dihydrourocanic acid **75** in hand, we turned our attention to the hydrolysis of the ester function in the eleuthoside **63**. To this end, treatment of **63** with excess NaOH in MeOH resulted in the smooth cleavage of the N-methylurocanic ester from the diterpenoid core (eq. 16). After considerable experimentation, it could be shown that a modification of the procedure reported by Danishefsky and co-workers[29] provided access to the desired dihydroeleuthoside **67**. Thus, the addition of a solution of DMAP, DCC and an excess of the dihydrourocanic acid **75** in *DMF* to the crude alcohol **76**, afforded the dihydro eleuthoside **67** in excellent yield (eq. 16). The spectroscopic data exhibited by this material was in accord with the assigned structure. The ^{1}H NMR spectrum included resonances corresponding to the protons at C-7' and C-5' of the imidazole ring at δ 7.30 and 6.63, respectively. Additionally, two 2-proton multiplets at δ 2.87 and 2.69 could be assigned to the protons at C-2' and C-3' of the

reduced urocanic ester moiety. The ^{13}C NMR spectrum of **67** included one carbonyl carbon resonance at δ 172.4 and additional resonances that were assigned to the C-4 ketal carbon at δ 116.5, the ispropylidene O-C-O carbon at δ 116.0 and the anomeric carbon (C-1") at δ 97.7.
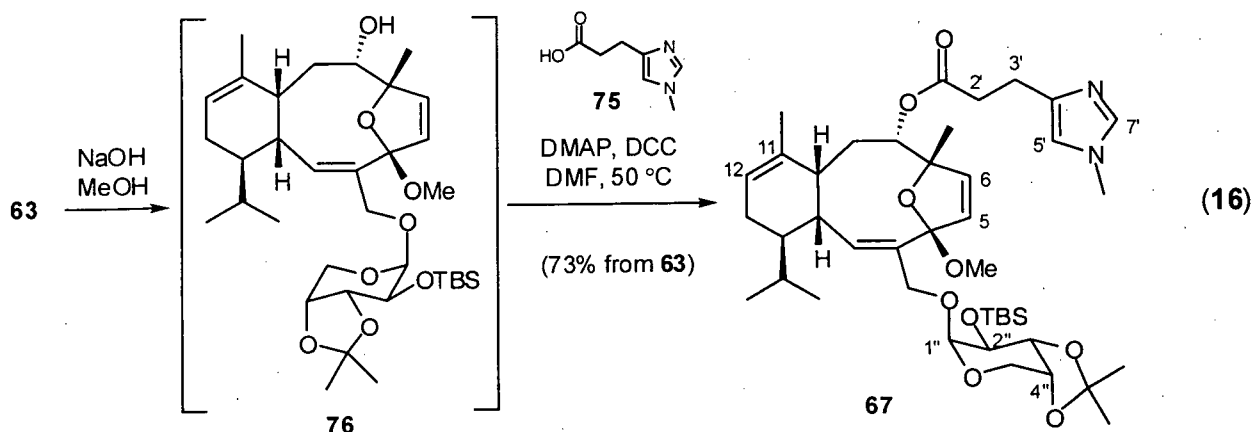
With the key coupling reaction successfully accomplished, it was pivotal to effect the deprotection and subsequent acetylation of the C-2" hydroxyl function in the dihydroeleuthoside **67**. In this regard, treatment of **67** with TBAF in THF resulted in the facile removal of the *t*-butyldimethylsilyl protecting group (eq. 17). The resulting alcohol **77** was then directly acetylated by the action of acetic anhydride in pyridine, to provide the acetonide of 2',3'-dihydroeleutherobin **78** in excellent yield. The spectroscopic data exhibited by this substance was in accord with the proposed structure. The ^{1}H NMR spectrum included a 3-proton singlet at δ 2.04 that was assigned to the methyl group of the C-2" acetate function. Additionally, a proton resonance at δ 4.88, which displayed coupling to the anomeric proton (H-1") at δ 4.79, could thus be assigned to H-2". The deshielding of the former proton by the appended acetate group provided further evidence that successful acetylation of the C-2" alcohol had occurred.
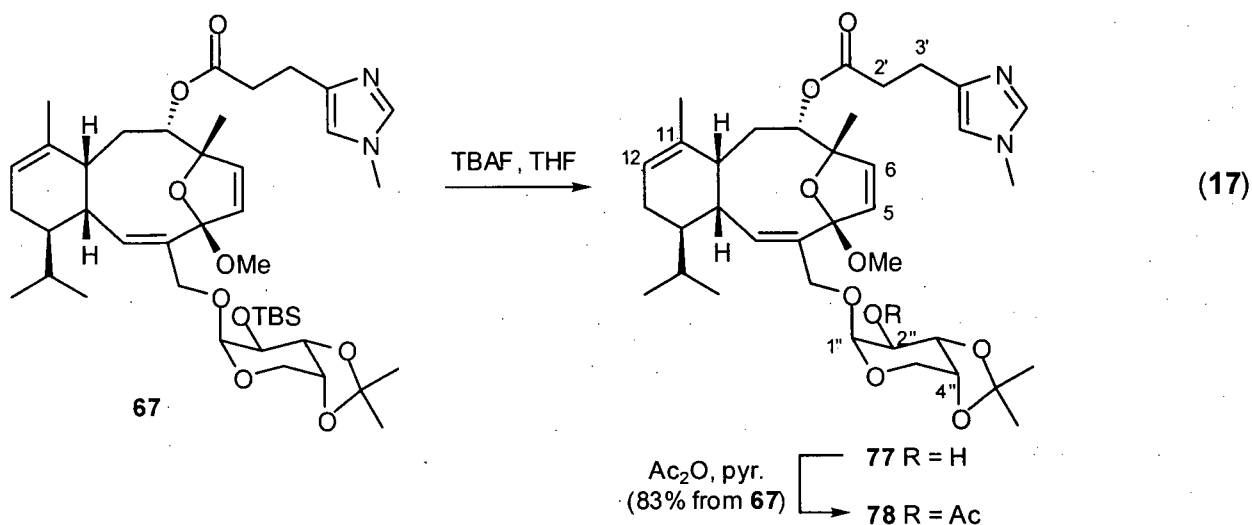
Removal of the acetonide protecting group and, consequently, completion of the synthesis of 2',3'-dihydroeleutherobin (62) was effected by heating a solution of the eleuthoside 78 in MeOH with a catalytic amount of PPTS (eq. 18).[29] Unfortunately, while the removal of the acetonide moiety had proceeded smoothly in the synthesis of 5,6,11,12-tetrahydroeleutherobin (61) (*vide supra*), treatment of the acetonide 78 in the same manner resulted in the production of 62 along with two byproducts. Analysis of the ^{1}H NMR spectrum of the crude reaction mixture, indicated that the byproducts were in fact isomers of the desired eleuthoside, in which the acetate function had migrated to the C-3" or C-4" hydroxyl groups on the arabinose unit. Fortunately, these substances were separable from 2',3'-dihydroelutherobin (62) by normal phase HPLC. In this manner the synthesis of 62 was completed and a quantity of this material sufficient to analyze the role played by the $\Delta^{2',3'}$ olefin in potentiating the antimitotic activity of the eleuthosides was obtained. As anticipated, in assays against MCF-7 breast cancer cells,[39] 62 (IC$_{50}$ = 20,000 nM) was found to be 1000-fold less active than eleutherobin (8) (IC$_{50}$ = 20 nM)[17] and, consequently, similar in activity to 5,6,11,12,2',3'-hexahydroeleutherobin (60) (IC$_{50}$ >100,000 nM) (Figure 4.18). These results confirmed our hypothesis regarding the significance of the $\Delta^{2',3'}$ olefin in mediating the antimitotic activity of the eleuthosides. The remarkable inactivity of

2',3'-dihydroeleutherobin (**62**) in the cell-based antimitotic assay was mirrored by the complete inability of this substance to promote the polymerization of purified bovine tubulin in a standard *in vitro* assay (Figure 4.19).[39]
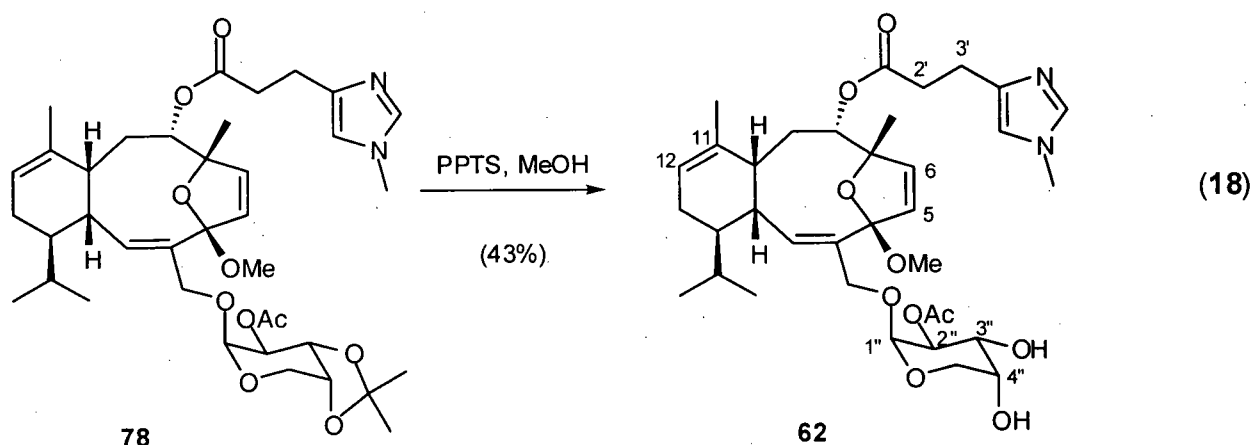
The spectroscopic data exhibited by **62** was in complete accord with the assigned structure. The ^{1}H NMR spectrum of **62** (Figure 4.20) displayed resonances for the $\Delta^{5,6}$ olefin at δ 6.07 (H-5) and 5.99 (H-6) and the $\Delta^{11,12}$ olefin at δ 5.26 (H-12). A resonance at δ 4.95 in the ^{1}H NMR spectrum of **62** displayed vicinal coupling ($J = 3.3$ Hz) with the anomeric proton (H-1") at δ 4.87 and was thus assigned to H-2". The large chemical shift of H-2" proton resonance supported the assignment of the appended acetate at C-2". Owing in large part to the acetate isomerization side reactions, which had accompanied the formation of **62**, the amount of 2',3'-dihydroeleutherobin (**62**) produced from the final deprotection reaction was insufficient to directly acquire a ^{13}C NMR spectrum. However, analysis of the results from a combination of HMQC and HMBC experiments allowed for the inverse detection and subsequent assignment of most of the carbon resonances. That the diterpenoid core and dihydrourocanic ester appendage were unaffected by the transformation of **78** into **62** was ascertained by the comparison of ^{1}H NMR spectra of 2',3'-dihydroeleutherobin (**62**) and eleutherobin (**8**) (Figure 4.20).
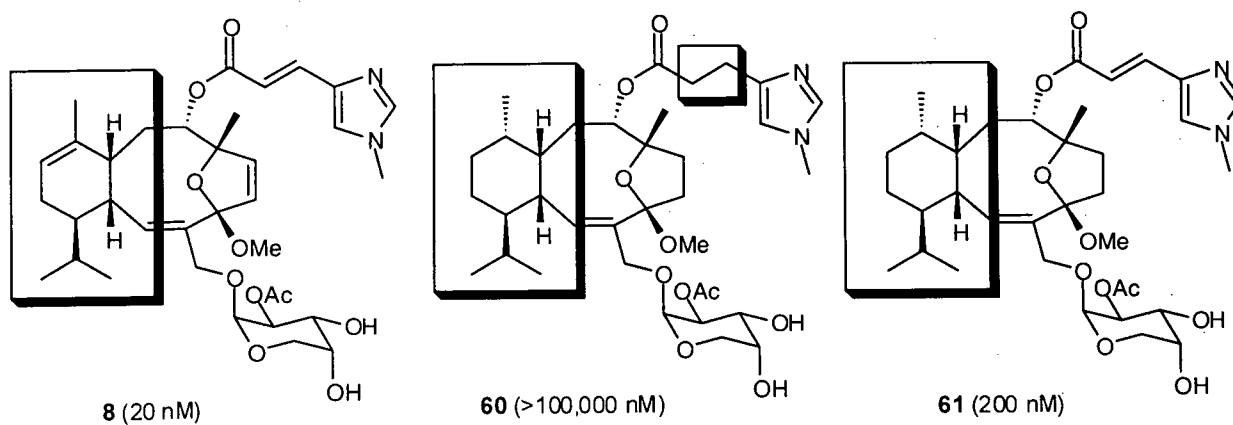
8 (20 nM)   60 (>100,000 nM)   62 (20,000 nM)
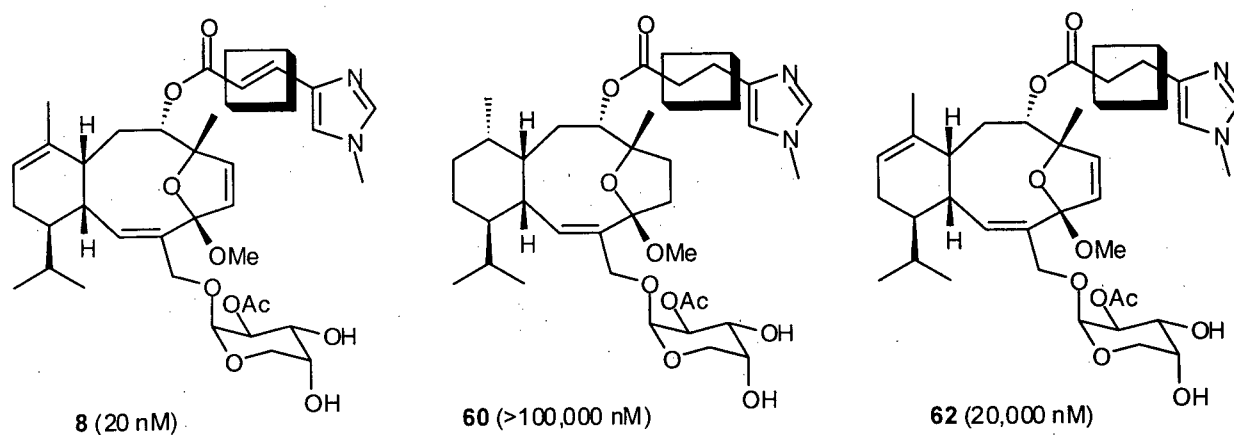
Figure 4.18. Eleutherobin (**8**), 5,6,11,12,2',3'-hexahydroeleutherobin (**60**) and 2',3'-dihydroeleutherobin (**62**). Concentrations in parentheses indicate the IC_{50} values for these compounds when screened against MCF-7 breast cancer cells.
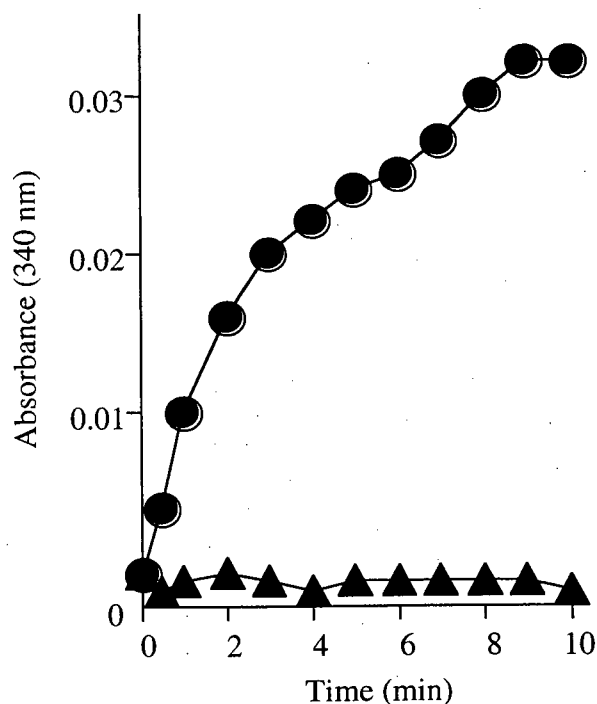
Figure 4.19. Microtubule stabilizing activity of eleutherobin ● (**8**) and 2',3'-dihydroeleutherobin ▲ (**62**). The ability of these substances to promote the polymerization of bovine tubulin is measured at 340 nm by the change in turbidity of microtubule protein.
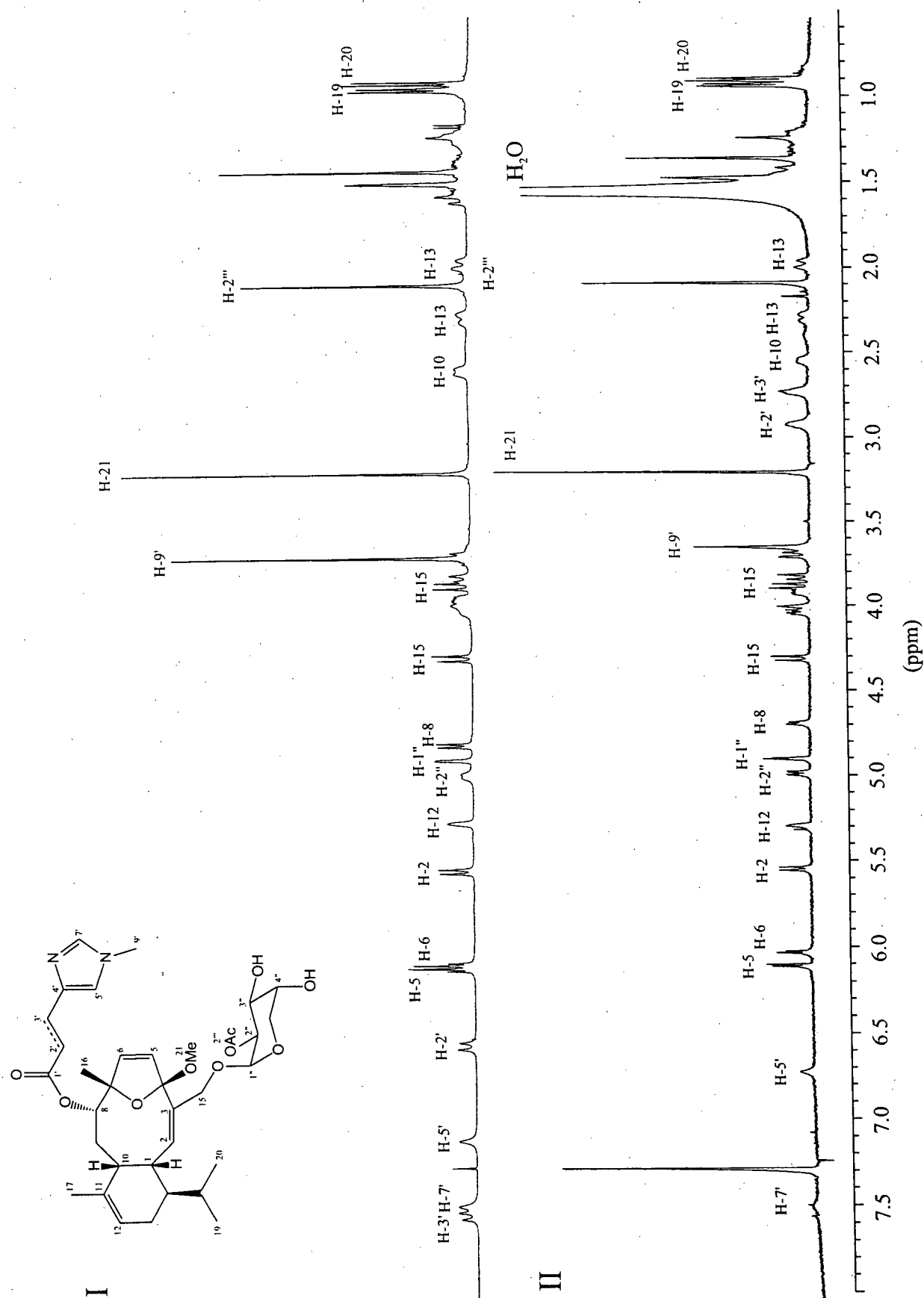
Figure 4.20. ^{1}H NMR spectra of (I) eleutherobin (**8**) recorded in CDCl$_3$ at 400 MHz and (II) 2',3'-dihydroeleutherobin (**62**) recorded in CDCl$_3$ at 500 MHz.

4.4 Conclusions

The Caribbean gorgonian *Erythropodium caribaeorum* is well known to produce a variety of diterpenoid secondary metabolites that inhibit mitosis.[35] Fractionation of the MeOH extract of *E. caribaeorum*, collected off the northwest coast of Dominica, led to the isolation of the known antimitotic agents sarcodictyin A (**4**),[12] eleutherobin (**8**),[17] desmethyleleutherobin (**32**) and *Z*-eleutherobin (**31**)[35] (Figure 4.21). Additionally, two novel diterpenoids, methylcaribaeorane (**35**) and the eleutherobin aglycon (**34**) were isolated from the non polar, sarcodictyin containing fractions of this extract. It was shown that the eleuthosides which possess a C-4 methyl ketal are in fact artifacts of the corresponding hemiketal natural product, generated during the MeOH extraction procedure. Thus, the novel hemiketal diterpenoids 15-hydroxy caribaeorane (**36**) and caribaeorane (**37**) are proposed to be early intermediates in the biogenesis of the sarcodictyins (e.g. **4**) and the eleuthosides (e.g. **32**). Moreover, the presence of **36** and **37** in the extracts of *E. caribaeorum* indicates that, biosynthetically, the *N*-methylurocanic ester is appended to the diterpenoid core of the latter substances prior to functionalization of C-15.
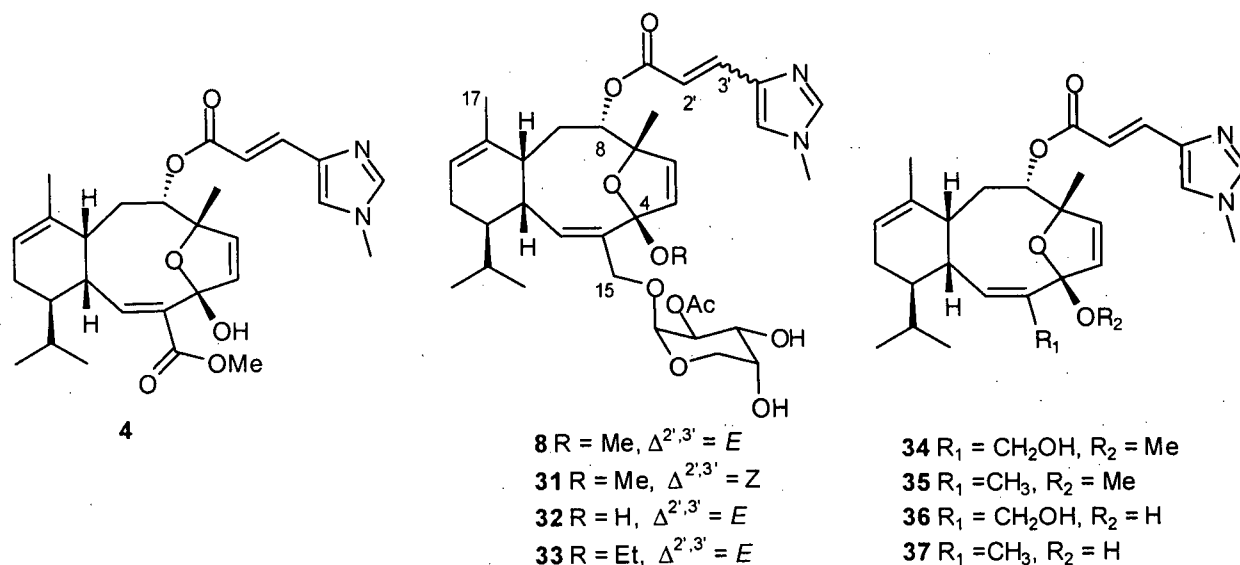
Figure 4.21. Antimitotic diterpenes from *E. caribaeorum.*

Having secured quantities of eleutherobin (**8**) and desmethyleleutherobin (**32**) sufficient to explore synthetic transformations of these substances, an investigation along this vein was initiated. The results gathered from this pursuit indicated that, with respect to antimitotic activity, a broad tolerance exists for substitutions at the C-4 ketal center of the eleuthosides. Additionally, while it has been proposed that the cyclohexene ring and its appended substituents constitute a crucial hydrophobic binding region of the eleuthosides,[33] the introduction of polar functionality at C-17 had a minimal effect on the biological activity of this substance.

A series of hydrogenated eleuthosides highlighted the significant role played by the $\Delta^{2',3'}$ olefinic function in potentiating antimitotic activity. Thus, hydrogenation of eleutherobin provided the hexahydroeleuthoside **60** (Figure 4.22), which was inactive in a cell based assay for antimitotic agents. The tetrahydroeleuthoside **61** and the dihydroeleuthoside **62** were procured through a series of synthetic transformations that originated with eleutherobin (**8**). Although, to a large extent, the tetrahydroeleuthoside **61** retained the biological activity of the parent compound **8**, remarkably the dihydroeleuthoside **62** was practically inactive (Figure 4.23).
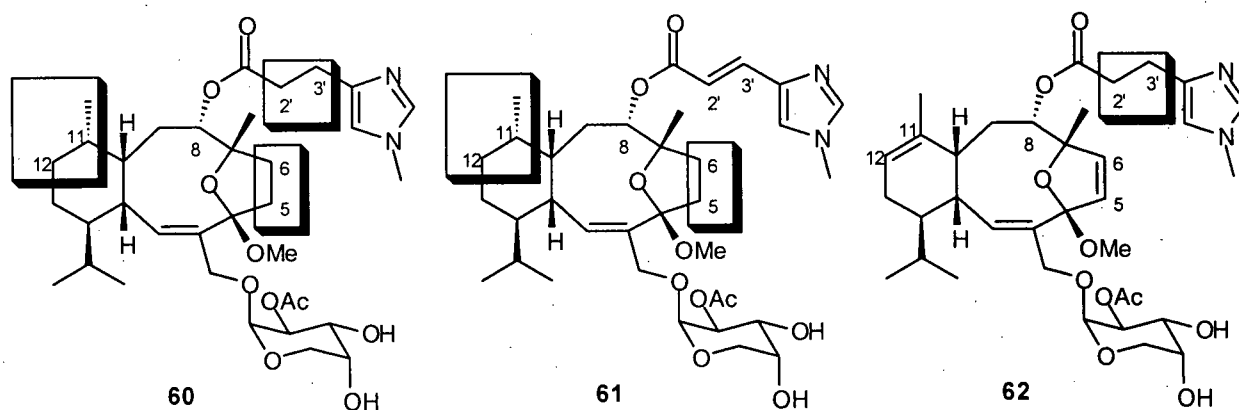
Figure 4.22. Selectively hydrogenated eleuthosides.
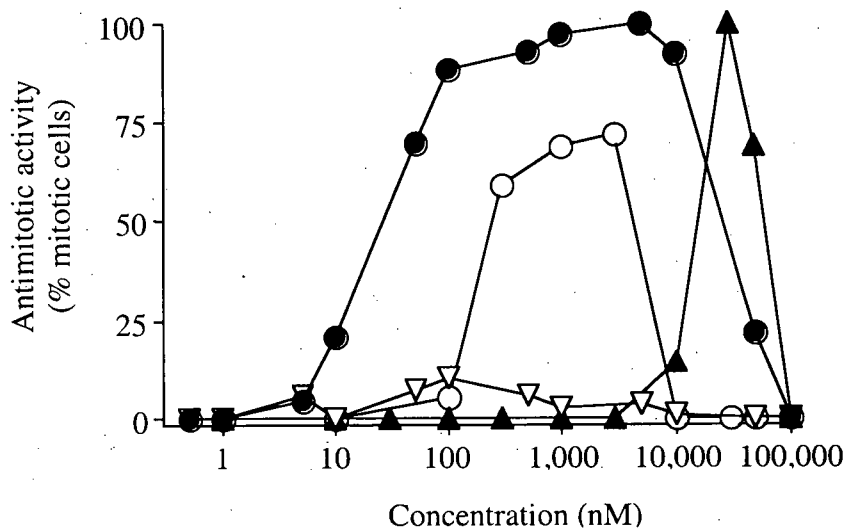
Figure 4.23. Antimitotic activity of (●) eleutherobin (**8**), (○) tetrahydroeleutherobin (**61**), (▲) dihydroeleutherobin (**62**) and (▽) hexahydroeleutherobin (**60**).

The pharmacophore models put forward to date have all suggested that the C-8 urocanic ester in the eleuthosides is important for their binding to tubulin,[30,31] however, the remarkably stringent requirement for the $\Delta^{2',3'}$ olefin of the urocanic ester function was unanticipated. From this result, it may be proposed that the binding of the eleuthosides to tubulin, and consequently their agency as antimitotic substances, relies heavily on interactions between the *N*-methylurocanic ester appendage and residues present in the taxol binding site on tubulin. Clearly, the flexibility and/or loss of conjugation in this appendage afforded by the reduction of the $\Delta^{2',3'}$ olefin, severely hinders the biological activity of these substances. This important feature of eleuthoside binding, along with the observed tolerance for the oxygenation at C-17 and substitutions at C-4, will have to be accommodated in future iterations of the pharmacophore models.

4.5 Experimental

For General Experimental, see Section 2.5.

<u>Isolation Procedure A (MeOH extracts).</u>

Samples of *Erythropodium caribaeorum* (6.4 kg wet weight) were collected off Prince Rupert Point, Dominica in September of 2000 using SCUBA at depths of 3-5 meters. The samples were frozen in Dominica at Ross University and transported back to the University of British Columbia in coolers packed with dry ice. The frozen material was placed in 4 large erlenmeyer flasks (2L) and immersed in MeOH (4 x 1.8 L). The MeOH was decanted after 24 hours and the soft-coral was immersed in fresh MeOH. The first MeOH extract was concentrated under reduced pressure to provide an orange residue. The residue was dissolved in EtOAc (250 mL) and H_2O (250 mL) and the phases were separated. The aqueous phase was then extracted with EtOAc (5 x 250 mL) and the combined organic phases were concentrated under reduced pressure. The resulting organic residue was dissolved in MeOH - H_2O (9:1, 250 mL) and extracted with hexane (100 mL). The MeOH - H_2O phase was then concentrated to provide a brown gum (33.3 g) and the hexane phase was concentrated to provide a brown oil (10 g). Following the above procedure, a second, third, fourth and fifth MeOH extract of the soft-coral provided 20.0 g, 14.3 g, 4.5 g and 2.0 g respectively from the MeOH - H_2O phase (total weight 74.1 g) and a total of 35.0 g from the hexane phase (total weight 45.0 g).

The brown gum derived from the first MeOH extract (33.3 g) was placed on a large column of silica gel (400 g) and the least polar compounds in the mixture were eluted with EtOAc (1.5 L). Eleutherobin and its analogues were then eluted with EtOAc - MeOH (17:3, 1 L) followed by EtOAc - MeOH (1:1, 1 L). Concentration of the combined EtOAc - MeOH filtrates provided 1.3

g of a crude, dark green oil. Fractionation of this oil by flash chromatography (100 g of silica gel) eluting with CH_2Cl_2 - MeOH (95:5, 1 L) then CH_2Cl_2 - MeOH (85:5, 250 mL) then CH_2Cl_2 - MeOH (11:9, 250 mL) provided 6 groups of fractions (from least to most polar): 8A (120 mg), 8B (81 mg), 8C (150 mg), 8D (171 mg), 8E (189 mg) and 8F (93 mg).

The components of fraction 8A were purified by flash chromatography (25 g of silica gel, 25:1 CH_2Cl_2 - MeOH) to provide 3 groups of fractions (from least to most polar): 8A-1 (15 mg), 8A-2 (40 mg) and 8A-3 (40 mg).

Purification of methylcaribaeorane (35) (R_F = 0.5, 50:1 CH_2Cl_2 - MeOH) from fraction 8A-1 by flash chromatography (15 g of silica gel, 50:1 CH_2Cl_2 - MeOH) provided, upon combination and concentration of the appropriate fractions, a residue which was further purified by flash chromatography (15 g of silica gel, 5:1 CH_2Cl_2 - MeCN). Final purification was achieved by normal phase HPLC (radial pac column, 85:15 CH_2Cl_2 - MeCN, 2 mL/minute, monitor at 230 nm, retention time 13 minutes) to provide 5 mg (0.00008% wet weight) of methylcaribaeorane (35) as a colorless solid which decomposed in $CDCl_3$ on standing. See below for spectral data.

Purification of eleutherobin aglycon (34) (R_F = 0.4, 50:1 CH_2Cl_2 - MeOH) from fraction 8A-2 by flash chromatography (15 g of silica gel, 50:1 CH_2Cl_2 - MeOH) provided, upon combination and concentration of the appropriate fractions, a residue which was further purified by flash chromatography (15 g of silica gel, 97:3 EtOAc - MeOH) to provide 25 mg (0.00039% wet weight) of eleutherobin aglycon (34) as a colorless solid ($[\alpha]_D$ −24.2). Spectral data (see below) was in accordance to that reported in the literature.[26]

Purification of sarcodictyin A (4) (R_F = 0.3, 50:1 CH_2Cl_2 - MeOH) from fraction 8A-3 by flash chromatography (15 g of silica gel, EtOAc) provided, upon combination and concentration of the appropriate fractions 30 mg (0.00031% wet weight) of sarcodictyin A (4) as a colorless solid. The spectroscopic data (^{1}H NMR, ^{13}C NMR) and HRFABMS (M+H) acquired from sarcodictyin A (4) was in accordance with that reported in the literature.[12]

The components of fraction 8C and 8D were combined and purified by flash chromatography (25 g of silica gel, 92:8 CH_2Cl_2 - MeOH) to provide 2 groups of fractions (from least to most polar): 8C-1 (80 mg) and 8C-2 (80 mg).

Purification of eleutherobin (**8**) (R_F = 0.25, 9:1 EtOAc - MeOH) and Z-eleutherobin (R_F = 0.3, 9:1 EtOAc - MeOH) from fraction 8C-1 by flash chromatography (15 g of silica gel, 92:8 CH_2Cl_2 - MeOH) provided, upon combination and concentration of the appropriate fractions, a residue which was further purified by flash chromatography (15 g of silica gel, 93:7 EtOAc - MeOH) to provide 50 mg (0.00078% wet weight) of eleutherobin (**8**) as a colorless solid and 7 mg (0.00011% wet weight) of Z-eleutherobin (**31**) as a colorless solid. The spectroscopic data (^{1}H NMR, ^{13}C NMR) and HRFABMS (M+H) acquired from eleutherobin (**8**) and Z-eleutherobin (**31**) were in accordance with that reported in the literature.[17,35]

Purification of desmethyleleutherobin (**32**) (R_F = 0.2, 10:1 CH_2Cl_2 - MeOH) from fraction 8C-2 by flash chromatography (15 g of silica gel, 9:1 CH_2Cl_2 - MeOH) provided, upon combination and concentration of the appropriate fractions, a residue which was further purified by flash chromatography (15 g of silica gel, 9:1 EtOAc - MeOH) to provide 40 mg (0.00063% wet weight) of desmethyleleutherobin (**32**) as a colorless solid. The spectroscopic data (^{1}H NMR, ^{13}C NMR) and HRFABMS (M+H) acquired from desmethyleleutherobin (**32**) was in accordance with that reported in the literature.[35]

Isolation Procedure B (EtOH extracts).

A small amount of the frozen soft-coral *Erythropodium caribaeorum* (68 g) was placed in an erlenmeyer flask (250 mL) and immersed in EtOH (250 mL). The EtOH was decanted after 24 hours and the soft-coral was immersed in fresh EtOH. After 4 additional EtOH extractions of the soft-coral, the combined EtOH extracts were concentrated under reduced pressure to provide an

orange residue. The residue was dissolved in EtOAc (25 mL) and H_2O (25 mL) and the phases were separated. The aqueous phase was extracted with EtOAc (5 x 25 mL) and the combined organic phases were concentrated under reduced pressure. The resulting residue was placed on a column of silica gel (40 g) and the least polar compounds in the mixture were eluted with EtOAc (250 mL). The ethyl ketal of eleutherobin **33** and its analogues were eluted with CH_2Cl_2 - EtOH (9:1, 100 mL) followed by CH_2Cl_2 - EtOH (5:1, 100 mL). Fractions with similar TLC characteristics (R_F = 0.4, 9:1 CH_2Cl_2 - MeOH) to eleutherobin were combined and concentrated to provide 2 mg of a residue that contained the ethyl ketal of eleutherobin **33** as its major constituent (approx. 60% pure). Purification of crude ethyl ketal of eleutherobin **33** by flash chromatography (15 g of silica gel, 9:1 EtOAc - EtOH) provided 1 mg of pure **33** (0.0015% wet weight) (see below for spectral data).

Methylcaribaeorane (**35**):
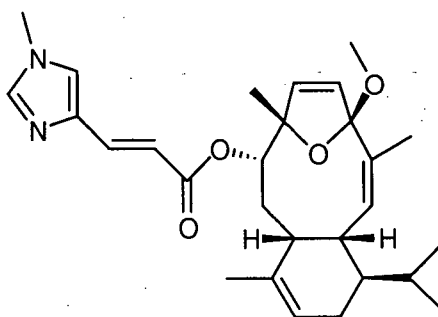
^{1}H-NMR (C_6D_6, 500 MHz) δ 7.95 (d, 1H, J = 15.4 Hz, H-3'), 7.26 (d, 1H, J = 15.4 Hz, H-2'), 6.72 (s, 1H, H-7'), 6.00 (s, 1H, H-5'), 5.95 (d, 1H, J = 5.8 Hz, H-6), 5.78 (d, 1H, J = 5.8 Hz, H-5), 5.49 (d, 1H, J = 9.7 Hz, H-2), 5.33 (m, 1H, H-12), 5.25 (d, 1H, J = 7.3 Hz, H-8), 4.30 (m, 1H, H-1), 3.18 (s, 3H, H-21), 2.95 (m, 1H, H-10), 2.37 (m, 1H, H-13), 2.25 (s, 3H, H-9'), 2.00 (m, 1H, H-9), 1.98 (m, 1H, H-13), 1.81 (m, 1H, H-9), 1.80 (s, 3H, H-15), 1.65 (s, 3H, H-17),

1.57 (m, 1H, H-18), 1.46 (s, 3H, H-16), 1.28 (m, 1H, H-14), 1.06 (d, 3H, J = 6.5 Hz, H-19), 0.89 (d, 3H, J = 6.5 Hz, H-20).

^{13}C-NMR (C$_6$D$_6$, 100.5 MHz) δ 167.1 (C-1'), 139.2 (C-4'), 139.2 (C-7'), 137.3 (C-3'), 134.9 (C-11), 134.8 (C-6), 134.0 (C-3), 131.3 (C-2), 130.1 (C-5), 122.6 (C-5'), 121.6 (C-12), 117.4 (C-4), 116.5 (C-2'), 90.5 (C-7), 82.2 (C-8), 49.5 (C-21), 43.3 (C-14), 39.6 (C-10), 34.6 (C-1), 32.3 (C-9), 31.9 (C-9'), 29.4 (C-18), 24.9 (C-16), 24.8 (C-13), 22.4 (C-15), 22.3 (C-17), 22.2 (C-20), 20.8 (C-19).

Exact mass calcd for C$_{28}$H$_{39}$O$_4$N$_2$ (HRFABMS, M+H): 467.2910; found: 467.2912.

The assignment of proton and carbon resonances observed in the ^{1}H and ^{13}C NMR spectra of methylcaribaeorane (**35**) are summarized in Tables 4.3 and 4.4. The assignments are based on the analysis of HMQC (Table 4.3), HMBC (Table 4.3), 1D-NOESY (Table 4.4) and 1D-TOCSY (Table 4.4) data.

Table 4.3. NMR data for methylcaribaeorane (**35**) (recorded in C_6D_6).
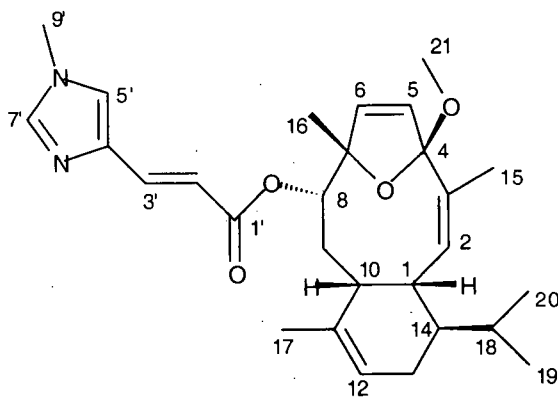
Carbon No.	^{13}C δ (ppm)[a]	^1H δ (ppm) (mult, J (Hz))[b,c]	HMBC[b]
1	34.6	4.30 (m)	H-9, H-13
2	131.3	5.49 (d, 9.7)	H-15
3	134.0		H-15
4	117.4		H-2, H-5, H-6, H-15, H-21
5	130.1	5.78 (d, 5.8)	
6	134.8	5.95 (d, 5.8)	H-8, H-16
7	90.5		H-5, H-6, H-8, H-9, H-16
8	82.2	5.25 (d, 7.3)	H-9, H-16
9	32.3	2.00 (m), 1.81 (m)	
10	39.6	2.95 (m)	H-8, H-9, H-17
11	134.9		H-17
12	121.6	5.33 (m)	H-17
13	24.8	2.37 (m), 1.98 (m)	
14	43.3	1.28 (m)	H-19, H-20
15	22.4	1.80 (s)	H-2
16	24.9	1.46 (s)	H-8
17	22.3	1.65 (s)	
18	29.4	1.57 (m)	H-19, H-20
19	20.8	1.06 (d, 6.5)	H-20
20	22.2	0.89 (d, 6.5)	H-19
21	49.5	3.18 (s)	
1'	167.1		H-8, H-3'
2'	116.5	7.26 (d, 15.4)	
3'	137.3	7.95 (d, 15.4)	
4'	139.2		H-2', H-5'
5'	122.6	6.00 (s)	H-9'
7'	139.2	6.72 (s)	H-5', H-9'
9'	31.9	2.25 (s)	

[a] Recorded at 100.5 MHz. [b] Recorded at 500 MHz. [c] Assignments based on HMQC data.

Table 4.4. NMR data for methylcaribaeorane (**35**) (recorded in C_6D_6).
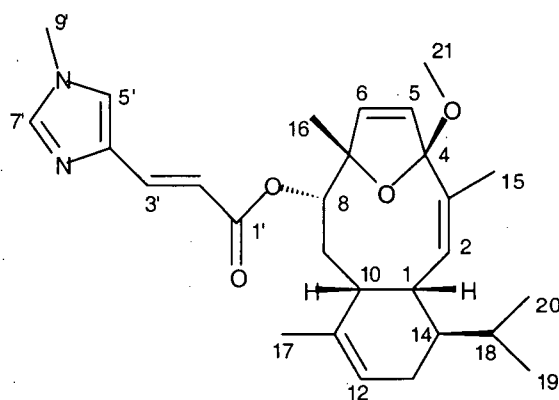
Proton No.	^1H δ (ppm) (mult, J (Hz))[a]	NOE[b]	1D-TOCSY[c]
1	4.30 (m)	H-10, H-19	H-2, H-10
2	5.49 (d, 9.7)	H-13, H-14, H-15	
3			
4			
5	5.78 (d, 5.8)		
6	5.95 (d, 5.8)		
7			
8	5.25 (d, 7.3)		H-9, H-10
9	2.00 (m), 1.81 (m)		
10	2.95 (m)		
11			
12	5.33 (m)		H-10, H-13, H-14, H-17
13	2.37 (m), 1.98 (m)		
14	1.28 (m)		
15	1.80 (s)	H-2, H-5	
16	1.46 (s)		
17	1.65 (s)		
18	1.57 (m)		
19	1.06 (d, 6.5)		
20	0.89 (d, 6.5)		
21	3.18 (s)		
1'			
2'	7.26 (d, 15.4)		
3'	7.95 (d, 15.4)		
4'			
5'	6.00 (s)		
7'	6.72 (s)		
9'	2.25 (s)		

[a] Recorded at 500 MHz. [b] Recorded as NOE difference at 400 MHz using 1D selective NOE experiments. [c] Recorded at 400 MHz using 1D selective TOCSY experiments.

Eleutherobin aglycon (**34**):
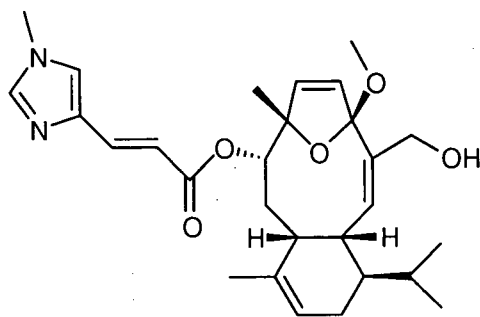
^{1}H-NMR (CDCl$_3$, 400 MHz) δ 7.52 (d, 1H, J = 15.4 Hz, H-3'), 7.45 (s, 1H, H-7'), 7.08 (s, 1H, H-5'), 6.54 (d, 1H, J = 15.4 Hz, H-2'), 6.21 (d, 1H, J = 6.0 Hz, H-6), 6.02 (d, 1H, J = 6.0 Hz, H-5), 5.56 (d, 1H, J = 9.4 Hz, H-2), 5.25 (m, 1H, H-12), 4.80 (d, 1H, J = 7.4 Hz, H-8), 4.16 (d, 1H, J = 12.0 Hz, H-15), 3.85-3.95 (m, 2H, H-1, H-15), 3.69 (s, 3H, H-21), 3.23 (s, 3H, H-9'), 2.67 (m, 1H, OH), 2.59 (m, 1H, H-10), 2.31 (m, 1H, H-13), 1.98 (m, 1H, H-13), 1.50-1.65 (m, 2H, H-9, H-18), 1.50 (s, 3H, H-17), 1.45 (s, 3H, H-16), 1.25-1.40 (m, 2H, H-9, H-14), 0.97 (d, 3H, J = 6.5 Hz, H-19), 0.91 (d, 3H, J = 6.5 Hz, H-20).

^{13}C-NMR (CDCl$_3$, 100.5 MHz) δ 166.7, 139.2, 138.5, 136.8, 136.4, 135.7, 135.1, 134.1, 129.2, 122.7, 121.4, 117.1, 116.0, 90.4, 81.5, 67.4, 49.6, 42.1, 38.7, 33.9, 33.6, 31.5, 29.0, 24.3, 23.9, 22.2, 22.1, 20.5.

Exact mass calcd for C$_{28}$H$_{39}$O$_5$N$_2$ (HRFABMS, M+H): 483.2859; found: 483.2860.

Preparation of the desurocanate methylcaribaeorane **40.**
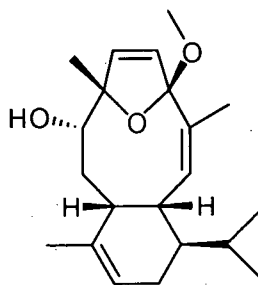
To a stirred solution of methylcaribaeorane (**35**) (1.0 mg, 0.002 mmol) in MeOH (1.0 mL) at room temperature, was added a solution of aqueous NaOH (5N, 50 μL, 0.25 mmol) and the reaction mixture was stirred overnight. The reaction mixture was then diluted with H_2O (10 mL) and EtOAc (10 mL) and the phases were separated. The aqueous phase was extracted with EtOAc (2 x 10 mL) and the combined organic phases were dried ($MgSO_4$) and concentrated under reduced pressure. Purification of the crude product by flash chromatography (15 g of silica gel, 4:1 hexane - EtOAc) and removal of trace amounts of solvent from the resulting solid provided 0.6 mg (90%) of the desurocanate methylcaribaeorane **40** as a colorless solid which readily decomposed on standing in $CDCl_3$.

^{1}H-NMR (C_6D_6, 400 MHz) δ 5.99 (d, 1H, J = 5.9 Hz, H-6), 5.74 (d, 1H, J = 5.9 Hz, H-5), 5.41 (dd, 1H, J = 9.3, 1.3 Hz, H-2), 5.36 (m, 1H, H-12), 4.15 (m, 1H, H-1), 3.47 (m, 1H, H-8), 3.19 (s, 3H, H-21), 2.35 (m, 1H, H-10), 2.28 (m, 1H, H-13), 1.97 (m, 1H, H-13), 1.80 (s, 3H, H-15), 1.62 (s, 3H, H-17), 1.50 (s, 3H, H-16), 1.50-1.72 (m, 4H, H-9, H-18, H-14, OH), 1.27 (m, 1H, H-9), 0.98 (d, 3H, J = 6.5 Hz, H-19), 0.93 (d, 3H, J = 6.5 Hz, H-20).

^{13}C-NMR (C_6D_6, 100.5 MHz) δ 134.8, 134.7, 134.4, 130.6, 129.7, 122.0, 117.1, 81.0, 49.4, 43.3, 39.8, 35.1, 34.3, 31.9, 29.6, 25.1, 24.9, 22.6, 22.3, 22.1, 20.7.

Exact mass calcd for $C_{21}H_{32}O_3$ (HRDCI$^+$MS): 332.2351; found: 332.2351.

Preparation of the desurocanate eleutherobin aglycon **43**.
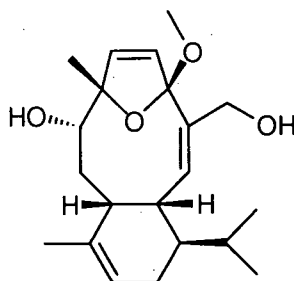
To a stirred solution of eleutherobin aglycon (**34**) (1.0 mg, 0.0062 mmol) in MeOH (1.0 mL) at room temperature, was added a solution of aqueous NaOH (5N, 50 μL, 0.25 mmol) and the reaction mixture was stirred overnight. The reaction mixture was then diluted with H_2O (10 mL) and EtOAc (10 mL) and the phases were separated. The aqueous phase was extracted with EtOAc (2 x 10 mL) and the combined organic phases were dried (MgSO$_4$) and concentrated under reduced pressure. Purification of the crude product by flash chromatography (15 g of silica gel, 3:2 hexane - EtOAc) and removal of trace amounts of solvent from the resulting solid provided 1.8 mg (83%) of the desurocanate eleutherobin aglycon **43** as a colorless solid.

^{1}H-NMR (C$_6$D$_6$, 400 MHz) δ 5.94 (d, 1H, J = 5.9 Hz, H-6), 5.68 (d, 1H, J = 5.9 Hz, H-5), 5.67 (d, 1H, J = 9.5 Hz, H-2), 5.31 (m, 1H, H-12), 4.00-4.20 (m, 3H, H-1, H-15, H-15), 3.44 (d, 1H, J = 6.1 Hz, H-8), 3.00 (s. 3H, H-21), 2.23-2.38 (m, 3H, OH, H-10, H-13), 1.93 (m, 1H, H-13), 1.59 (s, 3H, H-17), 1.43 (s, 3H, H-16), 1.42-1.62 (m, 3H, H-9, H-18, OH), 1.30 (m. 1H, H-14), 1.25 (m, 1H, H-9), 0.93 (d, 3H, J = 6.9 Hz, H-19), 0.90 (d, 3H, J = 6.7 Hz, H-20).

^{13}C-NMR (C$_6$D$_6$, 100.5 MHz) δ 138.5, 135.3, 134.3, 133.3, 129.5, 122.2, 117.2, 91.8, 80.9, 67.1, 49.2, 42.7, 39.6, 35.0, 34.1, 29.5, 24.8, 24.4, 22.6, 22.2, 20.6.

Exact mass calcd for C$_{21}$H$_{32}$O$_4$ (HRDCI$^+$MS): 348.2301; found: 348.2303.

Preparation of the eleutherobin acetonide **68.**
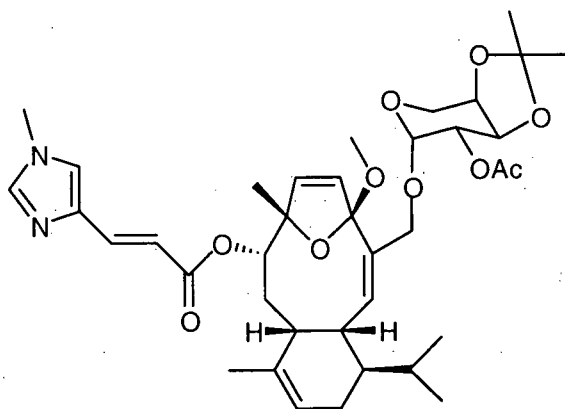
To a stirred solution of eleutherobin (**8**) (17 mg, 0.026 mmol) in dry CH$_2$Cl$_2$ (1.5 mL) and 2,2-dimethoxypropane (1.5 mL) at room temperature, was added a catalytic amount of PPTS (approx. 1 mg). After the reaction mixture had been stirred overnight, it was treated with saturated aqueous NaHCO$_3$ (10 mL) and the resultant mixture was diluted with EtOAc (10 mL). The phases were separated and the aqueous phase was extracted with EtOAc (2 x 10 mL). The combined organic phases were dried (MgSO$_4$) and concentrated. Purification of the crude product by flash chromatography (15 g of silica gel, 97:3 CH$_2$Cl$_2$ - MeOH) and removal of trace amounts of solvent from the resulting solid provided 14 mg (78%) of the eleutherobin acetonide **68** as a colorless solid.

^{1}H NMR (400 MHz, CDCl$_3$) δ 7.52 (d, 1H, J = 15.4 Hz), 7.45 (s, 1H), 7.08 (s, 1H), 6.54 (d, 1H, J = 15.4 Hz), 6.07 (d, 1H, J = 6.1 Hz), 6.06 (d, 1H, J = 6.1 Hz), 5.52 (d, 1H, J = 9.2 Hz), 5.25 (m, 1H), 4.89 (dd, 1H, J = 8.4, 3.4 Hz), 4.81 (d, 1H, J = 3.4 Hz), 4.80 (d, 1H, J = 8.2 Hz), 4.30 (m, 1H), 4.29 (d, 1H, J = 12.2 Hz), 4.21 (dd, 1H, J = 5.3, 2.3 Hz), 3.82-3.98 (m, 4H), 3.70 (s, 3H), 3.20 (s, 3H), 2.58 (m, 1H), 2.28 (m, 1H), 2.07 (s, 3H), 1.97 (m, 1H), 1.51-1.62 (m, 2H), 1.50 (s, 6H), 1.43 (s, 3H), 1.33 (s, 3H), 1.19-1.36 (m, 2H), 0.95 (d, 3H, J = 6.5 Hz), 0.90 (d, 3H, J = 6.5 Hz).

^{13}C NMR (100.5 MHz, CDCl$_3$) δ 170.2, 166.7, 139.2, 138.4, 137.4, 136.5, 134.1, 133.7, 132.6, 131.0, 122.8, 115.9, 115.8, 109.3, 92.8, 89.8, 81.4, 73.6, 73.2, 71.9, 69.1, 58.8, 49.6, 42.3, 38.7, 34.2, 33.6, 31.4, 29.3, 29.0, 28.0, 26.3, 24.4, 24.2, 22.2, 21.9, 21.1, 20.5.

Exact mass calcd for C$_{38}$H$_{53}$N$_2$O$_{10}$ (HRFABMS, M+H): 697.3700; found: 697.3696.

Preparation of 2"-*tert*-butyldimethylsilyloxyeleuthoside **63**.
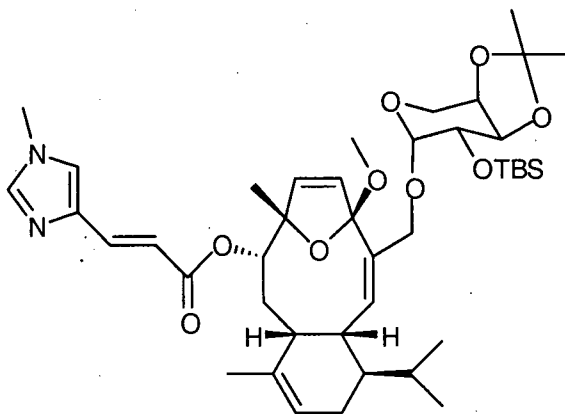
To a stirred solution of the eleutherobin acetonide **65** (12 mg, 0.017 mmol) in dry MeOH (2.0 mL) at room temperature, was added NaOMe (1 mg, 0.02 mmol). After the reaction mixture had

been stirred for 2 hours at room temperature, it was treated with saturated aqueous NH₄Cl (10 mL) and the resultant mixture was diluted with EtOAc (10 mL). The phases were separated and the aqueous phase was extracted with EtOAc (2 x 10 mL). The combined organic phases were dried (MgSO₄) and concentrated. Purification of the crude product by flash chromatography (15 g of silica gel, 97:3 CH₂Cl₂ - MeOH) and removal of trace amounts of solvent (vacuum pump) from the resulting liquid provided 11 mg of the desacetyleleuthoside **69** as an oil which was used in the next step without further purification.

To a stirred solution of the desacetyleleuthoside **69** (11 mg, 0.017 mmol), imidazole (10 mg, 0.15 mmol) and TBSCl (10 mg, 0.067 mmol) in dry CH₂Cl₂ (2 mL) at room temperature, was added a catalytic amount of DMAP. After the reaction mixture had been stirred overnight at room temperature, it was diluted with EtOAc (10 mL) and saturated aqueous NaHCO₃ (10 mL). The phases were separated and the aqueous phase was washed with EtOAc (2 x 10 mL). The combined organic phases were dried (MgSO₄) and concentrated. Purification of the crude product by flash chromatography (15 g of silica gel, 98.5:1.5 CH₂Cl₂ - MeOH) and removal of trace amounts of solvent (vacuum pump) from the resulting solid provided 9.1 mg (70% over 2 steps) of the 2"-*tert*-butyldimethylsilyloxyeleuthoside **63** as a colorless solid.

¹H NMR (400 MHz, CDCl₃) δ 7.52 (d, 1H, *J* = 15.3 Hz), 7.45 (s, 1H), 7.08 (s, 1H), 6.57 (d, 1H, *J* = 15.3 Hz), 6.10 (d, 1H, *J* = 5.7 Hz), 6.08 (d, 1H, *J* = 5.7 Hz), 5.59 (d, 1H, *J* = 9.5 Hz), 5.24 (m, 1H), 4.79 (d, 1H, *J* = 7.3 Hz), 4.61 (d, 1H, *J* = 3.1 Hz), 4.30 (d, 1H, *J* = 11.8 Hz), 4.17 (m, 1H), 4.11 (dd, 1H, *J* = 7, 7 Hz), 3.85-3.91 (m, 3H), 3.80 (d, 1H, *J* = 11.8 Hz), 3.72 (m, 1H), 3.69 (s, 3H), 3.19 (s, 3H), 2.59 (m, 1H), 2.29 (m, 1H), 1.95 (m, 1H), 1.45-1.64 (m, 2H), 1.49 (s, 6H), 1.42 (s, 3H), 1.33 (s, 3H), 1.19-1.26 (m, 2H), 0.96 (d, 3H, *J* = 6.5 Hz), 0.89 (d, 3H, *J* = 6.5 Hz), 0.85 (s, 9H), 0.08 (s, 3H), 0.02 (s, 3H).

^{13}C NMR (100.5 MHz, CDCl$_3$) δ 166.8, 139.2, 138.5, 136.2, 135.3, 134.1, 134.1, 133.4, 131.0, 122.8, 121.2, 116.0, 115.9, 108.6, 97.5, 89.8, 81.5, 76.8, 73.5, 71.8, 70.2, 59.4, 49.6, 42.5, 38.7, 34.1, 33.6, 31.6, 29.1, 28.2, 26.2, 25.9, 24.5, 24.2, 22.2, 22.0, 20.5, 18.1, -3.6, -4.5.

Exact mass calcd for C$_{42}$H$_{65}$N$_2$O$_9$Si (HRFABMS, M+H): 769.4459; found: 769.4459.

Preparation of the 5,6,11,12-tetrahydroeleuthoside **65.**
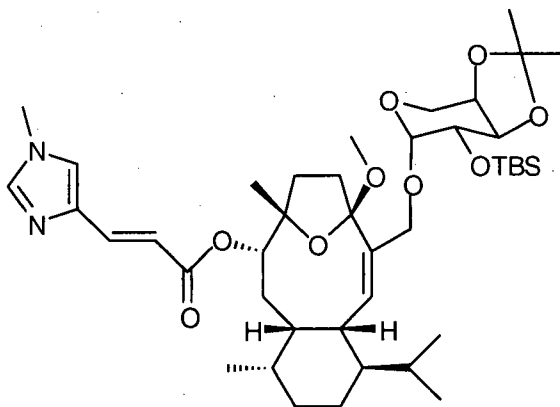
To a stirred solution of the 2"-*tert*-butyldimethylsilyloxyeleuthoside **63** (3.0 mg, 0.0039 mmol) in EtOAc (2.0 mL) was added Pd/BaSO$_4$ (5 wt. % Pd, 2 mg) and the resulting suspension was stirred under an atmosphere of H$_2$ (balloon) for 1 hour. The crude reaction mixture was filtered through a short plug of Celite®, and the Celite® was washed with EtOAc (20 mL). The filtrate was concentrated to provide the crude hydrogenation product as an oil that was used without further purification.

To a stirred solution of the crude hydrogenation product in MeOH (2.0 mL) at room temperature was added an aqueous solution of NaOH (5N, 0.05 mL, 0.25 mmol) and the mixture was stirred overnight. The reaction mixture was then treated with saturated aqueous NH$_4$Cl (5 mL) and the resulting mixture was diluted with EtOAc (10 mL). The phases were separated and the aqueous

phase was extracted with EtOAc (2 x 10 mL). The combined organic phases were dried (MgSO$_4$) and concentrated to provide the crude hydrolysis product as an oil, which was used without further purification.

A mixture of the crude hydrolysis product, triethylamine (0.015 mL, 0.11 mmol) and DMAP (1 mg, 0.008 mmol) were dissolved in a solution of the mixed anhydride **18** (0.2 M in CH$_2$Cl$_2$, 1 mL, 0.2 mmol) and stirred overnight at room temperature. The crude reaction mixture was placed directly on a column of silica gel (15 g) and the product was eluted with CH$_2$Cl$_2$ - MeOH (30:1), to provide 2.8 mg (93% over 3 steps) of the 5,6,11,12-tetrahydroeleuthoside **65** as a colorless solid.

^{1}H NMR (400 MHz, CDCl$_3$) δ 7.49 (d, 1H, J = 15.6 Hz), 7.43 (s, 1H), 7.06 (s, 1H), 6.53 (d, 1H, J = 15.6 Hz), 5.83 (d, 1H, J = 9.5 Hz), 4.64 (d, 1H, J = 3.4 Hz), 4.61 (d, 1H, J = 7.6 Hz), 4.08-4.20 (m, 3H), 4.88-4.95 (m, 2H), 3.78 (m, 1H), 3.70 (m, 1H), 3.69 (s, 3H), 3.62 (d, 1H, J = 12.2 Hz), 3.11 (s, 3H), 2.43 (m, 1H), 2.23-2.30 (m, 2H), 2.10 (m, 1H), 1.63-1.92 (m, 6H), 1.55 (s, 3H), 1.10-1.48 (m, 4H), 1.34 (s, 6H), 0.89 (d, 3H, J = 6.5 Hz), 0.87 (d, 3H, J = 6.5 Hz), 0.86 (s, 9H), 0.75 (d, 3H, J = 7.3 Hz), -0.08 (s, 3H), 0.04 (s, 3H).

^{13}C NMR (100.5 MHz, CDCl$_3$)[44] δ 167.0, 139.2, 137.3, 136.1, 132.7, 122.5, 116.4, 113.0, 108.5, 98.7, 86.7, 80.8, 76.5, 73.7, 72.0, 70.5, 59.1, 49.5, 46.1, 41.8, 39.8, 36.3, 34.0, 33.9, 33.6, 30.6, 28.5, 28.4, 28.4, 26.7, 26.3, 25.8, 21.6, 21.5, 18.0, 16.8, 16.1, -4.4, -4.7.

Exact mass calcd for C$_{42}$H$_{69}$N$_2$O$_9$Si (HRFABMS, M+H): 773.4772; found: 773.4774.

Preparation of the 5,6,11,12-tetrahydroeleuthoside **72.**
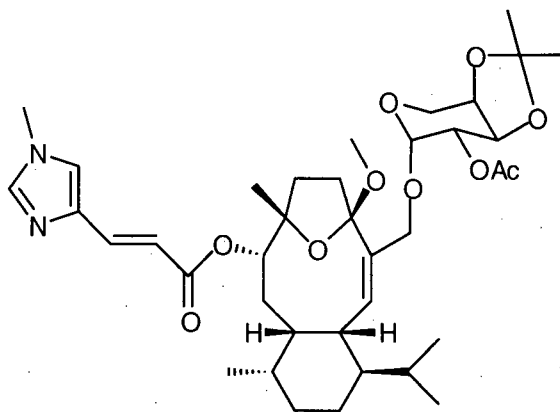
To a stirred solution of the 5,6,11,12-tetrahydroeleuthoside **65** (2.7 mg, 0.0035 mmol) in dry THF (3.0 mL) at room temperature, was added a solution of TBAF (1M in THF, 0.030 mL, 0.03 mmol). After 30 minutes, the reaction mixture was diluted with EtOAc (15 mL) and washed with brine (10 mL). The organic layer was dried ($MgSO_4$) and concentrated to provide the crude alcohol **71** as an oil, which was used without further purification.

To a stirred solution of the crude alcohol **71** in anhydrous pyridine (1.0 mL) was added acetic anhydride (0.05 mL, 0.5 mmol) and the reaction mixture was stirred overnight at room temperature. The reaction mixture was then concentrated, the crude residue was placed directly on a column of silica gel (15 g), and the product was eluted with CH_2Cl_2 - MeOH (30:1) to provide 2.4 mg (98% over 2 steps) of the 5,6,11,12-tetrahydroeleuthoside **72** as a colorless solid.

^{1}H NMR (400 MHz, $CDCl_3$) δ 7.49 (d, 1H, J = 15.5 Hz), 7.43 (s, 1H), 7.07 (s, 1H), 6.52 (d, 1H, J = 15.5 Hz), 5.78 (d, 1H, J = 9.2 Hz), 4.96 (d, 1H, J = 3.4 Hz), 4.89 (dd, 1H, J = 8.2, 3.4 Hz), 4.62 (d, 1H, J = 8.0 Hz), 4.30 (dd, 1H, J = 7,7 Hz), 4.23 (m, 1H), 4.10 (d, 1H, J = 11.8 Hz), 3.90-4.01 (m, 2H), 3.80 (m, 1H), 3.69 (s, 3H), 3.68 (m, 1H), 3.10 (s, 3H), 2.43 (m, 1H), 2.18-2.30 (m, 2H), 2.08 (s, 3H), 2.06 (m, 1H), 1.63-1.95 (m, 6H), 1.55 (s, 3H), 1.52 (s, 3H), 1.43 (m, 1H), 1.34 (s,

3H), 1.23 (m, 1H), 0.97-1.14 (m, 2H), 0.90 (d, 3H, J = 6.5 Hz), 0.88 (d, 3H, J = 6.8 Hz), 0.76 (d, 3H, J = 6.9 Hz).

^{13}C NMR (100.5 MHz, CDCl$_3$) δ 170.5, 167.0, 139.4, 139.2, 138.6, 136.2, 132.4, 122.5, 116.3, 112.8, 109.3, 94.9, 86.5, 80.7, 73.6, 73.2, 72.3, 70.1, 58.8, 49.6, 46.1, 41.1, 39.5, 36.3, 34.2, 33.9, 33.6, 30.5, 28.4, 28.3, 28.0, 26.6, 26.3, 21.6, 21.4, 21.0, 16.7, 16.1.

Exact mass calcd for C$_{38}$H$_{57}$N$_2$O$_{10}$ (HRFABMS, M+H): 701.4013; found: 701.4023.

Preparation of 5,6,11,12-tetrahydroeleutherobin (**61**).
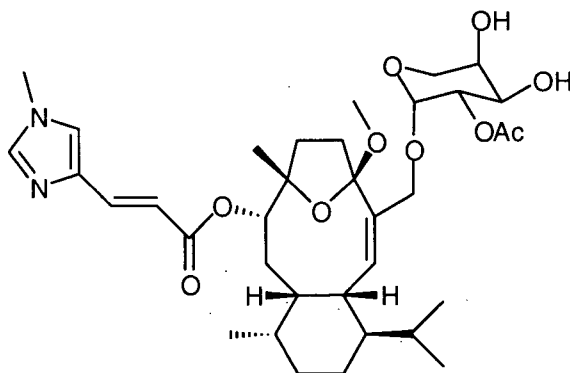
A stirred solution of the 5,6,11,12-tetrahydroeleuthoside **72** (1.5 mg, 0.0021 mmol) and PPTS (1.5 mg, 0.006 mmol) in dry MeOH (1.0 mL) was heated at 50°C overnight. The reaction mixture was then treated with saturated aqueous NaHCO$_3$ (10 mL) and the resultant mixture was diluted with EtOAc (10 mL). The phases were separated and the aqueous phase was extracted with EtOAc (2 x 10 mL). The combined organic phases were dried (MgSO$_4$) and concentrated. Purification of the crude product by flash chromatography (15 g of silica gel, 10:1 CH$_2$Cl$_2$ -

MeOH) and removal of trace amounts of solvent (vacuum pump) from the resulting solid provided 1.0 mg (72%) of 5,6,11,12-tetrahydroeleutherobin (**61**) as a colorless solid.

^{1}H NMR (500 MHz, CDCl$_3$) δ 7.49 (d, 1H, J = 15.6 Hz, H-3'), 7.43 (s, 1H, H-7'), 7.07 (s, 1H, H-5'), 6.53 (d, 1H, J = 15.6 Hz, H-2'), 5.80 (d, 1H, J = 9.5 Hz, H-2), 5.03 (d, 1H, J = 3.5 Hz, H-1"), 4.97 (dd, 1H, J = 3.5, 9.6 Hz, H-2"), 4.63 (d, 1H, J = 7.8 Hz, H-8), 4.11 (d, 1H, J = 11.9 Hz, H-15), 3.98-4.04 (m, 2H, H-3", H-4"), 3.85 (d, 1H, J = 12.0 Hz, H-5"), 3.82 (m, 1H, H-1), 3.73 (dd, 1H, J = 1.8, 12.0 Hz, H-5"), 3.71 (d, 1H, J = 11.9 Hz, H-15), 3.69 (s, 3H, H-9'), 3.11 (s, 3H, H-21), 2.62 (bs, 1H, C-3"-OH), 2.46 (m, 1H, H-5), 2.39 (bs, 1H, C-4"-OH), 2.26 (m, 1H, H-6), 2.24 (m, 1H, H-5), 2.10 (s, 3H, OCOCH$_3$), 2.06 (m, 1H, H-10), 1.90 (m, 1H, H-9), 1.89 (m, 1H, H-18), 1.82 (m, 1H, H-6), 1.69-1.74 (m, 3H, H-11, H-12, H-13), 1.45 (m, 1H, H-13), 1.34 (s, 3H, H-16), 1.22 (m, 1H, H-12), 1.13 (dd, 1H, J = 1.7, 14.3 Hz, H-9), 0.99 (m, 1H, H-14), 0.91 (d, 3H, J = 6.6 Hz, H-19), 0.88 (d, 3H, J = 6.6 Hz, H-20), 0.78 (d, 3H, J = 7.2 Hz, H-17).

^{13}C NMR (100.5 MHz, CDCl$_3$) δ 171.7 (O$\underline{C}$OCH$_3$), 166.9 (C-1'), 139.5 (C-2), 139.2 (C-7'), 139.1 (C-4'), 136.2 (C-3'), 132.4 (C-3), 122.5 (C-5'), 116.3 (C-2'), 112.8 (C-4), 95.3 (C-1"), 86.5 (C-7), 80.7 (C-8), 72.2 (C-2"), 69.9 (C-15), 69.5 (C-4"), 68.2 (C-3"), 62.0 (C-5"), 49.6 (C-21), 46.1 (C-14), 41.1 (C-5), 39.5 (C-10), 36.3 (C-9), 34.2 (C-1), 34.0 (C-9'), 33.6 (C-11), 30.5 (C-6), 28.4 (C-12), 28.3 (C-16), 26.6 (C-18), 21.6 (C-20), 21.4 (C-19), 21.0 (OCO$\underline{C}$H$_3$), 16.7 (C-13), 16.1 (C-17).

Exact mass calcd for C$_{35}$H$_{53}$N$_2$O$_{10}$ (HRFABMS, M+H): 661.3700; found: 661.3700.

Table 4.5. NMR data for 5,6,11,12-tetrahydroeleutherobin (**61**) (recorded in CDCl$_3$).
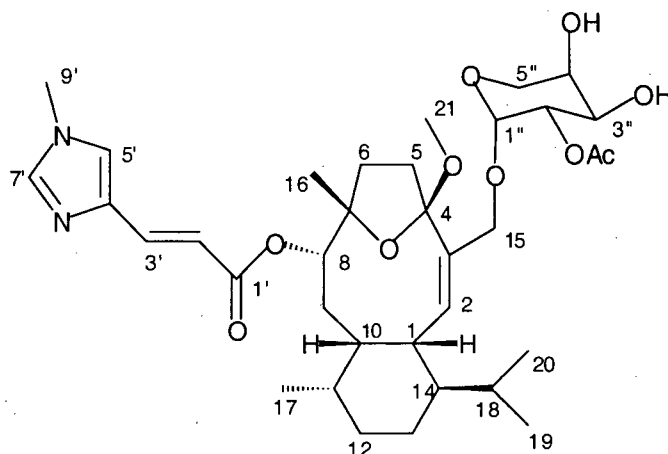
Carbon No.	^{13}C δ (ppm)^a	^{1}H δ (ppm) (mult, J (Hz))^{b,c}	HMBC^b
1	34.2	3.82 (m)	
2	139.5	5.80 (d, 9.5)	H-15
3	132.4		H-15
4	112.8		H-2, H-5, H-6, H-15, H-21
5	41.1	2.46 (m) 2.24 (m)	
6	30.5	2.26 (m) 1.82 (m)	H-8, H-16
7	86.5		H-8, H-16
8	80.7	4.63 (d, 7.8)	H-9, H-16
9	36.3	1.90 (m) 1.13 (dd, 1.7, 14.3)	
10	39.5	2.06 (m)	H-8, H-9, H-17
11	33.6	1.69 (m)	H-1, H-17
12	28.4	1.72 (m) 1.22 (m)	H-9, H-17
13	16.7	1.70 (m) 1.45 (m)	
14	46.1	0.99 (m)	H-2, H-19, H-20
15	69.9	4.11 (d, 11.9) 3.71 (d, 11.9)	H-2
16	28.3	1.34 (s)	H-8
17	16.1	0.78 (d, 7.2)	

^{a} Recorded at 100.5 MHz. ^{b} Recorded at 500 MHz. ^{c} Assignments based on HMQC data.

Table 4.5 (continued). NMR data for 5,6,11,12-tetrahydroeleutherobin (**61**) (recorded in CDCl₃).
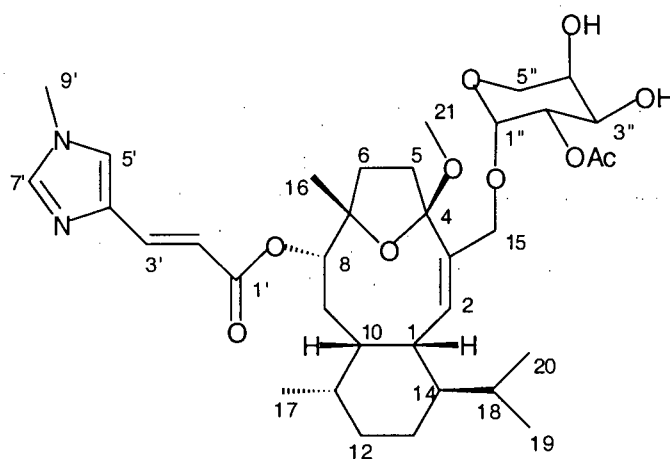
Carbon No.	¹³C δ (ppm)ᵃ	¹H δ (ppm) (mult, J (Hz))ᵇ,ᶜ	HMBCᵇ
18	26.6	1.89 (m)	H-19, H-20
19	21.4	0.91 (d, 6.6)	
20	21.6	0.88 (d, 6.6)	
21	49.6	3.11 (s)	
1'	166.9		H-8, H-3', H-2'
2'	116.3	6.53 (d, 15.6)	H-3'
3'	136.2	7.49 (d, 15.6)	
4'	139.1		H-2', H-3', H-5'
5'	122.5	7.07 (s)	H-7', H-9'
7'	139.2	7.43 (s)	H-5', H-9'
9'	34.0	3.69 (s)	
1"	95.3	5.03 (d, 3.5)	H-15, H-5"
2"	72.2	4.97 (dd, 3.5, 9.6)	
3"	68.2	4.00 (m) OH 2.62 (bs)	H-5"
4"	69.5	4.00 (m) OH 2.39 (bs)	H-5"
5"	62.0	3.85 (d, 12.0) 3.73 (dd, 1.8, 12.0)	H-1"
1'''	171.7		H-2'''
2'''	21.0	2.10 (s)	

ᵃ Recorded at 100.5 MHz. ᵇ Recorded at 500 MHz. ᶜ Assignments based on HMQC data.

Table 4.6. NMR data for 5,6,11,12-tetrahydroeleutherobin (**61**) (recorded in $CDCl_3$).
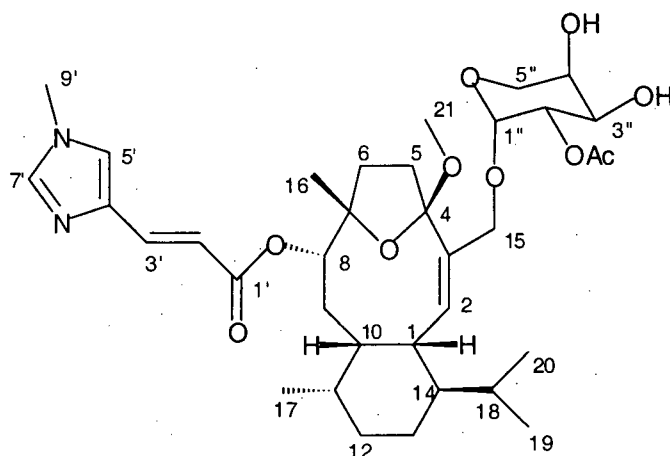
Proton No.	^{1}H δ (ppm) (mult, J (Hz))[a]	COSY[a]	NOE[b]
1	3.82 (m)	H-2, H-10	
2	5.80 (d, 9.5)	H-1	H-14, H-15, H-17
5	2.46 (m)	H-5, H-6	
	2.24 (m)	H-5, H-6	
6	2.26 (m)	H-5, H-6	
	1.82 (m)	H-5, H-6	
8	4.63 (d, 7.8)	H-9	
9	1.90 (m)	H-8, H-10	
	1.13 (dd, 1.7, 14.3)	H-8, H-10	
10	2.06 (m)	H-1, H-9, H-11	
11	1.69 (m)	H-10, H-12, H-17	
12	1.72 (m)	H-11, H-13	
	1.22 (m)	H-11, H-13	
13	1.70 (m)	H-12, H-14	
	1.45 (m)	H-12, H-14	
14	0.99 (m)	H-13, H-18	H-2
15	4.11 (d, 11.9)	H-15	
	3.71 (d, 11.9)	H-15	
16	1.34 (s)		
17	0.78 (d, 7.2)	H-11	H-2
18	1.89 (m)	H-14, H-19, H-20	
19	0.91 (d, 6.6)	H-18	
20	0.88 (d, 6.6)	H-18	

[a] Recorded at 500 MHz. [b] Recorded as NOE difference at 400 MHz using 1D selective NOE experiments.

Table 4.6 (continued). NMR data for 5,6,11,12-tetrahydroeleutherobin (**61**) (recorded in CDCl₃).
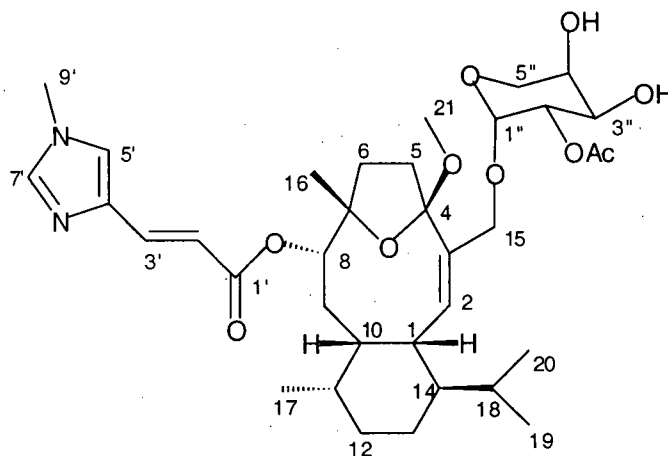
Proton No.	¹H δ (ppm) (mult, J (Hz))ᵃ	COSYᵃ	NOEᵇ
21	3.11 (s)		
2'	6.53 (d, 15.6)	H-3'	
3'	7.49 (d, 15.6)	H-2'	
5'	7.07 (s)		
7'	7.43 (s)		
9'	3.69 (s)		
1"	5.03 (d, 3.5)	H-2"	
2"	4.97 (dd, 3.5, 9.6)	H-1", H-3"	
3"	4.00 (m) OH 2.62 (bs)	H-2", H-4", OH	
4"	4.00 (m) OH 2.39 (bs)	H-3", H-5", OH	
5"	3.85 (d, 12.0) 3.73 (dd, 1.8, 12.0)	H-4", H-5" H-4", H-5"	
2'''	2.10 (s)		

ᵃ Recorded at 500 MHz. ᵇ Recorded as NOE difference at 400 MHz using 1D selective NOE experiments.

Preparation of the 2"-*tert*-butyldimethylsilyloxy-2',3'-dihydroeleuthoside **67**.
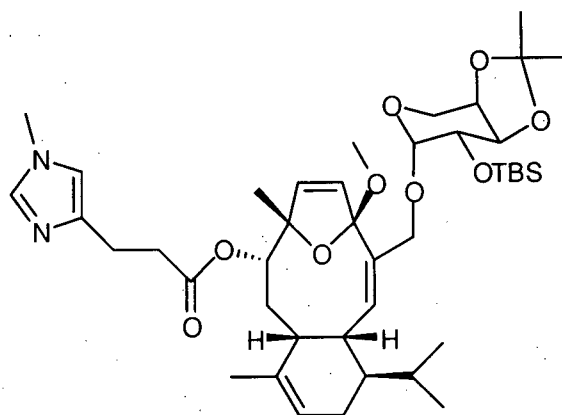
To a stirred solution of the 2"-*tert*-butyldimethylsilyloxyeleuthoside **63** (3.0 mg, 0.0039 mmol) in MeOH (1.0 mL) was added an aqueous solution of NaOH (5N, 0.05 mL, 0.25 mmol) and the mixture was stirred overnight at room temperature. The reaction mixture was then treated with saturated aqueous NH$_4$Cl (5 mL) and the resultant mixture was diluted with EtOAc (10 mL). The phases were separated and the aqueous phase was extracted with EtOAc (3 x 10 mL). The combined organic phases were dried (MgSO$_4$) and concentrated. The resulting organic residue was placed on a short plug of silica gel (10 g) and eluted with CH$_2$Cl$_2$ - MeOH (20:1) and the fractions containing the crude hydrolysis product **76** were combined and concentrated to provide an oil, which was used without further purification.

A stirred solution of the crude hydrolysis product **76**, 2,3-dihydro-*N*-methylurocanic acid (**75**) (2.0 mg, 0.013 mmol), DCC (1 mg, 0.0049 mmol) and a catalytic amount of DMAP in dry DMF (2.0 mL) was heated at 50°C overnight. After this time, the DMF was removed under reduced pressure. Purification of the crude product by flash chromatography (15 g of silica gel, 2:1 CH$_2$Cl$_2$ - EtOAc then 10:1 CH$_2$Cl$_2$ - MeOH) and removal of trace amounts of solvent (vacuum pump) from the resulting solid provided 2.2 mg (73% over 2 steps) of the 2"-*tert*-butyldimethylsilyloxy-2',3'-dihydroeleuthoside **67** as a colorless solid.

^{1}H NMR (400 MHz, CDCl$_3$) δ 7.30 (s, 1H), 6.63 (s, 1H), 6.07 (d, 1H, J = 5.9 Hz), 6.01 (d, 1H, J = 5.9 Hz), 5.57 (d, 1H, J = 9.4 Hz), 5.25 (m, 1H), 4.68 (d, 1H, J =6.1 Hz), 4.60 (d, 1H, J =3.2 Hz), 4.27 (d, 1H, J =12.0 Hz), 4.17 (m, 1H), 4.10 (dd, 1H, J = 7,7 Hz), 3.83-3.92 (m, 3H), 3.79 (d, J = 12.0 Hz, 1H), 3.70 (dd, 1H, J = 3.2, 7.2 Hz), 3.59 (s, 3H), 3.18 (s, 1H), 2.87 (m, 2H), 2.69 (m, 2H), 2.52 (m, 1H), 2.28 (m, 1H), 1.95 (m, 1H), 1.15-1.60 (m, 6H), 1.49 (s, 3H), 1.46 (s, 3H), 1.34 (s, 3H), 1.33 (s, 3H), 0.93 (d, 3H, J = 6.6 Hz), 0.89 (d, 3H, J = 6.3 Hz), 0.86 (s, 9H), 0.08 (s, 3H), 0.02 (s, 3H).

^{13}C NMR (100.5 MHz, CDCl$_3$) δ 172.4, 137.2, 135.2, 134.0, 133.9, 133.4, 131.0, 121.4, 116.5, 116.0, 108.6, 97.7, 89.6, 81.7, 76.8, 73.5, 71.9, 70.2, 59.5, 49.6, 42.5, 38.7, 34.2, 34.1, 33.2, 31.7, 29.8, 29.1, 28.2, 26.2, 25.9, 24.5, 24.1, 23.7, 22.2, 21.9, 20.6, 18.1, -4.5, -4.5.

Exact mass calcd for C$_{42}$H$_{67}$N$_2$O$_9$Si (HRFABMS, M+H): 771.4616; found: 771.4614.

Preparation of the 2',3'-dihydroeleuthoside **78.**
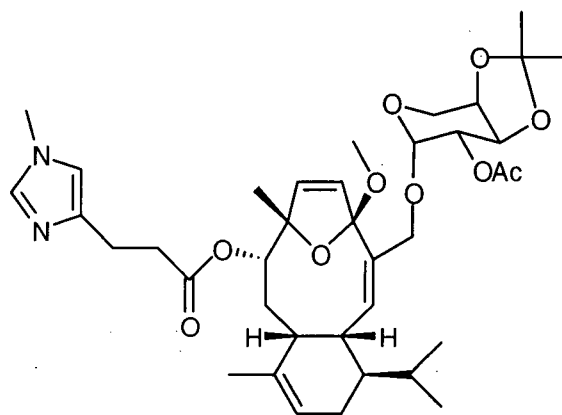
To a stirred solution of the 2"-*tert*-butyldimethylsilyloxy-2',3'-dihydroeleuthoside **67** (2.0 mg, 0.0026 mmol) in dry THF (2.0 mL) at room temperature, was added a solution of TBAF (1M in THF, 0.03 mL, 0.03 mmol). After the reaction mixture had stirred for 2 hours at room temperature, it was diluted with EtOAc (15 mL) and brine (10 mL). The phases were separated and the organic layer was dried ($MgSO_4$) and concentrated to provide the crude alcohol **77** as an oil, which was used without further purification.

To a stirred solution of the crude alcohol **77** in anhydrous pyridine (1.0 mL), was added acetic anhydride (0.05 mL, 0.5 mmol) and the reaction mixture was stirred overnight at room temperature. The reaction mixture was then concentrated under reduced pressure. Purification of the crude product by flash chromatography (15 g of silica gel, 30:1 CH_2Cl_2 - MeOH) and removal of trace amounts of solvent from the resulting solid provided 1.5 mg (83% over 2 steps) of the 2',3'-dihydroeleuthoside **78** as a colorless solid.

^{1}H NMR (400 MHz, $CDCl_3$) δ 7.32 (s, 1H), 6.63 (s, 1H), 6.05 (d, 1H, J = 5.7 Hz), 5.99 (d, 1H, J = 5.7 Hz), 5.50 (d, 1H, J = 9.5 Hz), 5.25 (m, 1H), 4.88 (dd, 1H, J = 3.4, 8.2 Hz), 4.79 (d, 1H, J = 3.4 Hz), 4.67 (d, 1H, J = 7.3 Hz), 4.25-4.31 (m, 2H), 4.21 (dd, 1H, J = 2.3, 5.3 Hz), 3.84-3.96 (m, 3H), 3.82 (d, 1H, J = 12.6 Hz), 3.59 (s, 3H), 3.18 (s, 3H), 2.88 (m, 2H), 2.68 (m, 2H), 2.55

(m, 1H), 2.28 (m, 1H), 2.04 (s, 3H), 1.96 (m, 1H), 1.15-1.80 (m, 4H), 1.51 (s, 3H), 1.47 (s, 3H), 1.34 (s, 3H), 1.33 (s, 3H), 0.92 (d, 3H, J = 6.5 Hz), 0.89 (d, 3H, J = 6.5 Hz).

^{13}C NMR (100.5 MHz, CDCl$_3$) δ 172.4, 170.2, 142.3, 137.6, 137.3, 133.9, 133.5, 132.6, 131.1, 121.4, 116.6, 115.8, 109.3, 92.7, 89.6, 81.7, 73.6, 73.2, 72.0, 69.1, 58.8, 49.6, 42.4, 38.6, 34.2, 33.2, 31.4, 29.7, 29.0, 28.0, 26.3, 24.4, 24.1, 23.6, 22.1, 21.8, 21.0, 20.5.

Exact mass calcd for C$_{38}$H$_{55}$N$_2$O$_{10}$ (HRFABMS, M+H): 699.3856; found: 699.3857.

Preparation of 2',3'-dihydroeleutherobin (62).
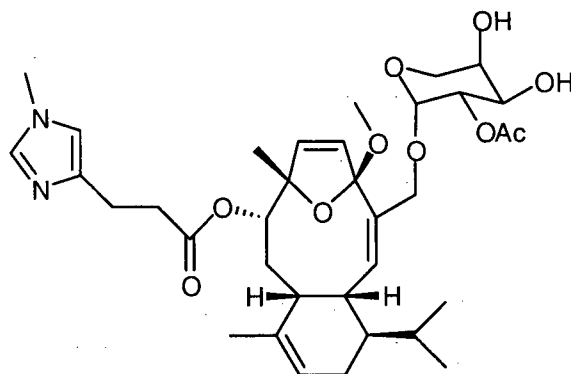
A stirred solution of the 2',3'-dihydroeleuthoside **78** (1.0 mg, 0.0014 mmol) and PPTS (1.5 mg, 0.006 mmol) in dry MeOH (1.0 mL) was heated at 50°C overnight. The reaction mixture was then treated with saturated aqueous NaHCO$_3$ (10 mL) and the resultant mixture was diluted with EtOAc (10 mL). The phases were separated and the aqueous phase was extracted with EtOAc (2 x 10 mL). The combined organic phases were dried (MgSO$_4$) and concentrated. Purification of the crude product by HPLC (NP radial pac column, 9:1 CH$_2$Cl$_2$ - MeOH, 1.25 mL/minute, monitor at 230 nm, rt = 8.6 minutes) and removal of trace amounts of solvent (vacuum pump)

from the resulting solid provided 0.4 mg (43%) of 2',3'-dihydroeleutherobin (**62**) as a colorless

solid.

^{1}H NMR (500 MHz, CDCl$_3$) δ 7.45 (s, 1H, H-7'), 6.68 (s, 1H, H-5'), 6.07 (d, 1H, J = 5.7 Hz, H-

5), 5.99 (d, 1H, J = 5.7 Hz, H-6), 5.51 (d, 1H, J = 9.6 Hz, H-2), 5.26 (m, 1H, H-12), 4.95 (dd,

1H, J = 3.3, 9.5 Hz, H-2"), 4.87 (d, 1H, J = 3.3 Hz, H-1"), 4.66 (d, 1H, J = 7.1 Hz, H-8), 4.28 (d,

1H, J = 12.3 Hz, H-15), 4.01 (dd, 1H, J = 9.5, 3.3 Hz, H-3"), 3.97 (m, 1H, H-4"), 3.89 (m, 1H,

H-1), 3.86 (d, 1H, J = 12.3 Hz, H-15), 3.80 (d, 1H, J = 12.5 Hz, H-5"), 3.67 (dd, 1H, J = 12.5,

2.0 Hz, H-5"), 3.63 (s, 3H, H-9'), 3.18 (s, 3H, H-21), 2.90 (m, 2H, H-2', H-2'), 2.71 (m, 2H, H-

3', H-3'), 2.54 (m, 1H, H-10), 2.28 (m, 1H, H-13), 2.08 (s, 3H, OCOCH$_3$), 1.96 (m, 1H, H-13),

1.15-1.60 (m, 4H, H-9, H-9, H-14, H-18), 1.47 (s, 3H, H-17), 1.35 (s, 3H, H-16), 0.93 (d, 3H, J =

6.4 Hz, H-19), 0.89 (d, 3H, J = 6.5 Hz, H-20).

^{13}C NMR (100.5 MHz, CDCl$_3$)[45] δ 171.3 (O$\underline{C}$OCH$_3$), 137.4 (C-2), 133.7 (C-11), 133.3 (C-6),

130.7 (C-5), 121.2 (C-12), 115.9 (C-4), 92.8 (C-1"), 89.6 (C-7), 81.7 (C-8), 71.6 (C-2"), 69.0 (C-

4"), 68.8 (C-15), 67.9 (C-3"), 61.9 (C-5"), 49.5 (C-21), 42.4 (C-14), 38.7 (C-10), 34.2 (C-1),

33.9 (C-3'), 33.4 (C-9'), 29.1 (C-18), 24.4 (C-13), 24.0 (C-16), 23.0 (C-2'), 22.0 (C-20), 21.7 (C-

17), 20.9 (OCO$\underline{C}$H$_3$), 20.4 (C-19).

Exact mass calcd for C$_{35}$H$_{51}$N$_2$O$_{10}$ (HRFABMS, M+H): 659.3543; found: 659.3543.

Preparation of 2,3-dihydro-*N*-methylurocanic acid ethyl ester (**74**).
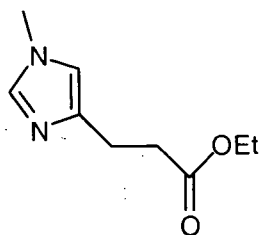
To a stirred solution of *N*-methyl urocanic acid ethyl ester (**73**) (136 mg, 0.76 mmol) in EtOAc (6.0 mL) was added Pd/BaSO$_4$ (5 wt. % Pd, 5 mg) and the resulting suspension was stirred overnight at room temperature under an atmosphere of H$_2$ (balloon). The reaction mixture was then filtered through Celite®, and the Celite® was washed with CH$_2$Cl$_2$ (50 mL). The filtrate was concentrated to afford the crude product which was further purified by flash chromatography (30 g of silica gel, 10:1 CH$_2$Cl$_2$ - MeOH) to provide 94 mg (70%) of 2,3-dihydro-*N*-methylurocanic acid ethyl ester (**74**) as a colorless oil.

^{1}H NMR (400 MHz, CDCl$_3$) δ 7.15 (s, 1H), 6.48 (s, 1H), 3.95 (q, 2H, *J* = 6.9 Hz), 3.45 (s, 3H), 2.70 (t, 2H, *J* = 7.6 Hz), 2.49 (t, 2H, *J* = 7.6 Hz), 1.07 (t, 3H, *J* = 6.9 Hz).

^{13}C NMR (100.5 MHz, CDCl$_3$) δ 172.9, 141.1, 136.8, 116.1, 59.8, 33.7, 32.8, 23.3, 13.8.

IR (neat) 3391, 2980, 1729, 1509, 1421, 1372, 1167, 1041, 823 cm^{-1}.

Exact mass calcd for C$_9$H$_{14}$N$_2$O$_2$: 182.1055; found: 182.1060.

Preparation of 2,3-dihydro-*N*-methylurocanic acid (**75**).
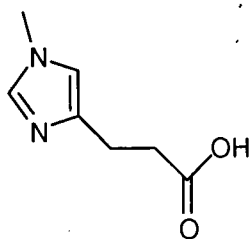
To a stirred solution of 2,3-dihydro- *N*-methylurocanic acid ethyl ester (**74**) (22 mg, 0.12 mmol) in THF (1.0 mL) and H_2O (1.0 mL) at room temperature was added LiOH•H_2O (5.0 mg, 0.13 mmol) and the resulting mixture was stirred overnight. The reaction mixture was then neutralized with aqueous HCl (1N) and the solvents were removed under reduced pressure. The crude acid **75** and LiCl mixture was used in the coupling reaction (*vide supra*) without further purification.

Preparation of the 17-hydroxyeleuthoside **56**.
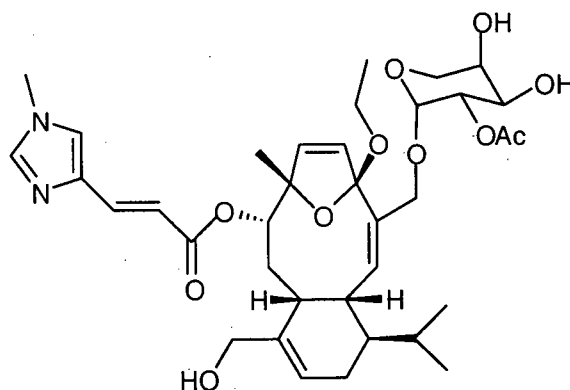
A stirred solution of eleutherobin (**8**) (2.2 mg, 0.0033 mmol) and SeO $_2$ (2 mg, 0.018 mmol), in dry EtOH (1.0 mL) was heated at reflux for 7 hours. The reaction mixture was then concentrated and the crude product was purified by normal phase HPLC (radial pac column, 92:8 CH_2Cl_2 -

MeOH, 1.25 mL/minute, monitor at 230 nm) to provide 1.0 mg (45%) of the 17-hydroxyeleuthoside **56** as a colorless solid.

^{1}H NMR (500 MHz, DMSO-d_6) δ 7.69 (s, 1H, H-7'), 7.57 (s, 1H, H-5'), 7.50 (d, 1H, J = 15.6 Hz, H-3'), 6.34 (d, 1H, J = 15.6 Hz, H-2'), 6.22 (d, 1H, J = 6.0 Hz, H-5), 6.09 (d, 1H, J = 6.0 Hz, H-6), 5.48 (m, 1H, H-12), 5.38 (d, 1H, J = 9.3 Hz, H-2), 4.91 (d, 1H, J = 6.1 Hz, C-3"-OH), 4.82 (dd, 1H, J = 3.4, 8.6 Hz, H-2"), 4.73 (d, 1H, J = 7.3 Hz, H-8), 4.69 (d, 1H, J = 3.4 Hz, H-1"), 4.39 (dd, 1H, J = 5.0, 5.0 Hz, C-17-OH), 4.17 (d, 1H, J = 12.3 Hz, H-15), 3.91 (m, 1H, H-1), 3.77 (d, 1H, J = 12.3 Hz, H-15), 3.63-3.75 (m, 4H, H-17, H-17, H-4", H-3"), 3.66 (s, 3H, H-9'), 3.59 (d, 1H, J = 12.2 Hz, H-5"), 3.43 (dd, 1H, J = 1.5, 12.2 Hz, H-5"), 3.33 (m, 2H, H-21, H-21), 2.56 (m, 1H, H-10), 2.29 (m, 1H, H-13), 2.02 (m, 1H, H-13), 2.02 (s, 3H, OCOCH$_3$), 1.59 (d, 1H, J = 13.6 Hz, H-9), 1.46 (m, 1H, H-18), 1.33 (s, 3H, H-16), 1.28 (m, 1H, H-9), 1.13 (m, 1H, H-14), 1.09 (t, 3H, J = 6.9 Hz, H-22), 0.94 (d, 3H, J = 6.3 Hz, H-19), 0.93 (d, 3H, J = 6.2 Hz, H-20).

^{13}C NMR (100.5 MHz, DMSO-d_6) δ 170.1 (O$\underline{C}$OCH$_3$), 165.8 (C-1'), 140.1 (C-7'), 137.7 (C-3'), 137.7 (C-11), 136.9 (C4'), 134.4 (C-2), 133.6 (C-3), 133.1 (C-5), 131.1 (C-6), 124.7 (C-5'), 120.4 (C-12), 115.3 (C-4), 113.6 (C-2'), 93.0 (C-1"), 89.2 (C-7), 80.2 (C-8), 70.8 (C-2"), 68.5 (C-3"), 67.8 (C-15), 66.2 (C-4"), 63.3 (C-5"), 63.1 (C-17), 57.0 (C-21), 41.7 (C-14), 36.2 (C-10), 33.2 (C-1), 33.2 (C-9'), 29.9 (C-9), 28.6 (C-18), 24.0 (C-16), 23.6 (C-13), 22.0 (C-20), 20.9 (OCO$\underline{C}$H$_3$), 20.2 (C-19), 15.3 (C-22).

Exact mass calcd for C$_{36}$H$_{51}$N$_2$O$_{11}$ (HRFABMS, M+H): 687.3499; found: 687.3500.

Table 4.7. NMR data for the 17-hydroxyeleuthoside **56** (recorded in DMSO-d_6).
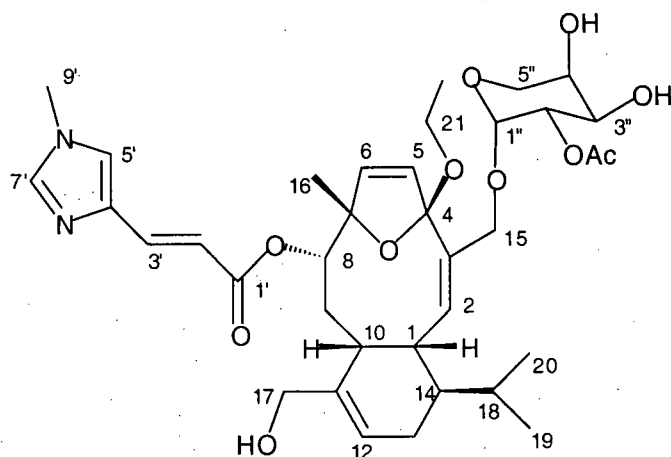
Carbon No.	^{13}C δ (ppm)[a]	^{1}H δ (ppm) (mult, J (Hz))[b,c]	COSY[b]
1	33.2	3.91 (m)	
2	134.4	5.38 (d, 9.3)	H-1
3	133.6		
4	115.3		
5	133.1	6.22 (d, 6.0)	H-6
6	131.1	6.09 (d, 6.0)	H-5
7	89.2		
8	80.2	4.73 (d, 7.3)	H-9
9	29.9	1.59 (d, 13.6)	H-9, H-10
		1.28 (m)	H-8, H-9, H-10
10	36.2	2.56 (m)	H-1, H-9
11	137.7		
12	120.4	5.48 (m)	H-13
13	23.6	2.02 (m)	H-12, H-14
		2.29 (m)	H-12, H-14
14	41.7	1.13 (m)	H-13, H-18
15	67.8	4.17 (d, 12.3)	H-15
		3.77 (d, 12.3)	H-15
16	24.0	1.33 (s)	
17	63.1	3.71 (m)	H-17, OH
		3.63 (m)	H-17, OH
		OH 4.39 (dd, 5.0, 5.0)	
18	28.6	1.46 (m)	H-14, H-19, H-20

[a] Recorded at 100.5 MHz. [b] Recorded at 500 MHz. [c] Assignments based on HMQC data.

Table 4.7 (continued). NMR data for the 17-hydroxyeleuthoside **56**
(recorded in DMSO-d_6).
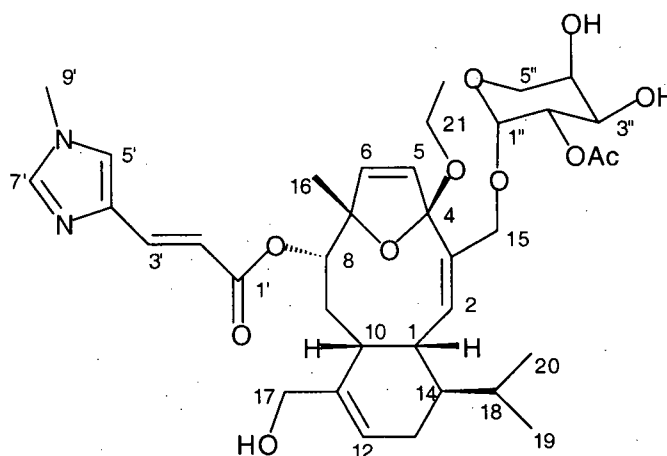
Carbon No.	^{13}C δ (ppm)[a]	^1H δ (ppm) (mult, J (Hz))[b,c]	COSY[b]
19	20.2	0.94 (d, 6.3)	H-18
20	22.0	0.93 (d, 6.2)	H-18
21	57.0	3.33 (m)	H-22
22	15.3	1.09 (t, 6.9)	H-21
1'	165.8		
2'	113.6	6.34 (d, 15.6)	H-3'
3'	137.7	7.50 (d, 15.6)	H-2'
4'	136.9		
5'	124.7	7.57 (s)	
7'	140.1	7.69 (s)	
9'	33.2	3.66 (s)	
1"	93.0	4.69 (d, 3.4)	H-2"
2"	70.8	4.82 (dd, 3.4, 8.6)	H-1", H-3"
3"	68.5	3.75 (m)	H-2", H-4", OH
		OH 4.91 (d, 6.1)	H-3"
4"	66.2	3.75 (m)	H-3", H-5", OH
		OH (3.72, m)	H-4"
5"	63.3	3.59 (d, 12.2)	H-4", H-5"
		3.43 (dd, 1.5, 12.2)	H-4", H-5"
1'''	170.1		
2'''	20.9	2.02 (s)	

[a] Recorded at 100.5 MHz. [b] Recorded at 500 MHz. [c] Assignments based on HMQC data.

Preparation of 5,6,11,12,2',3'-hexahydroeleutherobin (60).
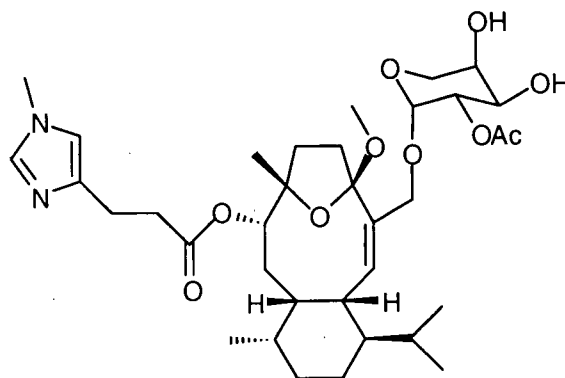
To a stirred solution of eleutherobin (**8**) (1.5 mg, 0.0023 mmol) in EtOAc (1.0 mL) was added Pd/BaSO$_4$ (5 wt. % Pd, 1 mg) and the resulting suspension was stirred under an atmosphere of H$_2$ (balloon) for 1 hour. The reaction mixture was then filtered through a short plug of Celite®, and the Celite® was washed with CH$_2$Cl$_2$ - MeOH (9:1, 15 mL). The filtrate was concentrated to afford a crude residue which was purified by normal phase HPLC (radial pac column, 93:7 CH$_2$Cl$_2$ - MeOH, 1.25 mL/minute, monitor at 230 nm) to provide 1.4 mg (90%) of 5,6,11,12,2',3'-hexahydroeleutherobin (**60**) as a colorless solid.

^{1}H NMR (500 MHz, CDCl$_3$) δ 7.35 (s, 1H, H-7'), 6.63 (s, 1H, H-5'), 5.78 (d, 1H, J = 9.3 Hz, H-2), 5.02 (d, 1H, J = 3.5 Hz, H-1"), 4.97 (dd, 1H, J = 3.5, 9.6 Hz, H-2"), 4.53 (d, 1H, J = 7.9 Hz, H-8), 4.09 (d, 1H, J = 12.0 Hz, H-15), 3.96-4.04 (m, 2H, H-3", H-4"), 3.84 (d, 1H, J = 12.2 Hz, H-5"), 3.76 (m, 1H, H-1), 3.72 (dd, 1H, J = 1.5, 12.2 Hz, H-5"), 3.70 (d, 1H, J = 12.0 Hz, H-15), 3.60 (s, 3H, H-9'), 3.09 (s, 3H, H-21), 2.85 (m, 2H, H-3', H-2'), 2.67 (m, 2H, H-2', H-3'), 2.43 (m, 1H, H-5), 2.22 (m, 1H, H-5), 2.17 (m, 1H, H-6), 2.08 (s, 3H, OCOCH$_3$), 1.99 (m, 1H, H-10), 1.83 (m, 1H, H-18), 1.80 (m, 1H, H-9), 1.78 (m, 1H, H-6), 1.72 (m, 1H, H-13), 1.70 (m, 1H, H-12) 1.68 (m, 1H, H-11), 1.45 (m, 1H, H-13), 1.25 (s, 3H, H-16), 1.24 (m, 1H, H-12), 0.99 (m,

1H, H-14), 0.98 (m, 1H, H-9), 0.88 (d, 3H, J = 6.5 Hz, H-19), 0.87 (d, 3H, J = 6.5 Hz, H-20), 0.76 (d, 3H, J = 7.0 Hz, H-17).

^{13}C NMR (100.5 MHz, CDCl$_3$) δ 172.6 (C-1') 171.6 (O$\underline{C}$OCH$_3$), 141.0 (C-7'), 139.6 (C-2), 137.1 (C-4'), 132.3 (C-3), 116.6 (C-5'), 112.8 (C-4), 95.1 (C-1''), 86.2 (C-7), 80.8 (C-8), 72.1 (C-2''), 69.8 (C-15), 69.4 (C-3''), 68.1 (C-4''), 62.0 (C-5''), 49.6 (C-21), 46.0 (C-14), 41.0 (C-5), 39.4 (C-10), 36.3 (C-9), 34.2 (C-1), 34.1 (C-11), 34.0 (C-2'), 33.6 (C-9'), 30.4 (C-6), 28.3 (C-12), 28.3 (C-16), 26.6 (C-18), 23.6 (C-3'), 21.6 (C-20), 21.4 (C-19), 21.0 (OCO$\underline{C}$H$_3$), 16.6 (C-13), 16.1 (C-17).

Exact mass calcd for C$_{35}$H$_{55}$N$_2$O$_{10}$ (HRFABMS, M+H): 663.3857; found: 663.3858.

Table 4.8. NMR data for 5,6,11,12,2',3'-hexahydroeleutherobin (**60**)
(recorded in CDCl$_3$).
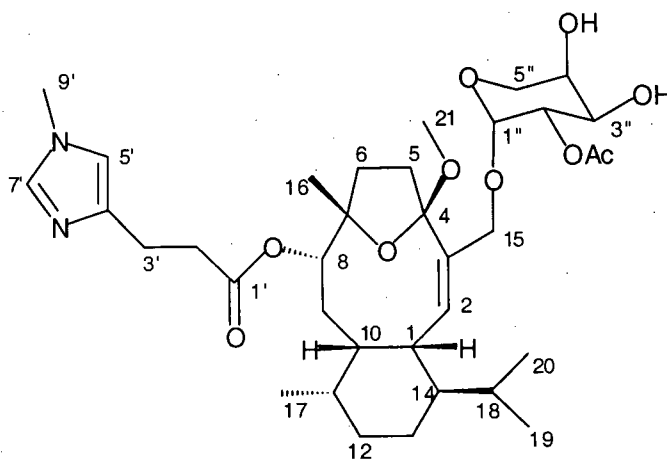
Carbon No.	^{13}C δ (ppm)[a]	^1H δ (ppm) (mult, J (Hz))[b,c]	HMBC[b]
1	34.2	3.76 (m)	
2	139.6	5.78 (d, 9.3)	H-1, H-15
3	132.3		H-1, H-15
4	112.8		H-1, H-2, H-21
5	41.0	2.43 (m)	
		2.22 (m)	
6	30.4	2.17 (m)	H-8, H-16
		1.78 (m)	
7	86.2		H-8, H-16
8	80.8	4.53 (d, 7.9)	H-9, H-16
9	36.3	1.80 (m)	
		0.98 (m)	
10	39.4	1.99 (m)	H-8, H-17
11	34.1	1.68 (m)	H-9, H-17
12	28.3	1.70 (m)	
		1.24 (m)	
13	16.6	1.72 (m)	
		1.45 (m)	
14	46.0	0.99 (m)	H-2, H-19, H-20
15	69.8	4.09 (d, 12.0)	H-2
		3.70 (d, 12.0)	
16	28.3	1.25 (s)	H-17

[a] Recorded at 100.5 MHz. [b] Recorded at 500 MHz. [c] Assignments based on HMQC data.

Table 4.8 (continued). NMR data for 5,6,11,12,2',3'-hexahydroeleutherobin (**60**) (recorded in CDCl₃).
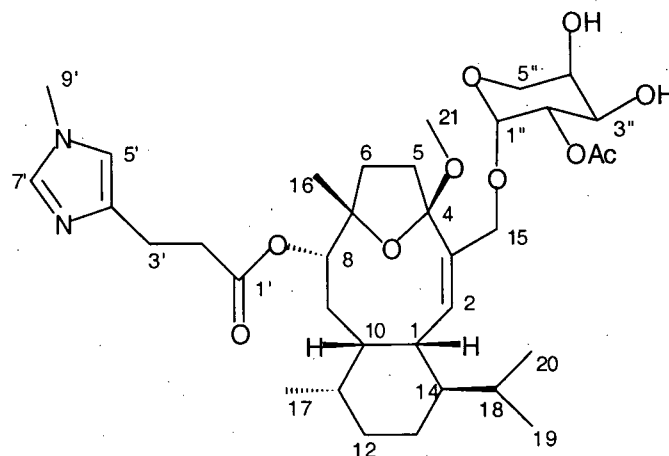
Carbon No.	^{13}C δ (ppm)[a]	^1H δ (ppm) (mult, J (Hz))[b,c]	HMBC[b]
17	16.1	0.76 (d, 7.0)	
18	26.6	1.83 (m)	
19	21.4	0.88 (d, 6.5)	
20	21.6	0.87 (d, 6.5)	
21	49.6	3.09 (s)	
1'	172.6		H-8, H-2'
2'	34.0	2.85 (m)	H-3'
		2.67 (m)	
3'	23.6	2.67 (m)	
		2.85 (m)	
4'	137.1		H-5', H-9'
5'	116.6	6.63 (s)	H-3', H-9'
7'	141.0	7.35 (s)	H-3', H-5'
9'	33.6	3.60 (s)	
1"	95.1	5.02 (d, 3.5)	H-5"
2"	72.1	4.97 (dd, 3.5, 9.6)	H-4"
3"	69.4	4.00 (m)	H-5"
4"	68.1	4.00 (m)	H-5"
5"	62.0	3.84 (d, 12.2)	H-3"
		3.72 (dd, 1.5, 12.2)	
1'''	171.6		H-2'''
2'''	21.0	2.08 (s)	

[a] Recorded at 100.5 MHz. [b] Recorded at 500 MHz. [c] Assignments based on HMQC data.

Table 4.9. NMR data for 5,6,11,12,2',3'-hexahydroeleutherobin (**60**)
(recorded in CDCl$_3$).
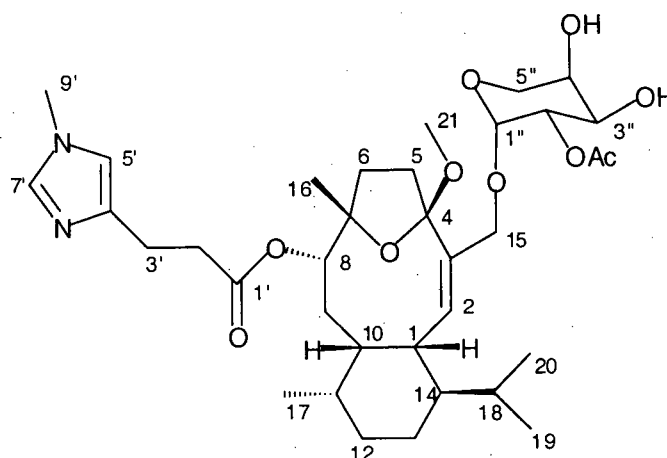
Proton No.	^{1}H δ (ppm) (mult, J (Hz))[a]	COSY[a]	NOE[b]
1	3.76 (m)	H-2, H-10	H-14, H-10, H-19
2	5.78 (d, 9.3)	H-1	H-14, H-15, H-17
5	2.43 (m)	H-5, H-6	
	2.22 (m)	H-5, H-6	
6	2.17 (m)	H-5, H-6	
	1.78 (m)	H-5, H-6	
8	4.53 (d, 7.9)	H-9	H-9, H-16
9	1.80 (m)	H-8, H-9	
	0.98 (m)	H-9	
10	1.99 (m)		
11	1.68 (m)	H-17	
12	1.70 (m)	H-12, H-13	
	1.24 (m)	H-12, H-13	
13	1.72 (m)	H-12, H-13, H-14	
	1.45 (m)	H-12, H-13	
14	0.99 (m)	H-13, H-18	
15	4.09 (d, 12.0)	H-15	H-15
	3.70 (d, 12.0)	H-15	H-5
16	1.25 (s)		
17	0.76 (d, 7.0)	H-11	
18	1.83 (m)	H-14, H-19, H-20	
19	0.88 (d, 6.5)	H-18	H-15

[a] Recorded at 500 MHz. [b] Recorded at 500 MHz using a 2D NOESY experiment.

Table 4.9 (continued). NMR data for 5,6,11,12,2',3'-hexahydroeleutherobin (**60**) (recorded in CDCl₃).
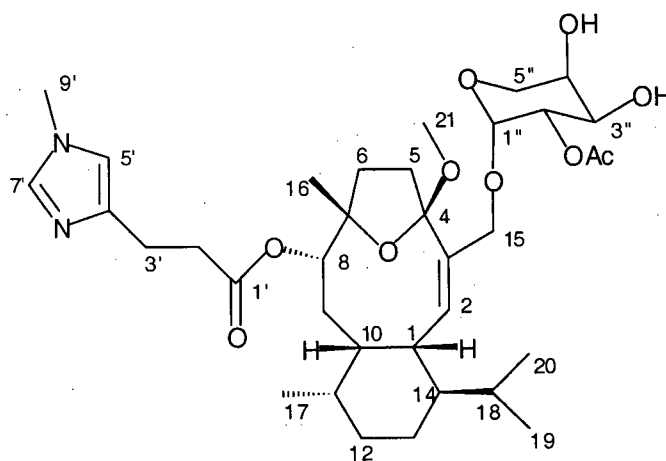
Proton No.	¹H δ (ppm) (mult, J (Hz))ᵃ	COSYᵃ	NOEᵇ
20	0.87 (d, 6.5)	H-18	
21	3.09 (s)		
2'	2.85 (m)	H-3'	
	2.67 (m)		
3'	2.67 (m)	H-2'	
	2.85 (m)		
5'	6.63 (s)		
7'	7.35 (s)		
9'	3.60 (s)		
1"	5.02 (d, 3.5)	H-2"	
2"	4.97 (dd, 3.5, 9.6)	H-1", H-3"	
3"	4.00 (m)	H-2", H-4"	
4"	4.00 (m)	H-3", H-5"	
5"	3.84 (d, 12.2)	H-4", H-5"	
	3.72 (dd, 1.5, 12.2)	H-4", H-5"	
2'"	2.08 (s)		

ᵃ Recorded at 500 MHz. ᵇ Recorded at 500 MHz using a 2D NOESY experiment.

Preparation of ketals of eleutherobin (procedure A).[46]

33 R = Et
46 R = n-Pr
47 R = i-Pr
48 R = n-Bu
49 R = ⌇⌇OH

50 R = ⌇⌇OH
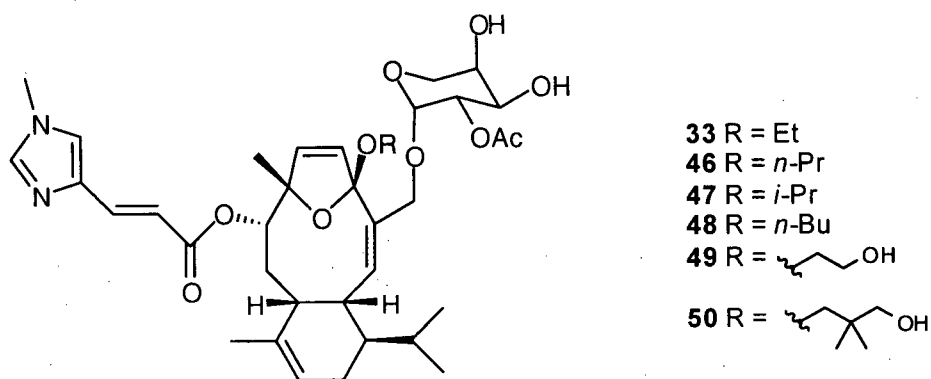
To a stirred solution of desmethyleleutherobin (**32**) in the appropriate anhydrous alcohol (1.0 mL) at room temperature was added excess PPTS (5 equivalents). After the reaction mixture had been stirred for 3 hours, it was treated with saturated aqueous $NaHCO_3$ (5 mL) and the resultant mixture was diluted with EtOAc (10 mL). The phases were separated and the aqueous phase was extracted with EtOAc (2 x 10 mL). The combined organic phases were dried ($MgSO_4$) and concentrated. Purification of the crude product by flash chromatography (20g of silica gel, 93:7 CH_2Cl_2 - MeOH) and removal of trace amounts of solvent from the resulting solids provided the desired ketal of eleutherobin.

Preparation of the ethyl ketal of eleutherobin **33.**

Following procedure A, a stirred solution of desmethyleleutherobin (**32**) (4.0 mg, 0.0061 mmol) in EtOH provided 3.6 mg (88%) of ethyl ketal of eleutherobin **33** as a colorless solid.

^{1}H NMR (400 MHz, $CDCl_3$) δ 7.51 (d, 1H, J = 15.7 Hz, H-3'), 7.44 (s, 1H, H-7'), 7.08 (s, 1H, H-5'), 6.54 (d, 1H, J = 15.7 Hz, H-2'), 6.12 (d, 1H, J = 5.9 Hz, H-5), 6.03 (d, 1H, J = 5.9 Hz, H-6), 5.53 (d, 1H, J = 9.2 Hz, H-2), 5.25 (m, 1H, H-12), 4.96 (dd, 1H, J = 3.4, 9.9 Hz, H-2"), 4.89 (d,

1H, J = 3.4 Hz, H-1"), 4.78 (d, 1H, J = 7.2 Hz, H-8), 4.30 (d, 1H, J = 12.2 Hz, H-15), 4.01 (dd, 1H, J = 3.6, 9.9 Hz, H-3"), 3.90-4.00 (m, 2H, H-1, H-4"), 3.86 (d, 1H, J = 12.2 Hz, H-15), 3.83 (d, 1H, J = 12.7 Hz, H-5"), 3.70 (s, 3H, H-9'), 3.68 (dd, 1H, J = 1.5, 12.7 Hz, H-5"), 3.44 (m, 2H, H-21, H-21), 2.59 (m, 1H, H-10), 2.28 (m, 1H, H-13), 2.10 (s, 3H, OCOCH$_3$), 1.97 (m, 1H, H-13), 1.50-1.61 (m, 2H, H-9, H-18), 1.50 (s, 3H, H-17), 1.41 (s, 3H, H-16), 1.39 (m, 1H, H-9), 1.23 (m, 1H, H-14), 1.18 (t, 3H, J = 7.1 Hz, H-22), 0.95 (d, 3H, J = 6.5 Hz, H-19), 0.91 (d, 3H, J = 6.5 Hz, H-20).

^{13}C NMR (100.5 MHz, CDCl$_3$) δ 171.4 (O$\underline{C}$OCH$_3$), 166.7 (C-1'), 139.2 (C-7'), 138.5 (C-4'), 137.3 (C-2), 136.4 (C-3'), 134.2 (C-11), 133.1 (C-6), 133.0 (C-3), 131.5 (C-5), 122.7 (C-5'), 121.3 (C-12), 115.9 (C-2'), 115.7 (C-4), 93.5 (C-1"), 89.8 (C-7), 81.5 (C-8), 71.8 (C-2"), 69.5 (C-4"), 69.1 (C-15), 68.2 (C-3"), 62.1 (C-5"), 57.7 (C-21), 42.5 (C-14), 38.7 (C-10), 34.3 (C-1), 33.6 (C-9'), 31.5 (C-9), 29.1 (C-18), 24.5 (C-13), 24.4 (C-16), 22.1 (C-20), 21.9 (C-17), 21.0 (OCO$\underline{C}$H$_3$), 20.6 (C-19), 15.5 (C-22).

Exact mass calcd for C$_{36}$H$_{51}$N$_2$O$_{10}$ (HRFABMS, M+H): 671.3544; found: 671.3545.

Preparation of the *n*-propyl ketal of eleutherobin **46.**

Following procedure A, a stirred solution of desmethyleleutherobin (**32**) (4.0 mg, 0.0061 mmol) in *n*-propanol provided 3.8 mg (91%) of the *n*-propyl ketal of eleutherobin **46** as a colorless solid.

^{1}H NMR (400 MHz, CDCl$_3$) δ 7.50 (d, 1H, J = 15.0 Hz, H-3'), 7.46 (s, 1H, H-7'), 7.10 (s, 1H, H-5'), 6.54 (d, 1H, J = 15.0 Hz, H-2'), 6.11 (d, 1H, J = 5.7 Hz, H-5), 6.03 (d, 1H, J = 5.7 Hz, H-6), 5.52 (d, 1H, J = 9.5 Hz, H-2), 5.26 (m, 1H, H-12), 4.96 (dd, 1H, J = 3.4, 9.9 Hz, H-2"), 4.89 (d, 1H, J = 3.4 Hz, H-1"), 4.78 (d, 1H, J = 7.2 Hz, H-8), 4.29 (d, 1H, J = 12.4 Hz, H-15), 3.92-4.05 (m, 3H, H-1, H-3", H-4"), 3.86 (d, 1H, J = 12.4 Hz, H-15), 3.82 (d, 1H, J = 12.6 Hz, H-5"), 3.70 (s, 3H, H-9'), 3.69 (m, 1H, H-5"), 3.33 (m, 2H, H-21, H-21), 2.59 (m, 1H, H-10), 2.28 (m, 1H, H-13), 2.09 (s, 3H, OCOCH$_3$), 1.97 (m, 1H, H-13), 1.50-1.63 (m, 4H, H-9, H-18, H-22, H-22), 1.50 (s, 3H, H-17), 1.41 (s, 3H, H-16), 1.39 (m, 1H, H-9), 1.23 (m, 1H, H-14), 0.95 (d, 3H, J = 6.5 Hz, H-19), 0.91 (d, 3H, J = 6.5 Hz, H-20), 0.89 (t, 3H, J = 7.4 Hz, H-23).

^{13}C NMR (100.5 MHz, CDCl$_3$) δ 171.4 (OCOCH$_3$), 166.8 (C-1'), 139.2 (C-7'), 138.4 (C-4'), 137.2 (C-2), 136.5 (C-3'), 134.3 (C-11), 133.1 (C-6), 133.0 (C-3), 131.6 (C-5), 122.8 (C-5'), 121.3 (C-12), 115.9 (C-2'), 115.6 (C-4), 93.5 (C-1"), 89.8 (C-7), 81.5 (C-8), 71.8 (C-2"), 69.5 (C-4"), 69.1 (C-15), 68.2 (C-3"), 63.9 (C-21), 62.1 (C-5"), 42.5 (C-14), 38.8 (C-10), 34.3 (C-1), 33.6 (C-9'), 31.5 (C-9), 29.1 (C-18), 24.5 (C-13), 24.4 (C-16), 23.2 (C-22), 22.1 (C-20), 21.9 (C-17), 21.0 (OCOCH$_3$), 20.6 (C-19), 10.8 (C-23).

Exact mass calcd for C$_{37}$H$_{53}$N$_2$O$_{10}$ (HRFABMS, M+H): 685.3700; found: 685.3701.

Preparation of the *n*-butyl ketal of eleutherobin 48.

Following procedure A, a stirred solution of desmethyleleutherobin (32) (4.0 mg, 0.0061 mmol) in *n*-butanol provided 3.6 mg (84%) of the *n*-butyl ketal of eleutherobin 48 as a colorless solid.

^{1}H NMR (400 MHz, CDCl$_3$) δ 7.52 (d, 1H, J = 15.3 Hz, H-3'), 7.45 (s, 1H, H-7'), 7.08 (s, 1H, H-5'), 6.54 (d, 1H, J = 15.3 Hz, H-2'), 6.11 (d, 1H, J = 5.7 Hz, H-5), 6.01 (d, 1H, J = 5.7 Hz, H-6), 5.52 (d, 1H, J = 9.5 Hz, H-2), 5.26 (m, 1H, H-12), 4.96 (dd, 1H, J = 3.4, 9.9 Hz, H-2"), 4.89 (d, 1H, J = 3.4 Hz, H-1"), 4.78 (d, 1H, J = 7.6 Hz, H-8), 4.28 (d, 1H, J = 12.2 Hz, H-15), 3.92-4.05 (m, 3H, H-1, H-3", H-4"), 3.85 (d, 1H, J = 12.6 Hz, H-15), 3.82 (d, 1H, J = 13.1 Hz, H-5"), 3.70 (s, 3H, H-9'), 3.69 (dd, 1H, J = 1.9, 13.1 Hz, H-5"), 3.37 (m, 2H, H-21, H-21), 2.60 (m, 1H, H-10), 2.28 (m, 1H, H-13), 2.09 (s, 3H, OCOCH$_3$), 1.97 (m, 1H, H-13), 1.48-1.63 (m, 4H, H-9, H-18, H-22, H-22), 1.50 (s, 3H, H-17), 1.41 (s, 3H, H-16), 1.30-1.43 (m, 3H, H-9, H-23, H-23), 1.23 (m, 1H, H-14), 0.95 (d, 3H, J = 6.5 Hz, H-19), 0.91 (d, 3H, J = 6.5 Hz, H-20), 0.89 (t, 3H, J = 7.6 Hz, H-24).

^{13}C NMR (100.5 MHz, CDCl$_3$) δ 171.4 (O$\underline{C}$OCH$_3$), 166.8 (C-1'), 139.2 (C-7'), 138.6 (C-4'), 137.2 (C-2), 136.4 (C-3'), 134.3 (C-11), 133.1 (C-6), 133.0 (C-3), 131.6 (C-5), 122.7 (C-5'), 121.3 (C-12), 115.9 (C-2'), 115.6 (C-4), 93.4 (C-1"), 89.8 (C-7), 81.5 (C-8), 71.8 (C-2"), 69.5 (C-4"), 69.0 (C-15), 68.2 (C-3"), 62.1 (C-5"), 61.9 (C-21), 42.5 (C-14), 38.8 (C-10), 34.3 (C-1), 33.6 (C-9'), 32.0 (C-22), 31.5 (C-9), 29.1 (C-18), 24.5 (C-13), 24.4 (C-16), 22.1 (C-20), 21.9 (C-17), 21.0 (OCO$\underline{C}$H$_3$), 20.6 (C-19), 19.5 (C-23), 13.9 (C-24).

Exact mass calcd for C$_{38}$H$_{55}$N$_2$O$_{10}$ (HRFABMS, M+H): 699.3857; found: 699.3859.

Preparation of ketals of eleutherobin (procedure B).

To a stirred solution of desmethyleleutherobin (**32**) in the appropriate alcohol (1.0 mL) and CH_2Cl_2 at room temperature was added excess PPTS (5 equivalents). After the reaction mixture had been stirred for 3 hours at room temperature, it was treated with saturated aqueous $NaHCO_3$ (5 mL) and the resultant mixture was diluted with EtOAc (10 mL). The phases were separated and the aqueous phase was extracted with EtOAc (2 x 10 mL). The combined organic phases were dried ($MgSO_4$) and concentrated. Purification of the crude product by flash chromatography (20g of silica gel, 93:7 CH_2Cl_2 - MeOH) and removal of trace amounts of solvent from the resulting solids provided the desired ketal of eleutherobin.

Preparation of the *i*-propyl ketal of eleutherobin 47.

Following procedure B, a stirred solution of desmethyleleutherobin (**32**) (2.0 mg, 0.003 mmol) in *i*-propanol and CH_2Cl_2 provided 1.2 mg (60%) of the *i*-propyl ketal of eleutherobin (**47**) as a colorless solid.

^{1}H NMR (400 MHz, $CDCl_3$) δ 7.52 (d, 1H, *J* = 15.3 Hz, H-3'), 7.45 (s, 1H, H-7'), 7.09 (s, 1H, H-5'), 6.53 (d, 1H, *J* = 15.3 Hz, H-2'), 6.11 (d, 1H, *J* = 5.7 Hz, H-5), 6.03 (d, 1H, *J* = 5.7 Hz, H-6), 5.54 (d, 1H, *J* = 9.2 Hz, H-2), 5.26 (m, 1H, H-12), 4.96 (dd, 1H, *J* = 3.4, 9.5 Hz, H-2"), 4.89 (d, 1H, *J* = 3.4 Hz, H-1"), 4.77 (d, 1H, *J* = 7.6 Hz, H-8), 4.28 (d, 1H, *J* = 12.0 Hz, H-15), 3.96-4.04 (m, 3H, H-1, H-3", H-4"), 3.79-3.89 (m, 3H, H-15, H-5", H-21), 3.70 (s, 3H, H-9'), 3.66-3.72

(m, 1H, H-5"), 2.59 (m, 1H, H-10), 2.27 (m, 1H, H-13), 2.09 (s, 3H, OCOCH$_3$), 1.97 (m, 1H, H-13), 1.50-1.63 (m, 2H, H-9, H-18), 1.50 (s, 3H, H-17), 1.41 (s, 3H, H-16), 1.39 (m, 1H, H-9), 1.23 (m, 1H, H-14), 1.16 (d, 3H, J = 6.1 Hz, H-22), 1.13 (d, 3H, J = 6.5 Hz, H-23), 0.94 (d, 3H, J = 6.5 Hz, H-19), 0.91 (d, 3H, J = 6.5 Hz, H-20).

^{13}C NMR (100.5 MHz, CDCl$_3$) δ 171.4 (O$\underline{C}$OCH$_3$), 166.7 (C-1'), 139.2 (C-7'), 137.5 (C-2), 136.4 (C-3'), 134.3 (C-11), 133.1 (C-6), 132.9 (C-3), 131.9 (C-5), 122.7 (C-5'), 121.3 (C-12), 116.1 (C-2'), 115.9 (C-4), 93.4 (C-1"), 89.9 (C-7), 81.7 (C-8), 71.8 (C-2"), 69.5 (C-4"), 68.9 (C-15), 68.1 (C-3"), 65.4 (C-21), 62.1 (C-5"), 42.5 (C-14), 38.8 (C-10), 34.3 (C-1), 33.6 (C-9'), 31.4 (C-9), 29.0 (C-18), 24.6 (C-22), 24.4 (C-13), 24.4 (C-16), 24.1 (C-23), 22.1 (C-20), 21.9 (C-17), 21.0 (OCO$\underline{C}$H$_3$), 20.5 (C-19).

Exact mass calcd for C$_{37}$H$_{53}$N$_2$O$_{10}$ (HRFABMS, M+H): 685.3700; found: 685.3702.

Preparation of the 2-hydroxyethyl ketal of eleutherobin **49**.

Following procedure B, a stirred solution of desmethyleleutherobin (**32**) (2.0 mg, 0.003 mmol) in ethylene glycol and CH$_2$Cl$_2$ provided 1.3 mg (60%) of the 2-hydroxyethyl ketal of eleutherobin **49** as a colorless solid.

^{1}H NMR (400 MHz, CDCl$_3$) δ 7.52 (d, 1H, J = 15.0 Hz, H-3'), 7.46 (s, 1H, H-7'), 7.09 (s, 1H, H-5'), 6.54 (d, 1H, J = 15.0 Hz, H-2'), 6.09 (m, 2H, H-5, H-6), 5.61 (d, 1H, J = 9.6 Hz, H-2), 5.26

(m, 1H, H-12), 4.94-5.01 (m, 2H, H-1", H-2"), 4.79 (d, 1H, J = 7.3 Hz, H-8), 4.22 (d, 1H, J =

12.2 Hz, H-15), 3.80-4.03 (m, 5H, H-1, H-3", H-4", H-15, H-5"), 3.65-3.78 (m, 3H, H-5", H-21,

H-21), 3.70 (s, 3H, H-9'), 3.56 (m, 2H, H-22, H-22), 2.59 (m, 1H, H-10), 2.28 (m, 1H, H-13),

2.10 (s, 3H, OCOCH$_3$), 1.98 (m, 1H, H-13), 1.50-1.65 (m, 2H, H-9, H-18), 1.51 (s, 3H, H-17),

1.43 (s, 3H, H-16), 1.38 (m, 1H, H-9), 1.23 (m, 1H, H-14), 0.96 (d, 3H, J = 6.5 Hz, H-19), 0.92

(d, 3H, J = 6.4 Hz, H-20).

Exact mass calcd for $C_{36}H_{51}N_2O_{11}$ (HRFABMS, M+H): 687.3493; found: 687.3490.

Preparation of the 2,2-dimethyl-3-hydroxypropyl ketal of eleutherobin 50.

To a stirred solution of desmethyleleutherobin (32) (1.5 mg, 0.0023 mmol) in 2,2-dimethyl-1,3-

propanediol (1.0 mL) and dry CH$_2$Cl$_2$ (1.0 mL) at room temperature, was added excess PPTS (3

mg, 0.012 mmol) and 4 Å molecular sieves. After the reaction mixture had been stirred for 3 ours

at room temperature, it was decanted, trreated with saturated aqueous NaHCO$_3$ (5 mL) and the

resultant mixture was diluted with EtOAc (10 mL). The phases were separated and the aqueous

phase was extracted with EtOAc (2 x 10 mL). The combined organic phases were dried (MgSO$_4$)

and concentrated. Purification of the crude product by flash chromatography (20g of silica gel,

EtOAc then 9:1 CH$_2$Cl$_2$ - MeOH) and removal of trace amounts of solvent from the resulting

solid provided 1.0 mg (60%) of the 2,2-dimethyl-3-hydroxypropyl ketal of eleutherobin (50) as a

colorless solid.

¹H NMR (400 MHz, CDCl₃) δ 7.52 (d, 1H, J = 15.6 Hz, 1H, H-3'), 7.45 (s, 1H, H-7'), 7.09 (s, 1H, H-5'), 6.54 (d, 1H, J = 15.6 Hz, H-2'), 6.10 (d, 1H, J = 5.9 Hz, H-5), 6.03 (d, 1H, J = 5.9 Hz, H-6), 5.53 (d, 1H, J = 9.5 Hz, H-2), 5.27 (m, 1H, H-12), 4.97 (dd, 1H, J = 3.4, 9.9 Hz, H-2''), 4.89 (d, 1H, J = 3.4 Hz, H-1''), 4.78 (d, 1H, J = 7.6 Hz, H-8), 4.23 (d, 1H, J = 12.2 Hz, H-15), 3.85-4.05 (m, 3H, H-1, H-3'', H-4''), 3.88 (d, 1H, J = 12.2 Hz, H-15), 3.82 (d, 1H, J = 13.0 Hz, H-5''), 3.64-3.70 (m, 1H, H-5''), 3.70 (s, 3H, H-9'), 3.38 (m, 2H, H-23, H-23), 3.26 (d, 1H, J = 9.4 Hz, H-21), 3.14 (d, 1H, J = 9.4 Hz, H-21), 2.57 (m, 1H, H-10), 2.25 (m, 1H, H-13), 2.10 (s, 3H, OCOCH₃), 1.97 (m, 1H, H-13), 1.50-1.63 (m, 2H, H-9, H-18), 1.50 (s, 3H, H-17), 1.43 (s, 3H, H-16), 1.39 (m, 1H, H-9), 1.23 (m, 1H, H-14), 0.95 (d, 3H, J = 6.5 Hz, H-19), 0.91 (d, 3H, J = 6.5 Hz, H-20), 0.88 (s, 3H, H-24), 0.87 (s, 3H, H-25).

¹³C NMR (100.5 MHz, CDCl₃) δ 171.4 (O$\underline{C}$OCH₃), 166.7 (C-1'), 139.3 (C-7'), 137.9 (C-2), 136.5 (C-3'), 134.3 (C-11), 133.3 (C-6), 132.4 (C-3), 131.2 (C-5), 122.8 (C-5'), 121.4 (C-12), 115.8 (C-2'), 115.7 (C-4), 93.5 (C-1''), 90.2 (C-7), 81.4 (C-8), 71.8 (C-2''), 70.6 (C-21), 69.8 (C-23), 69.4 (C-4''), 68.9 (C-15), 68.1 (C-3''), 62.2 (C-5''), 42.8 (C-14), 38.8 (C-10), 35.9 (C-22), 34.4 (C-1), 33.6 (C-9'), 31.5 (C-9), 29.2 (C-18), 24.5 (C-13), 24.5 (C-16), 22.1 (C-20), 22.0 (C-17), 22.0 (C-24), 21.8 (C-25), 21.0 (OCO$\underline{C}$H₃), 20.6 (C-19).

Exact mass calcd for $C_{39}H_{57}N_2O_{11}$ (HRFABMS, M+H): 729.3962; found: 729.3961.

4.6 References

(1)   Faulkner, D. J. *Chem. Rev.* **1993**, *93*, 1671.

(2)   For reviews on the chemistry of octacorals see: (a) Rodriguez, A. D. *Tetrahedron* **1995**, *51*, 4571. (b) Coll, J. C. *Chem. Rev.* **1992**, *92*, 613.

(3)   Miner, R. W. *Field Book of Seashore Life*; Putnam's Sons: New York, 1950.

(4)   Goldberg, W. M. *Bull. Mar. Sci.* **1973**, *23*, 465.

(5)   Fenical, W.; Pawlik, J. R. *Mar. Ecol. Prog. Ser.* **1991**, *75*, 1.

(6)   Burkholder, P. R.; Burkholder, L. M. *Science* **1958**, *127*, 1174.

(7)   Look, S. A.; Fenical, W.; Qi-tai, Z.; Clardy, J. *J. Org. Chem.* **1984**, *49*, 1417.

(8)   Kennard, O.; Watson, D. G.; Riva di Sanseverino, B.; Tursch, R.; Bosmans, R.; Djerassi, C. *Tetrahedron Lett.* **1968**, *9*, 2879.

(9)   See for example: Bernardelli, P.; Moradei, O. M.; Friedrich, D.; Yang, J.; Gallou, F.; Dyck, B. P.; Doskotch, R. W.; Lange, T.; Paquette, L. A. *J. Am. Chem. Soc.* **2001**, *123*, 9021 (and refererences cited therein).

(10)   Look, S. A.; Fenical, W.; Van Engen, D.; Clardy, J. *J. Am. Chem. Soc.* **1984**, *106*, 5026.

(11)   Pawlik, J. R.; Burch, M. T.; Fenical, W. *J. Exp. Mar. Biol. Ecol.* **1987**, *108*, 55.

(12)   D'Ambrosio, M.; Guerriero, A.; Pietra, F. *Helv. Chim. Acta* **1987**, *70*, 2019.

(13)   D'Ambrosio, M.; Guerriero, A.; Pietra, F. *Helv. Chim. Acta* **1988**, *71*, 964.

(14)   Ketzinel, S.; Rudi, A.; Schleyer, M.; Benayahu, Y.; Kashman, Y. *J. Nat. Prod.* **1996**, *59*, 873.

(15)   Hooper, G. J.; Davies-Coleman, M. T.; Schleyer, M. *J. Nat. Prod.* **1997**, *60*, 889.

(16)   The cytotoxic properties of eleutherobin, but not its tubulin stabilizing propoerties, were described in U.S. Letters Patent No. 5,473,057 issued December 5, 1995.

(17)   Lindel, T.; Jensen, P. R.; Fenical, W.; Long, B. H.; Casazza, A. M.; Carboni, J.; Fairchild, C. R. *J. Am. Chem. Soc.* **1997**, *119*, 8744.

(18)   Dewick, P. M. *Medicinal Natural Products*; John Wiley & Sons Ltd.: West Sussex, 1997.

(19)   See reference 16.

(20) Long, B. H.; Carboni, J.; Wasserman, A. J.; Cornell, L. A.; Casazza, A. M.; Jensen, P. R.; Lindel, T.; Fenical, W.; Fairchild, C. R. *Cancer Res.* **1998**, *58*, 1111.

(21) ter Haar, E.; Kowalski, R. J.; Hamel, E.; Lin, C. M.; Longley, R.; Gunaskera, S. P.; Rosenkranz, H. S.; Day, B. W. *Biochemistry* **1996**, *35*, 243.

(22) Bollag, D. M.; McQueney, P. A.; Zhu, J.; Hansens, O.; Koupal, L.; Liesch, J.; Goetz, M.; Lazarides, E.; Woods, C. *Cancer Res.* **1995**, *55*, 2325.

(23) Clomel, C.; Albanese, C.; Pastori, W.; Grandi, M.; Pietra, F.; D'Ambrosio, M.; Guerriero, A.; Battistini, C. Abstract No. 30, *Pro. Amer. Assoc. Can. Res.* **1997**, *38*, 5.

(24) Rayl, A. J. S. *The Scientist* **1999**, *13*, 1.

(25) Nicolaou, K. C.; Xu, J.-Y.; Kim, S.; Pfefferkorn, J.; Ohshima, T.; Vourloumis, D.; Hosokawa, S. *J. Am. Chem. Soc.* **1998**, *120*, 8661.

(26) Nicolaou, K. C.; Xu, J.-Y.; Kim, S.; Ohshima, T.; Hosokawa, S.; Pfefferkorn, J. *J. Am. Chem. Soc.* **1997**, *119*, 11353.

(27) Nicolaou, K. C.; Ohshima, T.; Hosokawa, S.; van Delft, F. L.; Vourloumis, D.; Xu, J.-Y.; Pfefferkorn, J.; Kim, S. *J. Am. Chem. Soc.* **1998**, *120*, 8674.

(28) Chen, X.-T.; Zhou, B.; Bhattacharya, S. K.; Gutteridge, C. E.; Pettus, T. R. R.; Danishefsky, S. *Angew. Chem. Int. Ed.* **1998**, *37*, 789.

(29) Chen, X.-T.; Bhattacharya, S. K.; Zhou, B.; Gutteridge, C. E.; Pettus, T. R. R.; Danishefsky, S. J. *J. Am. Chem. Soc.* **1999**, *121*, 6563.

(30) Nicolaou, K. C.; Winssinger, N.; Vourloumis, D.; Oshima, T.; Kim, S.; Pfefferkorn, J.; Xu, J.-Y.; Li, T. *J. Am. Chem. Soc.* **1998**, *120*, 10814.

(31) McDaid, H. M.; Bhattacharya, S. K.; Chen, X.-T.; He, L.; Shen, H.-J.; Gutteridge, C. E.; Band Horwitz, S.; Danishefsky, S. *Cancer Chemother. Pharmacol.* **1999**, *44*, 131.

(32) Giannakakou, P.; Gussio, R.; Nogales, E.; Downing, K. H.; Zaharevitz, D.; Bollbuck, B.; Poy, G.; Sackett, D.; Nicolaou, K. C.; Fojo, T. *Proc. Nat. Acad. Sci. U.S.A.* **2000**, *97*, 2904.

(33) Ojima, I.; Chakravarty, S.; Inoue, T.; Lin, S.; He, L.; Band Horwitz, S.; Kuduk, S. D.; Danishefsky, S. J. *Proc. Nat. Acad. Sci. U.S.A.* **1999**, *96*, 4256.

(34) He, L.; Jagtap, P. G.; Kingston, D. G. I.; Shen, H.-J.; Orr, G. A.; Band Horwitz, S. *Biochemistry* **2000**, *39*, 3972.

(35) Cinel, B.; Roberge, M.; Behrisch, H.; van Ofwegen, L.; Castro, C. B.; Andersen, R. J. *Org. Lett.* **2000**, *2*, 257.

(36) Roberge, M.; Cinel, B.; Anderson, H. J.; Lim, L.; Jiang, X.; Xu, L.; Kelly, M. T.; Andersen, R. J. *Cancer Res.* **2000**, *60*, 5052.

(37) Cinel, B.; Patrick, B. O.; Roberge, M.; Andersen, R. J. *Tetrahedron Lett.* **2000**, *41*, 2811.

(38) Humann, P. In *Reef Coral Identification*; Deloach, N., Ed.; New World Publications: Jacksonville, 1993.

(39) We thank Dr. Michel Roberge, Cristina Bigg, Tamsin Tarling and Lianne M. McHardy (of the Department of Biochemistry and Molecular Biology at UBC) for the testing of all eleuthosides for antimitotic activity, as described in reference 36, and for performing the *in vitro* tubulin polymerization assays.

(40) A compound similar in structure to the pyranose isomer has been reported and characterized by Dainshefsky and co-workers. See reference 29.

(41) Bhalerao, U. T.; Rapoport, H. *J. Am. Chem. Soc.* **1971**, *93*, 4835.

(42) Carey, F. A.; Sundberg, R. J. *Advanced Organic Chemistry, Part B: Reactions and Synthesis*; 3 ed.; Plenum Press: New York, 1993.

(43) Lauth-de Viguerie, N.; Sergueeva, N.; Damoit, M.; Mawlawi, H.; Riviere, M.; Lattes, A. *Heterocycles* **1994**, *37*, 1561.

(44) Owing to an insufficient amount of material, the resonance that typically appears at δ 138 ppm in the ^{13}C NMR spectra of the eleuthosides (C-4') was not observed.

(45) Due to an insufficient amount of material, ^{13}C NMR resonances for C-3, C-9, C-1', C-4', C-5', C-7' were not observed.

(46) The assignment of ^{1}H and ^{13}C NMR resonances for the various ketals are based on comparison of spectral data recorded on these substances to those reported for eleutherobin in ref. 17.

5. New Analogues of Okadaic Acid from the Sponge *Merriamum Oxeato*: First Examples of Diarrhetic Shellfish Poisons in Northeastern Pacific Ocean

5.1 Introduction

Diarrhetic shellfish poisoning (DSP) was first detected in northeastern Japan in 1978, where folklore had described the frequent occurrence of gastroenteritis after the ingestion of shellfish in late spring and early summer.[1] Yasamoto and co-workers connected these human symptoms to acetone-soluble toxins found in the digestive glands of the implicated shellfish. They also correlated the occurrence of DSP to the appearance of the dinoflagellate *Dinophysis fortii*, and thus named the toxins dinophysistoxins.[2] Since this time, DSP has been recognized as a growing problem for coastal communities around the world. In addition to public health concerns, the economic effect of DSP on commercial fisheries has become critical, as DSP outbreaks have resulted in the banning of shellfish harvests in some areas for up to several months.

Through chemical analysis, the occurrence of DSP has been connected to the accumulation of toxins produced by certain species of dinoflagellates including *Dinophysis acuminata, Procentrum lima, Procentrum maculosum, Protoceratium reticultum* and *Coolia sp.*[3] These microscopic planktonic algae are crucial food for filter-feeding shellfish such as oysters, mussels, scallops and clams, as well as sponges, all of which concentrate the dinophysistoxins. Recently, it has been shown that zooplankton are also capable of consuming the toxic dinoflagellates, thus transferring dinophysistoxins through the food web to higher trophic levels including pelagic fish and marine mammals.[4]

Although DSP is not fatal, a high rate of morbidity and increasing worldwide occurrence of DSP has necessitated the development of sensitive assays for detection and surveillance of

dinophysistoxins. The first causative toxin of DSP, dinophysistoxin 1 (1), was identified by Yasamoto and co-workers in 1982 (Figure 5.1). These researchers reported the isolation of 1 from the hepatopancreas of the mussel *Mytilus edulis*.[5] The structure of dinophysistoxin 1 (1) was elucidated through comparison of its spectral data to that previously reported for the toxins okadaic acid (2), isolated from the sponge *Halichondria okadai*,[6] and acanthifolicin (3), isolated from the Caribbean sponge *Pandaros acanthifolium*.[7] Structurally, these compounds belong to a family of polycyclic ethers whose biosynthesis derives from a C_{42} polyketide chain, which undergoes carbon deletion through both Bayer-Villiger oxidation and Favorski-type rearrangements to provide the common C_{38} backbone.[8] Since the initial report on the structure of dinophysistoxin 1 (1), numerous analogues, including dinophysistoxin 2 (4)[9] and dinophysistoxin 3 (5),[10] have been identified as dinoflagellate metabolites. In addition, two new structural classes of DSP toxins, the pectenotoxins (6)[10] and the yessotoxins (7)[11] have also been reported. Although both 6 and 7 are potent cytotoxins, neither has been shown to induce the onset of diarrhea and hence a reclassification as Hepatotoxic Shellfish Poisons (HSP) has been suggested.[3]

More recently, it has been reported that the dinophysistoxins and okadaic acid are potent inhibitors of serine/threonine family of phosphatases.[12] These phosphatases catalyze dephosphorylation and regulate cell cycle transitions from G_1 to S phase and from S to G_2 phase. Specifically, okadaic acid and the dinophysistoxins inhibit the PP family of protein phosphatases which include protein phosphatase-1 (PP1), -2A (PP2A) and -2B (PP2B).[12] X-ray crystallographic studies of okadaic acid bound to PP1 suggest these toxins adopt a cyclic conformation, which is maintained through an intramolecular hydrogen bond between the C-1 carboxylic acid and the C-24 hydroxyl group.[12] Consequently, structure activity studies have shown that both a free carboxylic acid and free C-24 hydroxyl group are essential for okadiac acid biological activity.

1 $R_1 = R_2 = CH_3$, $R_3 = H$
2 $R_1 = H$, $R_2 = CH_3$, $R_3 = H$
4 $R_1 = CH_3$, $R_2 = R_3 = H$
5 $R_1 = R_2 = CH_3$, $R_3 =$ Acyl
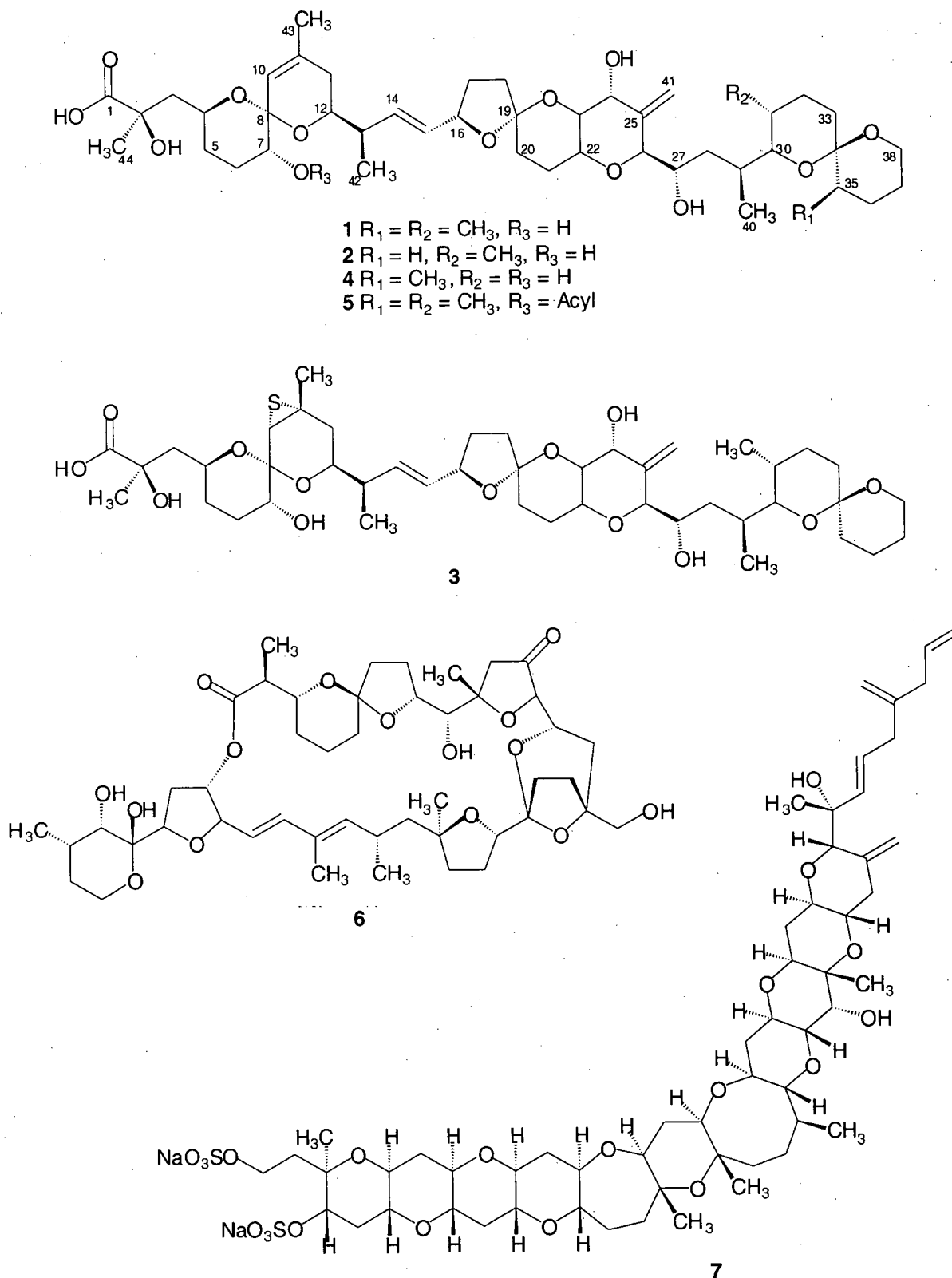
Figure 5.1. Causative toxins of Diarrhetic Shellfish Poisoning (DSP).

As these toxins present a danger not only to filter feeding organisms, but also to the producing dinoflagellate itself, their mechanism of storage in dinoflagellates has been investigated. Wright and co-workers were the first to isolate a water-soluble toxin, dinophysistoxin 4 (8), from the dinoflagellate *P. lima* collected in Mahone Bay, Nova Scotia.[13] The presence of a highly oxygenated, polysulfated carbon chain attached via an ester linkage to the known okadaic acid diol ester 9 results in a marked decrease in protein phosphatase inhibition activity. Consequently, it was proposed that intracellular storage of the dinophysistoxins as the less active sulfates may provide an effective self-protection mechanism for the host dinoflagellate. Observations of the free acid, okadaic acid (2), in the medium of *P. lima* cultures have also led researchers to propose that the less active sulfated dinophysistoxins, such as 8, undergo hydrolysis outside the dinoflagellate cell, yielding the hydrophobic, biologically active toxins, which cannot re-enter the cell. This theory has been supported by the identification of the water-soluble dinophysistoxins 5a (10) and 5b (11) from the dinoflagellate *P. maculosum*, collected in tropical waters.[14]

Biological screening of the extracts from a number of marine invertebrates collected in Jervis Inlet, British Columbia in the summer of 1999 for G2 checkpoint inhibition activity, led to chemical investigations of the sponge *Merriamum oxeato*. The following sections describe the isolation and structure elucidation of known compound dinophysistoxin 1 (1) and the new DSP toxins 27-O-acetyl okadaic acid (12) and 27-O-acetyl dinophysistoxin 1 (13).
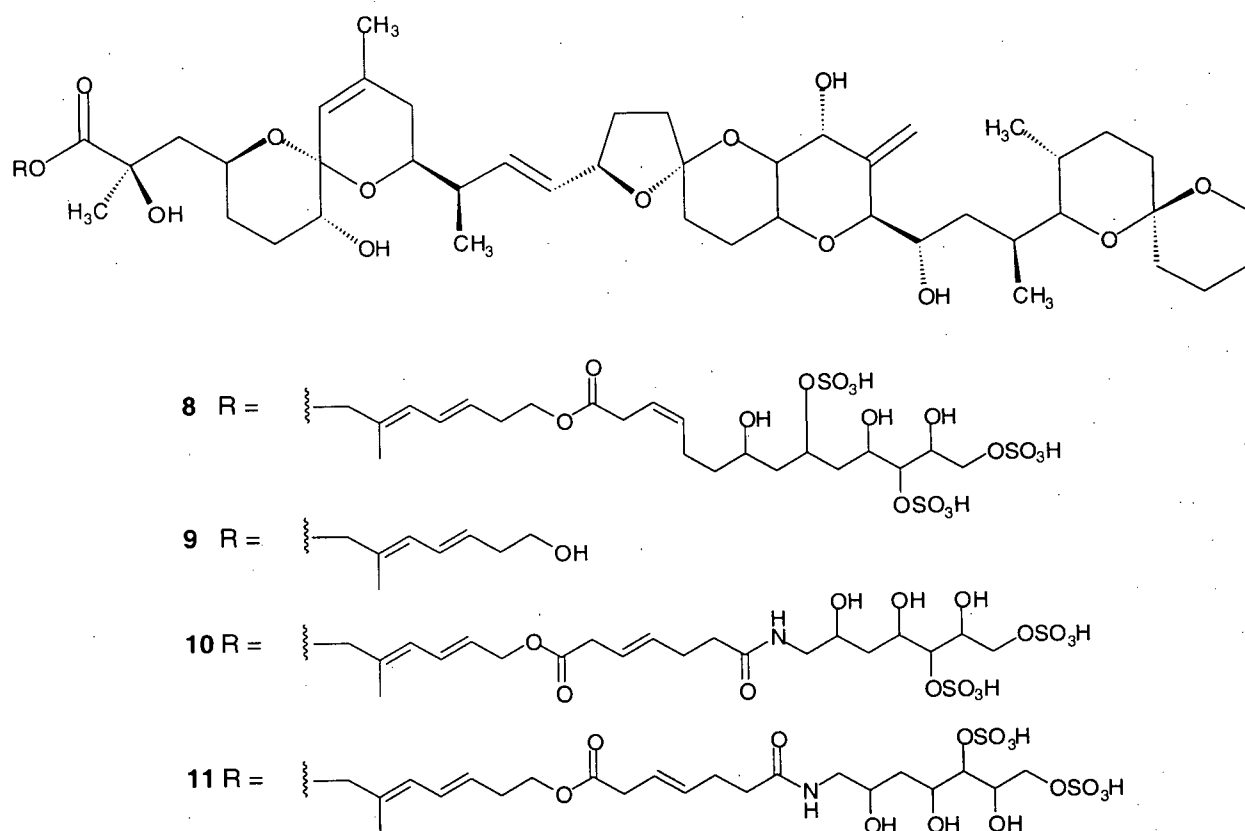
Figure 5.2. C-1 esters of okadaic acid (**2**).

5.2 Results and Discussion

Merriamum oxeato (class *Demospongia*, family *Myxillidae*) was first discovered in the Okhotsk Sea and documented by Koltun in a survey of siliceous-spiculed sponges of the northern and far-eastern seas of the USSR.[15] In the Pacific Northwest, *M. oxeato* is uncommon at depths accessible by SCUBA and there is only one previous report of *M. oxeato* in this area.[16] Specimens of *M. oxeato* were collected in August and September of 1999 in Agamemnon Channel, off Fearney Point, Nelson Island and in Jervis Inlet in January of 2000 off Ball Point, Hardy Island (Figure 5.3). Samples were immediately immersed in MeOH and transferred to the University of British Columbia.
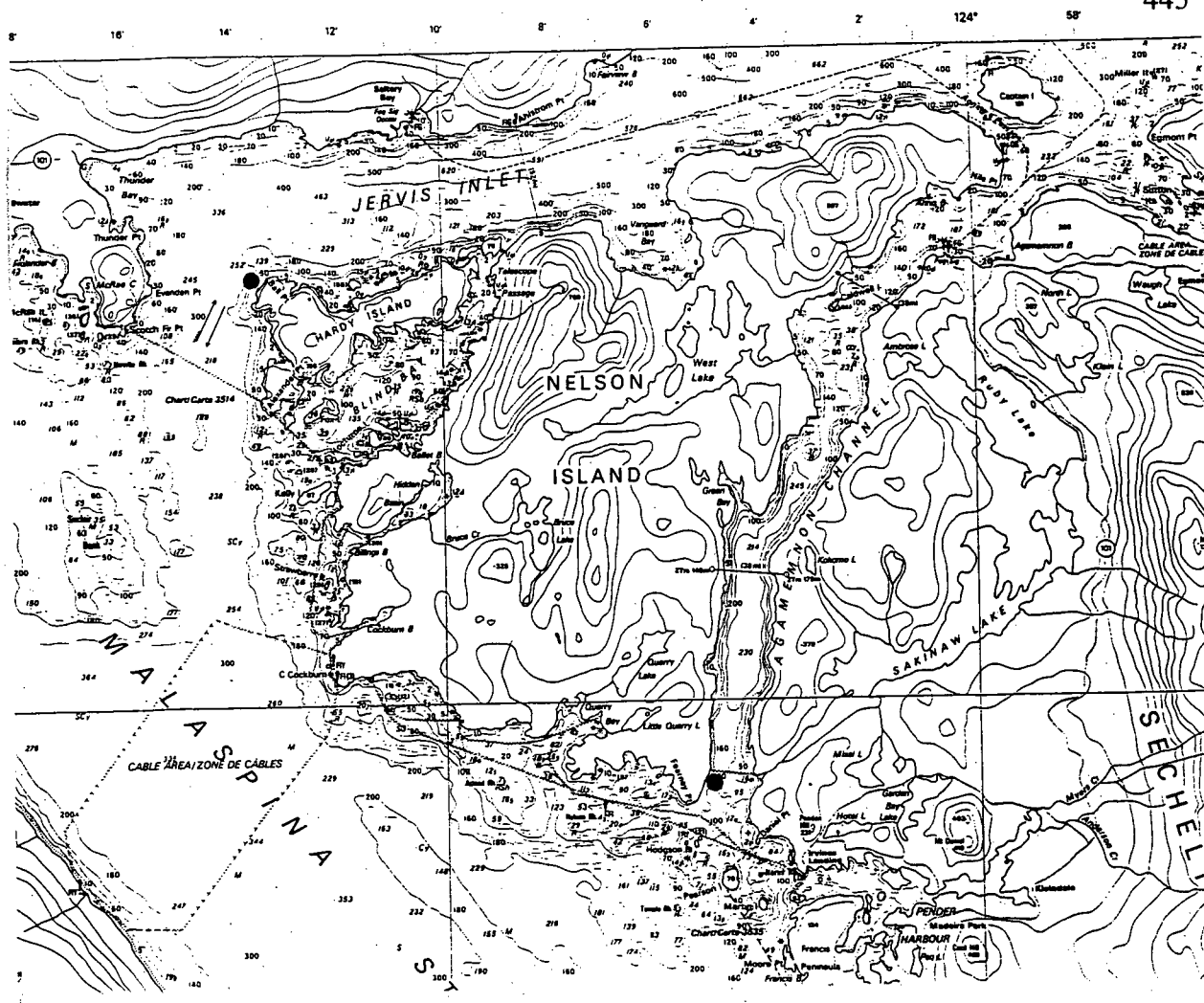
Figure 5.3. Map of collection sites (●) for *Merriamum oxeato.*

Fractionation of the MeOH extract of *M. oxeato* was closely monitored using the G2

checkpoint inhibition assay outlined in Section 1.3.[17] Exhaustive chromatography provided an

inseparable mixture of compounds which, collectively, exhibited G2 checkpoint inhibition

activity at nM concentrations. ^{1}H NMR analysis indicated the mixture was composed of 3

compounds closely related to okadaic acid (**2**). To facilitate further purification, 1/3

(approximately 0.5 mg) of the material was converted to the corresponding mixture of methyl

esters (PhH, MeOH, TMSCH$_2$N$_2$).[18] Unfortunately, while recording spectral data in CDCl$_3$ (the

solvent typically used for okadaic acid characterization) the mixture of methyl esters

decomposed, complicating a direct comparison between spectral data published for okadaic acid (2) and that of the mixture.

Undaunted, the remaining 2/3 of the crude mixture (approximately 1.0 mg) was converted to the corresponding mixture of methyl esters (see Experimental) and efforts towards their separation were undertaken. Separation of these substances by reverse phase HPLC provided pure samples of three analogues of okadaic acid, which were analyzed by ^{1}H NMR in deuteriobenzene (C_6D_6). The choice of C_6D_6 for spectroscopic analysis of these compounds provided certain advantages over $CDCl_3$. Primarily, deuteriobenzene is both inherently less acidic than $CDCl_3$ and a solid at 0 °C, thus less likely to aid in the decomposition of the methyl esters and more amenable to long term storage. In addition, the ^{1}H NMR spectroscopic resonance corresponding to residual H_2O (δ 0.40 ppm) in C_6D_6 does not interfere with aliphatic proton signals (in $CDCl_3$ the residual H_2O resonance appears at δ 1.54 ppm). However, the use of C_6D_6 necessitated reassignment of the diagnostic ^{1}H NMR resonances of okadaic acid (2), as spectral data reported for 2 and the dinophysistoxins is typically that acquired in $CDCl_3$. Fortunately, okadaic acid (2) is commercially available, and transformation of 2 into its methyl ester proceeded smoothly (PhH, MeOH, $TMSCH_2N_2$)[18] affording okadaic acid methyl ester (14) (Figure 5.2) as a standard for comparison of NMR spectral data. The structures of dinophysistoxin 1 methyl ester (15), 27-O-acetyl okadaic acid methyl ester (16) and 27-O-acetyl dinophysistoxin 1 methyl ester (17) were determined through spectroscopic analysis, particularly one and two dimensional NMR and mass spectrometry. Additionally, comparison of the spectral data recorded on these compounds to that of okadaic acid methyl ester (14) aided in confirming the structural assignments.

5.3 Dinophysistoxin 1 (1) and the methyl ester 15

1 R_1 = H, R_2 = CH$_3$
14 R_1 = CH$_3$, R_2 = H
15 R_1 = R_2 = CH$_3$
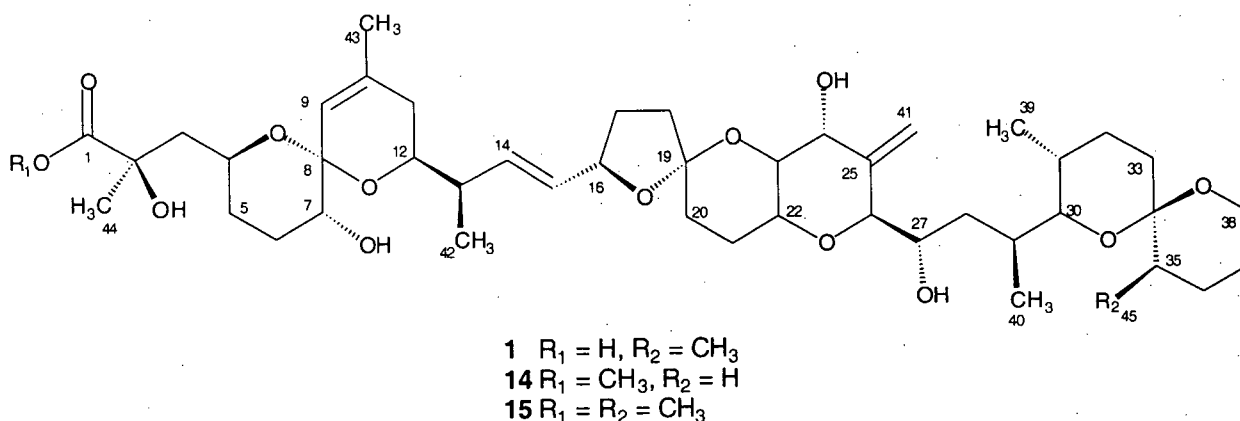
Dinophysistoxin 1 methyl ester (15), the most polar compound in the mixture, was isolated as a white film (200 µg) which gave an (M+H)$^+$ ion in HRFABMS at *m/z* 833.5053. The HRFABMS differed from that of okadaic acid methyl ester (14) (*m/z* 819.4895) by ≈14 mass units corresponding to the replacement of a proton with a methyl substituent. Comparison of ^{1}H NMR spectra recorded for 14 and dinophysistoxin 1 methyl ester (15) (Figure 5.4) confirmed the presence of an additional methyl doublet (δ 1.00, J = 6.7 Hz) in 15. As expected, ^{13}C NMR analysis proved unsuccessful on such small amounts of material, however, inverse detection of many of the carbon signals was possible through the execution of a HMQC experiment. From this data, the presence of seven appended methyl groups (δ 51.8 (C-46), 27.4 (C-44), 22.5 (C-43), 17.0 (C-45), 16.3 (C-40), 15.9 (C-42) and 10.9 (C-39)) was confirmed. Additionally, two protons that resonated at δ 3.68 and 3.57 displayed a common correlation into a single carbon resonance at δ 59.8 in the HMQC spectrum. This data allowed the assignment of the carbon resonance to C-38 (the only oxymethylene in the molecule) and, consequently, the proton resonances in the ^{1}H NMR spectrum of 15 at δ 3.68 and 3.57 were assigned to the protons on C-38. A subsequent HOHAHA experiment (Figure 5.5) provided connectivity between these protons and the additional methyl resonance at δ 1.00. Analysis of a COSY experiment (Figure 5.6) executed on this material permitted the connection of this additional methyl group to C-35.

Further analysis of COSY and HOHAHA spectral data, coupled with the known variations of methyl substitution patterns within the dinophysistoxin family of natural products (Figure 5.1), supported our structural assignment. Thus, the spectral data confirmed the structure of **15** as the methyl ester of the known toxin, dinophysistoxin 1 (**1**) (for ^{1}H and ^{13}C NMR data and assignments see Table 5.1).

Table 5.1. NMR data for dinophysistoxin 1 methyl ester (recorded in C_6D_6).

Carbon No.	^{13}C δ (ppm)[a,b]	^{1}H δ (ppm) (mult, J (Hz))[b]
1	n.o.	
2	n.o.	OH: 4.91 (s)
3	n.o.	2.09 (m); 1.78 (m)
4	71.9	4.15 (m)
5	n.o.	1.80 (m); 1.31 (m)
6	n.o.	2.08 (m); 1.60 (m)
7	68.5	3.46 (m)
8	n.o.	
9	122.5	5.31 (bs)
10	n.o.	
11	n.o.	1.51 (m); 1.33 (m)
12	70.9	3.81 (ddd, 4.8, 8.6, 8.6)
13	n.o.	2.13 (m)
14	135.6	5.82 (dd, 8.6, 15.2)
15	131.1	5.56 (dd, 7.8, 15.2)
16	79.1	4.62 (ddd, 7.4, 7.6, 7.8)
17	n.o.	2.03 (m); 1.49 (m)
18	n.o.	n.o.
19	n.o.	
20	n.o.	n.o.
21	n.o.	1.95 (m); 1.52 (m)
22	69.7	3.49 (m)
23	77.1	3.64 (dd, 9.4, 9.8)
24	71.2	4.32 (m); OH: 2.79 (d, 5.1)
25	n.o.	
26	85.1	3.97 (d, 9.4)
27	65.0	4.17 (m); OH: 2.57 (s)
28	n.o.	1.45 (m); 1.04 (m)
29	n.o.	2.33 (m)
30	75.0	3.42 (dd, 2.3, 10.4)

[a] From HMQC experiments. [b] Recorded at 500 MHz. n.o. (not observed).

Table 5.1 (continued). NMR data for dinophysistoxin 1 methyl ester (recorded in C_6D_6).

Carbon No.	^{13}C δ (ppm)[a,b]	^1H δ (ppm) (mult, J (Hz))[b]
31	n.o.	1.82 (m)
32	n.o.	n.o.
33	n.o.	n.o.
34	n.o.	
35	n.o.	1.50 (m)
36	n.o.	n.o.
37	n.o.	1.61 (m), 1.34 (m)
38	59.8	3.68 (ddd, 2.4, 10.5, 10.5); 3.57 (dd, 4.7, 10.5)
39	10.9	1.09 (d, 7.0)
40	16.3	1.22 (d, 6.5)
41	112.2	5.65 (bs); 4.90 (bs)
42	15.9	0.96 (d, 6.9)
43	22.5	1.36 (s)
44	27.4	1.52 (s)
45	17.0	1.00 (d, 6.7)
46	51.8	3.47 (s)

[a] From HMQC experiments. [b] Recorded at 500 MHz. n.o. (not observed).
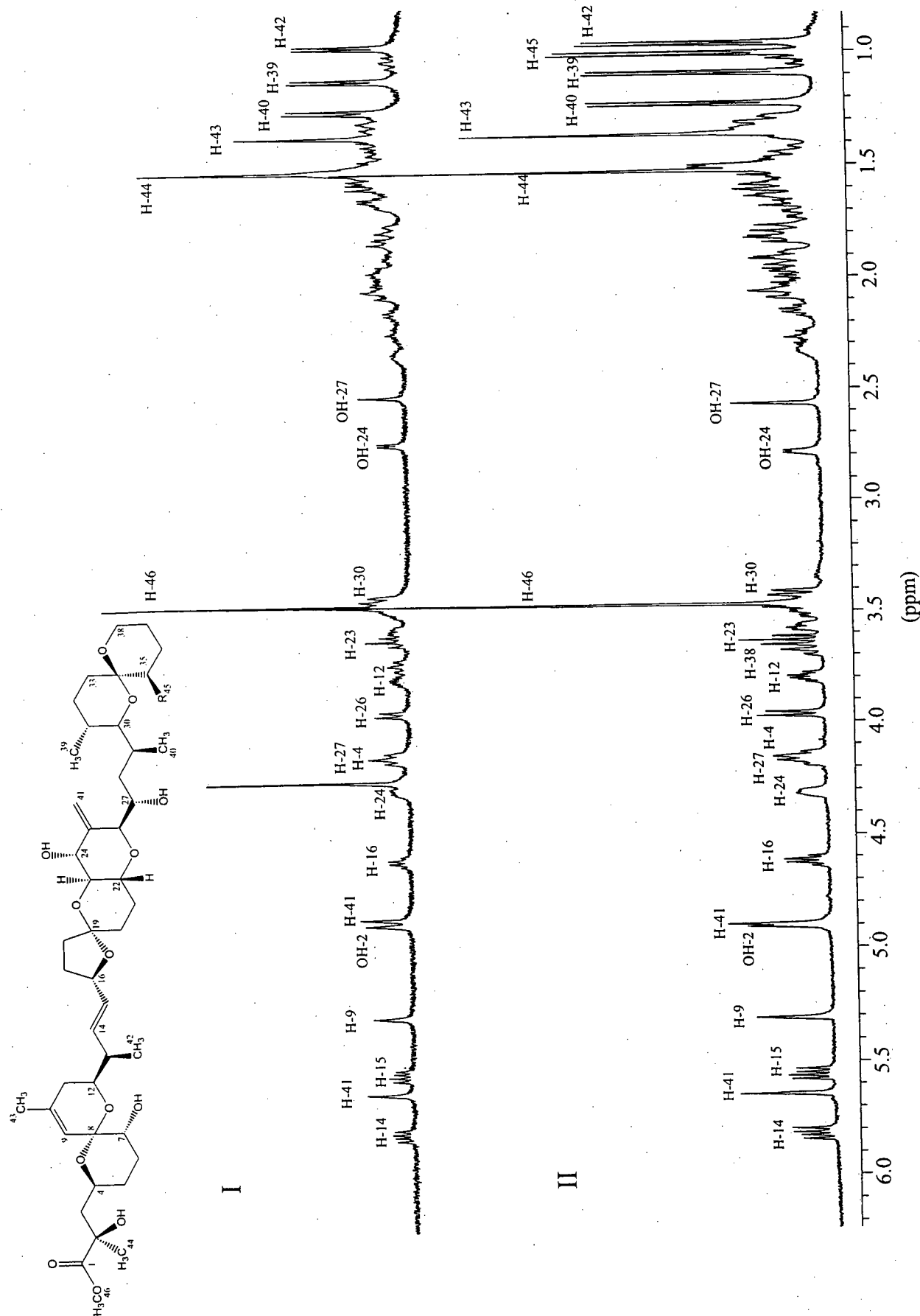
Figure 5.4. ^{1}H NMR spectra of (I) okadaic acid methyl ester (**14**, R=H) and (II) dinophysistoxin 1 methyl ester (**15**, R=CH$_3$) (recorded in C$_6$D$_6$ at 500 MHz).
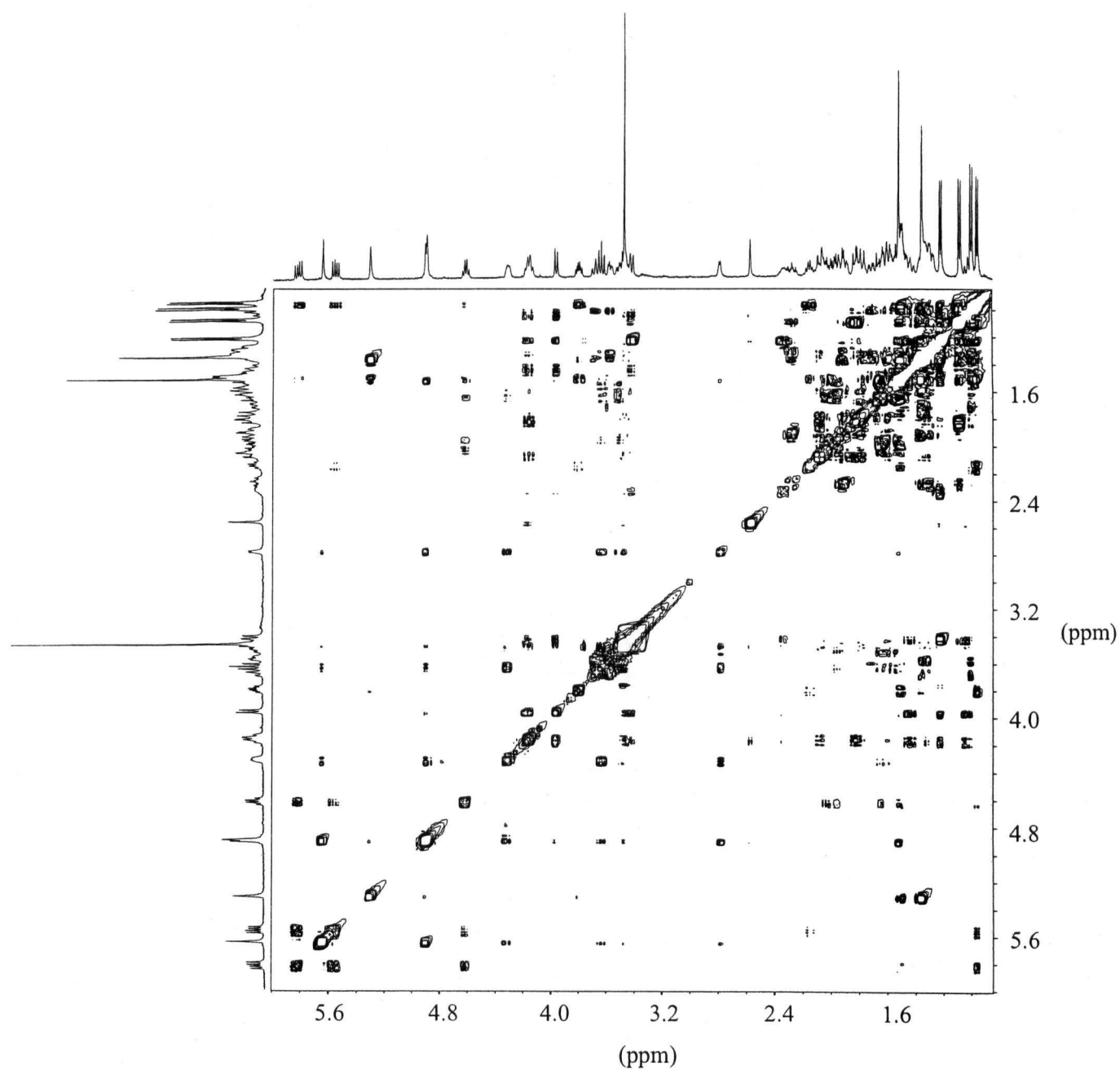
Figure 5.5. HOHAHA spectrum of dinophysistoxin 1 methyl ester (**15**) (recorded in C₆D₆ at 500 MHz).
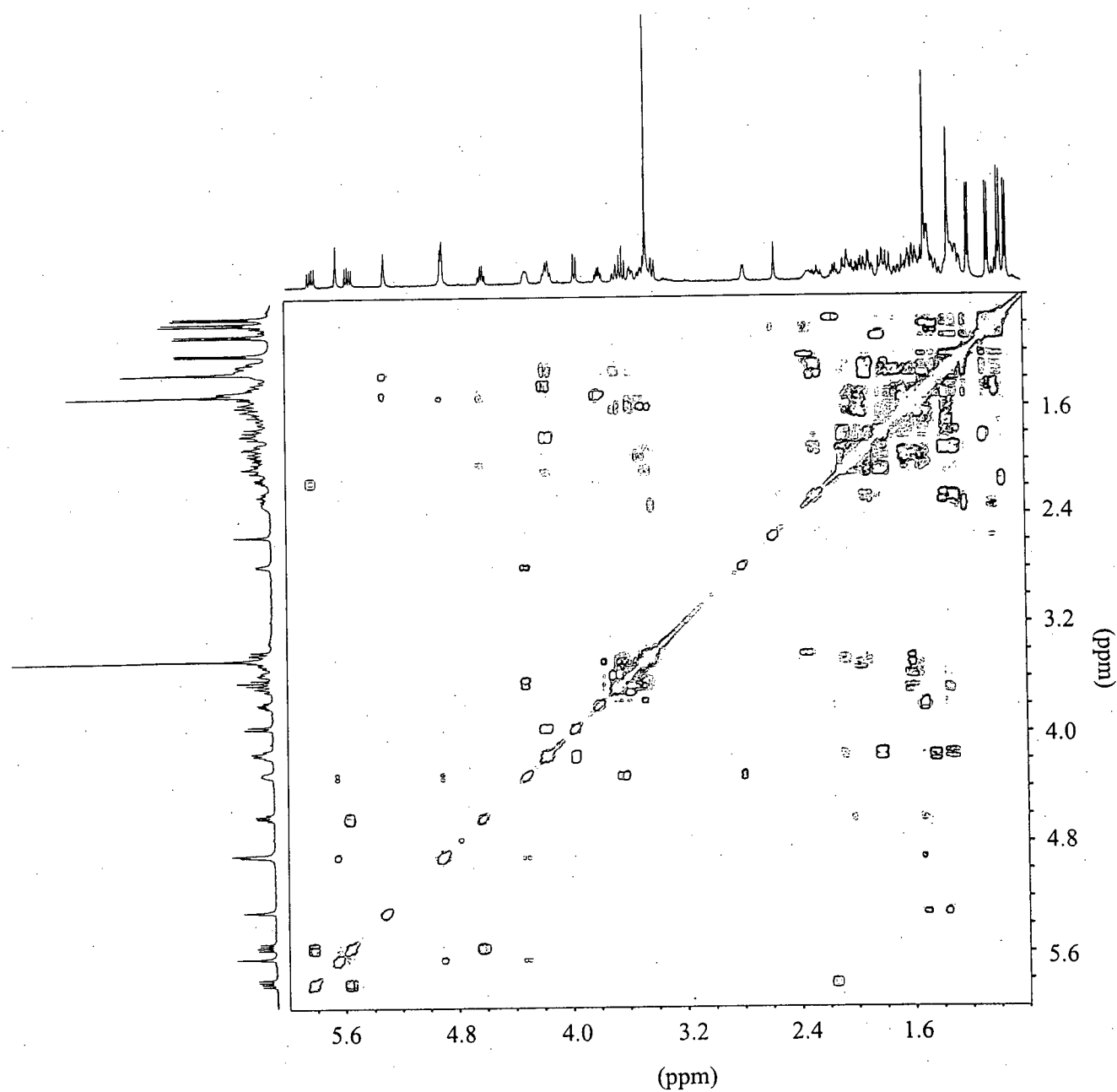
Figure 5.6. COSY spectrum of dinophysistoxin 1 methyl ester (**15**) (recorded in C_6D_6 at 500 MHz).

5.4 27-O-acetyl okadaic acid (12) and the methyl ester 16

12 R = H
16 R = CH₃

27-O-acetyl okadaic acid methyl ester (**16**) was isolated as a white film (300 µg) which gave an (M+H)⁺ ion in HRFABMS at m/z 861.5004. The HRFABMS differed from that of okadaic acid methyl ester (**14**) (m/z 819.4895) by 42 mass units, corresponding to the replacement of a proton with an acetate group. Comparison of ¹H NMR spectral data recorded for okadaic acid methyl ester (**14**) and 27-O-acetyl okadaic acid methyl ester (**16**) (Figure 5.7) indicated a downfield shift of H-27 from δ 4.16 ppm in that of **14** (Figure 5.4) to δ 5.85 ppm in that of **16** (Figure 5.7). Additional spectroscopic disparities between the spectra of **14** and **16** included the absence of the OH-27 proton resonance (δ 2.53 ppm in the ¹H NMR spectrum of **14**) in that of **16** and the presence of an additional methyl singlet (δ 1.79 ppm) in the ¹H NMR spectrum of **16**. As expected, ¹³C NMR analysis proved unsuccessful on such small amounts of material, however, inverse detection of many of the carbon signals was possible through both HMQC (Figure 5.8) and HMBC experiments. Analysis of HMBC correlations, indicated the methyl group, which resonated at δ 1.79 ppm, was attached to a carbonyl (δ 170.2 ppm). Additionally, the carbon resonance for C-27 was shifted downfield by 2.3 ppm (δ 67.3 ppm) when compared to the corresponding resonance for C-27 in the ¹³C NMR spectrum of dinophysistoxin 1 methyl ester (**15**) (see Table 5.2 for assignment of proton and carbon resonances). This data suggested an acetate residue was connected to okadaic acid core at OH-

27. 1D TOCSY experiments (Figure 5.9) allow the acquisition of ^{1}H NMR spectra of individual spin systems within a molecule and thus greatly simplified the ^{1}H NMR spectroscopic data acquired from **16** and aided in establishing connectivity in the okadaic acid core. The structure of the okadaic acid analogue was thus established as 27-O-acetyl okadaic acid methyl ester (**16**).

Table 5.2. NMR data for 27-O-acetyl okadaic acid methyl ester (**16**) (recorded in C_6D_6).

Carbon No.	^{13}C δ (ppm)[a,b]	^1H δ (ppm) (mult, J (Hz))[b]	HMBC[b]
1	177.2		H-44, H-46
2	75.9	OH: 4.89 (s)	H-44
3	45.5	n.o.	H-44
4	70.6	4.12 (m)	
5	n.o.	n.o.	
6	n.o.	n.o.	
7	68.6	3.42 (m)	
8	n.o.		
9	122.5	5.30 (s)	H-43
10	138.0		H-43
11	33.6	1.54 (m); 1.50 (m)	H-43
12	70.7	3.82 (ddd, 5.5, 9.3, 9.3)	H-42
13	42.7	2.14 (m)	H-15, H-42
14	135.4	5.82 (dd, 8.8, 15.5)	H-42
15	131.3	5.55 (7.8, 15.5)	
16	78.9	4.62 (ddd, 7.6, 7.6, 7.8)	H-14
17	n.o.	1.98 (m); 1.52 (m)	
18	n.o.	n.o.	
19	101.4		H-22
20	n.o.	n.o.	
21	n.o.	2.08 (m); 1.80 (m)	
22	70.1	4.13 (m)	
23	77.2	3.69 (dd, 9.8, 9.8)	
24	71.4	4.39 (m); OH: 2.83 (d, 4.7)	H-26, H-41
25	n.o.		
26	83.4	4.21 (d, 9.4)	H-41
27	67.3	5.85 (ddd, 2.0, 9.4, 9.4)	H-26
28	31.7	1.52 (m); 1.06 (dd, 10,2, 10.2)	H-40
29	34.2	1.81 (m)	H-40

[a] From HMBC and HMQC experiments. [b] Recorded at 500 MHz. n.o. (not observed).

Table 5.2 (continued). NMR data for 27-O-acetyl okadaic acid methyl ester (**16**) (recorded in C_6D_6).

Carbon No.	^{13}C δ (ppm)[a,b]	^1H δ (ppm) (mult, J (Hz))[b]	HMBC[b]
30	74.4	3.32 (dd, 2.0, 10.3)	H-39, H-40
31	28.0	n.o.	H-39
32	26.9	n.o.	H-39
33	n.o.	n.o.	
34	n.o.		
35	n.o.	n.o.	
36	n.o.	n.o.	
37	n.o.	1.49 (m); 1.38 (m)	
38	60.1	3.50 (m); 3.62 (m)	
39	10.5	0.98 (d, 6.6)	
40	16.2	1.18 (d, 6.2)	
41	112.3	5.68 (bs); 4.91 (bs)	H-26
42	15.9	0.97 (d, 6.7)	
43	22.4	1.36 (s)	
44	27.2	1.53 (s)	C_2-OH
46	51.7	3.49 (s)	
47	170.1		H-48
48	20.1	1.79 (s)	

[a] From HMBC and HMQC experiments. [b] Recorded at 500 MHz. n.o. (not observed).
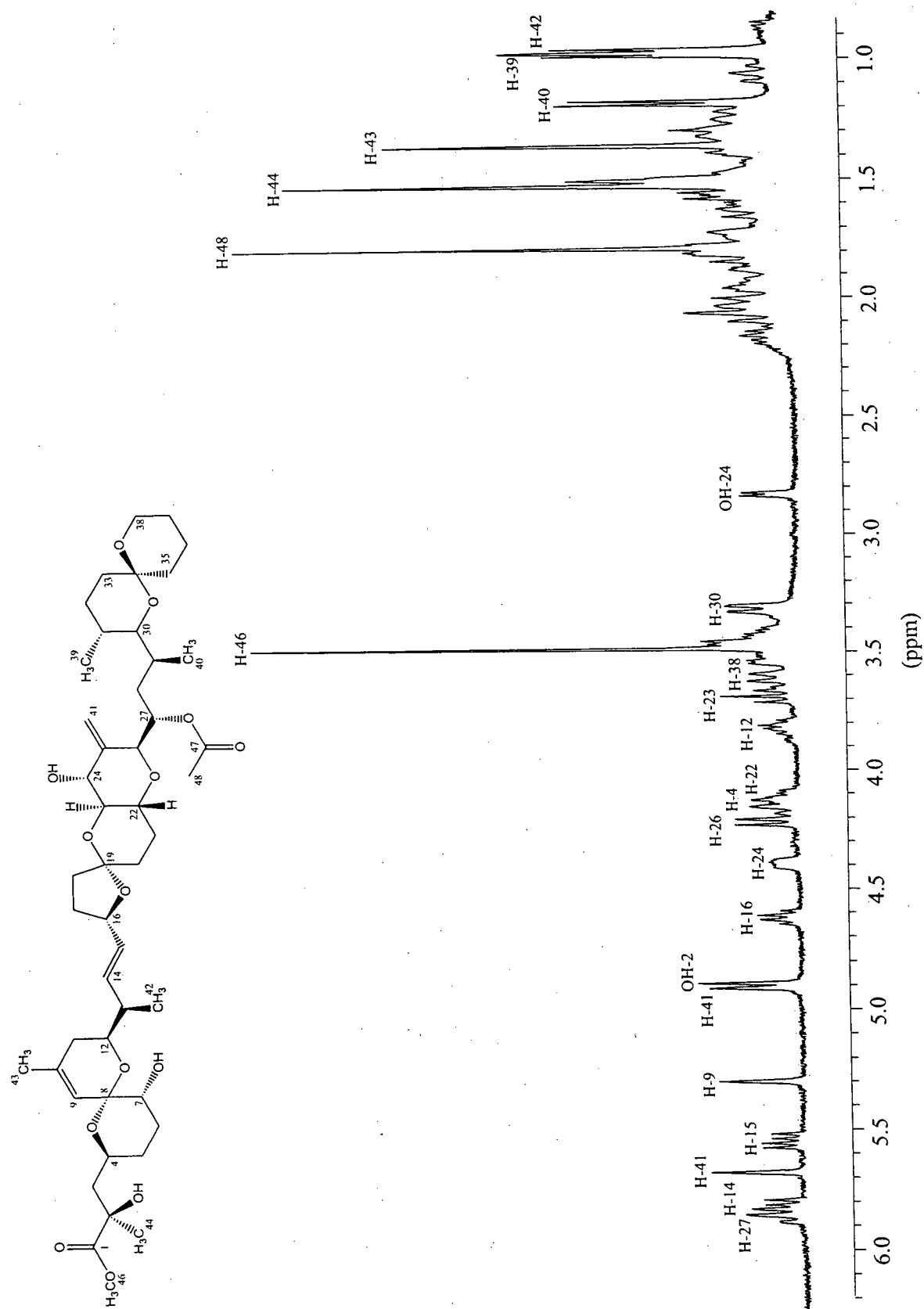
Figure 5.7. ^{1}H NMR spectrum of 27-O-acetyl okadaic acid methyl ester (**16**) (recorded in C_6D_6 at 500 MHz).

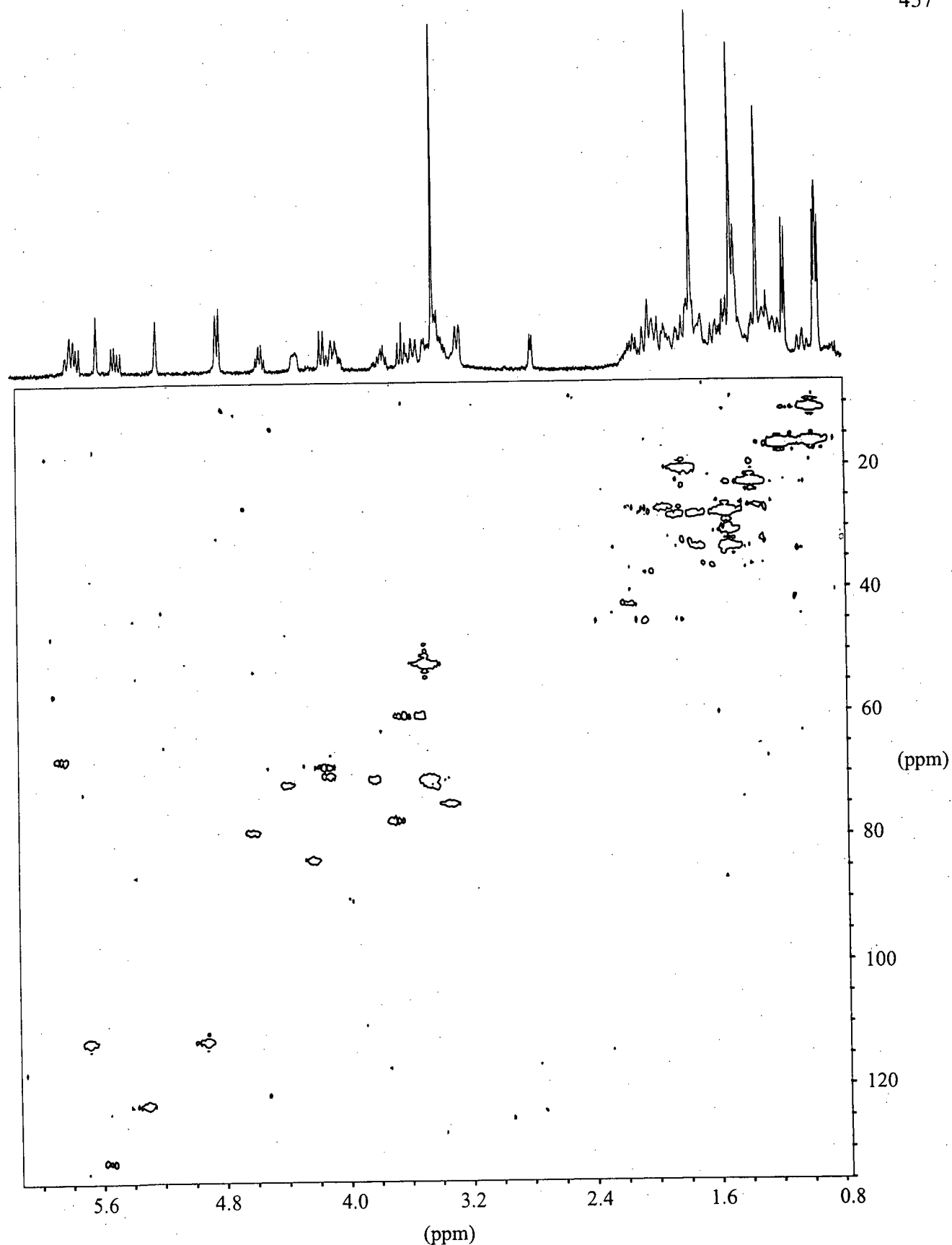**Figure 5.8.** HMQC spectrum of 27-O-acetyl okadaic acid
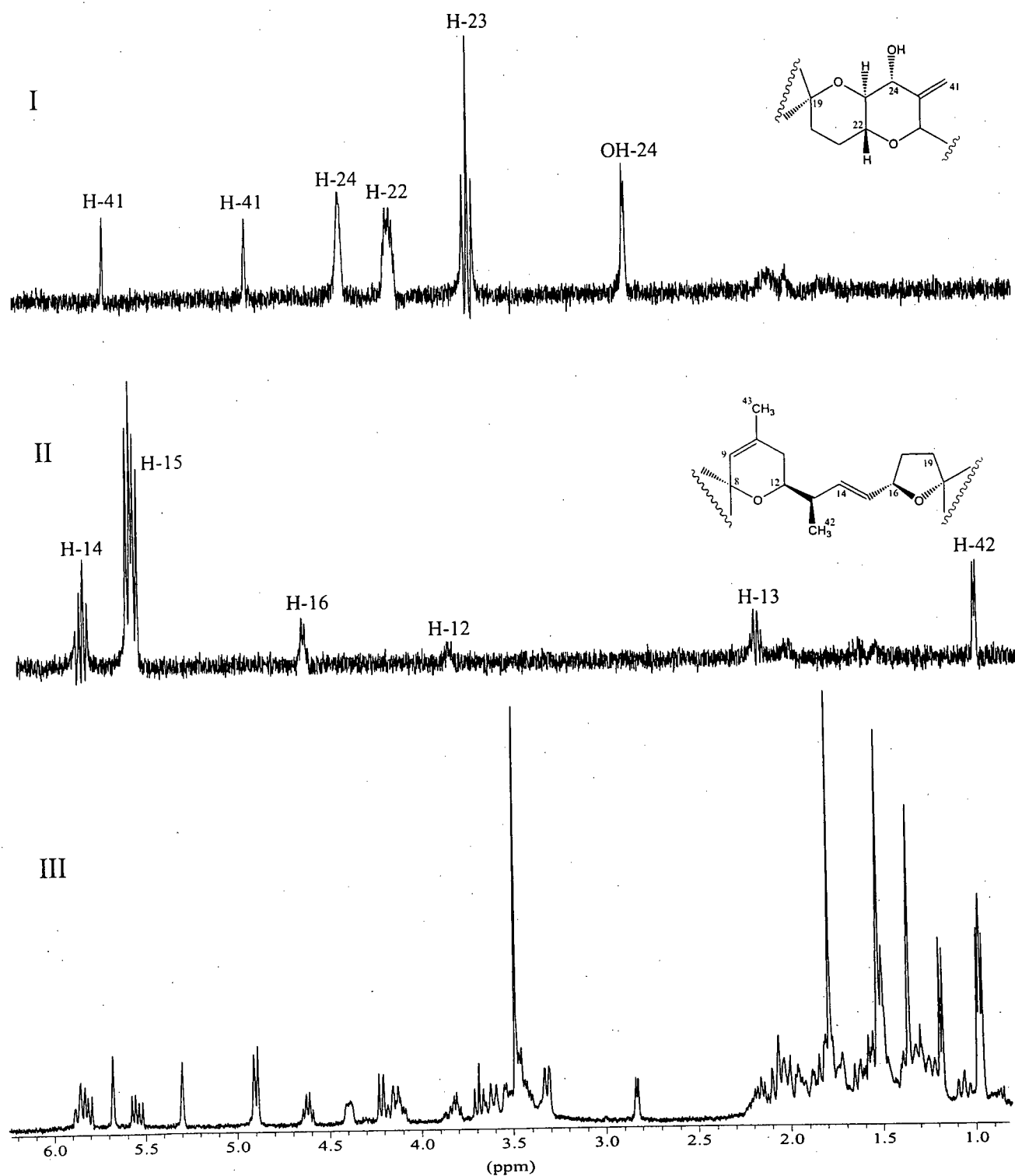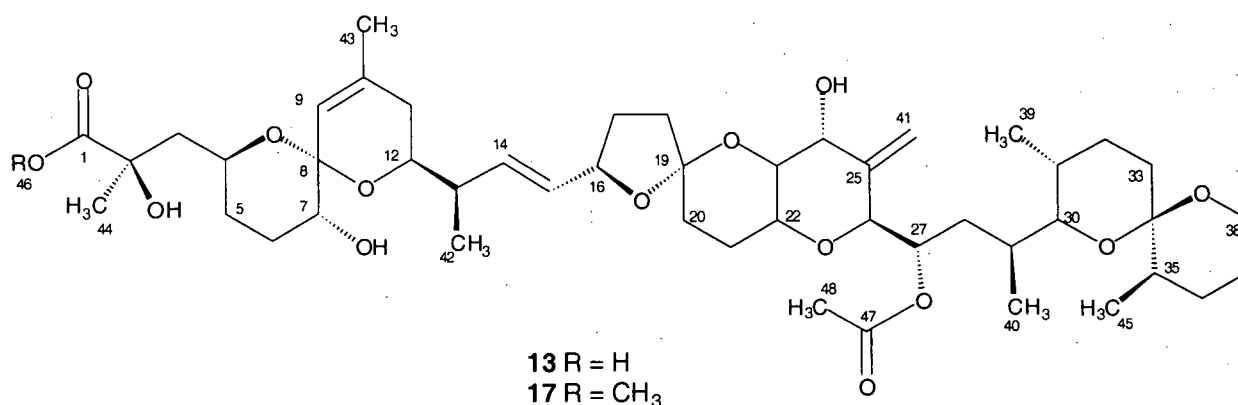methyl ester (**16**) (recorded in C_6D_6 at 500 MHz).

Figure 5.9. Selected 1D TOCSY experiments on 27-O-acetyl okadaic acid methyl ester (**16**).
I. Irradiation of H-24 (δ 4.39); II. irradiation of H-15 (δ 5.55); III. ¹H NMR spectrum
of 27-O-acetyl okadaic acid methyl ester (**16**) (all spectra recorded in C₆D₆ at 500 MHz).

5.5 27-O-acetyl dinophysistoxin 1 (13) and its methyl ester (17)

13 R = H
17 R = CH₃

27-O-acetyl dinophysistoxin 1 methyl ester (**17**), the least polar compound in the mixture, was isolated as a white film (300 μg) which gave an (M+H)⁺ ion in HRFABMS at *m/z* 875.5151. The HRFABMS differed from that of 27-O-acetyl okadaic acid methyl ester (**16**) (*m/z* 861.5004) by 14 mass units, corresponding to the replacement of a proton with a methyl substituent. Comparison of ¹H NMR spectral data recorded from **16** (Figure 5.4) and **17** (Table 5.3 and Figure 5.10) supported the presence of an additional methyl group (δ 0.97, *J* = 6.3 Hz) in the structure of **17**. Again, the large chemical shift observed for the proton resonance corresponding to H-27 (δ 5.86 ppm), a methyl singlet at δ 1.76 ppm and the absence of a resonance for OH-27 (δ 2.57 in the ¹H NMR spectrum of dinophysistoxin 1 methyl ester (**15**)) in the ¹H NMR spectrum of **17**, supported the attachment of an acetate group at OH-27. Analysis of HMQC (Figure 5.11) and HMBC spectral data verified the connectivity of the acetate methyl group, which resonated at δ 1.76 (¹H NMR), to a carbonyl carbon at δ 170.2 (¹³C NMR). Furthermore, the carbon resonance corresponding to C-27 was shifted downfield by 2.4 ppm (δ 67.4 ppm) when compared to that observed for C-27 in dinophysistoxin 1 methyl ester (**15**) (for assignments of proton and carbon resonances see Table 5.3). In the HMBC spectrum of **17**, the resonance at δ 0.97, which corresponded to a methyl substituent, displayed a correlation into a O-C-O carbon at δ 98.2. This data suggested the additional methyl substituent in this molecule

was attached to either C-18, C-20, C-33 or C-35. Further analysis of COSY spectral data (Figure

5.12) and a series of 1D TOCSY experiments (Figure 5.13), coupled with the known variations

of methyl substitution patterns within the dinophysistoxin family of natural products, permitted

for the connection of the additional methyl group (δ 0.97) to C-35. This data thus established the

structure of the dinophysistoxin 1 analogue as that depicted for 27-O-acetyl dinophysistoxin 1

methyl ester (17).

Table 5.3. NMR data for 27-O-acetyl dinophysistoxin 1 methyl ester (17)
(recorded in C_6D_6).

Carbon No.	^{13}C δ (ppm)^{a,b}	^1H δ (ppm) (mult, J (Hz))^b	HMBC^b
1	177.1		H-44, H-46
2	75.4	OH: 4.92 (s)	H-3, H-44
3	45.4	2.09 (m); 1.82 (m)	
4	71.8	4.14 (m)	
5	n.o.	1.81 (m); 1.29 (m)	
6	n.o.	1.87 (m); 1.57 (m)	
7	68.6	3.41 (ddd, 4.1, 10.6, 10.6)	
8	96.7		H-9
9	122.4	5.30 (s)	H-43
10	138.0		H-11, H-43
11	33.3	1.50 (m); 1.34 (m)	H-9, H-43
12	70.7	3.81 (ddd, 5.5, 9.0, 9.0)	H-42
13	42.9	2.14 (m)	H-12, H-14, H-15, H-42
14	135.7	5.82 (dd, 8.6, 15.2)	H-13, H-16, H-42
15	131.2	5.54 (dd, 7.5, 15.2)	H-12, H-13
16	78.9	4.62 (ddd, 7.3, 7.5, 7.5)	H-14, H-15
17	31.0	2.13 (m); 1.51 (m)	
18	n.o.	n.o.	
19	n.o.		
20	n.o.	n.o.	
21	26.5	2.02 (m); 1.94 (m)	
22	70.1	4.12 ((m)	H-26
23	77.2	3.69 (dd, 9.8, 9.8)	H-24
24	71.5	4.39 (m); OH: 2.85 (d, 5.1)	H-23, H-26, H-41
25	145.1		C_{24}-OH, H-26, H-41
26	83.5	4.21 (d, 9.5)	H-41
27	67.4	5.86 (ddd, 2.0, 9.5, 9.5)	H-26
28	33.9	1.53 (m); 1.08 (dd, 9.6, 9.6)	H-30, H-40
29	34.0	1.82 (m)	H-40

^{a}From HMBC and HMQC experiments. ^{b}Recorded at 500 MHz. n.o. (not observed).

Table 5.3 (continued). NMR data for 27-O-acetyl dinophysistoxin 1 methyl ester (**17**) (recorded in C_6D_6)

Carbon No.	^{13}C δ (ppm)^{a,b}	^1H δ (ppm) (mult, J (Hz))^b	HMBC^b
30	74.3	3.31 (dd, 2.0, 10.1)	H-39, H-40
31	28.1	1.72 (m)	H-39
32	26.8	n.o.	H-39
33	n.o.	n.o.	
34	98.2		H-45
35	39.6	1.43 (m)	H-45
36	37.3	2.02 (m); 1.62 (m)	
37	n.o.	1.54 (m); 1.26 (m)	
38	59.8	3.52 (m); 3.54 (m)	
39	10.5	0.99 (d, 6.7)	H-30
40	16.1	1.16 (d, 6.4)	
41	112.3	5.68 (bs); 4.90 (bs)	H-26
42	16.2	0.96 (d, 6.8)	
43	22.4	1.35 (s)	H-9
44	27.2	1.53 (s)	C_2-OH
45	16.2	0.97 (d, 6.3)	
46	51.7	3.48 (s)	
47	170.2		H-48
48	20.2	1.76 (s)	

^{a} From HMBC and HMQC experiments. ^{b} Recorded at 500 MHz. n.o. (not observed)
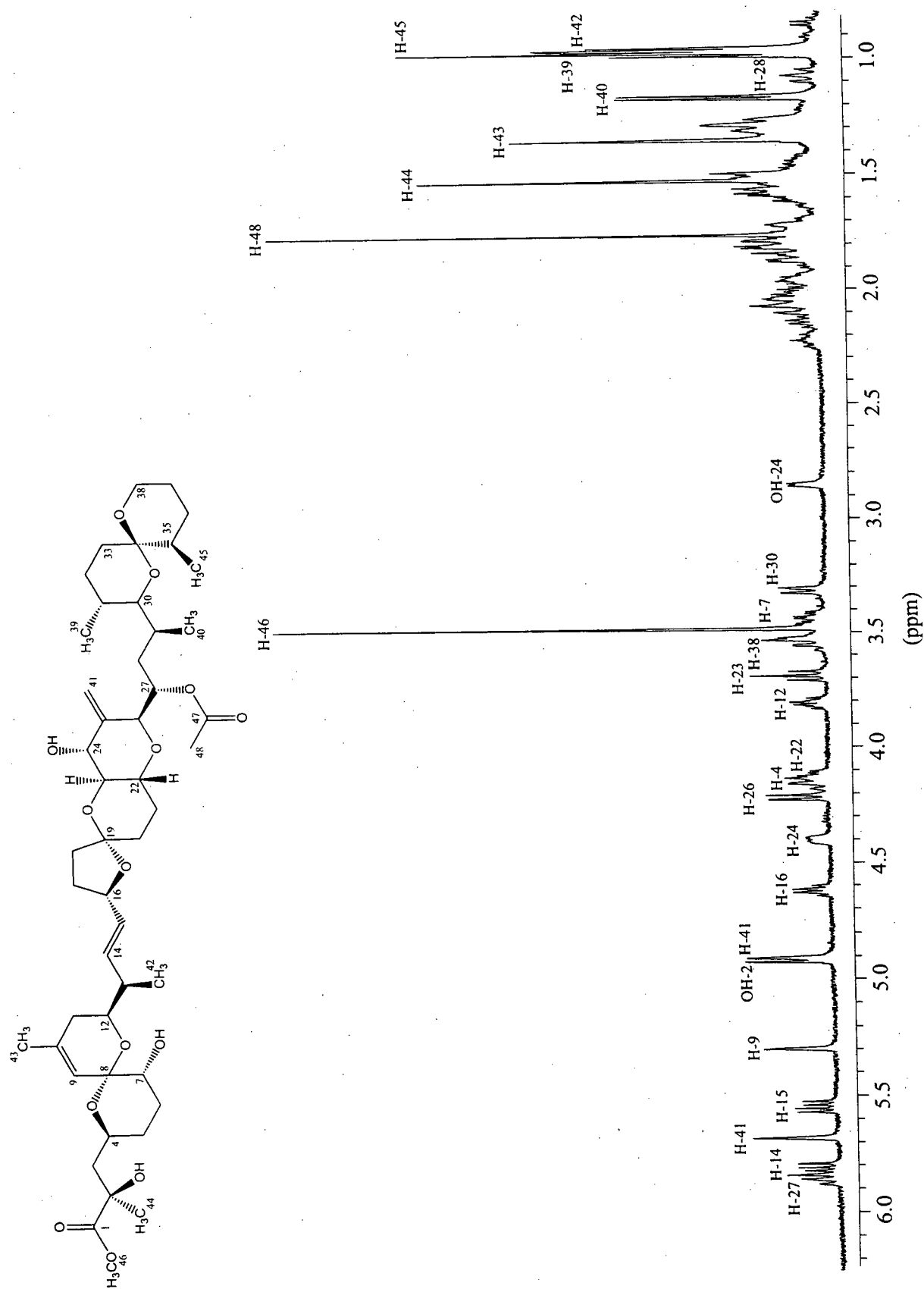
Figure 5.10. ^{1}H NMR spectrum of 27-O-acetyl dinophysistoxin 1 methyl ester (**17**) (recorded in C$_6$D$_6$ at 500 MHz).
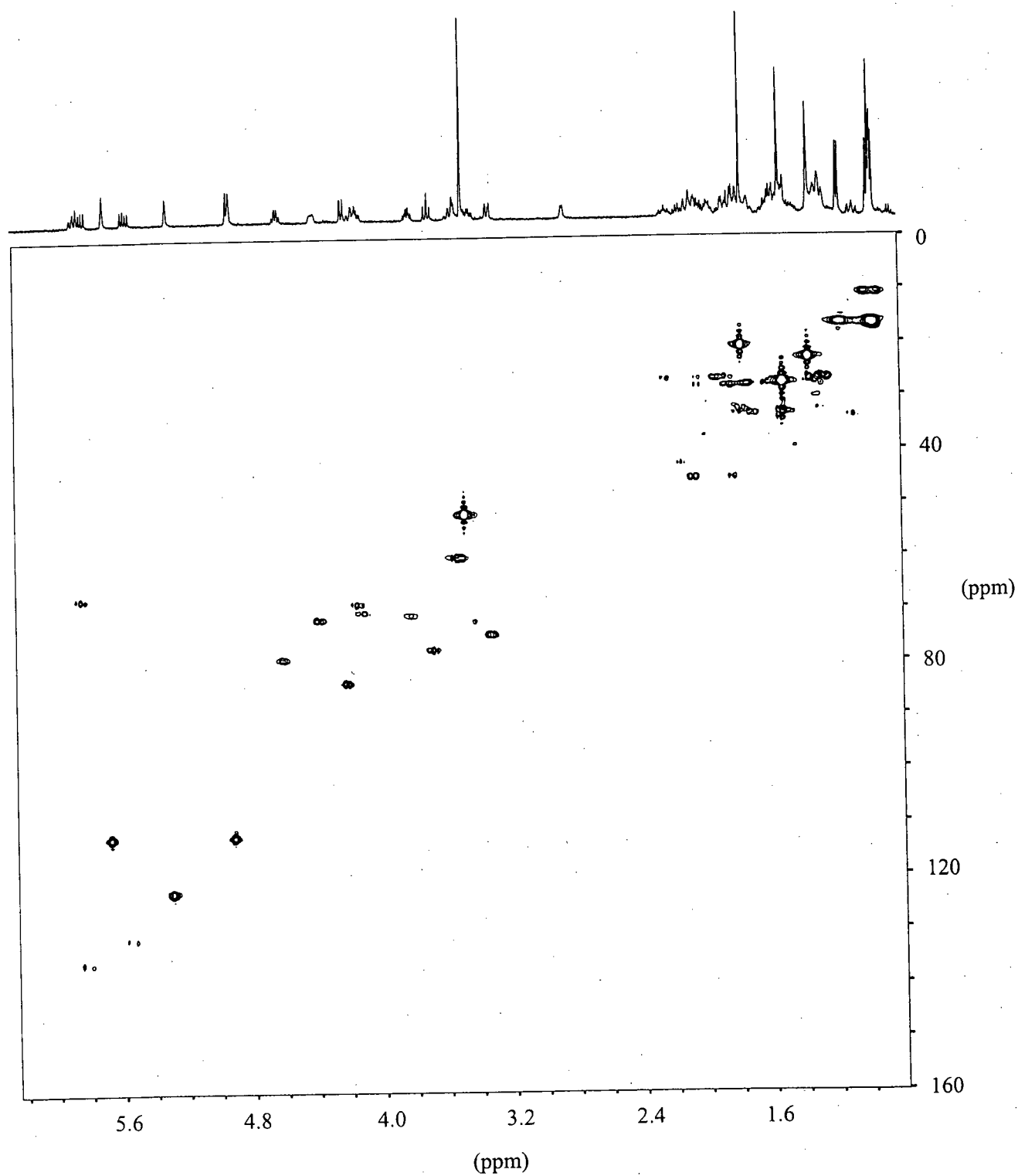
Figure 5.11. HMQC spectrum of 27-O-acetyl dinophysistoxin 1 methyl ester (**17**) (recorded in C_6D_6 at 500 MHz).

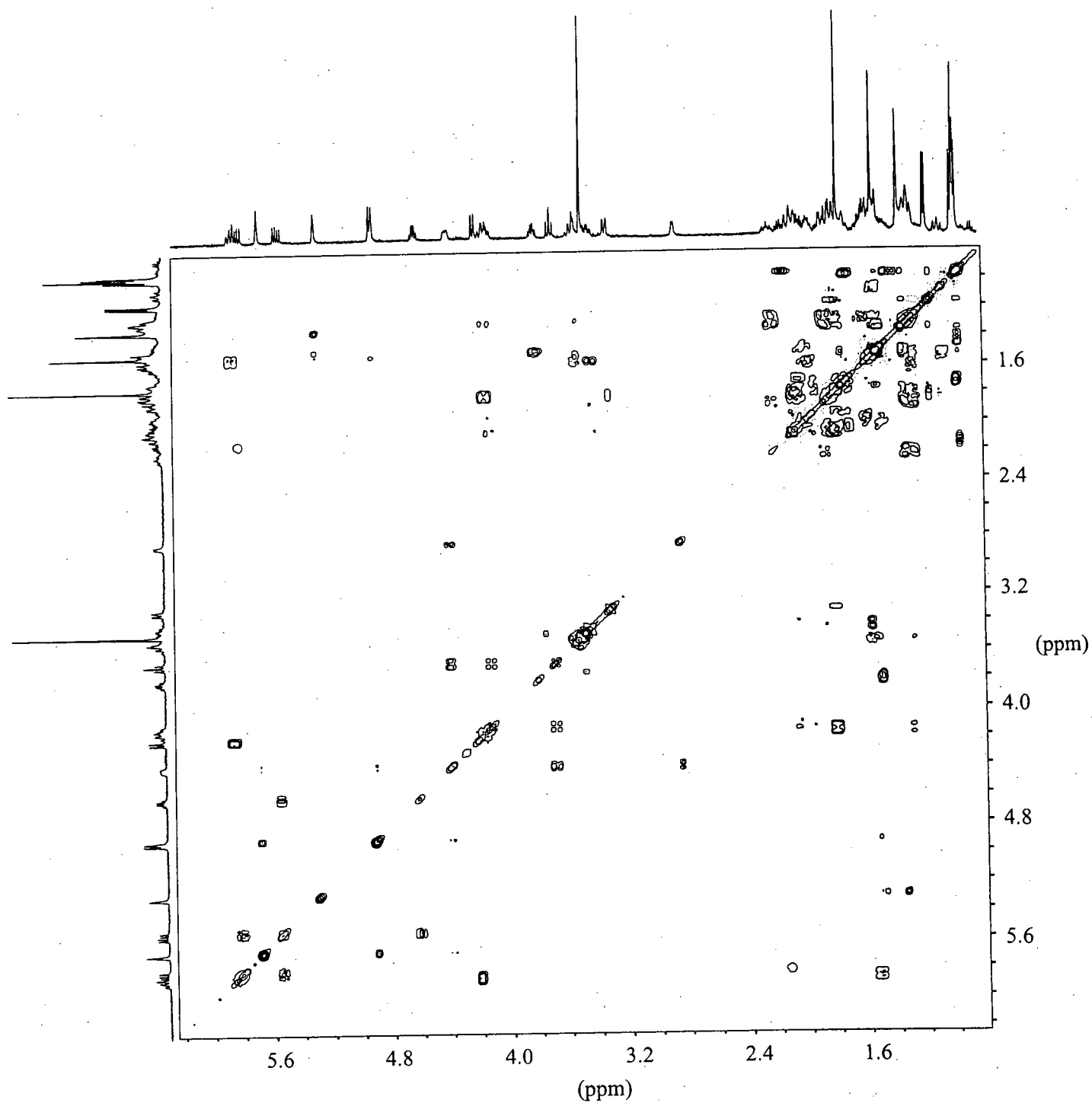**Figure 5.12.** COSY spectrum of 27-O acetyl dinophysistoxin 1 methyl ester (**17**) (recorded in C_6D_6 at 500 MHz).
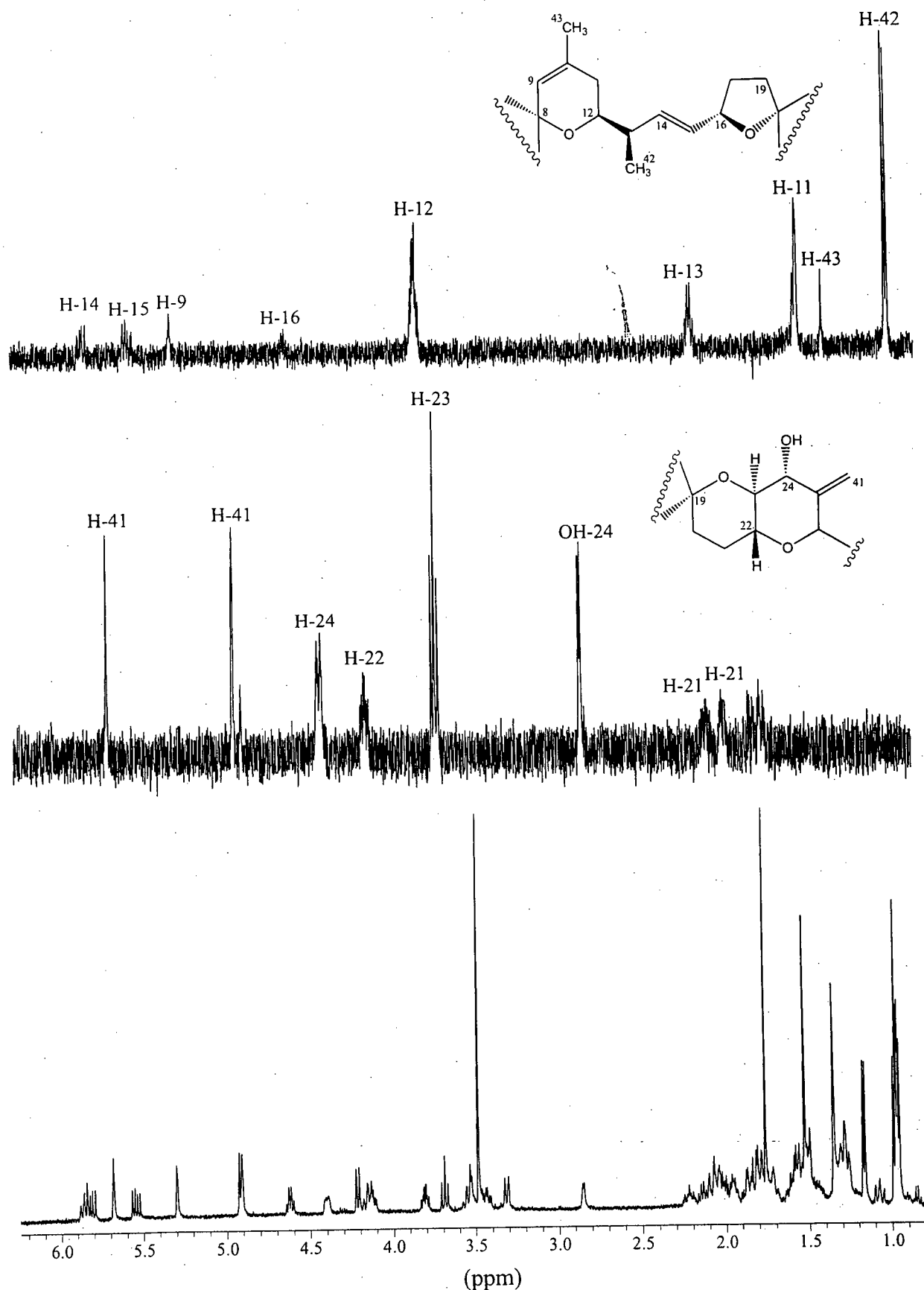
Figure 5.13. Selected 1D TOCSY experiments on 27-O-acetyl dinophysistoxin 1 methyl ester (**17**).
I. Irradiation of H-12 (δ 3.81); II. irradiation of H-23 (δ 3.69); III. ^{1}H NMR spectrum
of 27-O-acyl dinophysistoxin 1 methyl ester (**17**) (all spectra recorded in C_6D_6 at 500 MHz).

5.6 Biological Activity

Phosphorylation, catalyzed by protein kinases and dephosphorylation, catalyzed by protein phosphatases, are two of the most important regulatory processes in the cell cycle. Therefore, it is not surprising that the mixture containing dinophysistoxin 1 (**1**), 27-O-acetyl okadaic acid (**12**) and 27-O-acetyl dinophysistoxin 1 (**13**), all analogues of the potent inhibitor of protein phosphatase inhibitor okadaic acid (**2**), displayed strong activity in a cell based assay for G2 checkpoint inhibitors.

A number of reports indicate okadaic acid (**2**), at concentrations greater than 1 μM, is capable of increasing cellular levels of phosphorylated proteins by up to 400%[19] as well as inducing cells blocked in S phase or G_2 phase into premature mitosis.[20] While it has been proposed that **2** can overcome the S/G_2 checkpoint through modulation of a tyrosine kinase,[20] the effect of **2** on the G_2/M checkpoint is little understood and likely more complicated.[20,21,23] However, the phosphorylation and dephosphorylation of certain proteins must occur in an orderly fashion to ensure fidelity in the cell cycle. Therefore, it is not surprising that the disruption of these events by **2** leads to premature mitosis.

Compounds **1**, **12** and **13**, all analogues of okadaic acid, were isolated as an inseparable mixture and assayed as such for G2 checkpoint inhibition activity.[17] The dose dependence of G2 checkpoint inhibition was determined by exposing G2-arrested cells to different concentrations of the mixture of okadaic acid analogues for 4 hours and determining the number of cells that escaped G2 arrest. The mixture exhibited significant G2 checkpoint inhibition at concentrations as low as 1 nM and caused complete inhibition of the G2 checkpoint at 0.1 μM (see Figure 5.14). By comparison, the established G2 checkpoint inhibitor caffeine caused only 37% G2 checkpoint abrogation at a concentration of 2 mM. Consequently, the mixture of okadaic acid analogues are

much more efficacious than caffeine and represent the only compounds identified to date that are able to induce 100% of G2 arrested cells to enter mitosis.
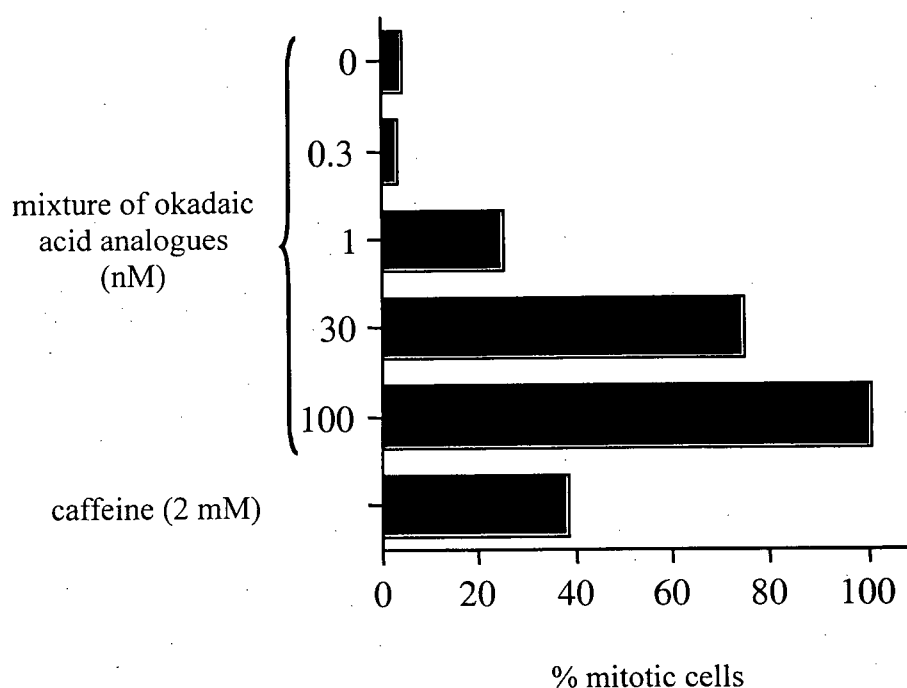

Figure 5.14. G2 checkpoint inhibition by **1, 12** and **13** and by caffeine.

5.7 Conclusions

MeOH extracts of the sponge *Merriamum oxeato* demonstrated strong G2 checkpoint inhibition activity in a screen of extracts from marine invertebrates collected in Jervis Inlet. Fractionation of the extract from *Merriamum oxeato* led to the isolation of a causative toxin of DSP, dinophysistoxin 1 (**1**), as well as the new toxins 27-O-acetyl okadaic acid (**12**) and 27-O-acetyl dinophysistoxin 1 (**13**) (Figure 5.15). The structures of **1, 12** and **13**, were determined by spectroscopic analysis (COSY, HMQC, HMBC, and 1D TOCSY) of the corresponding methyl esters **15, 16** and **17** and by comparison of their ^{1}H NMR data with that of okadaic acid methyl ester (**14**). Unfortunately, the parent carboxylic acids could not be separated, and, owing to the known inactivity of the corresponding methyl esters,[24] no biological testing was carried out on

the purified compounds. However, the mixture of carboxylic acids was shown to completely inhibit the G2 checkpoint at a concentration of 0.1 μM. Tachibana and co-workers have demonstrated, through the synthesis okadaic acid derivatives selectively acylated at C-1, C-7, C-24 and C-27, that acyl substituents at C-7 and C-27 of okadaic acid do not greatly affect its protein phosphatase inhibition activity.[12] Thus, the new toxins 27-O-acetyl okadaic acid (12) and 27-O-acetyl dinophysistoxin 1 (13) should have comparable activity to dinophysistoxin 1 (1) and okadaic acid (2) and must therefore be included among the DSP toxins.

1 R₁ = R₂ = H, R₃ = CH₃
12 R₁ = H, R₂ = Ac, R₃ = H
13 R₁ = H, R₂ = Ac, R₃ = CH₃
15 R₁ = CH₃, R₂ = H, R₃ = CH₃
16 R₁ = CH₃, R₂ = Ac, R₃ = H
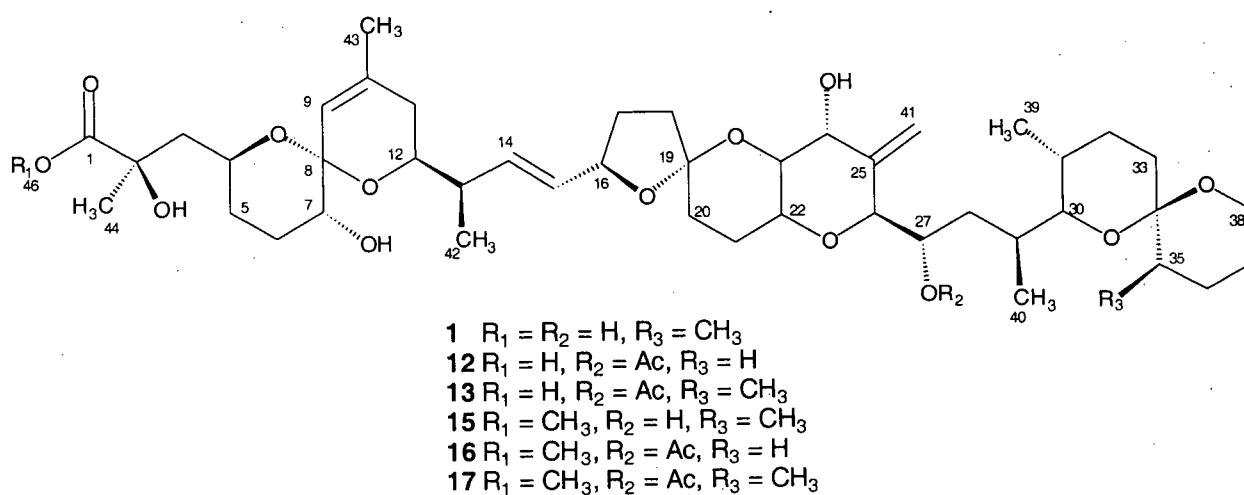17 R₁ = CH₃, R₂ = Ac, R₃ = CH₃

Figure 5.15. DSP toxins isolated from *Merriamum oxeato*.

It has recently been reported that some organisms that feed on toxic dinoflagellates may in fact have enzymes that are capable of detoxifying okadaic acid and the dinophysistoxins through chemical transformations. Suzuki and co-workers have reported the scallop *Patinopectin yessoensis*, when reared on the dinophysistoxin 1 (1) producing dinoflagellate *Dinophysis fortii*, rapidly converts 1 to 7-O-acyl dinophysistoxin 1 (18) (Figure 5.16).[25] Additionally, Wright and co-workers have reported the diatom *Thalassiosira weissflogii* is capable of transforming the toxic diol ester of okadaic acid (9), produced by *Prorocentrum Lima*, to the more polar oxidation products 19-22.[26] Analysis of the sponge *M. oxeato* collected in Jervis Inlet showed no sign of

DSP producing dinoflagellates,[27] thus the accumulation of acetylated dinoflagellate toxins (i.e. **1**, **12** and **13**) in the sponge tissue raises interesting questions. During the course of synthesizing a number of biotinylated okadaic acids, Tachibana and co-workers discovered the nucleophilicity of the three secondary hydroxyl groups in okadaic acid to decrease in the order C_7-OH > C_{24}-OH > C_{27}-OH.[28] The isolation of the two new analogues of okadaic acid, **12** and **13**, both acetylated at C_{27}-OH, indicate the acetylation of dinophysistoxin 1 (**1**) and okadaic acid (**2**) is likely controlled by enzymes, as the least nucleophilic hydroxyl group is selectively acetylated. Since there are no reports in the literature of dinoflagellate toxins acetylated at C_{27}-OH, it is possible that the sponge *Merriamum oxeato* is in fact capable of acetylating the parent toxins in a mechanism of self-defense. However, substantiation of this statement requires the identification of the DSP producing dinoflagellate and analysis of the toxins produced by this algae.
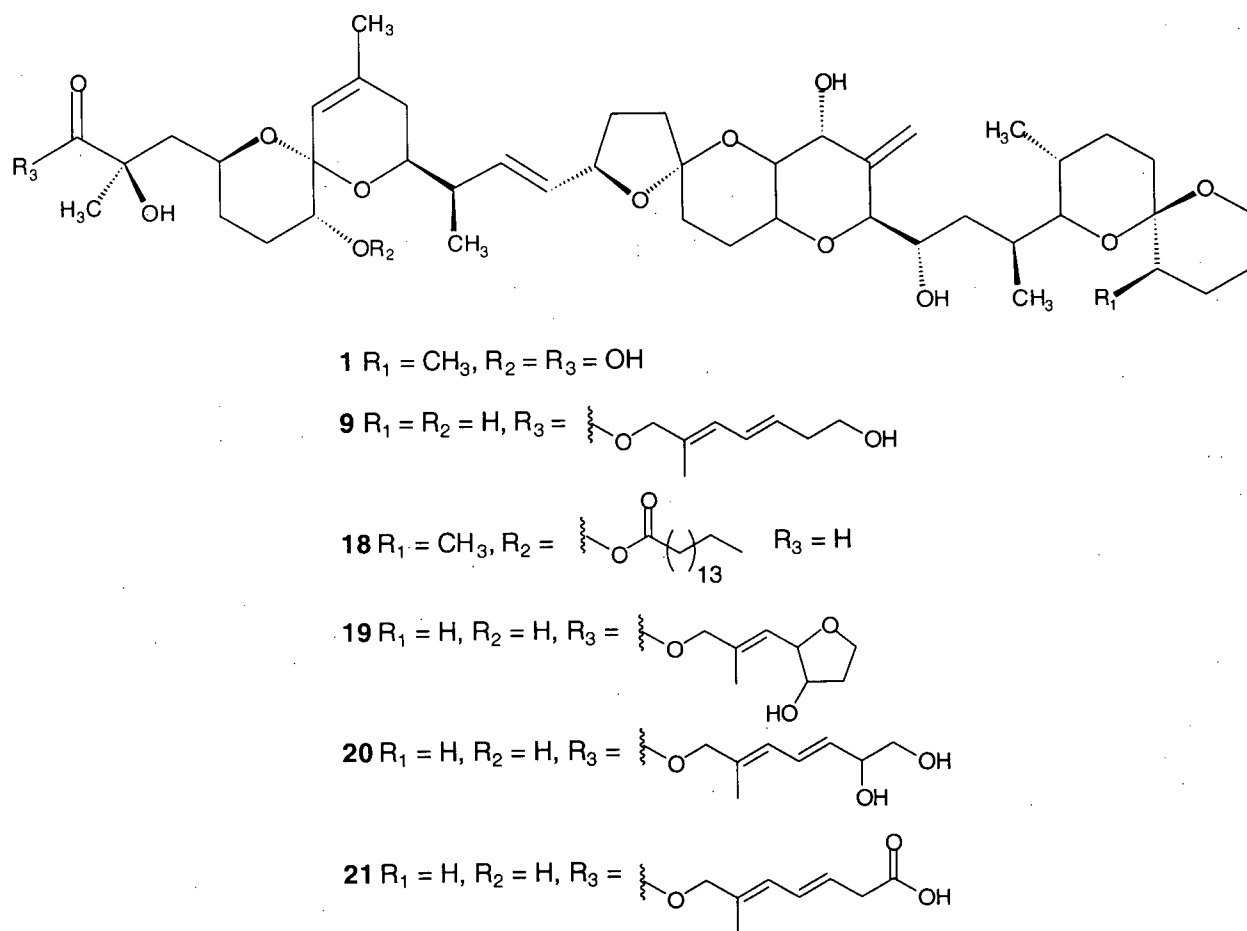
Figure 5.16. Biological transformation of DSP toxins through oxidation and acylation.

Regardless of origin, the isolation of dinophysistoxin 1 (**1**), 27-O-acetyl okadaic acid (**12**) and 27-O-acetyl dinophysistoxin 1 (**13**) are a concern and represent the first examples of DSP toxins in the North Eastern Pacific ocean. In British Columbia alone, 24,000 tonnes of shellfish were harvested in 1999, with a wholesale value of 159,000,000 dollars.[29] To avoid the possible public health and economic implications of a DSP outbreak, we must become increasingly vigilant in the monitoring of shellfish harvested in our coastal waters.

5.8 Experimental

For General Experimental see Section 2.5

Samples of *Merriamum oxeato* (1 kg wet weight) were collected off the northwest and southwest points of Nelson Island, in Jervis Inlet, British Columbia in September of 1999 and January of 2000 using SCUBA at depths of 25-30 meters. The samples were immediately immersed in MeOH and transported to the University of British Columbia. The MeOH was decanted after 24 hours and the sponge was immersed in fresh MeOH. After the sponge had been extracted 7 times (over 7 days) with MeOH, the combined extracts were concentrated to provide a green gum. The green gum was dissolved in H_2O (500 mL) and EtOAc (500 mL) and the phases were separated. The aqueous phase was washed with EtOAc (10 x 250 mL) and the combined organic phases were concentrated to provide a brown residue. The residue was dissolved in MeOH - H_2O (9:1, 100 mL) and extracted with hexane (3 x 50 mL). The MeOH - H_2O phase was then concentrated to provide a green residue and the combined hexane phases were concentrated to provide an orange oil.

The green residue from the MeOH - H_2O phase was placed on a short plug of reverse phase silica gel (10 g) and the most polar compounds in the mixture were eluted with MeOH - H_2O (1:5, 10 mL). Compounds of decreasing polarity were then eluted with MeOH - H_2O (2:5, 10 mL, fraction A), (4:5, 10 mL, fraction B), (1:1, 10 mL, fraction C), (5:3, 10 mL, fraction D), (5:1, 10 mL, fraction E), (5:0, 10 mL, fraction F); MeOH - EtOAc (5:1, 10 mL, fraction G) and EtOAc (10 mL, fraction H). A biological assay of the individual fractions, indicated fractions E and F contained compounds that inhibit the G2-checkpoint. Combination and concentration of fractions E and F provided a brown residue (25 mg) which was placed on a Sephadex LH-20 column and eluted with MeOH. Combination and concentration of all active fractions

(determined by biological assay) provided a beige residue (5 mg) which was placed on a Sephadex LH-20 column and eluted with EtOAc - MeOH - H$_2$O (25:5:1) to provide an inseparable mixture of compounds that included dinophysistoxin 1 (**1**), 27-O-acetyl okadaic acid (**12**) and 27-O-acetyl dinophysistoxin 1 (**13**) (total weight 1.5 mg, ^{1}H NMR ratio 2:3:3) as a white solid.

Preparation of dinophysistoxin 1 methyl ester (**15**), 27-O-acetyl okadaic acid methyl ester (**16**) and 27-O-acetyl dinophysistoxin 1 methyl ester (**17**).

To a stirred solution of the three okadaic acid analogues **1, 12** and **13** (1.0 mg, 0.001 mmol) in dry MeOH - benzene (1:7, 1.6 mL) at room temperature, was added a solution of (trimethylsilyl)diazomethane (2.0 M in hexane, 20 μL, 0.01 mmol). After 2 hours, the reaction mixture was concentrated under reduced pressure. Purification of the crude methyl esters by reverse phase HPLC (analytical column, 1 mL/minute, monitor at 204 nm, 78:20 MeOH - H$_2$O) provided 0.2 mg (0.00002% wet weight) of dinophysistoxin 1 methyl ester (**15**) as a white solid (retention time 14 minutes), 0.3 mg (0.00003% wet weight) of 27-O-acetyl okadaic acid methyl ester (**16**) as a white solid (retention time 20.4 minutes) and 0.3 mg (0.00003% wet weight) of 27-O-acetyl dinophysistoxin 1 methyl ester (**17**) as a white solid (retention time 26.5 minutes).

Dinophysistoxin 1 methyl ester (**15**): (RP-TLC: R$_F$ = 0.6, 8:1 MeOH - H$_2$O) Exact mass calcd for C$_{46}$H$_{73}$O$_{13}$ (HRFABMS, M+H): 833.5051; found: 833.5053.

27-O-Acetyl okadaic acid methyl ester (**16**): (RP-TLC: R$_F$ = 0.55, 8:1 MeOH - H$_2$O) Exact mass calcd for C$_{47}$H$_{73}$O$_{14}$ (HRFABMS, M+H): 861.5000; found: 861.5004.

27-O-Acetyl dinophysistoxin 1 methyl ester (**17**): (RP-TLC: R_F = 0.5, 8:1 MeOH - H_2O) Exact

mass calcd for $C_{48}H_{75}O_{14}$ (HRFABMS, M+H): 875.5157; found: 875.5151.

5.9 References

(1)   Yasumoto, T.; Oshima, Y.; Yamaguchi, M. *Bull. Japan. Soc. Sci. Fish.* **1978**, *44*, 1249.

(2)   Yasumoto, T.; Oshima, Y.; Sugawara, W.; Fukuyo, Y.; Oguri, H.; Igarashi, T.; Fujita, N. *Bull. Japan. Soc. Sci. Fish.* **1980**, *46*, 1405.

(3)   Daranas, A. H.; Norte, M.; Fernandez, J. J. *Toxicon* **2001**, *39*, 1101.

(4)   Maneiro, I.; Frangopulos, M.; Guisande, C.; Fernandez, M.; Reguera, B.; Riveiro, I. *Mar. Ecol.-Prog. Ser.* **2000**, *201*, 155.

(5)   Murata, M.; Shimatani, M.; Sugitani, H.; Oshima, Y.; Yasumoto, T. *Bull. Japan. Soc. Sci. Fish.* **1982**, *48*, 549.

(6)   Tachibana, K.; Scheuer, P. J.; Tsukitani, Y.; Kikuchi, H.; Engen, D. V.; Clardy, J.; Gopichand, Y.; Schmitz, F. J. *J. Am. Chem. Soc.* **1981**, *103*, 2469.

(7)   Schmitz, F. J.; Prasad, R. S.; Gopichand, Y.; Hossain, M. B.; Helm, D. v. d.; Schmidt, P. *J. Am. Chem. Soc.* **1981**, *103*, 2467.

(8)   Wright, J. L. C.; Hu, T.; Mclachlan, J. L.; Needham, J.; Walter, J. A. *J. Am. Chem. Soc.* **1996**, *118*, 8757.

(9)   Hu, T.; Doyle, J.; Jackson, D.; Marr, J.; Nixon, E.; Pleasance, S.; Quilliam, M. A.; Walter, J. A.; Wright, J. L. C. *J. Chem. Soc. Chem. Commun.* **1992**, 39.

(10)   Yasumoto, T.; Murata, M.; Oshima, Y.; Sano, M.; Matsumoto, G. K.; Clardy, J. *Tetrahedron* **1985**, *41*, 1019. ---

(11)   Murata, M.; Kumagai, M.; Lee, J. S.; Yasumoto, T. *Tetrahedron Lett.* **1987**, *28*, 5869.

(12)   Maynes, J. T.; Bateman, K. S.; Cherney, M. M.; Das, A. K.; Luu, H. A.; Holmes, C. F. B.; James, M. N. G. *J. Biol. Chem.* **2001**, *276*, 44078.

(13)   Hu, T.; Curtis, J. M.; Walter, J. A.; Wright, J. L. C. *J. Chem. Soc. Chem. Commun.* **1995**, 597.

(14)   Hu, T.; Curtis, J. M.; Walter, J. A.; McLachlan, J. L.; Wright, J. L. C. *Tetrahedron Lett.* **1995**, *36*, 9273.

(15)   Koltun, V. M. *Siliceous-spiculed Sponges of the Northern and Far-Eastern Seas of the USSR*; Opredeliteli po Faune SSSR:, 1959; Vol. 67.

(16)   Bill Austin (Director, Marine Ecology Station, Cowichan Bay, British Columbia), personal communication, **1999**.

(17) We thank Dr. Michel Roberge and members of his research group in the Department of Biochemistry and Molecular Biology at UBC for performing the biological assessment of new DSP toxins applying methods described in: Roberge, M.; Berlinck, R. G. S.; Xu, L.; Anderson, H. J.; Lim, L. Y.; Curman, D.; Stringer, C. M.; Friend, S. H.; Davies, P.; Vincent, I.; Haggarty, S. J.; Kelly, M. T.; Britton, R.; Piers, E.; Andersen, R. J. *Cancer Res.* **1998**, *58*, 5701.

(18) Hashimoto, N.; Aoyama, T.; Shioiri, T. *Chem. Pharm. Bull.* **1981**, *29*, 1475.

(19) Yamashita, K.; Yasuda, H.; Pines, J.; Yasumoto, K.; Nishitani, H.; Ohtsubo, M.; Hunter, T.; Sugimura, T.; Nishimoto, T. *EMBO J.* **1990**, *9*, 4331.

(20) Ghosh, S.; Schroeter, D.; Paweletz, N. *Exp. Cell Res.* **1996**, *227*, 165.

(21) Zheng, B.; Woo, C. F.; Kuo, J. F. *J. Biol. Chem.* **1991**, *266*, 10031.

(22) Zeng, Y.; Forbes, K. C.; Wu, Z. Q.; Moreno, S.; Piwnica-Worms, H.; Enoch, T. *Nature* **1998**, *395*, 507.

(23) Guo, X. W.; Th'ng, J. P. H.; Swank, J. A.; Anderson, H. J.; Tudan, C.; Bradbury, E. M.; Roberge, M. *EMBO J.* **1995**, *14*, 976.

(24) Takai, A.; Murata, M.; Torigoe, K.; Isobe, M.; Mieskes, G.; Yasumoto, T. *Biochem. J.* **1992**, *284*, 539.

(25) Suzuki, T.; Ota, H.; Yamasaki, M. *Toxicon* **1999**, *37*, 187.

(26) Hu, T.; Burton, I.; Curtis, J. M.; Quilliam, M. A.; Walter, J. A.; Windust, A. J.; Wright, J. L. C. *Tetrahedron Lett.* **1999**, *40*, 3981.

(27) Max Taylor (Professor Earth and Ocean Sciences), personal communication, **1999**.

(28) Konoki, K.; Sugiyama, N.; Murata, M.; Tachibana, K.; Hatanaka, Y. *Tetrahedron* **2000**, *56*, 9003.

(29) "The 1999 British Columbia Seafood Industry Year in Review," BC Fisheries, 1999.